The role of Nef-mediated CD3 downmodulation during HIV-1 viral spread

Dejan Mesner

Division of Infection and Immunity
University College London

A thesis submitted for the degree of
Doctor of Philosophy

June 2020

Declaration

I, Dejan Mesner, confirm that the work presented in this thesis is my own. Where information has been derived from other sources, I confirm that this has been indicated in the thesis.

The work from this thesis has since been published in the Proceedings of the National Academy of Sciences as a research article – Mesner, D., Hotter, D., Kirchhoff, F., & Jolly, C. (2020). Loss of Nef-mediated CD3 down-regulation in the HIV-1 lineage increases viral infectivity and spread. *Proceedings of the National Academy of Sciences of the United States of America*, 117(13), 7382–7391.

Acknowledgements

First and foremost, I would like to thank my supervisor Dr Clare Jolly for constant help, support and guidance, but also patience during this project. I am also thankful for having the opportunity to work and be part of the Jolly lab. I would also like to thank my thesis committee members Prof Greg Towers and Prof Mala Maini for helpful guidance and constructive discussions that help the project to evolve. I would also like to thank Dr Laura McCoy for all the help and support with the antibodies and Env work.

I would like to acknowledge the Jolly lab members, AK, Xenia, Maitreyi, Tafhima and Shimona for help with the experimental work and helpful discussions and for always answering all my questions. I would also like to acknowledge the McCoy and Towers lab members for helpful discussions during our lab meetings. Special thanks also goes to the Maini Lab members, Anna, Laura and Allice for teaching and guidance with flow cytometry.

Finally, I also need to thank all my friends and family for all the support during this time which helped me finish the project.

Abstract

HIV-1 most efficiently disseminates by direct cell-cell transmission that occurs at virological synapses (VS) formed between infected and uninfected CD4+ T cells. Previous work has shown that VS formation triggers antigen-independent T cell receptor (TCR) signalling in infected T cells to drive viral spread. Interestingly, the viral accessory protein Nef of HIV-2 and most SIV lineages, but not HIV-1, downmodulates CD3 - the signalling component of TCR complex. This impairs signalling at the immunological synapse and may interfere with antiviral responses and prevent aberrant immune activation. Why HIV-1 lost this potential immune evasion strategy remains incompletely understood. This question was addressed using chimeric HIV-1 viruses expressing SIVsmm Nef proteins and mutants thereof that differ specifically in their ability to downmodulate CD3. The results show that retained CD3 expression on infected cells resulted in enhanced viral cell-cell spread compared to viruses that downmodulate CD3 expression. Retained CD3 expression resulted in increased expression of functional envelope trimers (Env) on the surface of infected cells, increased Env incorporation into virions and thus increased virion infectivity, which was found to be the determinant for enhancement of viral spread. Increased Env expression and virion infectivity was shown to be dependent on VS formation and cell activation, thus explaining the role of CD3 and TCR signalling in this process. It was also observed that during cell-cell spread the presence of CD3 on infected cells correlated with enhanced TCR signalling at the VS, increased cell activation, as well as increased cell death. In addition to SIVsmm, SIVmac and HIV-2 Nef chimeric viruses were also examined, as they originate from zoonotic transmissions from SIVsmm. Interestingly, SIVmac and HIV-2 Nef viruses did not show any differences in cell-cell spread, virion infectivity or cell activation that correlated with CD3 downmodulation as observed for SIVsmm Nef viruses. The reason for this remains unknown; however, it suggests that there may be additional species-specific Nef determinants that contribute to efficient viral spread. Taken together, the results suggest that HIV-1 might have lost Nef-mediated CD3 downmodulation activity to allow for more efficient viral replication while losing the ability to suppress T cell activation and cell death, which possibly contributes to increased viral pathogenicity of HIV-1.

Impact statement

Primate lentiviruses have acquired and evolved different accessory genes to manipulate their host to order to support efficient viral replication and dissemination, while balancing this with the need to modulate the host environment towards immune evasion. I have examined the role of one such accessory protein: Nef and its ability to downmodulate surface expression of CD3, a key feature that distinguishes the pandemic HIV-1 lineage form most other primate lentiviruses. The data in this Thesis suggests that loss of this otherwise conserved feature contributes to more efficient viral spread, which helps to explain why HIV-1 lost this function of Nef. Importantly, it was also observed that loss of CD3 downmodulation results in increased T cell activation and cell death, which possibly contributes to increased viral pathogenicity of HIV-1 and less efficient immune evasion. Comparing Nef proteins from different lineages, this work highlights the plasticity of accessory protein function between different lentiviruses and evolution of multiple pathways that support efficient viral spread and thus provides new insights into lineage-specific differences in Nef function. This work also provides further understanding into the role of Nef and TCR signalling in immune activation and pathogenesis, which could be harnessed to develop new therapeutic strategies. Furthermore, the results also suggested that TCR signalling might impact on Env trafficking and virion incorporation, which mediates the infectivity of the virus. Currently the pathways of intracellular trafficking of Env and its virion incorporation are not well understood. The chimeric Nef virus used in this study could therefore be used to further dissect and understand the biology of Env. In turn, this knowledge could have important implication for development of novel vaccine or cure strategies. The interplay between the host and the virus is highly complex and extremely difficult to dissect through *in vitro* studies; however, this work highlights the value of comparative virology to gain new insight into the biology of HIV-1 and to inform our understanding into the evolution of this important human pathogen.

Table of contents

Declaration **2**

Acknowledgements **3**

Abstract **4**

Impact statement **5**

Table of contents **6**

List of figures **10**

List of tables **14**

Abbreviations **15**

1 Introduction **21**

1.1 Primate lentiviruses **21**

1.1.1 Zoonosis and origins of HIV 21

1.1.2 HIV and SIV genome organisation 23

1.2 HIV and SIV infections *in vivo* **26**

1.2.1 HIV-1 infection 26

1.2.2 HIV-2 infection 29

1.2.3 SIV infection 30

1.3 HIV-1 viral life cycle **33**

1.3.1 Virion structure 34

1.3.2 Entry 34

1.3.3 Reverse transcription, uncoating and integration 37

1.3.4 Viral gene expression 40

1.3.5 Env expression and trafficking 41

1.3.6 Assembly, budding and maturation 42

1.3.7 Restriction factors 47

1.4 Lentiviral accessory proteins **54**

1.4.1 Vif 54

1.4.2 Vpr and Vpx 55

1.4.3 Vpu 57

1.4.4 Nef 59

1.5 HIV-1 dissemination **70**

1.5.1 T cell virological synapse 71
1.5.2 Macrophage-T cell virological synapse 78
1.5.3 Dendritic cell-T cell synapse 79
1.5.4 Filopodia and nanotubes 80
1.6 T cell activation 82
1.6.1 The immunological synapse 82
1.6.2 TCR signalling cascade 83
1.6.3 Homotypic T cell-T cell contacts 88
1.6.4 Signalling at the virological synapse 89
1.7 Aim of the project 92
2 Materials and methods 93
2.1 Proviral constructs 93
2.2 Cell culture 94
2.2.1 Primary CD4+ T cell isolation and activation 94
2.3 Virus stock preparation 95
2.3.1 Plasmid preparation 95
2.3.2 Virus production and purification 96
2.3.3 Virus titration 96
2.4 Virus infection 97
2.5 Flow cytometry 97
2.6 Cell-cell spread assay 99
2.7 Virus release and infectivity 99
2.7.1 SG-PERT assay 100
2.7.2 Infectivity assay 101
2.8 Immunofluorescence microscopy 101
2.9 SERINC antagonism assay 102
2.10 Immunoblot analysis 103
2.10.1 Sample preparation 103
2.10.2 SDS-PAGE 103
2.10.3 Immunoblotting 103
2.11 Analysis of mRNA expression 104
2.11.1 Sample preparation 104
2.11.2 cDNA synthesis 104
2.11.3 RT-qPCR 105

2.12 Env trafficking 106
2.12.1 Env internalisation assay 106
2.12.2 Env recycling assay 106
2.13 Antibody neutralisation assay 106
2.14 CD3ζ knock-down 107
2.15 Infected T cell activation assay 108
2.16 TCR signalling assay 108
2.16.1 Donor-target cell co-culture 108
2.16.2 Flow cytometry analysis 109
2.17 Statistical analysis 109
3 Retained CD3 expression results in increased viral spread, virion infectivity and T cell activation 110
3.1 Introduction 110
3.2 Results 113
3.2.1 Validation of the phenotype of Nef chimeric viruses 113
3.2.2 Retained CD3 expression on infected cells results in increased viral spread 119
3.2.3 Retained CD3 expression results in increased Env expression and virion infectivity 127
3.2.4 Manipulation of Env expression and virion infectivity 138
3.2.5 Retained CD3 expression results in increased T cell activation during cell-cell spread 145
3.2.6 Phosphorylation changes in ZAP70, ERK, AKT and S6 during virological synapse formation 155
3.2.7 Retained CD3 expression results in increased T cell death during cell-cell spread 159
3.3 Discussion 164
3.3.1 Env expression, virion incorporation and infectivity 164
3.3.2 T cell activation and cell signalling 168
3.3.3 Cell death 173
4 Viral spread, virion infectivity and T cell activation by SIVmac and HIV-2 Nef chimeric viruses 175
4.1 Introduction 175
4.2 Results 178
4.2.1 Validation of the phenotype of SIVmac Nef chimeric viruses 178
4.2.2 Viral spread of SIVmac Nef chimeric viruses 181

4.2.3 Retained CD3 expression of SIVmac Nef viruses results in decreased Env expression and virion infectivity 186
4.2.4 Viral spread of SIVmac Nef chimeric viruses in Jurkat T cells 192
4.2.5 T cell activation during cell-cell spread of SIVmac Nef chimeric viruses 192
4.2.6 Phosphorylation changes in ZAP70, ERK, AKT and S6 during virological synapse formation of SIVmac Nef viruses 197
4.2.7 T cell death during cell-cell spread of SIVmac Nef chimeric viruses 202
4.2.8 Validation of the phenotype of HIV-2 Nef chimeric viruses 202
4.2.9 Viral spread of HIV-2 Nef chimeric viruses 205
4.2.10 T cell activation during cell-cell spread of HIV-2 Nef chimeric viruses 209
4.2.11 T cell death during cell-cell spread of HIV-2 Nef chimeric viruses 211

4.3 Discussion 212

5 Conclusions and future work 220

5.1 Summary 220

5.2 Relationship between Vpu and Nef function 221

5.3 CD3, immune activation and viral pathogenicity 223

5.4 Future directions 226

5.5 Final remarks 228

6 References 229

List of figures

Figure 1.1: Zoonotic transmissions and origins of HIV....22

Figure 1.2: Genomic organisation of primate lentiviruses....24

Figure 1.3: Acquisition of *vpu* and *vpx* during primate lentiviral evolution....25

Figure 1.4: HIV-1 viral life cycle....33

Figure 1.5: Env structure and fusion mechanism....35

Figure 1.6: HIV-1 virion assembly, budding and maturation....43

Figure 1.7: Nef structure and sequence motifs important for Nef function....60

Figure 1.8: Lentiviral Nef proteins and CD3 downmodulation....65

Figure 1.9: HIV-1 dissemination....71

Figure 1.10: The T cell virological synapse....73

Figure 1.11: TCR signalling....85

Figure 1.12: Comparison of the immunological and virological synapse....90

Figure 3.1: SIVsmmFBr L4 and K2 *nef* alleles and NL4.3 Nef chimeric viruses....112

Figure 3.2: Infection of primary CD4+ T cells with Nef chimeric viruses....114

Figure 3.3: CD3, CD4, CD28, and CXCR4 downmodulation by Nef chimeric viruses 116

Figure 3.4: Nef chimeric viruses have similar ability to antagonise SERINC5 and SERINC3....118

Figure 3.5: Cell-cell spread assay and gating strategy to analyse flow cytometry data 120

Figure 3.6: Retained CD3 expression on infected cells results in increased viral cell-cell spread 121

Figure 3.7: CD4+ T cells infected with Nef chimeric viruses form virological synapses at similar frequencies 123

Figure 3.8: Primary HIV-1 *nef* alleles have similar downmodulation and cell-cell spread properties compared to NL4.3 *nef*....125

Figure 3.9: Cell-cell spread assay with IL-7 treated and resting target cells....126

Figure 3.10: Retained CD3 expression on infected cells results in increased virion infectivity 128

Figure 3.11: Retained CD3 expression results in increased Env incorporation into virions 130

Figure 3.12: Retained CD3 expression results in increased expression of Env and Gag mRNA.....132

Figure 3.13: Retained CD3 expression results in increased intracellular and surface expression of Env.....133

Figure 3.14: Kinetics of Env internalisation by Nef chimeric viruses.....135

Figure 3.15: Kinetics of Env recycling by Nef chimeric viruses.....136

Figure 3.16: Antibody neutralisation of Nef chimeric viruses 137

Figure 3.17: Viral spread, Env expression and virion infectivity are independent of CD3-modulation in Jurkat T cells.....139

Figure 3.18: Env expression and virion infectivity are not affected by T cell stimulation in activated infected cells 141

Figure 3.19: Env expression and virion infectivity is increased by T cell stimulation in IL-7 treated infected cells 142

Figure 3.20: CD3 knock-down reduces T cell activation, surface Env expression and virion infectivity.....144

Figure 3.21: Retained CD3 expression results in increased T cell activation during cell-cell spread in donor and target cells. 146

Figure 3.22: Changes in T cell activation in donor cells during cell-cell spread.....148

Figure 3.23: Retained CD3 expression results in increased expression of GFP and Gag during cell-cell spread in donor and target cells.....150

Figure 3.24: Blocking virological synapse formation reduces viral gene expression and T cell activation. 151

Figure 3.25: Retained CD3 expression does not correlate with increased expression of CD25, CD95, CD98, and Glut1 during cell-cell spread in donor and target cells.....153

Figure 3.26: Changes in expression of CD25, CD95, CD98, and Glut1 in donor cells during cell-cell spread 154

Figure 3.27: Flow cytometry assay to detect phosphorylation changes in ZAP70, ERK, AKT and S6 upon donor-target cell conjugate formation 156

Figure 3.28: Retained CD3 expression results in increased phosphorylation of ERK and S6 in donor-target cell conjugates.....158

Figure 3.29: Retained CD3 expression results in increased cell death during cell-cell spread in donor and target cells.....161

Figure 3.30: Apoptosis is enhanced in GFP+ population during cell-cell spread, but it does not correlate with CD3 expression 163

Figure 3.31: Retained CD3 expression results in increased Env surface expression and virion incorporation.....166

Figure 3.32: Retained CD3 expression at the VS results in increased T cell activation and viral spread.....170

Figure 4.1: Sequence alignment of SIVsmm, SIVmac and HIV-2 *nef* alleles.....177

Figure 4.2: Validation of SIVmac Nef chimeric viruses 179

Figure 4.3: SIVmac Nef chimeric viruses have similar ability to antagonise SERINC5 181

Figure 4.4: Cell-cell spread of SIVmac Nef chimeric viruses 182

Figure 4.5: CD4+ T cells infected with Nef chimeric viruses form virological synapses at similar frequencies 184

Figure 4.6: Cell-cell spread of SIVmac Nef chimeric viruses in IL-7 treated cells.....185

Figure 4.7: Virion infectivity and virus release of SIVmac Nef chimeric viruses.....187

Figure 4.8: Env virion incorporation, synthesis and processing of SIVmac Nef chimeric viruses.....188

Figure 4.9: Env and Gag mRNA expression of SIVmac Nef chimeric viruses.....189

Figure 4.10: Surface Env expression of SIVmac Nef chimeric viruses.....190

Figure 4.11: Neutralisation of SIVmac Nef chimeric viruses.....191

Figure 4.12: Viral spread, Env expression, virion infectivity and release of SIVmac Nef chimeric viruses in Jurkat T cells 193

Figure 4.13: T cell activation (CD69, phospho-S6, CD38, PD-1) during cell-cell spread in donor and target cells infected with SIVmac Nef chimeric viruses.....195

Figure 4.14: T cell activation (CD25, CD95, CD98, Glut1) during cell-cell spread in donor and target cells infected with SIVmac Nef chimeric viruses.....196

Figure 4.15: Expression of GFP and Gag during cell-cell spread in donor and target cells infected with SIVmac Nef chimeric viruses 198

Figure 4.16: Phosphorylation of ZAP70, ERK, AKT and S6 in donor-target cell conjugates 199

Figure 4.17: Lck relocalisation by Nef chimeric viruses 201

Figure 4.18: Cell death during cell-cell spread in donor and target cells infected with SIVmac Nef chimeric viruses 203

Figure 4.19: Validation of HIV-2 Nef chimeric viruses.....204

Figure 4.20: Cell-cell spread of HIV-2 Nef chimeric viruses.....206

Figure 4.21: Virion infectivity and virus release of HIV-2 Nef chimeric viruses 208

Figure 4.22: Viral spread of HIV-2 Nef chimeric viruses in Jurkat T cells 208

Figure 4.23: T cell activation (CD69, CD38, CD25) during cell-cell spread in donor and target cells infected with HIV-2 Nef chimeric viruses 210

Figure 4.24: Expression of GFP and Gag during cell-cell spread in donor and target cells infected with HIV-2 Nef chimeric viruses.....211

Figure 4.25: Cell death during cell-cell spread in donor and target cells infected with HIV-2 Nef chimeric viruses.....212

List of tables

Table 2.1: Different *nef* alleles used in this thesis 93

Table 2.2: Antibodies used for flow cytometry 98

Table 2.3: SG-PERT reaction set-up 100

Table 2.4: SG-PERT PCR cycling parameters 100

Table 2.5: Antibodies used for microscopy 102

Table 2.6: Antibodies used for immunoblotting 104

Table 2.7: RT-qPCR cycling parameters 105

Table 2.8: Antibodies used for TCR signalling assay 109

Abbreviations

Ab	Antibody
ADAP	Adhesion and degranulation promoting adaptor protein
Ag	Antigen
agm	African green monkey
AIDS	Acquired immunodeficiency syndrome
AKT	ARK thymoma kinase, also known as PKB
ANOVA	Analysis of variance
AP-1	Adaptor protein 1; can also mean Activator protein 1
APC	Antigen presenting cell; can also mean Allophycocyanin
APOBEC	Apolipoprotein B mRNA editing enzyme catalytic polypeptide
ATCC	American type culture collection
BCL-10	B-cell lymphoma 10 protein
BV	Brilliant^{TM} Violet dye
c/p/dSMAC	Central/peripheral/distal supramolecular activation complex
CA	Capsid
Ca^{2+}	Calcium
CARMA1	CARD-containing MAGUK protein 1
CCR5	C-C chemokine receptor 5
CD	Cluster of differentiation
CDC42	Cell division control protein 42 homologue
cDNA	Complementary DNA
CFAR	Centre for AIDS reagents
cpz	Chimpanzee
CRAC	Calcium release-activated calcium channel
CT	Cytoplasmic tail
CTD	C-terminal domain
CTL	Cytotoxic T lymphocyte
CXCR4	C-X-C chemokine receptor 4
Cy3/5	Cyanine 3/5
DAG	Diacylglycerol
DC	Dendritic cell

DMEM	Dulbecco's modified eagle medium
DMSO	Dimethyl sulphoxide
DNA	Deoxyribonucleic acid
dNTP	deoxynucleotide triphosphate
drl	Drill
ds	Double stranded
EDTA	Ethylene diaminetetracetic acid
eIF4	Eukaryotic translation initiation factor 4
ELISA	Enzyme linked immunoabsorbant assay
Env	Envelope
ER	Endoplasmic reticulum
ERK	Extracellular signal-regulated kinase
ESCRT	Endosomal sorting complex required for transport
F-actin	Actin filaments
FACS	Fluorescence activated cell sorting
FCS	Foetal calf serum
FDA	Food and drug administration
FSC-A/W/H	Forward scatter area/width/height
FWB	FACS wash buffer
GADS	GRB2-related adaptor protein 2
Gag	Group-specific antigen
GALT	Gut associated lymphoid tissue
GBP	Guanylate-binding protein
GFP	Green fluorescent protein
gor	Gorilla
gp41	Envelope glycoprotein of 120 kDa
gp160	Envelope glycoprotein of 160 kDa
gp41	Envelope glycoprotein of 41 kDa
GRB2	Growth factor receptor-bound protein 2
gsn	Greater spot-nosed monkey
h	Hour
HA	Hemagglutinin
HB	Helix bundle

HIV	Human immunodeficiency virus
HUSH	Human silencing complex
ICAM	Intercellular adhesion molecule
IF	Immunofluorescence
IFN	Interferon
Ig	Immunoglobulin
IL-2	Interleukin 2
IL-7	Interleukin 7
IN	Integrase
IP_3	Inositol triphosphate
IRES	Internal ribosomal entry site
IS	Immunological synapse
ITAM	immunoreceptor tyrosine-based activation motif
ITK	IL-2-inducible T cell kinase
JNK	Jun N-terminal kinase
kb	Kilobase
KD	Knock-down
kDa	Kilo Dalton
LAT	Linker for activation of T cells
LB	Luria Bertani
Lck	Lymphocyte-specific protein tyrosine kinase
LEDGF/p75	Lens epithelium-derived growth factor
LFA-1	Lymphocyte function-associated antigen 1
LTR	Long terminal repeat
MA	Matrix
mac	Rhesus macaque
MACS	Magnetic activated cell sorting
MALT1	Mucosa-associated lymphoid tissue lymphoma translocation protein 1
MAPK	Mitogen activated protein kinase
MARCH	Membrane associated RING-CH domain protein
MEKK	MAP/ERK kinase kinase
MFI	Mean fluorescence intensity
MHC	Major histocompatibility complex

min	Minute
MKK	MAPK kinase
MLV	Murine leukaemia virus
mnd	Mandrill
MOI	Multiplicity of infection
mon	Mona monkey
MTOC	Microtubule organising centre
mTORC	Mammalian target of rapamycin complex
mus	Moustached money
MxB	Myxovirus resistance protein B
n/a	Not applicable
Nef	Negative regulatory factor
NF-κB	nuclear factor kappa-light-chain-enhancer of activated B cells
NFAT	Nuclear factor of activated T cells
NIBSC	National institute of biological standards and control
NIH	National institute for health
NMR	Nuclear magnetic resonance
NNRTI	Non-nucleoside reverse transcriptase inhibitor
NPC	Nuclear pore complex
NRTI	Nucleoside reverse transcription inhibitor
NTD	N-terminal domain
Nup	Nucleoporin
ORF	Open reading frame
P-TEFb	Positive transcription elongation factor b
p.i.	Post-infection
p38	p38 MAP kinase
PBMC	Peripheral blood mononuclear cells
PBS	Phosphate buffered saline
pbs	Primer binding site
PCR	Polymerase chain reaction
PDK1	Phosphoinositide-dependent kinase 1
PE	Phycoerythrin
PerCP	Peridinin-Chlorophyll protein

PFA	Paraformaldehyde
PHA	Phytohemagglutinin
PI	Protease inhibitor
PI3K	phosphoinositide 3-kinase
PIP_2	Phosphatidylinositol 4,5-bisphosphate
PIP_3	Phosphatidylinositol 3,4,5-risphosphate
PKCθ	Protein kinase Cθ
PLCγ1	Phospholipase Cγ1
PM	Plasma membrane
pMHC	Peptide complexed with major histocompatibility complex
Pol	Polymerase
PPT	Polypurine tract
qPCR	Quantitative polymerase chain reaction
Ras	Rat sarcoma oncogene protein
RASGRP1	RAS guanyl-releasing protein 1
rcm	Red-capped mangabey
Rev	Regulator of expression of virion proteins
RLU	Relative light units
RNA	Ribonucleic acid
RNAi	RNA interference
RPMI	Roswell Park Memorial Institute medium
RT	Reverse transcriptase; can also mean room temperature
SAMHD1	Sterile α-motif and HD domain-containing protein 1
SDF-1	Stromal cell-derived factor 1
SDS-PAGE	Sodium dodecyl sulphate polyacrylamide gel electrophoresis
SERINC	Serine incorporator
shRNA	Small hairpin RNA
siRNA	Small interfering RNA
SIV	Simian immunodeficiency virus
SLP76	SH2 domain containing leukocyte protein of 76kDa
smm	Sooty mangabey
SOS1	Son of sevenless homologue 1
ss	Single stranded

SSC-A	Side scatter area
TAR	Transactivation responsive region
Tat	Transactivator protein
TBS	Tris buffered saline
TCR	T cell receptor
TGN	Trans Golgi network
TRIM5α	Tripartite motif 5 alpha
UTR	Untranslated region
Vif	Viral infectivity factor
VLP	Virus-like particle
Vpr	Viral protein R
Vpu	Viral protein U
Vpx	Viral protein X
VS	Virological synapse
VSVg	Vesicular stomatitis virus glycoprotein
WASP	Wiskott–Aldrich syndrome protein
WHO	World health organisation
WT	Wild type
ZAP70	Zeta-chain-associated protein kinase 70

1 Introduction

1.1 Primate lentiviruses

Lentiviruses are a member of retrovirus family (*Retroviridae*), which is characterised by single-stranded viral RNA genome that is converted to double-stranded DNA by viral reverse transcriptase enzyme and integrated into host genomic DNA (Stover & Watson, 2015). A common feature of lentiviruses compared to other retroviruses is their ability to infect non-dividing cells (Stover & Watson, 2015). This Thesis focuses on primate lentiviruses, which infect humans and non-human primates. Infection of humans is caused by human immunodeficiency virus (HIV) and results (if untreated) in acquired immune deficiency syndrome (AIDS) (Barré-Sinoussi et al., 1983). Simian immunodeficiency viruses (SIV) are highly prevalent and infect more than 40 species of African apes and monkeys in the wild (Klatt et al., 2012). Other examples of lentiviruses include bovine immunodeficiency virus, feline immunodeficiency virus and equine infectious anaemia virus (Stover & Watson, 2015).

The main targets of HIV and SIV infection are CD4+ T cells and to lesser extent macrophages and dendritic cells (Alkhatib et al., 1996; Kaur et al., 1998; Maddon et al., 1986; Smed-Sörensen et al., 2005). Loss of CD4+T cells during HIV infection leads to immunodeficiency and subsequent progression to disease (AIDS), which manifests as infectious and oncological complications (Brenchley et al., 2006). As of 2019, approx. 38 million people worldwide are living with HIV and since the beginning of the pandemic in 1980s approx. 75 million people have been infected and approx. 35 million have died from AIDS-related illnesses (*UNAIDS Fact Sheet*, 2019). By contrast, some monkey species are resistant to SIV-mediated CD4+ T cell depletion and do not develop AIDS-like disease despite high levels of viral replication, suggesting virus-host adaptation (Chahroudi et al., 2012).

1.1.1 Zoonosis and origins of HIV

HIV is the result of a series of cross-species zoonotic transmissions. Broadly, this has given rise to two different human immunodeficiency viruses: HIV-1 and HIV-2 which are genetically distinct (Clavel et al., 1986). HIV-1 is classified into 4 groups: M, N, O, P, which originated from 4 independent zoonotic transmissions (Sharp & Hahn, 2011). Phylogenetic analysis revealed that HIV-1 groups M and N originated from SIVcpz

infecting the central subspecies of chimpanzees (*Pan troglodytes troglodytes*) while HIV-1 groups O and P originated from SIVgor infecting western lowland gorillas (*Gorilla gorilla gorilla*) (Gao et al., 1999; Keele et al., 2006; Plantier et al., 2009; Simon et al., 1998). SIVgor itself most likely resulted from zoonotic transmission from central chimpanzees into gorillas (Takehisa et al., 2009). Phylogenetic analysis of SIVcpz showed it originated from a recombination event between precursor of SIVrcm infecting red-capped mangabeys and precursor of SIVgsn/mon/mus lineage infecting closely related *Cercopithecus* monkeys (greater spot-nosed, mona and mustached monkeys) (Bailes et al., 2003). More recent phylogenetic analysis also suggests that origin of SIVcpz might be tripartite, resulting from a recombination between SIVrcm, SIVgsn/mon/mus and an unknown SIV (Bell & Bedford, 2017). HIV-2 was transmitted to humans from SIVsmm infected sooty mangabeys (*Cercocebus atys*) in nine independent transmissions to give HIV-2 groups A-I (Ayouba et al., 2013; Gao et al., 1994; Hirsch et al., 1989). Zoonotic transmission to humans most likely occurred via contact with infected blood during bushmeat hunting and butchering (Sharp & Hahn, 2011).

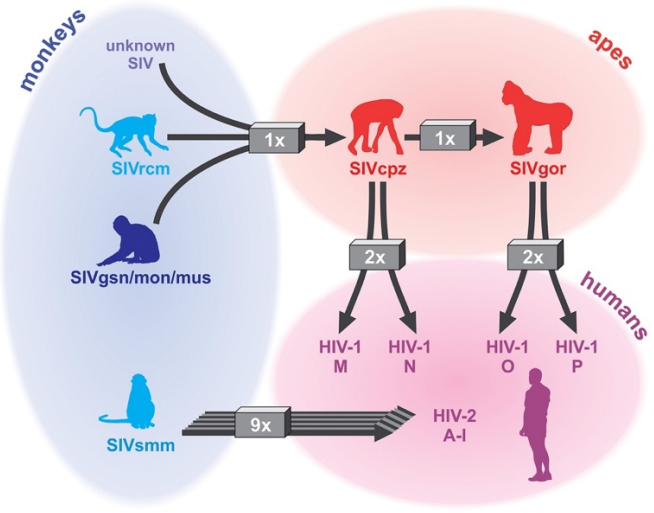

Figure 1.1: Zoonotic transmissions and origins of HIV

SIVcpz resulted from a recombination event between a precursor of SIVrcm, SIVgsn/mon/mus and possibly another unknown SIV. SIVcpz was transmitted to humans to give HIV-1 groups M and N, and to gorillas to give SIVgor. SIVgor was transmitted to humans to give HIV-1 groups O and P. SIVsmm was transmitted to humans to give HIV-2 groups A-I. Taken from (Sauter & Kirchhoff, 2019).

Out of all HIV strains, only HIV-1 group M is pandemic and accounts for more than 98% of infections worldwide (Sauter & Kirchhoff, 2019). By contrast, HIV-1 groups N, O and P are largely restricted to Central West Africa. Group O accounts for approx. 100,000

cases, whereas group N and P viruses are particularly rare, with only a handful of documented cases (Mourez et al., 2013). Due to genetic diversity group M viruses are further classified into nine subtypes: A, B, C, D, F, G, H, J, K (as well as circulating recombinants thereof) and their distribution varies geographically (Geretti, 2006). For example, subtype B is the most prevalent in North America and Europe, whereas subtype C and to a lesser extent subtype A are most common in Africa (Geretti, 2006). HIV-2 is also mainly restricted to West Africa and only groups A and B show significant spread in the population with approx. 1-2 million infections (Visseaux et al., 2016).

The first cases of AIDS were reported in New York, USA in 1981 (Friedman-Kien et al., 1981) and HIV was identified as causative agent of AIDS in 1983 (Barré-Sinoussi et al., 1983). However, sequencing of historic tissue samples, phylogenetic analysis and modelling suggested that chimpanzee-to-human transmission of HIV-1 group M viruses most likely occurred at the beginning of 20th century (1910-1920s) in Cameroon with initial spread in Kinshasa, DRC in 1960s (Faria et al., 2014; Worobey et al., 2008). Interestingly, the time and place of HIV-1 group O emergence is thought to be similar to group M (Faria et al., 2014); however, only the later became pandemic. The reasons why only group M became better adapted for transmission and spread in the human population remain incompletely understood and will be discussed further in Section 1.3. By contrast, the history of SIVcpz infections in chimpanzees is thought to be much longer. Given that SIVcpz phylogenetic analysis suggests one common ancestor of SIVcpz and only two out of four chimpanzee subspecies are infected (*Pan troglodytes troglodytes* and *Pan troglodytes schweinfurthii*), this places the emergence of SIVcpz approx. 100-500 thousand years ago (Bailes et al., 2003; Sauter & Kirchhoff, 2019). Furthermore, analysis of evolution and positive selection of host genes suggests that SIVs have been infecting other African monkey species for at least 5-10 million years (Compton et al., 2013; McCarthy et al., 2015).

1.1.2 HIV and SIV genome organisation

The HIV/SIV viral genome is positive-sense single-stranded RNA, approx. 10 kb long, which contains 8-9 genes encoding for 14-15 proteins depending on the viral lineage. The proviral genome is flanked by two long terminal repeats (LTR), which act as promoters to drive viral transcription (Burnett et al., 2009). The structural and enzymatic genes: *gag, pol* and *env* are common to all retroviruses. *Gag* gene encodes for matrix, capsid, nucleocapsid and p6 proteins, which are required for virion formation and

structure. *Env* gene encodes for envelope glycoprotein (transmembrane and surface subunit), which is required for virus entry. *Pol* gene encodes for enzymes reverse transcriptase, protease and integrase. Primate lentiviruses also contain two regulatory genes *tat* and *rev*, and at least three accessory genes: *vif, vpr* and *nef*, which are required for efficient viral replication. Additionally, some primate lentiviruses also contain *vpu* or *vpx* accessory genes. Function of these proteins will be examined in detail in Section 1.4.

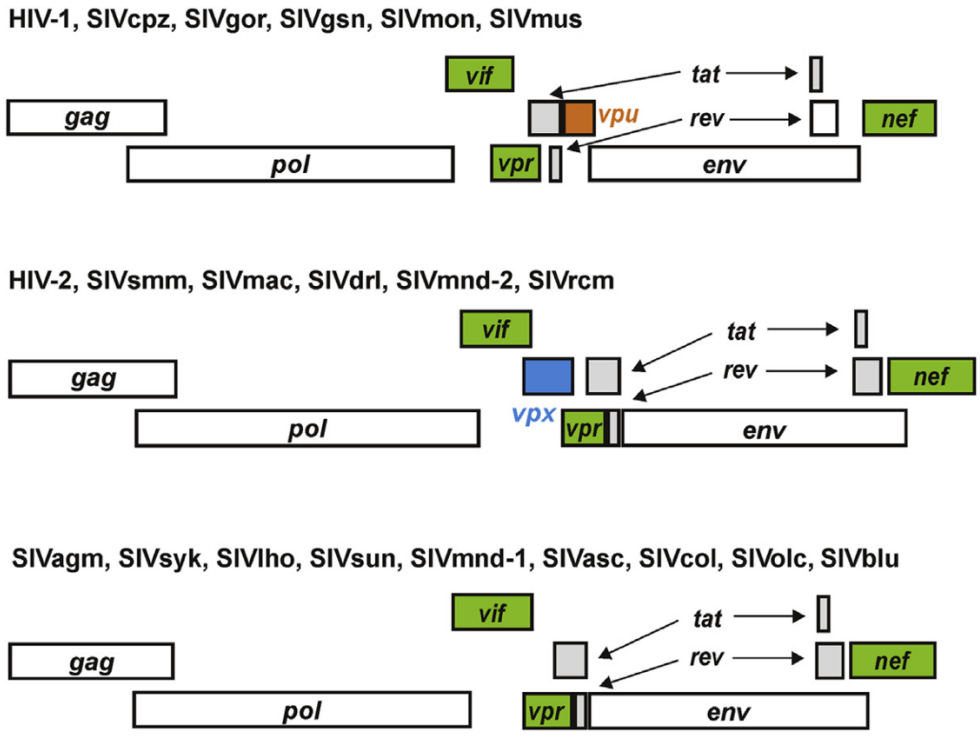

Figure 1.2: Genomic organisation of primate lentiviruses

The structural and enzymatic genes (*gag, pol* and *env*) are shown in white and are common to all retroviruses. The regulatory genes *tat* and *rev* common to all primate lentiviruses are shown in grey. The accessory genes *vif, vpr*, and *nef* are also common to all primate lentiviruses and are shown in green. *Vpu* gene (orange) is only found in the HIV-1/SIVcpz lineage and closely related SIVgsn/mon/mus infecting *Cercopithecus* monkeys. *Vpx* gene (blue) is only found in the HIV-2/SIVsmm and related SIVrcm/drl/mnd2 linages. Taken from (Sauter & Kirchhoff, 2014).

Based on presence of different accessory genes primate lentiviruses can be divided into three groups (Figure 1.2). Viruses in the first group contain *vif, vpr, nef* and *vpu* genes. These viruses are: HIV-1, SIVcpz, SIVgor, SIVgsn/mon/mus. It is believed that *vpu* was first acquired by a precursor of the SIVgsn/mon/mus lineage and was then transferred to HIV-1/SIVcpz lineage after recombination with SIVrcm (Figure 1.3) (Bailes et al., 2003). The presence of *vpu* gene thus distinguishes the HIV-1 lineage from most other

primate lentiviral lineages. Viruses in the second group contain *vif, vpr, nef* and *vpx* genes. *Vpx* likely originated from a duplication of *vpr* gene (Tristem et al., 1990) and can be found in two related linages: HIV-2, SIVsmm and SIVmac infecting rhesus macaques; and SIVrcm, SIVdrl infecting drills and SIVmnd2 infecting mandrills (Etienne et al., 2013). Phylogenetic analysis suggests that *vpx* emerged once during primate lentiviral evolution, prior to the separation of HIV-2/SIVsmm and SIVrcm/drl/mnd2/ lineages (Etienne et al., 2013). *Vpx* was lost during the recombination of SIVrcm and SIVgsn/mon/mus and is thus absent in the HIV-1/SIVcpz lineage (Figure 1.3). The rest of the SIVs are in the third group and contain only *vif, vpr* and *nef* genes (prototype SIV). For example, SIVagm infecting African green monkeys, SIVsyk infecting Sykes' monkeys, SIVsun infecting sun-tailed monkeys, SIVcol infecting guereza colobus monkeys, SIVblu infecting blue monkeys, etc (Peeters & Courgnaud, 2003; Sauter & Kirchhoff, 2014).

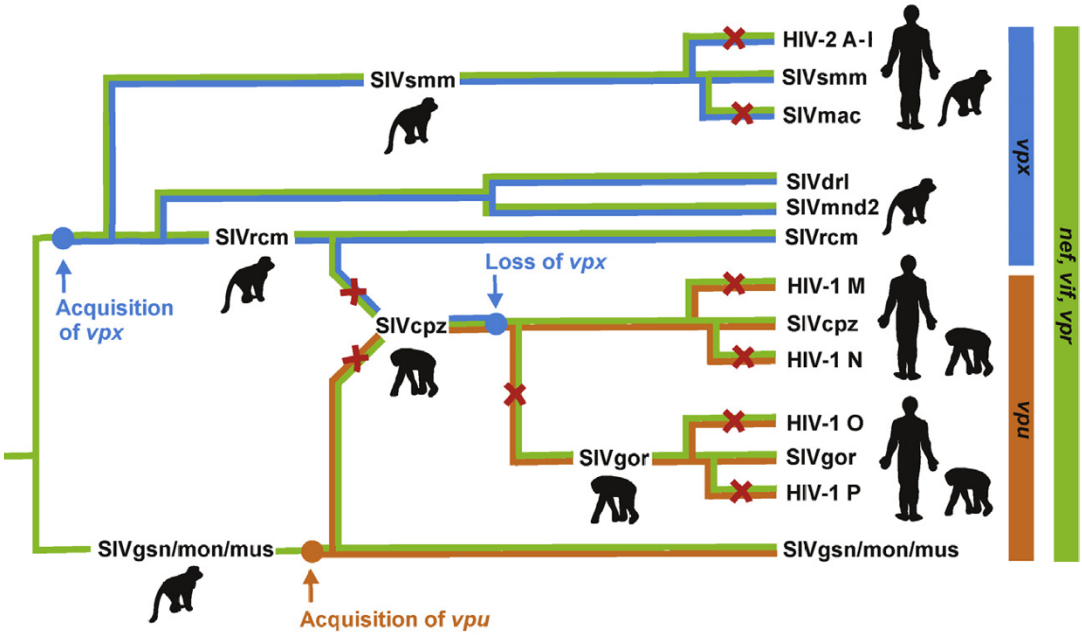

Figure 1.3: Acquisition of *vpu* and *vpx* during primate lentiviral evolution

The diagram shows acquisition of *vpx* gene in the HIV-2/SIVsmm and SIVrcm/drl/mnd2 lineages, shown in blue. HIV-2 and SIVmac originate from zoonotic transmission from SIVsmm. *Vpu* was acquired by a precursor of SIVgsn/mon/mus, shown in orange. The recombination of SIVgsn/mon/mus and SIVrcm resulted in gain of *vpu* and loss of *vpx* genes in the HIV-1/SIVcpz lineage. SIVcpz was transmitted to gorillas (SIVgor) and to humans (HIV-1 M and N). SIVgor was also transmitted to humans (HIV-1 O and P). Red crosses indicate zoonotic transmissions. All primate lentiviruses contain *vif, vpr* and *nef* genes, shown in green. Adapted from (Sauter & Kirchhoff, 2014).

1.2 HIV and SIV infections *in vivo*

1.2.1 HIV-1 infection

Like all primate lentiviruses, HIV-1 mainly infects CD4+ T cells. Infection and cell tropism is primarily determined by the presence of the CD4 molecule on the surface of target cells that is the receptor for viral entry (Maddon et al., 1986) alongside C-C chemokine receptor 5 (CCR5) that acts as a coreceptor (Alkhatib et al., 1996). However, for some viruses the coreceptor C-X-C chemokine receptor 4 (CXCR4) is used instead of CCR5 (Feng et al., 1996). This distinction has been defined as viruses being either CCR5-tropic (R5) or CXCR4-tropic (X4). In addition to CD4+ T cells, macrophages and dendritic cells also express these receptors and can thus become infected by HIV-1. Although macrophages represent only a minor population of HIV-1 infected cells in the body, they are thought to be an important viral reservoir due to their long-term survival after infection (Watters et al., 2013). Productive infection of dendritic cells is largely restricted due to high activity of innate immune sensors (TLR7/9) and viral restriction factors, particularly dNTP hydrolase SAMHD1, which inhibits reverse transcription (Laguette et al., 2011; Manches et al., 2014; Smed-Sörensen et al., 2005). However, dendritic cells can capture and carry the virus to infect CD4+ T cells *in trans* during immunological synapse formation (Geijtenbeek et al., 2000), which will be discussed further in Section 1.5.

1.2.1.1 Transmission

In an infected individual, HIV-1 can be found in blood, cervicovaginal and rectal secretions, semen and breastmilk. Therefore, the virus can be transmitted via multiple routes: sexual contact, percutaneous or intravenous inoculation and maternal-infant transmission during pregnancy (*in utero*), childbirth or breastfeeding (Shaw & Hunter, 2012). Approx. 80% of people get infected through sexual contact, therefore HIV-1 is primarily a sexually transmitted infection. The remaining 20% of infections are mainly contributed to maternal-infant transmission and intravenous inoculation (Cohen et al., 2011). The probability of infection greatly depends on the stage of HIV infection, viral load, existing co-infections and route of transmission. For example, the probability of penile-vaginal transmission (per exposure event) is 1:200-1:2000, whereas the probability of penile-rectal transmission is much higher, 1:20-1:300 (Shaw & Hunter, 2012). Genetic analysis of viral quasi-species during acute infection revealed that in approx. 80% of sexual transmissions, the infection is established by a single virion, termed transmitted/founder virus (Keele et al., 2008; Salazar-Gonzalez et al., 2009). By contrast, during intravenous transmission multiple transmitted/founder viruses (up to 16)

are usually responsible for establishing the initial infection (Bar et al., 2010). This suggest that mucosal barriers present a significant bottleneck for viral transmission. Taken together with relatively low probability of transmission via sexual contact, these data suggest that initial HIV-1 infection is a rare event.

1.2.1.2 Clinical features of infection and pathogenesis

After successful transmission, HIV-1 infection can be divided into three phases: acute, latent and AIDS. In the acute phase the virus replicates rapidly, allowing for detection of viral RNA in the blood approx. one week post-transmission (Fiebig et al., 2003; Shaw & Hunter, 2012). Subsequently, Gag p24 antigen (2 weeks post-transmission) and anti-HIV-1 antibodies (3-4 weeks post-transmission) can be detected to allow clinical diagnosis (Fiebig et al., 2003; Shaw & Hunter, 2012). During the acute phase, the infection is first established at the mucosal epithelia (depending in the route of transmission) and then spreads to draining lymph nodes and the gastrointestinal tract (i.e. gut-associated lymphoid tissue, GALT) before becoming systemic (Cohen et al., 2011). The main targets of infection are memory CCR5+ CD4+ T cells (Douek et al., 2002). The initial viral spread with peak blood viremia (20-30 days post-transmission) is associated with rapid depletion of CD4+ T cells, particularly in the GALT (Brenchley et al., 2004; Mehandru et al., 2004; Schacker et al., 1996). At this stage, infected individual may present with flu-like symptoms (Schacker et al., 1996) that are reflective of seroconversion. Depletion of GALT CD4+ T cells is thought to cause intestinal epithelium breakdown, which allows microbial translocation in the blood stream (Brenchley et al., 2006). This is thought to cause chronic immune activation during HIV-1 infection, although the extent of contribution of microbial translocation to HIV-1 induced inflammation remains controversial (Younas et al., 2016).

In the latent phase of infection, after the acute viremia the plasma viral load drops and reaches a set-point, due to (limited) immune control by cytotoxic T lymphocytes (CTL) and humoral immune responses (Fiebig et al., 2003; Goonetilleke et al., 2009; Wei et al., 2003). CD4+ T cell count also recovers slightly and remains relatively stable or slowly declines for months to years depending on the individual (Shaw & Hunter, 2012; Younas et al., 2016). In majority of infections the immune system cannot produce a neutralising antibody response to control the infection due to rapid virus evolution and generation of escape mutants (Wei et al., 2003). In about 50% of cases chronic infection is associated with coreceptor switch (mutations in the envelope glycoprotein), meaning that the virus

starts using CXCR4 instead of CCR5 as the coreceptor or is CCR5/CXCR4 dual-tropic (Brumme et al., 2005). This expands viral tropism to naïve CD4+ T cell population and is thus associated with more aggressive disease and poor prognosis (Brumme et al., 2005).

In the final stage, progression to AIDS occurs and is classified as blood CD4+ T cell count of less than 200 cells/ml (Castro et al., 1993). At this stage an infected individual, due to immune deficiency, cannot control other infections and malignancies (e.g. pneumonia, candidiasis, tuberculosis, lymphoma, Kaposi's sarcoma), eventually leading to death (Luetkemeyer et al., 2010).

1.2.1.3 Treatment and prevention

Several classes of HIV-1 antiviral drugs have been developed, which drastically improved survival rates and disease prognosis of HIV-1 infected individuals. The first HIV-1 antiviral drug, zidovudine (AZT) targeting the viral reverse transcriptase (RT) was approved in 1987 (Furman et al., 1986). However, it was ineffective due to rapid development of viral drug resistance (Larder et al., 1995). The first combination antiretroviral therapy was approved 1996 and consisted of three viral enzyme inhibitors: zidovudine and zalcitabine targeting RT, and saquinavir targeting the viral protease (Collier et al., 1996). The triple combination antiretroviral therapy is required as HIV-1 has high mutation rate and viral escape mutants emerge quickly, resulting in viral drug resistance if only one or two antiretroviral drugs are administered (Autran et al., 1997). There are four major classes of antiretroviral drugs used in the clinic targeting viral RT, protease and integrase. First, nucleotide reverse transcriptase inhibitors (NRTIs) are dNTP analogues targeting the active site of RT and thus inhibiting reverse transcription by causing premature chain termination (Clair et al., 1987). Current Food and Drug Administration (FDA) approved NRTIs are: abacavir, emtricitabine, lamivudine, tenofovir and zidovudine. Second, non-nucleotide reverse transcriptase inhibitors (NNRTIs) bind to RT proximal to the active site, inducing a conformational change and thus inhibiting the enzyme (Kohlstaedt et al., 1992). Current FDA approved NNRTIs are: efavirenz, etravirine, nevirapine and rilpivirine. Third, protease inhibitors (PIs) prevent Gag polyprotein cleavage and virion maturation, thus producing non-infectious viral particles (Kempf et al., 1995). Current FDA approved PIs are: atazanavir, darunavir, fosamprenavir, ritonavir, saquinavir and tipranavir. Fourth and most recent are integrase inhibitors (INIs), which inhibit DNA strand transfer reaction and thus prevent viral

integration into host DNA (Espeseth et al., 2000). Current FDA approved INIs are: dolutegravir, raltegravir, elvitegravir and bictegravir.

The combination antiretroviral therapy in most cases results in almost complete suppression of viral replication (below the limit of detection of viral RNA in blood, <50 copies/ml of plasma) and significantly restores the CD4+ T cell numbers (Cihlar & Fordyce, 2016). Currently, where the antiretroviral therapies are available, HIV-1 infected individuals have normal life expectancy (Trickey et al., 2017). The combination antiretroviral therapy is also used to prevent HIV-1 infection in recently exposed individuals (post-exposure prophylaxis) or to prevent transmission in high risk groups (pre-exposure prophylaxis) (Ford et al., 2014; Wilton et al., 2015). Importantly, the antiretroviral therapy is not curative, resulting in viral replication rebound after treatment interruption (Cihlar & Fordyce, 2016). The reason for this is the presence of a viral reservoir consisting of an unknown population of latently infected cells, which after treatment interruption can become actively infected and produce infectious virus (Pitman et al., 2018). Therefore, current efforts to cure HIV-1 include strategies to reactivate the latent reservoir (latency-reversal agents) and thus kill all infected cells in the body (Pitman et al., 2018). However, these strategies have so far been unsuccessful. Furthermore, ongoing viral replication in sanctuary sites where drug penetrance is low (e.g. central nervous system) may also contribute to viral persistence, but this remains controversial due to the challenges associated with sampling different anatomical compartments (Fletcher et al., 2014; Letendre et al., 2008). Another strategy to prevent HIV-1 infection is vaccine development, which has so far also been unsuccessful, mainly due to great genetic diversity of HIV-1, high rate of viral mutations and difficulty of eliciting a neutralising antibody response (Gao et al., 2018). To date, the most successful HIV-1 vaccine clinical trial (RV144 in Thailand) resulted in modest 31% protection efficacy (Robb et al., 2012).

1.2.2 HIV-2 infection

HIV-1 and HIV-2 have similar modes of transmission, cellular tropism, replication pathways and both cause AIDS; however, HIV-2 infection is generally considered less pathogenic and has lower probability of progression to AIDS (Marlink et al., 1994; Nyamweya et al., 2013; Olesen et al., 2018). HIV-2 mainly infects CD4+ T cells by using CD4 as receptor for viral entry but has extended coreceptor usage and in addition to CCR5/CXCR4 can also utilise CCR1, CCR2, CCR3, CCR8, CXCR6 chemokine

receptors (Shi et al., 2005). HIV-2 has same routes of transmission compared to HIV-1, but is characterised by significantly lower transmission rates, most likely due to lower viral loads in HIV-2 infected individuals (Gottlieb et al., 2006; Popper et al., 2000). Indeed, a significant proportion of HIV-2 infected individuals present with undetectable plasma viral load (Popper et al., 2000; Soriano et al., 2000; van der Loeff et al., 2010). Lower viral loads are thought to reflect better immune control of HIV-2 infection. This is shown by better innate immune responses (production of TNF-α and type-1 interferons), better T cell responses (polyfunctional Gag-specific CD4+ and CD8+ T cells) and better humoral immune responses, resulting in production of neutralising antibodies (Duvall et al., 2007, 2008; Nuvor et al., 2006; Rodriguez et al., 2007). Consistent with better immune control and lower viral loads there is less chronic immune activation observed in HIV-2 infection (Hanson et al., 2005). Overall, this results in lower morbidity and mortality associated with the infection and slower disease progression, with majority of infected individuals becoming long-term non-progressors (Jaffar et al., 1997; Marlink et al., 1994; Olesen et al., 2018; Thiébaut et al., 2011; van der Loeff et al., 2010). It is important to note that HIV-1 and HIV-2 are different viruses, originating from different SIVs with different set of acceory genes, therefore inherent differences between the viruses may contribute to the observed differences in clinical course of disease. Regarding HIV-2 treatment, same antiretroviral drugs as for HIV-1 are generally active, although with different potency, except for NNRTIs, which are inactive against HIV-2 RT, so different combinations of drugs are required (Peterson & Rowland-Jones, 2012).

1.2.3 SIV infection

More than 40 species of African apes and monkeys are infected with SIV, with generally high prevalence of infection in the wild (Klatt et al., 2012). Due to relatively long evolutionary history of SIV infections in monkeys (5-10 million years) they are considered “natural’ infections, particularly in comparison to HIV, which has been infecting humans for only about 100 years and is thus considered a “non-natural” infection (Brenchley et al., 2010; McCarthy et al., 2015; Worobey et al., 2008). SIV infections are generally considered to be non-pathogenic as despite high levels of viral replication, infected monkeys do not develop AIDS-like disease (Chahroudi et al., 2012). Importantly, good evidence to support this statement only exists for sooty mangabeys and African green monkeys, and to lesser extent mandrills.

1.2.3.1 Sooty mangabey and African green monkey

Sooty mangabeys (SM) and African green monkeys (AGM) are best studied models of non-pathogenic lentiviral infections. Like pathogenic HIV-1 infection, SIVsmm and SIVagm infections present with high levels of viral replication and no robust immune control of the virus (Dunham et al., 2006; Li et al., 2010; Silvestri et al., 2003). However, SIV-infected SM and AGM do not show high levels of chronic immune activation, maintain normal CD4+ T cell counts and do not progress to disease (Kaur et al., 1998; Pandrea et al., 2007b; Silvestri et al., 2003; Sodora et al., 2009; Sumpter et al., 2007). SIVs also use CCR5 is the main coreceptor for viral entry (Riddick et al., 2010). The acute infection is (like HIV-1) also associated with depletion of CCR5+CD4+ T cells in the GALT; however SM and AGM have much lower initial frequency of GALT CCR5+CD4+ T cells (3-5%) compared to humans (50%), resulting in proportionally smaller T cell depletion (Gordon et al., 2007; Pandrea et al., 2007a, 2007b). As a result, SM and AGM maintain intact mucosal barriers and do not show microbial translocation, which contributes to low levels of immune activation (Brenchley et al., 2006). Additionally, infection of memory CD4+ T cells is reduced by two mechanisms: SM have low levels of CCR5 expression and AGM have low levels of CD4 expression on memory T cells (Beaumier et al., 2009; Paiardini et al., 2011). Coreceptor switch to CXCR4 usage is almost never observed, which maintains healthy naïve cell population (Milush et al., 2007; Schmökel et al., 2013). Together these mechanisms contribute to improved T cell homeostasis and preserve the immune function during infection. Moreover, both SM and AGM have been shown to have fully functional double negative (CD4-CD8-) helper T cells, which are therefore resistant to infection (Milush et al., 2011; Sundaravaradan et al., 2013; Vinton et al., 2011). This further exemplifies high levels of natural host adaptation to SIV infection that protects SM and AGM from the development of disease.

1.2.3.2 Rhesus macaque

SIVmac infection of rhesus macaques (RM) is considered to be a non-natural infection. This is because SIVmac originates from experimental infection of RM with tissue homogenates from SIVsmm infected SM (Apetrei et al., 2005; Murphey-Corb et al., 1986). Infected RM show high levels of viral replication, no robust immune control of the virus, chronic immune activation, progressive CD4+ T cell depletion and thus develop AIDS-like disease (Dunham et al., 2006; Estes et al., 2008; Kaur et al., 1998; Münch et al., 2001; Silvestri et al., 2003a; Watson et al., 1997). RM are thus used as a model of pathogenic SIV infection. Similarly, experimental (non-natural) infection of pigtailed macaques with SIVagm also resulted in pathogenic infection and AIDS-like disease

(Goldstein et al., 2005). Like SIVsmm or SIVagm, acute SIVmac infection also results in depletion of CCR5+CD4+ T cells in the GALT; however, RM have high proportion of CCR5+ GALT CD4+ T cells, which results in dramatic loss of CD4+T cells in the gut (Pandrea et al., 2007a, 2007b). This is thought to cause breakdown of mucosal barriers and subsequent microbial translocation, which contributes to chronic immune activation (Brenchley et al., 2006). Moreover, RM memory CD4+ T cells express high levels of CCR5 coreceptor, which allows for enhanced infection of the central memory pool, thus disrupting normal T cell homeostasis and contributing to the pathogenesis (Okoye et al., 2007). Furthermore, when SM were infected with SIVmac virus they showed relatively high levels of viral replication, but no progressive CD4+ T cell depletion and did not progress to AIDS-like disease, similar to natural SIVsmm infection (Kaur et al., 1998). Taken together, this suggest that poor host adaptation, rather than intrinsic high virulence of SIVmac might be responsible for pathogenic infection of RM.

1.2.3.3 Chimpanzee and gorilla

SIV infection of African apes, chimpanzees and gorillas, is not well studied. Phylogenetic and evolutionary analysis suggests that SIVcpz has been infecting chimpanzees for about 100-500 thousand years (Sauter & Kirchhoff, 2019), which classifies it as a natural infection. Despite this, limited evidence exists that SIVcpz infection causes CD4+ T cell depletion, AIDS-like disease and increased mortality of chimpanzees in the wild (Keele et al., 2009). SIV infection of gorillas is even less well studied. Phylogenetic analysis suggests that SIVgor transmitted from chimpanzees at least 200 years ago and possibly much earlier (Takehisa et al., 2009). Immunological features of SIVgor infection are currently unknown; however, given the SIVcpz data and relatively short history of infection, one can speculate that SIVgor infection is also pathogenic.

1.3 HIV-1 viral life cycle

This Section discusses HIV-1 viral life cycle as the work in this Thesis focuses on HIV-1 replication; however, HIV-2 and SIVs have similar viral life cycles. As shown in Figure 1.4, HIV-1 must complete a series of steps in its life cycle in order to replicate: (1) receptor and coreceptor binding, fusion and entry into host cell cytoplasm; (2) reverse transcription of viral genome, capsid uncoating, nuclear import and integration; (3) viral gene expression; (4) virion assembly, budding and maturation.

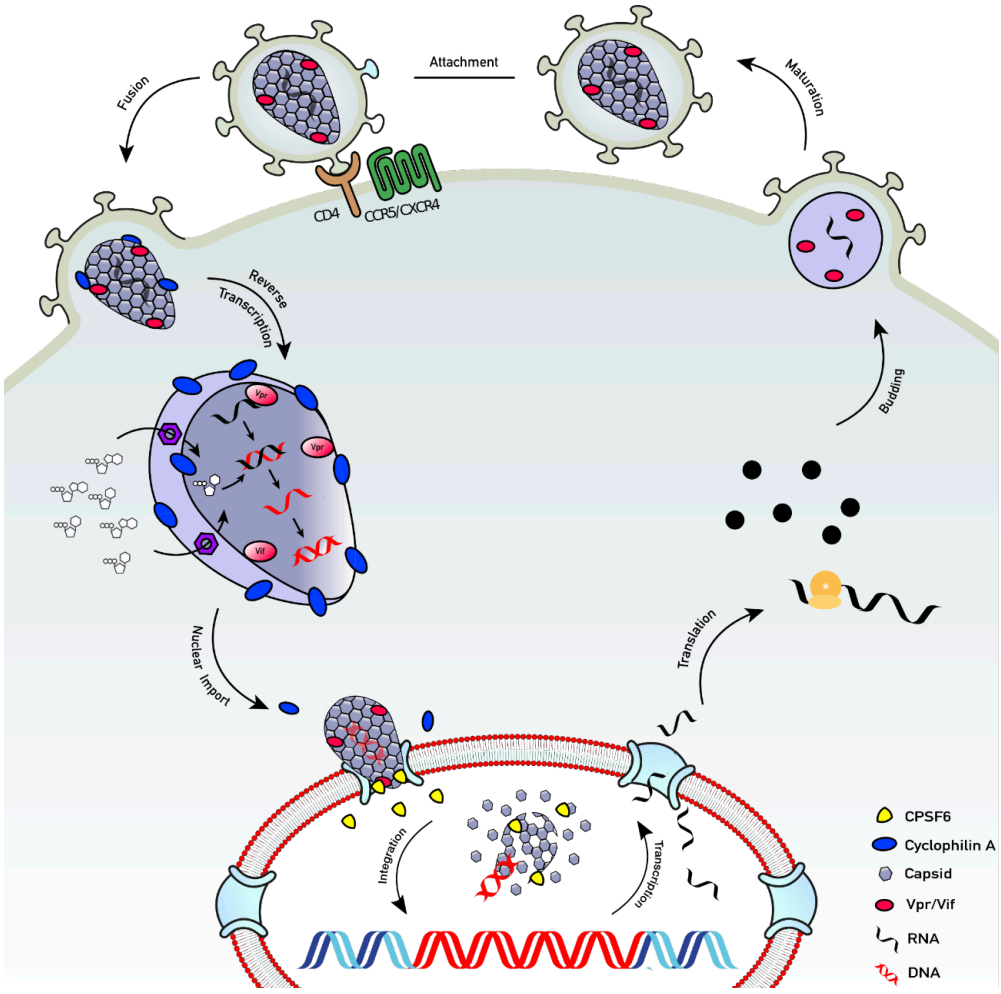

Figure 1.4: HIV-1 viral life cycle

Envelope glycoprotein binds the CD4 receptor and CCR5/CXCR4 coreceptor, which results in viral fusion and release of the capsid core into the host cell cytoplasm. Inside the capsid core viral RNA genome is transcribed into double stranded DNA. Capsid uncoating might happen at the nucler pore or inside the nucleus where the viral DNA is integrated into the host genome. Capsid recruits cellular proteins cyclophilin A and CPSF6 to avoid inate immune detection and ensure optimal viral integration. Transcription and translation of viral DNA results produces viral proteins resulting in assembly and budding of progeny virus. In nascent viral particels viral protease cleaves the structural polyproteins to produce mature infectious virions. Adapted from (Sumner et al., 2017).

1.3.1 Virion structure

The size of mature HIV-1 virion is approx. 145 nm in diameter (Briggs et al., 2003). Viral envelope is a lipid bilayer derived from the host cell plasma membrane, which incorporates multiple host cell proteins and 7-10 envelope glycoprotein (Env) trimers that mediate viral entry (Chojnacki et al., 2012; Linde et al., 2013; Zhu et al., 2003). Associated with the inner leaflet of the envelope lipid bilayer is a layer of matrix protein (MA) that stabilised the virion structure. Inside the virion there is a conical capsid core formed out of hexameric capsid protein (CA). Inside the capsid core there are two copies of single stranded viral RNA genome, bound to nucleocapsid protein (NC) and viral enzymes, reverse transcriptase (RT) and integrase (IN). Viral protease (PR) and viral accessory protein Vpr are also incorporated into the virion (reviewd in Freed, 2015).

1.3.2 Entry

HIV-1 entry into host cell occurs predominantly by fusion at the plasma membrane and is mediated by the envelope glycoprotein (Env). Fusion in the endosomal compartment remains controversial and is most likely restricted to macrophages (Herold et al., 2014; Miyauchi et al., 2009; van Wilgenburg et al., 2014). Env is a dimer of gp120 and gp41 subunits, which form Env trimers that are required for viral entry (Hallenberger et al., 1992). The gp120 subunit binds the receptor CD4 and coreceptor CCR5 or CXCR4 (Alkhatib et al., 1996; Feng et al., 1996; Maddon et al., 1986). Initial virion attachment can also be supported by nonspecific Env interactions with the extracellular matrix (heparan sulphate proteoglycan) or by adhesion molecules (ICAM-1 and LFA-1) that are incorporated into the virion (Saphire et al., 2001); however, these are termed attachment factors that may help overcome electrostatic repulsion between viral and cellular membranes, and are not bona fide HIV-1 receptors.

As shown in Figure 1.5, Env surface subunit gp120 contains five conserved (C1-C5) and five variable loop (V1-V5) domains and is heavily glycosylated (Leonard et al., 1990; Lyumkis et al., 2013; Ward & Wilson, 2017). The gp41 subunit contains the fusion machinery and consists of the N-terminal ectodomain, the transmembrane domain and the cytoplasmic C-terminal domain. The ectodomain contains the fusion peptide, two helical heptad-repeat domains (HR1 and HR2) that are separated by the disulphide loop (DLS) hinge, and the membrane-proximal external region (MPER). (Ward & Wilson, 2017). There are 25-30 glycans in gp120 and 3-5 glycans in gp41 subunit (discussed

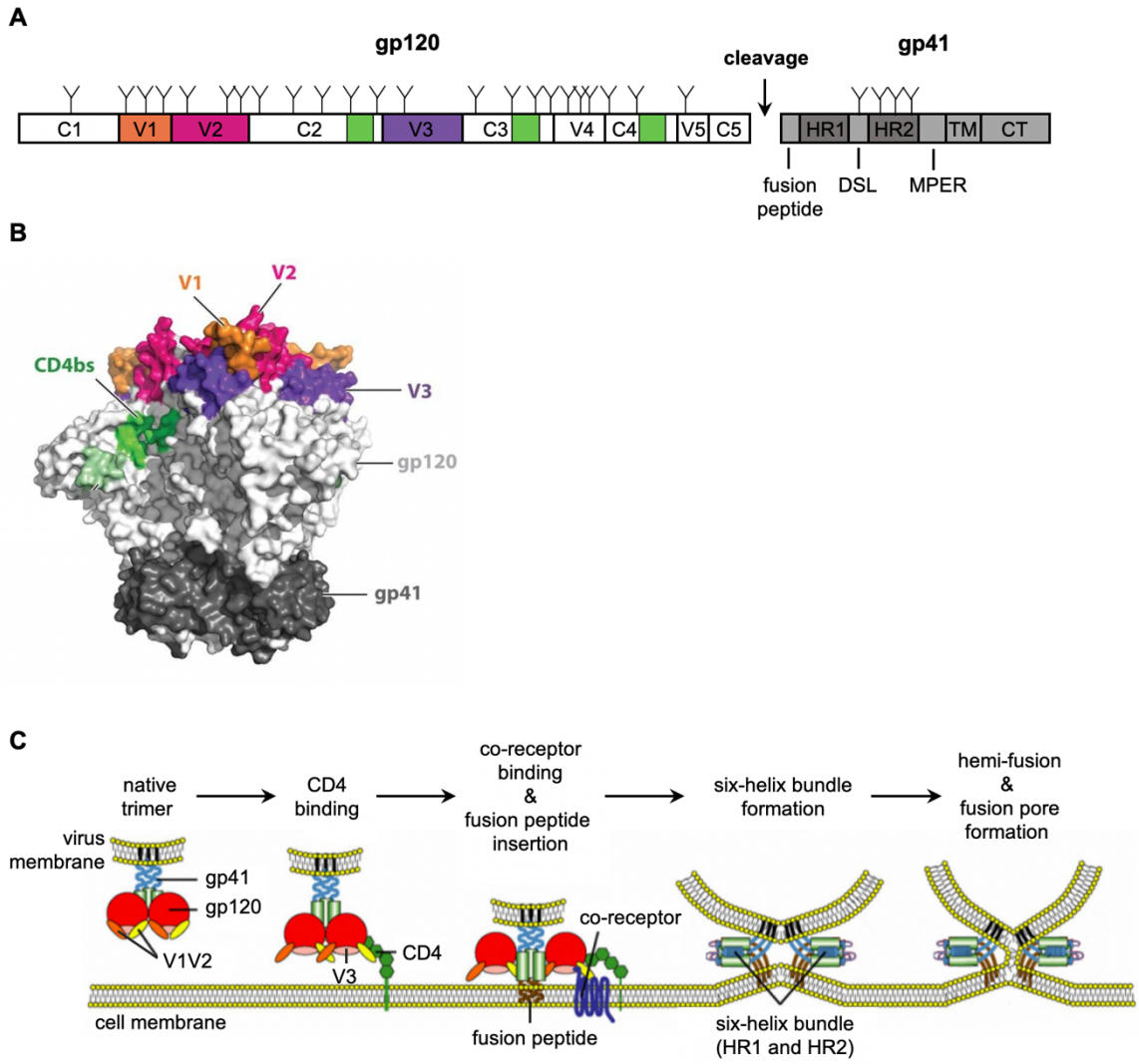

Figure 1.5: Env structure and fusion mechanism

(A) Schematic representation of gp120 and gp41 linear structure. Shown are conserved domains (C1-C5) and variable loops (V1-V5) in the gp120 subunit. Regions containing CD4 binding site (C2, C3 and C4) are shown in green. The gp41 subunit consists of fusion peptide, two heptad-repeat domains (HR1 and HR2), disulphide loop (DSL) hinge region, membrane-proximal external region (MPER), transmembrane helix and cytoplasmic tail (CT). Furin cleavage site is between the C5 domain and fusion peptide. N-linked glycan are depicted above the sequence. **(B)** Crystal structure of Env trimer (PDB 4ZMJ). The gp120 subunit is shown in light grey and the gp41 subunit (ectodomain only) is shown in dark grey. V1, V2 and V3 loops are shown in orange, magenta and purple, respectively. The CD4 binding site (CD4bs) is shown in green. NB Colour scheme matches that in panel (A). Taken from (Burton & Hangartner, 2016). **(C)** Fusion mechanism of viral and host cell membrane. CD4 binding to gp120 induces conformational changes, particularly in V1 and V2 loops, opening up the trimer and exposing the V3 loop, which is then able to bind the co-receptor CCR5 or CXCR4. Co-receptor binding stabilises the open CD4-bound conformation and anchors the Env in close proximity to the host cell membrane. CD4 binding also induces gp41 refolding resulting in fusion peptide insertion into the host cell membrane and dissociation of gp120 subunits. HR1 and HR2 domains from each trimer fold together to form a six-helix bundle, which results in hemi-fusion and finally fusion of viral and host cell membranes. Adapted from (Tilton & Doms, 2010).

further in Section 1.3.5), which comprise about half of the total Env mass and act as "glycan shield" to mask antibody epitopes and thus act as an immune evasion strategy (Burton & Hangartner, 2016; Leonard et al., 1990). Env is cleaved by cellular furin protease between C5 and the fusion peptide at a highly conserved polybasic K/R-X-K/R-R motif to produce gp120 and gp41 subunits (Dubay et al., 1995). The N-terminus (C1) and the C-terminus (C5) of gp120 loop together and non-covalently interact with gp41 subunit in a four-helix collar binding pocket formed around HR1 and HR2 domains (Julien et al., 2013; Lyumkis et al., 2013; Pancera et al., 2014). Single-molecule FRET studies revealed that trimeric gp120 subunits are conformationally dynamic, fluctuating between 3 states: open, intermediate and closed conformation (Munro et al., 2014). Consistent with crystallographic studies, CD4 binding induced open Env conformation and binding of neutralising antibodies recognising various epitopes on gp120 stabilised the closed conformation, which likely explains their neutralisation ability (Munro et al., 2014). Interestingly, lab-adapted (NL4.3) and clinical isolate (JR-FL) Env showed differences in intrinsic flexibility, where JR-FL Env was substantially less flexible, thus possibly explaining its decreased sensitivity to neutralising antibodies.

CD4 binding site on the Env is a quaternary epitope formed by sequences in C2, C3 and C4 domains (Figure 1.5) and its conformation depends on neighbouring gp120 monomers (Kwon et al., 2012; Lyumkis et al., 2013). Co-crystal and cryo-EM studies have shown that CD4 binds Env via the N-terminal domain 1 (D1), which induces extensive conformational changes in Env: gp120 subunits assume open conformation, V1V2 loops rotate to expose V3 loop, bridging sheet in C4 is formed and HR1 domains from each gp41 subunit rearrange to form a tighter three-helix bundle (Kwong et al., 1998; Lyumkis et al., 2013; Ozorowski et al., 2017). The V3 loop that is exposed upon CD4 binding is then able to interact with the co-receptor CCR5 or CXCR4. The cryo-EM structure of Env-CD4-CCR5 ternary complex revealed that V3 loop binds the CCR5 chemokine binding pocket in a manner similar to its native ligand CCL5 and that CCR5 N-terminal domain makes additional interactions with the bridging sheet in gp120 (Shaik et al., 2019). The specificity for CCR5 or CXCR4 coreceptor binding is primarily determined by the sequence of the V3 loop, where X4-tropic viruses have more positively charged residues in V3 loop, consistent with CXCR4 chemokine binding pocket being more negatively charged compared to CCR5 (Cocchi et al., 1996; Rosen et al., 2006; Shaik et al., 2019). Interestingly, the comparison of the cryo-EM structures showed no additional conformational changes in gp120 or gp41 upon CCR5 binding compared to binding of CD4 alone (Shaik et al., 2019). This was also observed previously comparing

crystal structures of Env in complex with CD4 and 17b antibody, which recognises CD4-induced epitope and thus mimics the co-receptor binding (Ozorowski et al., 2017). Taken together these studies negate previously proposed mechanism where the co-receptor binging induces further conformational changes in the Env needed for fusion (Tilton & Doms, 2010). The current model therefore proposes that co-receptor binding acts primarily to stabilise the Env-CD4 complex in the pre-fusion conformation and to anchor it in close proximity to the host cell membrane thus allowing productive fusion, Comparing current Env structures in native and pre-fusion states (complexed with CD4, 17b or CCR5) suggests that binding of CD4 alone triggers sufficient conformational changes that result in gp41 refolding concomitant with gp120 dissociation from gp41 (Lyumkis et al., 2013; Moore et al., 1990; Ozorowski et al., 2017; Pancera et al., 2014; Shaik et al., 2019). As shown in Figure 1.5, this results in insertion of the hydrophobic fusion peptide into the host cell membrane, which brings together HR1 and HR2 domains from each gp41 subunit in the trimer to form a six-helix bundle (from previously formed three-helix bundle) (Melikyan et al., 2000; Pancera et al., 2014; Sabin et al., 2010). Formation of the six-helix bundle pulls the viral and host cell membranes in close proximity and enables hemi-fusion and the formation of the fusion pore (Melikyan et al., 2000). Expansion of the fusion pore then allows the delivery of capsid cores in the host cell cytoplasm.

1.3.3 Reverse transcription, uncoating and integration

HIV-1 viral genome is positive-sense single-stranded +ssRNA, which needs to be converted into double-stranded DNA before integration into host genomic DNA. These processes are mediated by viral reverse transcriptase (RT) and integrase (IN) enzymes, which are together with the two copies of viral RNA enclosed within the capsid core.

1.3.3.1 Capsid structure and function

The capsid core is a fullerene-like closed conical structure composed of capsid protein (CA) assembled in approx. 200 hexamers and 12 pentamers, which stabilise the capsid curvature (Zhao et al., 2013). It was previously thought that capsid cores disassemble (known as CA uncoating) immediately after cytoplasmic entry. However, new evidence suggests that reverse transcription occurs within the capsid core and that completion of DNA synthesis by RT might trigger uncoating (Rankovic et al., 2017). In support of this, it was shown that capsid hexamers contain a central electrostatic channel which allows the transport of dNTPs into the core required for reverse transcription (Jacques et al.,

2016). The N-terminal domain of capsid (cytosolic side) binds cyclophilin A (a peptidyl-prolyl cis-trans isomerase), which is thought to be required for efficient reverse transcription, capsid core stability and immune evasion (Hatziioannou et al., 2005; Kim et al., 2019; Liu et al., 2016; Rasaiyaah et al., 2013; Sokolskaja et al., 2004). Capsid uncoating (at least partially) is thought to occur at the nuclear pore during nuclear import or potentially inside the nucleus (Bejarano et al., 2019; Burdick et al., 2020; Francis & Melikyan, 2018; Peng et al., 2014; Schaller et al., 2011). It is thought that intact capsid core in the cytoplasm protects the viral RNA and DNA intermediates from the detection by cytosolic RNA and DNA sensors (e.g. RIG-I, cGAS, IFI16) and thus prevents innate immune activation (Berg et al., 2012; Monroe et al., 2014; Rasaiyaah et al., 2013; Sumner et al., 2017).

1.3.3.2 Reverse transcription

HIV-1 viral genome is positive-sense single-stranded +ssRNA, which is converted into double-stranded DNA by viral reverse transcriptase (RT). RT consist of the structural p51 subunit and the catalytic p66 subunit, which contains polymerase and RNase H domains (Lightfoote et al., 1986). The initial reverse transcription occurs near the 5' end of the viral RNA where host cell $tRNA_{Lys3}$ acts as a primer, hybridised at the primer binding site (PBS) (Isel et al., 1996). The RNA in resulting DNA:RNA hybrid is degraded by RNase H activity of RT, which results in production of minus-strand DNA. The viral genome is flanked by two identical long terminal repeat (LTR) sequences, which means that 5' and 3' ends have the same sequence. This enables the newly synthesised minus-strand DNA to act as a primer and hybridise on the 3' end of the RNA template (first strand transfer) (Panganiban & Fiore, 1988). Since HIV-1 has two copies of viral genome, the template hybridisation during strand transfer can occur on either of the two viral genomes (strand switching). This results in reverse transcription of the rest of the RNA template. The RNA in resulting DNA:RNA hybrid is again degraded by RNase H activity, except for two short polypurine tracts (ppt), which are resistant to RNase activity (Hungnesi et al., 1992). The RNA in ppt sequences now acts as a primer for synthesis of the plus-strand DNA and is degraded after the completion of plus-strand DNA (Charneau et al., 1992). Next, PBS sequences from each end of plus- and minus-strand DNA hybridise (second strand transfer) to form a circular DNA stricture that enables full extension of plus- and minus-strand DNA by RT, which generates full length LTR sequences (reviewed in Hu & Hughes, 2012). The final product is double-stranded DNA, which is ready to integrate into host genome.

1.3.3.3 Nuclear import

Capsid core containing reverse transcribed viral genome enters the nucleus through the nuclear pore complex (NPC). Whether the capsid core disassembles (fully or partially) at the NPC or whether the intact core enters the nucleus remains controversial (Bejarano et al., 2019; Burdick et al., 2020; Francis & Melikyan, 2018; Kane et al., 2018; Peng et al., 2014). Since CA can be deteteced in the nucleus, this argues against full uncoating at the NPC (Bejarano et al., 2019; Burdick et al., 2020; Chen et al., 2016). However, it remains a subject of debate how the CA core could enter the nucleus since the size of the intact core (75 nm) is larger than the NPC pore (50 nm) (Bui et al., 2013; Zhao et al., 2013). CA was shown to be an important determinant for nuclear entry and integration site selection (Achuthan et al., 2018; Schaller et al., 2011). Nup358, a component of the NPC, interacts with CA via its cyclophilin-like domain, which is thought to displace cyclophilin A bound to CA (Bichel et al., 2013). Next, CA interacts with Nup153 component of the NPC. Nup153 is located at the nuclear side of the NPC and interacts with CA via its FG (phenylalanine-glycine) repeats (Matreyek et al., 2013; Price et al., 2014). In the nucleus CA interacts with an mRNA-processing protein cleavage and polyadenylation specificity factor 6 (CPSF6). It is thought that CPSF6 binding to CA displaces Nup153 since they share the same binding site (Price et al., 2014). CPSF6 binding was shown to be crucial for efficient nuclear import and optimal viral integration into gene-dense, transcriptionally active regions in the host chromatin (Achuthan et al., 2018; Bejarano et al., 2019; Price et al., 2012; Schaller et al., 2011).

1.3.3.4 Integration

Integration of viral DNA into host genome is mediated by the viral integrase enzyme (IN). IN monomers form a tetrameric complex with the viral DNA, called intasome, where two IN molecules bind each end of the viral DNA (Hare et al., 2010). IN was also shown to interact with host cell factor LEDGF/p75, which promotes targeting of integration into transcriptionally active regions in the host genome (Cherepanov et al., 2003; Marini et al., 2015). First, IN catalyses the processing of blunt-ended viral DNA: two nucleotides are removed from each 3’ end, generating 5’ end overhangs (Brown et al., 1989; Fujiwara & Mizuuchi, 1988). Next, during the strand transfer reaction, IN catalyses the 3’ end hydroxy group nucleophilic attack on 5’ phosphodiester bond in the target DNA, resulting in covalent attachment and insertion of viral DNA into host DNA (Hare et al., 2010). The sites of insertion are five nucleotides apart in the target DNA. The strand reaction thus creates a 5-nucleotide gap in the target DNA and a 2-nucleotide overhang in the viral DNA on each side of insertion. The host cell DNA repair machinery fills in the

gaps and cleaves the overhangs to complete the integration, which results in the duplication of the five-nucleotide host sequence on each end of insertion (reviewed in Lusic & Siliciano, 2017). Integrated viral DNA is termed the provirus.

In the nucleus, linear unintegrated viral DNA can also undergo circularisation mediated by the host cell DNA repair machinery to form 1-LTR or 2-LTR circles, containing one or two LTR sequences. 1-LTR circle formation is mediated by the MRN complex and 2-LTR circle formation is mediated by components of the non-homologous end joining machinery (Kilzer et al., 2003; Li et al., 2001). Whether viral gene expression can occur from the non-integrated viral DNA remains a subject of debate (Geis & Goff, 2019; Saenz et al., 2004; Thierry et al., 2016; Zhu et al., 2018).

1.3.4 Viral gene expression

Expression of viral genes is driven by the LTR sequence and regulated by viral transactivator (Tat) and regulator of expression of virion proteins (Rev) proteins. The viral genome contains two LTR sequences, containing U3, R and U5 elements. The transcription starts at R element of 5' LTR and terminates at the R element of 3' LTR, therefore 5' LTR acts as the promoter for transcription (Klaver & Berkhout, 1994). The U3 element contains binding sites for transcription factors: NF-κB, SP1, AP-1 and NFAT, and the core promoter containing TATA box (Burnett et al., 2009; Rittner et al., 1995; Williams et al., 2007). Since viral transcription depends on cellular transcription factors it is tightly linked to cell activation. Transcription factor binding results in transcription initiation by RNA polymerase II. Initially, mRNA transcripts are fully spliced and code for Tat, Rev and Nef proteins. Importantly, the majority of initial transcription elongation is halted at the 5' end, which produces a stem loop structure containing the transactivation region (TAR) element (Wei et al., 1998). Tat binds to TAR element and recruits positive transcription elongation factor b (P-TEFb), which enables transcription elongation and production of full-length mRNA transcripts (Berkhout et al., 1989; Wei et al., 1998). This results in accumulation of Tat and sustained viral transcription.

Splicing of viral mRNA results in approx. 40 differently spliced transcripts due to alternative usage of splice acceptor and donor sites (Emery et al., 2017). Broadly, they can be categorised as fully spliced (encoding Tat, Rev, Nef), partially spliced (encoding Vif, Vpr, Vpu, Env) and unspliced transcripts (encoding Gag and Gag-Pol polyproteins).

Normally, unspliced and partially spliced mRNA is retained in the nucleus. However, Rev (expressed from fully spliced mRNA) overcomes this restriction and enables the nuclear export of partially spliced and unspliced transcripts (Malim et al., 1989). Rev contains both nuclear export and nuclear import signals, which enables its trafficking between the cytoplasm and the nucleus. Rev binds to Rev-responsive element (RRE) in the *env* gene, which is present in all partially and unspliced transcripts, thus enabling their nuclear export (Nasioulas et al., 1994).

In the cytoplasm viral mRNA is translated to produce viral proteins. Translation is mainly cap-dependent, where the 40S ribosomal subunit scans for the start codon and recruits the 60S subunit to initiate the translation (Bolinger & Boris-Lawrie, 2009). Env is expressed from *vpu-env* bicistronic mRNA and translation of *env* was thought to occur as a result of leaky scanning of the 40S subunit through the *vpu* start codon (Schwartz et al., 1990). Interestingly, more recent data shows that presence of a conserved minimal ORF (start codon followed by a stop codon) immediately upstream of *vpu* start codon promotes translation of downstream *env* gene by mechanism of ribosome shunting (Krummheuer et al., 2007). This mechanism does not impact on Vpu expression; however, it is dependent on weak *vpu* initiation site, consistent with the leaky scanning mechanism. Expression of *pol* gene (encoding for RT, integrase and protease) occurs through the programmed ribosomal frameshift at the *gag* stop codon, resulting in production of Gag-Pol precursor polyprotein (Jacks et al., 1988).

1.3.5 Env expression and trafficking

Env undergoes extensive processing and intracellular trafficking in order to produce infectious Env trimers that are incorporated into nascent viral particles. Env is synthesised as a gp160 precursor in the endoplasmic reticulum (ER). The gp160 precursor contains an ER signal peptide sequence that targets it for insertion into the ER membrane, resulting in formation of one transmembrane helix near the C-terminus (Berman et al., 1988). During translation, gp160 is glycosylated mostly with N-linked and some O-linked glycans (Bernstein et al., 1994; Leonard et al., 1990). Monomeric gp160 assembles into trimers, although a small proportion of dimers and tetramers can also be observed (Earl et al., 1990). Trimeric and glycosylated gp160 is then trafficked to the Golgi network to undergo further processing. The host protease furin cleaves the gp160 precursor to yield the soluble gp120 domain and the transmembrane gp41 domain (Dubay et al., 1995). Furin cleavage occurs at a highly conserved polybasic K/R-X-K/R-

R motif and is required to produce an infectious, fusion-competent Env. There are 25-30 glycans in gp120 and 3-5 glycans in gp41, which are further processed and modified in the Golgi (Lyumkis et al., 2013; Montefiori et al., 1988). Extensive Env glycosylation is thought to be an important immune evasion strategy as it masks protein epitopes from antibody recognition.

At the plasma membrane, Env is rapidly endocytosed to limit cell surface expression and thus evade immune recognition (Anand et al., 2019; Chung et al., 2008; Prévost et al., 2018). Env endocytosis is mediated by two endocytic motifs found in the cytoplasmic tail of gp41: membrane-proximal YxxL motif recognised by the clathrin adaptor AP-2 and C-terminal LL motif recognised by the clathrin adaptor AP-1 (Berlioz-Torrent et al., 1999; Boge et al., 1998; Byland et al., 2007; Egan et al., 1996; Wyss et al., 2001). Once endocytosed, Env can be targeted for lysosomal degradation or recycled back to the plasma membrane via the endosomal recycling compartment (ERC) or the trans-Golgi network (TGN). Trafficking through the ERC is mediated by FIP1C and Rab14 endosomal proteins, where FIP1C was shown to interact with gp41 cytoplasmic tail (Kirschman et al., 2018; Qi et al., 2013, 2015). Env trafficking to the TGN is mediated by the retromer complex and is dependedent on gp41 cytoplasmic tail interaction with Vps26 and Vps35 retromer components (Groppelli et al., 2014). Recycling of Env between the plasma membrane and the endosomal compartments is thought to be important for Env virion incorporation (discussed below). In addition to cleaved gp120/gp41 heterotrimers, Env at the plasma membrane exists in multiple nonfunctional forms: monomers, dimers, tetramers, uncleaved gp160 or gp41 stumps (Moore et al., 2006). These additional, nonfunctional forms are thought to act as immune decoys to induce non-neutralising antibodies and thus contributing to immune evasion (Sanders & Moore, 2017).

1.3.6 Assembly, budding and maturation

1.3.6.1 Gag assembly and genome encapsidation

Gag polyprotein is crucial for virion assembly and budding from the plasma membrane. In fact, Gag expression alone, without other viral proteins, results in formation of virus-like particles that are released from the PM (Gheysen et al., 1989). Gag consists of 4 domains: matrix (MA), capsid (CA), nucleocapsid (NC) and p6, where NC domain is surrounded by two spacer peptides, SP1 and SP2 (Figure 1.6). GagPol precursor is produced at 1:20 ratio to Gag, as a result of programmed ribosomal frameshift and

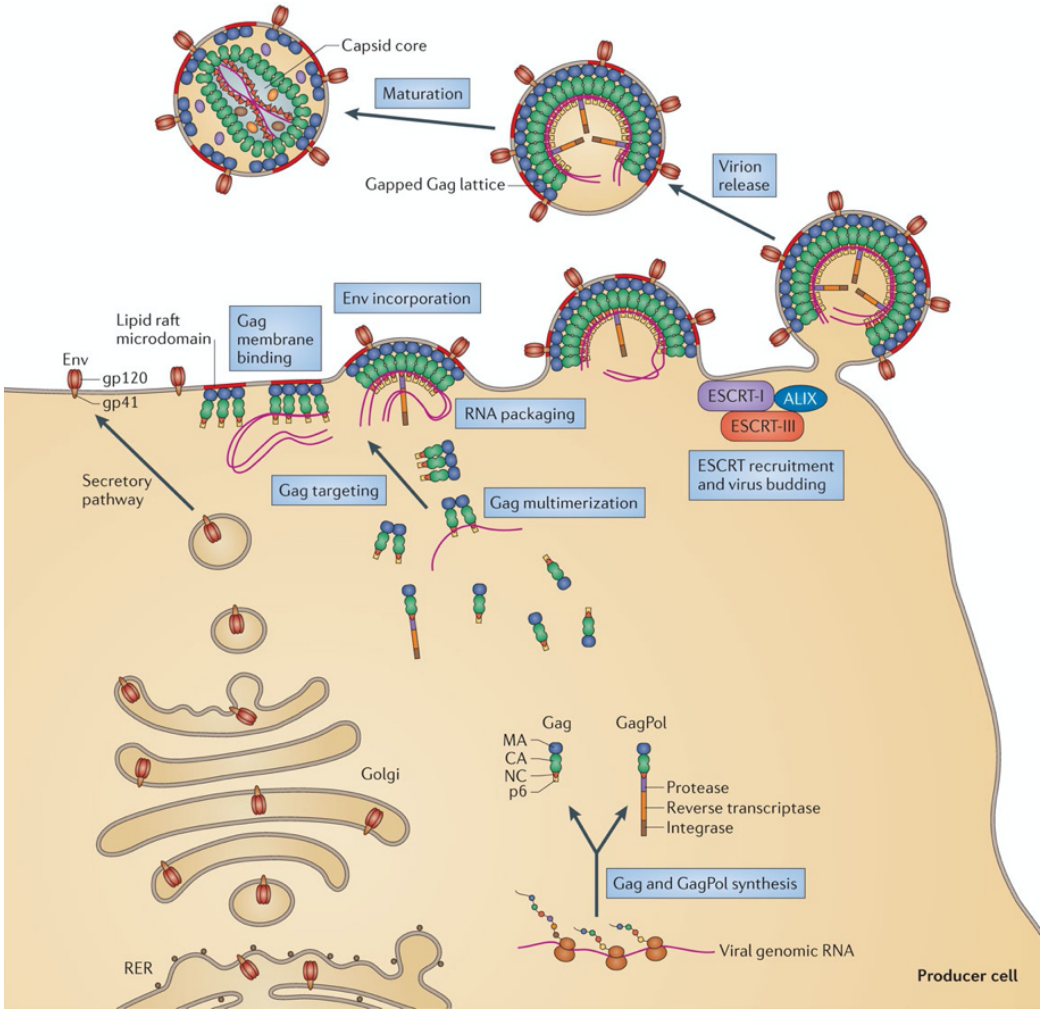

Figure 1.6: HIV-1 virion assembly, budding and maturation

Gag and GagPol precursors are synthesised in the cytoplasm and targeted to the PM via MA interaction with the membrane phospholipids. MA is also attached to the membrane with the insertion of the myristoyl anchor. NC binds the viral RNA ensuring its packinging into virions. Gag multimerization is triggered by MA interactions and viral RNA binding, which results in formation of lipid raft microdomains that serve as virus assembly sites. Env virion incorporation remains incompletely understood, but likely involves specific targeting of Env to the virus assembly sites and is further mediated by Env-MA interactions. The p6 domain of Gag recruits ESCRT-I (TSG101) and ALIX complexes, which in turn recruit ESCRT-III complexes and VPS4 that mediate membrane scission, resulting in virion release from the PM. Virion maturation is mediated by the viral protease enzyme which cleaves Gag and GagPol polyproteins into individual subunits. This results in formation of mature capsid core that encapsidates the viral genome, RT and integrase. Taken from (Freed, 2015).

ensures incorporation of RT, integrase and protease into the virion (Jacks et al., 1988). Gag and GagPol are synthesised in the cytoplasm and targeted to the plasma membrane (PM) by the MA domain, although the precise mechamism remains unknown. At the PM, a cluster of basic residues in MA interacts with negatively charged phosphatidylinositol-4,5-bisphosphate (PIP_2) found on the inner leaflet of PM (Mücksch et al., 2017; Ono et

al., 2004). This interaction causes insertion of the myristoyl tag at the N-terminus of MA into the PM, thus anchoring Gag and GagPol in the membrane (Saad et al., 2006). Gag localisation to the PM recruits cholesterol-, sphingolipid- and tetraspanin-rich lipid microdomains known as lipid rafts, which serve as platforms for virion assembly (Halwani et al., 2003; Hogue et al., 2011; Mercredi et al., 2016; Nguyen & Hildreth, 2000).

The HIV-1 genome consists of two copies of viral RNA and their incorporation is ensured by viral RNA dimerisation and NC binding (Lu et al., 2011; Nikolaitchik et al., 2013). The 5' untranslated region contains a dimer initiation signal and packaging sequences known as ψ-element, which ensures viral genome encapsidation (Chen et al., 2009; Moore et al., 2009). The NC contains two zinc-finger-like domains, which preferentially bind dimeric RNA (Nikolaitchik et al., 2013). RNA dimerization and NC binding can occur in the cytoplasm or at the PM (Moore et al., 2009; Nikolaitchik et al., 2013). At the PM, Gag-RNA interactions help Gag multimerization and start nucleation of virion assembly (Kutluay & Bieniasz, 2010). Morover, CA interactions are crucial for Gag oligomerization and formation of immaure Gag lattice, which presumably consists of Gag trimers (Alfadhli et al., 2009; Tedbury et al., 2013).

1.3.6.2 Env incorporation

Incorporation of Env into nascent virions is poorly understood. So far, four models of Env incorporation have been proposed: passive incorporation, direct Gag-Env interaction, indirect Gag-Env interaction and Gag-Env co-targeting model (Checkley et al., 2011). Importantly, these models are not mutually exclusive and different mechanisms can contribute to efficient Env incorporation. The first model suggests that Env is passively incorporated into virions by virtue of its expression in the PM. This comes from observations that mutations of endocytic motifs in gp41 cytoplasmic tail (CT), which increase Env surface expression, result in increased Env virion incorporation (Boge et al., 1998; Byland et al., 2007; Day et al., 2004; Groppelli et al., 2014; Qi et al., 2013). Additionally, gp41 CT deletion does not impair Env virion incorporation in model cell lines (e.g. HeLa, HEK 293T), further suggesting passive incorporation (Freed & Martin, 1995; Murakami & Freed, 2000a; Qi et al., 2015). However, gp41 CT is required for Env incorporation in some T cell lines and more importantly, in primary T cells or monocyte-derived macrophages, which argues against the passive model of incorporation (Akari et al., 2000; Groppelli et al., 2014; Murakami & Freed, 2000a; Qi et al., 2015). In fact, cell type-specific requirement for gp41 CT implicates cellular factors being responsible

for Env incorporation, which is consistent with the co-targeting and indirect interaction models. The Gag-Env co-targeting model suggests that Env is targeted to the same PM microdomains as Gag, resulting in its incorporation. It is known that virus assembly and budding occurs at lipid rafts (discussed above) and that Env can be found clustering at these microdomains (Bhattacharya et al., 2006; Muranyi et al., 2013); however, less is known how Env is trafficked to these assembly sites. In support of this model, it was shown that disrupting Env endocytic trafficking, either via the endosomal recycling compartment or the trans-Golgi network, results in differences in Env virion incorporation (Groppelli et al., 2014; Kirschman et al., 2018; Qi et al., 2013). This suggest that Env recycling is required for optimal Env incorporation, possibly by trafficking Env to the virus assembly sites. Another study showed that coexpressing HIV-1 Env glycoprotein and Ebola glycoprotein together with Gag resulted in segregation of both glycoproteins to separate PM microdomains, which produced virions with either viral glycoprotein, but not both (Leung et al., 2008). Targeting of Env to specific microdomains thus further supports the Env-Gag co-targeting model. By contrast, the indirect Gag-Env interaction model proposes that a cellular factor acts as a bridge between Env and Gag, thus recruiting Env into virus assembly sites. Several cellular factors (apart from the endocytic machinery) have been suggested to interact with gp41 CT, such as TIP47, Dlg1 and α-catenin; however, their exact role in Env incorporation and potential Gag interaction remains poorly defined (Checkley et al., 2013; Kim et al., 1999; Lopez-Vergès et al., 2006; Perugi et al., 2009). This model has the least evidence in its support. By contrast, there is good evidence to support the direct Gag-Env interaction model. Several studies using genetic, biochemical and microscopy approaches have suggested that there is a direct interaction between gp41 CT and the MA domain, which traps the Env in the Gag multimeric lattice as virions bud from the PM, thus ensuring Env incorporation (Alfadhli et al., 2019; Buttler et al., 2018; Chojnacki et al., 2017; Freed & Martin, 1995; Murakami & Freed, 2000b; Pezeshkian et al., 2019; Tedbury et al., 2013). For example, MA mutants that are defective for Env incorporation can be rescued by mutations or deletions in gp41 CT and vice versa (Alfadhli et al., 2019; Freed & Martin, 1995; Murakami & Freed, 2000b; Tedbury et al., 2013). Deletion of gp41 CT or MA mutations result in free movement of Env and loss of trapping in the Gag lattice (Buttler et al., 2018; Muranyi et al., 2013; Pezeshkian et al., 2019). Virion maturation and cleavage of Gag results in increased mobility of Env in the virion, consistent with loss of Env-Gag interactions and trapping in the Gag lattice (Chojnacki et al., 2017). Importantly, the biochemical evidence for direct gp41 CT-MA interaction remains controversial due to likelihood of nonspecific gp41 interactions. Likewise, microscopy studies of Env mobility and genetic studies of Env incorporation rescue mutants do not prove direct Env-Gag

interaction, but rather show a role for MA in accommodating Env and its long CT during virion assembly and budding. Taken together, these studies show that optimal Env incorporation is likely achieved by multiple mechanisms and is likely cell type-dependent, whereby Env trafficking and targeting to virus assembly sites results in potential Env-Gag interaction that ensures Env incorporation into nascent virions.

1.3.6.3 Budding

Once Env, Gag, GagPol and viral RNA are assembled, virion budding is mediated by p6 domain of Gag and cellular ESCRT machinery (Figure 1.6). Endosomal sorting complex required for transport (ESCRT) machinery is involved in membrane scission reactions, such as during multivesicular body formation or cytokinesis (Hanson et al., 2009). First, p6 contains three “late domains”: P(T/S)AP and YPXL which recruit TSG101 as part of ESCRT-I complex and ALIX protein (Fujii et al., 2009; Garrus et al., 2001; Gottlinger et al., 1991; Huang et al., 1995; Martin-Serrano et al., 2001). This recruits ESCRT-III complexes and VPS4 protein (Bleck et al., 2014; Jouvenet et al., 2008). Finally, this enables ESCRT-III oligomerisation and formation of long spiral arrays which are thought to mediate elongation of the membrane at the neck of the bud and final scission of the membrane, which releases the nascent virion from the PM (Bleck et al., 2014; Jouvenet et al., 2008; van Engelenburg et al., 2014). Additionally, p6 also recruits viral accessory protein Vpr via the LXSLFG motif, which results in Vpr incorporation into virions (Bachand et al., 1999).

1.3.6.4 Maturation

After virus budding, maturation is mediated by the viral protease enzyme (PR) and is essential for production of infectious virions. PR is incorporated into virion as GagPol precursor and functions as a dimer, where the catalytic site is formed in the dimer interface (Wlodawer & Erickson, 1993). PR cleaves Gag and GagPol precursors into individual subunits. The cleavage efficiency varies between the cleavage sites, which results in ordered and sequential proteolytic processing cascade (Kaplan et al., 1993; Pettit et al., 1994). Cleavage of Gag releases CA subunits, which reassemble into hexamers to form a fullerene-like conical core, known as the capsid core (Frank et al., 2015; Li et al., 2000). Matrix stays associated with the membrane and NC stays associated with the RNA genome. The newly formed capsid core encapsidates the viral genome together with the RT and IN enzymes.

1.3.7 Restriction factors

Host cells have evolved a multitude of viral restriction factors that target viruses at different steps in the life cycle and thus prevent their replication. HIV-1 uses the accessory proteins Vif, Vpr, Nef and Vpu to directly counteract or antagonise some of these restriction factors, which will be discussed further in Section 1.4. By contrast, some of these restriction factors are not directly antagonised and may therefore reduce viral fitness. Restriction factors are often induced by type-1 interferon (IFN) response (IFNα, IFNβ). This is induced by innate immune detection of pathogens by pattern-recognition receptors (PRR), which results in expression of IFN-stimulated genes (ISGs), many of which are restriction factors, thus inhibiting viral replication (Schoggins et al., 2011).

1.3.7.1 IFITM proteins

Interferon-inducible transmembrane proteins (IFITMs) inhibit viral fusion of diverse enveloped viruses, such as influenza A, Dengue and hepatitis C virus, possibly by regulating the fluidity of host cell membranes; however, the precise mechanism of inhibition is still unknown (Desai et al., 2014). HIV-1 entry is restricted by IFITM1, 2 and 3; however, the restriction is less potent compared to other viruses (Lu et al., 2011). IFITM1 is localised at the plasma membrane, whereas IFITM2 and 3 are localised in the endosomal compartments (Jia et al., 2012). CCR5-tropic HIV-1 is more susceptible to restriction by IFITM1, whereas CXCR4-tropic viruses are more susceptible to restriction by IFITM2 and 3 (Foster et al., 2016; Wang et al., 2017; Wu et al., 2017). This suggest that CXCR4-tropic viruses might fuse in the endosomal compartments; however, precise subcellular localisation of HIV-1 entry remains controversial. Transmitted/founder viruses (CCR5-tropic) were shown to be particularly resistant to IFITM inhibition, which was shown to confer their resistance to interferon treatment. By contrast, matched antibody escape Env mutants (6-months post-transmission, chronic viruses) were more susceptible to inhibition by IFITM2 and 3 (without the change of coreceptor usage) and were also more sensitive to interferon treatment. (Foster et al., 2016). Together this shows that IFITM activity is an important barrier for HIV-1 entry, particularly during transmission, and that viruses have to balance the evasion of adaptive immune responses and innate antiviral restriction.

1.3.7.2 SERINC3/5

Serine incorporator proteins (SERINC) are a family of 5 membrane proteins containing 10-11 transmembrane helices. They were originally thought to mediate serine incorporation into membrane lipids (Inuzuka et al., 2005); however, this observation was challenged by recent studies showing no effect on cell or virus membrane lipid composition in presence or absence of SERINCs (Chu et al., 2017; Trautz et al., 2017). Therefore, at present SERINCs have unknown cellular function. SERINC5 and to lesser extent SERINC3 inhibit HIV-1 entry and the mechanism of inhibition remains incompletely understood (Rosa et al., 2015; Usami et al., 2015). It is important to note that there are no available antibodies against SERINCs, therefore exogenously expressed and tagged SERINC proteins are used in research, which can result in various artefacts associated with overexpression. Recently, a Jurkat T cell line was generated to tag endogenous SERINC5 via CRISPR/Cas9 gene editing (Passos et al., 2019). Interestingly, it was shown that IFN treatment does not change SERINC5 mRNA or protein levels, but rather increases SERINC5 surface expression and thus promotes its restriction activity. SERINC3/5 associate with lipid rafts and are incorporated into nascent viral particles (Passos et al., 2019; Schulte et al., 2018). During entry into target cells, SERINC3/5 inhibit fusion, possibly by interfering with fusion pore formation or expansion; however, the exact mechanism remains poorly defined (Rosa et al., 2015; Sood et al., 2017; Usami et al., 2015). Several primary R5-tropic Env isolates were shown to be resistant to SERINC inhibition, which mapped to V1/V2 and V3 loop regions in Env (Beitari et al., 2017; Usami & Göttlinger, 2013). The presence of SERINC5 also increases virus sensitivity to Env MPER-targeting neutralising antibodies, suggesting a conformational change in Env in the presence of SERINCs (Beitari et al., 2017; Pye et al., 2020; Sood et al., 2017). Moreover, specific mutations in SERINC5 extracellular loops were shown to allow for virion incorporation, but prevent its restriction activity and sensitisation to neutralising antibodies (Pye et al., 2020). Taken together, these data suggest that SERINC5 is likely interacting with Env, altering its conformation or stability and thus interfering with viral fusion. To overcome this restriction, primate lentiviruses encode Nef protein, which downmodulates plasma membrane expression of SERINC3/5 and thus prevent their virion incorporation (Rosa et al., 2015; Usami et al., 2015). This will be discussed in Section 1.4.

1.3.7.3 TRIM5α

Tripartite motif protein 5α (TRIM5α) recognises a variety or retroviral capsids as they enter the cytoplasm and acts as an immune sensor (Pertel et al., 2011; Stremlau et al.,

2004). TRIM5α restriction was shown to be species-specific such that SIV capsids are restricted in human cells, and vice versa HIV-1 capsids are restricted in monkey cells (Keckesova et al., 2006; Stremlau et al., 2004; Ylinen et al., 2005). TRIM5α restriction is thus proposed to present a major barrier in zoonotic transmission. TRIM5α contains a PRYSPRY domain that binds to CA, which leads to assembly of hexagonal TRIM5α lattice on the capsid cores and triggers TRIM5α auto-ubiquitinoylation by its E3 ubiquitin ligase RING domain (Fletcher et al., 2015; Stremlau et al., 2006). TRIM5α ubiquitinoylation triggers innate immune activation (via NF-κB activation) and targets capsid cores for proteasomal degradation, thus inhibiting reverse transcription and viral replication (Kim et al., 2019; Lascano et al., 2016; Pertel et al., 2011). HIV-1 was thought to be relatively insensitive to TRIM5α restriction due to poor recognition of HIV-1 capsid by TRIM5α (Keckesova et al., 2006; Kim et al., 2019; Kratovac et al., 2008; Stremlau et al., 2004). Particularly in primary CD4+ T cells, cyclophilin A interaction with CA was shown to be crucial to block TRIM5α restriction (Kim et al., 2019). Interestingly, it was recently shown that induction of antiviral state by type-1 IFN can lead to activation of immunoproteasome, which in turn activates TRIM5α for effective restriction of viral capsids and inhibition of HIV-1 infection (Jimenez-Guardeño et al., 2019). By contrast, HIV-2 capsids are more sensitive to restriction due to better recognition and binding by TRIM5α (Takeuchi et al., 2013; Ylinen et al., 2005). This is thought to partially contribute to poor viral replication and improved immune control of HIV-2 infection *in vivo* (Nyamweya et al., 2013).

1.3.7.4 APOBEC3

Apolipoprotein B mRNA editing enzyme catalytic polypeptide 3 proteins (APOBEC3) are a family of 7 cytidine deaminases (APOBEC3A-H) that inhibit diverse retroviruses by causing guanosine to adenosine (G to A) hypermutation in the viral genome (Chiu & Greene, 2008; Sheehy et al., 2002). APOBEC3 proteins are constitutively expressed, however their expression can be enhanced by type-1 IFN response (Koning et al., 2009). APOBEC3G is most potent and well-studied inhibitor of HIV-1 replication; however, ABOBEC3D/F/H can also restrict its replication (Dang et al., 2006; Harris et al., 2003; Mangeat et al., 2003; Zheng et al., 2004). APOBEC3 enzymes are incorporated into the virion by interaction with viral RNA and the NC subunit (Huthoff et al., 2009). APOBEC3 enzymes act during reverse transcription where they deaminate the cytidine residues in the minus-strand DNA, thus causing G to A mutations in the plus-strand DNA (Harris et al., 2003; Mangeat et al., 2003). This results in defective hypermutated provirus

(premature stop codons or missense mutations), producing non-functional viral proteins. APOBEC3G was also shown to directly inhibit reverse transcription by several mechanisms including primer tRNA binding, strand transfer reactions and direct binding to RT enzyme (Bishop et al., 2008; Pollpeter et al., 2018). APOBEC3 enzymes are therefore potent restriction factors of HIV-1 replication. To overcome this restriction, lentiviruses encode viral accessory protein Vif, which targets APOBEC3 proteins for proteasomal degradation (Sheehy et al., 2003; Yu et al., 2003). The mechanism of Vif antagonism will be discussed in Section 1.4.

1.3.7.5 SAMHD1

Sterile alpha motif (SAM) and HD-domain-containing protein 1 (SAMHD1) hydrolyses dNTPs into deoxynucleosides and inorganic triphosphate. This depletes cellular levels of dNTPs, thus inhibiting reverse transcription (Goldstone et al., 2011). The SAM domain is involved in protein and nucleic acid interactions, and the HD domain has hydrolase activity. SAMHD1 is primarily active in myeloid cells: dendritic cells and macrophages, and in resting CD4+ T cells, which restricts HIV-1 infection in these cells (Baldauf et al., 2012; Hrecka et al., 2011; Laguette et al., 2011). Interestingly, it was suggested there is another block to reverse transcription in resting primary CD4+ T cells (but not in macrophages) that is SAMHD1-independent (Baldauf et al., 2017). The full mechanism of HIV-1 restriction in resting CD4+ T cells thus remains to be determined. SAMHD1 is active as a tetramer, which is regulated by GTP binding, and is inactivated by phosphorylation (Ji et al., 2014). SAMHD1 phosphorylation is cell cycle dependent and mediated by cell cycle kinases CDK1 and 2 (Cribier et al., 2013). SAMHD1 phosphorylation (inactivation) in CD4+ T cells can also be mediated by cell activation (via T cell receptor signalling) or by common γ-chain cytokines (e.g. IL-2, IL-7, IL-15), which relieves the block to infection (Coiras et al., 2016; Manganaro et al., 2018). By contrast, macrophages were shown to cycle between the G0 and G1-like phase, without cell cycle progression (Mlcochova et al., 2017). In G1-like phase, SAMHD1 is phosphorylated by CDK1, which allows HIV-1 infection. HIV-1 does not antagonise SAMHD1; however, HIV-2 uses Vpx and some SIVs use either Vpr or Vpx to antagonise SAMHD1, which will be discussed in Section 1.4.

1.3.7.6 MxB

Myxovirus resistance B protein (MxB) is induced by type-1 IFN response and can restrict HIV-1 nuclear entry (Goujon et al., 2013; Kane et al., 2013). MxB is located at the nuclear

envelope and oligomerises to form higher-order structures (Busnadiego et al., 2014; Fribourgh et al., 2014). MxB restricts the nuclear entry by interacting with CA, which is dependent on CA interaction with cyclophilin A (Goujon et al., 2013; Kane et al., 2013). MxB localisation at the nuclear envelope and interaction with the NPC components is important for the restriction of the nuclear import (Dicks et al., 2018; Kane et al., 2018; Schulte et al., 2015); however, the precise mechanism of restriction remains unknown.

1.3.7.7 HUSH complex

Human silencing hub (HUSH) complex consists of three subunits: TASOR, MPP8 and periphilin, which act to epigenetically silence gene expression via chromatin remodelling. MPP8 recognises existing histone methylation in the chromatin and TASOR recruits SETDB1 methyl transferase, resulting in histone methylation (H3K9me3) and spreading of this repressive mark on the chromatin (Tchasovnikarova et al., 2015). The HUSH complex was shown to repress more than 900 genes and also LINE-1 transposable elements (Liu et al., 2018; Tchasovnikarova et al., 2015). In addition to cellular genes, the HUSH complex was also shown to silence HIV-1 proviral gene expression (Chougui et al., 2018; Yurkovetskiy et al., 2018). The repression was shown to be heterogeneous as only a proportion of cells in infected population become repressed. The reason for this remains poorly understood and might depend on site of proviral integration as the HUSH complex acts mainly to spread repressive marks on the chromatin. The HUSH complex is thought to be involved in latency establishment as HUSH antagonism results in reactivation of latent provirus (Chougui et al., 2018; Yurkovetskiy et al., 2018). Further, the HUSH complex was also shown to mediate silencing of gene expression from unintegrated retroviral DNA (2-LTR circles) from murine leukaemia virus (Zhu et al., 2018). Unintegrated HIV-1 DNA was also shown to be associated with repressive histone methylation (H3K9me3) and whether this is also mediated by HUSH complex remains to be investigated (Geis & Goff, 2019). HIV-1 does not antagonise HUSH complex; however, HIV-2 uses Vpx and some SIVs use either Vpr or Vpx to antagonise HUSH complex, which will be discussed in Section 1.4.

1.3.7.8 GBP2/5

Guanylate binding proteins (GBP) are a family of IFN-inducible GTPases with activity against diverse pathogens (Kim et al., 2012). GBP5 and to lesser extent GBP2 inhibit proteolytic cleavage of the Env gp160 precursor by furin protease. GBP2/5 expression is induced by both type-1 and type-2 IFN and reduces the proteolytic activity of furin

(Braun et al., 2019; Krapp et al., 2016). GBP2/5 were shown to interact with furin, but the exact mechanism of inhibition remains unknown (Braun et al., 2019). Furin inhibition results in production and virion incorporation of uncleaved gp160, thus reducing virion infectivity. Since GBP2/5 target furin they exert broad antiviral activity against viral envelope proteins that require furin cleavage, such as influenza A, Zika and measles virus (Braun et al., 2019).

1.3.7.9 MARCH proteins

Membrane associated RING-CH proteins (MARCH) are a family of 11 proteins with RING-finger E3 ubiquitin ligase activity that downmodulate several membrane proteins from the cell surface (e.g. transferrin receptor, MHC-II, TRAIL) via ubiquitination and degradation of target proteins (Fujita et al., 2013; Tze et al., 2011). MARCH8 is constitutively expressed, whereas MARCH1/2 are induced by type-1 IFN (Zhang et al., 2019). MARCH1/2/8 act to reduce plasma membrane expression of Env (Tada et al., 2015; Zhang et al., 2019). This is achieved via Env binding and internalisation, but without causing its degradation. Reduced plasma membrane expression of Env results in reduced Env virion incorporation and reduced virion infectivity. Whether MARCH proteins also induce Env ubiquitination remains unknown.

1.3.7.10 Tetherin

Tetherin is a transmembrane protein that restricts virion release of diverse enveloped viruses, such as retroviruses, Ebola, Marburg and Lassa virus (Jouvenet et al., 2009; Neil et al., 2008; Sakuma et al., 2009; van Damme et al., 2008). Tetherin is constitutively expressed and is upregulated by type-1 and type-2 IFN response, but also via TLR3, TLR8 and IL-27 signalling (Bego et al., 2012; Guzzo et al., 2012). Tetherin forms dimers and consists of the N-terminal cytoplasmic tail, transmembrane α-helix, coiled-coil ectodomain and a C-terminal glycosyl-phosphatidylinositol (GPI) anchor, which targets it to lipid rafts, where the viruses assemble (Kupzig et al., 2003). As the virions bud from the PM, the GPI anchor of tetherin gets incorporated in the virion membrane whilst the transmembrane domain stays associated with the host PM (Hammonds et al., 2010; Neil et al., 2008; Perez-Caballero et al., 2009; van Damme et al., 2008). This physically tethers the nascent virions to the cell surface and prevents their release. Tethered virions are also exposed to antibody recognition, which can result in antibody-dependent cell cytotoxicity (ADCC) (Alvarez et al., 2014). Furthermore, tetherin retention of viral particles was shown to induce an innate immune response via activation of NF-κB

signalling and downstream proinflammatory gene expression (Cocka & Bates, 2012; Galão et al., 2012). Tetherin is expressed in two isoforms: the long (full-length) and the short isoform missing the initial 12 residues in the N-terminal cytoplasmic tail. Both isoforms were shown to inhibit particle release, but only the long isoform is able to induce NF-κB signalling (Cocka & Bates, 2012; Galão et al., 2012). This is due to the di-tyrosine motif in the cytoplasmic tail that functions as a hemi-immunoreceptor tyrosine-based activation motif (hemITAM), such as found in C-type lectin receptors. Tetherin signalling is induced by retention of viral particles and coupled to the cortical actin cytoskeleton via RICH2 adaptor, which results in phosphorylation of hemITAM by Syk kinase and propagation of downstream signalling via TRAF2, TRAF6 and TAK1 complex that activates NF-κB (Galão et al., 2014). Tetherin is a potent viral restriction factor and is antagonised by lentiviral accessory proteins Vpu or Nef, which will be discussed in Section 1.4. Interestingly, HIV-2 uses its Env to antagonise tetherin.

1.4 Lentiviral accessory proteins

1.4.1 Vif

Viral infectivity factor (Vif) is a viral accessory protein found in all primate lentiviruses. It is crucial for viral replication *in vivo* and *in vitro* as it antagonises the host restriction factors APOBEC3D/F/G/H enzymes, which would otherwise cause genomic hypermutation and production of defective virus (Gabuzda et al., 1992; Harris et al., 2003; Mangeat et al., 2003; Sheehy et al., 2002). Vif acts as an adaptor protein between APOBEC3 and the Cullin5 E3 ubiquitin ligase complex, which causes APOBEC3 polyubiquitination and targeting for proteasomal degradation (Sheehy et al., 2003; Yu et al., 2003). Assembly of the Vif-Cullin5 ligase complex is mediated by the cellular transcription factor CBF-β (Zhang et al., 2012). Additionally, Vif was shown to antagonise APOBEC3 enzymes by inhibiting their mRNA translation or virion incorporation (Goila-Gaur et al., 2008; Stopak et al., 2003).

Vif antagonism of APOBEC3 enzymes presents an important barrier for zoonotic transmissions of SIVs and HIV. For example, most SIV Vif proteins are unable to efficiently antagonise chimpanzee APOBEC3 enzymes; however, the recombination between SIVrcm and SIVgsn/mon/mus that gave rise to SIVcpz virus resulted in generation of a hybrid, elongated Vif protein that was able to counteract chimpanzee APOBEC3 enzymes (Etienne et al., 2013). This adaptation also facilitated SIVcpz transmission into humans as SIVcpz Vif is generally active against human APOBEC3 proteins, except for APOBEC3H (Etienne et al., 2013; Zhang et al., 2017). By contrast, Vif antagonism is unlikely to have posed a significant barrier in HIV-2 zoonosis as SIVsmm Vif is able to antagonise human APOBEC3 enzymes (Letko et al., 2013).

Recently Vif has been shown to possess a second function by dysregulating a major cellular protein phosphatase PP2A. Vif recruits members of the phosphatase regulatory subunit (PPP2R5A-E) to the Cullin5 ubiquitin ligase complex, resulting in their proteasomal degradation (Greenwood et al., 2016). This results in reduced activity of PP2A and hence increased phosphorylation of more that 200 cellular proteins, particularly the substrates of aurora kinases (Greenwood et al., 2016; Naamati et al., 2019). This activity was shown to be conserved between diverse SIV Vif proteins (Greenwood et al., 2016); however, the importance of this function for the virus or the host cell remains unknown.

1.4.2 Vpr and Vpx

Viral protein R (Vpr) is a small accessory protein found in all primate lentiviruses. Viral protein X (Vpx) is related and structurally similar to Vpr and is found only in related HIV-2/SIVsmm and SIVrcm/drl/mnd2 lentiviral lineages (Schwefel et al., 2014). Vpx is thought to originate from Vpr gene duplication, which likely occurred after the separation of HIV-2/SIVsmm and SIVrcm/drl/mnd2 lineages from SIVagm lineage (Etienne et al., 2013; Tristem et al., 1990). Both Vpr and Vpx are incorporated into nascent viral particels via interaction with p6 domain of Gag (Selig et al., 1999). In the host cell, Vpr/Vpx target various host cell proteins for proteasomal degradation to enhance viral replication. They achive this by acting as adaptors to recruit cellular proteins to DCAF1-Cullin4 E3 ubiquitin ligase complex (via DCAF1 binding) and thus target them for proteasomal degradation (le Rouzic et al., 2007; Srivastava et al., 2008).

While the precise cellular function orf Vpr remains to be fully-eluciated, HIV-1 Vpr was recently shown to cause broad host cell proteome remodelling by promiscuous targeting of at least 38 proteins for degradation via DCAF1-Cullin4 complex, which results (indirectly) in changes in abundance of almost 2,000 cellular proteins (Greenwood et al., 2019). Vpr targets include: UNG2 (uracil DNA glycosylase) and HLTF (DNA translocase) both involved in DNA repair and ZGPAT involved in chromatin remodelling (Lahouassa et al., 2016; Maudet et al., 2013; Schröfelbauer et al., 2005). Vpr has long been observed to cause G2/M cell cycle arrest in dividing cells (Jowett et al., 1995), which has been attributed to degradation of several proteins involved in cell cycle control and progression: SLX4 complex (including MUS81 and EME1), MCM10, SMN1, CDCA2, and ZNF267 (Berger et al., 2015; Greenwood et al., 2019; Laguette et al., 2014; Romani et al., 2015; Zhou et al., 2016). Importantly, it remains unknown how targeting DNA repair or cell cycle arrest contributes to viral replication either *in vivo* or *in vitro*, thus the role of Vpr remains enigmatic. Vpr is clearly important for the virus as it gets incorporated into virions; however, its precise function in viral replicaiton remains unknown and is thus an active area of HIV-1 research. Interestingly, one case of infection with Vpr-defective virus has been reported, which showed delayed seroconversion, poor viral replication and no disease, indicating that Vpr function is important for viral replication *in vivo* (Ali et al., 2018). Furthermore, recent data suggests that Vpr might be involved in antagonism of innate immune sensing, possibly by preventing IRF3 and NF-κB nuclear translocation (Khan et al., 2020).

Vpx and some Vpr proteins were shown to degrade restriction factor SAMHD1 via targeting to DCAF1-Cullin4 complex and thus enhancing viral replication in dendritic cells, macrophages and resting CD4+ T cells. (Baldauf et al., 2012; Hrecka et al., 2011; Laguette et al., 2011). Vpx from both HIV-2/SIVsmm and SIVrcm/drl/mnd2 lentiviral lineages is able to degrade SAMHD1 in their respective host; however, the antagonism is species specific. For example, SIVrcm Vpx cannot degrade human SAMHD1 (Lim et al., 2012). Antagonism of SAMHD1 likely precedes the emergence of Vpx as Vpr from related SIVagm, SIVgsn/mon/mus and SIVdeb/syk lineages also degrade SAMHD1 in their respective hosts (Lim et al., 2012; Sakai et al., 2016). Again, the antagonism is species-specific and phylogenetic analysis indicates positive selection in SAMHD1, which maps to Vpr/Vpx sensitivity, thus showing the importance of SAMHD1 restriction (Lim et al., 2012).

Another function of Vpx and some Vpr proteins is HUSH complex degradation, which relieves the transcriptional repression of proviral DNA (Chougui et al., 2018; Yurkovetskiy et al., 2018). Similar to SAMHD1, the TASOR subunit of HUSH complex is targeted to DCAF1-Cullin4 complex resulting in proteasomal degradation. This function is conserved in Vpxs from both HIV-2/SIVsmm and SIVrcm/drl/mnd2 lineages, and is also present in Vpr from related SIVagm and SIVgsn/mon/mus linages and more distant SIVlst/sun and SIVcol lineages (Yurkovetskiy et al., 2018). Importantly, lentiviral Vpr/Vpx function has only been tested against human HUSH complex; however, given that diverse Vpr proteins have anti-HUSH activity (unlike SAMHD1 antagonism) this might suggest that HUSH antagonism is a common feature of primate lentiviruses. Why HUSH and SAMHD1 antagonism was lost in the HIV-1/SIVcpz lineage remains unknown. HIV-1 infection of dendritic cells and macrophages can be enhanced by delivering Vpx *in trans* (as VLPs) to enable efficient reverse transcription. Interestingly, this was shown to induce sensing of viral DNA products by cGAS or IFI16, resulting in innate immune response (Jønsson et al., 2017; Lahaye et al., 2013; Yoh et al., 2015). Similarly, degradation of HUSH complex can result in expression of transposable elements and endogenous retroviruses and thus triggering of innate immune responses (Liu et al., 2018; Robbez-Masson et al., 2018). These observations thus suggest that antagonism of SAMHD1 and HUSH might also have a negative effect on viral relication by triggering an innate immune response. Having to balance efficient viral replication and immune evasion this may therefore explain why HIV-1 evolved away from SAMHD1 and HUSH antagonism.

1.4.3 Vpu

Viral protein U (Vpu) is a small accessory protein found only in HIV-1/SIVcpz and related SIvgsn/mon/mus lineages. Vpu interacts with multiple cell surface proteins, most notably tetherin, to target them for degradation and thus enhance viral replication (Sugden et al., 2016). Additionally, it antagonises NF-κB signalling to prevent innate immune activation (Galão et al., 2012; Sauter et al., 2015). Vpu is a membrane protein, consisting of N-terminal transmembrane helix and two cytoplasmic α-helices and is found mainly in the ER, the TGN and endosomal compartments (Dubé et al., 2009). It contains a conserved dual serine motif that is phosphorylated by CK-II kinase and the ExxxLL motif that mediates interaction with AP-1 and AP-2 clathrin adaptors of the endocytic machinery (Kueck & Neil, 2012; Ulrich Schubert et al., 1994). Phosphorylation of the dual serine motif enables Vpu interaction with the β-TrCP adaptor of the SCF-β-TrCP E3 ubiquitin ligase complex (Margottin et al., 1998)

Vpu downmodulates surface expression of tetherin to enable efficient virion release and prevent tetherin-induced NF-κB activation and resulting proinflamatory gene expression (Galão et al., 2012, 2014; Neil et al., 2008; van Damme et al., 2008). The transmembrane helix of Vpu interacts with the transmembrane helix of tetherin and recruits AP-1 complex via the ExxxLL motif to promote targeting to late endosomes (Kueck et al., 2015; Kueck & Neil, 2012; Vigan & Neil, 2010). This occurs mainly in the TGN, thus Vpu can target both newly synthesised and recycling pools of tetherin. Additionally, Vpu recruits the SCF-β-TrCP complex, which mediates tetherin ubiquitination and targets it for ESCRT-mediated endosomal degradation (Jia et al., 2014; Kueck et al., 2015; Mitchell et al., 2009). The short isoform of tetherin, lacking the cytoplasmic tail, is thus resistant to endosomal degradation; however, the interaction with Vpu still reduces its surface expression (Weinelt & Neil, 2014).

Tetherin antagonism is species specific and thus presented a major barrier to HIV/SIV zoonotic transmissions. Interestingly, most SIV lineages use their Nef proteins to downmodulate tetherin in their respective hosts; however, SIVgsn/mon/mus Nefs are inactive in tetherin antagonism and instead use Vpu to downmodulate tetherin (Sauter et al., 2009; Zhang et al., 2009). Upon transmission to chimpanzees, SIVcpz Vpu was unable to antagonise chimpanzee tetherin, but instead SIVcpz evolved Nef to downmodulate tetherin (Sauter et al., 2009; Zhang et al., 2009). Upon subsequent

transmission to humans, HIV-1 Nef protein was inactive against human tetherin, because of a short deletion in tetherin cytoplasmic tail, which conferred resistance to Nef-mediated downmodulation (Zhang et al., 2009). HIV-1 M group thus evolved Vpu to antagonise tetherin (Neil et al., 2008; van Damme et al., 2008), and HIV-1 O group (despite having Vpu) evolved Nef to overcome human tetherin resistance (Kluge et al., 2014). Interestingly, HIV-2 evolved Env to antagonise human tetherin (Heusinger et al., 2018; le Tortorec & Neil, 2009). By contrast to Vpu, HIV-2 envelope is thought to interact with tetherin ectodomain via the gp41 extracellular domain and targets it for endocytosis, which is dependent on the endocytic motif in gp41 cytoplasmic tail. Taken together, this suggests that tetherin antagonism is a necessary function for efficient viral replication and thus primate lentiviruses evolved multiple strategies to antagonise this restriction factor.

In addition to preventing tetherin-mediated NF-κB activaiton, Vpu can also direcly target the NF-κB complex and thus further supress innate immune responses. Lack of Vpu-mediated NF-κB antagonism results in expression of IFNs and ISGs, which inhibits viral replication (Langer et al., 2019; Sauter et al., 2015). Vpu was shown to stabilise the inhibitory subunit IκB and thus prevent NF-κB activation and nuclear translocation (Hotter et al., 2017; Sauter et al., 2015). Stabilisation of IκB is thought to occur in β-TrCP-independent manner; however, the mechanism of inhibition is not well understood. This function of Vpu was shown to be conserved across all lentiviral lineages, thus highlighting its importance for viral replication.

One other well-defined function of Vpu is to degrade CD4. This prevents inhibitory Env-CD4 interactions in the host cells that can result in production of non-infectious Env, expose CD4-induced antibody epitopes and thus mediate ADCC or tether nascent viral particles at the PM (Ross et al., 1999; Smalls-Mantey et al., 2013; Veillette et al., 2014; Willey et al., 1992). Additionally, CD4 downmodulation prevents superinfection of the host cell (Wildum et al., 2006). In the ER, the cytoplasmic domain of Vpu interacts with CD4 cytoplasmic tail, which recruits the SCF-β-TrCP complex that mediates CD4 ubiquitination (Bour et al., 1995; Margottin et al., 1998). Firstly, this inhibits the anterograde trafficking of CD4 and sequesters it in the ER, which recruits the ERAD machinery that targets CD4 for proteasomal degradation (Magadán et al., 2010; Ulrich Schubert et al., 1998). Vpu also downmodulates surface expression of several immunoreceptors: NTB-A, PVR and CD1d to evade NK and NKT cell immune responses

(Matusali et al., 2012; Moll et al., 2010; Shah et al., 2010). Vpu sequesters these immunoreceptors in the TGN and the endosomal compartments, but it does not cause their degradation. Furthermore, Vpu was also shown to downmodulate and degrade alanine transporter SNAT1, which was shown to inhibit CD4+ T cell proliferation (Matheson et al., 2015). This might therefore represent another immune evasion strategy.

1.4.4 Nef

Negative factor (Nef) is a small (27-32 kDa) accessory protein found in all primate lentiviruses. Despite its original naming “negative factor”, Nef is required for efficient viral replication *in vitro* and *in vivo*. Notably, individuals infected with Nef-defective viruses showed poor viral replication and lack of disease progression (Deacon et al., 1995; Kirchhoff et al., 1995). Similarly, Nef was crucial for maintenance of high viral loads and development of simian AIDS in SIVmac infected rhesus macaques (Kestler et al., 1991). Nef downmodulates a variety of cell surface molecules to enhance viral replication and evade immune responses. Additionally, Nef interacts with cellular kinases to perturb T cell activation and actin cytoskeleton.

Nef functions as an adaptor between host cell proteins and AP-1 or AP-2 clathrin adaptors of the endocytic machinery to trigger endocytosis of target proteins and thus downmodulate their cell surface expression (Craig et al., 1998; Schwartz et al., 1996). As shown in Figure 1.7, Nef contains N-terminal myristoyl anchor that inserts it in the membrane and basic residues in the unstructured N-terminal region further stabilise interaction with negatively charged lipids in the membrane (Geyer et al., 1999; Yu & Felsted, 1992). This Nef localisation to cellular membranes is necessary for its function. Nef interacts with clathrin adaptors AP-1/2 via the ExxxLL motif in the C-terminal loop (Craig et al., 1998), while SIV and some HIV-2 Nefs also contain an additional YxxL endocytic motif in the unstructured N-terminal region. In addition to AP1 and AP2, Nef also interacts with other endocytic adaptors: phosphofurin acidic cluster sorting protein 1 (PACS-1), β subunit of COPI coatomers (β-COP) and vacuoloar ATPase V1H to further promote endocytosis of target proteins (Figure 1.7) (Lu et al., 1998; Munch et al., 2005; Piguet et al., 1999, 2000).

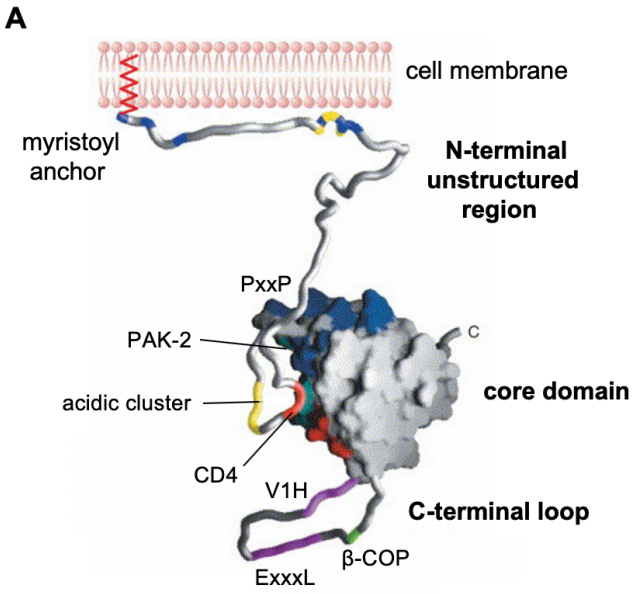

B

```
          myristoylation
HIV-1   MGGKWSKSSVIGWPAVRERMRRAE-------------PAADGVGAVSRDLEKHGAITSS- 46
SIVsmm  ..AAG..KRSKPRGGL...LLK.RGETYGRLWEGLEEGYSQSR.GLG..WNL.SSEGQGY 60
                                    YxxL
                                    CD4 PACS-1          PxxP
HIV-1   -------------------NTAANNAACAWLEAQEEEEVGFPVTPQVPLRPMTYKAAVDLS 88
SIVsmm  NEGQFMNTPWRNPARERERKLKYRQQNMDDVDDDDN.L..VS.R.KT..A.S..L.I.M. 120
                      CD4
                          PAK-2
HIV-1   HFLKEKGGLEGLIHSQRRQDILDLWIYHTQGYFPDWQNYTPGPGVRYPLTFGWCYKLVPV 148
SIVsmm  ..I........IYYDE..HR...IYLEKEE.II...........I...MF...LW..... 180
          CD3                     CD3
              β-COP    ExxxL          V1H
HIV-1   EPDKVEEANKGENTSLLHPVSLHGMDDPEREVLEWRFDSRLAFHHVARELHPEYFKNC*- 206
SIVsmm  HVS--..QTD.THC.V..AQTYQW..PWG...A....PQ..YTYE.FIR...E.GSKSG 238
                                                  MHC-I

HIV-1   ------------------------- 206
SIVsmm  LSEEEVRRRLTARGLLKMADKKETS 263
```

Figure 1.7: Nef structure and sequence motifs important for Nef function.

(A) Structure of HIV-1 Nef. The model of Nef membrane association is based on two NMR structures (1QA5 and 2NEF). The model shows N-terminal myristoyl anchor, N-terminal unstructured region, globular core domain, which interacts with Nef target proteins and C-terminal flexible loop, which interacts with components of the endocytic machinery. Highlighted are important motifs for Nef function (described in panel B). Adapted from (Arold & Baur, 2001). **(B)** Amino acid sequence alignment of HIV-1 (NL4.3) and SIVsmm (FBr 75wL4) Nef. Highlighted are important motifs for Nef interaction with: AP-2 and AP-1 clathrin adaptors (YxxL and ExxxLL), PACS-1 (acidic cluster), β-COP (di-acidic motif, EE), V1H (di-acidic motif, DD), SH3 domain of Src-family kinases (PxxP) and PAK-2 (RR and PxxP). SIV Nef proteins interact with CD4 via residues $P_{73}A$, with MHC-I via Y221, and with CD3 via I123 and L146. HIV-1 Nef proteins interact with CD4 via residues $W_{57}L$, whereas PxxP and acidic cluster motifs (PACS-1) are important for MHC-I downmodulation. Dots indicate identity and dashes indicate gaps introduced to optimise the alignment.

The best characterised targets of Nef are: SERINC3/5, tetherin, CD4, CD3, CD28, CXCR4 and MHC-I. Additionally, Nef interacts with SH3 domain of Src-family kinases via conserved PxxP motif (Collette et al., 2000), and interaction with PAK-2 kinase involved in actin remodelling is mediated via PxxP and di-arginine motifs (Haller et al., 2007). Thus, Nef can be considered a promiscuous binding partner for many components of the host cell trafficking and endocytic machinery. This adaptor function explains why it has been reported to target a large number of cellular proteins and processes.

1.4.4.1 SERINC5/3 downmodulation

Nef has long been observed to increase virion infectivity (Chowers et al., 1994; Münch et al., 2007; Tokunaga et al., 1998) but the mechanism remained unknown until two studies published in 2015 identified SERINC3 and 5 as the targets of HIV-1 Nef (Rosa et al., 2015; Usami et al., 2015). Specifically, it was shown that Nef induces endocytosis of SERINC3/5 from the plasma membrane of cells, which prevents their virion incorporation and thus enhances virion infectivity. As discussed earlier, there are no available SERINC antibodies, therefore exogenous expression of tagged SERINCs is used in research. Recently, Jurkat T cell line was generated containing tagged endogenous SERINC5 (Passos et al., 2019). Interestingly it was shown that Nef, in addition to preventing endogenous SERINC5 virion incorporation, may also counteract virion-associated SERINC5 to enhance virion infectivity and a similar mechanism of Nef-mediated antagonism of virion incorporated SERINC5 was previously proposed using exogenously expressed SERINC5 (Trautz et al., 2016). Taken together, this suggests that Nef might use multiple mechanisms to counteract SERINC5 restriction and the exact mechanistic details remain to be uncovered. SERINC3/5 endocytosis is mediated via the ExxxLL motif in Nef and AP-2 adaptor complex and results in SERINC retargeting to late endosomes (Rab7+ compartment) and lysosomes, but without their degradation (Rosa et al., 2015; Shi et al., 2018; Trautz et al., 2016; Usami et al., 2015). Nef is thought to interact with intracellular loop 4 of SERINC5, which was determined by domain-swap experiments between human SERINC5 and Nef-resistant frog SERINC5 (Dai et al., 2018). By contrast, residues in Nef required for SERINC5 binding have not been well defined. Notably, Nef antagonism of SERINC5 is not species-specific as diverse primate lentiviral Nef proteins are able to counteract both human and different monkey species SERINC5 orthologs (Heigele et al., 2016), which suggests that SERINC antagonism did not present a barrier to zoonotic transmissions. Likewise, SERINC5 restriction of viral infectivity was shown to be conserved as diverse primate and non-primate SERINC5

proteins, including mouse, frog and zebrafish SERINC5 orthologs are able to restrict HIV-1 infectivity (Dai et al., 2018; Heigele et al., 2016). Interestingly, the potency of Nef-mediated SERINC5 antagonism varies and was shown to correlate to some extent with prevalence of SIV infection in different monkey species in the wild (Heigele et al., 2016). This suggest that SERINC restriction presents an important selective pressure for viral transmission and viral fitness in general, even in the absence of species-specific Nef-SERINC phenotypes. Moreover, HIV-2 Nefs were shown to be particularly weak antagonists of SERINC3/5 compared to HIV-1 Nef, which one may speculate to contribute to the relatively poor viral replication of HIV-2 observed *in vivo* (Heigele et al., 2016). This is an intriguing observation as SIVsmm Nef (which transmitted to HIV-2) is a potent antagonist of human SERINC5 and why HIV-2 Nef partially lost this ability remains unknown. Moreover, certain HIV-1 Nef mutants that are associated with viral escape from CTL responses were shown to be defective for SERINC5 antagonism, which resulted in low virion infectivity (Jin et al., 2019) and shows the importance of balancing viral replication and efficent immune evasion. Notably, these Nef mutants were isolated form HIV-1 elite controllers, which are characteresid by effiecient long-term control of viral replication. Therefore, it is possible to speculate that immune pressure selection of Nef variants defective in SERINC5 antagonism activity might contributed to better control of viral replication in these individuals.

1.4.4.2 Tetherin downmodulation

Most SIV Nef proteins antagonise the restriction factor tetherin in their respective monkey species (Jia et al., 2009; Sauter et al., 2009; Zhang et al., 2009). The exceptions are SIVgsn/mon/mus, which use their Vpu to counteract tetherin. As discussed in the previous Section, lentiviral antagonism of tetherin is species specific and thus is proposed to have presented a major barrier to zoonotic transmissions. Nef binds to the tetherin cytoplasmic tail and recruits the AP-2 adaptor complex via the ExxxLL motif, which results in tetherin endocytosis (Serra-Moreno et al., 2013; Zhang et al., 2011). Human tetherin has a five-amino acid deletion in the cytoplasmic tail which renders it resistant to Nef-mediated downmodulation (Zhang et al., 2009). Notably, HIV-1 O group Nef (transmitted from SIVgor) evolved to target an adjacent region in tetherin cytoplasmic tail and mainly prevents anterograde transport from the TGN, which is mediated by the ExxxLL motif and the AP-1 adaptor complex (Kluge et al., 2014; Morris et al., 2018).

1.4.4.3 CD4 downmodulation

CD4 downmodulation is a conserved feature of all primate lentiviral Nef proteins. CD4 downmodulation prevents superinfection and inhibitory Env-CD4 interactions in the host cell that can result in virion tethering at the PM or expose Env epitopes for ADCC (Ross et al., 1999; Veillette et al., 2014; Wildum et al., 2006). The CD4 cytoplasmic tail contains a di-leucine endocytic motif; however, to induce endocytosis the endocytic motif requires phosphorylation, which is dependent on T cell activation (Pitcher et al., 1999). Nef is able to bind CD4 endocytic motif in the absence of phosphorylation and recruits AP-2 complex via its ExxxLL motif, which results in CD4 endocytosis and lysosomal degradation (Aiken et al., 1994; Garcia & Miller, 1991; Greenberg et al., 1997). Notably, CD4 downmodulation is not species-specific as diverse SIV Nefs can downmodulate human CD4 (Hua & Cullen, 1997; Munch et al., 2005). Interestingly, different residues in Nef core domain were shown to be important for CD4 downmodulation: residues $P_{73}A$ in SIV Nefs and residues $W_{57}L$ in HIV-1 Nefs (Figure 1.7B), which suggests different mode of CD4 interaction between different Nefs (Hua & Cullen, 1997; Iafrate et al., 2000).

1.4.4.4 CD3 downmodulation

HIV-2 and most SIV Nef proteins downmodulate CD3 expression from the surface of infected cells, whereas HIV-1 Nef does not have this ability. Therefore, one of the most intriguing questions regarding Nef activity is the evolutionary relationship between lentiviral Nefs in their ability to downregulate CD3 surface expression. CD3 complex is the signalling component of the T cell receptor (TCR) complex and thus mediates T cell activation (discussed in Section 1.6). Nef-mediated CD3 downmodulation in infected cells *in vitro* was shown to suppress T cell activation induced by TCR crosslinking (via PHA or CD3/CD28 stimulation) and also reduce apoptosis of stimulated infected cells (Khalid et al., 2012; Schindler et al., 2006; Schmökel et al., 2013). CD3 downmodulation was also shown to impair formation and signalling at the immunological synapse between infected T cells and antigen presenting cells (Arhel et al., 2009). Therefore, it was postulated that Nef-mediated CD3 downmodulation interferes with antiviral immune responses and prevents aberrant immune activation that is observed in SIV and HIV-2 infection *in vivo*. Although SIVsmm Nef is able to downmodulate CD3, rare cases have been reported where SIVsmm Nef lost this ability during *in vivo* infection of sooty mangabeys, which was associated with increased immune activation and loss of CD4+ T cells (Schindler et al., 2008; Schmökel et al., 2013; Sumpter et al., 2007). This might therefore suggest a protective role of CD3 downmodulation against immunopathology. Indeed, efficient Nef-mediated CD3 downmodulation was also shown to dampen

immune activation and inflammatory responses during *in vivo* SIV infection of two other monkey species: African green monkeys and rhesus macaques (Joas et al., 2018, 2020). Additionally, CD3 downmodulation was particularly important for efficient viral immune evasion and subsequent maintenance of high viral loads in SIVmac infected macaques (Joas et al., 2020). In humans, maintained Nef-mediated CD3 downmodulation activity in viraemic HIV-2 patients correlated with preserved CD4+ T cell counts (Khalid et al., 2012), which is consistent with protective role of CD3 downmodulation against aberrant immune activation and immunopathology. Whether loss of Nef-mediated CD3 downmodulation contributes to viral pathogenesis in HIV-1 infection remains a matter of speculation.

Notably, as shown by phylogenetic analysis in Figure 1.8, Nef-mediated CD3 downmodulation was lost twice during primate lentivirus evolution. First it occurred in the SIVgsn/mon/mus lineage, and second after the transmission to chimpanzees in the HIV-1/SIVcpz lineage (Schindler et al., 2006). SIVrcm Nef, the precursor of SIVcpz Nef, was shown to downmodulate CD3 expression less potently compared to other SIVs, which might have facilitated the loss of this function upon transmission to chimpanzees (Schindler et al., 2006). Reasons why this potential immune evasion strategy was lost remains poorly understood. Given that Nef-mediated CD3 downmodulation activity was lost twice suggests a strong selective pressure against this function in SIVgsn/mon/mus and HIV-1/SIVcpz lineages. Interestingly, loss of Nef-mediated CD3 downmodulation in these lineages coincided with acquisition of *vpu* gene (Figure 1.8). As discussed above, Vpu prevents immune activation by inhibiting NF-κB activation both via tetherin antagonism and via stabilisation of inhibitory IκB subunit (Galão et al., 2012; Langer et al., 2019; Sauter et al., 2015). This means that viruses without CD3 downmodulation ability still have a mechanism to suppress immune activation, which is via Vpu activity. By contrast, having two mechanism to suppress NF-κB activation: via both CD3 downmodulation and Vpu has been hypothesised it could result in too much suppression and thus inhibit viral replication (Heusinger & Kirchhoff, 2017); however, this remains to be investigated. Taken together, this led to hypothesis that acquisition of Vpu facilitated or even necessitated loss of Nef-mediated CD3 downmodulation (Heusinger & Kirchhoff, 2017; Kirchhoff, 2009). Importantly, this remains a matter of debate and it is unclear why either of the strategies to supress immune activation should be better. Whether loss of Nef-mediated CD3 downmodulation confers any replicative advantage to HIV-1 will be explored in this Thesis.

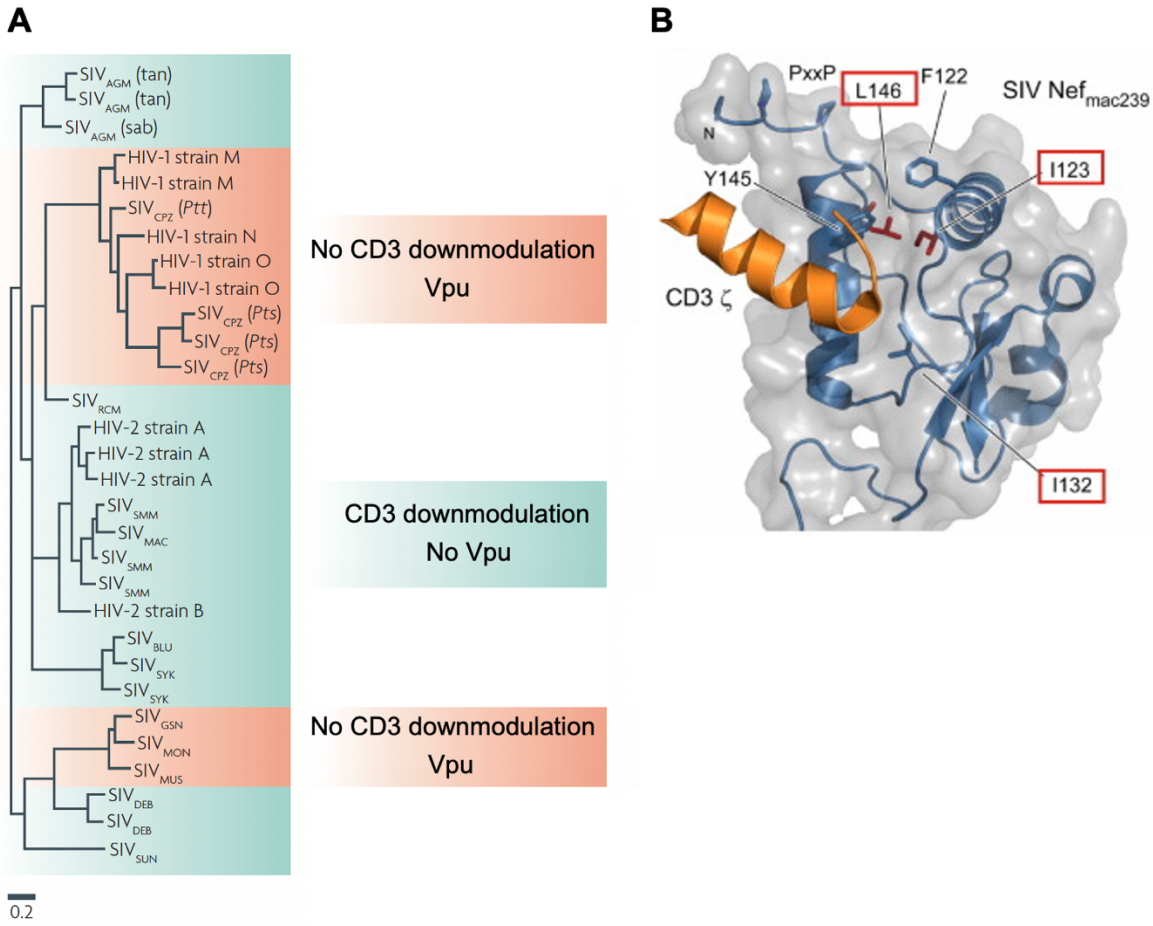

Figure 1.8: Lentiviral Nef proteins and CD3 downmodulation

(A) Phylogenetic analysis of HIV-1, HIV-2 and SIV Nef proteins. Loss of Nef-mediated CD3 downmodulation occurred twice in the lentiviral evolution: first in the SIVgsn/mon/mus lineage, and second after transmission to chimpanzees in the HIV-1/SIVcpz lineage. This also coincided with acquisition of *vpu* gene. Orange therefore indicates viruses that lost Nef-mediated CD3 downmodulation ability and have *vpu* gene. Green indicates viruses with Nef-mediated CD3 downmodulation and no *vpu* gene. For example: SIVagm, SIVrcm and HIV-2/SIVsmm lineage. Scale bar shows 0.2 substitutions per site. Adapted from (Kirchhoff, 2009). **(B)** Co-crystal structure of SIVmac239 Nef in complex with the first ITAM of CD3ζ (PDB 3IK5). Nef is shown in blue and grey. CD3ζ is shown in orange. Highlighted are important residues in Nef for CD3ζ binding: I123, I132 and L146. Adapted from (Schmökel et al., 2013).

Nef interacts with the ζ chain of CD3 complex to induce its endocytosis and targeting for lysosomal degradation. As shown in Figure 1.8B, Nef recognises and binds CD3ζ cytoplasmic tail primarily in the first immunoreceptor tyrosine-based activation motif (ITAM) (Howe et al., 1998; Kim et al., 2010; Schaefer et al., 2000). Analysis of naturally occurring SIVsmm and HIV-2 Nef mutants showed that residues I123, I132 and L146 in Nef core domain are crucial for CD3ζ binding (Khalid et al., 2012; Schmökel et al., 2013).

Differences in accessibility of CD3ζ ITAM and Nef binding at the PM compared to CD4 downmodulation result in steric hindrance at the PM and Nef cannot use the ExxxLL motif, but instead uses the N-terminal YxxL motif to recruit AP-2 adaptor complex and induce CD3 endocytosis (Manrique et al., 2017; Swigut et al., 2003). Notably, CD3 downmodulation is not species-specific as diverse SIV Nef proteins are able to downmodulate human CD3 (Munch et al., 2005; Schindler et al., 2006).

1.4.4.5 CD28 and CXCR4 downmodulation

In addition to targeting CD3 to modulate immune activation, Nef also downmodulates the costimulatory molecule CD28 from the surface of infected cells to prevent efficient T cell co-stimulation at the immunological synapse. To do this, Nef binds CD28 cytoplasmic tail and recruits AP-2 adaptor complex to induce CD28 endocytosis (Leonard et al., 2011; Swigut et al., 2001). HIV-1 Nef proteins were shown to have only modest activity in CD28 downmodulation, whereas SIV and HIV-2 are more potent in this activity (Khalid et al., 2012; Munch et al., 2005). Inability to efficiently supress T cell co-stimulation might contribute to increased and chronic immune activation that is observed in HIV-1 infection and this remains to be investigated.

Downmodulation of CXCR4 chemokine receptor reduces migration to SDF-1 (also known as CXCL12), which is involved in lymphocyte retention in lymphoid tissues and migration to sites of inflammation (Kucia et al., 2004). This interferes with immune responses and is therefore considered to be another viral immune evasion strategy. Nef induces CXCR4 endocytosis via ExxxLL motif and recruitment of AP-2 adaptor complex (Hrecka et al., 2005; Venzke et al., 2006). SIV Nef proteins were shown to be particularly active in CXCR4 downmodulation, whereas HIV-1 and HIV-2 Nefs show only modest activity. Again, the consequence of this difference for *in vivo* infection remains unknown. Interestingly, HIV-1 Nef was shown to interfere with chemokine signalling downstream of CXCR4 by activating Rac signalling via DOCK2-ELMO1 complex and thus inhibiting SDF-1 chemotaxis (Janardhan et al., 2004). This strategy was proposed to compensate for weak downmodulation of CXCR4 by HIV-1 Nef

1.4.4.6 MHC-I downmodulation

Lentiviral Nef proteins downmodulate surface expression of MHC-I to evade cellular immune responses. It was initially observed that Nef only downmodulates MHC-I alleles

HLA-A and HLA-B to evade CD8+ T cell responses, whilst maintaining HLA-C and HLA-E expression to evade NK cell responses (Cohen et al., 1999; le Gall et al., 1998). However, this observation was recently challenged as some primary HIV-1 Nef isolates were shown to effectively downmodulate HLA-E (van Stigt Thans et al., 2019). This reduced the recognition of infected cells by CD8+ T cells but increased their susceptibility to NK cell killing; however, the importance of this function for replication *in vivo* remains unclear. Efficient Nef-mediated MHC-I downmodulation was shown to be crucial for evasion of immune responses and maintenance of high viral loads during *in vivo* SIV infection of sooty mangabeys or rhesus macaques (Münch et al., 2001; Schindler et al., 2008; Swigut et al., 2004). Nef interferes with anterograde trafficking of MHC-I by sequestering it in the TGN and targeting it for lysosomal degradation (Roeth et al., 2004; Schwartz et al., 1996). HIV-1 Nef forms a ternary complex with MHC-I cytoplasmic tail and AP-1 adaptor complex to induce recognition of the cryptic tyrosine-based sorting motif in MHC-I by the AP-1 complex (Jia et al., 2012; Roeth et al., 2004). Nef interacts with AP-1 via the PxxP motif and the acidic cluster, which was also shown to mediate interaction with PACS-1 endocytic adaptor and is important for MHC-I downmodulation (Jia et al., 2012; Noviello et al., 2008; Piguet et al., 2000). By contrast, SIV Nef uses the C-terminal domain to downmodulate MHC-I, where the conserved tyrosine residue (Y221) is crucial for this activity (Munch et al., 2005; Swigut et al., 2000); however, the precise interaction between Nef, AP-1 and MHC-I remains poorly defined.

1.4.4.7 Interaction with cellular kinases

Lentiviral Nef proteins interact with Src-family kinases (SFK): Lck, Fyn, Hck and Lyn; however, the consequences of this interaction for the host cell or viral replication remain poorly understood. Nef binds the SH3 domain of SFKs via the conserved PxxP motif (Arold et al., 1998; Collette et al., 2000; Greenway et al., 1996; Haller et al., 2007; Lee et al., 1995; Saksela et al., 1995). The binding also depends on residues surrounding the PxxP motif, therefore different HIV-1, HIV-2 and SIV Nefs have varying affinities towards different kinases. Whether this interaction has inhibitory or activating effect on the kinase function remains a matter of debate. In infected cells, Nef was shown to induce hyperresponsiveness to stimulation (such as TCR activation) that results in increased activity of transcription factors (NFAT, NF-κB, c-Jun/c-Fos) and increased production of cytokines (Fenard et al., 2005; Fortin et al., 2004; Schrager & Marsh, 1999; Wang et al., 2000). This was dependent on the PxxP motif, which suggests the involvement of SFKs, but the exact mechanism was not defined. Nef was also shown to cause Lck relocalisation from the PM to the TGN (Haller et al., 2007; Rudolph et al.,

2009). This was suggested to activate downstream Ras-ERK signalling pathway and thus compensate for the relocalisation of Lck (Hung et al., 2007; Pan et al., 2012). Although this is consistent with observations of Nef-induced hyperresponsiveness, the mechanism of ERK activation remains unknown. Moreover, Nef has been implicated in stimulating NF-κB activity and proviral transcription, which was again dependent on the PxxP motif, thus suggesting involvement of the SFKs (Fortin et al., 2004; Herbein et al., 2008; Mangino et al., 2011; Sauter et al., 2015). Notably, this effect was suppressed by Vpu-mediated inhibition of NF-κB in the late stages of viral life cycle, thus suggesting Nef acts upstream of Vpu (IκB stabilisation) and early in the life cycle (Sauter et al., 2015). Intriguingly, conflicting reports also show Nef having inhibitory effect (Bandres & Ratner, 1994; Niederman et al., 1993) or no activity (Witte et al., 2008; Yoon & Kim, 1999) against NF-κB activation. While these discrepancies might be reconciled by differences in cell lines or T cell activation used in different studies, the exact role of Nef in NF-κB activation remains unknown and perhaps implies it is dependent on the cell activation status. Although the exact role of Nef-SH3 domain interaction remains puzzling, intact PxxP motif is important for enhanced viral replication *in vitro* (Carl et al., 2000; Fackler et al., 2006; Homann et al., 2009; Meuwissen et al., 2012). By contrast, mutation of PxxP motif in SIVmac Nef was dispensable for viral replication or disease progression during *in vivo* infection of macaques (Carl et al., 2000; Lang et al., 1997). Taken together, the conservation of PxxP motif and the interaction with the SFKs implies that manipulation of cellular kinases is important for viral replication; however, the exact mechanism remains a matter of debate.

Lentiviral Nef proteins also interact with cellular kinase PAK-2 to inhibit cytoskeleton remodelling. Nef binds PAK-2 via the PxxP and di-arginine motifs (Figure 1.7), which results in PAK-2 activation and hyper-phosphorylation of actin-severing factor cofilin (Krautkrämer et al., 2004; Nunn & Marsh, 1996; Stolp et al., 2009, 2010). This in turns inhibits cofilin and prevents F-actin remodelling, which is required for cell motility and chemotaxis or during immunological synapse formation (Rudolph et al., 2009; Stolp et al., 2009). Indeed, Nef-PAK-2 interaction resulted in reduced migration to SDF-1, CCL-19 and CCl-21 chemokines and impaired F-actin ring formation upon TCR crosslinking. Therefore, this might represent another viral strategy of immune evasion; however, its importance *in vivo* remains unknown. Moreover, Nef-mediated activation of PAK-2 was shown to enhance viral replication *in vitro*; however, the precise mechanism remains unknown (Meuwissen et al., 2012; Olivieri et al., 2011; Rudolph et al., 2009).

Given that PAK-2 activation is a conserved feature of primate lentiviruses, this suggest that inhibition of actin remodelling is important for viral replication.

In summary, Nef is an intriguing viral accessory protein that exerts a diverse array of functions that converge on dysregulating host cells during viral infection, often by manipulating cell surface protein expression to enhance viral replication and immune evasion. While Nef targets a range of cellular proteins, this is often achieved by recruitment of a few key host proteins (for example the clathrin adaptor AP-2), thus explaining how such a small accessory protein can exert such a plethora of effects on the host cell.

1.5 HIV-1 dissemination

HIV-1 can infect a new target cell either as a cell-free virion or via cell-cell spread (Sattentau, 2008). During cell-free infection, virions that have budded from the plasma membrane of an infected cell move through the liquid phase by diffusion until they attach and bind to a target cell to initiate new infection (Figure 1.9). Importantly, it is now known that the dominant mode by which HIV-1 disseminates to infect new target cells is by highly-efficient cell-cell spread. Cell-cell spread occurs at so-called virological synapses (VS), which are virus-induced contacts between infected and uninfected cells that allow for polarised viral budding and highly efficient transfer of virions across the synapse to infect new target cells (Chen et al., 2007; Jolly et al., 2004) (Figure 1.9). Formation of the VS brings the two cells in close physical contact, where the virus buds from the PM of the infected cell, thus viral transfer is not associated with cell-cell fusion. The name "virological synapse" was coined due to parallels with the immunological or neurological synapse where information (in this case virus) is transmitted by polarised secretion (in this case viral budding) (Jolly & Sattentau, 2004). HIV-1 is therefore thought to exploit and manipulate the ability of immune cells to communicate via cell-cell contact as observed in lymphoid tissues where T cells are densely packed and frequently interact. Interestingly, HIV-1 was known to utilise cell-cell spread for a number of years (Dimitrov et al., 1993; Gupta et al., 1989; Sato et al., 1992); however, whether this was an artefact of using polarised cells such as epithelial cell lines was not clear and as such the discovery of the VS and mechanisms of cell-cell spread remained unknown and largely unstudied. In addition to cell-cell spread at the VS, HIV-1 can also spread by cell-cell means through cellular projections such as filopodia and membrane nanotubes, or through "infectious synapses" formed between dendritic cells and T cells (McDonald et al., 2003; Sowinski et al., 2008). Interestingly, two other retroviruses, human T-lymphotropic virus 1 (HTLV-1) and murine leukaemia virus (MLV) were also shown to use cell-cell spread for viral dissemination. HTLV-1 infects T cells and was shown to form a structure similar to HIV-1 VS to infect target cells (Igakura et al., 2003; Yamamoto et al., 1982). MLV infects B cells and was also shown to form VS between infected and uninfected cells both *in vitro* and *in vivo* (Jin et al., 2009; Sewald et al., 2012, 2015). By contrast, whether other non-M HIV-1 groups (N, O and P), HIV-2 and related SIVs also exploit cell-cell spread to more efficiently disseminate and whether they induce formation of VS analogous to HIV-1 M group is unknown and remains an important question.

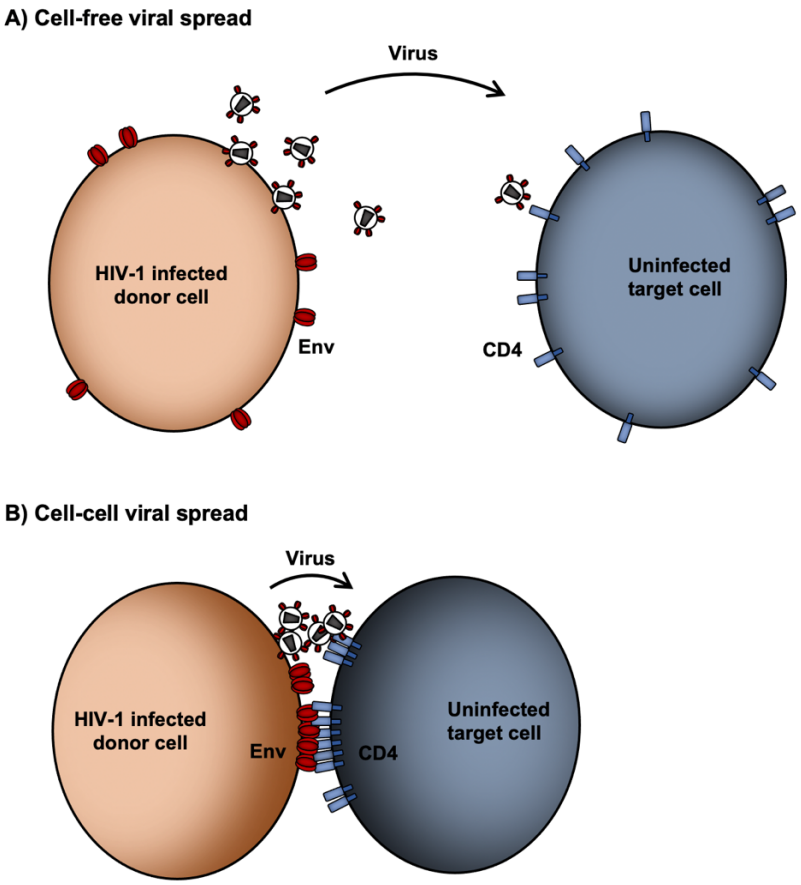

Figure 1.9: HIV-1 dissemination

(A) During cell-free viral spread virions bud from the infected cell and diffuse through the extracellular space until they encounter and bind to an uninfected target cells to initiate infection. **(B)** Cell-cell viral spread occurs through the formation of the VS, which is mediated by Env-CD4 interactions that bring the infected and uninfected cell in close physical contact. Viral budding is polarised at the synapse and results in highly efficient viral spread and infection of target cells.

1.5.1 T cell virological synapse

1.5.1.1 Structure and formation

Infected CD4+ T cells can readily spread HIV-1 to uninfected target CD4+ T cells via formation of a virological synapse (VS), which is depicted in Figure 1.10. The formation of the VS is triggered by binding of Env on infected cell (referred to as a donor cell) and CD4 on the uninfected cell (referred to as a target cell), which brings the two cells in direct physical contact (Jolly et al., 2004). This contact is further stabilised by adhesion molecule interactions mediated by the integrin LFA-1 and its cognate ICAM ligands (ICAM-1 and to lesser extent ICAM-3), which are expressed on both donor and target T cells (Chen et al., 2007; Jolly et al., 2007b; Sourisseau et al., 2007). Inhibition of either Env-CD4 or LFA-1-ICAM interactions reduces VS formation and inhibits cell-cell spread.

This was demonstrated using blocking antibodies, inhibitory peptides and CD4 or LFA-1 knock-out cell lines, which resulted in lack of Env or Gag polarisation and thus inhibition of cell-cell spread (Chen et al., 2007; Jolly et al., 2004, 2007b; Rudnicka et al., 2009). Live cell imaging showed that VS formation results in a stable cell-cell contact that is maintained for approx. one hour (after which the cells separate), whereas non-specific contacts between uninfected T cells last only approx. 2 min (Groppelli et al., 2015; Martin et al., 2010). Transfer of viral Gag protein to the target cell also occurs within one hour as shown by fixed cell microscopy (Jolly et al., 2004) and was also demonstrated by live cell imaging using GFP-tagged Gag protein (Hubner et al., 2009). Env-CD4 interaction at the VS could theoretically results in cell fusion of donor and target cell and formation of syncytia but this is not seen (Jolly et al., 2004). Cell fusion is thought to be inhibited by tetraspanins (such as CD9 and CD81) that are enriched at the VS and block cell-cell fusion (Jolly & Sattentau, 2007; Roy et al., 2014; Weng et al., 2009). Moreover, electron microscopy of VS shows budding of nascent virions into the synaptic cleft, further establishing that transfer of viral proteins to target cell is not dependent on cell fusion (Jolly et al., 2004, 2011; Martin et al., 2010).

The VS is characterised as a cell-cell conjugate with polarisation of viral Env and Gag proteins in donor cell and CD4 in target cell to the site of cell contact (Figure 1.10). This polarisation is an active process and requires actin and tubulin cytoskeleton remodelling (Chen et al., 2007; Jolly et al., 2004, 2007a; Rudnicka et al., 2009). Specifically, it was shown that actin is enriched at the VS and inhibition of actin and tubulin network using inhibitors dimished Gag and Env polarisation and reduced cell-cell spread. Furthermore, formation of the VS was also shown to induce polarisation of cellular organelles (Golgi, mitochondria, microtubule organising centre) and calcium signalling, which was absent in the target cell or in contacts between uninfected cells, thus suggesting specific and active contact-induced cellular remodelling (Groppelli et al., 2015; Jolly et al., 2011). This suggests that polarisation of viral proteins at the synapse is a regulated and active process; however, what mediates the accumulation of Gag and Env is incompletely understood and three models have been proposed. First, Gag and Env colocalise with lipid rafts, which are enriched at the VS and depletion of cholesterol disrupting lipid raft integrity inhibits Gag and Env polarisation to the VS (Jolly & Sattentau, 2005). This suggests that PM remodelling might be one mechanism mediating Gag and Env polarisation. Second, viral proteins might be trafficked from intracellular compartments to the site of cell-cell contact which was shown by live cell imaging as formation of Gag clusters or “buttons” at the synapse (Hubner et al., 2009).

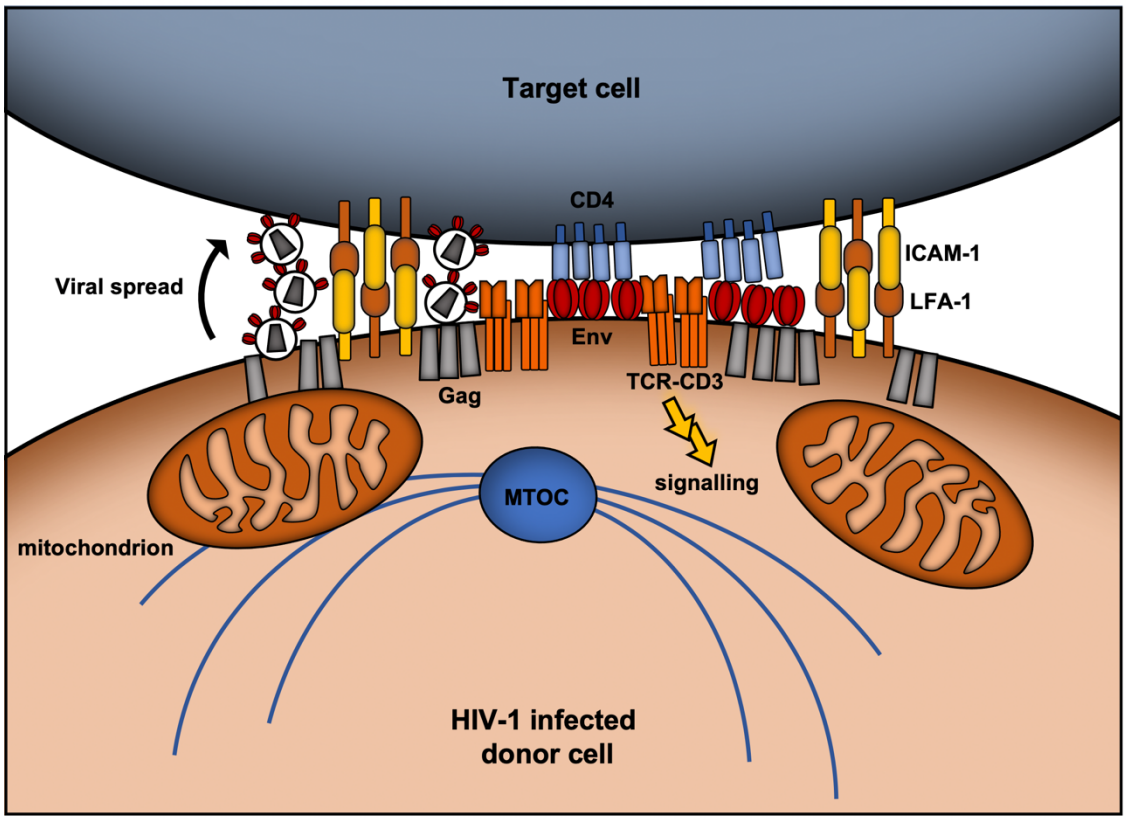

Figure 1.10: The T cell virological synapse

Diagram shows a VS formed between an infected donor CD4+ T cell and an uninfected target CD4+ T cell. The formation of synapse is mediated by Env and CD4 interactions and stabilised by interactions between adhesion molecules LFA-1 and ICAM-1. Env and Gag are enriched at the synapse. Clustering of TCR-CD3 complexes at the synapse triggers TCR signalling, which supports efficient viral spread. The synapse formation also triggers polarisation of MTOC and mitochondria to the site of cell contact, which supports polarised virus budding into the synapse. Nascent virions diffuse across the synapse to infect the target cell.

Third, Gag has been shown to be recruited or enriched to the uropods of T cells, which are rear-end structures of polarised migrating T cells (Llewellyn et al., 2010). Gag-enriched uropods were shown to preferentially form contacts with uninfected target cells, which resulted in VS formation and inhibition of uropod formation reduced cell-cell spread. Importantly, these models of polarisation and not mutually exclusive and it is likely that a combination of different mechanism meditates polarisation of Env and Gag. Alternatively, the mechanism might differ between different T cells depending on their polarity and migration. Moreover, how polarisation of Gag and Env to the synapse is coordinated is unknown. Intracellular Env that is recruited to the synapse was shown to be associated with secretory vesicles and inhibition of the regulated secretory pathway was shown to reduce cell-cell spread, thus suggesting that HIV-1 likely hijacks this pathway for Env polarisation and efficient viral spread (Jolly et al., 2011). Moreover, Env

at the VS was also shown to be associated with contact-induced polarisation of the microtubule organising centre (MTOC) where Env was seen in vesicles clustered around the MTOC and associated with the VS-proximal Golgi apparatus and recycling endosomes (Starling & Jolly, 2016). Thus, contact-induced polarisation of the MTOC and associated organelles also likely contributes to efficient delivery and polarisation of Env to the contact zone and enhanced virus budding at the VS, thus supporting efficient cell-cell spread. Interestingly, as described in Section 1.3.6, optimal Env virion incorporation is thought to require Env trafficking through the Golgi and recycling endosomal compartments (Groppelli et al., 2014; Kirschman et al., 2018). These observations raise a possibility that Env trafficking and virion incorporation is coupled to VS formation and cell-cell spread. This is an intriguing hypothesis that warrants further investigation.

In addition to viral proteins, as mentioned above, the MTOC, mitochondria, Golgi network and secretory vesicles are also polarised to the synapse in the HIV-1 infected T cell (Groppelli et al., 2015; Jolly et al., 2011; Rudnicka et al., 2009; Starling & Jolly, 2016). Importantly, the polarisation of cell organelles is not observed in contacts formed between uninfected cells showing that the polarisation is contact-specific. What triggers VS polarisation is incompletely understood. Integrin LFA-1 binding to its ligand, ICAM molecules, induces signalling activation in the β2 subunit (CD18) that results in cytoskeleton rearrangements (Hogg et al., 2011). It was shown that LFA-1 engagement in the infected cell triggers polarisation of the MTOC to the synapse, which is mediated via activation of ZAP70 kinase (Sol-Foulon et al., 2007; Starling & Jolly, 2016). MTOC polarisation is thought to coordinate the recruitment of Golgi, mitochondria and other organelles to the synapse, thus supporting VS formation and efficient viral spread. Polarisation of mitochondria is an active process, requiring microtubule rearrangements and occurs within minutes of VS formation as shown by live cell imaging (Groppelli et al., 2015). Mitochondrial polarisation with associated calcium signalling was shown to transiently increase intracellular Ca^{2+} levels at the VS and thus support formation of stable VS and efficient cell-cell spread, which was blocked using inhibitros of mitochondrial calcium signalling. Concomitant with mitochondrial polarisation, Gag protein was also shown to be recruited to the synapse, which required mitochondrial calcium signalling, thus further suggesting that Gag polarisation is an active process (Groppelli et al., 2015). Overall, polarisation of cellular organelles and recruitment of Env and Gag proteins to the VS results in polarised virus budding into the synaptic cleft,

where virions diffuse towards the target cell to initiate new infection (Hubner et al., 2009; Jolly et al., 2004, 2011, Martin et al., 2010).

In addition to LFA-1 signalling, VS formation was also shown to trigger antigen-independent TCR signalling in both donor and target cell (Len et al., 2017). Specifically, the TCR-CD3 complex was shown to cluster at the synapse and mediate activation of Lck, ZAP70 and multiple downstream components of the TCR signalling pathway, which was required for efficient cell-cell spread. TCR signalling at the VS will be discussed further in Section 1.6. Whether TCR signalling directly contributes to cellular organelle and viral protein polarisation to the VS was not investigated; however, it is likely that multiple proteins and pathways contribute to the polarisation. Moreover, what triggers dissociation and release of the VS is also unknown. Live cell imaging showed that T cell polarisation is lost (as evidenced by Gag and mitochondria redistribution) when the cells disengage (Groppelli et al., 2015); however, what constitutes the stop signal remains unknown.

1.5.1.2 Efficiency

Cell-cell spread offers an advantage for HIV-1 compared to cell-free infection due to its high efficiency. In fact, experimental data shoes that cell-cell spread is at least an order of magnitude (10-100 times) more efficient compared to equivalent cell-free infection (Chen et al., 2007; Dimitrov et al., 1993; Jolly et al., 2007b; Martin et al., 2010; Mazurov et al., 2010; Sourisseau et al., 2007). This is usually measured by transwell experiments where donor and target cells are separated by a porous membrane and compared to wells where donor and target cells are allowed to interact. Moreover, incubation of donor and target cell co-cultures with continuous gentle shaking, which prevents cell-cell contact resulted in greatly diminished viral spread, thus further illustrating the efficiency of cell-cell spread (Sourisseau et al., 2007). Notably, the effect size varies between reports depending on the exact experimental setup and the type of cells used (different T cell lines or primary cells). Increased efficiency of cell-cell spread is evident as both faster kinetics of infection and greater numbers of infected target cells. This is thought to be achieved by polarised virus budding, high multiplicity of infection, enrichment of viral receptors and coreceptors at the cell contact, and close proximity of donor and target cell, which minimises the distance needed for virus to travel. Furthermore, as TCR signalling was shown to be triggered at the VS, this also raises a possibility that cell-cell spread influences the permissivity of the target cell and this remains to be explored. As

multiple viruses bud in the synapse this results in high multiplicity of infection that can result in multiple provirus integrations in the target cell (del Portillo et al., 2011; Russell et al., 2013). Importantly, these studies examined T cell lines, which are highly permissive to infection, therefore this might overestimate viral integration compared to primary T cells. Whether the same occurs *in vivo* remains unclear and a matter of debate. Some reports suggest that infected cells *in vivo* isolated from the peripheral blood or lymph nodes only carry a single provirus (Josefsson et al., 2011, 2013), whereas infected cells isolated from the spleen were shown to have an average of 3 to 4 integrated proviruses (Gratton et al., 2000; Jung et al., 2002).

The high efficiency of cell-cell spread is also evident by resistance to antiretroviral drugs and neutralising antibodies. Compared to cell-free infection, cell-cell spread was shown to be relatively resistant to RT inhibitors, particularly NRTIs, but sensitive to protease inhibitors (Agosto et al., 2014; Sigal et al., 2011; Titanji et al., 2013, 2017). This is thought to be due to high multiplicity of infection that can overwhelm the inhibitors, thus requiring higher inhibitor concentration compared to cell-free infection. That protease inhibitors are equally effective at blocking cell-cell and cell-free infection is somehow expected given that the inhibition of protease-mediated viral maturation leads to the production of non-infectious virions that are thus unable to infect target cells, regardless of the route of viral spread (Titanji et al., 2013). Importantly, testing clinically relevant combinations of antiretrovirals showed that combination therapy markedly increases the potency of weak inhibitors during cell-cell spread, which likely explains the effectiveness of combination therapy in clinical settings (Agosto et al., 2014; Titanji et al., 2017). This has important implications for HIV-1 treatment and design of antiviral regimes, which need to be able to suppress high viral multiplicity of infection during cell-cell spread. Moreover, cell-cell viral spread was shown to be more resistant to neutralising antibodies compared to cell free infection (Chen et al., 2007; Gupta et al., 1989; Malbec et al., 2013; Martin et al., 2010; McCoy et al., 2014; Zhong et al., 2013). Viral transfer at the VS is thought to reduce the time that the virus is exposed to the humoral immune factors, which mediates reduced antibody sensitivity of cell-cell spread.

Interestingly, cell-cell spread was also shown to overcome activity of certain host cell restriction factors. Tetherin restricts the release of budding virions from the PM and is antagonised by Vpu (Neil et al., 2008). Cell-cell spread was shown to overcome tetherin restriction compared to cell-free infection, either by tetherin overexpression or deletion

of Vpu (Jolly et al., 2010; Zhong et al., 2013). Interestingly, *vpu*-defective viruses showed increased VS formation and enhanced viral spread and conversely, tetherin knock-down resulted in reduced cell-cell spread (Jolly et al., 2010). It was shown that tetherin is enriched at the VS and it increases surface levels of Env, presumably by tethering nascent virions at the PM, which mediates more efficient VS formation. Indeed, previous reports observed selection of *vpu*-defective viruses *in vitro*, which was shown to mediate more efficient viral spread (Gummuluru et al., 2000; Klimkait et al., 1990; Schubert et al., 1995). Notably, since those initial studies on tetherin, Vpu and cell-cell spread it was found that tetherin also activates NF-κB signalling, which is antagonised by Vpu (Galão et al., 2012). Loss of tetherin antagonism might therefore be an efficient strategy for viral replication *in vitro*; however, *in vivo* tetherin antagonism is likely more important to prevent innate immune activation and induction of an antiviral state. In support of this idea, the tetherin antagonism function of Vpu was shown to be largely intact in primary *vpu* alleles isolated form infected individuals (Pickering et al., 2014). Moreover, cell-cell spread was also shown to overcome restriction factor TRIM5α. Rhesus macaque TRIM5α was shown to potently inhibit HIV-1 infection by targeting incoming viral capsids in the cytoplasm (Stremlau et al., 2004). Interestingly, expression of rhesus TRIM5α in human cells restricts cell-free infection but not cell-cell spread, suggesting that this mode of viral can overcome TRIM5α restriction (Richardson et al., 2008). The effect of other more recently identified restriction factors (e.g. SERINCs, MxB) on HIV-1 cell-cell spread at the VS has been largely unstudied but would be an interesting area for future research.

In addition to driving more efficient viral dissemination (which confers obvious advantages to the virus), HIV-1 cell-cell spread was also shown to enhance cell death of target cells. Using tonsil-derived T cells, the Greene lab has previously shown that cell-cell spread mediated non-productive or abortive infection of resting CD4+ T cells, which resulted in pyroptotic cell death and was not observed with cell-free infection (Galloway et al., 2015). Abortive infection was shown to result in production incomplete RT products that are detected by IFI16 DNA sensor, which triggers pyroptosis (Doitsh et al., 2014; Monroe et al., 2014). This might be due to high efficiency of cell-cell spread, which enables (abortive) infection of nonpermissive cells, thus triggering cell death. Therefore, cell-cell spread might represent a major mechanism of T cell depletion that is observed *in vivo*, especially in the lymphoid tissues where T cells are densely packed together. Overall, these observations show that cell-cell spread is advantageous for HIV-1, resulting in highly efficient viral transmission and resistance to neutralising antibodies,

antiretroviral drugs and restriction factors, but can also enhance cell death and thus contribute to pathogenesis.

1.5.1.3 *in vivo* evidence

Cell-cell spread is thought to be the predominant mode of HIV-1 dissemination in an infected individual (Agosto et al., 2015; Sattentau, 2008; Zhong et al., 2013); however, the direct evidence for VS formation and cell-cell spread *in vivo* is limited. This is due to technical difficulties of accessing lymphoid tissues in humans and an inability to do direct *in vivo* infection studies in humans, therefore so far only indirect evidence exists for cell-cell spread occurring *in vivo*. Histological examination of lymph nodes from HIV-1 infected individuals showed clustering of infected T cells (Schacker et al., 2000, 2001), thus suggesting preferential infection of neighbouring cells, which is consistent with cell-cell spread. Intravital microscopy in humanized mouse model showed that HIV-1 infected T cells migrate in lymph nodes but also form stable contacts with uninfected cells that are dependent on Env-CD4 interaction, which is indicative of cell-cell spread (Murooka et al., 2012). Moreover, using sphingosine 1-phosphate receptor antagonist to block the recirculation of T cells from the lymph nodes into the periphery reduced plasma viral loads, which suggest that cell-cell spread is required for efficient viral dissemination. Another study using humanized mouse model and electron microscopy showed that HIV-1 infected T cells in the GALT form close contacts with uninfected target cell (Ladinsky et al., 2014). This was accompanied with polarised virus budding and presence of LFA-1 and ICAM-1 molecules at the site of cell contact, which suggests formation of VS. A related model of retroviral infection using Friend murine leukaemia virus and intravital microscopy also showed formation of stable contacts between infected and uninfected cells (Sewald et al., 2012). This was dependent on the expression of Env and resulted in polarisation of Gag to the site of cell contact, which is again indicative of VS formation. This result was further confirmed in another study using a related murine leukaemia virus and intravital microscopy, which showed VS formation and cell-cell viral spread in the lymph node (Sewald et al., 2015). Taken together, present evidence strongly suggests that cell-cell spread of HIV-1 can occur *in vivo*; however, its importance for viral replication *in vivo* remains a matter of debate.

1.5.2 Macrophage-T cell virological synapse

Macrophages are also targets of HIV-1 infection and can infect T cells via cell-cell spread. Macrophages have been observed to infect CD4+ T cells in contact dependent

manner, whereas cell-free infection under the same conditions was greatly reduced (Carr et al., 1999; Sharova et al., 2005), again demonstrating the high efficiency of cell-cell spread. This was shown to occur through transient adhesive contacts that were mediated by Env-CD4 interaction (Groot et al., 2008). These contacts resemble the T cell-T cell VS and show polarisation of Gag, Env and CD4 to the synapse; however, the mechanistic details of the synapse structure and formation are less well studied. Interestingly, it was shown that viral assembly and budding in macrophages takes place in deep membrane invaginations that are connected to the extracellular space and can present virus at the VS, thus mediating efficient viral spread (Bennett et al., 2009; Deneka et al., 2007; Gousset et al., 2008). Cell-cell spread from macrophages is highly efficient and results in high multiplicity of infection of T cells *in vitro* (Duncan et al., 2013, 2014). Consistently, this mode of viral transmission was thus shown to be resistant to treatment with antiretroviral drugs (RT and integrase inhibitors) or neutralising antibodies. This may therefore have important implications for viral persistence and eradication *in vivo*. Furthermore, infected T cells can also transmit the virus to macrophages. Interestingly this was shown to occur via engulfment of infected T cells, which results in productive infection of macrophages (Baxter et al., 2014). Macrophages engulf both healthy and damaged or dying infected T cells, where the capture does not depend on Env-CD4 interaction and receptors mediating the capture remain unknown. Again, this mode of cell-cell spread is much more efficient compared to equivalent cell-free infection. Importantly, the significance of viral transmission between macrophages and T cells *in vivo* is unknown; however, given the long lifespan of macrophages and high efficiency of cell-cell spread, this might contribute to the establishment of the latent reservoir and viral persistence.

1.5.3 Dendritic cell-T cell synapse

Dendritic cells (DC) are poor targets of HIV-1 infection, presumably due to high activity of innate immune sensors and restriction factor SAMHD1 (Laguette et al., 2011; Sмed-Sörensen et al., 2005). DCs express multiple immunoreceptors that can capture HIV-1 virions including: DC-SIGN, DCIR, CD169 (Siglec-1) and syndecan-3 (de Witte et al., 2007; Geijtenbeek et al., 2000; Izquierdo-Useros et al., 2012; Lambert et al., 2008). Captured virus can be endocytosed or can be carried on the cell surface for up to several days (Geijtenbeek et al., 2000; Sandgren et al., 2013). The virus is often observed in deep membrane invaginations found on DCs (Felts et al., 2010; McDonald et al., 2003). Virus-laden DCs can interact with CD4+ T cells and infect them *in trans* (Cameron et al.,

1992; Geijtenbeek et al., 2000; Pope et al., 1994). This occurs through so-called infectious synapse, which is characterised by concentration of virions on the DC and polarisation of CD4 and CCR5/CXCR4 coreceptors on the T cell to the site of cell contact (Arrighi et al., 2004; McDonald et al., 2003; Turville et al., 2004). Viral transfer at the synapse occurs in the absence of antigen-dependent signalling and the mechanism of recruitment of viral particles and viral receptors to the synapse remains unknown. Since DCs normally patrol mucosal sites and capture pathogens for antigen presentation it has been proposed that DCs carry HIV-1 from the site of infection to the lymph nodes where they infect CD4+ T cells *in trans* (Manches et al., 2014). Whether this occurs *in vivo* in humans remains a matter of speculation. Interestingly, a similar mechanism of *trans* infection has been observed for murine leukaemia virus (MLV), which can be used as a model retrovirus and infects B cells in mice. During *in vivo* infection, macrophages were shown to capture MLV virions by CD169 and carried the virus to the lymph nodes where they infected B cells *in trans* (Sewald et al., 2015). Whether macrophages also mediate HIV-1 trans-infection in humans remains unknown.

1.5.4 Filopodia and nanotubes

Filopodia are long and narrow membrane extensions formed between two cells that allows for cell-cell communication and transport of ligands (Önfelt et al., 2004). Cell-cell spread mediated by filopodia was first observed in MLV model of retroviral infection (Sherer et al., 2007). Formation of filopodial bridges between infected and uninfected cell was dependent on Env-receptor interaction and resulted in transfer of virions across the outer (extracellular) surface of filopodia (Sherer et al., 2007); however precise mechanism of this transfer remains unknown. Additionally, filopodia have also been observed in HIV-1 infection, forming between DCs and T cells to mediating efficient viral transfer (Do et al., 2014; Felts et al., 2010; Nikolic et al., 2011). This suggest that HIV-1 might exploit natural ability of immune cells to transport ligands through filopodia. Moreover, HIV-1 was also shown to spread between T cells though membrane nanotubes. These membrane structures form when T cell interact and subsequently disengage, are 5-10 times longer than filopodia and contain a cell-cell junction (Sowinski et al., 2008). The formation of nanotubes was not dependent on Env-CD4 interaction and resulted in fast and efficient transfer of virus across the nanotube to infect the target cell. Nanotube-mediated cell-cell spread was also observed between infected and uninfected macrophages, which can form both nanotubes and filopodia (Eugenin et al., 2009). In infected T cell cultures *in vitro,* it was estimated that viral transfer mediated by

filopodia or nanotubes accounts for only about 10% of cell-cell spread (Rudnicka et al., 2009) but may provide a mechanism for longer range viral transfer. Overall, this shows that HIV-1 can exploit these forms of immune cell contact for efficient viral dissemination; however, the importance of this mode of viral spread *in vivo* also remains a matter of speculation.

1.6 T cell activation

T cell activation is mediated through the formation of a structure called the immunological synapse (IS) that allows signalling through the T cell receptor (TCR). The IS is formed between T cells and antigen presenting cells (APC), such as dendritic cells, macrophages or B cells and allows for communication between the immune cells, which is required for orchestration of the immune response.

1.6.1 The immunological synapse

The formation of the IS is highly specific and tightly regulated to prevent aberrant immune activation. IS formation is initiated by the TCR recognising a specific peptide bound to the MHC molecule (pMHC) presented by the APC (Dustin et al., 1997; Katz et al., 1973; Kupfer & Singer, 1989). There are two classes of MHC molecules: CD4+ T cells recognise MCH-II via the CD4 coreceptor and CD8+ T cells recognise MHC-I via the CD8 coreceptor (Gao et al., 1997; Kruisbeek et al., 1985; Swain et al., 1983). The IS formation results in formation of three distinct supramolecular activation complexes (SMAC) on the T cell (Monks et al., 1998). First, the central SMAC (cSMAC) contains the TCR and the costimulatory or inhibitory receptors. Second, the proximal SMAC (pSMAC) surrounds the cSMAC and contains adhesion molecules such as LFA-1 and ICAM-1 that stabilise the cell-cell contact at the IS. Third, the distal SMAC (dSMAC) surrounds the pSMAC and contains the actin ring and large membrane molecules CD43, CD44 and CD45. Organisation of these structures allows the triggering of TCR signalling, cytoskeleton remodelling and T cell activation (discussed further in the next Section). In naïve T cells, IS formation and TCR signalling results in activation of gene expression required for effector function, increased cellular metabolism and cell proliferation (Iezzi et al., 1998; Poo et al., 1988). Importantly, TCR signalling is also crucial for T cell development in the thymus (Molina et al., 1992) and for homeostatic proliferation of naïve T cells (Seddon et al., 2000). In activated CD4+ T cells, TCR signalling results in polarised secretion of effector cytokines (e.g. IL-2, IFN-γ, IL-4 or IL-17) into the synapse or in case of CD8+ T cells, secretion of lytic granules (granzyme, perforin) towards the target cell (Kupfer et al., 1994; Poo et al., 1988). This is mediated by the polarisation of MTOC to the synapse and concomitant recruitment of mitochondria, Golgi apparatus and secretory vesicles, which stabilises the IS and allows for polarised secretion of cytokines or lytic granules (Dustin et al., 1997; Kupfer et al., 1987; Quintana et al., 2007). In this regard, the IS and the VS share many similarities: both show clustering of receptors and adhesion molecules at the synapse, cytoskeleton remodelling,

polarisation of cellular organelles and polarised secretion or budding into the synapse. The main differences are the receptors (Env-CD4 vs TCR-pMHC), the target cell (T cell vs APC) and secreted material (virus vs cytokines).

In addition to the TCR-pMHC interaction, T cell activation is fine-tuned and regulated by signalling via costimulatory and inhibitory receptors. In fact, efficient T cell activation requires costimulatory signalling, which can be mediated via multiple receptors, such as CD28, ICOS, CD27, CD2, OX40 (Chen & Flies, 2013). The signalling depends on the immune context and the cognate ligands presented by the APC (CD80, CD86, ICOS-L, CD70, CD48, CD58, OX40-L, etc.) and results in differential T cell proliferation, differentiation, effector function and survival. T cells also express inhibitory receptors such as CTLA-4, PD1, TIM3 and LAG3 that negatively modulate T cell activation, which is important for terminating an immune response or establishing immune tolerance (Odorizzi & Wherry, 2012). The signalling is again dependent on the cognate ligands presented by the APC (CD80, CD86, PD-L1/L2, galectin 9, etc.) and can result in inhibition of proliferation and effector function, tolerance and exhaustion. The outcome of TCR signalling and cell activation is also regulated by the so-called third signal (TCR signalling and costimulation being the first and second signal), which is mediated via secreted cytokines (IL-12, IL-4, IL-6, etc) and determines the differentiation pathway and effector function, such as Th1 or Th2 response (Curtsinger & Mescher, 2010).

1.6.2 TCR signalling cascade

The TCR does not have any catalytic activity, therefore the TCR signalling is initiated by the activation of upstream kinases Lck and ZAP70. TCR complex consists of variable α and β chains that recognise the pMHC and the CD3 complex consisting of six subunits arranged in dimers: $\gamma\varepsilon$, $\delta\varepsilon$ and $\zeta\zeta$, where the ζ-chains are the main signal-transducing components (Figure 1.11) (Call et al., 2002; Irving & Weiss, 1991). Lck exists in equilibrium between active and inactive forms, which is regulated by phosphorylation (Nika et al., 2010; Schoenborn et al., 2011; Straus & Weiss, 1992). Active Lck is phosphorylated on the residue Y394, which is mediated by Lck (autophosphorylation) or Fyn kinase. Dephosphorylation can be mediated by multiple phosphatases, most importantly CD45, which results in inactive, primed Lck conformation. Lck can be further inhibited by inhibitory phosphorylation at the residue Y505 mediated by CSK kinase. Lck (active or inactive form) is associated with the coreceptors CD4 or CD8 (Veillette et al.,

1988). Binding of TCR to pMHC allows coreceptor binding to non-variable region on the MHC and thus brings Lck in close proximity to the TCR-CD3 complex (Bjorkman et al., 1987; Irving & Weiss, 1991). Lck phosphorylates the immunoreceptor tyrosine-based activation motifs (ITAMs) on CD3 subunits, which is required for propagation of TCR signalling (Figure 1.11) (van Oers et al., 1996). Despite decades of research, how TCR signalling is initiated is still a matter of debate. Based on the experimental observations, three major models of TCR signalling initiation have been proposed, which are not mutually exclusive (Courtney et al., 2018). First, the mechanosensor model states that TCR-pMHC binding results in conformational changes in the TCR complex that allow for phosphorylation of CD3 chains by Lck. Recently, this has been supported by several studies showing that high-affinity ligands induce reorganisation of CD3 chains that allows for more efficient ITAM phosphorylation by Lck (Lee et al., 2015; Liu et al., 2014). Second, the serial engagement model proposes that the signalling initiation requires activation of a threshold number of TCRs within a limited time period. This is achieved by serial engagement of pMHC with multiple TCRs and thus explains how very low density of pMCH molecules on APCs can trigger TCR signalling (Huang et al., 2013; Pielak et al., 2017; Valitutti et al., 1995). Third, the kinetic segregation model states that TCR signalling is initiated by the formation of the IS and spatial reorganisation of membrane molecules that results in formation of distinct SMAC structures (Davis & van der Merwe, 2006). Specifically, tight TCR-pMHC and LFA-1-ICAM-1 interactions (cSMAC and pSMAC) bring opposing plasma membranes in close proximity, which results in steric exclusion of large and rigid extracellular domains of membrane phosphatases such as CD45 (Chang et al., 2016; James & Vale, 2012; Johnson et al., 2000; Varma et al., 2006). Segregation of CD45 thus prevents inhibitory dephosphorylation of Lck, which can therefore accumulate in cSMAC in its active form, thus enabling phosphorylation of CD3 ITAMs. As these models are not mutually exclusive it is likely that several of the described mechanism cooperate to achieve the high sensitivity and specificity of TCR signalling that allows for discrimination between self and non-self.

TCR signalling is propagated by ZAP70, which binds the phosphorylated ITAMs on CD3ζ (van Oers et al., 1994). This results in active conformation of ZAP70 that is further stabilised by phosphorylation by Lck (Pelosi et al., 1999; van Oers et al., 1996).

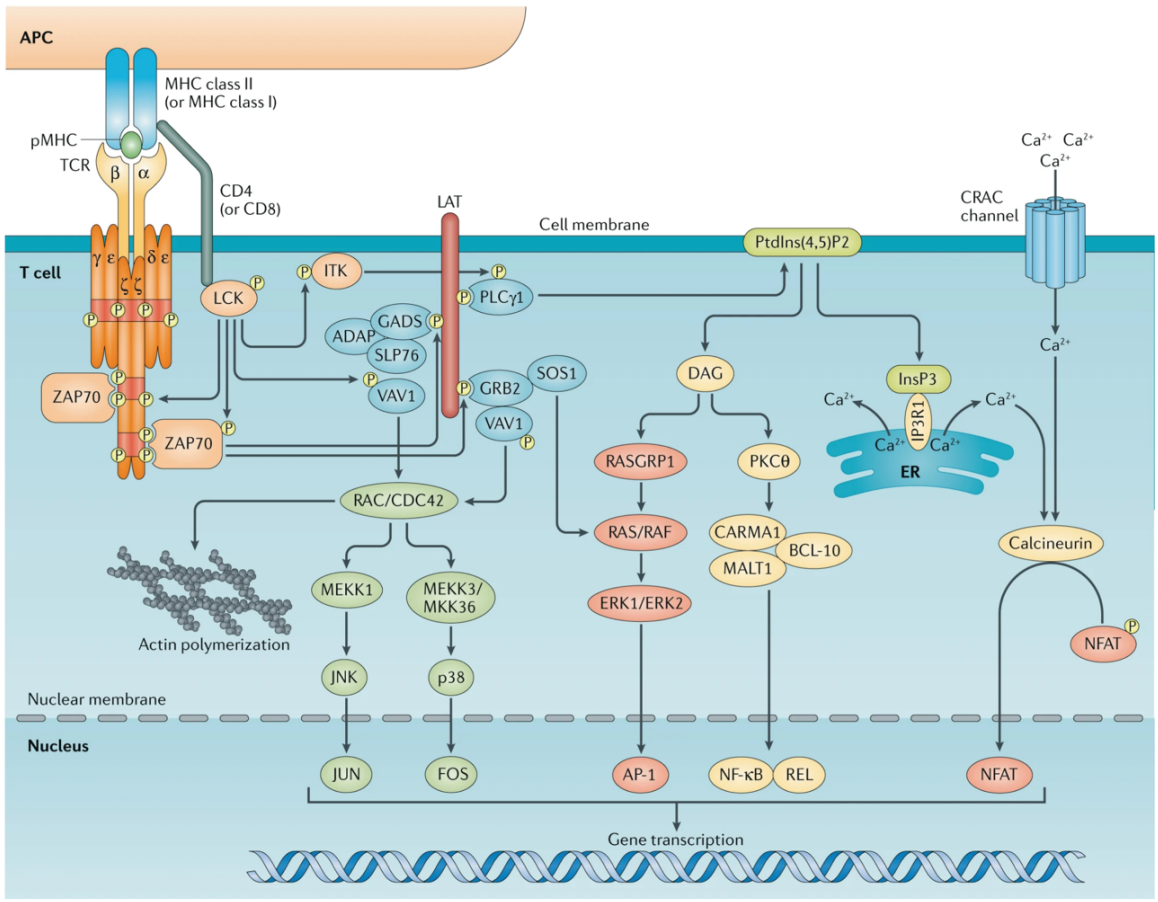

Figure 1.11: TCR signalling

T cell expresses TCR-CD3 complex (consisting of α, β, γ, δ, ε and ζ chains), which recognises its cognate peptide in complex with MHC (pMHC) that is presented by the APC. The pMHC is also recognised by the TCR coreceptors CD4 or CD8, which recruits Lck to the CD3 complex, resulting in phosphorylation of CD3 ITAMs. This recruits ZAP70, which is further activated by Lck phosphorylation. ZAP70 phosphorylates LAT, which can then act as a scaffold for SLP76, PLC1, GRB2, GADS, VAV1, ADAP and SOS1, thus forming the LAT signalosome. VAV1 activates RAC and CDC42 GTPases, which results in actin cytoskeleton remodelling and activation of MAP kinase pathways. This results in activation of JNK and p38 MAP kinases, which activate transcription factors JUN and FOS that form dimeric AP-1 complex. Lck also activates ITK, which activates PLCγ1 at the LAT signalosome. Active PLCγ1 cleaves phosphatidylinositol 4,5-bisphosphate, PtdIns(4,5)P2 into secondary messenger molecules inositol 1,4,5-trisphosphate (InsP3) and diacylglycerol (DAG). InsP3 binds to IP3R1 and releases calcium, Ca^{2+} from the ER into the cytoplasm. This opens CRAC channels at the PM, which further increases cytosolic Ca^{2+} and activates calcineurin, which results in activation and nuclear translocation of transcription factor NFAT. DAG activates PKCθ, which activates the CBM complex (CARMA1, BCL-10 and MALT1) leading to activation and nuclear translocation of transcription factor NF-κB. DAG also activates RASGRP1. This activates Ras, which is additionally activated by SOS1, and results in sustained activation of Ras pathway. This leads to activation of ERK and transcription factor FOS, part of AP-1 complex. Activation of transcription factors AP-1, NF-κB and NFAT results in transcription of multiple genes. Taken from (Gaud et al., 2018).

Activated ZAP70 is then able to phosphorylate the transmembrane adaptor molecule LAT, which serves as a scaffold for other adaptor and effector molecules and thus results in the formation of the LAT signalosome (Horejsi et al., 2004). LAT phosphorylation generates binding sites for phospholipase PLCγ1 and adaptor molecules GRB2 and GADS, which in turn recruit SLP76, SOS1, VAV1 and ADAP (Figure 1.11). Microscopy studies revealed that LAT forms microclusters which are important for efficient TCR signalling and contribute to signal amplification and diversification (Balagopalan et al., 2015). VAV1 activates RAC and CDC42 GTPases, which triggers cytoskeleton rearrangements via activation of WASP and PAK, resulting in actin ring formation in the dSMAC (Barda-Saad et al., 2010). ADAP activates SKAP55 and RAP1 which induces active conformation of LFA-1 and thus increases ICAM binding, which stabilises the cell-cell contact at the synapse (Hogg et al., 2011). In turn, LFA-1 binding to ICAM induces intracellular signalling via ZAP70, which together with activity of VAV1 and PKCθ (discussed bellow) induces polarisation of MTOC to the synapse (Sims et al., 2007; Soede et al., 1998).

Downstream TCR signalling also activates three major transcription factors: NFAT, NF-κB and the activator protein 1 (AP-1), which is a dimer of JUN and FOS family transcription factors. The MAP kinase pathway is activated by RAC/CDC42 via MEKK1 and 3, which results in downstream activation of JNK and p38 kinases, which in turn activate transcription factors JUN and FOS, respectively (Inder et al., 2008). ITK kinase is activated by Lck and interacts with membrane phospholipid phosphatidylinositol 3,4,5-trisphosphate (PIP_3) and SLP76 to associate with the signalosome (Andreotti et al., 2010). There, ITK fully activates PLCγ1 (associated with LAT) which is then able to cleave phosphatidylinositol 4,5-bisphosphate (PIP_2) into two secondary messenger molecules: inositol 1,4,5-trisphosphate (IP_3) and diacylglycerol (DAG) (Berridge & Irvine, 1984; Gonen et al., 2005). IP_3 dissociates into the cytoplasm and binds to its receptor, IP3R in the ER, which releases Ca^{2+} into the cytoplasm (Lockyer et al., 2001). The increase in cytoplasmic calcium opens CRAC Ca^{2+} channels at the PM, resulting in influx of extracellular Ca^{2+}, thus further increasing intracellular Ca^{2+} concentration (Lioudyno et al., 2008). Calmodulin binds Ca^{2+} and activates calcineurin phosphatase, which results in dephosphorylation and nuclear translocation of NFAT transcription factor (Aramburu et al., 1999; Shaw et al., 2010). The second branch of PLCγ1 response is mediated via DAG, which stays associated with the membrane. DAG activates PKCθ kinase, which activates the CBM complex (CARMA1, BCL-10 and MALT1) lading to activation of TAK1

and degradation of IκB, which allows for NF-κB transcription factor activation and nuclear translocation (Coudronniere et al., 2000). DAG also activates RasGRP, resulting in activation of Ras GTPase (Bivona et al., 2003). The Ras pathway is additionally activated by SOS1 (recruited to LAT via GRB2) which directly activates Ras (Das et al., 2009), leading to activation of Raf and MEK, which in turn phosphorylate and activate ERK kinase. ERK is a master regulator of cell growth, survival and proliferation and thus phosphorylates many cellular targets including several transcription factors, such as FOS (Wang & Prywes, 2000). Overall, TCR signalling activation of transcription factors NFAT, NF-kB and AP-1 leads to transcription of numerous genes required for T cell effector function and proliferation.

Another major branch of TCR signalling is the phosphoinositide 3-kinase (PI3K) pathway. PI3K is activated by Lck and Ras and importantly by signalling via costimulatory molecules such as CD28 or ICOS (Ward et al., 1993). These receptors are activated by their ligands CD80/CD86 and ICOS-L, respectively, presented on the APC (Greenwald et al., 2005). PI3K phosphorylates PIP_2 phospholipid to obtain PIP_3, which activates PH domain containing proteins (Vanhaesebroeck et al., 1997). As described earlier, PIP3 contributes to activation of ITK, which activates PLCγ1. Additionally, PIP_3 stimulates PDK1, which together with DAG activates PKCθ (Coudronniere et al., 2000; Mora et al., 2004). PDK1 also stimulates AKT kinase, also known as PKB (which also binds PIP_3) by phosphorylation on residue T308 (Stokoe et al., 1997). Full AKT activity requires additional phosphorylation on residue S473, which is mediated by mTORC2 complex. Like ERK, AKT has many cellular targets and regulates glucose, amino acid and lipid metabolism in addition to cell growth, survival and proliferation (Ramsay & Cantrell, 2015; Sinclair et al., 2013). Notably, many of these AKT activities are mediated by activation of mTORC1 complex, which controls cellular metabolism and protein expression (Finlay et al., 2012; Hukelmann et al., 2016; Navé et al., 1999). Protein synthesis is regulated by phosphorylation and activation of ribosomal S6 subunit and transcription initiation factors (eIF4B, eIF4G, eIF4E) (Chapman & Chi, 2015; Mora et al., 2004). Furthermore, there is a crosstalk between ERK and AKT pathways as ERK has been shown to also activate mTORC1 and directly phosphorylate S6 subunit (Pende et al., 2004; Roux et al., 2007). As mentioned above, PI3K signalling is in part mediated by costimulatory signalling, which ensures optimal T cell activation and effector function (Costello et al., 2002). Importantly, this activity can be opposed by inhibitory receptors such as PD-1 and CTLA-4, which are activated by their ligands PD-L1/L2 and CD80/CD86, respectively, presented on the APC (Butte et al., 2007; Park et al., 2010).

Activation of these receptors results in activation of phosphatases SHP1, SHP2 and PP2A, which inhibit PI3K and AKT kinases, but also PLCγ1 and PKCθ, thus resulting in inhibition of T cell activation (Rudd et al., 2009; Yokosuka et al., 2012). This can mediate termination of an immune response or induce anergy and tolerance.

TCR signalling results in broad spectrum T cell activation and is characterised by upregulation of many cell surface receptors. CD69 is upregulated very early (6-12 h) post-stimulation and regulates tissue retention of T cells (Caruso et al., 1997; Kumar et al., 2017). CD69 inhibits sphingosine 1-phosphate receptor (S1PR), which mediates lymphocyte tissue egress (Matloubian et al., 2004). Inhibitory receptors PD1 and CTLA-4 are also upregulated upon activation and regulate the immune response (Chikuma et al., 2009; Rudd et al., 2009). Depending on the differentiation stage, T cell activation results in production of IL-2, a homeostatic cytokine involved in cell survival and proliferation (Robb et al., 1981). CD25 and CD38 are upregulated later, 2-3 days post stimulation (Caruso et al., 1997; Motamedi et al., 2016). CD25 is IL-2 receptor (IL-2R) α-chain, which forms a complex with IL-2R$\beta\gamma$, resulting in formation of high-affinity IL-2 receptor and thus increased cell survival and proliferation (Chastagner et al., 1996). CD38 is a cyclic ADP ribose hydrolase and is involved in calcium signalling, signal transduction and cell adhesion (Chini et al., 2002). Cell activation also results in increased cell metabolism, which requires import of nutrients. This is characterised by upregulation of various metabolite transporters, such as Glut1 (glucose), CD71 (transferrin) and CD98 (neutral amino acids), which support increased metabolic capacity of activated cells (Caruso et al., 1997; Loisel-Meyer et al., 2012; Motamedi et al., 2016; Nii et al., 2001; Sinclair et al., 2013).

1.6.3 Homotypic T cell-T cell contacts

In addition to the classical interaction between the T cell and the APC at the IS, homotypic T cell interactions were also reported to have a function in normal immune system (Brod et al., 1990). Activated CD4+T cells were shown to form stable homotypic contacts that were more transient compared to the classical IS, but also resulted in recruitment of MTOC to the contact zone and polarised secretion of IL-2 (Ramming et al., 2009; Sabatos et al., 2008). This interaction was dependent on LFA-1 engagement and resulted in increased T cell proliferation and survival; however, whether TCR signalling was triggered was not directly investigated. Similarly, homotypic CD8+T cell

contacts between activated cells were shown to result in polarised secretion of IFNγ and increased cell proliferation and effector function (Gérard et al., 2013). Taken together, these studies show that T cells have a capacity to engage in homotypic contacts, triggering a response reminiscent of that at the classical IS and thus contribute in the propagation of the immune response.

1.6.4 Signalling at the virological synapse

The IS and the VS share many similarities, such as polarisation of receptors, adhesion molecules and cellular organelles (Piguet & Sattentau, 2004), which is shown in Figure 1.12. The observations of active T cell remodelling at the VS and polarisation of cytoskeleton, organelles and virus assembly provided the initial indirect evidence for signalling at the VS (Chen et al., 2007; Jolly et al., 2004, 2007a, 2011; Rudnicka et al., 2009). Mitochondrial polarisation and associated calcium flux in the donor cell at the VS gave the first direct evidence for activation of signalling at the VS (Groppelli et al., 2015). Together with data showing LFA-1-induced MTOC polarisation in infected cells (Starling & Jolly, 2016) led to a study to perform global, unbiased analysis of signalling via mass spectrometry based phoshoproteomics to map signalling at the VS over time in both infected and uninfected cells (Len et al., 2017). This approach identified 134 proteins with phosphorylation changes in the donor cell and 124 differentially phosphorylated proteins in the target cell, of which 58 proteins overlapped between both cells. Notably, it was also shown that VS formation triggers TCR signalling in both donor and target cell, which occurs in the absence of TCR-pMHC interaction and supports efficient viral spread (Len et al., 2017). This was further validated by immunoblotting and using knock-out cell lines deficient in TCR, Lck or ZAP70 expression. In addition to TCR signalling, donor cells also showed activation of pathways associated with CD28, ICOS and actin cytoskeleton signalling. Similarly, target cells also showed activation of CD28, RAC/CDC42 and actin cytoskeleton signalling. Importantly, it was shown that CD3 clusters at the VS and TCR signalling was dependent on CD3 expression; however, the mechanism of TCR signalling activation remains unclear. Since donor and target cells are held closely together by Env-CD4 and LFA-1-ICAM interactions, this may allow triggering of antigen-independent signalling, consistent with the kinetic segregation model of TCR signalling. Importantly, whether segregation of CD45 occurs at the VS remains to be investigated.

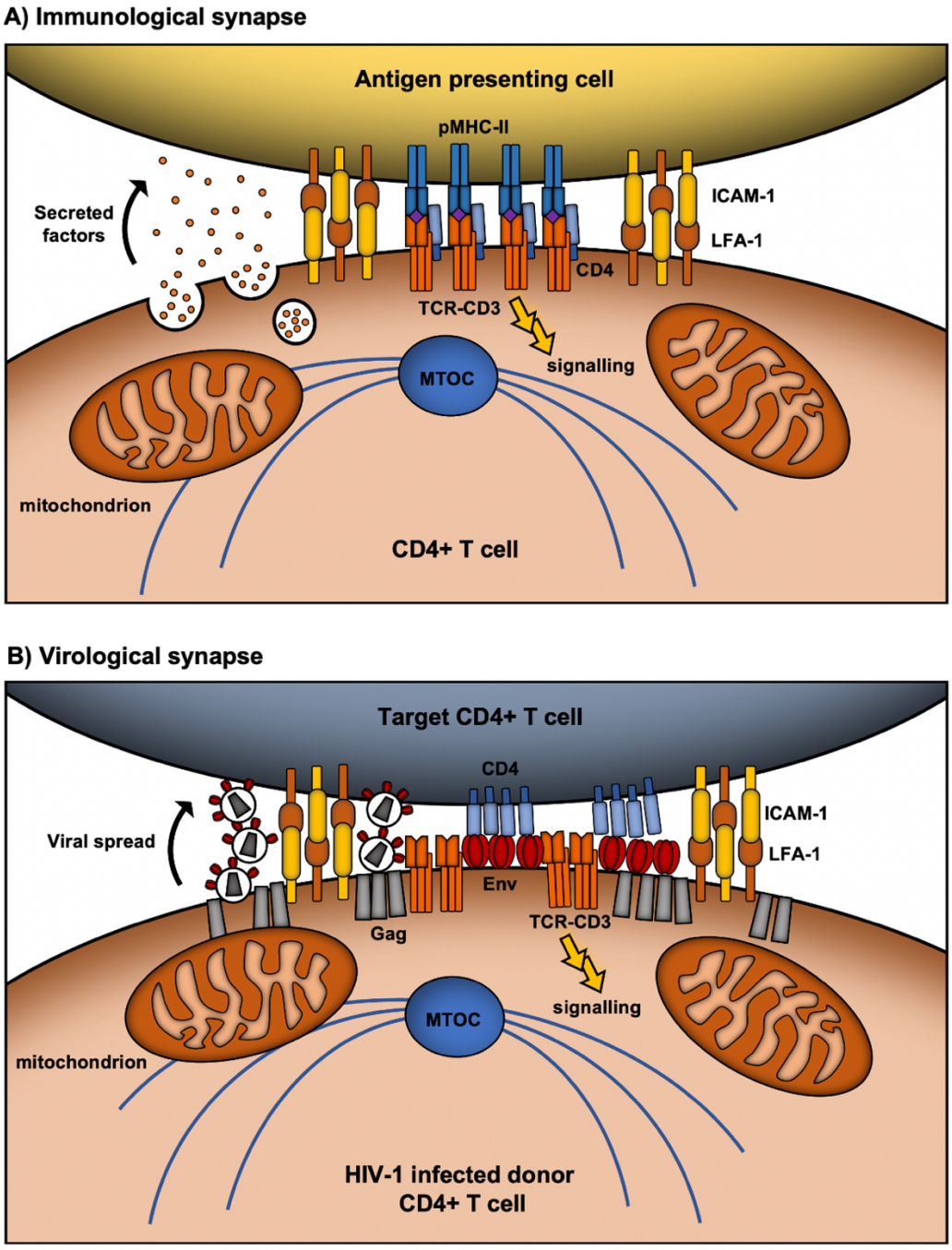

Figure 1.12: Comparison of the immunological and virological synapse

(A) The immunological synapse (IS) formed between a CD4+ T cell and antigen presenting cell (APC). TCR-CD3 complex and CD4 on the T cell bind to pMHC-II complex (antigen) on the APC, which forms the cSMAC. Costimulatory receptors and ligands are also clustered in the cSMAC (not shown). The IS is further stabilised by LFA-1 and ICAM-1 interactions (pSMAC). The exclusion of large membrane phosphatases, such as CD45 in the dSMAC is not shown. The formation of the IS triggers TCR signalling and polarisation of organelles such as MTOC and mitochondria, which results in polarised secretion of cytokines and other secreted factors. **(B)** The virological synapse (VS) as shown in Figure 1.10. Here, the contact between the donor and target cell is mediated by Env-CD4 interactions and further stabilised by LFA-1 and ICAM-1 interactions. The VS formation triggers antigen-independent TCR signalling and polarisation of viral proteins (Env and Gag) and organelles, such as MTOC and mitochondria, which results in polarised virus assembly and budding into the synapse to infect the target cell.

Moreover, as mentioned above, engagement of LFA-1 was shown to be sufficient to trigger MTOC polarisation at the VS (Starling & Jolly, 2016). This was depended on activation of Lck and ZAP70 kinases, which again shows involvement of cell signalling at the VS that is similar to the IS. Furthermore, experiments using gp120 and ICAM-1 supported lipid bilayers, thus mimicking infected donor cell, showed activation of TCR signalling in the target cell (Deng et al., 2016; Vasiliver-Shamis et al., 2009). Notably, this reductionist model of the VS showed activation of multiple TCR signalling components, such as Lck, ZAP70, PLCγ1 and AKT, but without calcium signalling that is associated with complete TCR activation. This is again consistent with the kinetic segregation model and antigen-independent signalling at the VS; however, it suggests that VS formation does not activate TCR signalling as potently compared to the IS, possibly due to the lack of TCR-pMHC interaction and signalling through costimulatory receptors. Taken together, these observations suggest that formation of VS triggers TCR signalling, similar as the IS; however, the precise mechanism remains to be uncovered.

1.7 Aim of the project

The focus of this Thesis is to investigate to role of CD3 downmodulation in HIV-1 cell-cell spread. As discussed in Section 1.4.4, Nef of HIV-2 and most SIV lineages, but not HIV-1, downmodulates CD3, which impairs signalling at the immunological synapse and may interfere with antiviral responses and prevent aberrant immune activation. Why HIV-1 does not employ this potential immune evasion strategy remains incompletely understood. Interestingly, it was shown that formation of HIV-1 VS triggers TCR signalling to drive efficient viral spread. Given the present evidence, I hypothesised that loss of Nef-mediated CD3 downmodulation in HIV-1 lineage contributes to the TCR signalling at the VS and thus enable more efficient viral spread. The role of CD3 downmodulation in cell-cell spread was investigated using different SIVsmm, SIVmac and HIV-2 *nef* alleles that differ in their ability to downmodulate CD3. Specifically, the effect of CD3 downmodulation on viral replication, T cell activation and cell death was examined. Chapter 3 describes the results obtained with SIVsmm *nef* alleles and Chapter 4 describes results obtained with SIVmac and HIV-2 *nef* alleles.

2 Materials and methods

2.1 Proviral constructs

Replication competent HIV-1 NL4.3 IRES-GFP proviral constructs carrying a panel of *nef* alleles were gift from Frank Kirchhoff (Ulm University, Germany). These constructs containing different *nef* alleles followed by an internal ribosome entry site (IRES) and the enhanced green fluorescent protein (GFP) reporter gene (Figure 3.1) were generated by splice-overlap extension PCR as described previously (Schindler et al., 2006). It was previously confirmed that these constructs express Nef proteins in human CD4+ T cells at similar levels and proportional to GFP expression (Khalid et al., 2012; Schindler et al., 2006; Schmökel et al., 2013). The proviral constructs were cloned into pBR bacterial expression vector containing ampicillin resistance gene. The integrity of all *nef* alleles was confirmed by sequence analysis (described below). *Nef* alleles used in this study are listed in Table 2.1. *Nef*-defective control construct carries NL4.3 *nef* gene with mutated start codon and premature codons introduced at positions 4, 5, 73 and 74 of NL4.3 *nef* ORF.

Table 2.1: Different *nef* alleles used in this thesis

Lentiviral lineage	*nef* allele	AA residues (CD3 downmod.)	Abbreviation	GenBank accession #
HIV-1	NL4-3 *nef*-defective	n/a	*nef*-defective	n/a
	NL4.3	n/a	NL4.3	M19921
	NA7	n/a	NA7	DQ242535
	SF2	n/a	SF2	K02007
SIVsmm	FBr 75wL4 (WT)	I123 L146	L4 IL	KF478046.1
	FBr 75wL4	L123 F146	L4 LF	n/a
	FBr 304wK2	I123 L146	K2 IL	n/a
	FBr 304wK2 (WT)	L123 F146	K2 LF	KF478022.1
SIVmac	239 (WT)	I123 L146 D158	ILD	M33262
	239	L123 F146 N158	LFN	n/a
HIV-2	RH2-1 D8 (WT)	I132	D8 I	JQ746633.1
	RH2-1 D8	T132	D8 T	n/a
	RH2-1 A8	I132	A8 I	n/a
	RH2-1 A8 (WT)	T132	A8 T	JQ746634.1

2.2 Cell culture

HEK 293T/17 cells (abbreviated hereon as 293T cells) (Pear et al., 1993) were obtained from American Type Culture Collection (ATCC). HeLa TZM-bl cells (expressing luciferase and beta-galactosidase under the control of HIV-1 LTR) (Wei et al., 2002) were obtained from Centre for AIDS Reagents (CFAR). 293T and HeLa TZM-bl cells were grown in Dulbecco's modified Eagle's medium (DMEM; Gibco) supplemented with 10% fetal calf serum (FCS; Labtech) and 100 U/ml Penicillin-Streptomycin (Gibco) to obtain complete DMEM medium. Cells were passaged every 3-4 days (until reaching confluency) using trypsin (Gibco) to detach the cells and diluted (1:10) in fresh culture medium.

Jurkat CE6.1 T cells (Schneider et al., 1977) were obtained from ATCC and grown in Roswell Park Memorial Institute 1640 (RPMI) medium (Gibco) supplemented with 10% FCS (Labtech) and 100 U/ml Penicillin-Streptomycin (Gibco) to obtain complete RPMI medium. Cells were passaged once a week when cells had reached 1-2x10^6 cells/ml by diluting in fresh medium (diluted to a density of 1x10^5 cells/ml).

Primary CD4+ T cells were isolated (described below) from buffy coats from anonymous, healthy donors, provided by the NHS Blood and Transplant Service. Cells were maintained in complete RPMI medium supplemented with 10 IU/ml IL-2 (National Institute of Biological Standards and Controls; NIBSC).

All cell cultures were maintained in humidified incubator at 37°C with 5% CO_2. Unless otherwise stated, cells were centrifuged at 500 x g for 5 min at RT.

2.2.1 Primary CD4+ T cell isolation and activation

Peripheral blood mononuclear cells (PBMC) were isolated from buffy coats by density gradient centrifugation. The blood (25 ml) was layered over 15 ml of Ficoll Paque Plus (GE Healthcare) and centrifuged at 1,000 x g for 20 min at room temperature (RT) with no brake. The layer of PBMCs was removed with Pasteur pipette and isolated cells were washed twice in Dulbecco's phosphate buffered saline (PBS; Gibco) by centrifugation at 500 x g for 5 min. Red blood cells (RBC) were lysed in 10 ml RBC Lysis Buffer (Biolegend) for 15 in at RT and washed twice in PBS. After washing, cells were resuspended in freezing medium (10% dimethyl sulfoxide [DMSO; Sigma] in FCS) and transferred to cryovials (5x10^7 cell/vial) and frozen in isopropanol bath container at -80°C until transferring to liquid nitrogen store for long-term storage.

After thawing, PBMCs were resuspended and washed twice in warm RPMI medium. Cells were treated with DNAse1 (200 KU/5x10^7 cells; Sigma) for 20-30 min at 37°C to disrupt cell aggregates that formed during freezing and thawing process. After DNAse treatment cells were washed twice in PBS and filtered through 70 μm MACS SmartStrainer (Miltenyi Biotec) filter. CD4+ T cells were isolated by negative selection using MojoSort Human CD4+ T Cell Isolation kit (Biolegend) according to manufacturer's instructions and using LS separation columns (Miltenyi Biotec). The purity of CD+ T cells isolations was routinely checked by flow cytometry (described below) to detect CD3+CD4+ cells, which showed 92-96% purity in most preparations.

Unless otherwise stated, primary CD4+ T cells were activated for 4-5 days by CD3/CD28 stimulation. Nunclon T25 flasks (Thermo Fisher Scientific) were coated with 5 μg anti-CD3 antibody (clone OKT3, Biolegend) in 5 ml PBS for 2 h at 37°C (flask in horizontal position) and washed with RPMI medium. Isolated CD4+ T cells were transferred to coated flask (10-15x10^6 cells/flask) in 10 ml complete RPMI medium supplemented with IL-2 (10 IU/ml) in the presence of 2 μg/ml soluble anti-CD28 antibody (clone CD28.2, Biolegend). After 3 days of activation, cells were centrifuged to remove half of the activation culture medium and resuspended in fresh medium (with IL-2) at density of 1x10^6 cells/ml and incubated for another 1-2 days (flask in vertical position). Isolated CD4+ T cells that were not activated (resting) were cultured in complete RPMI medium, supplemented with IL-2 (10 IU/ml), at density of 2x10^6 cells/ml.

2.3 Virus stock preparation

2.3.1 Plasmid preparation

Proviral plasmids were produced in *E. coli* JM109 competent cells (>10^8cfu/μg, Promega). JM109 cells (20 μl) were incubated with 100-200 ng of plasmid DNA on ice for 30 min. The bacteria were transformed by heat-shock at 42°C for 45 s and then incubated on ice for 5 min. Bacteria were then plated on Luria Bertani (LB) agar plates containing 100 μg/ml ampicillin and incubated overnight (16 h). The next day, 3 ml starter culture of LB broth (containing 100 μg/ml ampicillin) was inoculated with a single colony from the overnight plate and incubated at 30°C with shaking for 8 h. The starter culture was transferred (1:1000 dilution) into 200 ml LB (with ampicillin) and incubated at 30°C with shaking overnight (16 h). Cultures were then centrifuged at 6000 x g for 20min at 4°C to pellet the bacteria.

Plasmid DNA was extracted using Qiagen Plasmid Maxiprep kit according to manufacturer's instructions. Purified plasmid DNA was resuspended in 300 μl nuclease-free water. DNA concentration was measured using the NanoDrop 2000 Spectrophotometer (Thermo Fisher) according to the manufacturer's instructions.

The integrity of *nef* genes in the proviral constructs was confirmed by sequencing. Plasmid samples and primers were sent for sequencing to Source Bioscience (Cambridge, UK) and prepared according to company's instructions. Primers flanking the *nef* gene corresponded to 3'-end of *env* gene (forward primer) and 5'-end of *gfp* reporter gene (reverse primer). Primer sequence:

Forward: 5'-GTAGCTGAGGGGACAGATAGG-3'
Reverse: 5'-GATATAGACAAACGCACACCGG-3'

Sequence identity was confirmed by aligning sample sequences with Nef sequences from NCBI GenBank database (accession numbers listed in Table 2.1) using Clustal Omega online alignment tool.

2.3.2 Virus production and purification

293T cells ($1x10^7$ per T175 flask) were grown in 16 ml culture medium and transfected with 9 μg provial DNA using 30 μl Fugene 6 (Promega) and 500 μl Opti-MEM medium (Gibco). Virus containing supernatants were collected 48h and 72h post-transfection and filtered through 0.45 μm filter. Viral supernatants were purified by ultracentrifugation using Sorvall Discovery (Hitachi) at 23,000 rpm for 2 h at 4°C through a sucrose cushion (20% (w/v) sucrose in PBS). Virus pellets were resuspended in complete RPMI medium (concentrated 4-fold) and stored in liquid nitrogen.

2.3.3 Virus titration

Virus stock infectivity was quantified using HeLa TZM-bl reporter cell assay to obtain $TCID_{50}$ values as described previously (Wei et al., 2002). Briefly, TZM-bl cells were plated in Nunclon-White 96-well plate ($1x10^4$/well) overnight and infected with 4-fold serial dilution (100 μl/well) of viral stocks in triplicates. 48 h post-infection culture supernatants were removed and cells were lysed in 50 μl Luciferase lysis buffer (Promega). Luciferase Bright-Glo substrate (50ul, Promega) was added to measure luciferase activity in relative light units (RLU) using PheraStar (MBG Labtech) luminometer. $TCID_{50}$/ml values were determined as virus stock fold-dilution to give RLU

reading of 2.5-fold above the background (uninfected control) using Excel (Microsoft) macro (available at http://www.hiv.lanl.gov/content/nab-reference-strains/TCID501.xls).

2.4 Virus infection

Jurkat or primary CD4+ T cells were infected with Nef chimeric viruses by spinoculation. Cells were seeded in 96-well U bottom plate at density $2.5x10^5$ cells/well and centrifuged to remove culture medium. Cells were mixed with purified virus stock to yield the multiplicity of infection MOI=0.1, as calculated from $TCID_{50}$/ml values (described above). Cells were centrifuged at 1,200 x *g* for 2h at RT and washed after the spinoculation. Cells were resuspended in complete culture medium and incubated for 48 h (unless otherwise stated) until further manipulation and analysis.

2.5 Flow cytometry

Cells were first washed in PBS and then stained with surface antibodies in 50 μl PBS, for 30min at 4°C. Cell viability dye Zombie UV (1:500 dilution; Biolegend) was included in all stains to detect dead cells. Antibodies used in this thesis (and their dilution factors) are listed in Table 2.2. For detection of Env, cells were washed after primary Ab stain and incubated with the secondary fluorophore-conjugated Ab (50 μl PBS, 30min at 4°C). Next, cells were washed in FACS wash buffer (FWB; 1% FCS and 0.1% sodium azide in PBS) and fixed in 100 μl of 4% methanol-free formaldehyde (Thermo Fisher) for 30min at 4°C. Cells were then washed and resuspended in FWB and analysed by flow cytometry.

Alternatively, for detection of intracellular antigens cells were permeabilised with 200 μl Permeabilization Wash Buffer (Biolegend) for 20 min at RT. Cells were then stained with antibodies in 50 μl of the permeabilization buffer for 30min at 4°C, washed twice in permeabilization buffer and resuspended in FWB before flow cytometry.

For detection of apoptosis, cells were washed in Annexin V binding buffer (eBioscience) and stained with Annexin V-PE/Cy7 (1:100; eBioscience) in 50 μl Annexin V binding buffer for 30 min at 4°C. Cells were then washed and fixed in 4% formaldehyde (made in Annexin V binding buffer) for 30 min at 4°C, washed and analysed by flow cytometry.

Flow cytometry analysis was done using LSR Fortessa X-20 cytometer (Becton Dickinson, BD). Compensation was performed using CompBeads (BD) according to manufacturer's instructions. For GFP and Zombie UV markers cells were used instead of beads. Compensation was calculated by FACSDiva software (BD). Data was analysed using FlowJo V10 software (BD). Gating strategy to identify infected cells is described in Figure 3.2 and Figure 3.5.

Table 2.2: Antibodies used for flow cytometry

Target	Antibody clone	Fluorophore	Supplier	Dilution	Stain
CD4	SK3	BV605	Biolegend	1:100	Surface, (1° Ab) 50 μl PBS
CD3	UCHT1	BV711	Biolegend	1:100	
CD28	CD28.2	APC/R700	BD	1:50	
CXCR4	12G5	APC	Biolegend	1:150	
CD25	M-A251	PE/Dazzle 594	Biolegend	1:200	
CD69	FN50	APC/Fire 780	Biolegend	1:100	
CD38	HIT2	PerCP/Cy5.5	Biolegend	1:150	
PD-1	EH12.2H7	PE/Cy7	Biolegend	1:100	
CD95	DX2	PE/Dazzle 594	Biolegend	1:150	
CD98	REA387	PE/Vio770	Miltenyi Biotec	1:150	
Env	PGT151	unconjugated	*in house*[1]	1:200	
Env	PG9	unconjugated	*in house*[1]	1:200	
Flag-tag	L5	PE/Cy7	Biolegend	1:150	
Human IgG	Polyclonal	Cy5	Bethyl	1:200	Surface, (2° Ab) 50 μl PBS
Human IgG	Polyclonal	PE	Jackson Immuno	1:100	
Gag p24	KC57-RD1	PE	Beckman Coulter	1:200	Intracellular, 50 μl Perm. buffer
Env	50-69	unconjugated	CFAR[2]	1:100	
Glut1	EPR3915	Alexa Fluor 647	Abcam	1:600	
CD247	6B10.2	PE	Biolegend	1:150	
Phospho-S6	N7-548	PE	BD	1:20	
HA-tag	16B12	PE	Biolegend	1:200	

[1] Gift from Laura McCoy (UCL), stock concentration 1 mg/ml.

[2] Donated by Dr S. Zoller-Pazner and Dr M. Gorny.

2.6 Cell-cell spread assay

For short-term (24h) cell-cell spread assay, T cells were infected for 48h (donor cells) and analysed for GFP expression by flow cytometry to quantify the number of GFP+ cells using Precision Count Beads (Biolegend) according to manufacturer's instructions. The day before, uninfected T cells (target cells) were labelled with 2.5 μM Cell Proliferation Dye eFluor 450 (Thermo Fisher Scientific) according to manufacturer's instructions. Labelled target cells were cultured overnight and counted by flow cytometry (together with donor cells) using the counting beads. Before the co-culture, the input of donor and target cells was normalised to account for variability between different PBMC donors and viruses in initial infection rates. To do so, GFP+ donor cells and labelled target cells were mixed in 1:4 ratio to achieve approx. 10% GFP+ cells in the donor-target cell co-culture. This was confirmed by flow cytometry analysis at 0h post-mix. Co-cultures were then incubated for 24h and analysed by flow cytometry.

For long-term spreading infection assays, donor cells were analysed for GFP expression by flow cytometry at 24h post-infection (p.i.) to count the number of GFP+ cells as described above. To account for different initial infection levels between PBMC donors and viruses, number of GFP+ cells in all cell cultures was adjusted to 2% with autologous uninfected CD4+ T cells. Cells were incubated up to 7 days p.i. and analysed by flow cytometry at various time points.

2.7 Virus release and infectivity

Jurkat or primary CD4+ T cells were infected for 48 h. Number of infected (GFP+) cells in the culture was quantified by flow cytometry using counting beads (as described above). Culture supernatant was collected and centrifuged at 800 x g for 5 min to remove all cell debris. Virus release was quantified as supernatant reverse transcriptase (RT) activity measured by a qPCR-based SYBR Green I-based product-enhanced reverse transcriptase (SG-PERT) assay (Pizzato et al., 2009), as described below. RT activity was normalized to the number of GFP+ cells to account for differences in infection levels. This was used as a measure of virus release/budding in the supernatant. Infectivity of viral supernatants was measured using luciferase assay on HeLa TZM-bl reporter cell line to obtain RLU values (described below). RLU values were normalised to RT activity (to account for differences in budding) to give a measure of virion (particle) infectivity. Alternatively, to account for differences in infection, RLU values were normalised to number of GFP+ cells to give a measure of total supernatant infectivity.

2.7.1 SG-PERT assay

SG-PERT assay was used to measure supernatant RT content as a surrogate for number of viral particles as described previously (Pizzato et al., 2009). Briefly, 5 μl of virus supernatant was lysed using 5 μl lysis buffer and Riblock RNAase Inhibitor (0.4 U/μl; Thermo Fisher Scientific). Virus lysate was diluted 1:20 using nuclease-free water. Quantitect SYBR Green PCR Master Mix (Qiagen) was used together with MS2 forward and reverse primers (Sigma) and MS2 RNA template (Roche) to set up the reactions as described in Table 2.1. Recombinant HIV-1 RT enzyme (Sigma) was used to make 10-fold serial dilution standards from 10^8 to 10^2 pU/μl RT activity. 7500 Real-Time PCR System (Applied Biosystems) was used to run the quantitative polymerase chain reaction (qPCR) reaction. Reaction parameters are described in Table 2.4.

Table 2.3: SG-PERT reaction set-up

Component		Stock concentration	Volume per reaction (μl)
Master mix	Quantitect SYBR Green Master Mix	n/a	12.5
	Forward MS2 primer	100 μM	0.125
	Reverse MS2 primer	100 μM	0.125
	MS2 RNA	0.7 μM	0.125
	Riblock RNAse inhibitor	4 U/μl	0.125
Sample (virus lysate or RT standard)		n/a	12
		Total volume	25

Table 2.4: SG-PERT PCR cycling parameters

Step	Temperature (°C)	Time	Number of cycles
RT	42	20 min	1
Initial heat-activation	95	15 min	
Denaturation	95	10 s	40
Annealing	60	30 s	
Extension	72	15 s	

2.7.2 Infectivity assay

Viral supernatant infectivity was determined by luciferase assay using HeLa TZM-bl reporter cell line, as described for virus stock titration (Section 2.3.3). Briefly, viral supernatants were diluted in a 2-fold serial dilution (1:4, 1:8, 1:16) and used to infect TZM-bl cells in triplicates (100 μl/well). Luciferase activity was measured 48 h p.i. using Bright-Glo substrate (Promega). RLU values were normalised (by dilution factors) and averaged to obtain average RLU/μl values for viral supernatants.

2.8 Immunofluorescence microscopy

For virological synapse (VS) quantification, primary CD4+ T cells were infected for 48 h. Uninfected CD4+ T cells (target cells) were labelled with 10 μM CellTracker Blue CMAC dye (Thermo Fisher Scientific) according to manufacturer's instructions. Donor and target cells were counted using counting beads (described in Section 2.6) and mixed in 1:1 ratio (total $6x10^5$ cells) in 100 μl RPMI medium supplemented with 1% FCS. Non-blocking Env antibody (1:100; clone 50-69) was added to enable detection of Env at the VS. Donor-target cell culture was quickly pulsed in the centrifuge and transferred to poly-L-lysine coated coverslips and incubated for 1 h at 37°C. Coverslips (VWR) were coated by incubation with 2.5% poly-L-lysine (Sigma) solution in water for 1 h at 37°C, dried and placed into a 24-well plate for further use. After 1 h incubation, cells were fixed with 4% methanol-free formaldehyde in PBS (1 ml/well) for 30 min at 4°C and washed thrice with 1 ml of 1% bovine serum albumin (BSA; Sigma) in PBS solution (BSA/PBS). Cells were then permeabilized with 0.1% Triton X-100 (Sigma) in BSA/PBS and washed thrice with BSA/PBS. Samples were stained in 200 μl of BSA/PBS with anti-Gag antisera (1:1000) for 1 h at RT and washed thrice in BSA/PBS. Primary antibodies were detected with fluorescent secondary antibodies in 200 μl BSA/PBS for 30 min at RT and washed thrice in BSA/PBS and once in water. Antibodies used for microscopy are listed in Table 2.5. After washing, coverslips were dried and mounted on microscope slides with ProLong Gold Antifade mounting solution without DAPI (Thermo Fisher Scientific). Images were acquired on DeltaVision Elite image restoration microscope (Applied Precision) with softWoRx 5.0 software. Image processing was performed using Huygens Professional 4.0 and Adobe Photoshop 7 software. VS was defined as a donor-target cell conjugate with Gag and Env polarized towards the cell-cell contact (Jolly et al., 2004). VS formation was quantified as a percentage of donor-target cell conjugates forming the VS out of total number of donor-target cell conjugates. At least 30 VS were counted for each sample.

For Lck localisation, CD4+ T cells were infected ($2.5x10^5$ cells/virus) for 48 h, washed and incubated on poly-L-lysine coated coverslips for 1h at 37°C as described above. After fixation and permeabilisation, cells were stained in 100 μl BSA/PBS with anti-Lck antibody (1:400, Table 2.5). After secondary antibody stain and washes, coverslips were mounted with ProLong Gold Antifade mounting solution with DAPI (Thermo Fisher Scientific). Images were acquired as described above.

Table 2.5: Antibodies used for microscopy

Target	Antibody clone	Fluorophore	Supplier	Dilution
Gag p17 & p24	Rabbit antisera	Unconjugated	CFAR[1]	1:1000
Env gp41	Human mAb 50-69	Unconjugated	CFAR[2]	1:100
Lck	Rabbit mAb 73A5	Unconjugated	Cell Signaling	1:400
Rabbit IgG	Polyclonal	Cy3	Jackson Immuno	1:200
Human IgG	Polyclonal	Cy5	Bethyl	1:200

[1] Donated by Dr G. Reid. [2] Donated by Dr S. Zoller-Pazner and Dr M. Gorny.

2.9 SERINC antagonism assay

SERINC5 and SERINC3 expression vectors (pcDNA based) were gifted from Massimo Pizzato (University of Trento, Italy). SERINC proteins were HA-tagged at the N-terminus (intracellular tag) and Flag-tagged in the fourth extracellular loop (extracellular tag) as described previously (Pye et al., 2020). SERINC plasmids were prepared as described in Section 2.3.1. 293T cells were seeded in 24-well plates ($2x10^5$cells/well in 0.5 ml culture medium) and transfected with 120 ng proviral DNA, 0-20 ng SERINC DNA and empty pcDNA vector to equalize DNA content using 3 μl Fugene 6 and 45 μl Opti-MEM medium. Transfected cells and virus containing supernatants were collected at 48h post-transfection. Virion infectivity was measured as described in Section 2.7. Cells were detached using 5 mM EDTA solution in PBS and analysed by flow cytometry (as described in Section 2.5) for SERINC expression using Flag and HA epitope tags.

2.10 Immunoblot analysis

2.10.1 Sample preparation

A small aliquot of infected cell culture was used to measure infection levels by flow cytometry. Infected cells ($1.2x10^6$) were washed twice in PBS and lysed in 35 μl RIPA cell lysis buffer (150 mM NaCl, 50 mM Tris pH 8, 1% (v/v) NP-40, 0.5% (w/v) deoxycholate, 0.1% (w/v) SDS, 1mM phenylmethylsulphonyl fluoride [PMSF]). Lysates were centrifuged at 13,000 x g for 10 min at 4°C to remove cell debris and to pellet the nucleus and supernatants were collected. Protein concentration was measured using Pierce BCA Protein Kit (Thermo Fisher Scientific) according to the manufacturer's instructions. Virus-containing supernatants (1 ml) were purified through a sucrose cushion by centrifugation at 13,000 x g for 2 h at 4°C. Virus pellets were lysed in 20 μl 1X protein loading buffer (50 mM Tris-HCl pH 6.8, 2% (w/v) SDS, 10% (v/v) glycerol, 0.1% (w/v) bromophenol blue, 100 mM β-mercaptoethanol).

2.10.2 SDS-PAGE

To separate samples by sodium dodecyl sulphate polyacrylamide gel electrophoresis (SDS-PAGE), 40 μg of cell lysate (mixed with 6X protein loading buffer) and 20 μl of virus lysate was heated at 95°C for 5 min. The samples were loaded on NuPAGE 4-12% gradient gel (Thermo Fisher Scientific) in NuPAGE MES SDS running buffer (Thermo Fisher Scientific) and run at 120 V for approx. 90 min. PageRuler Plus prestained protein ladder (Thermo Fisher Scientific) was used to estimate protein size.

2.10.3 Immunoblotting

After SDS-PAGE, proteins were transferred to Protran 0.45 μm nitrocellulose membrane (GE Healthcare) by electrophoresis at 100 V for 60 min in transfer buffer (25 mM Tris-HCl, 250 mM glycine, 20% [v/v] methanol). Membranes were cut to detect gp120 separately to gp41, Gag and tubulin, and blocked overnight at 4°C in 5% (w/v) milk protein solution in 0.01% (v/v) Tween-20 in PBS (PBST). Membranes were then stained with primary antibodies in 5 ml of 5% milk protein in PBST for 1 h at RT and washed thrice in PBST. Antibodies used for immunoblotting are listed in Table 2.6. Primary antibodies were detected with appropriate fluorescent secondary antibodies (Table 2.6) in 5 ml of 5% milk protein in PBST for 1 h at RT and washed thrice in PBST and once in PBS. Membranes were imaged with Odyssey Infrared Imager (Licor) and immunoblots

were analysed with Image Studio Lite software.

Table 2.6: Antibodies used for immunoblotting

Target	Antibody clone	Fluorophore	Supplier	Dilution
Env gp120	Rabbit antisera	Unconjugated	CFAR[1]	1:1000
Env gp41	Human mAb 246-D	Unconjugated	CFAR[2]	1:500
Gag	Rabbit antisera	Unconjugated	CFAR[3]	1:3000
α-tubulin	Mouse mAb DM1A	Unconjugated	Sigma	1:10,000
Rabbit IgG	ab216773	IRDye 800CW	Abcam	1:10,000
Mouse IgG	ab216772	IRDye 800CW	Abcam	1:10,000
Human IgG	925-68078	IRDye 680RD	Licor	1:10,000

[1] Donated by Dr S. Ranjibar. [2] Donated by Dr S. Zoller-Pazner and Dr M. Gorny.

[3] Donated by Dr G. Reid.

2.11 Analysis of mRNA expression

2.11.1 Sample preparation

Infected cells were analysed by flow cytometry 48h post-infection to count GFP+ cells using counting beads as described above. For each sample 10^5 GFP+ cells from the infected cell culture were mixed with appropriate number of autologous uninfected cells to obtain $1.2x10^6$ cells in total per sample. This gave identical proportions of infected cells (8% GFP+ cells) in all samples to facilitate comparison between different PBMC donors and viruses. Cells were washed twice in PBS and cellular RNA was extracted using RNeasy Mini Kit (Qiagen) according to manufacturer's instructions. Samples were eluted in 30 μl nuclease-free water and treated with RQ1 RNase-Free DNase (Promega) according to manufacturer's instructions to degrade DNA. Samples were stored at -80°C until used.

2.11.2 cDNA synthesis

To synthesise complementary DNA (cDNA), RNA concentration in each sample was measured using Nanorop and 800 ng of RNA was used in each reaction containing 2.5 μM random hexamer primers (Invitrogen) and 500 μM dNTP mix (Invitrogen) in 13 μl nuclease-free water. Samples with no RNA or no RT added were included as controls.

Primers were annealed at 65°C for 5 min. Reverse transcription reaction was set up by adding 4 µl 5X First Strand buffer, 50 U Superscript IV reverse transcriptase, 5 mM DTT and 40 U RNase OUT (all purchased from Invitrogen) to obtain 20 µl of total reaction volume. The samples were first incubated at 50°C for 10 min and then at 80°C for 10min to stop the reaction. Samples were diluted 1:4 in nuclease-free water for further analysis.

2.11.3 RT-qPCR

Real-time quantitative polymerase chain reaction (RT-qPCR) was set-up using 4.5 µl cDNA sample, 2X Fast SYBR Green Master Mix (Invitrogen) and 250 nM of each primer (Sigma) to make up 10 µl total reaction volume. Primers used for RT-PCR were as follows:

Env forward: 5'-GCCTCAATAAAGCTTGCCTTGA-3';
Env reverse: 5' GATTACTATGGACCACACAACTATTG-3'

Gag forward: 5'-GGACATCAAGCAGCCATGCAAAT-3'
Gag reverse: 5'-GCTATGTCACTTCCCCTTGGTTCTCT-3'

GAPDH forward: 5'-ACATCGCTCAGACACCATG-3'
GAPDH reverse: 5'-TGTAGTTGAGGTCAATGAAGGG-3'

RT-qPCR was performed using 7500 Real-Time PCR System (Applied Biosystems) and cycling parameters are shown in Table 2.7. The threshold cycle (Ct) values of *gapdh* gene were compared against *env* or *gag* genes using the $2^{-\Delta\Delta Ct}$ method to calculate the relative expression of *env* and *gag* genes.

Table 2.7: RT-qPCR cycling parameters

Step	Temperature (°C)	Time	Number of cycles
Initial denaturation	95	20 s	1
Denaturation	95	3 s	40
Extension	60	30 s	

2.12 Env trafficking

2.12.1 Env internalisation assay

The Env internalisation assay was performed as described previously (Anand et al., 2019). Briefly, infected CD4+ T cells ($2.5x10^5$ cells/virus) were washed in PBS and stained with anti-Env PGT151 Ab (5 µg/ml) and cell viability dye (1:1500, Zombie UV) in 50 µl PBS for 45 min on ice and then washed twice in ice-cold RPMI medium. To start Env internalisation, cells were incubated in 150 µl complete RPMI medium at 37°C for 0-120 min. Env internalisation was stopped by adding methanol-free formaldehyde directly to the cell culture to obtain 2% final formaldehyde concentration. Cells were fixed for 1 h at 4°C and washed in PBS. For 0 min time-point (T_{0min}) control, cells were fixed after initial Ab incubation, without incubation at 37°C. The remaining Ab-Env complexes on the cell surface were detected with anti-human IgG Cy5-conjugated secondary antibody (Table 2.2) in 50 µl PBS for 30 min at 4°C. Cells were washed and resuspended in FWB and analysed by flow cytometry.

2.12.2 Env recycling assay

Infected CD4+T cells ($2.5x10^5$ cells/virus) were washed in PBS and stained with Env PGT151 Ab (5 µg/ml) in 100 µl complete RPMI medium for 60min at 37°C to allow for Env internalisation. Cells were washed twice in ice-cold PBS and surface Env was stained with anti-human IgG PE-conjugated secondary antibody (Table 2.2) and Zombie UV cell viability dye (1:500) in 50 µl PBS for 30min on ice. This measured baseline (T_{0min}) surface Env expression. Cells were then washed twice in cold RPMI medium and incubated with anti-human IgG Cy5-conjugated secondary antibody (Table 2.2) for 0-120 min in 100 µl complete RPMI medium at 37°C to label Env that was being recycled back to the cell surface. For T_{0min} control, cells were kept on ice and stained with Cy5-conjugated secondary antibody without incubation at 37°C. Cells were washed in ice-cold FWB and fixed in 2% formaldehyde for 1 h at 4°C and analysed by flow cytometry.

2.13 Antibody neutralisation assay

Primary CD4+ T cells were infected for 48 h and virus-containing supernatants were filtered through a 0.45 µm filter and stored at -80°C until used for antibody neutralisation assay. Virus stock produced in 293T cells was used for comparison. The neutralisation was performed as described previously (Montefiori, 2009). First, virus supernatant

infectivity was measured using HeLa TZM-bl reporter cell assay (described in section 2.7.2) to determine the amount of supernatant to give RLU reading 20-times above the background (uninfected control). Equal amounts of infectious supernatant were incubated with 7-fold serial dilutions (starting at 7 μg/ml) of PG9 or PGT151antibodies (gift from Laura McCoy, UCL) in total volume of 100 μl complete DMEM medium and incubated at 37°C for 1h. HeLa TZM-bl reporter cells were seeded the day before in 96-well plates (10^4 cell/well) in 100 μl DMEM medium. The virus-antibody mixture was added to TZM-bl cells (200 μl total culture medium) and luciferase activity was measured 48 h later using Bright-Glo substrate (described in Section 2.7.2). Antibody neutralisation was calculated as percent decrease in luciferase activity compared to the corresponding virus only control. The half maximal inhibitory concentration (IC_{50}) values were calculated by non-linear regression analysis (sigmoid curve interpolation) using Prism software (GraphPad).

2.14 CD3ζ knock-down

CD3ζ (CD247) knock-down (KD) was achieved by RNAi using ON-TARGET plus SMARTpool siRNA oligonucleotides (Dharmacon) designed against CD247, which included 4 siRNA oligos (sequences shown below). Non-targeting siRNA (Dharmacon) was used as a control. Primary CD4+ T cells were activated for 4 days before the KD and $2x10^6$ cells/condition were electroporated with 250 pmol siRNA oligos using Neon Transfection System (Thermo Fisher Scientific) according to manufacturer's instructions. Briefly, cells were resuspended in 100 μl Buffer T and mixed with siRNA before electroporation (3 pulses, 1600 V, 10 ms). After electroporation, cells were incubated for 4 h in 12 ml complete RPMI medium (with IL-2) without Penicillin-Streptomycin to ensure high cell survival. After 4 h, cells were transferred to 96-well plate ($2.5x10^5$ cells/well) and cultured in fresh RPMI medium (with IL-2 and Penicillin-Streptomycin). CD247 KD efficiency was checked 48 h after by flow cytometry (Table 2.2) and cells were infected with viruses.

CD274-targeting siRNA oligo sequences:
5'-GAAGAGAGGAGUACGAUGU-3', 5'-AGGAAGGCCUGUACAAUGA-3',
5'-GGCCAGAACCAGCUCUAUA-3', 5'-GCGGAGGCCUACAGUGAGA-3'.

2.15 Infected T cell activation assay

The infected T cell activation assay was done using either pre-activated or resting infected cells. For the assay with pre-activated cells, primary CD4+ T cells were activated for 5 days by CD3/CD28 stimulation (described in Section 2.2.1) and infected with viruses for 24 h until used in the activation assay (described below). For the assay with resting cells, primary CD4+ T cells were after isolation treated with 20 ng/ml IL-7 (Miltenyi Biotec) and 10 IU/ml IL-2 (NIBSC) in complete RPMI medium for 4 days. Cells were then infected with viruses for 48h and cultured in medium containing IL-7 and IL-2 until used in the activation assay.

For the infected cell activation assay, Nunclon 96-well plates (Thermo Fisher Scientific) were coated with 0.5 μg/ml anti-CD3 Ab (clone OKT3, Biolegend) in 50 μl PBS per well for 2 h at 37°C. Plates were washed twice in complete RPMI medium to remove unbound antibody. Infected cells were washed in RPMI medium and transferred to coated plates (2.5x105 cells/well) and cultured in fresh culture medium containing 2 μg/ml anti-CD28 Ab (clone CD28.2, Biolegend) and supplemented with 10 IU/ml IL-2. For untreated control, infected cells were transferred to mock treated wells (PBS only) and cultured in fresh culture medium without anti-CD28 Ab. Cells were harvested 24 h post-activation and analysed by flow cytometry. Culture supernatants were analysed for virion infectivity.

2.16 TCR signalling assay

2.16.1 Donor-target cell co-culture

Primary CD4+ T cells were infected for 48 h (donor cells). Uninfected cells (target cells) were labelled 24 h before co-culture with 2.5 μM Cell Proliferation Dye eFluor 450 (Thermo Fisher Scientific) according to manufacturer's instructions. After the overnight culture (48 h p.i.) labelled target cells and donor cells were centrifuged and resuspended in 1% FCS RPMI medium (for about 2 h until the co-culture experiment) to allow for better detection of signalling. A small aliquot of cells was taken for counting by flow cytometry using the counting beads (Section 2.6). Before the co-culture, donor and target cells were stained with Zombie UV cell viability dye (1:500, 10^6 cells/ml) in Hank's balanced salt solution (HBSS, Gibco) for 15 min at RT and washed in 1% FSC RPMI medium. Donor and target cells were mixed in 1:1 ratio (total of $3x10^5$ cells/condition) in 100 μl 1% FSC RPMI medium and incubated at 37°C for 20 min. For the time course protocol, donor and target cells were preincubated on ice for 5 min, then mixed and incubated on ice for further 15 min to allow for conjugate formation without activation of

cell signalling. Co-cultures were then warmed to 37°C for 0-40 min. For 0 min time-point cells were fixed after incubation on ice, without incubation at 37°C. As a positive control cells were stimulated with 5 μl/ml soluble anti-CD3 Ab (OKT3) and 2 μg/ml anti-CD28 Ab (CD28.2). Signalling activation was stopped by adding methanol-free formaldehyde directly to the co-cultures to obtain 4% final formaldehyde concentration. Cells were fixed for 10 min at 37°C and for further 20min at 4°C.

2.16.2 Flow cytometry analysis

For flow cytometry analysis, cells were washed in PBS and permeabilised with 200 μl ice-cold methanol-based TruePhos buffer (Biolegend) for 30-60 min on ice. Cells were centrifuged at 1000 x g for 10 min to remove TruePhos buffer and washed twice in PBS (standard spin). Cells were stained with phosho-specific antibodies (Table 2.8) in 50 μl PBS for 30 min at 4°C, washed and resuspended in FWB and analysed by flow cytometry (Section 2.5). Gating strategy to identify phosphorylation changes in infected cell conjugates is described in Figure 3.27.

Table 2.8: Antibodies used for TCR signalling assay

Target	Phosphorylation site	Antibody clone	Fluorophore	Supplier	Dilution
ZAP70	pY319	17A	PE/Cy7	BD	1:50
ERK	pT202/Y204	6B8B69	PerCP/Cy5.5	Biolegend	1:50
AKT	pT308	D25E6	Alexa Fluor 647	Cell Signaling	1:100
AKT	pS473	M89-61	PE/CF594	BD	1:50
S6	pS235/S236	N7-548	PE	BD	1:20

2.17 Statistical analysis

Statistical significance was calculated using paired or unpaired student's *t* test. For multiple comparisons, one-way analysis of variance (ANOVA) with Sidak's multiple comparisons test was performed. Statistical significance was assumed when $p<0.05$. All statistical analyses were calculated using Prism 6 software (GraphPad).

3 Retained CD3 expression results in increased viral spread, virion infectivity and T cell activation

3.1 Introduction

The lentiviral accessory protein Nef of HIV-2 and most SIV lineages, but not HIV-1, downmodulates CD3 - the signalling component of T cell receptor (TCR) complex (Schindler et al., 2006). This impairs signalling at the immunological synapse and may interfere with antiviral responses and prevent aberrant immune activation (Arhel et al., 2009). Why HIV-1 does not employ this potential immune evasion strategy remains incompletely understood. In this Chapter I investigated if retained CD3 expression conferred any advantage for viral replication. Specifically, I addressed the following question - if virus induced downregulation of CD3 from the surface of infected cells confers an important immune evasion strategy, is there any selective advantage for HIV-1 not to do this that may explain why loss of this Nef function has been retained in the HIV-1 lineage?

HIV-1 most efficiently disseminates by direct cell-cell transmission that occurs at virological synapses (VS) formed between infected and uninfected cells (Jolly et al., 2004, 2007a; Sourisseau et al., 2007). VS formation is mediated by engagement of viral envelope glycoprotein (Env) on infected (donor) cell with CD4 on uninfected (target) cell with an additional contribution of adhesion molecule interactions mediated by the integrin LFA-1 and its cognate ICAM ligands (Chen et al., 2007; Jolly et al., 2007b; Sourisseau et al., 2007). This results in polarised virus assembly and budding from the infected cell towards uninfected target cell, resulting in rapid and efficient infection of target cells (Groppelli et al., 2015; Hubner et al., 2009; Jolly et al., 2007a, 2011; Martin et al., 2010). Previous work from our lab has shown that VS-formation triggers antigen-independent TCR signalling in infected T cells to drive viral spread (Len et al., 2017). This was partially dependent on TCR/CD3 complex expression as efficient signalling at the VS and HIV-1 cell-cell spread was abrogated in TCR knock-down Jurkat cell line. Given these results, it was hypothesised that the inability of HIV-1 Nef to downregulate CD3 contributes to the activation of TCR/CD3 signalling at the virological synapse and thus allowing more efficient cell-cell spread. Therefore, the role of Nef-mediated viral manipulation of CD3 during viral spread was investigated.

It was previously shown impossible to engineer HIV-1 Nef to downmodulate CD3, without disrupting other Nef functions (Manrique et al., 2017). In effort to do so, HIV-1 SF2 Nef was made to downmodulate CD3 by constructing a SF2-SIVmac239 Nef chimera (Manrique et al., 2017). However, this Nef chimera was unable to downmodulate surface expression of CD4, CD28, MHC-I or CXCR4 and unable to enhance virus infectivity, which would confound the analysis and interpretation of the data in this thesis. Therefore, SIVsmm (infecting sooty mangabeys) *nef* alleles were used that differ in their ability to downmodulate surface CD3 expression. Although CD3 downmodulation is a conserved feature of most SIV Nef proteins, rare cases of SIVsmm *in vivo* infections have been reported where *nef* alleles lost the ability to downmodulate CD3 expression (Schindler et al., 2008; Schmökel et al., 2013). Schmökel et al. described several *nef* alleles that were isolated during a course of *in vivo* infection of a sooty mangabey infected with SIVsmmFBr virus. As illustrated in Figure 3.1A, at early time points (≈1.5 years) during this infection the animal had a normal CD4+ T cell count and high blood viremia, consistent with normal SIVsmm infection. *Nef* alleles at that time showed normal CD3 downmodulation ability. One *nef* allele from this group, FBr 75wL4 (abbreviated to L4) was used in this thesis. By contrast, late infection (≈6 years) was marked by very low CD4+ T cell counts (with a corresponding drop in viral load) and was associated with loss of Nef-mediated CD3 downmodulation, while other Nef functions remained intact. One *nef* allele from this group, FBr 304wK2 (abbreviated to K2) was used in this thesis. Notably, the loss of CD3 downmodulation was also associated with mutations in Env that allowed for efficient use of CXCR4 co-receptor (in addition to CCR5, GPR15 and CXCR6 that are commonly used by SIVsmm), which is also rarely observed in SIVsmm infection, and was proposed it enhanced CD4+ T cell death. Further *in vitro* analysis confirmed that the retention of CD3 on the cell surface resulted in increased in T cell activation and cell death following TCR cross-linking of infected CD4+ T cells (Schindler et al., 2006; Schmökel et al., 2013). However, whether retained CD3 expression conferred any replicative advantage to the virus, which might explain selection of this phenotype *in vivo*, was not addressed.

Nef sequence and functional analyses showed that L4 and K2 Nefs are closely related and differ only in 10 amino acids, two of which were identified as crucial for CD3 downmodulation: I123 and L146, whereas mutation to L123 and F146 resulted in loss of CD3 downmodulation (Figure 3.1B) (Schmökel et al., 2013). Therefore, point mutations (I123L/L146F and L123I/F146L) in L4 and K2 *nef* alleles were made by site-directed mutagenesis to specifically disrupt CD3 downmodulation (Figure 3.1C) (Schmökel et al.,

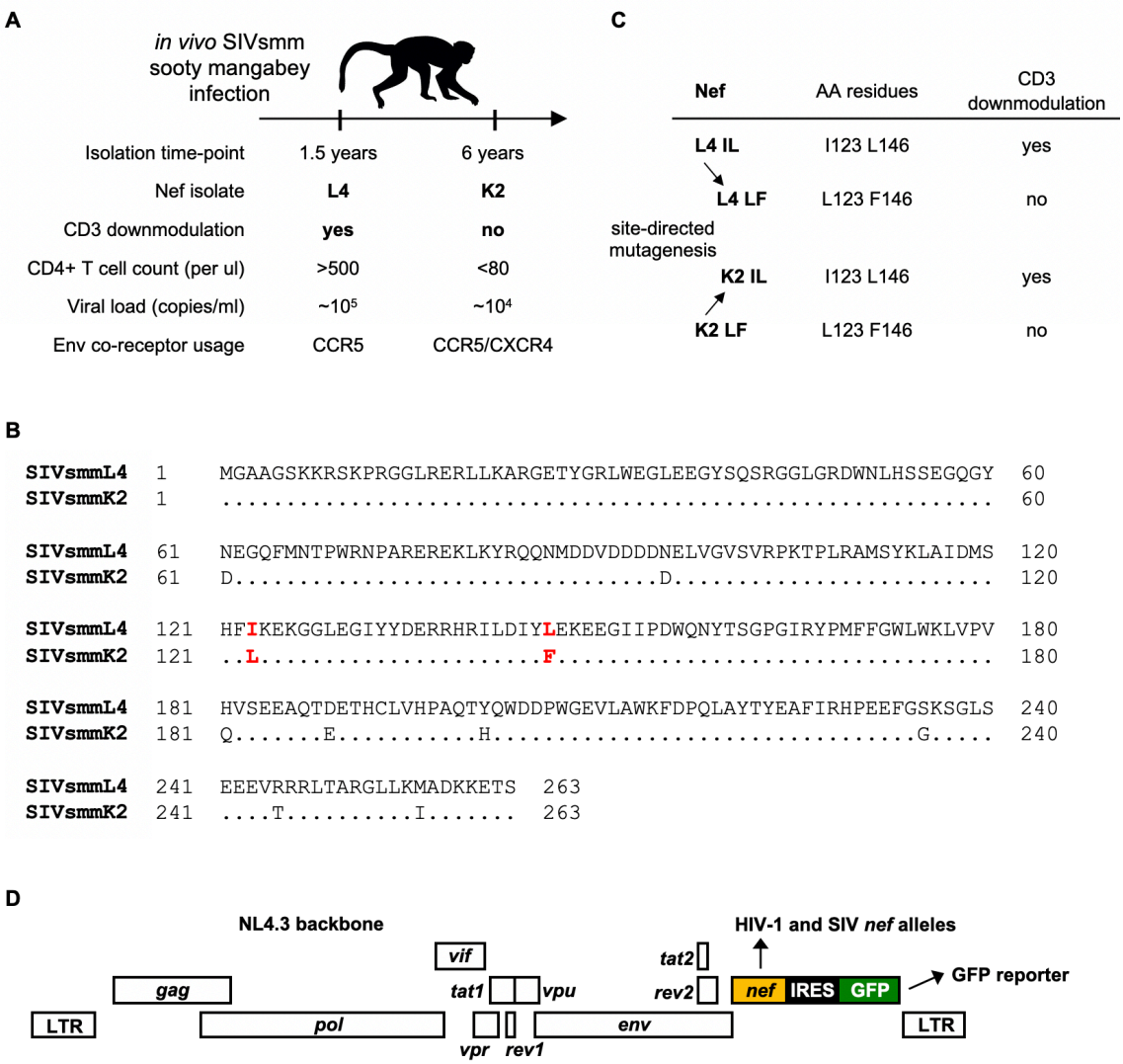

Figure 3.1: SIVsmmFBr L4 and K2 *nef* alleles and NL4.3 Nef chimeric viruses

(A) Two SIVsmmFBr *nef* alleles isolated during *in vivo* sooty mangebey infection: L4 (75 weeks post-infection, ≈1.5 years) and K2 (304 weeks post-infection, ≈6 years). Table shows their CD3 downmodulation abilitiy, viral load, CD4+ T cell count and predominant Env tropism at the time of isolation. **(B)** Alignment of SIVsmmFBr L4 and K2 Nef sequences. Dots indicate sequence identity. Highlighted in red are residues crucial for CD3 downmodulation: I123 and L146. Mutation to L123/F146 abolishes Nef CD3 downmodulation ability. **(C)** Generation of L4 and K2 point-mutants by site-directed mutagenesis that differ CD3 downmodulation ability. L4 IL (I123/L146) and LF (L123/F146) *nef* alleles were generated, together with K2 IL (I123/L146) and K2 LF (L123/F146) *nef* alleles. **(D)** SIVsmm *nef* alleles or HIV-1 NL4.3 *nef* (WT and nef-defective) were inserted into replication competent NL4.3 backbone with an IRES-driven GFP reporter gene to produce Nef chimeric viruses.

2013). To simplify the naming, *nef* alleles that are able to downmodulate CD3 are referred to in this Chapter as IL Nef (I123/L146) and *nef* alleles that are unable to downmodulate CD3 are referred to as LF Nef (L123/F146). As previously reported (Schindler et al., 2006), these nef alleles have been cloned into HIV-1 NL4.3 backbone

co-expressing different *nef* alleles and green fluorescent protein (GFP) reporter gene from a bicistronic RNA (Figure 3.1D). The panel of *nef* alleles studied in this Chapter included SIVsmm Nefs (L4 IL and LF, K2 IL and LF) together with the parental NL4.3 *nef* and a *nef*-defective control (*nef*-, no Nef expression). Producing these Nef chimeric viruses thus allowed us to determine the role of CD3 downmodulation on HIV-1 cell-cell spread, irrespective of other viral genes or Env tropism.

3.2 Results

3.2.1 Validation of the phenotype of Nef chimeric viruses

In order to assess the impact of differences in Nef mediated CD3 downmodulation it was necessary to first validate the phenotype of the chimeric viruses provided by our collaborator Frank Kirchhoff (Schmökel et al., 2013). A panel of *nef* alleles cloned into HIV-1 NL4.3 IRES-GFP proviral construct (Schindler et al., 2006) were first sequenced, which confirmed their sequence identity, and then assessed for the ability to infect primary CD4+ T cells. To do this, 293T cells were transfected with viral plasmids and virions were harvested and titrated prior to infection of primary CD4+ T cells. To characterise the virus produced from 293T cells, virion infectivity was measured by titrating the viral supernatants on HeLa-TZMbl reporter cell line and normalising the RLU values to supernatant RT activity (measured by SG-PERT assay) as a measure of viral content. Figure 3.2A shows that all Nef chimeric proviruses produce infectious virus. Consistent with published data (Chowers et al., 1994; Münch et al., 2007), *nef*-defective virus had significantly lower infectivity compared to NL4.3 Nef virus, and all L4 and K2 Nef viruses showed slightly higher infectivity compared to NL4.3 Nef virus. Importantly, there was no difference in the relative infectivity of IL and LF viruses produced from 293T cells. Next, primary CD4+ T cells were isolated from PBMCs of normal healthy donors, activated with anti-CD3/CD28 antibodies and infected with equal infectious doses of Nef chimeric viruses (*nef*-defective, NL4.3, L4 IL and LF, K2 IL and LF). After 48h primary CD4+ T cells were analysed by flow cytometry to quantify the percentage of HIV-1 infection and Nef activity. Infected cells were identified as single, live lymphocytes that are positive for Gag and/or GFP expression (Figure 3.2B-E). Analysis of infected primary CD+ T cells showed broadly similar percentages of Gag+ or GFP+ cells between cells infected with the different Nef chimeric viruses (Figure 3.2F-G). Cells infected with *nef*-defective virus showed lower infection levels as measured by Gag expression when compared to other Nef-containing viruses; however, this difference was smaller when

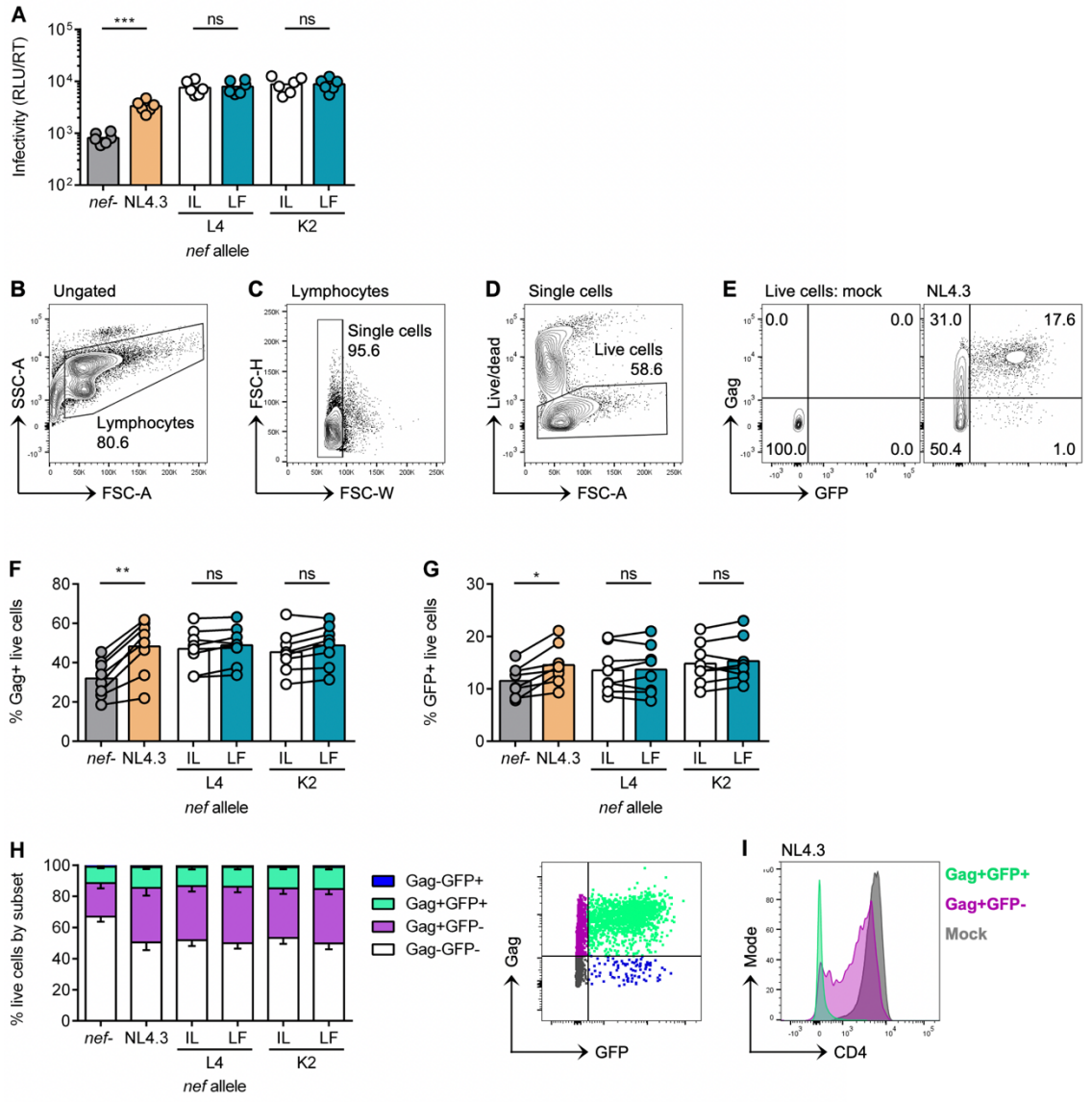

Figure 3.2: Infection of primary CD4+ T cells with Nef chimeric viruses

(A) Nef chimeric viruses were produced by transfection of HEK293T cells. Viral infectivity (RLU) was measured by titration on HeLa-TZMbl reporter cell line and normalised to supernatant RT activity, a measure of viral content. **(B-I)** Primary CD4+ T cells were activated with anti-CD3/CD28 antibodies for 4-5 days, infected with Nef chimeric viruses for 48h and analysed by flow cytometry. **(B-E)** Gating strategy to analyse flow cytometry data. **(B)** Lymphocytes were gated based on their forward- and side-scatter properties (FSC-A vs SSC-A). **(C)** Doublets were excluded based on their forward scatter properties (FSC-W vs FSC-H). **(D)** Live single cells were gated as Live/dead dye (Zombie UV) negative. **(E)** Infected live cells were identified as Gag+ or GFP+. Uninfected (mock) control was used to set the gates. **(F)** Percentage of Gag+ live cells. **(G)** Percentage of GFP+ live cells. **(H)** Percentage of live cells in the four subsets defined by expression of Gag and GFP. Shown is a representative dot plot of flow cytometry data. **(I)** Surface expression of CD4 in NL4.3 Nef virus infected cells. Histogram shows CD4 expression in Gag+GFP- and Gag+GFP+ population compared to mock infected control. Bars show mean and lines join paired results from the same PBMC donor. Error bars show mean ± SEM. Groups were compared using paired *t*-test (ns, P>0.05; *, P<0.05; **, P<0.01; ***, P<0.001).

measuring GFP expression. Analysing expression patterns of Gag and GFP showed that only a subpopulation of Gag+ cells expressed GFP, and almost all GFP+ cells were also Gag+ (Figure 3.2E, H). To better understand the discrepancy in Gag and GFP expression, surface CD4 expression was measured in Gag+GFP+ and Gag+GFP- populations. Productively infected cells show downmodulation of surface CD4, which requires expression of viral Nef or Vpu proteins (Wildum et al., 2006; Willey et al., 1992). Analysing expression of CD4 in Gag+GFP+ and Gag+GFP- populations showed that only a small proportion of Gag+GFP- cells downmodulated CD4, whereas most of the Gag+GFP+ cells downmodulated CD4 (Figure 3.2I), indicating productive infection. This suggests that the Gag+GFP- population may represent newly-infected cells which do not yet express GFP (and do not downmodulate CD4) or perhaps reflects the detection of viral capsids (Gag) that have been transferred into cells during spinoculation, thus resulting in positive Gag signal (Terahara et al., 2012). Therefore, expression of GFP, which better reflects productive infection, was used in the majority of further experiments and unless otherwise stated to identify infected cells.

To determine the ability of Nef chimeric viruses to downmodulate surface expression of CD3, CD4, CD28, and CXCR4 primary CD4+ T cells infected with Nef chimeric viruses (or uninfected mock control) were analysed by flow cytometry to measure expression of these surface markers. Figure 3.3A shows that, as expected, L4 and K2 IL Nef expressing viruses were able to downmodulate surface expression of CD3 and reduced the number of CD3+ infected cells to less than 20%. By contrast, L4 and K2 LF Nefs are unable to downmodulate CD3 expression as evidenced by more than 90% of cells remaining CD3+, similar to the percentage of CD3+ cells in mock infected (uninfected) control. Furthermore, and as expected, *nef*-defective and NL4.3 Nef viruses were unable to downmodulate CD3, in agreement with HIV-1 NL4.3 Nef having lost this function. CD4 surface staining showed that all *nef*-containing viruses (NL4.3, L4 IL, L4 LF, K2 IL and K2 LF) retained the ability to downmodulate CD4 (Figure 3.3B) when compared to uninfected cells. The partial downregulation of CD4 by *nef*-defective virus (≈50% CD4+ infected cells), is attributed to the presence of HIV-1 Vpu that can mediate CD4 degradation (Willey et al., 1992). Turning to CD28, it was found that L4 and K2 parental and mutant Nef viruses downmodulated CD28 to similar extents (≈30% CD28+ infected cells, Figure 3.3C), whereas NL4.3 Nef was less able to do so (≈70% CD28+ infected cells) in agreement with published data (Munch et al., 2005).

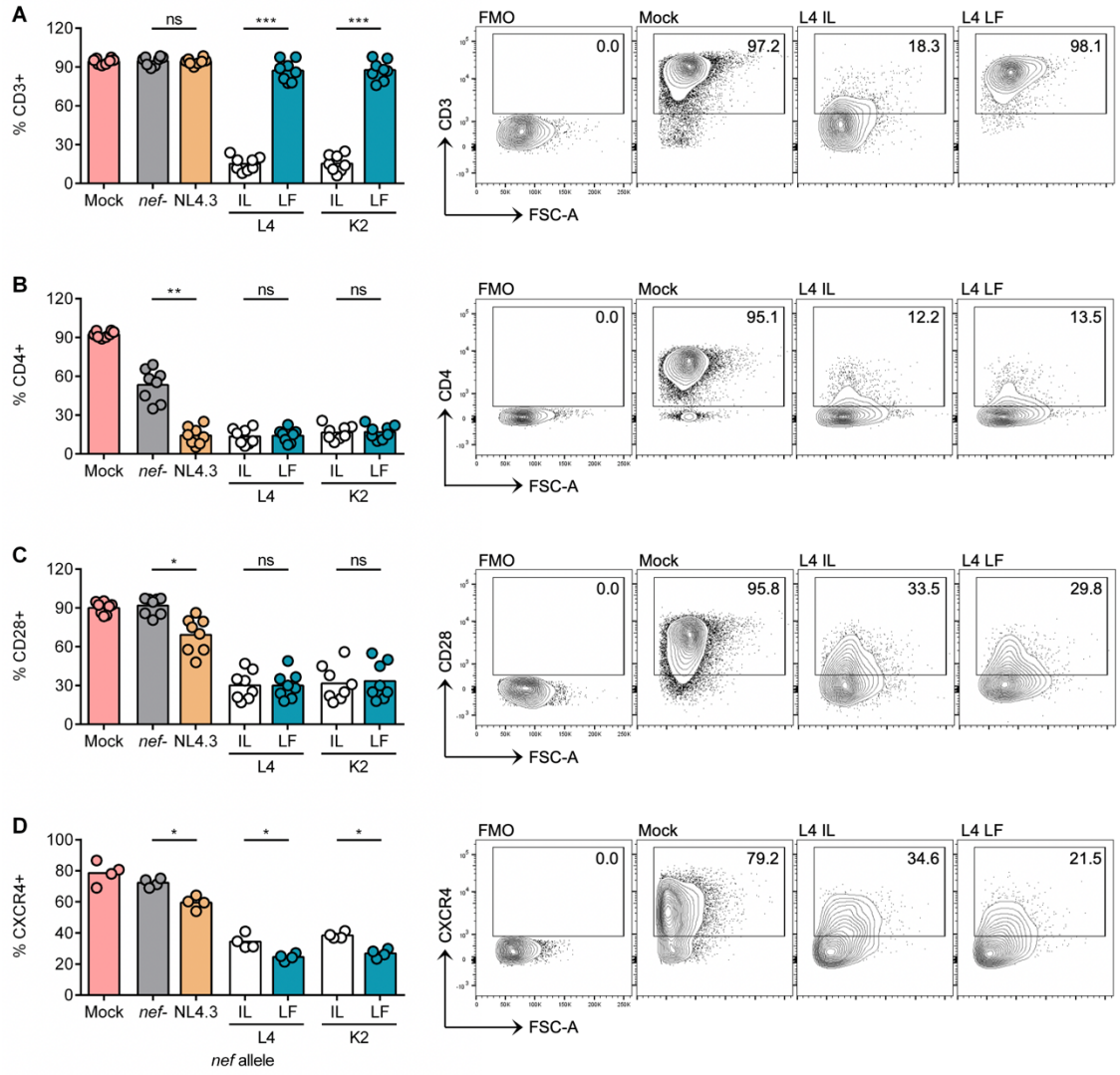

Figure 3.3: CD3, CD4, CD28, and CXCR4 downmodulation by Nef chimeric viruses

Primary CD4+ T cells were infected with Nef chimeric viruses and analysed by flow cytometry 48h post-infection. Shown is percentage of positive cells of live, Gag+GFP+ population for **(A)** CD3, **(B)** CD4, **(C)** CD28, and **(D)** CXCR4 surface markers. Mock is uninfected control and total live population was analysed. Right-hand side panels show representative flow cytometry plots. FMO controls were used to set the gates. Bars show mean and symbols show results from an individual PBMC donor. Groups were compared using paired *t*-test (ns, P>0.05; *, P<0.05; **, P<0.01; ***, P<0.001).

Similarly, NL4.3 Nef was also less able to downmodulate CXCR4 (≈60% CXCR4+ infected cells, Figure 3.3D) compared to L4 and K2 Nef viruses, again as expected (Hrecka et al., 2005; Schmökel et al., 2013). While it was observed that L4 and K2 LF Nef viruses appeared better able to downmodulate CXCR4 compared to their IL Nef counterparts this difference was very small. Together these results validate the expected phenotype of this panel of Nef chimeric viruses, and show that manipulation of CD3

downregulation by site-directed mutagenesis of L4 and K2 Nefs had specific effects on downmodulation of CD3.

It has been shown that lentiviral Nefs antagonise the host restriction factors SERINC3 and SERINC5 (Rosa et al., 2015; Usami et al., 2015). SERINC5 and to a lesser extent SERINC3 reduces virion infectivity by inhibiting viral fusion (Rosa et al., 2015; Sood et al., 2017; Usami et al., 2015), which requires their incorporation into nascent viral particles. Nef antagonises SERINCs activity by downmodulating their surface expression and thus reducing incorporation into viral particles, thereby increasing viral infectivity (Rosa et al., 2015; Trautz et al., 2016; Usami et al., 2015). Because the focus of the work described in this Chapter was to assess the effects of Nef-mediated downregulation of CD3 on HIV-1 replication and spread between T cells, it was important to determine whether the *nef* alleles used in this study showed any differences in SERINCs antagonism or restriction of viral infectivity that may impact on future experiments and interpretation of the data. To test the ability of Nef chimeric viruses to antagonise host restriction factors SERINC5/3, 293T cells were co-transfected with viral plasmids alongside increasing doses of dual-tagged SERINC5/3 expressing plasmid (Pye et al., 2020). In this assay, the presence of increasing doses of SERINC will reduce the infectivity of progeny virus if SERINC is not antagonised by Nef (Heigele et al., 2016; Rosa et al., 2015). Flow cytometry analysis confirmed a dose-dependent increase in the amount of total SERINC5 expressed in transfected cells measured by intracellular staining for HA-tagged SERINC5 (Figure 3.4A). The presence of over-expressed SERINC5 resulted in up to a 300-fold reduction in infectivity of *nef*-defective virus that was rescued by expression of functional Nef (Figure 3.4B) in agreement with previous reports (Rosa et al., 2015). The fact that all Nef-expressing viruses also showed a dose-dependent decrease in infectivity at high doses of SERINC5 plasmid likely reflects the fact that substantial overexpression of SERINC5 can overwhelm Nef activity. Importantly, Figure 3.4B shows that there was no significant difference between IL and LF Nef viruses in infectivity in the presence or absence of SERINC5 overexpression. Nef antagonises SERINC5/3 by downmodulating their cell surface expression and preventing their incorporation into nascent viral particles. Flow cytometry analysis of SERINC5 cell surface expression (detected by extracellular Flag-tag) showed that all Nef expressing viruses were able to downmodulate SERINC5 from the cell surface (Figure 3.4C). Importantly, there was no difference between IL and LF Nef viruses in the amount of cell surface SERINC5 (Figure 3.4C) suggesting these *nef* alleles are equally able to antagonise SERINC5.

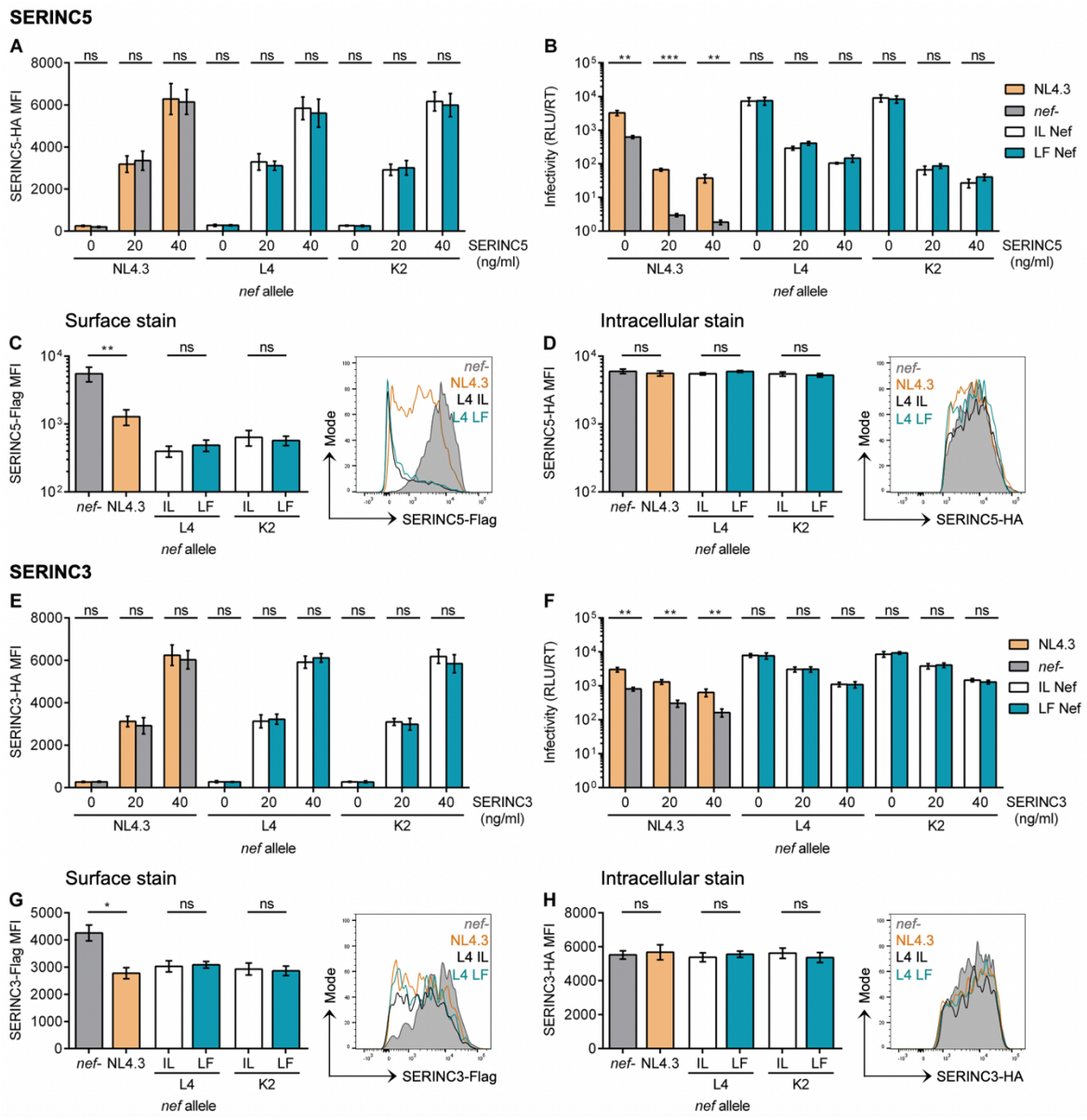

Figure 3.4: Nef chimeric viruses have similar ability to antagonise SERINC5 and SERINC3

HEK293T cells were co-transfected with Nef chimeric proviruses and increasing doses of plasmid encoding dual-tagged SERINC5 or SERINC3 (n=3). Cells and virus supernatants were harvested 48h post-transfection. Virion infectivity (RLUs) was measured using HeLa-TZMbl reporter cell assay and normalised to supernatant RT activity. Flow cytometry was used to measure total SERINC expression (intracellular HA-tag) or surface SERINC expression (extracellular Flag-tag). **(A-D)** SERINC5 restriction and antagonism. **(A)** MFI of SERINC5 HA-tag in live, GFP+ population. **(B)** Virion infectivity in the presence of SERINC5. **(C)** MFI of SERINC5 Flag-tag, and **(D)** MFI of SERINC5 HA-tag in GFP+HA-tag+ cells transfected with 20 ng/ml SERINC5 plasmid. **(E-H)** SERINC3 restriction and antagonism. **(E)** MFI of SERINC3 HA-tag in live, GFP+ population. **(F)** Virion infectivity in the presence of SERINC3. **(G)** MFI of SERINC3 Flag-tag, and **(H)** MFI of SERINC3 HA-tag in GFP+HA-tag+ cells transfected with 20 ng/ml SERINC3 plasmid. Histograms show representative flow cytometry data. Error bars show mean ± SEM of 3 independent experiments. Groups were compared using unpaired *t*-test (ns, P>0.05; *, P<0.05; **, P<0.01; ***, P<0.001).

This is consistent with the similar levels of infectivity that were observed in Figure 3.4B. Similar levels of total SERINC5 expression was confirmed by staining for intracellular HA-tag (Figure 3.4D). Consistent with published data (Heigele et al., 2016), NL4.3 Nef is less able to downmodulate SERINC5 compared to SIVsmm Nef. Similar results were also observed with over-expression of SERINC3 (Figure 3.4E-H), showing there was no difference between IL and LF Nef viruses in their ability to antagonise SERINC3. However, as previously reported (Heigele et al., 2016; Rosa et al., 2015), it was observed that SERINC3 was a weaker antagonist of virion infectivity compared to SERINC5 (Figure 3.4B). Furthermore, all Nef-expressing viruses are less able to downmodulate SERINC3 surface expression compared to SERINC5 (Figure 3.4C). Taken together, these results show that Nef mutations disrupting CD3 downmodulation do not affect SERINC5/3 antagonism.

3.2.2 Retained CD3 expression on infected cells results in increased viral spread

To investigate the effect of CD3 downmodulation on cell-cell spread, primary CD4+ T cells infected with Nef chimeric viruses (donor cells) were co-cultured with autologous uninfected, pre-labelled target cells (Figure 3.5A). Cell-cell spread is the dominant mode of HIV-1 dissemination in cell culture (Chen et al., 2007; Hubner et al., 2009; Jolly et al., 2004, 2007a; Sourisseau et al., 2007), therefore this well-established assay mainly measures cell-cell viral spread, with minimal contribution from cell-free virus infection (Jolly et al., 2010; Sourisseau et al., 2007). Donor cells were infected for 48h and the number of infected, GFP+ cells was quantified by flow cytometry (Figure 3.5B). To account for differences in initial infection between different PBMC donors, GFP+ donor and target cells were mixed in 1:4 ratio to obtain approx. 10% GFP+ donor cells in donor-target cell co-culture (Figure 3.5C). Viral spread was measured 24h post-mix (single round of replication) by flow cytometry to identify Gag+ or GFP+ target cells. Target cells were identified as live single cells positive for Target dye (Figure 3.5D-J). Quantifying Gag expressing target cells (Figure 3.6B), showed that NL4.3 Nef virus spread significantly better to target T cells compared to *nef*-defective virus, consistent with the observations that the lack of Nef results in reduced viral infectivity (Chowers et al., 1994; Münch et al., 2007) (Figure 3.2). Notably, L4 and K2 IL Nef viruses, which downmodulate CD3 from infected cells, were significantly impaired in cell-cell spread when compared to L4 and K3 LF Nef viruses that retain CD3 which spread significantly better (≈2-fold increase, Figure 3.6B). Treating co-cultures with the RT inhibitor Efavirenz resulted in an

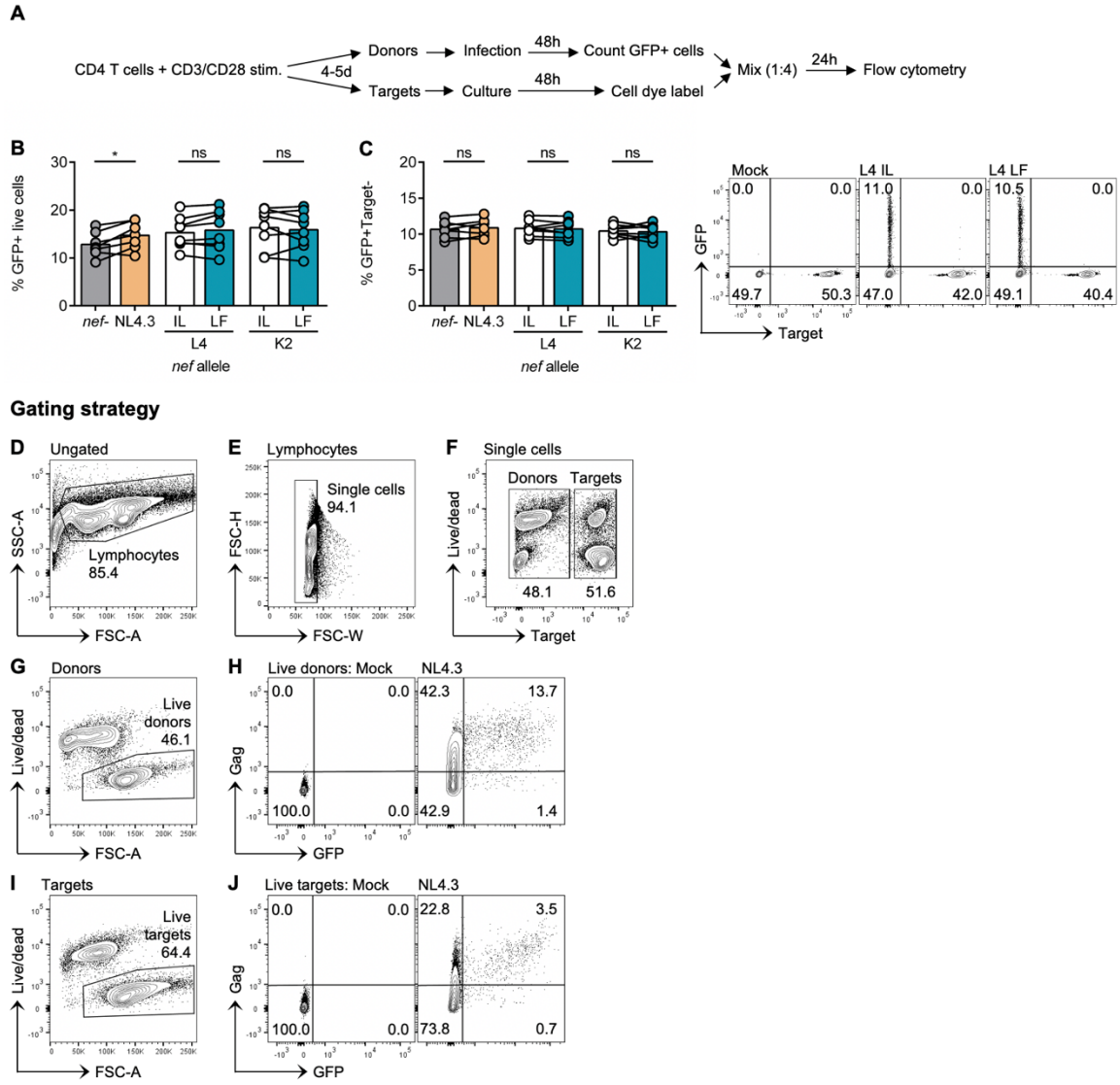

Figure 3.5: Cell-cell spread assay and gating strategy to analyse flow cytometry data

(A) Schematic of the cell-cell spread assay. Primary CD4+ T cells were activated with CD3/CD28 antibodies for 4-5 days. Donor cells were infected with Nef mutant viruses for 48h and analysed by flow cytometry to count GFP+ cells. Autologous target cells were labelled with cell dye and mixed with infected donor cells in 1:4 ratio (GFP+ donor cell:target cell). Cells were analysed by flow cytometry at 0h and 24h post-mix. **(B)** Percentage of GFP+ live donor cells at 48h post-infection, before target cell co-culture. **(C)** Percentage of GFP+ donor cells in target cell co-culture (GFP+Target-) at 0h post-mix. Shown are representative flow cytometry plots. **(D-J)** Gating strategy to analyse flow cytometry data. Shown is an example from NL4.3 infected co-culture at 24h post-mix. **(D)** Lymphocytes were gated based on their forward- and side-scatter properties (FSC-A vs SSC-A). **(E)** Doublets were excluded based on their forward scatter properties (FSC-W vs FSC-H). **(F)** Donor cells were gated as target dye (CPDe450) negative cells and target cells were gated as target dye positive cells. **(G)** Live donor cells were gated as Live/dead dye (Zombie UV) negative. **(H)** Infected live donor cells were identified as Gag+ or GFP+. Mock infected donor cells were used to set the gates. **(I)** Live target cells were gated as Live/dead dye negative. **(J)** Infected live target cells were identified as Gag+ or GFP+. Mock infected target cells were used to set the gates. Bars show mean and lines join paired results from the same PBMC donor. Groups were compared using paired *t*-test (ns, P>0.05; *, P<0.05; **, P<0.01; ***, P<0.001).

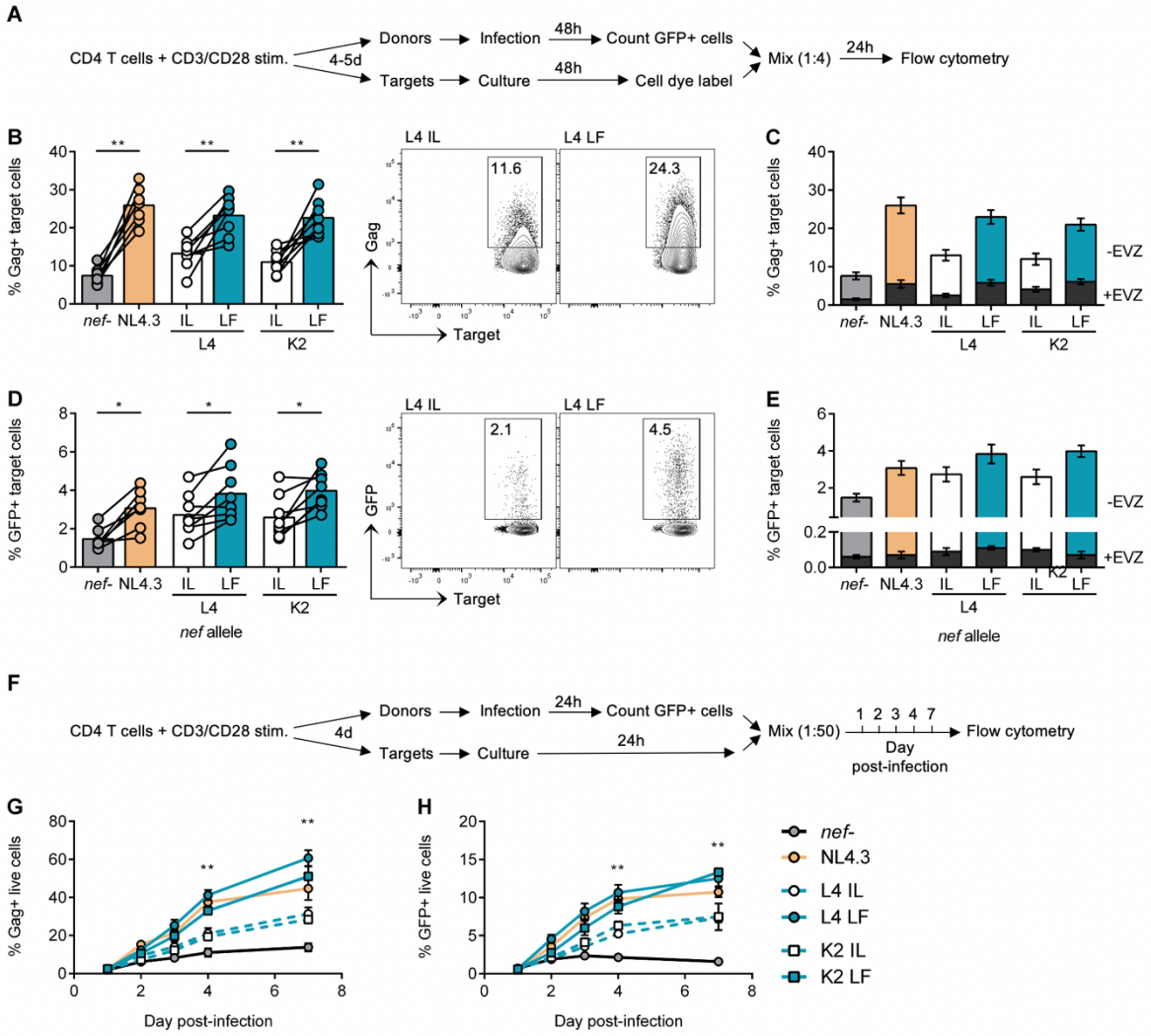

Figure 3.6: Retained CD3 expression on infected cells results in increased viral cell-cell spread

(A) Schematic of the 24h cell-cell spread assay (as described in Figure 3.5). CD4+ T cells infected with indicated viruses were mixed with autologous, pre-labelled target cells and analysed 24h post-mix by flow cytometry (n=8). **(B)** Percentage of Gag+ target cells. **(C)** Donor and target cells were co-cultured in the presence or absence of 5 μM Efavirenz (± EVZ). Superimposed grey bars show percentage of Gag+ target cells in presence of Efavirenz. **(D)** Percentage of GFP+ target cells. **(E)** Percentage of GFP+ target cells in presence of 5 μM Efavirenz (superimposed grey bars). Shown are representative flow cytometry plots. **(F)** Schematic of the long-term cell-cell spread assay. CD4+ T cells were infected with Nef chimeric viruses for 24h and analysed by flow cytometry to count GFP+ cells. Infection levels in cell culture were adjusted to 2% GFP+ cells with autologous, unlabelled, uninfected cells. Spreading infection was quantified by flow cytometry until 7 days post-infection (n=3). **(G)** Percentage of Gag+ live cells. **(H)** Percentage of GFP+ live cells. IL and LF Nef viruses were compared for statistical significance at days 4 and 7 post-infection. Bars show mean and lines join paired results from the same PBMC donor. Error bars show mean ± SEM. Groups were compared using paired *t*-test (ns, P>0.05; *, P<0.05; **, P<0.01; ***, P<0.001).

approximately 5-fold reduction of Gag+ target cells (Figure 3.6C), confirming that this assay predominantly detects a Gag signal coming from *de novo* Gag synthesis that requires RT, indicative of productive infection of target cells. In support of this, similar results were obtained when measuring infection levels by LTR-driven expression of GFP which also showed L4 and K2 LF Nef viruses spread significantly better than their IL mutant counterparts (Figure 3.6D). Treating co-cultures with Efavirenz almost completely abrogated detection of GFP+ target cells (Figure 3.6E), again showing that this assay is measuring productive infection. Of note, the percentage of GFP+ target cells was approximately 6-fold lower than that measured by intracellular Gag staining of target cells. A similar trend was also observed in the donor cell population (Figure 3.2, Figure 3.5H).

To determine whether differences in viral spread between IL and LF Nef viruses would diminish over time (i.e. whether the IL viruses would reach the same level of viral spread as the LF viruses) and to further confirm that IL and LF viruses showed difference in viral spread, a longer term spreading infection assay was performed. To do this, primary CD4+ T cells were infected with virus and infection levels adjusted to 2% GFP+ cells at 24h post-infection with autologous uninfected cells to equalise infection levels (Figure 3.6F). Viral spread was then measured by quantifying the percentage of Gag+ or GFP+ cells by flow cytometry over 7 days post-infection. L4 and K2 LF Nef viruses showed more efficient viral spread and accelerated replication kinetics compared to their IL Nef counterparts as measured by expression of both Gag and GFP (Figure 3.6G-H). Taken together, these data show that retained CD3 expression on infected donor cells results in increased viral spread to target T cells.

Viral cell-cell spread occurs through formation of the virological synapse (VS) in which virus assembly and budding from infected cells is polarised towards uninfected target cells that are in close physical contact (Jolly et al., 2004). VS can be visualised by immunofluorescence microscopy and defined by polarisation of the HIV-1 proteins Gag and Env to the site of donor-target cell contact (Jolly et al., 2004). To investigate if the increased cell-cell spread observed in Figure 3.6 was due to increased formation of VS in the donor-target cell co-cultures, primary CD4+ T cells infected with Nef chimeric viruses were mixed with autologous uninfected pre-labelled target T cells, incubated on coverslips for 1h, stained and analysed by immunofluorescent microscopy. As shown in Figure 3.7, examination of VS formation revealed no difference in the frequency or

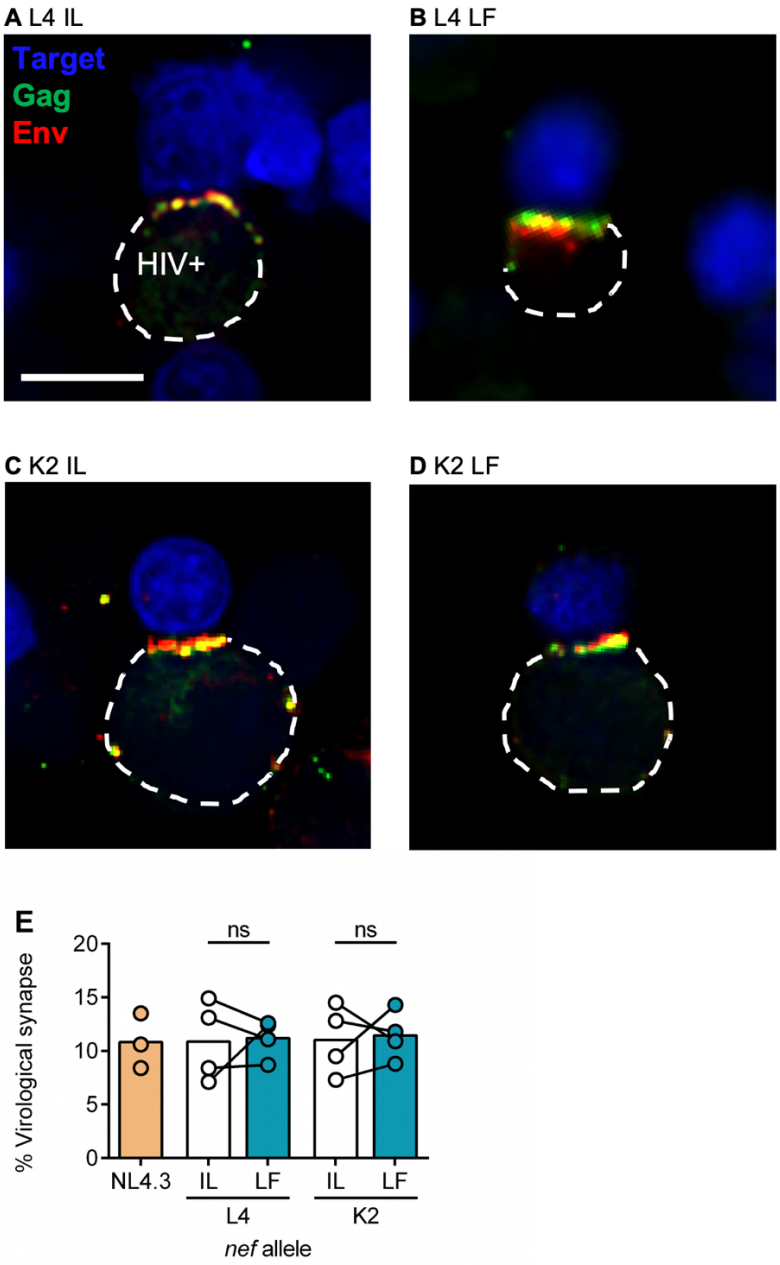

Figure 3.7: CD4+ T cells infected with Nef chimeric viruses form virological synapses at similar frequencies

CD4+ T cells were infected with Nef chimeric viruses for 48h. Autologous uninfected target cells were labelled with cell tracing dye and mixed with infected donor cells at 1:1 ratio. Cells were incubated on coverslips for 1h before fixation and antibody staining for immunofluorescence microscopy. Virological synapse (VS) was defined as infected donor cell-target cell conjugate with Gag and Env polarised towards the cell-cell contact. **(A-D)** Target cell dye is shown in blue, Gag is shown in green, Env is shown in red, and donor cell outline is shown with white, dashed line. Scale bar is 5 μm. Shown are representative images (single slice) of VS for **(A)** L4 IL, **(B)**, L4 LF, **(C)** K2 IL, and **(D)** K2 LF Nef chimeric viruses. **(E)** Quantification of microscopy data. Shown is percentage of conjugates forming VS out of all donor-target cell conjugates. Minimum of 30 VS were counted for each PBMC donor. Bars show mean and lines join paired results from the same PBMC donor. Groups were compared using paired *t*-test (ns, P>0.05; *, P<0.05).

appearance of VS formed between IL and LF Nef viruses and target T cells. All Nef chimeric viruses are able to form donor-target cell conjugates with polarised Gag and Env proteins to the site of cell-cell contact to similar levels (Figure 3.7E). Thus, the increased cell-cell spread appears not to be due to increased VS formation.

Having used NL4.3 Nef chimeric virus, which is a lab-adapted HIV-1 strain, it was next investigated whether HIV-1 primary *nef* alleles show similar results. To do this, Nef chimeric constructs containing NA7 and SF2 *nef* alleles (Levy et al., 1984; Mariani & Skowronski, 1993) were measured for their downmodulation abilities and viral spread into target T cells. It was observed that NA7 and SF2 Nef chimeric viruses downmodulated surface expression of CD4, CD28, and CXCR4 to similar level seen for NL4.3 Nef virus, and were similarly unable to downmodulate CD3 (Figure 3.8A-D). Furthermore, NL4.3, NA7 and SF2 Nef virions showed equivalent levels of infectivity when produced from 293T cells (Figure 3.8E) and similar levels of viral cell-cell spread between primary CD4+ T cells as measured by Gag and GFP expression in target T cells (Figure 3.8F-H). Taken together, these results show that the HIV-1 Nef chimeric viruses behave in a similar manner when containing lab-adapted NL4.3 *nef* allele or primary NA7 and SF2 *nef* alleles.

Next, a cell-cell spread assay was performed using primary CD4+ T cells that were not activated by anti-CD3/CD28 antibodies (as in the previous experiments) to investigate if a bigger difference in viral spread could be observed. CD3/CD28-mediated activation was used to make T cells permissive to initial HIV-1 infection; however, it provides a very potent stimulus which might diminish the effect of CD3 downmodulation during cell-cell spread. Therefore, donor primary CD4+ T cells were instead treated with IL-7 to make them permissive to cell-free virus infection, but without causing robust T cell activation (Coiras et al., 2016). IL-7 has been shown to allow for HIV-1 infection of resting CD4+ T cells, which has been attributed to phosphorylation of the lentiviral restriction factor SAMHD1, thus elevating cellular dNTP levels allowing for efficient HIV-1 reverse transcription (Baldauf et al., 2012; Coiras et al., 2016). Infected donor cells were then co-cultured with autologous uninfected, IL-7 treated, pre-labelled target cells (Figure 3.9A) and viral spread was quantified by flow cytometry 48h post-mix. Similar to what was seen using CD3/CD28 activated cells, both L4 and K2 LF viruses (which retain CD3 expression on infected cells) spread significantly better compared to their IL Nef counterparts when infection quantified either by percentage of Gag+ or GFP+ target cells

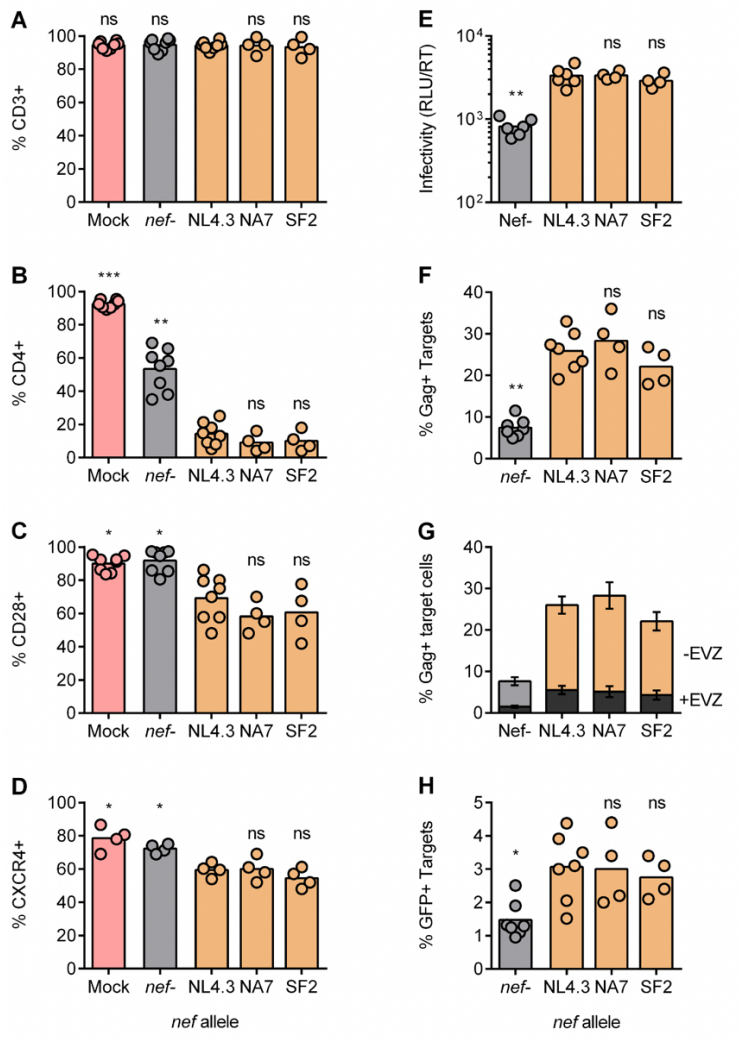

Figure 3.8: Primary HIV-1 *nef* alleles have similar downmodulation and cell-cell spread properties compared to NL4.3 *nef*

(A-D) Primary CD4+ T cells were infected with Nef chimeric viruses and analysed by flow cytometry 48h post-infection. Shown is percentage of positive cells of live, Gag+GFP+ population for **(A)** CD3, **(B)** CD4, **(C)** CD28, and **(D)** CXCR4 surface markers. Mock is uninfected control and total live population was analysed. **(E)** HEK293T cells were transfected with Nef chimeric proviruses and virus supernatant was collected 48h post-transfection. Virion infectivity (RLUs) was measured using HeLa-TZMbl reporter cell assay and normalised to supernatant RT activity. **(F-H)** CD4+ T cells infected with indicated viruses were mixed with autologous, pre-labelled target cells and analysed 24h post-mix by flow cytometry. **(F)** Percentage of Gag+ target cells. **(G)** Donor and target cells were co-cultured in the presence or absence of 5 μM Efavirenz (± EVZ). Superimposed grey bars show percentage of Gag+ target cells in presence of Efavirenz. **(H)** Percentage of GFP+ target cells. Bars show mean and symbols show results from an individual PBMC donor. Error bars show mean ± SEM. All groups were compared against NL4.3 using one-way ANOVA with Sidak's multiple comparisons test (ns, P>0.05; *, P<0.05; **, P<0.01; ***, P<0.001).

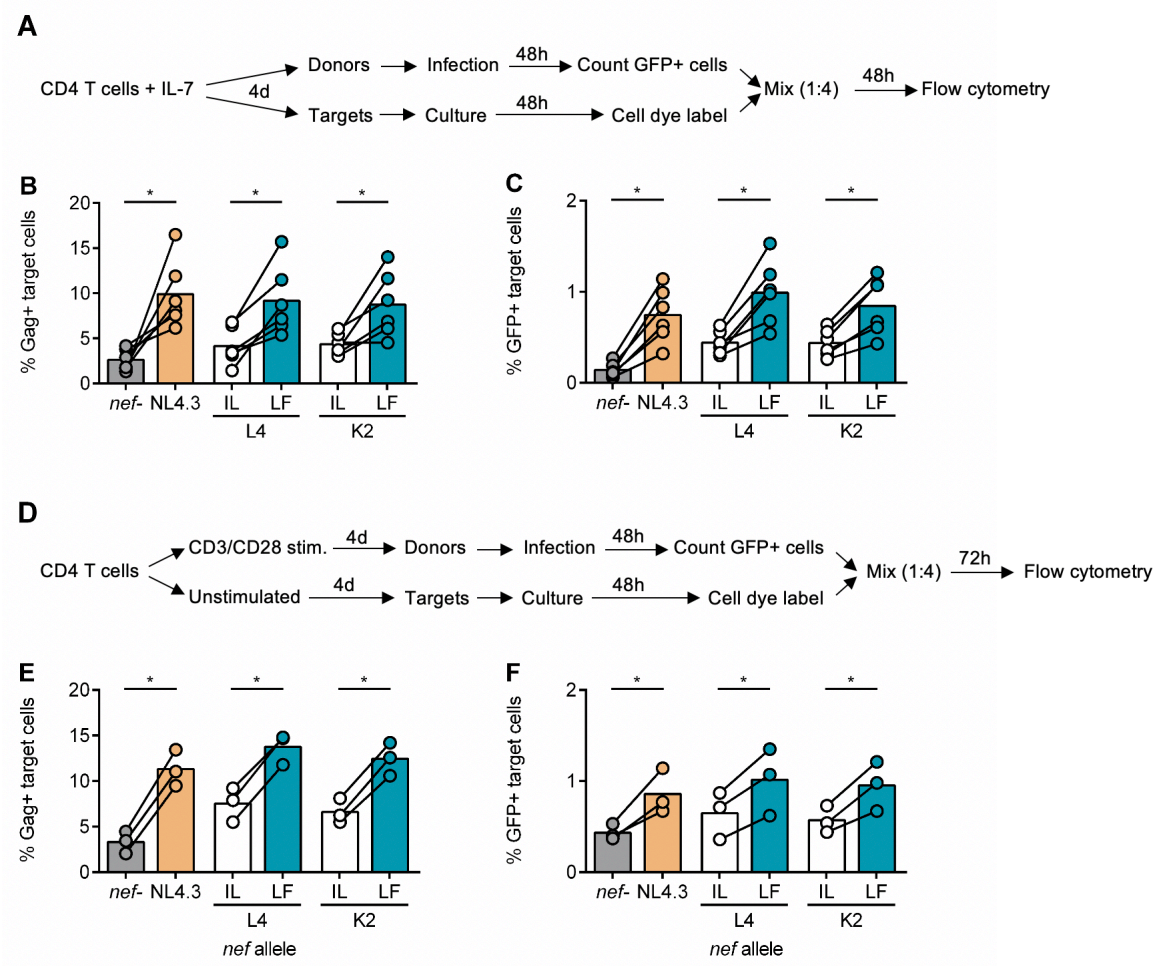

Figure 3.9: Cell-cell spread assay with IL-7 treated and resting target cells

(A-C) Viral spread into IL-7 treated targets cells. **(A)** Schematic of the cell-cell spread assay. Primary CD4+ T cells were treated with IL-7 for 4 days. Donor cells were infected with Nef mutant viruses for 48h and analysed by flow cytometry to count GFP+ cells. Target cells were labelled with cell dye and mixed with infected donor cells in 1:4 ratio (GFP+ donor cell:target cell). Cells were analysed by flow cytometry at 48h post-mix. **(B)** Percentage of Gag+ target cells. **(C)** Percentage of GFP+ target cells. **(D-F)** Viral spread into resting target cells. **(D)** Schematic of the cell-cell spread assay. Primary CD4+ T cells were split between donor cells, which were stimulated with CD3/CD28 antibodies for 4 days, and target cells, which were unstimulated. Donor cells were infected with Nef mutant viruses for 48h and analysed by flow cytometry to count GFP+ cells. Target cells were labelled with cell dye and mixed with infected donor cells in 1:4 ratio (GFP+ donor cell:target cell). Cells were analysed by flow cytometry at 72h post-mix. **(E)** Percentage of Gag+ target cells. **(F)** Percentage of GFP+ target cells. Bars show mean and lines join paired results from the same PBMC donor. Groups were compared using paired *t*-test (ns, P>0.05; *, P<0.05; **, P<0.01; ***, P<0.001).

(Figure 3.9B-C). NL4-3 Nef virus also spread much better compared to *nef*-defective virus, consistent with the observations that the lack of Nef results in reduced viral infectivity. Notably, the difference in viral spread between IL and LF viruses was about 2-fold, similar to what was observed with CD3/CD28 activated CD4+ T cells (Figure 3.6).

However, by contrast to CD3/CD28 activation experiments, cell-cell spread using IL-7 treated cells showed a lower percentage of either Gag+ (23% vs 9%, 2.5-fold reduction) or GFP+ (4% vs 1%, 4-fold reduction) target cells overall. This suggests that while IL-7 treatment can make T cells somewhat permissive, it does not make them as permissive for HIV-1 infection as classical T cell activation, leading to a lower overall percentage of Gag+ and GFP+ target cells. In a second experimental system, CD3/CD28 stimulated donor cells were used but were co-cultured with resting target cells that were not made permissive with anti-CD3/CD28 stimulation or IL-7 but instead only treated with IL-2 to ensure their survival (Figure 3.9D). Viral spread was quantified by flow cytometry 72h post-mix to ensure sufficient levels of infection were detected. Once again, L4 and K2 LF viruses, which retain CD3 expression, showed significantly better viral spread compared to their IL Nef counterparts, as measured by percentage of Gag+ or GFP+ target cells (Figure 3.9E-F). Similar to data from IL-7 treated target cells, a 2-fold difference between IL and LF Nef viruses was seen but with much lower numbers of Gag+ and GFP+ target cells compared to CD3/CD28 stimulated cells, indicating reduced permissivity of resting T cells for infection. Taken together, these data show that mode of T cell activation does not change the relative differences in viral spread that result from differential CD3 modulation of IL and LF Nef viruses; however, the mode of T cell activation does affect the absolute levels of viral spread, presumably by altering cellular permissivity. Since IL-7 treated or resting target T cells did not show greater differences in cell-cell spread assay, CD3/CD28 activated T cells were used for the subsequent experiments.

3.2.3 Retained CD3 expression results in increased Env expression and virion infectivity

To investigate how Nef-mediated modulation of CD3 expression affects viral spread, virus release from infected cells and virion infectivity were analysed. CD4+ T cells were infected with Nef chimeric viruses and incubated for 48h before virus containing culture supernatants and infected cells were collected and analysed. Virus release/budding from infected cells was quantified by measuring the amount RT activity present in the supernatants using an SG-PERT assay. RT activity measurements were normalised to the number of infected (GFP+) cells as quantified by flow cytometry. Figure 3.10A shows broadly similar levels of virus released from cells infected with either IL or LF Nef viruses. Although K2 IL and K2 LF Nef viruses showed a slight significant difference this was not seen for L4 IL and LF and the small effect size makes this unlikely to explain the

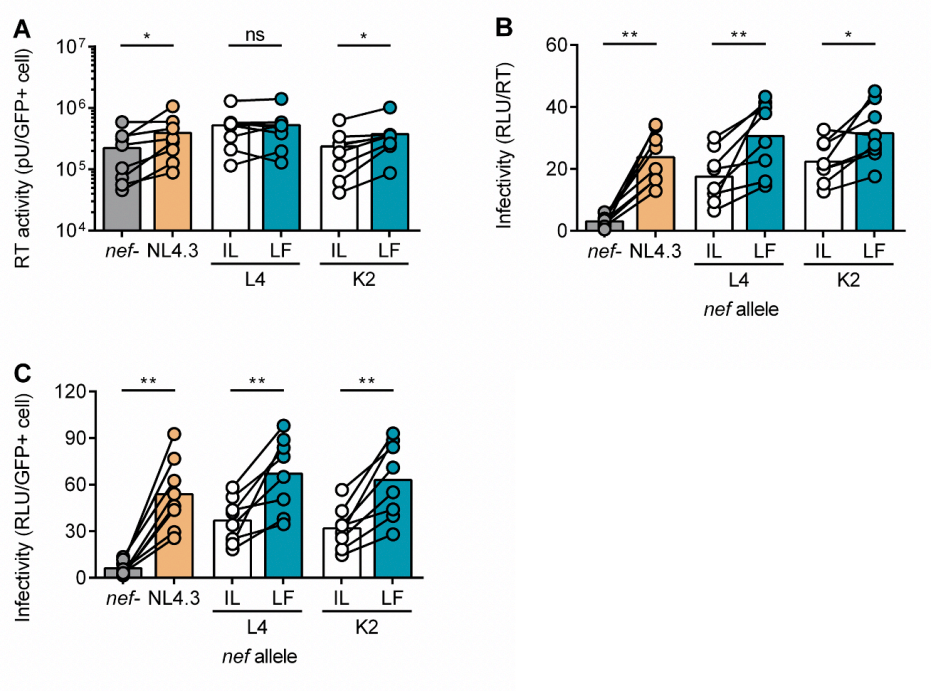

Figure 3.10: Retained CD3 expression on infected cells results in increased virion infectivity

Primary CD4+ T cells were infected with Nef chimeric viruses and culture supernatants collected at 48h post-infection. Number of GFP+ cells in cell culture was analysed by flow cytometry. **(A)** Virus release was measured by supernatant RT activity and normalised to number of infected GFP+ cells. **(B)** Virion infectivity (RLUs) was measured using HeLa-TZMbl reporter cell assay and normalised to supernatant RT activity as measured in (A). **(C)** Supernatant infectivity (RLUs) was measured as in (B) and normalised to number of infected GFP+ cells (as measured in (A)). Bars show mean and lines join paired results from the same PBMC donor. Groups were compared using paired *t*-test (ns, P>0.05; *, P<0.05; **, P<0.01; ***, P<0.001).

difference in cell-cell spread seen in Figure 3.6. By contrast, quantification of virion infectivity measured by titrating the supernatants on HeLa-TZMbl reporter cell line revealed significantly greater virion infectivity of L4 and K2 LF Nef viruses, which retain CD3 expression, compared to their IL Nef counterparts (Figure 3.10B). As expected, NL4.3 Nef virus displayed significantly higher virion infectivity compared to *nef*-defective virus that can be attributed to the lack of SERINC antagonism in the absence of Nef (Rosa et al., 2015; Usami et al., 2015). Importantly, for this analysis the RLU values were normalised to supernatant RT activity to account for any differences in viral budding. By contrast, normalising RLU values to number of infected (GFP+) cells (to account for differences in infection levels) gives a measure of total supernatant infectivity. Similar to virion infectivity, L4 and K2 Nef viruses showed increased supernatant infectivity compared to IL Nef viruses (Figure 3.10C). Consistent with increased viral release and virion infectivity, NL4.3 Nef virus showed significantly higher supernatant infectivity compared to *nef*-defective control. From these data it can be concluded that particle

infectivity is greater if virions are produced from primary CD4+ T cells that retain CD3 expression compared to cells where the virus downmodulates CD3. Taken together with the quantification of VS formation, these data suggest that the increase in cell-cell spread of viruses that retain CD3 expression on infected cells is likely due to increased virion infectivity.

Next, the mechanism of increased viral infectivity was addressed to gain insight why virions produced in the presence of CD3 expression were more infectious. Having already excluded differences in SERINC5/3 antagonism (Figure 3.4), and knowing that HIV-1 infection of cells is mediated by the envelope glycoprotein (Env), experiments were performed to measure Env expression, processing and incorporation into virions. CD4+ T cells infected with Nef chimeric viruses were incubated for 48h and then cell culture supernatants and cells were harvested for analysis. Immunoblot analysis of sucrose-gradient purified virions showed increased incorporation of both Env subunits, gp120 and gp41 into nascent particles in L4 and K2 LF viruses, which retain CD3 expression, compared to their IL Nef counterparts (Figure 3.11A-C). Quantification of immunoblots by densitometry analysis of three independently prepared viral preparations from three independent PBMC donors showed a significant increase in Env gp120 and gp41 incorporation into virions when normalised by the viral capsid protein Gag p24. This increase in Env content is consistent with observation that these viruses are more infectious (Figure 3.10). To understand the differences in Env virion incorporation, Env synthesis and processing were examined by immunoblot analysis of cell lysates (Figure 3.11D). Infected cells were analysed by flow cytometry to confirm similar levels of infection between Nef chimeric viruses (Figure 3.11E). Env gp160 precursor is cleaved by cellular furin to obtain processed gp120 and gp41 subunits (Braun et al., 2019; Dubay et al., 1995). Quantifying ratio of gp160/gp120 showed no difference in processing between IL and LF Nef viruses (Figure 3.10F). Env synthesis was quantified as ratio of total Env (gp160 + gp120) or gp41 normalised to cellular protein tubulin (Figure 3.11G-H). L4 and K2 LF Nef viruses, which retain CD3 expression, showed a modest increase in Env synthesis compared to IL Nef viruses. Similarly, quantifying Gag expression, L4 and K2 LF Nef viruses showed increased ratios of Gag protein p55 normalised to tubulin compared to their IL Nef counterparts (Figure 3.11I). By contrast, quantifying ratios of total Env (gp160 + gp120) or gp41 normalised to Gag protein p55 showed no difference between IL and LF Nef viruses (Figure 3.11J-K). This is consistent with the observation that both Env and Gag protein levels are increased in

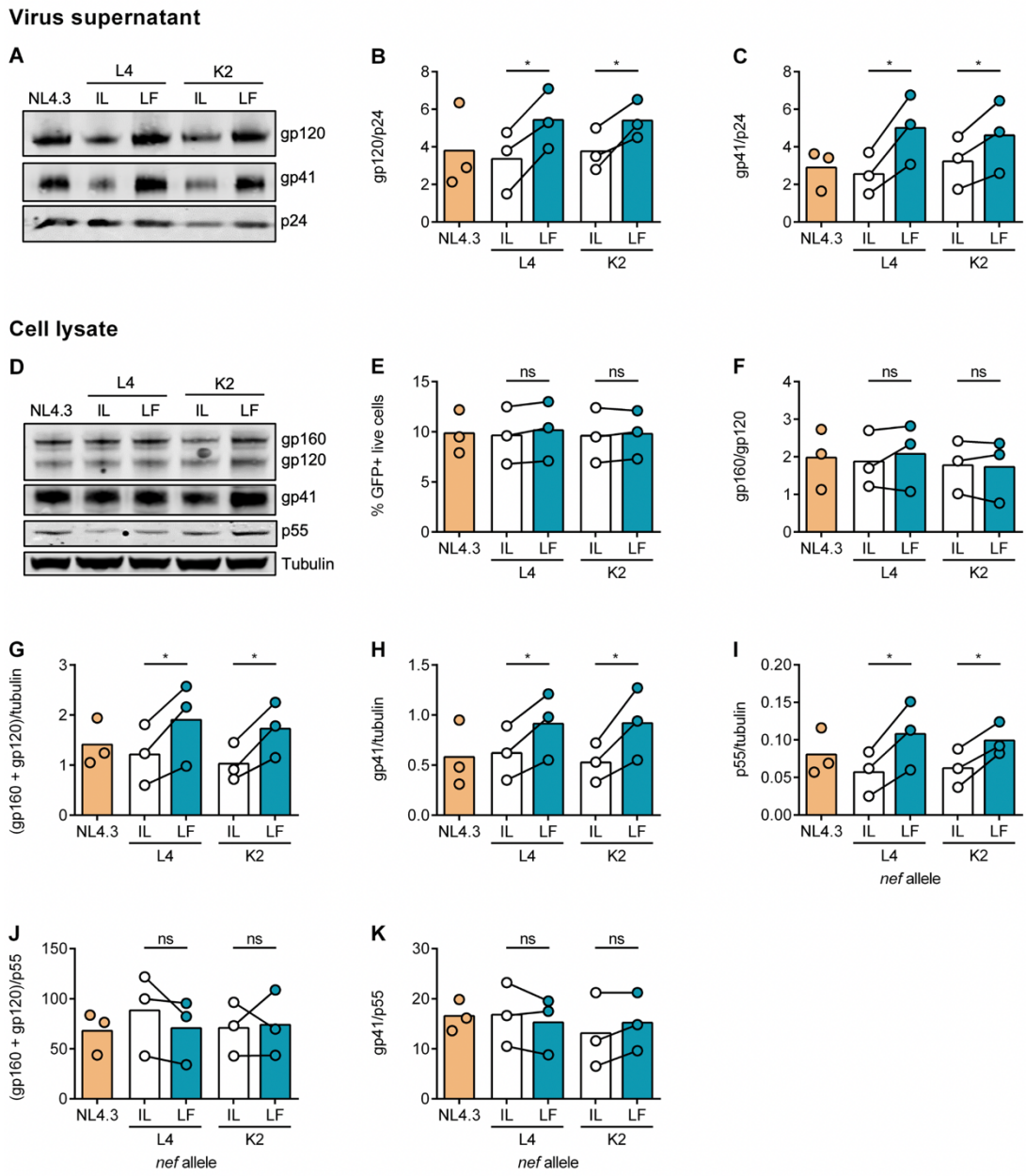

Figure 3.11: Retained CD3 expression results in increased Env incorporation into virions

Primary CD4+ T cells were infected with Nef chimeric viruses. Cells and culture supernatants were collected at 48h post-infection for immunoblot and flow cytometry analysis. **(A-C)** Immunoblotting of virus purified from cell culture supernatants. **(A)** Representative immunoblot shows detection of Env gp120, Env gp41 and Gag p24. **(B)** Quantification of gp120 incorporation normalized to p24. **(C)** Quantification of gp41 incorporation normalized to p24. **(D-K)** Immunoblot analysis of infected cell lysates. **(D)** Representative immunoblot shows detection of Env gp160, Env gp120, Env gp41, Gag p55 and tubulin. **(E)** Percentage of GFP+ live cells in the infected cell cultures as measured by flow cytometry prior to cell lysis. **(F)** Quantification of Env cleavage, shown as ratio of gp160/gp120. **(G)** Quantification of Env (gp160+gp120) expression normalised to tubulin. **(H)** Quantification of Env gp41 expression normalised to tubulin. **(I)** Quantification of Gag p55 expression normalised to tubulin. **(J)** Quantification of Env (gp160+120) normalised to p55. **(K)** Quantification of Env gp41 expression normalised to p55. Bars show mean and lines join paired results from the same PBMC donor. Groups were compared using paired *t*-test (ns, P>0.05; *, P<0.05; **, P<0.01; ***, P<0.001).

LF Nef virus infected cells. Taken together, these results suggest that retained CD3 expression results in increased Env incorporation into virions.

Having observed (slight) differences in Env and Gag protein expression by immunoblotting, this phenotype was further examined using more quantitative techniques (quantitative PCR and flow cytometry). First, the expression of Env and Gag mRNA was analysed by qRT-PCR. As above, CD4+ T cells were infected for 48h and analysed by flow cytometry to confirm similar infection levels between Nef chimeric viruses (Figure 3.12A). Percentage of infected (GFP+) cells was equalised to 8% in all infected cultures (using autologous uninfected cells) to facilitate the comparison between viruses and PBMC donors. Env and Gag mRNA expression was normalised to a housekeeping gene GAPDH mRNA levels. Increased expression of both Env and Gag mRNA was observed in cells infected with L4 and K2 LF Nef viruses, which retain CD3 expression, compared to IL Nef viruses (Figure 3.12B-C). By contrast, no differences in Env mRNA expression were observed when normalised to Gag mRNA (Figure 3.12D), consistent with observation that both Env and Gag mRNA expression is increased for LF Nef viruses. Taken together, this data is consistent with the immunoblot analysis and shows that retained CD3 expression results in increased expression of Env and Gag mRNA, and suggests that the increase of Env and Gag protein is likely due to increased transcription of viral genes. However, this does not explain the specific increased Env incorporation into virions produced in the presence of CD3 on infected cells as expression of both Env and Gag was increased.

Env is expressed on the plasma membrane of infected cells where it gets incorporated into viral particles as they bud from the cell surface. Increased Env incorporation may therefore reflect an increase in Env surface expression on infected cells. To explore this, and further validate the immunoblot and qPCR data, Env protein expression was analysed by flow cytometry. As above, CD4+ T cells were infected for 48h and analysed by flow cytometry to detect total Env expression (intracellular stain) and surface Env expression. Intracellular Env stain was performed using 50-69 Ab clone, recognising fixation-insensitive, linear epitope in the gp41 domain of Env (Yuan et al., 2009). L4 and K2 LF viruses, which retain CD3 expression showed increased levels of intracellular Env compared to IL Nef viruses (Figure 3.13A). This is consistent with immunoblot and qRT-PCR analysis of Env expression. Because virions assemble at and bud from the plasma

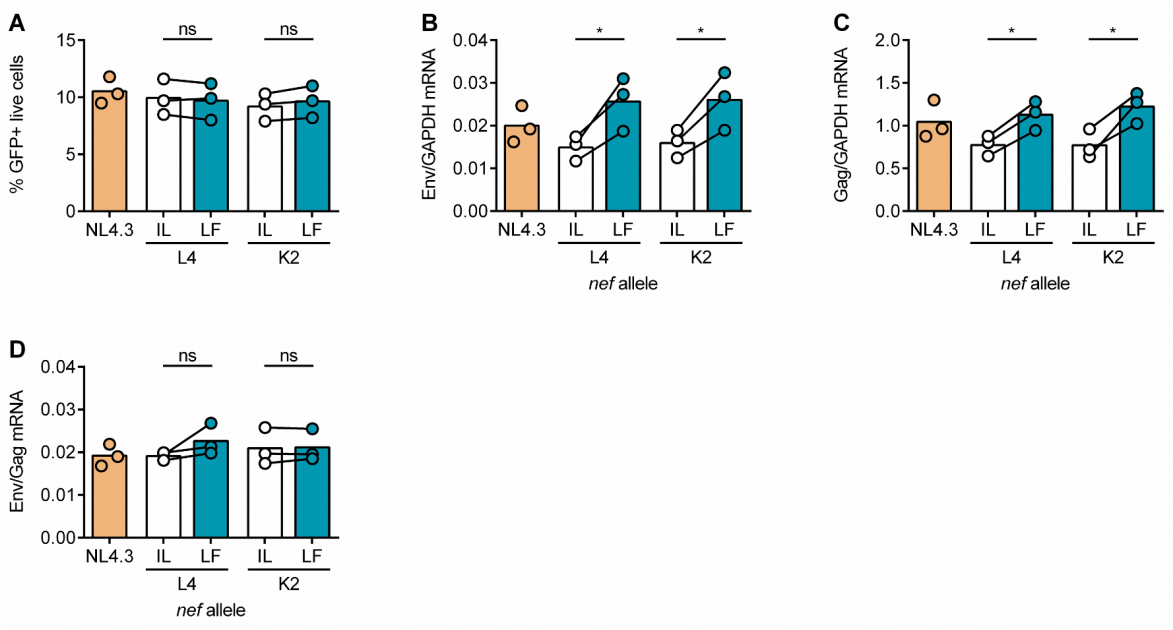

Figure 3.12: Retained CD3 expression results in increased expression of Env and Gag mRNA

Primary CD4+ T cells infected with Nef chimeric viruses were collected at 48h post-infection for flow cytometry analysis to equalise percentage of GFP+ live cells in all samples using autologous uninfected cells. Cells were then analysed by qRT-PCR for Env, Gag, and GAPDH mRNA expression. **(A)** Percentage of GFP+ live cells before mixing with uninfected cells to equalise infection levels. **(B)** Env mRNA relative expression normalized to GAPDH. **(C)** Gag mRNA relative expression normalized to GAPDH. **(D)** Env mRNA relative expression normalized to Gag. Bars show mean and lines join paired results from the same PBMC donor. Groups were compared using paired *t*-test (ns, P>0.05; *, P<0.05; **, P<0.01; ***, P<0.001).

membrane, cell surface expression of Env trimers was next analysed. Surface staining was performed using two conformation-sensitive, broadly neutralising antibodies (bnAbs) that recognise functional Env trimers: PGT151 (cleaved trimer) and PG9 (trimer apex) (Burton et al., 2009; Falkowska et al., 2014). Increased expression of surface Env (as recognised by both antibodies and quantified by the Env MFI) was observed on cells infected with L4 and K2 LF viruses, which retain CD3 expression, when compared to IL Nef viruses (Figure 3.13B-C). This is consistent with increased levels of total (intracellular) Env and taken together this suggest that retained CD3 expression results in increased intracellular and surface expression of Env, which is consistent with (and might explain) higher Env virion incorporation and increased infectivity of these viruses (L4 and K2 LF Nef).

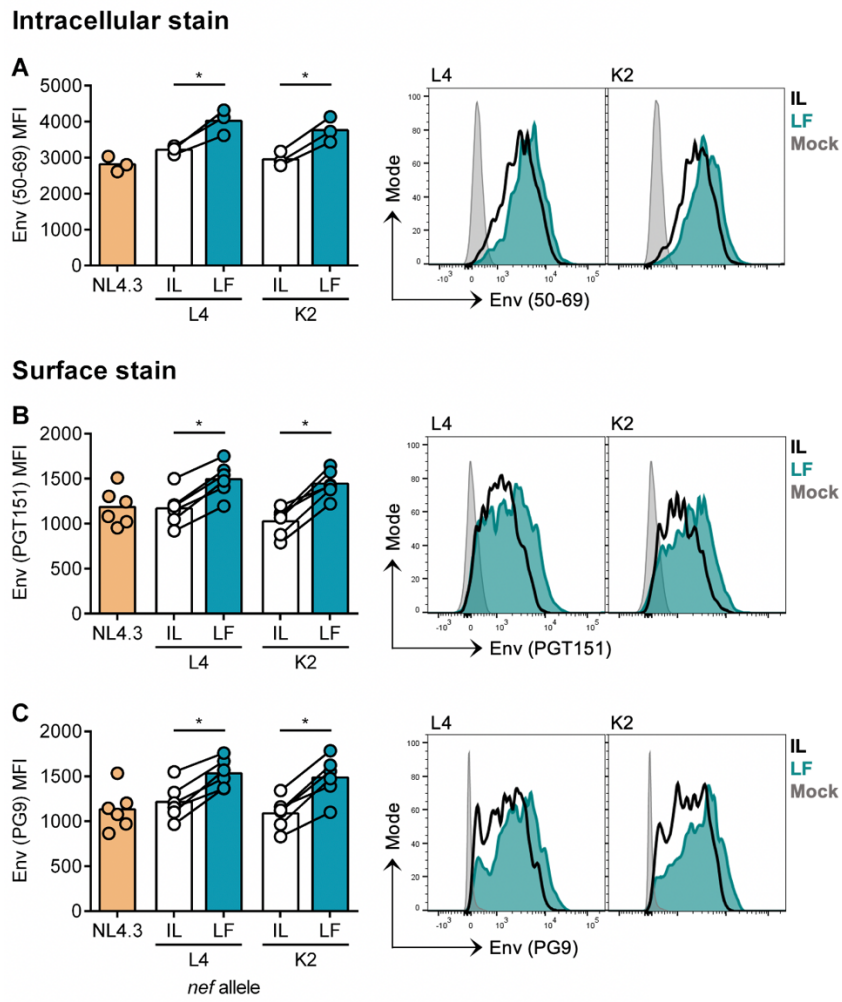

Figure 3.13: Retained CD3 expression results in increased intracellular and surface expression of Env

(A-C) Primary CD4+ T cells infected with Nef chimeric viruses were collected at 48h post-infection for flow cytometry analysis of intracellular and surface Env expression. **(A)** Expression (MFI) of intracellular Env as detected by 50-69 Ab. **(B-C)** Expression (MFI) of surface Env as detected by **(B)** PGT151 Ab, and **(C)** PG9 Ab. Right-hand side panels show representative flow cytometry plots. Mock is uninfected control. Bars show mean and lines join paired results from the same PBMC donor. Groups were compared using paired *t*-test (ns, P>0.05; *, P<0.05; **, P<0.01; ***, P<0.001).

Surface Env is trafficked rapidly between the plasma membrane and the endosomal compartments (Checkley et al., 2011). This is mediated by the presence of endocytic motifs in the Env cytoplasmic tail (membrane proximal YxxL and a C-terminal LL) that are recognised by the clathrin adaptor AP-2, leading to internalisation (Berlioz-Torrent et al., 1999; Boge et al., 1998; Byland et al., 2007; Egan et al., 1996). This limits Env surface expression, and has been proposed as a mechanism to avoid immune detection and antibody-dependent cell-mediated cytotoxicity (ADCC) (Anand et al., 2019; Prévost et al., 2018). Moreover, it has been suggested that Env internalisation and subsequent

sorting to the TGN and/or recycling compartments is required for efficient Env incorporation into virions (Groppelli et al., 2014; Kirschman et al., 2018; Qi et al., 2015). Therefore, to further examine differences in Env surface expression, the kinetics of surface Env internalisation and recycling back to the plasma membrane were investigated. To observe Env internalisation, infected CD4+ T cells were stained with Env PGT151 antibody on ice to label surface Env. Cells were then incubated at 37°C to allow Env internalisation and the remaining surface Env was detected with a fluorescently-labelled secondary antibody by flow cytometry (Figure 3.14A). Comparing the baseline Env surface signal at T_{0min} and the Env signal at various time points following incubation at 37°C allows quantification of Env retention/internalisation as measured by loss of Env signal. Figure 3.14B shows broadly similar levels of Env internalisation for all Nef chimeric viruses as measured by decrease of surface Env over 120min incubation period. However, because L4 and K2 LF Nef viruses had higher baseline levels (T_{0min}) of surface Env compared to IL Nef viruses (consistent with observations in Figure 3.13), it was necessary to normalise the signal for each virus to T_{0min} (set to 100%) and plot the data as the loss of signal over time (Figure 3.14C). This revealed a proportionally greater reduction in surface Env over time for LF viruses (which retain CD3 expression) compared to IL viruses (which downmodulate CD3). This difference was most pronounced after 120min of incubation, and is plotted in Figure 3.14D. These data suggest that L4 and K2 LF Nef viruses, which retain CD3 expression, may have faster kinetics of Env internalisation. Moreover, it suggests that LF Nef viruses do not have higher expression of surface Env because Env is actively retained on the cell surface.

After surface Env is internalised, it is recycled through the endosomal and Golgi compartments back to the plasma membrane (Groppelli et al., 2014; Kirschman et al., 2018; Qi et al., 2013). Having observed differences in Env internalisation, the kinetics of Env recycling were next investigated. To do this, infected CD4+ T cells were incubated with Env PGT151 Ab at 37°C for 1h to allow for Env internalisation, thus labelling surface and total (internalised/recycling) Env (Figure 3.15A). Initial (baseline) level of surface Env was detected with PE-labelled secondary Ab, stained on ice. Cells were then incubated at 37°C for up to 120min in the presence of Cy5-labelled secondary Ab that allows for the detection of recycling (intracellular) Env that was inaccessible to the first (PE-conjugated) antibody but has subsequently recycled back to the cell surface and is now accessible to the second (Cy5-conjugated) antibody. Figure 3.15B shows increasing levels of Cy5-labelled surface Env over time, indicating Env recycling back to

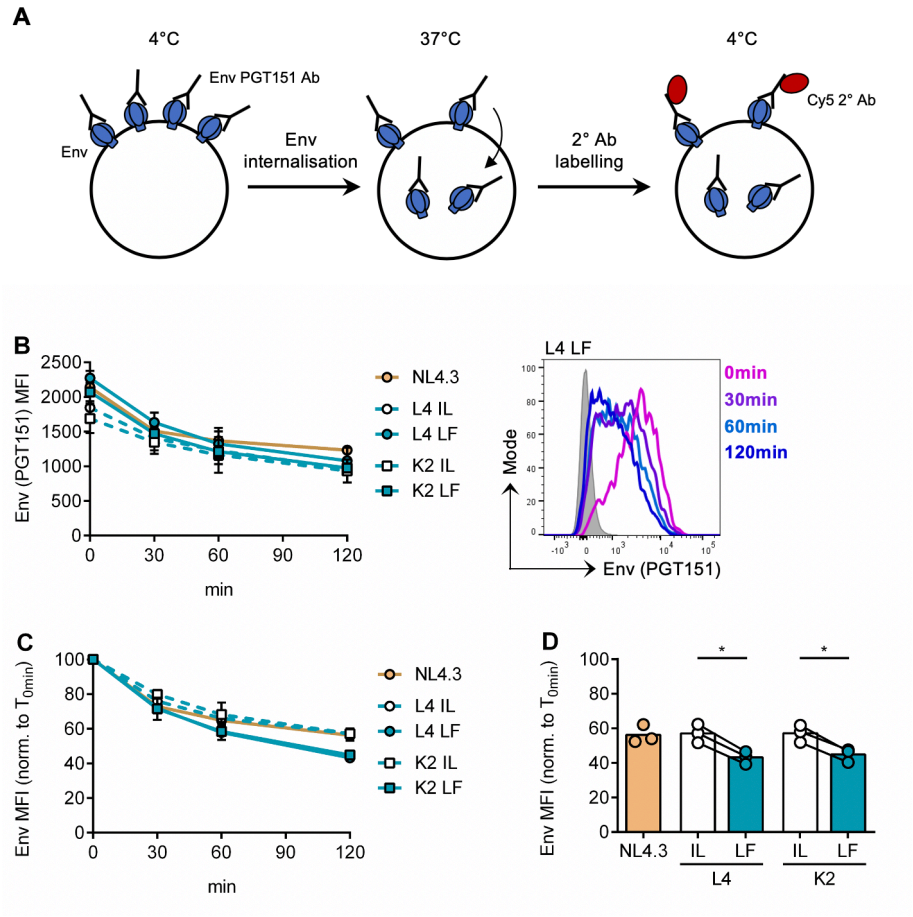

Figure 3.14: Kinetics of Env internalisation by Nef chimeric viruses

(A) Schematic of Env internalisation assay. Infected primary CD4+ T cells were stained on ice with anti-Env PGT151 Ab to label surface Env (n=3). Cells were then incubated for 0-120min at 37°C to allow for Env internalisation. The remaining surface Env was detected with Cy5-labelled 2° Ab and cells were analysed by flow cytometry. **(B)** Surface expression of Env (MFI) in the infected GFP+ cells after incubation at 37°C for the indicated time period. Right-hand side panel shows a representative histogram for L4 LF Nef virus. **(C)** Env MFI values from (B) normalised to T_{0min}. Baseline (T_{0min}) Env MFI for each virus was set as 100% and data show the percentage signal relative to 100% for each time point. **(D)** Normalised Env MFI at 120min. Error bars show mean ± SD. Bars show mean and lines join paired results from the same PBMC donor. Groups were compared using paired *t*-test (ns, P>0.05; *, P<0.05; **, P<0.01; ***, P<0.001).

the plasma membrane. L4 and K2 LF Nef viruses showed higher levels of surface Cy5-labelled Env at all time points compared to IL Nef viruses. A similar trend was observed when Env MFI values were normalised to T_{0min} (Figure 3.15C). Interestingly, LF Nef viruses showed greater proportional increase in surface Env staining compared to IL Nef viruses and this difference was most pronounced after 120min of incubation (Figure 3.15D). This suggests that L4 and K2 LF Nef viruses, which retain CD3 expression, have faster kinetics of Env recycling compared to IL Nef viruses. Together with the Env internalisation data (Figure 3.14), these results suggest that retained CD3 expression in

LF Nef virus infected cells results in faster kinetics of Env trafficking between the plasma membrane and recycling compartments.

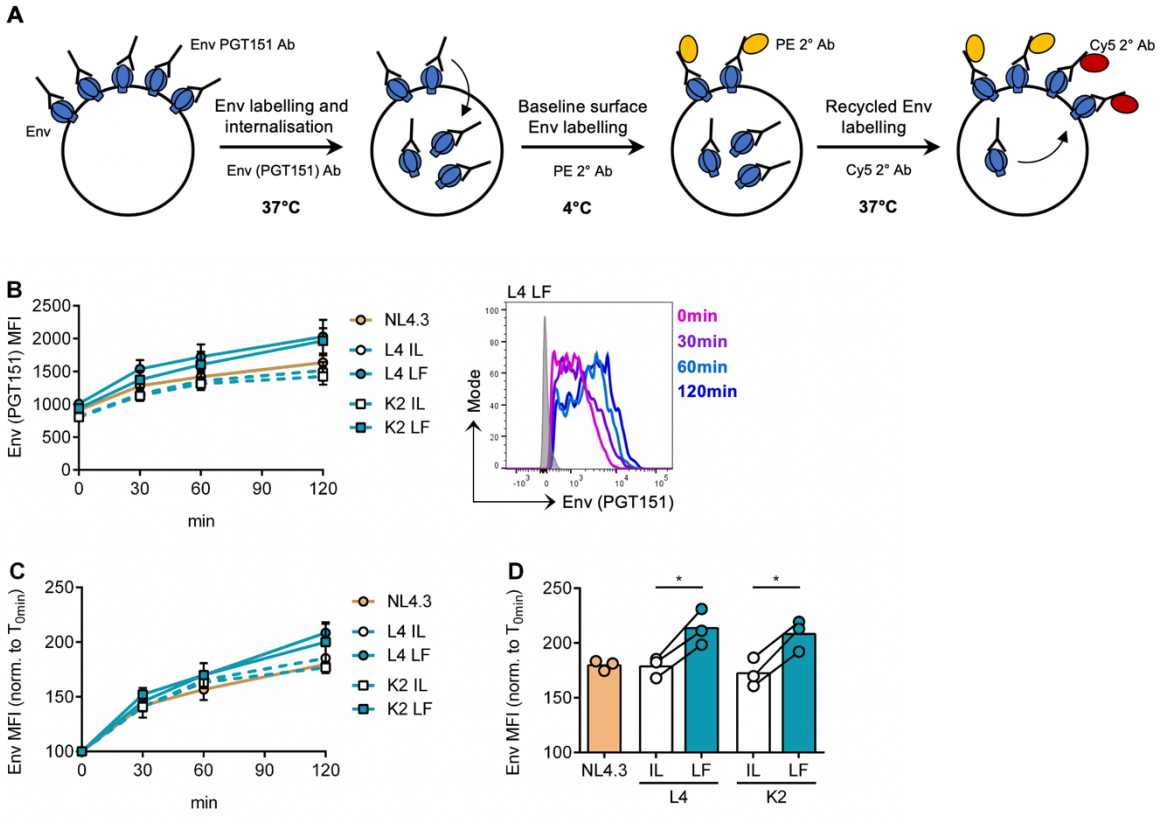

Figure 3.15: Kinetics of Env recycling by Nef chimeric viruses

(A) Schematic of Env recycling assay. Infected primary CD4+ T cells were stained at 37°C with anti-Env PGT151 Ab to allow for Env internalisation, thus labelling both surface and internalised/recycling Env (n=3). Cells were stained on ice with PE-labelled 2° Ab to label surface Env at baseline. Cells were then incubated for 0-120min at 37°C to allow for Env recycling. Increase in recycled surface Env was detected using Cy5-labelled 2° antibody and cells were analysed by flow cytometry. **(B)** Surface expression of Env (MFI) as detected by Cy5-labelled 2° antibody in the infected GFP+ cells after incubation at 37°C for the indicated time periods. Right-hand side panel shows a representative histogram for L4 LF Nef virus. **(C)** Env MFI values from (B) normalised to T_{0min}. Baseline (T_{0min}) Env MFI for each virus was set as 100% and data show the percentage signal relative to 100% for each time point. **(D)** Normalised Env MFI at 120min. Error bars show mean ± SD. Bars show mean and lines join paired results from the same PBMC donor. Groups were compared using paired *t*-test (ns, P>0.05; *, P<0.05; **, P<0.01; ***, P<0.001).

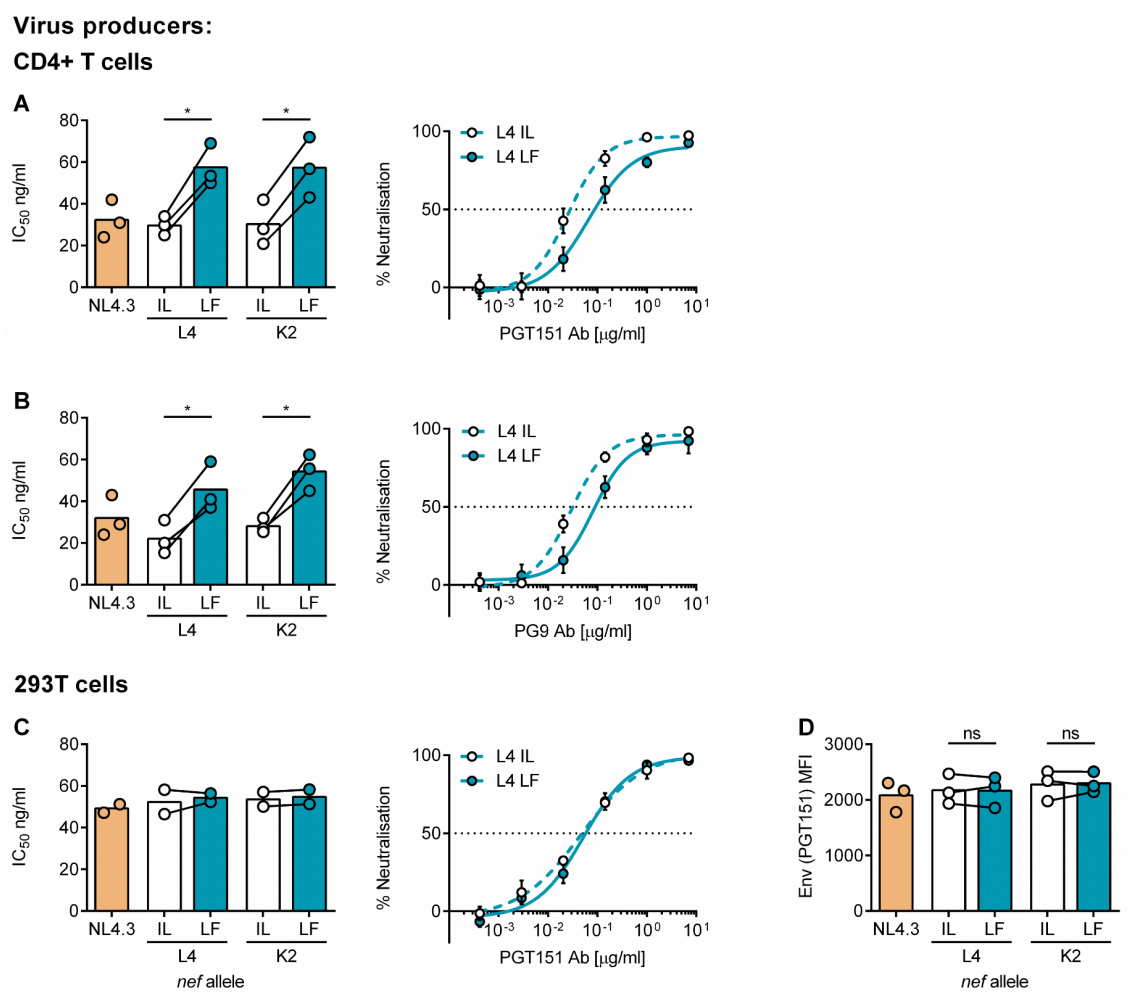

Figure 3.16: Antibody neutralisation of Nef chimeric viruses

Virus produced from primary CD4+ T cells and HEK293T cells was analysed by neutralisation assays. These were performed using HeLa-TZMbl reporter cell line with equal amounts of infectious supernatant and increasing amounts of bnAbs. IC_{50} values were calculated by non-linear regression analysis of the neutralisation curves. **(A-B)** Primary CD4+ T cells were infected with Nef chimeric viruses and cell culture supernatants were collected at 48h post-infection for antibody neutralisation analysis. Shown are IC_{50} values for **(A)** PGT151 Ab, and **(B)** PG9 Ab. **(C)** HEK293T cells were transfected with Nef chimeric proviruses and virus supernatants collected at 48h post-transfection for antibody neutralisation analysis. Shown are IC_{50} values for PGT151 Ab. Right-hand panels show representative examples of neutralisation curves. **(D)** HEK239T cells were analysed for surface expression (MFI) of Env (PGT151 Ab) at 48h post-transfection. Bars show mean and lines join paired results from the same PBMC donor. Error bars show mean ± SD. Groups were compared using paired *t*-test (ns, P>0.05; *, P<0.05; **, P<0.01; ***, P<0.001).

To further confirm that increased Env trimer surface expression correlates with increased Env virion incorporation (as measured by immunoblot analysis), incorporation of functional Env trimers into virions was analysed by antibody neutralisation assay. The standardised Ab neutralisation assay was performed using HeLa-TZMbl reporter cell line (Montefiori, 2009) and PGT151 and PG9 Ab (described above). Equal amounts of

infectious virus produced from CD4+ T cells were titrated against increasing doses of antibodies to obtain neutralisation curves and to calculate IC_{50} values. L4 and K2 LF Nef viruses, which retain CD3 expression, are harder to neutralise, thus have higher IC_{50} values compared to IL Nef viruses (Figure 3.16A-B). Higher IC_{50} values are consistent with increased Env trimer incorporation into virions, which thus require more antibody for neutralisation. This result is consistent with immunoblot analysis, showing increased Env virion incorporation in LF Nef viruses (Figure 3.11). As a control, virus produced from 293T cell transfection was used in the neutralisation assay. No differences in IC_{50} values were observed between IL and LF Nef viruses (Figure 3.16C). This is consistent with observations that these viruses are equally infectious when produced from 293T cells (Figure 3.2), and express equal levels of surface Env in 293T cells (Figure 3.16D). Taken together, these results show that retained CD3 expression on infected CD4+ T cells results in production of virus that is harder to neutralise, which correlates with increased surface Env expression and Env virion incorporation.

3.2.4 Manipulation of Env expression and virion infectivity

To gain insight into the mechanism of increased Env expression, it was examined whether the effect of CD3 modulation on Env expression and viral infectivity was specific to primary CD4+ T cells or whether this could also be observed using T cell lines. To investigate this, Jurkat T cells, which are a commonly used model T cell line for HIV-1 infection, were used to measure Env expression, viral infectivity and spread. Jurkat cells were infected with Nef chimeric viruses and analysed by flow cytometry 48h post infection. It was confirmed that L4 and K2 IL Nef viruses were able to downmodulate CD3 expression in these cells, while NL4.3, and L4 and K2 LF Nef viruses retained CD3 expression (Figure 3.17A). However, no differences in surface Env expression (detected by PGT151 and PG9 Abs) or virion infectivity were observed between IL and LF Nef viruses (Figure 3.17D-F). To further validate this phenotype, cell-cell spread was measured (as described in Figure 3.5), which showed similar numbers of Gag+ or GFP+ target cells in all infected cultures (Figure 3.17B-C). Together these data show that Env expression, virion infectivity and viral spread is independent of CD3-modulation in a Jurkat cell line.

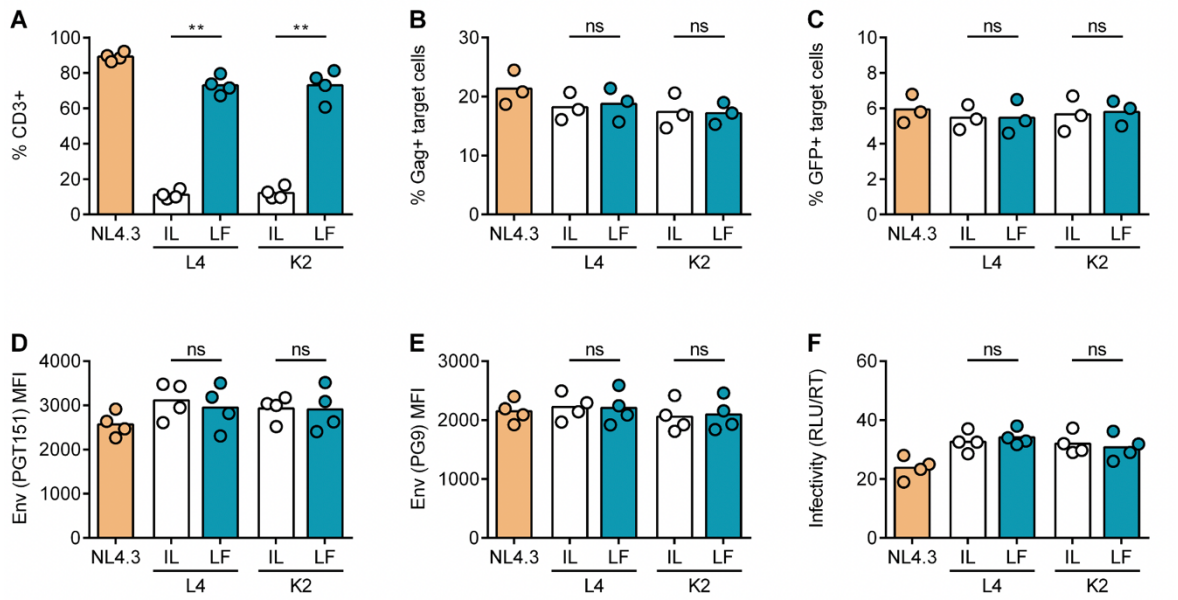

Figure 3.17: Viral spread, Env expression and virion infectivity are independent of CD3-modulation in Jurkat T cells

Jurkat T cells were infected with Nef chimeric viruses were analysed by flow cytometry 48h post-infection. **(A)** Percentage of CD3+ cells in infected (GFP+) population. **(B-C)** Jurkat cells infected with indicated viruses were mixed with autologous pre-labelled target cells and analysed by flow cytometry at 24h post-mix as described in Figure 3.6. Shown is percentage of **(B)** Gag+ target cells, and **(C)** GFP+ target cells at 24h post-mix. **(D-E)** Surface expression (MFI) of Env as detected by **(D)** PGT151 Ab, and **(E)** PG9 Ab. **(F)** Virus supernatant was collected at 48h post-infection and analysed for virion infectivity as described in Figure 3.10. Bars show mean and symbols show individual replicates. Groups were compared using unpaired *t*-test (ns, P>0.05; *, P<0.05; **, P<0.01; ***, P<0.001).

The inability to detect any differences between IL and LF viruses using Jurkat cells may reflect the fact that these cells are a transformed and constitutively (hyper) activated T cell line (Gioia et al., 2018), which may mask the effect of Nef-mediated CD3-modulation. Having shown that the effect of Nef-mediated enhancement of Env expression and viral infectivity was restricted to primary CD4+ T cells, the interplay between CD3 expression, T cell activation and enhanced virion infectivity was examined. Specifically, we hypothesised that co-culture of infected and uninfected primary CD4+ T cells may trigger the TCR/CD3 complex during cell-cell contact (Len et al., 2017), leading to CD3 dependent differences between IL and LF viruses. The TCR/CD3 complex drives T cell activation following formation of immunological synapse with an antigen-presenting cell (Dustin & Depoil, 2011). Similarly, TCR signalling is triggered during virological synapse formation (Len et al., 2017). As such, retained CD3 expression on infected cells could allow triggering of TCR signalling and T cell activation during VS formation, thus boosting viral gene expression and enabling more efficient viral spread. Therefore, to explore how

T cell activation affects Env expression and virion infectivity, it was examined whether Env expression and virion infectivity could be boosted by stimulating infected primary CD4+ T cells. Activated CD4+ T cells were infected with Nef chimeric viruses and 24h post-infection re-stimulated with anti-CD3/CD28 Abs or left untreated. Cells were analysed by flow cytometry 24h post-stimulation (Figure 3.18A). Equal levels of infection were observed across all cell cultures, with a slight decrease in cell viability in the stimulated condition, (Figure 3.18B-C), consistent with activation-induced cell death (Zhan et al., 2017). T cell activation was confirmed by upregulation of the activation marker CD69 in all stimulated cell cultures compared to untreated control (Figure 3.18D). CD3/CD28 stimulation increased CD69 expression further in cells infected with viruses that retain CD3 expression (NL4.3, L4 LF and K2 LF) compared to viruses that downmodulate CD3 (L4 IL and K2 IL) (52% vs 65% CD69+ infected cells). This is consistent with the idea that CD3-retaining cells are better able to respond to CD3 stimulation. Similarly, increased expression of CD69 was observed in the untreated condition for viruses that retain CD3 expression compared to viruses that downmodulate CD3 (36% vs 18% CD69+ infected cells). This is consistent with the hypothesis that CD3 expression on infected cells allows triggering of TCR signalling and T cell activation during VS formation between infected and uninfected T cells in cell culture. Next, viral gene expression was analysed following CD3/CD28 stimulation by measuring GFP and Env MFI in the infected cell (GFP+) population. No differences between stimulated and unstimulated cells were observed in expression of GFP or Env between the viruses (Figure 3.18E-F). Similarly (and consistent with equal levels of Env expression), no stimulation-dependent enhancement of virion infectivity was observed (Figure 3.18G). These data show that despite apparent T cell activation (CD69 upregulation), there is no further increase in viral gene expression (GFP reporter and Env) and virion infectivity following CD3/CD28 stimulation.

One confounder to the above experiment is that the cells were already activated (initial CD3/CD28 stimulation) to make primary T cells permissive to HIV-1 infection, thus it is possible that the second activation may not be able to further boost viral gene expression. To test this idea, the experimental setup was modified to stimulate CD4+ T cells with IL-7 only to make them permissive for HIV infection, without inducing robust T cell activation (Coiras et al., 2016) in order to see if subsequent CD3/CD28 stimulation would result in a stimulation-dependent increase in viral gene expression and virion infectivity. IL-7 stimulated CD4+ T cells were infected for 48h and then stimulated with

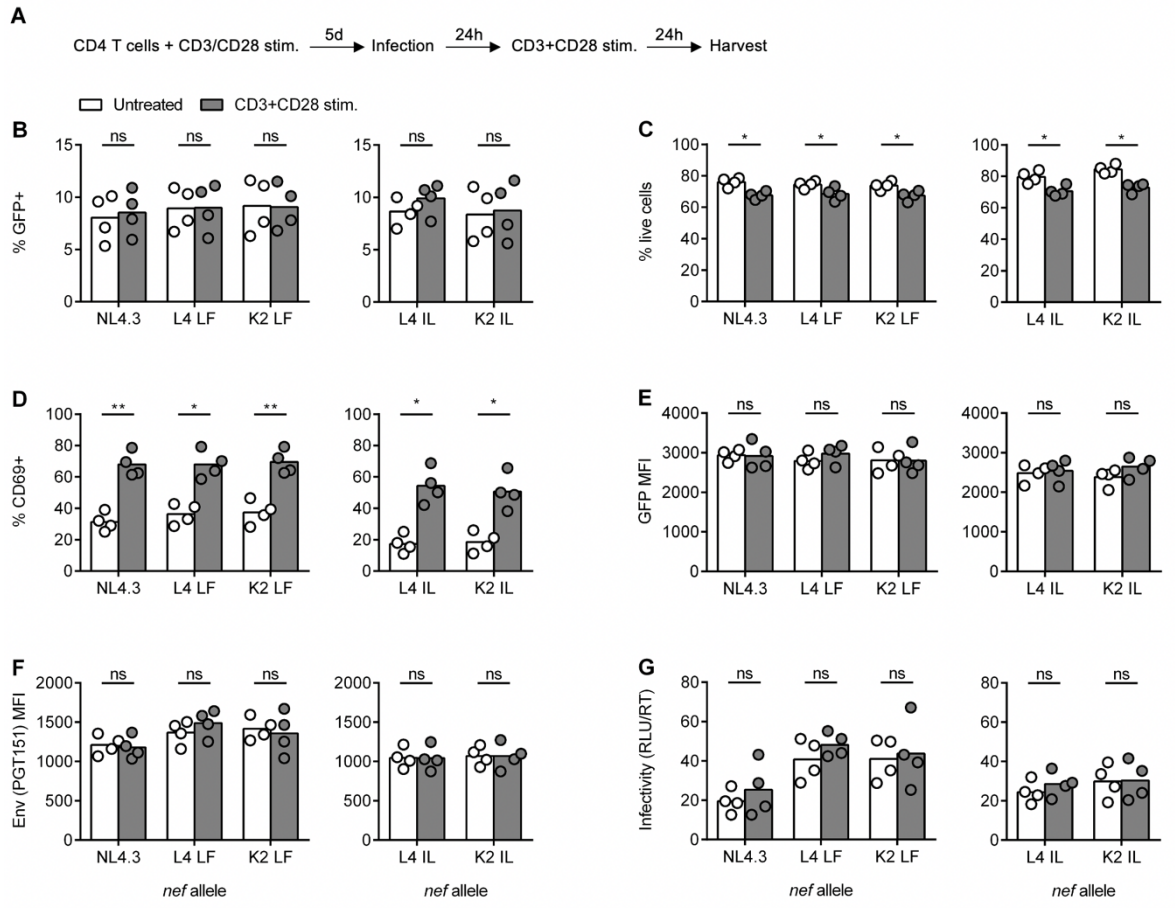

Figure 3.18: Env expression and virion infectivity are not affected by T cell stimulation in activated infected cells

Resting CD4+ T cells were stimulated with anti-CD3/CD28 antibodies for 5 days and then infected with Nef chimeric viruses. 24h post-infection cells were re-stimulated with anti-CD3/CD28 antibodies for 24h or left untreated. **(A)** Schematic of the experimental setup. **(B-F)** Cells were analysed by flow cytometry at 24h post-stimulation to measure percentage of (B) GFP+ live cells, **(C)** live cells, **(D)** CD69+ live cells, and expression (MFI) of **(E)** GFP, and **(F)** Env trimers (PGT151 Ab) in GFP+ population. **(G)** Virus supernatant was collected at 24h post-stimulation and analysed for virion infectivity as described in Figure 3.10. Bars show mean and symbols show individual PBMC donors. Groups were compared using paired *t*-test (ns, P>0.05; *, P<0.05; **, P<0.01; ***, P<0.001).

CD3/CD28 antibodies for 24h and analysed by flow cytometry (Figure 3.19A). Partial CD3 downmodulation in IL Nef virus infected (GFP+) cells (≈30% CD3+ infected cells) was observed 48 post-infection, prior to stimulation (Figure 3.19B). Equal levels of infection were confirmed across all cell cultures, with a small decrease in cell viability observed in the stimulated condition (Figure 3.19C-D). T cell activation was confirmed by marked upregulation of CD69 on stimulated cells (≈90% CD69+) in all infected cell cultures (Figure 3.19E). Notably, under these conditions C3/CD28 stimulation of infected

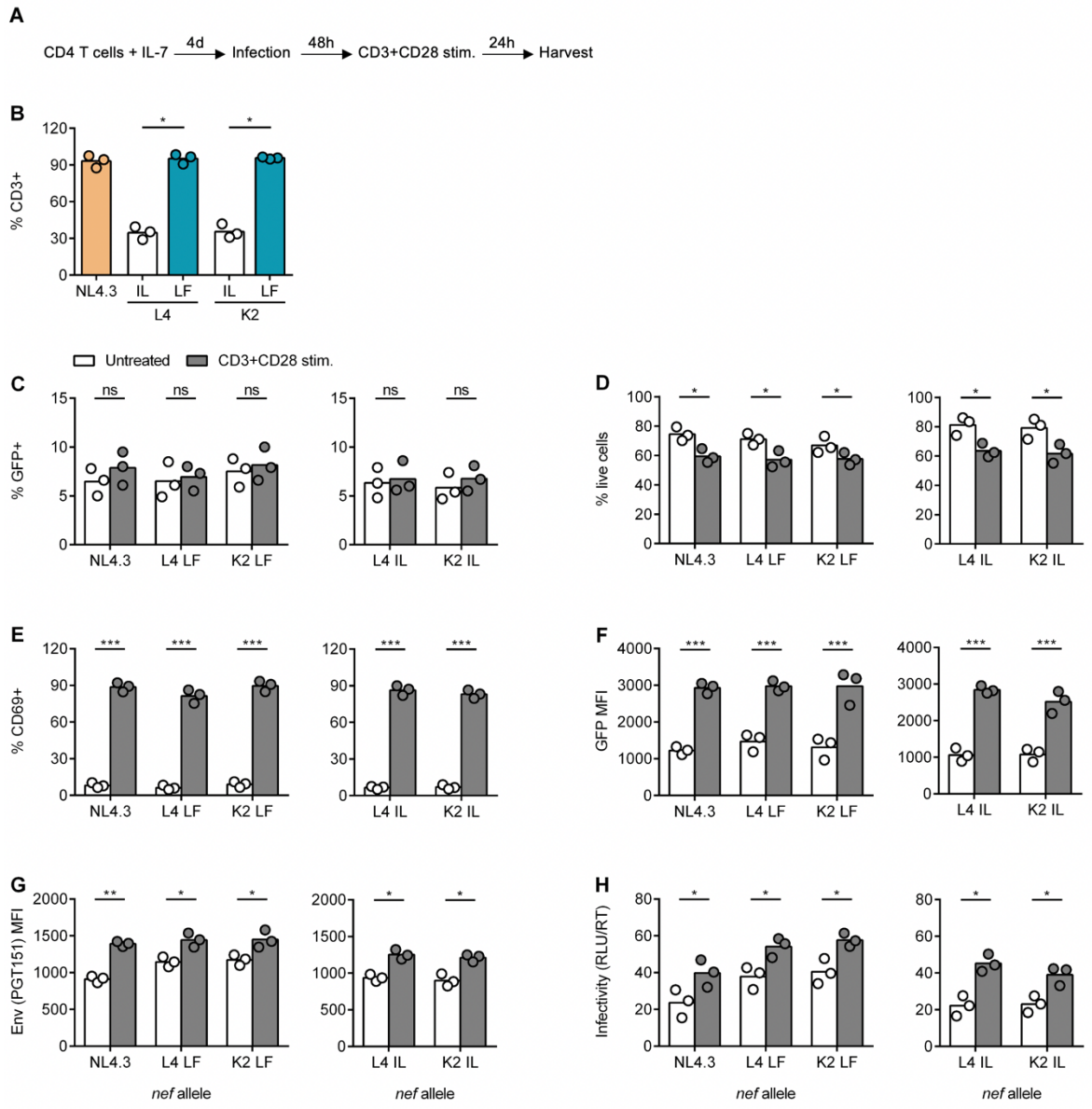

Figure 3.19: Env expression and virion infectivity is increased by T cell stimulation in IL-7 treated infected cells

Resting CD4+ T cells were treated with IL-7 for 4 days and then infected with Nef chimeric viruses. 48h post-infection cells were stimulated with anti-CD3/CD28 antibodies for 24h or left untreated. **(A)** Schematic of the experimental setup. **(B)** Percentage of CD3+ cells in infected (GFP+) population at 48h post-infection. **(C-G)** Cells were analysed by flow cytometry at 24h post-stimulation to measure percentage of **(C)** GFP+ live cells, **(D)** live cells, **(E)** CD69+ live cells, and expression (MFI) of **(F)** GFP, and **(G)** Env trimers (PGT151 Ab) in GFP+ population. **(H)** Virus supernatant was collected at 24h post-stimulation and analysed for virion infectivity as described in Figure 3.10. Bars show mean and symbols show individual PBMC donors. Groups were compared using paired *t*-test (ns, P>0.05; *, P<0.05; **, P<0.01; ***, P<0.001).

cells resulted in increased expression of GFP and Env when compared to untreated controls (Figure 3.19F-G). The fact that this effect was seen across all Nef viruses,

including CD3-downmodulating IL Nef viruses, is most likely explained by a proportion of the IL Nef infected cells still expressing CD3 at the time of stimulation (Figure 3.19B), meaning they had yet to downregulate CD3 and were thus able to respond to stimulation. Despite this, slightly higher expression of GFP and Env can still be observed for viruses that retain CD3 expression (NL4.3, L4 LF and K2 LF) compared to CD3-dowmnodulating viruses (L4 and K2 IL) (Figure 3.19F-G). This was expected as CD3 expressing cells should be better able to respond to CD3 stimulation. Similar to the increase in GFP and Env expression, increased virion infectivity was also observed in the stimulated condition, again with higher increase for CD3-retaining viruses (Figure 3.19H). These data show that inducing robust T cell activation in resting, IL-7 treated infected cells results in increased viral gene expression (GFP reporter and Env) and virion infectivity.

To confirm that the differences in Env expression and virion infectivity are due to Nef-mediated modulation of CD3 expression, and not due to other yet unidentified function of residues 123 and 146 in Nef, RNAi was used to knock-down (KD) CD3 expression in primary CD4+ T cells. Activated CD4+ T cells were electroporated with siRNA to deplete CD3ζ (or non-targeting siRNA) and infected with Nef chimeric viruses (Figure 3.20A). Flow cytometry analysis confirmed reduced expression of CD3ζ 48h after KD, as well as corresponding reduction in CD3ε expression, with negligible change in CD4 expression (Figure 3.20B). Cells were then infected for 48h and analysed by flow cytometry. It was confirmed that CD3ζ KD did not affect HIV-1 infection levels or cell viability in infected cell cultures (Figure 3.20C-D). Reduced CD3ε expression was confirmed at 48h post-infection in CD3 KD cells infected with viruses that do not downmodulate CD3 (NL4.3, L4 LF and K2 LF) compared to control KD (Figure 3.20E). Of note, CD3ζ KD did not reduce CD3 expression to the same levels as observed in cells infected with L4 and K2 IL Nef viruses (≈2000 vs ≈800 CD3 MFI). Next, the effect of CD3 depletion on T cell activation and viral gene expression was analysed by measuring the expression of CD69, GFP and Env. CD3ζ KD resulted in reduced T cell activation compared to control KD as measured by CD69 expression, and reduced viral gene expression as measured by GFP reporter expression in cells infected with viruses that do not downmodulate CD3: NL4.3, L4 LF and K2 LF (Figure 3.20F-G). This effect was very small or insignificant in L4 and K2 IL viruses that already downmodulate CD3 expression. Consistent with reduced CD69 and GFP expression, CD3ζ KD also resulted in reduced surface expression of Env in cells infected with viruses that do not downmodulate CD3 (Figure 3.20H). This effect was still observed, albeit to smaller extent, for viruses that already

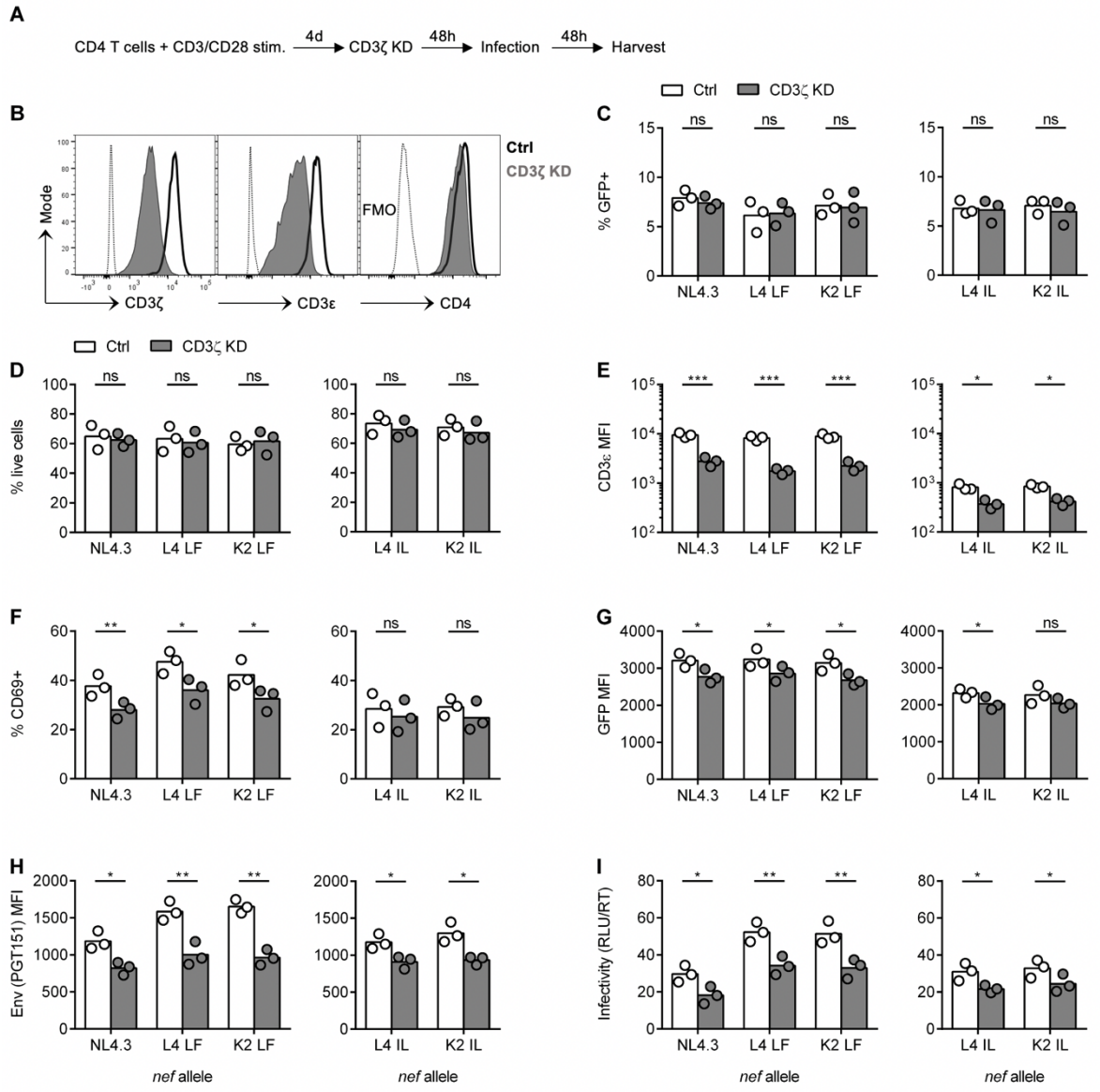

Figure 3.20: CD3 knock-down reduces T cell activation, surface Env expression and virion infectivity
Activated primary CD4+ T cells were electroporated with siRNA targeting CD3ζ (CD247) or a non-targeting control for 48h and infected with indicated viruses. **(A)** Schematic of the experimental setup. **(B)** Representative histograms show flow cytometry analysis of intracellular expression of CD3ζ (CD247) and surface expression of CD3ε, and CD4 at 48h post-knockdown. **(C-H)** 48h post-infection cells were analysed by flow cytometry to measure **(C)** percentage of GFP+ live cells, **(D)** percentage of live cells, and expression of **(E)** CD3ε, **(F)** CD69, **(G)** GFP, and **(H)** Env trimers (PGT151 Ab) in GFP+ population. **(I)** Virus supernatant was collected at 48h post-infection and analysed for virion infectivity as described in Figure 3.10. Bars show mean and symbols show individual PBMC donors. Groups were compared using paired *t*-test (ns, P>0.05; *, P<0.05; **, P<0.01; ***, P<0.001).

downmodulate CD3 expression (L4 and K2 IL). Reduced Env expression for these viruses is likely due to further decrease in CD3 expression by CD3ζ KD (≈800 vs ≈400 CD3 MFI, Figure 3.20E). Consistent with reduced Env expression, CD3ζ KD also

reduced virion infectivity (Figure 3.20I). Again, this effect was greater for viruses that do not downmodulate CD3 expression (NL4.3, L4 LF and K2 LF) compared to viruses that do (L4 IL and K2 IL). Taken together, these data show that RNAi-mediated CD3ζ depletion phenocopies Nef-mediated CD3 downmodulation in infected cells. This confirms that the observed phenotype of these viruses is specific to their CD3-modulation abilities. Furthermore, CD3ζ-depletion mediated reduction in viral gene expression and infectivity is in agreement with previous experiments which showed activation- and CD3-dependent enhancement of viral gene expression and infectivity.

3.2.5 Retained CD3 expression results in increased T cell activation during cell-cell spread

Previous work showed that HIV-1 cell-cell spread between T cells results in activation of T cell signalling in the infected donor and target cell, which is mediated in part by the TCR/CD3 complex (Len et al., 2017). Furthermore, previous experiments in this chapter (Figure 3.18, 3.20) showed CD3-dependent differences in T cell activation and viral gene expression in infected cells. Thus, it was further explored how retained CD3 expression affects T cell activation during cell-cell spread. To do so, the same experimental setup was used as for the cell-cell spread assay described in Figure 3.5. The expression of activation markers in infected (GFP+) donor and target cell population after 24h of co-culture (to allow for cell-cell contact and VS formation) was measured. The analysis included some of the classical cell surface activation markers: CD69, CD38, and PD-1, which are increased early after activation (Caruso et al., 1997; Chikuma et al., 2009), as well as phosphorylation of ribosomal S6 protein (phospho-S6), activated by downstream TCR signalling (Chapman & Chi, 2015). Figure 3.21A-D shows that donor-target cell co-culture resulted in increased expression of CD69, CD38, PD-1, and phospho-S6 in NL4.3 Nef virus infected donor cells compared to uninfected (mock) cells. This is consistent with previous observations showing that cell-cell viral spread induces T cell signalling (Len et al., 2017). Notably, the increase in expression of CD69, CD38, PD-1, and S6 phosphorylation in donor T cells infected with L4 and K2 LF Nef viruses, which retain CD3 expression, was greater than that observed for the IL Nef counterparts, suggesting a contribution of CD3 expression to this phenotype. Next, target cells in the co-culture were also analysed, and a similar trend was seen in the newly infected target cell population (Figure 3.21E-H). Here, increased expression of CD69, PD-1, and S6 phosphorylation in L4 and K2 LF Nef virus infected target cells was observed when compared to IL Nef virus infected cells. By contrast, CD38 remained unchanged between

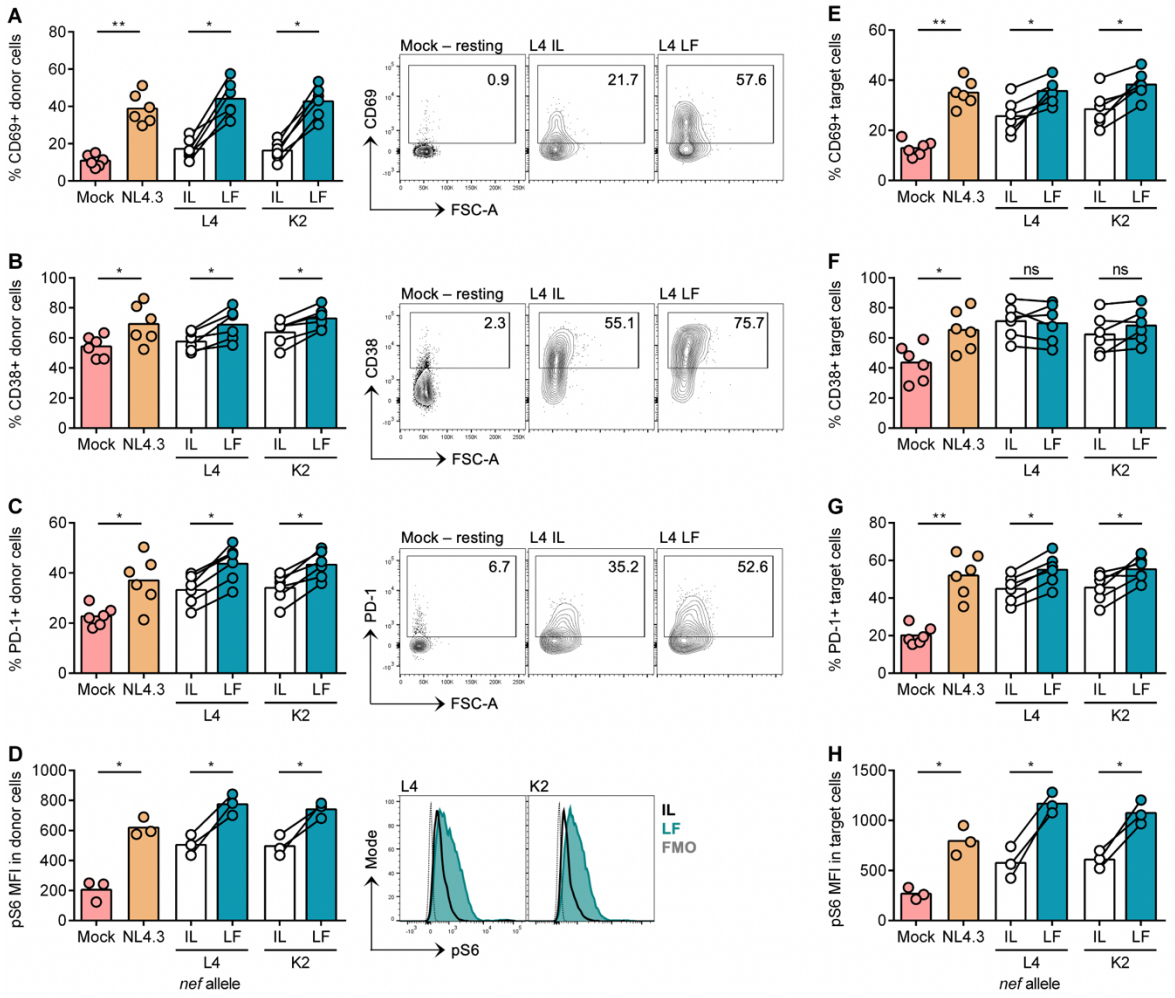

Figure 3.21: Retained CD3 expression results in increased T cell activation during cell-cell spread in donor and target cells.

Primary CD4+ T cells infected with indicated viruses were mixed with autologous pre-labelled target cells and analysed by flow cytometry 24h post-mix as described in Figure 3.5. **(A-D)** Infected (GFP+) donor cell population was analysed for expression of activation markers. Show is percentage of positive donor cells for **(A)** CD69, **(B)** CD38, **(C)** PD-1, and **(D)** MFI of phospho-S6 (pS6). Right-hand side panels show representative flow cytometry plots. Uninfected (mock) resting CD4+ T cells are shown for comparison. **(E-H)** Infected (GFP+) target cell population was analysed for expression of activation markers. Show is percentage of positive target cells for **(E)** CD69, **(F)** CD38, **(G)** PD-1, and **(H)** MFI of phospho-S6 (pS6). Mock is uninfected control and total live population of donor or target cells was analysed. Bars show mean and lines join paired results from the same PBMC donor. Groups were compared using paired *t*-test (ns, P>0.05; *, P<0.05; **, P<0.01; ***, P<0.001).

IL and LF Nef viruses, possibly due to already high expression of this marker on all infected cells. Observing CD3-dependent differences in the expression of activation markers in the newly-infected target cells was somewhat unexpected, because at the beginning of co-culture experiment, target cells in all infected cell cultures express CD3, and should thus respond similarly to cell-cell spread induced activation. A possible

explanation for this observation is that increased viral spread of LF Nef viruses (Figure 3.6) is also associated with enhanced transfer of viral particles across the VS and accelerated replication kinetics, thus resulting in increased T cell activation of target cells. Alternatively, donor-target cell cross-talk may occur at the VS, thus enhanced signalling in the donor cell may result in secretion of other factors leading to enhanced signalling and activation of target cells.

To address whether increased T cell activation observed in donor cells after 24h of co-culture (Figure 3.21) was induced by cell-cell contact, expression of activation markers in infected donor cells was quantified at 0h post-mix (48h post-infection), before donor and target cells had time to interact. Increased expression of CD69, CD38, PD-1, and S6 phosphorylation was apparent in NL4.3 Nef infected donor cells compared to mock infected cells. This is consistent with previous observation showing HIV-1 infected cells are hyperactivated (Cavrois et al., 2017; Corneau et al., 2017; Pardons et al., 2019; Rato et al., 2017). However, increased expression of these markers in donor cells infected with L4 and K2 LF Nef viruses, which retain CD3 expression, was also apparent when these viruses were compared to their IL Nef counterparts (Figure 3.22A-D). This observation is consistent with previous observations in this Chapter showing that retained CD3 expression on infected cells at 48h post-infection already resulted in increased Env expression and increased virion infectivity. Since donor cell cultures were only 10-20% GFP+ at 48h post-infection (Figure 3.5B), there would be enough opportunity for infected-uninfected donor cell contact during this period to allow for activation of T cell signalling. To further examine changes in T cell activation, expression of CD69, CD38, PD-1, and phosho-S6 was compared in infected donor cells at 0h and 24h post-mix with target cells. Comparing expression of CD69 and S6 phosphorylation (Figure 3.22E,H), both markers showed increased expression over time in all infected cell cultures. Moreover, the increase was greater in LF Nef infected cells, which retain CD3 expression, and are thus better able to trigger TCR signalling. The increase observed in IL Nef infected cells is likely due to incomplete CD3 downmodulation by these viruses (Figure 3.3A). This increase in cell activation over time (as measured by CD69 expression and S6 phosphorylation) is consistent with the hypothesis that continuous donor-target cell contact is triggering T cell activation, which is increased by retained CD3 expression. By contrast, decreased expression of PD-1 over time was observed in the infected donor cells (Figure 3.22G). This is consistent with rapid upregulation of PD-1 upon T cell activation, which diminishes over time (Chikuma et al., 2009). Notably, the decrease in PD-1 expression over time appeared to be smaller in LF

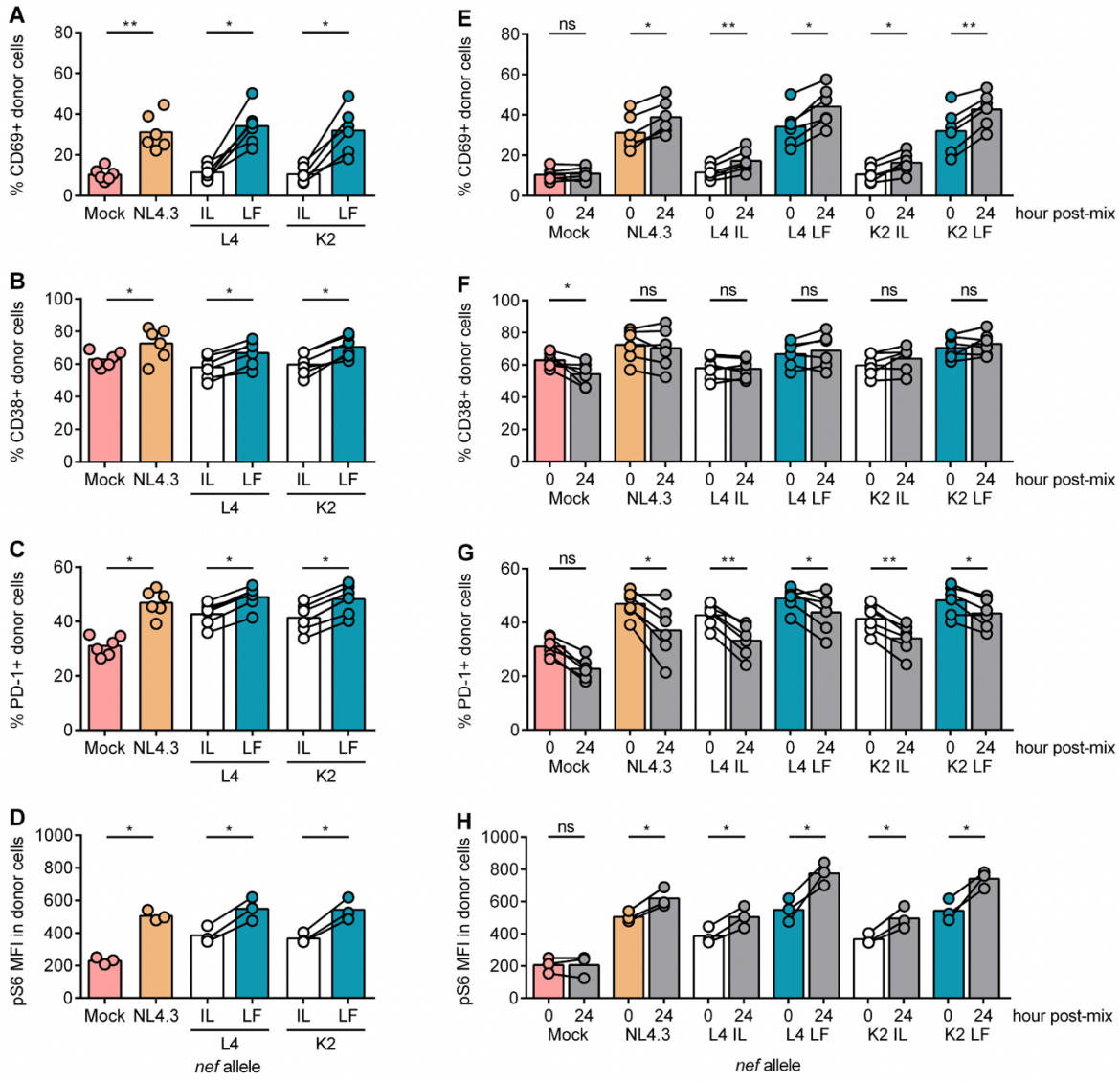

Figure 3.22: Changes in T cell activation in donor cells during cell-cell spread

Donor cells were analysed for expression of activation markers as described in Figure 3.21 at 0h post-mix. **(A-D)** Infected (GFP+) donor cell population was analysed for expression of activation markers. Shown is percentage of positive donor cells for **(A)** CD69, **(B)** CD38, **(C)** PD-1, and **(D)** MFI of phospho-S6 (pS6). **(E-H)** Shown is comparison of activation marker expression at 0h post-mix (as shown in panels A-D) and at 24h post-mix (as shown in Figure 3.21A-D). Percentage of positive infected donor cells for **(E)** CD69, **(F)** CD38, **(G)** PD-1, and **(H)** MFI of pS6. Mock is uninfected control and total live population of donor cells was analysed. Bars show mean and lines join paired results from the same PBMC donor. Groups were compared using paired *t*-test (ns, P>0.05; *, P<0.05; **, P<0.01; ***, P<0.001).

Nef infected cells, which retain CD3 expression. Although multiple factors are like to affect PD-1 expression, this is again consistent with the hypothesis that continuous donor-target cell contact is triggering T cell activation in a CD3-dependent manner. Interestingly, no significant time-dependent changes were observed in the expression of

CD38 for any of Nef viruses (Figure 3.22F). This suggests that the difference in CD38 expression was established early during infection and was maintained during the time period investigated.

HIV-1 viral gene expression is tightly linked to T cell activation (Gagne et al., 2019; Sauter et al., 2015; Shan et al., 2017; Stevenson et al., 1990; Weiss et al., 2014). Having observed CD3-dependent differences in T cell activation during cell-cell spread, it was investigated if increased T cell activation correlates with increased viral (or GFP-reporter) gene expression in cells that retain CD3 expression. As above, LTR-driven expression of Gag and GFP was measured in infected donor and target cells during cell-cell spread. L4 and K4 LF Nef virus infected donor cells, which retain CD3 expression, showed higher GFP MFI (GFP+ population) and higher Gag MFI (Gag+ population) at 0h and 24h post-mix compared to IL Nef viruses (Figure 3.23A-D). This is consistent with observation that these cells also showed increased T cell activation at both time points (Figure 3.22). Moreover, this is also consistent with increased Env expression of CD3-retaining viruses (Figure 3.13). Similarly, higher GFP MFI and Gag MFI in L4 and K2 LF Nef virus infected target cells was apparent at 24h post-mix (Figure 3.23E-F). Again, this is consistent with higher activation status of these cells (Figure 3.21E-H). Taken together, these results show that retained CD3 expression in infected cells results in increased expression of Gag and GFP proteins during cell-cell spread, consistent with increased T cell activation of these cells. Furthermore, target cells infected with LF Nef viruses, which retain CD3 expression, showed both increased percentage of GFP+ and Gag+ cells (Figure 3.6), and increased expression (MFI) of GFP and Gag proteins.

CD3-expression dependent differences in T cell activation (Figure 3.22) and viral gene expression (Figure 3.13, Figure 3.23) were already apparent before donor-target cell co-culture (i.e. 0h post-mix or 48h post-infection). Thus, it was hypothesised that continuous infected-uninfected cell contact may be triggering T cell activation, which was observed in infected (donor) cell culture at 48h post-infection. To test this, activated CD4+T cells were infected with Nef chimeric viruses and CD4/Env blocking antibodies were added at 4h and 20h post-infection to block VS formation and cell-cell contact mediated by Env on infected cells engaging CD4 on target cells (Figure 3.24A). Cells were analysed by flow cytometry 44h post-infection to measure expression of viral genes (GFP and Env) and activation markers. Addition of CD4 and Env blocking antibodies prevents the

formation of VS between infected and uninfected cells (Chen et al., 2007; Jolly et al., 2004; McCoy et al., 2014) and should thus reduce T cell activation and viral gene

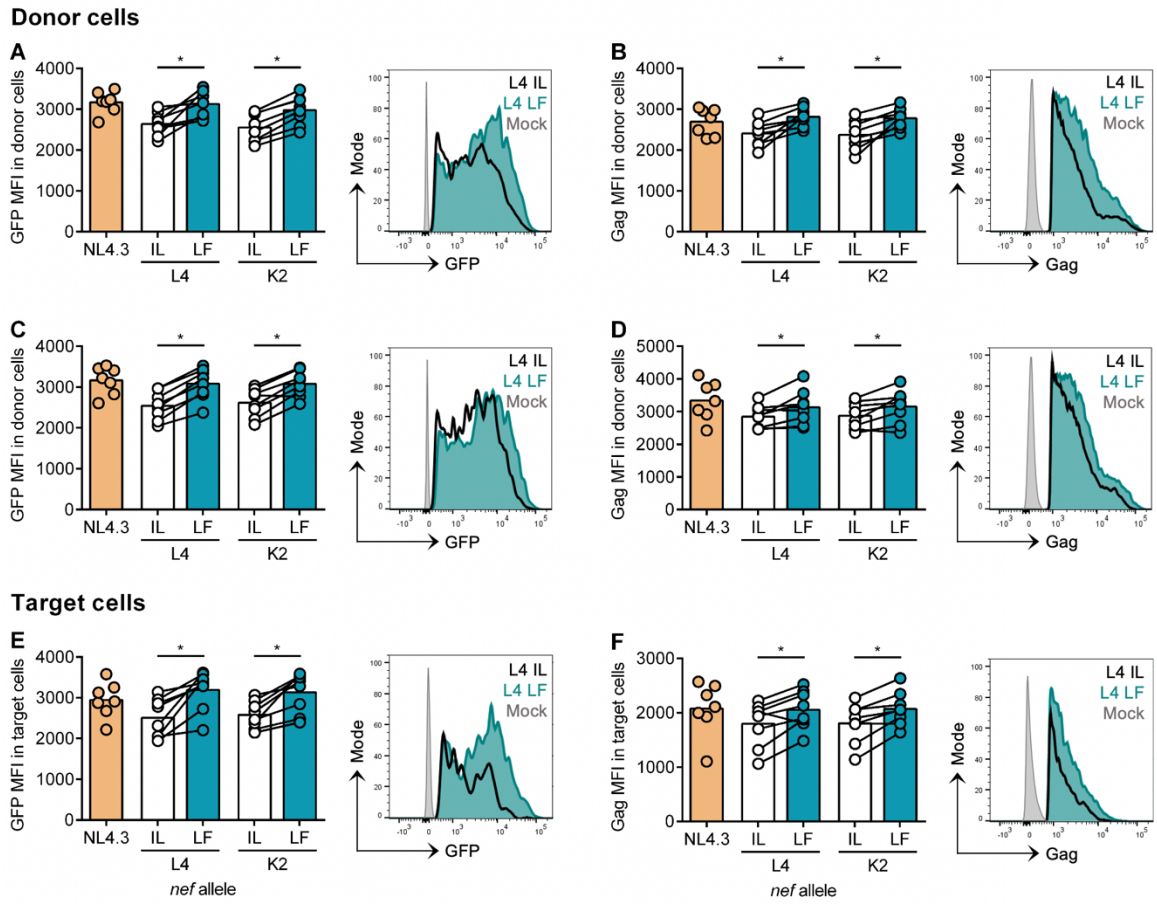

Figure 3.23: Retained CD3 expression results in increased expression of GFP and Gag during cell-cell spread in donor and target cells

Primary CD4+ T cells infected with indicated viruses were mixed with autologous pre-labelled target cells and analysed by flow cytometry 0h and 24h post-mix as described in Figure 3.6. **(A)** GFP MFI in GFP+ donor cells at 0h post-mix. **(B)** Gag MFI in Gag+ donor cells at 0h post-mix. **(C)** GFP MFI in GFP+ donor cells at 24h post-mix. **(D)** Gag MFI in Gag+ donor cells at 24h post-mix. **(E)** GFP MFI in GFP+ target cells at 24h post-mix. **(F)** Gag MFI in Gag+ target cells at 24h post-mix.

expression. A neutralising llama antibody (J3 clone) against Env was used to enable later detection (with secondary Ab) of Env with human PGT151 Ab. J3 Ab recognises Env CD4-binding site and does not compete with PGT151 Ab recognising gp120-gp41 interface (McCoy et al., 2012). Importantly, J3 has been shown to block cell-cell spread and VS formation (McCoy et al., 2014). Firstly, Ab block treatment resulted in reduced numbers of GFP+ cells compared to untreated (PBS treated) control (Figure 3.24B) showing that this neutralising Ab had an inhibitory effect on VS formation and viral cell-

cell spread, and suggesting that viral spread occurred during last 24h of infection, which was blocked by the Ab treatment.

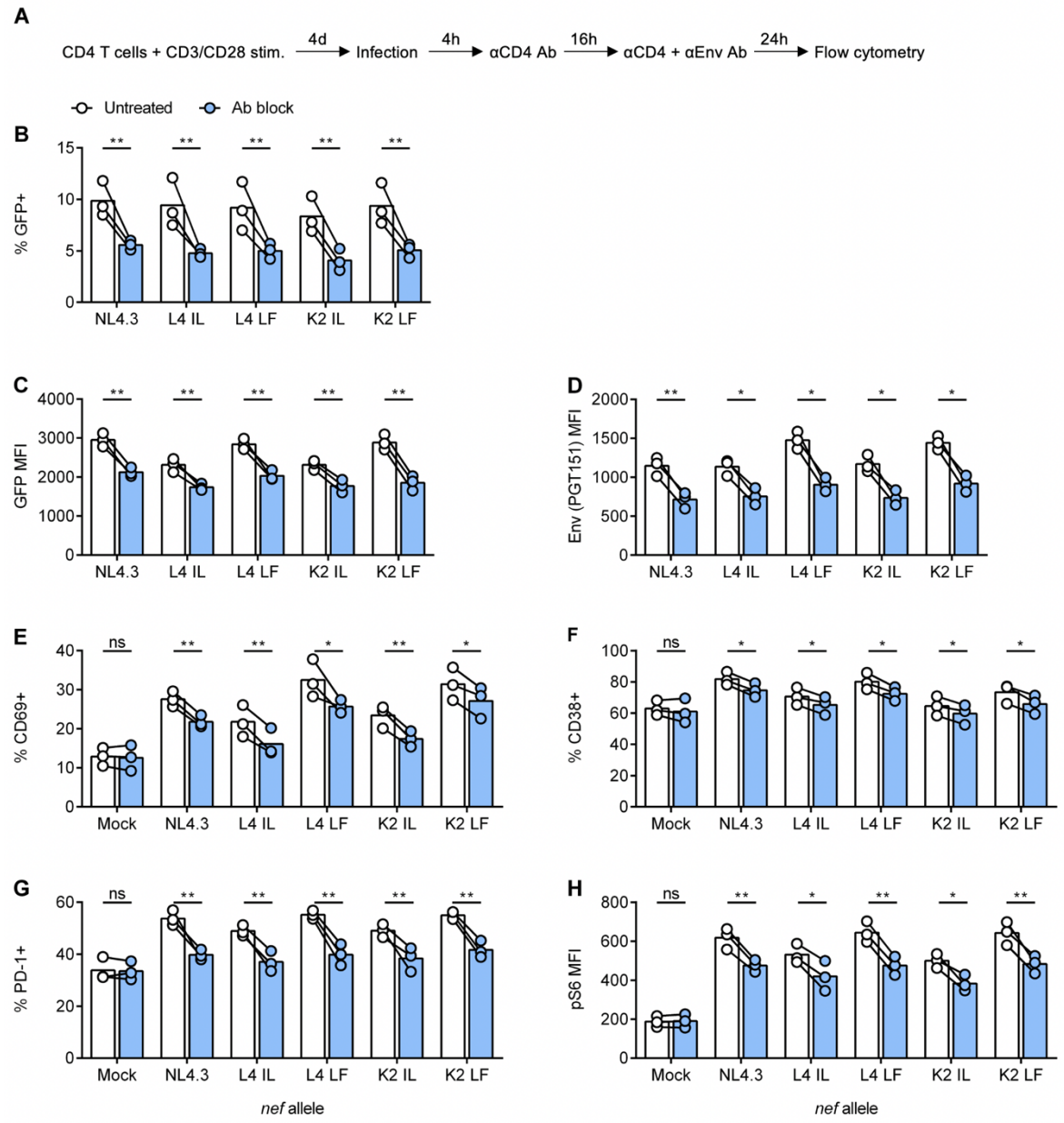

Figure 3.24: Blocking virological synapse formation reduces viral gene expression and T cell activation.

Primary CD4+ T cells were infected with Nef chimeric viruses. CD4 (Q4120, 20 μg/ml) and Env (J3, 5 μg/ml) blocking antibodies were added at 4h and 16h post-infection. Cells were analysed by flow cytometry 44h post-infection. **(A)** Schematic of the experimental setup. **(B)** Percentage of GFP+ live cells. **(C-G)** Infected (GFP+) donor cell population was analysed for expression of GFP, Env and activation markers. Show is **(C)** GFP MFI, **(D)** surface Env (PGT151 Ab) MFI, percentage of positive cells for **(E)** CD69, **(F)** CD38, **(G)** PD-1, and **(H)** pS6 MFI. Bars show mean and lines join paired results from the same PBMC donor. Groups were compared using paired *t*-test (ns, P>0.05; *, P<0.05; **, P<0.01; ***, P<0.001).

Notably, the infected (GFP+) population showed reduced expression of viral genes (GFP reporter and Env) and reduced expression of activation markers CD69, CD38, PD-1 and S6 phosphorylation in cultures treated with Ab block compared to untreated control (Figure 3.24C-H). This confirms the hypothesis that infected-uninfected cell contact triggers T cell activation and increases viral gene expression. Consistent with previous observations in this Chapter, L4 and K2 LF Nef virus infected cells showed higher expression of GFP, Env, and the activation markers compared to IL Nef viruses (Figure 3.22-23). Notably, reduced expression of the viral genes and the activation markers was observed across all Nef viruses, irrespective of their CD3 downmodulation ability. This is likely due to incomplete CD3 downmodulation of IL Nef viruses early during the infection (24h post-infection), thus allowing for cell-cell spread driven T cell activation, which can be reduced by blocking Ab treatment.

Having observed increased T cell activation as measured by expression of CD69, CD38, PD-1, and S6 phosphorylation, the panel of activation markers was expanded to better characterise T cell activation changes during cell-cell spread. The expanded panel included two other classical activation markers: CD25 (IL-2Rα) and CD95 (Fas), and two metabolic activation markers: CD98 (amino acid transporter) and Glut1 (glucose transporter) (Aries et al., 1995; Loisel-Meyer et al., 2012; Matheson et al., 2015; Palmer et al., 2017). Having observed increased viral gene expression, it was hypothesised that this might correlate with increased metabolic capacity and upregulation of nutrient transporters in infected cells. As described in Figure 3.21, expression of these markers was measured in infected (GFP+) donor and target cells at 24h post-mix. Increased expression of all markers was observed in both donor and target cells infected with NL4.3 Nef virus compared to mock infected control (Figure 3.25). Interestingly, no significant difference in expression of these markers was observed between IL and LF Nef viruses in either donor or target cells. This suggests that upregulation of these markers is independent of cell-cell spread and VS formation, and is likely caused by infection alone. This is consistent with previous observations showing that HIV-1 infected cells show increased activation phenotype (Cavrois et al., 2017; Corneau et al., 2017; Pardons et al., 2019). Another possibility is that cells with high expression of CD25/CD95/CD98/Glut1, i.e. highly-activated cells are preferentially infected or are better able to support productive infection (Rato et al., 2017).

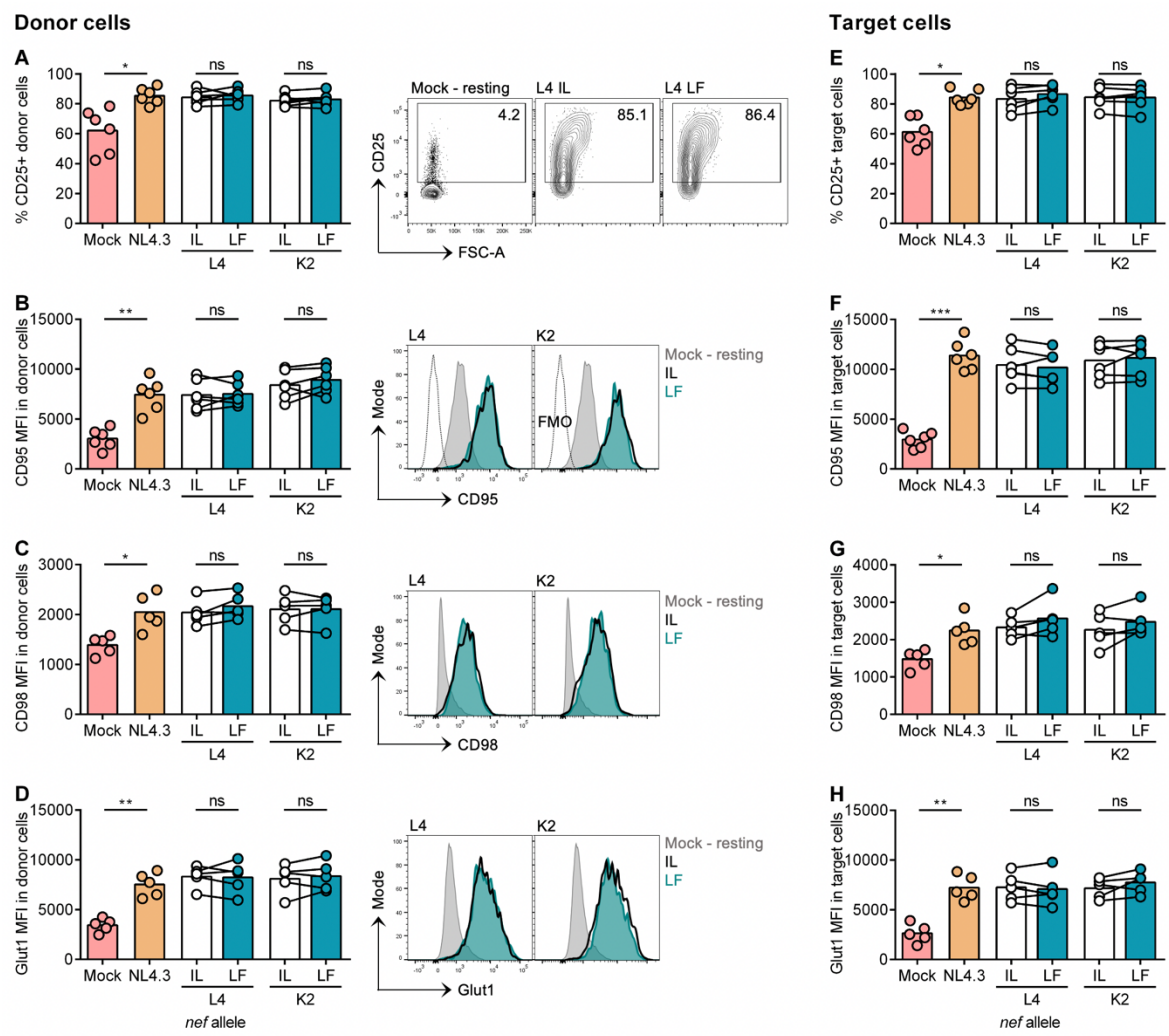

Figure 3.25: Retained CD3 expression does not correlate with increased expression of CD25, CD95, CD98, and Glut1 during cell-cell spread in donor and target cells.

Primary CD4+ T cells infected with indicated viruses were mixed with autologous pre-labelled target cells and analysed by flow cytometry 24h post-mix as described in Figure 3.6. **(A-D)** Infected (GFP+) donor cell population was analysed for expression of activation markers. Show is percentage of positive donor cells for **(A)** CD25, and MFI of **(B)** CD95, **(C)** CD98, and **(D)** Glut1. Right-hand side panels show representative flow cytometry plots. Uninfected (mock) resting CD4+ T cells are shown for comparison. **(E-H)** Infected (GFP+) target cell population was analysed for expression of activation markers. Show is percentage of positive target cells for **(E)** CD25, and MFI of **(F)** CD95, **(G)** CD98, and **(H)** Glut1. Mock is uninfected control and total live population of donor or target cells was analysed. Bars show mean and lines join paired results from the same PBMC donor. Groups were compared using paired *t*-test (ns, P>0.05; *, P<0.05; **, P<0.01; ***, P<0.001).

To further examine this phenotype of T cell activation, expression of CD25, CD95, CD98, and Glut1 was compared in infected donor cells at 0h and 24h post-mix with target cells. Expression of these activation markers in infected donor cells at 0h post mix again showed no differences between IL and LF Nef viruses (Figure 3.26A-D).

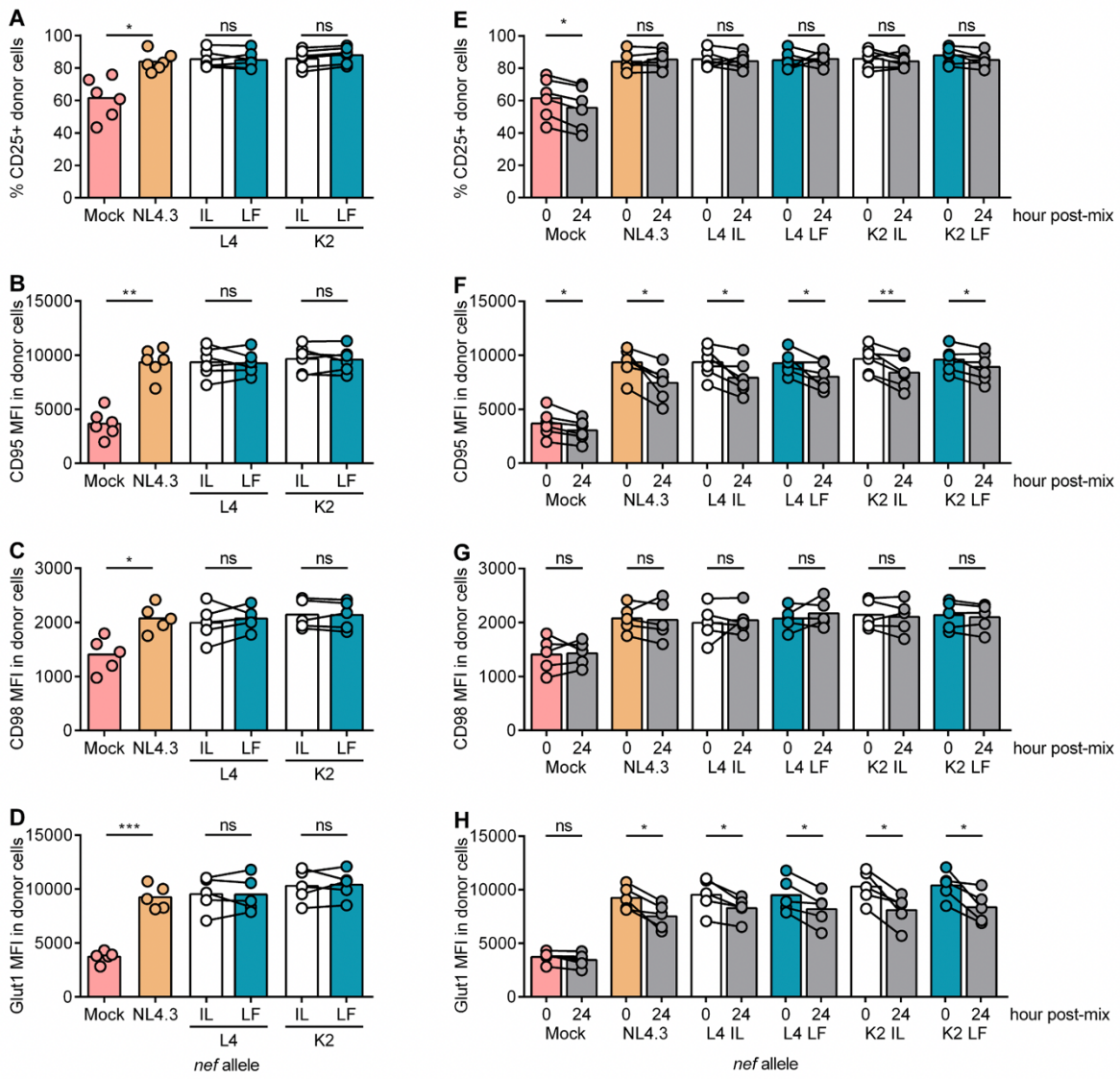

Figure 3.26: Changes in expression of CD25, CD95, CD98, and Glut1 in donor cells during cell-cell spread

Donor cells were analysed for expression of activation markers as described in Figure 3.25 at 0h post-mix. **(A-D)** Infected (GFP+) donor cell population was analysed for expression of activation markers. Show is percentage of positive donor cells for **(A)** CD25, and MFI of **(B)** CD95, **(C)** CD98, and **(D)** Glut1. **(E-H)** Shown is comparison of activation marker expression at 0h post-mix (as shown in panels A-D) and at 24h post-mix (as shown in Figure 3.25A-D). Percentage of positive infected donor cells for **(E)** CD25, and MFI of **(F)** CD95, **(G)** CD98, and **(H)** Glut1. Mock is uninfected control and total live population of donor cells was analysed. Bars show mean and lines join paired results from the same PBMC donor. Groups were compared using paired *t*-test (ns, P>0.05; *, P<0.05; **, P<0.01; ***, P<0.001).

However, NL4.3 infected donor cells showed increased expression of all four activation markers compared to mock infected control. Comparing expression of CD25 and CD98 in infected donor cells over time (Figure 3.26E,G) showed no significant changes in both markers in all infected cell cultures. Conversely, decreased expression of CD95 and

Glut1 over time was observed in all infected cell cultures (Figure 3.26F,H), similarly as observed for the expression of PD-1 (Figure 3.22G). Taken together, this suggests that upregulation of CD25, CD95, CD98, and Glut1 is independent of cell-cell spread induced T cell activation and is perhaps caused by infection alone.

3.2.6 Phosphorylation changes in ZAP70, ERK, AKT and S6 during virological synapse formation

To further explore CD3-dependent changes in T cell activation during cell-cell spread, activation of TCR signalling at the VS was examined. Previous work has shown that HIV-1 activates TCR signalling at the virological synapse to support viral spread (Len et al., 2017). This was done using mass spectrometry and immunoblotting approaches. Therefore, to enable a more high-throughput and quantitative analysis of TCR signalling at the virological synapse, a flow cytometry-based assay was developed. This allowed for discrimination of rare donor-target conjugates from the bulk population. Briefly, primary CD4+ T cells were infected (donor cells) and mixed with pre-labelled uninfected target cells and allowed to interact over a time course until formaldehyde fixation (Figure 3.27A). Infected donor-target conjugates (D:T GFP+) were identified as live lymphocyte doublets that are positive for GFP (infected donor cell) and Target dye (target cell) expression (Figure 3.27B-E). To validate the specificity of donor-target cell interaction, donor and target cells were preincubated with CD4 and Env blocking antibodies to prevent the VS formation (Figure 3.27F). Indeed, number of D:T GFP+ conjugates was reduced approx. 4-fold compared to untreated control during antibody blockade of the VS. To further validate this approach, phosphorylation changes in the TCR signalling pathway were measured over a time course and compared the changes in different donor-target doublet populations (Figure 3.27G-J). Cells were stained with phospho-specific antibodies to detect phosphorylation of ZAP70 (pY319), ERK (pT202/pY204), AKT (pT308 and pS473), and S6 (pS235/pS236). Notably, all phosphorylation sites examined here represent activating (not inhibitory) phosphorylation changes. These proteins and phosphorylation sites were chosen as they represent well-studied and key components of TCR signalling, with validated antibodies available. Moreover, ZAP70, ERK and AKT were previously found to be activated in infected cells during VS formation (Len et al., 2017). Phosphorylation of ZAP70, ERK, AKT, and S6 increased over time in D:T GFP+ population, with peak changes observed after 20min (or 5min for ZAP70) of co-culture (Figure 3.27G-K). This is consistent with signalling being triggered at the virological synapse, which results in phosphorylation of these proteins. By contrast, no

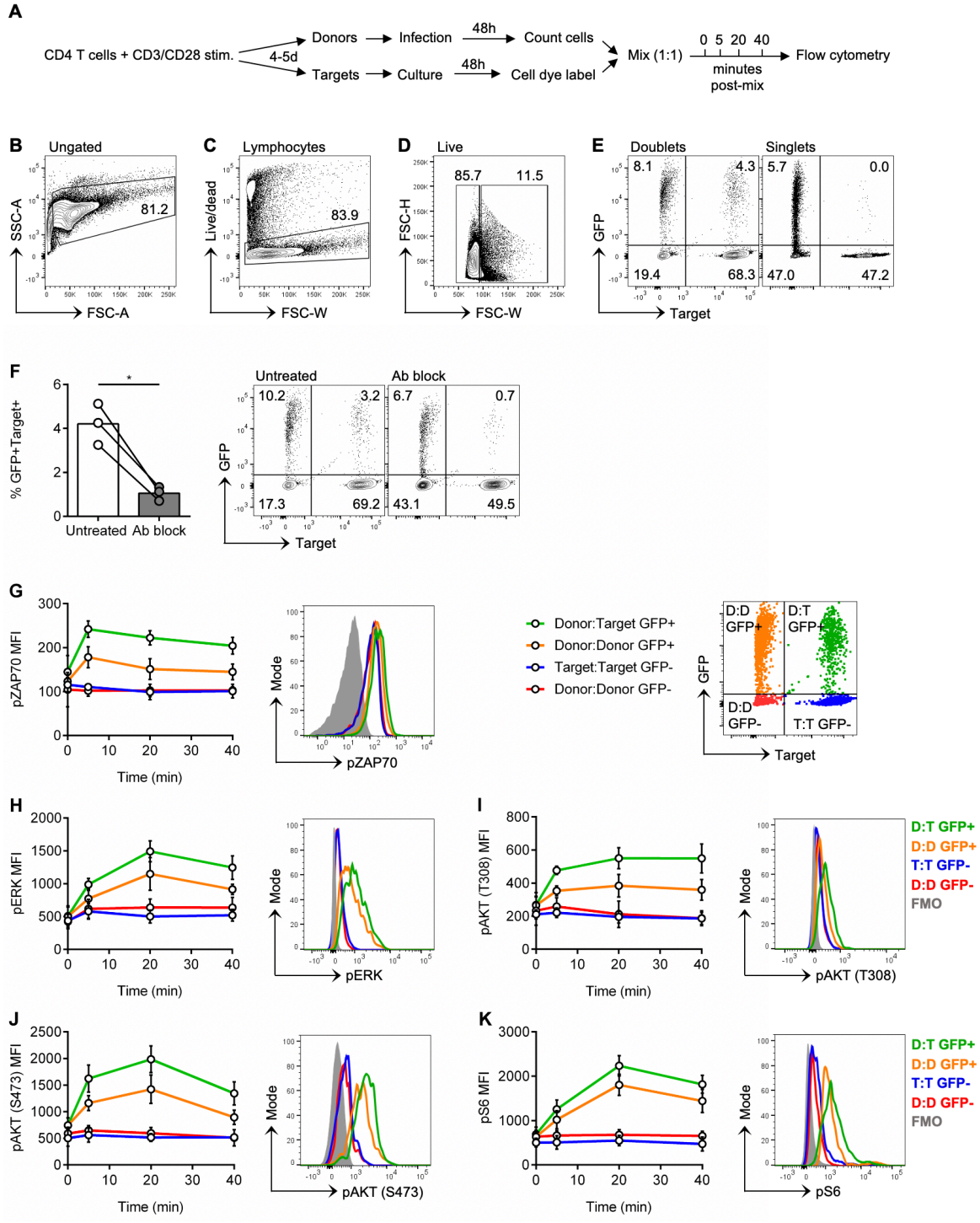

Figure 3.27: Flow cytometry assay to detect phosphorylation changes in ZAP70, ERK, AKT and S6 upon donor-target cell conjugate formation

Primary CD4+ T cells infected with NL4.3 Nef chimeric virus were mixed with autologous pre-labelled target cells for 0-40min and analysed by flow cytometry to detect phosphorylation changes in phospho-ZAP70 (pZAP70), phospho-ERK (pERK), phospho-AKT (pAKT), and phospho-S6 (pS6). **(A)** Schematic of the experimental setup. **(B-E)** Gating strategy to analyse flow cytometry data. **(B)** Lymphocytes were gated based on their forward- and side-scatter properties (FSC-A vs SSC-A). **(C)** Live cells were gated as live/dead dye negative population. **(D)** Singlets and doublets were gated based on their forward scatter properties (FSC-W vs FSC-H). **(E)** Infected donor cell-target cell conjugates were identified as GFP+Target dye+

doublets. **(F)** Donor and target cell cultures were pre-incubated with CD4 (Q4120, 10 μg/ml) and Env (2G12, 10 μg/ml) blocking antibodies and co-cultured for 20min. Shown is percentage of infected donor cell-target cell conjugates (GFP+Target+) in doublet population. **(G-J)** Analysis of phosphorylation changes over time in the four populations of doublets: Donor:Target GFP+ (GFP+Target+), Donor:Donor GFP+ (GFP+Target-), Donor:Donor GFP- (GFP-Target-), and Target:Target GFP- (GFP-Target+). Shown are MFI values of **(G)** pZAP70 (Y319), **(H)** pERK (T202/Y204), **(I)** pAKT (T308), **(J)** pAKT (S473), and **(K)** pS6 (S235/S236). Error bars show mean ± SEM from three PBMC donors. Bars show mean and lines join paired results from the same PBMC donor. Groups were compared using paired *t*-test (ns, P>0.05; *, P<0.05; **, P<0.01; ***, P<0.001).

phosphorylation changes were observed in doublet populations formed by nonspecific contacts between uninfected donor cells (D:D GFP-) or target cells (T:T GFP-). Interestingly, increase in phosphorylation of ZAP70, ERK, AKT and S6 in infected donor-donor doublet population (D:D GFP+) was also observed. This can be explained by the fact that only 15-20% of donor cells were GFP+, which means that uninfected donor cells can also act as targets to form virological synapse and activate the TCR signalling. These data show that phosphorylation changes in specific donor-target conjugates can be measured using this flow cytometry-based assay.

Retained CD3 expression results in increased cell activation of infected cells during cell-cell spread (Figure 3.21), thus it was investigated whether CD3-dependent phosphorylation changes can be observed in infected donor-target cell conjugates (D:T GFP+) by comparing IL and LF viruses in this assay. First, a time course experiment was performed (as described above) using L4 IL and LF Nef virus infected cells (Figure 3.28A-E). L4 LF infected donor-target cell conjugates showed slightly higher phosphorylation of ERK, AKT, and S6 over the 40min time course compared to IL Nef virus. This experiment also confirmed that 20min time point is optimal (or sufficiently optimal for ZAP70) for measuring all five phosphorylation changes, which was therefore used in further experiments. Figure 3.28F-J shows higher phosphorylation of all five markers in NL4.3 infected donor-target conjugates compared to mock infected control forming nonspecific donor-target doublets. This further confirmed specificity of this assay. Furthermore, higher phosphorylation of ERK and S6 in L4 and K2 LF Nef infected conjugates, which retain CD3 expression, was observed compared to their IL Nef counterparts (Figure 3.28G,J). The observed effect was modest, but significant, and is consistent with observed higher phosphorylation of S6 in donor and target cells during cell-cell spread (Figure 3.21). By contrast, ZAP70 phosphorylation showed no CD3-dependent differences. This was surprising given the central role of CD3 expression in

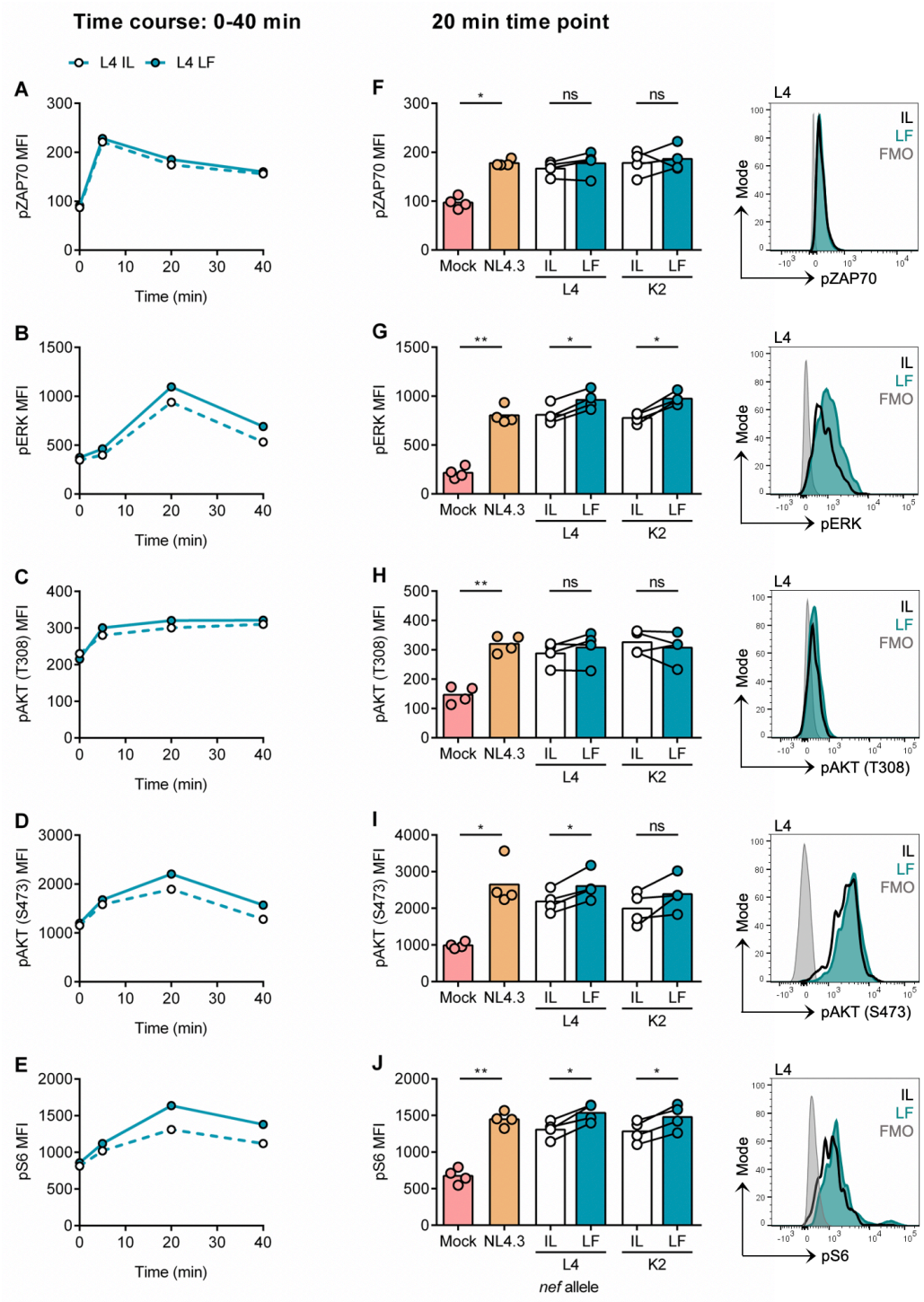

Figure 3.28: Retained CD3 expression results in increased phosphorylation of ERK and S6 in donor-target cell conjugates

Primary CD4+ T cells infected with Nef chimeric viruses were mixed with autologous pre-labelled target cells and analysed by flow cytometry to detect phosphorylation changes in pZAP70, pERK, pAKT, pS6 as described in Figure 3.27. **(A-E)** Phosphorylation changes in infected donor cell-target cell conjugates at 0-40min post-mix. Shown is a representative example for L4 IL and LF Nef viruses (n=1). Shown are MFI values of **(A)** pZAP70 (Y319), **(B)** pERK (T202/Y204), **(C)** pAKT (T308), **(D)** pAKT (S473), and **(E)** pS6 (S235/S236). **(F-J)** Phosphorylation changes in infected donor cell-target cell conjugates at 20min post-mix. Shown are MFI values of **(F)** pZAP70 (Y319), **(G)** pERK (T202/Y204), **(H)** pAKT (T308), **(I)** pAKT (S473),

and **(J)** pS6 (S235/S236). Right-hand side panels show representative flow cytometry plots. Mock is uninfected cells and total live doublet population was analysed. Bars show mean and lines join paired results from the same PBMC donor. Groups were compared using paired *t*-test (ns, P>0.05; *, P<0.05; **, P<0.01; ***, P<0.001).

TCR signalling activation. This might be due to transient activation of ZAP70 upon TCR signalling activation or poor detection of ZAP70 phosphorylation by this assay (very low MFI values), which would hinder the detection of any CD3-dependent differences. Alternatively, integrin signalling (LFA-1 and ICAM-1 interaction at the VS) has been shown to activate ZAP70 (Evans et al., 2011; Li et al., 2009; Starling & Jolly, 2016), which would also mask any CD3-dependent differences. Alternatively, this also raises a possibility that ZAP70 activation at the VS is not mediated via TCR-CD3 activation. Next, observing phosphorylation of AKT at S473 site (activating phosphorylation in the regulatory domain) showed increased phosphorylation in L4 LF Nef virus infected conjugates compared to L4 IL Nef (Figure 3.28G). However, no significant difference was apparent between K2 IL and LF Nef viruses. This might be due to small absolute differences in MFI values, which makes comparison of small number of replicates difficult. By contrast, no significant changes in phosphorylation of AKT at T308 site (activating phosphorylation in the kinase domain) were observed between IL and LF Nef viruses (Figure 3.28F). This might be in part due to poor detection of phosphorylation at this site, as shown by very small MFI values. Alternatively, this may reflect low phosphorylation at this site as detected in this experimental setup. Of note, phosphorylation at both sites is required for maximal AKT activity, but phosphorylation at either site can activate AKT kinase activity (Manning & Toker, 2017). Taken together, these data show that retained CD3 expression correlates with increased phosphorylation of ERK and S6 in donor-target conjugates during VS formation, which is consistent with increased T cell activation observed during cell-cell spread. By contrast, phosphorylation of ZAP70 and AKT was independent of CD3 expression.

3.2.7 Retained CD3 expression results in increased T cell death during cell-cell spread

HIV-1 cell-cell spread results in increased kinetics of viral replication and spread (Chen et al., 2007; Martin et al., 2010; Sourisseau et al., 2007). Thus contact-induced T cell signalling during cell-cell spread might also have pathogenic consequences leading to T cell death and dysfunction. It has been shown that both T cell hyper-activation and HIV infection cause cell death (Galloway et al., 2015; Zhan et al., 2017). Having observed

that retained CD3 expression correlates with increased cell-cell spread and increased T cell activation, it was investigated whether the same correlation exists for cell death. As described in Figure 3.5, flow cytometry was used to measure cell death (using a cell viability dye) in donor and target cells during cell-cell spread. L4 and K2 LF Nef virus infected donor cells, which retain CD3 expression, showed higher levels of cell death compared to their IL Nef infected counterparts at 24h post-mix (Figure 3.29A), which correlates with increased viral spread in these cultures. As expected, all infected cell cultures showed more cell death compared to mock infected control. A similar trend was seen in target cell population at 24h post-mix (Figure 3.29B). L4 and K2 LF Nef infected cultures showed increased target cell death compared to IL Nef viruses, again correlating with viral spread. Overall, lower levels of cell death were seen for target cells compared to donor cells, with the latter having been infected for longer. Thus, increased viral spread of LF Nef viruses results in increased cell death of both donor and target cells.

To address whether increased cell death of donor cells observed after 24h of co-culture was induced by cell-cell spread, cell death in infected donor cell cultures was analysed before donor-target co-culture (0h post-mix). Notably, increased cell death in L4 and K2 LF Nef infected donor cells compared to IL Nef viruses was already apparent at 0h post-mix (48h post-infection, Figure 3.29C), which is consistent with increased T cell activation of these cells. Importantly, these cultures also showed similar infection levels between all Nef viruses (Figure 3.5B). Comparing donor cell death over time (0-24h post-mix), all infected cultures showed time-dependent increase in the number of dead donor cells (Figure 3.29D), most likely due to viral spread. This increase was highest for L4 and K2 LF Nef viruses, which correlates with retained CD3 expression and with increased viral spread of these viruses (Figure 3.6).

It was hypothesised that continuous infected-uninfected cell contact, resulting in viral spread and T cell activation, triggers cell death that was observed in infected (donor) cell culture at 48h post-infection. If this was correct, blocking infected-uninfected cell contact would decrease cell death in infected cell culture. As described above (Figure 3.24), preventing VS formation using CD4/Env blocking antibodies (Ab block) decreases viral spread, viral gene expression and T cell activation. Consistent with these observations, Ab block treated cell cultures showed decreased levels of cell death in donor cells compared to untreated control (Figure 3.29E).

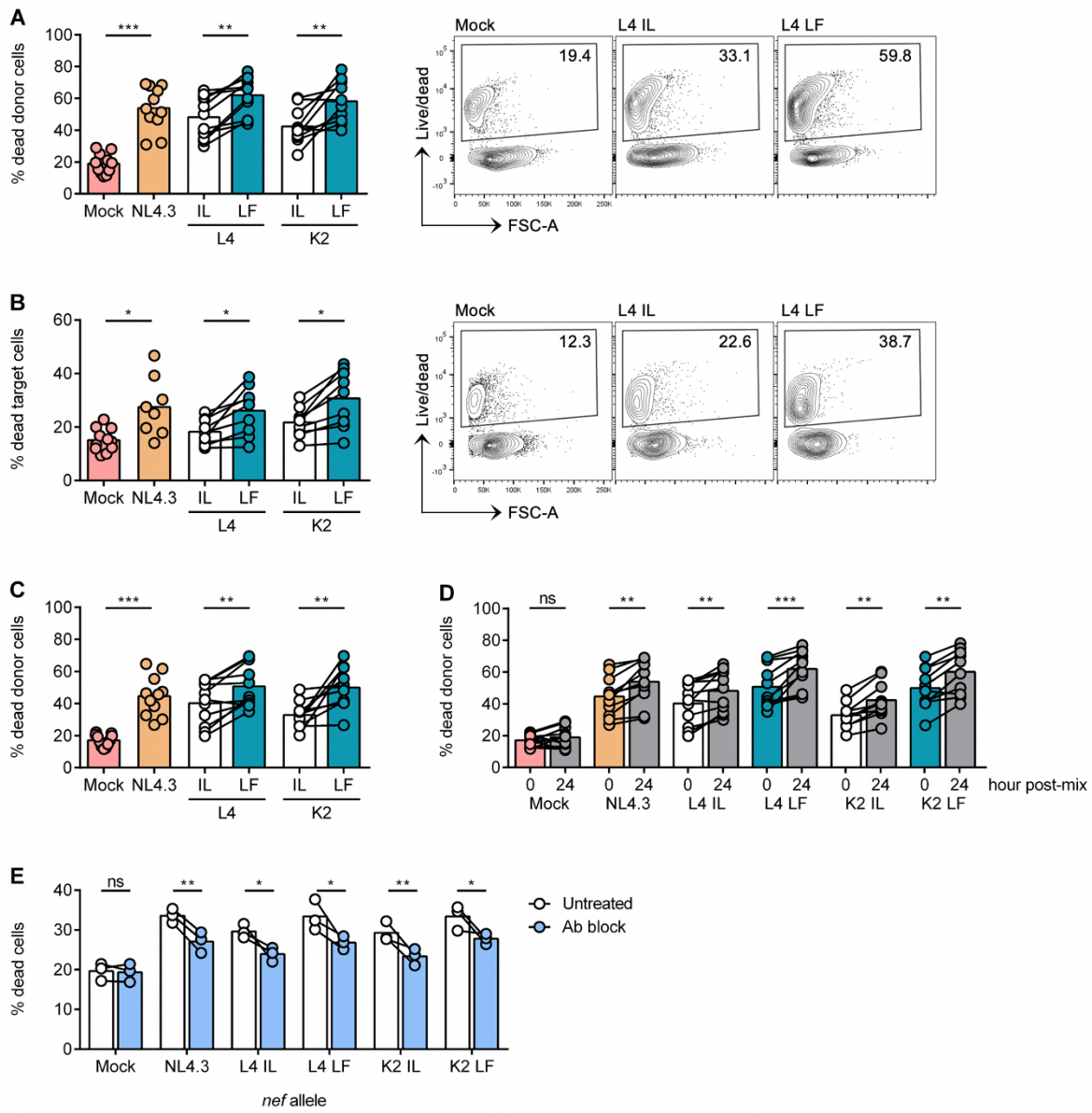

Figure 3.29: Retained CD3 expression results in increased cell death during cell-cell spread in donor and target cells.

Primary CD4+ T cells infected with indicated viruses were mixed with autologous pre-labelled target cells and analysed by flow cytometry at 0h and 24h post-mix as described in Figure 3.6. **(A)** Percentage of dead donor cells at 24h post-mix. **(B)** Percentage of dead target cells at 24h post-mix. Right-hand side panels show representative flow cytometry plots. **(C)** Percentage of dead donor cells at 0h post-mix. **(D)** Shown is comparison of cell death in donor cells at 0h post-mix (as shown in panel C) and at 24h post-mix (as shown in panel A). **(E)** Infected cell culture was treated with CD4 and Env blocking antibodies as described in Figure 3.24. Shown is percentage of dead cells at 44h post-infection. Mock is uninfected control. Bars show mean and lines join paired results from the same PBMC donor. Groups were compared using paired *t*-test (ns, P>0.05; *, P<0.05; **, P<0.01; ***, P<0.001).

Together these data show that viral spread results in increased cell death in HIV-1 infected donor T cells that can be reduced by blocking cell-cell contact.

To further define differences observed in cell death, the mechanism of cell death was investigated. Apoptosis is one of the mechanisms of cell death and is characterised by cell surface expression of Annexin V (Zhang et al., 2005). As described in Figure 3.5, flow cytometry was used to measure expression of Annexin V and cell viability marker (live/dead marker) in donor and target cell populations after 24h of co-culture. Apoptotic cells upregulate Annexin V and have an intact cell membrane, thus showing low expression of live/dead cell marker, which as a membrane impermeable dye. Dead cells lose the cell membrane integrity, thus showing high expression of both live/dead marker and Annexin V. This state (Annexin V+Live/dead marker+) can be reached via different cell death pathways: apoptosis, necrosis or pyroptosis (Crowley et al., 2016). Figure 3.30A revealed that donor cells showed Annexin V expression predominantly in the dead cell population (live/dead marker+), with minimal contribution from the live cell population. As a control, uninfected cells were treated with Etoposide to induce apoptosis (Figure 3.30B) (Karpinich et al., 2002). Etoposide treatment increased expression of Annexin V in the live cell population compared to DMSO treated control, consistent with the induction of apoptosis. Analysing Annexin V expression in donor cells after 24h of co-culture showed a broadly similar percentage of Annexin V+ live donor cells in all infected cell cultures (Figure 3.30C). Similar levels of Annexin V expression were also observed in uninfected cell cultures. Together, this suggests that apoptosis is unlikely to be responsible for differences in cell death observed between the different Nef viruses (Figure 3.29). By contrast, higher expression levels of Annexin V were observed when analysing the infected (GFP+) donor cell population (Figure 3.30D), suggesting that a significant proportion of infected cells die via apoptosis. However, no difference was observed between IL and LF Nef viruses, suggesting that this occurs in a CD3-independent manner. A similar trend in Annexin V expression was observed in total live and infected (GFP+) target cell population (Figure 3.30E-F), again showing no differences between IL and LF Nef viruses, but higher expression of Annexin V was observed in GFP+ population compared to total live population. Taken together, these data suggest that differences in overall levels of cell death in infected cell cultures are not due to apoptosis; however, a significant proportion of infected cells die via apoptosis.

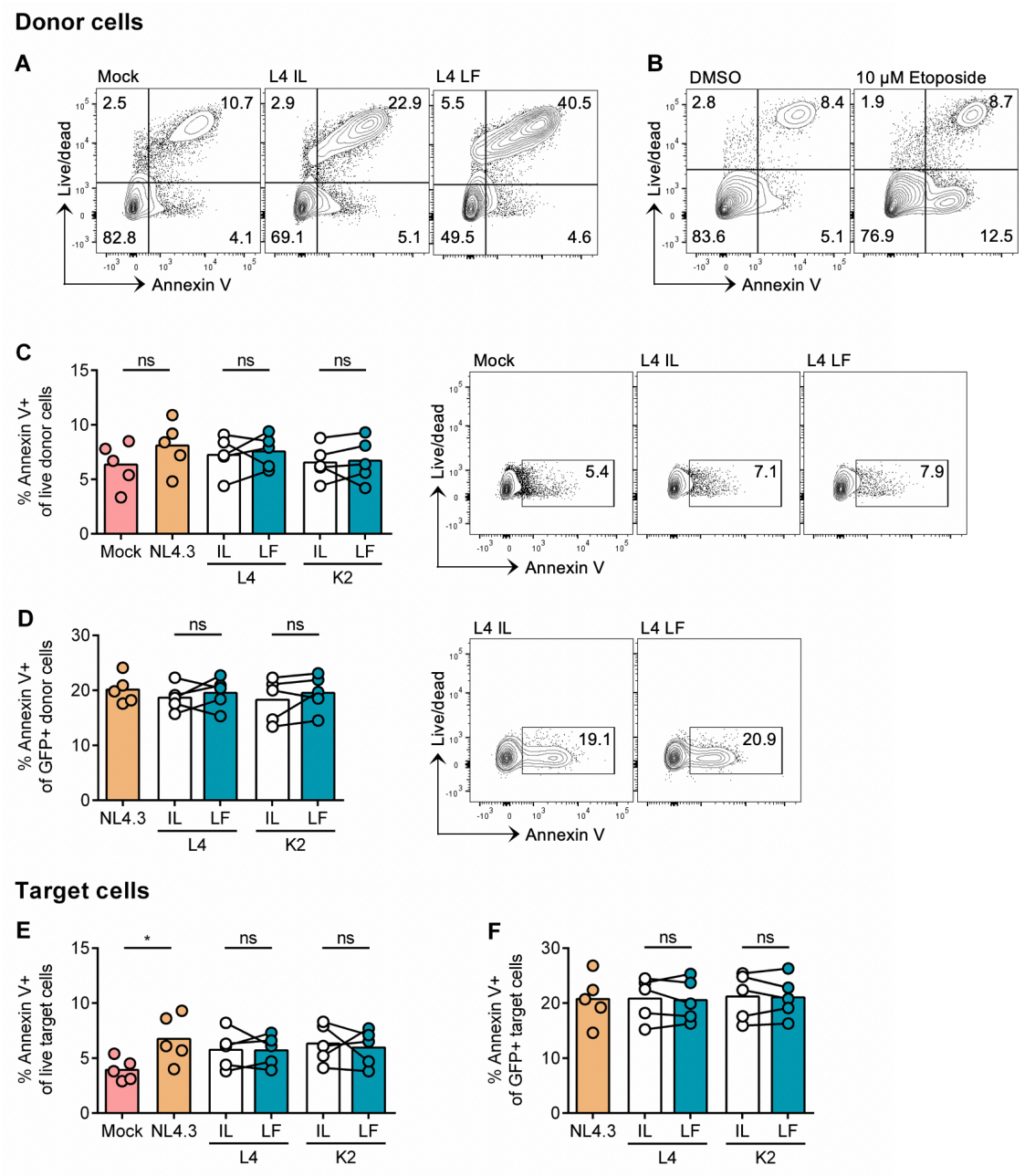

Figure 3.30: Apoptosis is enhanced in GFP+ population during cell-cell spread, but it does not correlate with CD3 expression

Primary CD4+ T cells infected with indicated viruses were mixed with autologous pre-labelled target cells and analysed by flow cytometry at 24h post-mix as described in Figure 3.5. **(A)** Annexin V and live/dead cell marker expression in infected donor cells. Total single cell population was analysed. Shown are representative flow cytometry plots for L4 IL and LF Nef chimeric viruses. **(B)** Uninfected (mock) cells were treated with DMSO or 10 µM Etoposide for 16h and analysed for expression of Annexin V and live/dead cell marker. **(C)** Percentage of Annexin V+ cells in live donor cell population. **(D)** Percentage of Annexin V+ cells in GFP+ donor cell population. **(E)** Percentage of Annexin V+ cells in live target cell population. Right-hand side panels show representative flow cytometry plots. **(F)** Percentage of Annexin V+ cells in GFP+ target cell population. Mock is uninfected control. Bars show mean and lines join paired results from the same PBMC donor. Groups were compared using paired *t*-test (ns, P>0.05; *, P<0.05; **, P<0.01; ***, P<0.001).

3.3 Discussion

The results in this Chapter show the consequences of differential Nef-mediated CD3 (down)modulation for HIV-1 viral spread, T cell activation and cell death. It was hypothesised that retained CD3 expression on infected cells (LF Nef viruses) would result in triggering of TCR/CD3 signalling and T cell activation during the VS formation and cell-cell spread, thus supporting more efficient viral spread. Indeed, retained CD3 expression on infected cells (LF Nef) resulted in increased T cell activation, viral gene expression, virion infectivity, cell-cell spread and cell death compared to viruses that downmodulated CD3 (IL Nef). The main finding of this Chapter is that retained CD3 expression on virus-producing primary CD4+ T cells resulted in greater cell-cell spread because virus produced by these cells incorporated more Env into virions and thus showed increased particle infectivity. By contrast, virus budding/release and the frequency of VS formation remained largely similar between viruses that either retain or downmodulate CD3 expression, suggesting that increased virion infectivity was the main factor responsible for enhanced viral spread.

3.3.1 Env expression, virion incorporation and infectivity

Retained CD3 expression and greater virion infectivity of LF Nef viruses correlated with increased Env expression in the cell and increased Env incorporation into virions (summarised in Figure 3.31). Env virion incorporation was measured directly by immunoblot analysis of purified virions and indirectly by Ab neutralisation assay, both of which showed increased Env incorporation into LF Nef viruses. This was not due to increased furin-mediated cleavage of Env gp160 to processed gp120 and gp41 subunits as shown by immunoblot analysis of cell lysates. Increased expression of Env was evident both on the transcriptional level (mRNA) and protein level. Importantly, flow cytometry analysis showed increased levels of cell surface Env for LF Nef viruses. Env is a limiting factor in viral infectivity due to low cell surface expression and low virion incorporation, 7-10 Env trimers per viral particle (Chojnacki et al., 2012; Zhu et al., 2003), that has been suggested to be an immune evasion strategy. Low Env expression on the cell surface is due to the presence of endocytic motifs in the cytoplasmic tail that mediate interactions with the clathrin adaptor AP-2, leading to endocytic uptake of surface exposed Env, (Anand et al., 2019; Boge et al., 1998; Byland et al., 2007; Day et al., 2004; Egan et al., 1996). Once endocytosed, there is good evidence that Env recycles back to the plasma membrane, possibly after trafficking via recycling compartments and/or the TGN (Groppelli et al., 2014; Kirschman et al., 2018; Qi et al., 2013).

Mechanisms of Env incorporation into nascent virions are poorly understood and factors which mediate low virion incorporation remain unknown. However, disrupting Env endocytosis has been shown to increase Env surface expression, which in turn results in increased Env virion incorporation and virion infectivity (Boge et al., 1998; Day et al., 2004; Groppelli et al., 2014; Kirschman et al., 2018). Given that Env is a limiting factor in viral infectivity, this provides one possible explanation how increased surface Env expression results in increased virion incorporation and virion infectivity. Moreover, analysis of Env trafficking between the plasma membrane and intracellular compartments showed faster kinetics of Env internalisation (endocytosis) and recycling back to the plasma membrane for LF Nef viruses, which correlates with their increased Env virion incorporation and infectivity. Previous work has shown that Env recycling through the endosomal compartments is required for efficient Env virion incorporation (Kirschman et al., 2018). It was suggested that during recycling Env is delivered to virus assembly domains at the plasma membrane, thus promoting Env virion incorporation. The caveat is that this work was done in HeLa cells and the requirements for Env incorporation in CD4+ T cells might be different. However, this model provides another possible explanation how faster kinetics of Env recycling might result in increased Env virion incorporation in LF Nef viruses. Taken together, both faster kinetics of Env recycling and increased expression of cell surface Env are possible mechanisms mediating increased Env incorporation into nascent virions (Figure 3.31)

Another question is what mediates increased surface expression of Env? As stated above, analysis of Env internalisation showed faster Env internalisation kinetics for LF Nef viruses (retained CD3 expression) compared to IL Nef viruses. This suggests that increased surface Env expression is not simply due to active retention of Env by CD3 on the cell surface. Interestingly, previous reports have suggested that there may be an Env-CD3 interaction, as evidenced by co-immunoprecipitation and super-resolution microscopy (Luo et al., 2016; Yakovian et al., 2018); however, the importance of this interaction for Env trafficking, conformation, virion incorporation and infectivity remains to be investigated. Data in this Chapter showed relatively abundant expression of Env even in the presence of almost complete CD3 downmodulation (IL Nef viruses), which suggests that Env does not simply get endocytosed together with CD3. Analysis of Env recycling back to the plasma membrane also showed faster Env recycling kinetics for LF Nef viruses (retained CD3 expression) compared to IL Nef viruses. This may be explained either by faster Env internalisation alone as was detected for LF Nef viruses,

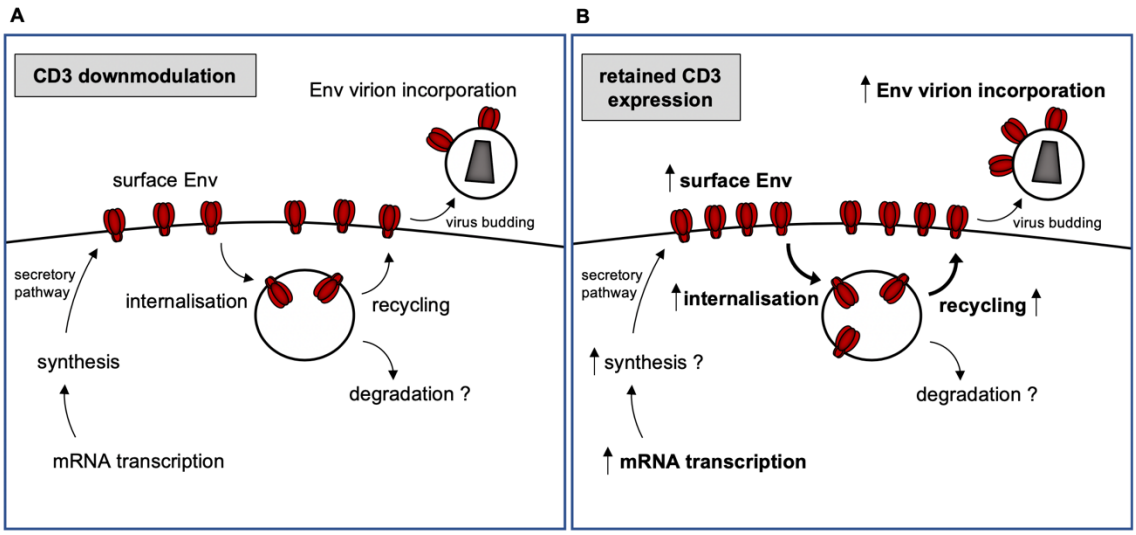

Figure 3.31: Retained CD3 expression results in increased Env surface expression and virion incorporation

Schematic diagram of Env trafficking and virion incorporation. Env mRNA transcription results in protein translation and synthesis of Env, which is transported through the Golgi network to the plasma membrane via the secretory pathway. Surface Env is readily internalised (endocytosis) to endosomes where it is recycled back to the plasma membrane (via TGN or the endosomal recycling compartment) or sorted for lysosomal degradation. Surface Env is incorporated into nascent virions and mechanisms mediating Env incorporation remain poorly understood. The diagrams show these processes of Env trafficking for **(A)** viruses that downmodulate CD3 (IL Nef) and **(B)** for viruses that retain CD3 expression (LF Nef). Comparing panels (A) and (B) shows that retained CD3 expression results in increased expression of Env mRNA and possibly increased synthesis of Env protein. CD3 expression also results in faster kinetics of Env internalisation and recycling. Altogether this leads to increased Env surface expression and Env virion incorporation, which ultimately contributes to increased virion infectivity. The contribution of Env degradation in the recycling pathway was not measured.

or faster internalisation coupled with differences in intracellular sorting (Env being targeted for lysosomal degradation or recycled back to the plasma membrane), with the caveat that the latter was not formally tested. Thus, faster kinetics of Env recycling and differences in intracellular sorting might explain increased levels of surface Env for LF Nef viruses. Another explanation for increased levels of surface Env is increased Env synthesis. This is consistent with increased expression of Env that was evident both on the transcriptional level (mRNA) and protein level. Although immunoblot analysis did not convincingly show differences in cellular Env expression, this was further confirmed by flow cytometry analysis that showed increased levels of intracellular Env for LF Nef viruses. However, greater levels of intracellular Env might also reflect faster kinetics of Env internalisation by LF Nef viruses. Taken together, increased levels of surface Env are likely mediated by increased Env synthesis coupled with faster kinetics of Env

internalisation and recycling, the latter also being important for Env incorporation (Figure 3.31).

As noted above, virus budding/release in the supernatant remained largely similar between viruses that either retain or downmodulate CD3 expression. This was somewhat surprising as retained CD3 expression correlated with increased expression of Gag. This suggests that Gag is not a limiting factor in virus budding as it is expressed abundantly and suggests that infected primary CD4+ T cells maybe producing virus at maximum capacity. Alternatively, host factors involved in viral budding, such as ESCRT machinery (Demirov & Freed, 2004) might be a limiting factor, thus increased expression of Gag does not result in increased virus release. However, it is possible that virus release is enhanced at the VS and differs for IL and LF Nef viruses, and this cannot be distinguished by measuring virus release in bulk supernatant. Further experiments would be required to test this hypothesis.

CD3 downmodulation did not result in diminished formation of VS. Instead, all Nef viruses formed VS at similar frequency. This is at odds with previous observations showing that infected TCR knock-out Jurkat cells formed fewer VS with uninfected target cells compared to WT Jurkat cells (Len et al., 2017). Importantly, this cell line was deficient for TCR-β subunit (but also lacking surface expression of CD3ε and CD4) and was generated by chemical mutagenesis (Chung & Strominger, 1995), which might have resulted in other off-target mutations. Additionally, the requirements (i.e. signalling, cell adhesion) for VS formation might be different between Jurkat and primary CD4+ T cells. Moreover, it was previously shown that LFA-1 signalling (resulting from LFA-1 and ICAM-1 interaction at the VS) is sufficient for polarisation of Gag and Env at the VS (Starling & Jolly, 2016). Altogether, this could explain why no differences were observed in VS formation between Nef mutant viruses. Alternatively, it is possible that duration of donor-target cell contact is different between IL and LF Nef viruses and live cell imaging experiments would be required to confirm this. Another possibility is that retained CD3 expression results in polarisation of more Env and Gag protein to the VS, which could result in enhanced viral spread. This could also explain increased Env virion incorporation of LF Nef viruses. Although no obvious differences in amount of Env or Gag at the VS were apparent, this was not formally tested and further, more quantitative microscopy experiments would be required to test this hypothesis.

Importantly, increased virion infectivity was not due to differences in Nef antagonism of SERINC proteins, as both IL and LF Nef viruses showed similar ability to downmodulate SERINC5/3 expression, and were equally restricted by SERINC5/3 overexpression. One limitation of this experiment was that no (good) anti-SERINC antibody was available, therefore tagged SERINC protein was overexpressed in 293T cells in order to assess SERINC inhibition and antagonism. However, this assay of SERINC overexpression in 293T cells is the current "gold-standard" assay to study SERINC restriction that is employed by many groups and so is well-established (Beitari et al., 2017; Heigele et al., 2016; Kmiec et al., 2018; Rosa et al., 2015; Sood et al., 2017; Usami et al., 2015). However, it cannot be excluded that Nef-mediated downmodulation efficiency or kinetics of regulation of endogenous SERINCs are different in primary CD4+ T cells compared to 293T cells. While the domains in Nef responsible for SERINC5 antagonism have not been mapped there is no evidence to suggest that this involves residues I123 and L146 that interact with CD3 based on the results presented in this Chapter, and the work of others (Ananth et al., 2019; Kmiec et al., 2018; Manrique et al., 2017; Pye et al., 2020). IL and LF Nef viruses were also confirmed to downmodulate CD4 and CD28 (this thesis), and MHC-I (Schmökel et al., 2013; Yu et al., 2015) to a similar extent, thus suggesting that observed phenotype of these viruses was dependent on their CD3 modulation. The exception here was CXCR4, which was observed to be downmodulated slightly better by LF Nef viruses (retained CD3 expression). This was also observed in the original study (Schmökel et al., 2013) where they isolated these *nef* alleles and it was proposed this was due to the expanded CXCR4 tropism of these viruses. However, the difference in downmodulation between IL and LF Nef viruses was very small and *in vitro* experiments in this thesis are unlikely to be affected by differences in chemokine signalling and cell migration, thus the difference in CXCR4 downmodulation is unlikely to affect the phenotype of these viruses.

3.3.2 T cell activation and cell signalling

Retained CD3 expression on infected cells (LF Nef viruses) resulted in increased donor cell activation during cell-cell spread. This was measured as upregulation of activation markers CD69, CD38, PD-1 and phosphorylation of S6 ribosomal protein. Previous observations showed that VS formation activates components of TCR-CD3 signalling pathway (Len et al., 2017), which is consistent with upregulation of the activation markers measured here. Interestingly, expression of activation markers CD25, CD95, CD98 and Glut1 was not affected by CD3 expression, which suggests that CD3-dependent

activation of T cell signalling during cell-cell spread only activates specific pathways, resulting in upregulation of a selected repertoire of activation markers. This might be due to weaker activation of TCR signalling at the VS compared to the immune synapse given the lack of TCR-pMHC interaction and CD28 co-stimulation at the VS. Previous studies showed that, as expected, Nef-mediated CD3 downmodulation results in diminished responsiveness of infected cells to PHA- or CD3/CD28-mediated stimulation (Schindler et al., 2006; Schmökel et al., 2013) Importantly, results here show CD3-dependent differences in cell activation occurred during cell-cell spread, in the absence of exogenous CD3 stimulation. Ribosomal S6 protein is activated by phosphorylation downstream of AKT/mTOR and RAS/ERK signalling pathways (triggered by TCR signalling and other stimuli) and results in increased protein translation/synthesis (Chapman & Chi, 2015; Roux et al., 2007). This is consistent with, and might go some way to explain, the increased expression of viral LTR-driven genes (Env, Gag and GFP reporter) in LF Nef infected cells. Importantly, viral gene transcription is also linked to cell activation as HIV-1 LTR contains binding sites for AP-1, NFAT and NF-κB transcription factors, which are activated by TCR-CD3 signalling (Burnett et al., 2009; Sauter et al., 2015). Indeed, increased expression of Env and Gag mRNA was observed for LF Nef viruses, which retain CD3 expression. Thus, increased cell activation may likely explain the increased transcription and translation of viral genes.

Further work in this Chapter showed that preventing infected-uninfected cell contact (VS formation) using Env and CD4 blocking antibodies reduced T cell activation (expression of CD69, CD38, PD-1, phosho-S6) and expression of Env and induction of the GFP reporter. This further supports the hypothesis that cell activation is being induced by infected-uninfected cell contact. Similarly, inducing T cell activation by CD3/CD28 stimulation in infected resting (IL-7-treated) cells also led to increased viral (LTR-driven) protein expression (Env and GFP reporter) and enhanced virion infectivity. Taken together these data provides a plausible explanation for how retained CD3 expression on infected cells and subsequent activation of TCR-CD3 signalling during cell-cell contact could result in increased expression of viral proteins, ultimately leading to increased Env virion incorporation and infectivity. Schematic representation of this model is shown in Figure 3.32. Importantly, RNAi-mediated depletion of CD3 expression reduced T cell activation, viral gene expression (Env and GFP reporter) and virion infectivity, thus phenocopying the effect of Nef-mediated CD3 downmodulation. This further confirmed that differences between IL and LF Nef viruses are specific to their

CD3-downmodulaiton abilities and not due to yet unidentified function of Nef mediated by these residues.

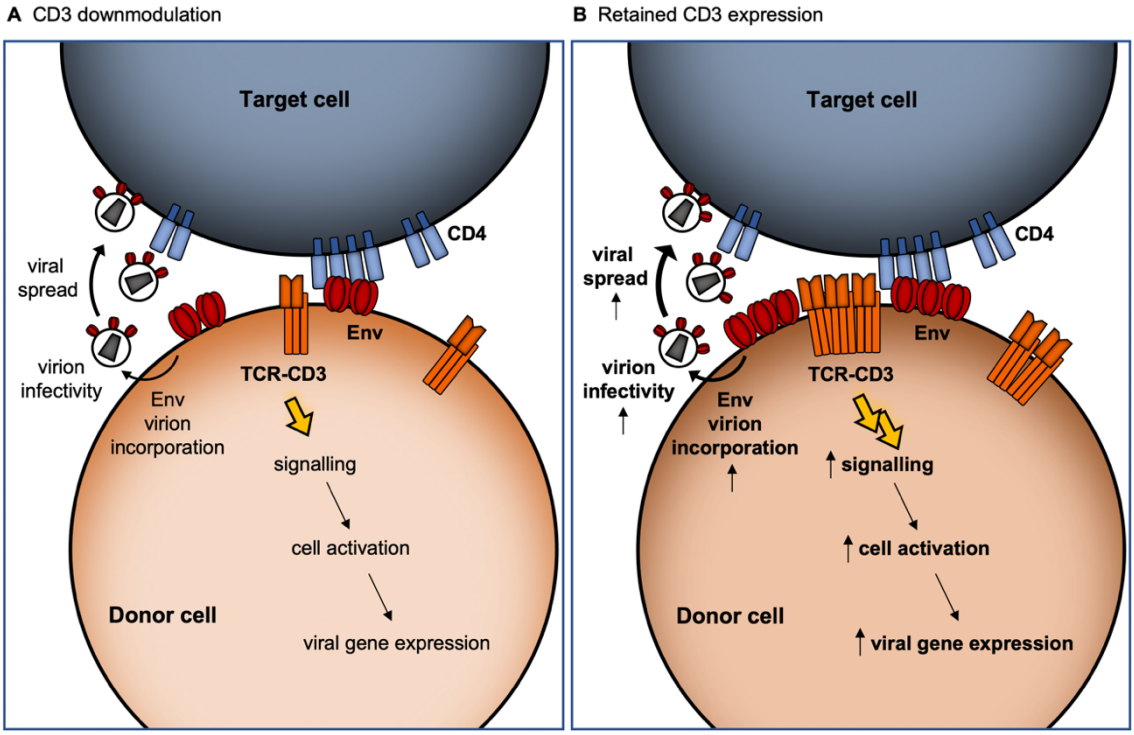

Figure 3.32: Retained CD3 expression at the VS results in increased T cell activation and viral spread
The VS formation is mediated by interaction of Env (infected donor cell) with CD4 (uninfected target cell) and is further stabilised by ICAM-1 and LFA-1 interactions (not shown). This triggers TCR signalling resulting in cell activation. The two diagrams show the VS of cells infected with **(A)** viruses that downmodulate CD3 (IL Nef) and **(B)** with viruses that retain CD3 expression (LF Nef). Comparing panels (A) and (B) shows that retained CD3 expression results in enhanced activation of signalling. This leads to increased cell activation and viral gene expression, Env and Gag. Most importantly, this results in increased surface Env expression and Env virion incorporation. Ultimately, production of virions with higher particle infectivity results in enhanced viral spread.

Notably, CD3-dependent differences were also apparent (except for CD38 upregulation) in target cells (Figure 3.21), which was somewhat surprising as all target cells express CD3 at the time of VS formation. Retained CD3 expression results in increased donor cell activation, which may contribute to enhanced transfer of viral particles across the VS or enhanced donor-target cell cross-talk at the VS, thus resulting in increased cell activation of target cells. Both scenarios are intriguing and warrant further investigation.

Interestingly, the effect of Nef-mediated CD3-modulation on Env expression and virion infectivity was restricted to primary CD4+ T cells and was not observed using Jurkat T cells, or 293T cells, which are both commonly used in HIV research. 293T cells do not express TCR-CD3 complex, thus this observation was not surprising. Jurkat cells, however, express CD3 (which can be downmodulated by IL Nefs), yet CD3-depedendent differences in Env expression and virion infectivity were not observed in this system. Jurkat cells lack expression of PTEN and SHIP1 phosphatases, which results in constitutively active PI3K/AKT pathway (Gioia et al., 2018), a major branch of downstream TCR-CD3 signalling. This hyper-activated status of Jurkat cells may explain why the effect of CD3 modulation on Env expression and viral infectivity was not observed this system. If these effects (Env expression and infectivity) are mediated by activation of TCR-CD3 signalling and Jurkat cells are already hyper-activated, then no effect may be apparent. This finding further highlights the importance of cell activation in these processes. Notably, most of experiments in this Chapter used primary CD4+ T cells that were mitogenically activated to make them permissive for initial viral infection. Given the Jurkat cell data, this might suggest that cell activation would also mask the effect of CD3-modulation in primary cells. However, *in vitro* stimulation with CD3/CD28 antibodies results in heterogeneous activation of cell in the culture, where not all cells are robustly activated. Moreover, cell activation decreases over time with cells gradually returning to resting state. Thus, it is possible to speculate that at the time of experiments, a significant population of cells was in state of “limited” or “reduced” cell activation, which likely explains why the effect of CD3 expression and TCR signalling was observed in primary CD4+ T cells.

Previous work has shown (using phospho-proteomic approaches) that formation of VS activates components of TCR signalling pathway (e.g. Lck, AKT, ERK) in both donor and target cells (Len et al., 2017). This was proposed to occur independently of antigen presentation by MHC-II. However, human CD4+ T cells (unlike in mice) can present self-antigen (via HLA-DR) to other CD4+ T cells (Kambayashi & Laufer, 2014). However, whether this potential TCR-pMHC interaction contributes to the triggering of TCR signalling at the VS was not investigated. The kinetic segregation model of TCR signalling proposes that close cell-cell contact at the immune synapse (mediated by TCR-pMHC interactions) drives size-exclusion (segregation) of inhibitory CD45 phosphatase from the cell interface, thus allowing for phosphorylation of kinases to trigger signalling (Davis & van der Merwe, 2006). In the case of the VS, donor-target cell contact is mediated by Env-CD4 and LFA-1-ICAM-1 interactions (Jolly et al., 2004,

2007b). Sustaining donor and target cells in close contact in such manner may allow triggering of antigen-independent signalling, consistent with the kinetic segregation model of TCR signalling. However, whether segregation of CD45 occurs at the VS remains to be investigated. Supporting this idea, another study showed that maintaining CD4+ T cells in close contact in the absence of TCR ligand (using supported lipid bilayers) drives CD45 segregation and triggers TCR signalling (Chang et al., 2016). Furthermore, experiments using gp120 and ICAM-1 supported lipid bilayers (mimicking infected donor cell) showed activation of TCR signalling in the target cell (Deng et al., 2016; Vasiliver-Shamis et al., 2009). This is consistent with the kinetic segregation model and antigen-independent signalling at the VS. However, further work is needed to test if kinetic segregation of phosphatases occurs at the VS.

In this Chapter, TCR signalling at the VS was examined by flow cytometry and showed increased phosphorylation of ZAP70, ERK, AKT and S6 in infected donor-target cell conjugates compared to mock control (forming non-specific conjugates). This is consistent with previous observations (Deng et al., 2016; Len et al., 2017; Vasiliver-Shamis et al., 2009) and supports the hypothesis that formation of the VS triggers T cell signalling. Notably, retained CD3 expression on infected cells (LF Nef viruses) resulted in increased phosphorylation of ERK and S6. This is consistent with increased expression of activation markers on these cells and supports the hypothesis that retained CD3 expression contributes to activation of signalling at the VS. Surprisingly, no CD3-dependent differences were observed in phosphorylation of ZAP70. This might be explained by transient activation of ZAP70 and poor detection of phosphorylation at this site by flow cytometry. Additionally, integrin signalling resulting from LFA-1-ICAM-1 interaction might also contribute to ZAP70 activation (Evans et al., 2011; Li et al., 2009; Starling & Jolly, 2016), which could mask any CD3 dependent differences and further experiments are required to investigate this possibility. Similarly, no major differences were observed in phosphorylation of AKT. Since S6 can be phosphorylated downstream of both ERK and AKT signalling cascades (Pende et al., 2004; Roux et al., 2007), this suggest that increased activation of S6 is possibly regulated via ERK at the VS. Altogether, CD3-dependent differences in phosphorylation were modest, which was somewhat surprising given the central role of CD3 complex in TCR signalling. However, this assay cannot distinguish between phosphorylation events in donor and target cells. Thus, it is possible that target cells have greater contribution to the measured signal since they do express CD3. Moreover, IL Nef viruses do not completely downmodulate CD3 (≈20% CD3+ infected cells), thus it is possible that CD3-expressing infected cells

preferentially form VS, which would skew the results. Further experiments using imaging flow cytometry would be required to dissect donor/target cell signalling contributions and CD3 expression at the VS.

Integrating these observations suggests a model where retained CD3 expression on infected cells during VS formation and cell-cell spread results in increased T cell signalling and activation (Figure 3.32). This supports more efficient expression of viral genes, most importantly Env as it is a limiting factor in viral infectivity. Increased Env surface expression and intracellular trafficking results in increased Env incorporation into nascent virions, thus mediating increased viral infectivity (Figure 3.31). Better understanding of mechanisms regulating Env trafficking and virion incorporation is required to fully understand the role of CD3 and T cell signalling in this process. During cell-cell spread, production and release of virions with higher infectivity would increase the probability of virus fusion and target cell infection, thus resulting in increased viral spread. It is also possible that retained CD3 expression and increased donor cell activation could result in greater number of released virions at the VS, or enhanced donor-target cell cross-talk that would make the target cell more permissive for the infection, thus increasing viral spread. Either or both mechanisms could act in concert with increased virion infectivity to enhance viral spread and further experiments are required to investigate this. These observations also suggest that cell-cell contact induced expression of Env and virion incorporation may present a possible mechanism for the virus to limit excessive exposure of Env and thus evade humoral immune responses. This is an intriguing scenario that warrants further investigation.

3.3.3 Cell death

Retained CD3 expression by LF Nef viruses resulted in increased cell death of donor cells during cell-cell spread. This is most likely explained by increased cell activation of donor cells, which is also contributing to enhanced viral spread. Since levels of cell death increased during cell-cell spread this suggest that cell death is triggered by cell contact. Indeed, cell-cell spread has been shown to enhance T cell death compared to cell-free infection (Galloway et al., 2015). Similarly, retained CD3 expression (LF Nef viruses) also resulted in increased target cell death. Since these cells showed both increased cell activation and viral spread, the relative contribution of each factor to cell death cannot be estimated. Interestingly, data from HIV infected patients suggests that CD4+T cell depletion is more closely corelated with immune cell activation than with viral load (Giorgi

et al., 1999; Sousa et al., 2002), suggesting that aberrant cell activation plays an important role in T cell death. Importantly, experiments in this Chapter were not designed to determine the cause of cell death, rather the data shows a positive correlation between cell activation, viral spread and cell death. Regarding the mechanism of cell death, the data here suggest that apoptosis is not responsible for observed differences in cell death, thus implicating other mechanisms, potentially necrosis or pyroptosis. Indeed, pyroptosis has been identified as the main mechanism of cell death in non-productively infected cells (Doitsh et al., 2014). Further experiments are thus required to define the mechanisms of increased contact-induced cell death.

Notably, loss of Nef-mediated CD3 downmodulation correlated with CD4+ T cell depletion during *in vivo* sooty mangabey infection from which L4 and K2 *nef* alleles were isolated (Schmökel et al., 2013), and our data recapitulates this result. It is therefore possible to speculate that increased viral replication and cell activation caused accelerated loss of CD4+ T cells in these animals. However, this study also identified extended viral tropism (CXCR4 co-receptor usage) of these viruses as a possible factor contributing to CD4+ T cell depletion. CCR5 is expressed predominantly on memory T cells, which are better able to support lentiviral infection (Brenchley et al., 2004; Paiardini et al., 2011; Veazey et al., 2000). By contrast, CXCR4 is also expressed on naïve T cells, which are less able to support infection, thus potentially explaining increased cell death and CD4+ T cell depletion (Brenchley et al., 2004; Doitsh & Greene, 2016; Milush et al., 2007). Importantly, the viruses used in this thesis were also CXCR4-tropic (NL4.3 backbone). This obviates differences in co-receptor usage as a contributor to the differences in cell death mediated by IL and LF viruses, but the effect of viral tropism on cell death *in vivo* remains unclear. Indeed, a switch to CXCR4 co-receptor usage in chronic HIV-1 patients has been linked to accelerated CD4+ T cell depletion and disease progression (Connor et al., 1997; Moore et al., 2004). Further experiments using Nef chimeric viruses with CCR5-tropic backbone are required to dissect the contribution of CD3-modulaiton and Env tropism to cell death.

4 Viral spread, virion infectivity and T cell activation by SIVmac and HIV-2 Nef chimeric viruses

4.1 Introduction

This Chapter expands the investigation of viral spread and T cell activation using SIVmac and HIV-2 Nef chimeric viruses that differ in their ability to downmodulate surface expression of CD3. Specifically, do chimeric viruses expressing SIVmac and HIV-2 Nef proteins also show CD3-dependent differences in viral spread and T cell activation? This is of interest given that SIVmac and HIV-2 are closely related to SIVsmm.

SIVsmm is a naturally occurring virus infecting sooty mangabeys, which do not develop AIDS-like disease, despite high levels of viral replication (Chahroudi et al., 2012; Rey-Cuillé et al., 1998; Sodora et al., 2009). It was proposed this is in part due to CD3 downmodulation by SIVsmm Nef, which prevents aberrant immune activation and protects from CD4+ T cell depletion (Schindler et al., 2008; Schmökel et al., 2013). However, multiple host factors have been identified that might protect sooty mangabeys from developing a pathogenic infection (Milush et al., 2011; Paiardini et al., 2011; Palesch et al., 2018; Sundaravaradan et al., 2013). SIVmac originated from a forced laboratory transmission of SIVsmm into rhesus macaques and as such is not a natural infection of rhesus macaques (Murphey-Corb et al., 1986). By contrast natural zoonotic transmissions of SIVsmm to humans have given rise to HIV-2 (Ayouba et al., 2013; Gao et al., 1994) and this has occurred on multiple independent occasions, resulting in HIV-2 groups A-I. Similar to SIVsmm Nef, SIVmac and HIV-2 Nef proteins are able to downmodulate CD3 (Schindler et al., 2006). By contrast to SIVsmm, SIVmac and HIV-2 infections in their respective hosts are usually pathogenic (Feldmann et al., 2009; Jaffar et al., 1997; Kaur et al., 1998). However, as described in Chapter 1, HIV-2 infection is generally considered to be less pathogenic compared to HIV-1, and a great proportion of infected individuals become long-term nonprogressors (Jaffar et al., 1997; Marlink et al., 1994; van der Loeff et al., 2010). These observations demonstrate that inter-species transmissions of SIVsmm into non-natural hosts can gave rise to pathogenic infections (SIVmac and HIV-2) and highlights a complex interplay between virus and host that is yet to be fully understood.

To study the effect of CD3 downmodulation by SIVmac Nef, mutant Nefs were generated that differ in their ability to downmodulate CD3. SIVmac239 molecular clone Nef chimeric

viruses were generated as described previously (Joas et al., 2020; Yu et al., 2015). Wild-type SIVmac239 Nef with residues I123, L146 and D158 (abbreviate herein as ILD Nef) is able to downmodulate surface expression of CD3 (Figure 4.1). Based on SIVsmm L4 and K2 mutant *nef* analysis (Figure 3.1) homologous mutations I123L, L146F and D158N were introduced into the SIVmac239 *nef* gene by site-directed mutagenesis (abbreviate herein as LFN Nef) to selectively disrupt the CD3 downmodulation ability (Joas et al., 2020; Yu et al., 2015). The D158N substitution had no significant effect on Nef function and was introduced to allow the detection of reversions in Nef during *in vivo* infection (Joas et al., 2020).

Unlike SIVmac Nef mutants that were made by rationale design based on SIVsmm Nef, the HIV-2 nef alleles (like SIVsmm L4 and K2) were isolated from natural *in vivo* infections (Khalid et al., 2012). This study described naturally occurring HIV-2 *nef* alleles that differ in their ability to downmodulate CD3 and it was observed that in viremic HIV-2 patients low CD4+ T cell counts correlated with loss of Nef-mediated CD3 downmodulation (Khalid et al., 2012). This might suggest a protective role of CD3 downmodulation in HIV-2 infection. Interestingly, two *nef* alleles that were isolated from one HIV-2 patient (RH2-1) with blood viremia and low CD4+ T cell count differed in their ability to downmodulate CD3. HIV-2 RH2-1 D8 Nef was able to downmodulate CD3 and A8 Nef lost this ability (retained CD3 expression). D8 and A8 *nef* alleles differed only in 14 amino acids (Figure 4.1) of which one mutation (I132T) was shown to be sufficient to disrupt CD3 downmodulation (Khalid et al., 2012). Analysis of SIVmac Nef crystal structure in complex with CD3ζ showed that Nef I123 residue interacts with the ζ-chain. This likely explains how I132T mutation in HIV-2 Nef disrupts the Nef-CD3 interaction and results in loss of CD3 downmodulation (Khalid et al., 2012). To specifically disrupt CD3 downmodulation, point mutations (I132T and T132I) in D8 and A8 *nef* alleles were made by site-directed mutagenesis. To simplify the naming, HIV-2 *nef* alleles that are able to downmodulate CD3 are referred to in this Chapter as D8 and A8 I Nef (I132) and *nef* alleles that are unable to downmodulate CD3 are referred to as D8 and A8 T Nef (T132). As described in Chapter 3, a panel of SIVmac and HIV-2 *nef* alleles: mac239 ILD and LFN, D8 I and T, A8 I and T, together with parental NL4.3 and *nef*-defective control was cloned into HIV-1 NL4.3 IRES-GFP proviral construct (Schindler et al., 2006), allowing to determine the role of CD3 downmodulation on HIV-1 cell-cell spread, irrespective of other viral genes.

```
                    myristoylation                          YxxL
SIVsmm L4 IL     1  MGAAGSKKRSKPRGGLRERLLKARGETYGRLWEGLEEGYSQSRGGLGRDWNLHSSEGQGY  60
SIVsmm K2 LF     1  ..........................................................  60
SIVmac239 ILD    1  ..G.I.MR..R.S.D..Q...R.........LGEV.D.....P...DKGLSSL.C...K.  60
HIV-2 D8 I       1  ...S....H...SQ.......R.S...C.GRCN.SGGE....Q..S..EQSSP.C...R.  60
HIV-2 A8 T       1  ...S......R.LQ.......R.S...C.GHCN.SGGE....Q..S..EQSSP.C...R.  60

                                  CD4               acidic cluster    PxxP
SIVsmm L4 IL    61  NEGQFMNTPWRNPARERKLKYRQQNMDDVDDDDNELVGVSVRPKTPLRAMSYKLAIDMS  120
SIVsmm K2 LF    61  D..........................D...............................  120
SIVmac239 ILD   61  .Q..Y........E.....A..K.....I.EE.DD........V....T..........  120
HIV-2 D8 I      61  QQ.D......KT..A...RDL.K.......SE.EG....HIT.RV.....T....V...  120
HIV-2 A8 T      61  QQ.D......KT..A...RDL.K.......SE.EG....H.T.RV...T.T....VN..  120

                                    PAK-2
SIVsmm L4 IL   121  HFIKEKGGLEGIYYDERRHRILDIYLEKEEGIIPDWQNYTSGPGIRYPMFFGWLWKLVPV  180
SIVsmm K2 LF   121  ..L......................F..................................  180
SIVmac239 ILD  121  ..............SA.......................D.........KT.........  180
HIV-2 D8 I     121  .........D...S.......T.......V........H...V..................  180
HIV-2 A8 T     121  .........D.T..S.......T..............H...V..................  180

                     β-COP    ExxxLΦ        V1H                MHC-I
SIVsmm L4 IL   181  HVSEEAQTDETHCLVHPAQTYQWDDPWGEVLAWKFDPQLAYTYEAFIRHPEEFGSKSGLS  240
SIVsmm K2 LF   181  Q.......E.......H..........................G.....  240
SIVmac239 ILD  181  N..D...E..E.Y.M.....S...........T......YV.Y..........  240
HIV-2 D8 I     181  N.LQ.--GE.D...L.....SRF..H..T.V.R....M..HE.T.........H....P  238
HIV-2 A8 T     181  NDLQ.--GE.D...L.....SRF..H..T.V....SM..HE.T.........H....P  238

SIVsmm L4 IL   241  EEEVRRRLTARGLLKMADKKETS  263
SIVsmm K2 LF   241  ....T..........I.......  263
SIVmac239 ILD  241  ..............N.......R  263
HIV-2 D8 I     239  .D.WKAK.K...IPFS         254
HIV-2 A8 T     239  .K.WKAK.K...IPFS         254
```

Figure 4.1: Sequence alignment of SIVsmm, SIVmac and HIV-2 *nef* alleles

Shown is amino acid sequence alignment of SIVsmm FBr L4 IL and K2 LF, SIVmac239 ILD, HIV-2 RH2-1 D8 I and A8 T *nef* alleles. Nef proteins that do not downmodulate CD3 are highlighted in red (SIVsmm K2 LF and HIV-2 D8 T). Shaded bars indicate amino acids directly involved in CD3 downmodulation (I123, I132, L146). Alignment of sequences also highlights important motifs for Nef interaction with: AP-2 (YxxL and ExxxLΦ), PACS (acidic cluster), β-COP (di-acidic motif, EE), V1H (DD), CD4 (PA), MHC-1 (Y221), SH3 domain of Src-family kinases (PxxP) and PAK-2 (RR). Dots indicate identity and dashes indicate gaps introduced to optimise the alignment.

Because, SIVmac and HIV-2 viruses originated from zoonotic transmissions of SIVsmm (Gao et al., 1994; Murphey-Corb et al., 1986), the *nef* alleles are closely related, with relatively high sequence similarity (Figure 4.1). A sequence alignment of the *nef* alleles viruses used in this Chapter and Chapter 3 is shown on Figure 4.1. This alignment highlights residues and sequence motifs involved in Nef interaction with the host endocytic machinery: AP-2 (YxxL and ExxxLΦ), PACS (acidic cluster), β-COP (di-acidic motif, EE), and V1H (DD). Residues important for downmodulation of CD3 (I123, I132, L146), CD4 ($P_{73}A$), MHC-1 (Y221) are also highlighted (Munch et al., 2005). Additionally, Nef interacts with SH3 domain of Src-family kinases (PxxP) and PAK-2 (RR) to

deregulate cell signalling, activation and the actin cytoskeleton (Haller et al., 2007; Olivieri et al., 2011; Rudolph et al., 2009; Stolp et al., 2010). Importantly, this sequence analysis shows that the known residues involved in the interaction with major Nef targets are conserved between the SIVsmm, SIVmac and HIV-2 *nef* alleles used in this thesis.

4.2 Results

4.2.1 Validation of the phenotype of SIVmac Nef chimeric viruses

The first part of this Chapter investigates viral spread of SIVmac Nef chimeric viruses. In order to assess the impact of differences in Nef-mediated CD3 downmodulation it was necessary to first validate the chimeric viruses provided by our collaborator Frank Kirchhoff (Joas et al., 2020; Yu et al., 2015). SIVmac 239 ILD and LFN *nef* alleles cloned into HIV-1 NL4.3 IRES-GFP proviral construct (Schindler et al., 2006) were first sequenced, which confirmed their sequence identity. To validate and characterise the SIVmac 293 ILD and LFN variants (as described in Chapter 3), 293T cells were transfected with viral plasmids and viruses were titrated prior to infection of primary CD4+ T cells. The virus produced from 293T cells was characterised by measuring virion infectivity (as described in Figure 3.2), which showed that NL4.3, SIVmac ILD and LFN proviruses produce infectious virus with no observable difference between SIVmac ILD and LFN mutant pair (Figure 4.2A). Consistent with previous observations (Figure 3.2) and published data (Chowers et al., 1994; Münch et al., 2007), *nef*-defective virus had significantly lower infectivity compared to NL4.3 Nef virus. Both SIVmac Nef viruses showed slightly higher infectivity compared to NL4.3 Nef virus (1.6-fold increase; p=0.0021), which is consistent with previous observations (Heigele et al., 2016; Joas et al., 2020). Next, primary CD4+ T cells isolated from healthy PBMC donors were activated with anti-CD3/CD28 antibodies and infected with equal infectious doses of Nef chimeric viruses (*nef*-defective, NL4.3, SIVmac ILD, SIVmac LFN). After 48h primary CD4+ T cells were analysed by flow cytometry to quantify the percentage of HIV-1 infection and Nef activity. Infected cells were identified as single, live lymphocytes that are positive for Gag and/or GFP expression (gating strategy shown in Figure 3.2). Analysis of infected CD4+ T cells showed broadly similar percentages of Gag+ or GFP+ cells between cells infected with the different Nef-containing chimeric viruses (Figure 4.2B-C). Cells infected with *nef*-defective virus showed lower infection levels as measured by Gag expression when compared to other Nef-containing viruses; however, this difference was smaller when measuring GFP expression. As described in Chapter 3 (Figure 3.2), GFP+ cells

better represent productively infected population, thus expression of GFP was used in the majority of further experiments (unless otherwise stated) to identify infected cells.

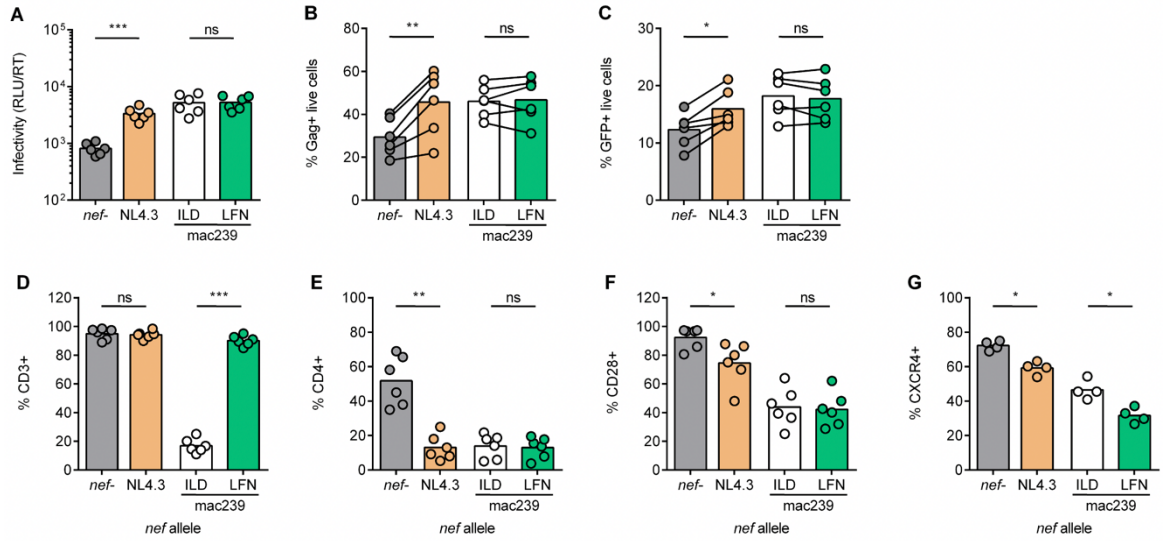

Figure 4.2: Validation of SIVmac Nef chimeric viruses

(A) Nef chimeric viruses were produced by transfection of HEK293T cells. Viral infectivity (RLU) was measured by titration on HeLa-TZMbl reporter cell line and normalised to supernatant RT activity, a measure of viral content. **(B-G)** Primary CD4+ T cells were activated with anti-CD3/CD28 antibodies for 4-5 days, infected with Nef chimeric viruses for 48h and analysed by flow cytometry. **(B)** Percentage of Gag+ live cells. **(C)** Percentage of GFP+ live cells. Percentage of live, GFP+ cells positive for **(D)** CD3, **(E)** CD4, **(F)** CD28, and **(G)** CXCR4 surface markers. Bars show mean and lines join paired results from the same PBMC donor. Groups were compared using paired *t*-test (ns, P>0.05; *, P<0.05; **, P<0.01; ***, P<0.001).

To determine the ability of SIVmac ILD and SIVmac LFN to downmodulate surface expression of CD3, CD4, CD28, and CXCR4, primary CD4+ T cells were infected with *nef*-defective, NL4.3, SIVmac ILD and LFN Nef chimeric viruses (or uninfected mock control) and analysed by flow cytometry to measure expression of these surface markers. For simplicity, SIVmac ILD is hereon abbreviated as ILD and SIVmac LFN is abbreviated as LFN. Figure 4.2D shows that, as expected, ILD Nef expressing virus was able to downmodulate surface expression of CD3 and reduced the number of CD3+ infected cells to less than 20%. By contrast, LFN Nef was unable to downmodulate CD3 expression as evidenced by more than 90% of cells remaining CD3+, similar to the percentage of CD3+ cells in *nef*-defective and NL4.3 Nef virus infected cells. CD4 surface staining (Figure 4.2E) showed that all Nef-containing viruses (NL4.3, ILD and LFN) retained the ability to downmodulate (≈15% CD4+ infected cells). As described in Chapter 3, the partial downregulation of CD4 by *nef*-defective virus (≈50% CD4+ infected

cells), is attributed to the presence of HIV-1 Vpu that can mediate CD4 degradation (Willey et al., 1992). CD28 surface expression analysis (Figure 4.2F) showed that ILD and LFN Nef viruses downmodulated CD28 to similar extent (≈40% CD28+ infected cells), whereas as shown in Chapter 3, NL4.3 Nef was less able to do so (≈70% CD28+ infected cells), which is in agreement with published data (Munch et al., 2005; Yu et al., 2015). Similarly, ILD and LFN Nef viruses were able to downmodulate CXCR4 (Figure 4.2G), however it was observed that LFN Nef virus was better able to downmodulate CXCR4 compared to its ILD Nef counterpart, consistent with previous observations (Hrecka et al., 2005; Joas et al., 2020). Together these results validate the expected phenotype of SIVmac Nef chimeric viruses, and show that generation of ILD and LFN Nef mutants by site-directed mutagenesis had specific effect on downmodulation of CD3, with a modest effect on CXCR4 downmodulation. This was also observed for SIVsmm chimeric viruses (Figure 3.3), suggesting that mutations disrupting CD3 interaction may also impact on CXCR4 downmodulation.

As described in Chapter 3, the ability of Nef chimeric viruses to antagonise host restriction factors SERINC5 impacts on viral infectivity. Therefore, antagonism of SERINC5 by ILD and LFN Nef chimeric viruses was tested. To do this, 293T cells were co-transfected with viral plasmids alongside increasing doses of dual-tagged SERINC5 expressing plasmid (Pye et al., 2020). In this assay, the presence of increasing doses of SERINC5 reduces the infectivity of progeny virus if SERINC5 is not antagonised by Nef (Heigele et al., 2016; Rosa et al., 2015). Flow cytometry analysis confirmed a dose-dependent increase in the amount of total SERINC5 expressed in transfected cells measured by intracellular staining for HA-tagged SERINC5 (Figure 4.3A). In agreement with previous reports (Heigele et al., 2016; Rosa et al., 2015), SERINC5 over-expression resulted in up to a 300-fold reduction in infectivity of *nef*-defective virus that was rescued by expression of functional Nef (Figure 4.3B). Importantly, there was no significant difference in infectivity between ILD and LFN Nef viruses in in the presence or absence of SERINC5 overexpression (Figure 4.3B). Flow cytometry analysis of SERINC5 cell surface expression (detected by extracellular Flag-tag) showed that ILD and LFN Nef viruses were equally able to remove SERINC5 from the cell surface as evidenced by similar amounts of cell surface SERINC5 (Figure 4.3C). This is consistent with the similar levels of infectivity that were observed in Figure 4.3B. Similar levels of total SERINC5 expression was confirmed by staining for intricellular HA-tag (Figure 4.3D). Consistent with published data (Heigele et al., 2016), NL4.3 Nef is less able to downmodulate SERINC5 surface expression compared to SIVmac Nef (2.7-fold reduction; p=0.0074).

Taken together, these results show that Nef mutations disrupting CD3 downmodulation in SIVmac do not affect SERINC5 antagonism.

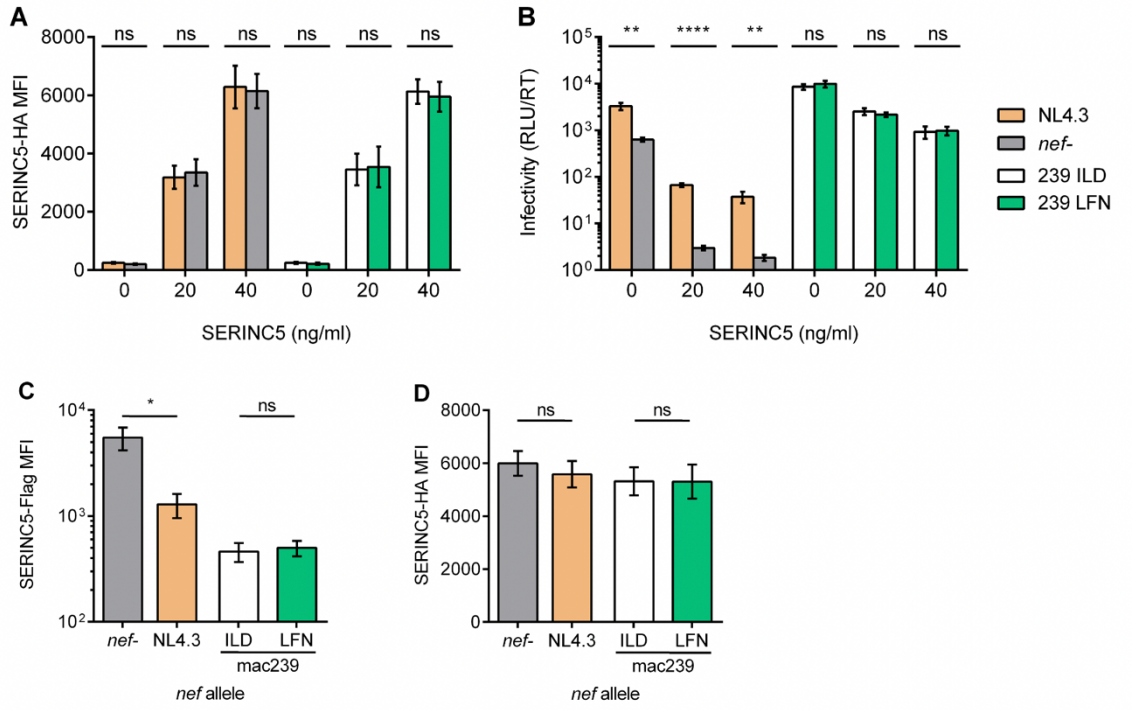

Figure 4.3: SIVmac Nef chimeric viruses have similar ability to antagonise SERINC5

HEK293T cells were co-transfected with Nef chimeric proviruses and increasing doses of plasmid encoding dual-tagged SERINC5 (n=3). Cells and virus supernatants were harvested 48h post-transfection. Virion infectivity (RLUs) was measured using HeLa-TZMbl reporter cell assay and normalised to supernatant RT activity. Flow cytometry was used to measure total SERINC expression (intracellular HA-tag) or surface SERINC expression (extracellular Flag-tag). **(A)** MFI of SERINC5 HA-tag in live, GFP+ population. **(B)** Virion infectivity in the presence of SERINC5. **(C)** MFI of SERINC5 Flag-tag (surface expression), and **(D)** MFI of SERINC5 HA-tag (intracellular expression) in GFP+HA-tag+ cells transfected with 20 ng/ml SERINC5 plasmid. Error bars show mean ± SEM. Groups were compared using unpaired *t*-test (ns, P>0.05; *, P<0.05; **, P<0.01; ***, P<0.001).

4.2.2 Viral spread of SIVmac Nef chimeric viruses

To investigate the effect of CD3 downmodulation on cell-cell spread, primary CD4+ T cells infected with Nef chimeric viruses (donor cells) were co-cultured with autologous uninfected, pre-labelled target cells as described in Chapter 3 (Figure 3.5). Donor cells were infected for 48h and the number of infected, GFP+ cells was quantified by flow cytometry. To account for differences in initial infection between different PBMC donors, donor and target cells were mixed in 1:4 ratio to obtain approx. 10% GFP+ donor cells in donor-target cell co-culture. Viral spread was measured 24h post-mix (single round of

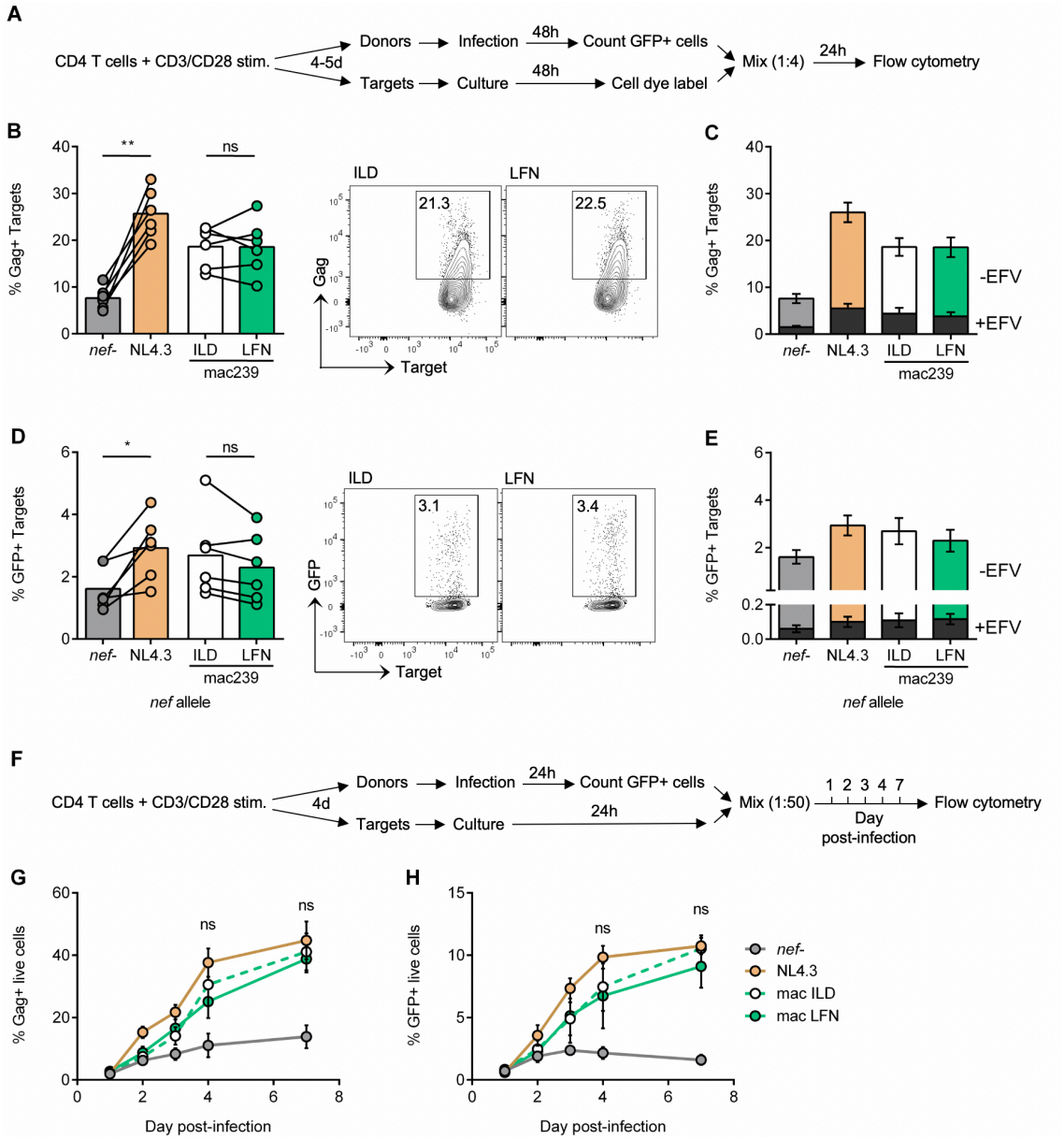

Figure 4.4: Cell-cell spread of SIVmac Nef chimeric viruses

(A) Schematic of the 24h cell-cell spread assay. CD4+ T cells infected with indicated viruses were mixed with autologous, pre-labelled target cells in 1:4 ratio (GFP+ donor cell:target cell). Cells were analysed by flow cytometry at 0h and 24h post-mix. (n=6). **(B)** Percentage of Gag+ target cells. **(C)** Donor and target cells were co-cultured in the presence or absence of 5 μM Efavirenz (± EFV). Superimposed grey bars show percentage of Gag+ target cells in presence of Efavirenz. **(D)** Percentage of GFP+ target cells. **(E)** Percentage of GFP+ target cells in presence of 5 μM Efavirenz (superimposed grey bars). Shown are representative flow cytometry plots. **(F)** Schematic of the long-term cell-cell spread assay. CD4+ T cells were infected with Nef chimeric viruses for 24h and analysed by flow cytometry to count GFP+ cells. Infection levels in cell culture were adjusted to 2% GFP+ cells with autologous, unlabelled, uninfected cells. Spreading infection was quantified by flow cytometry until 7 days post-infection (n=3). **(G)** Percentage of Gag+ live cells. **(H)** Percentage of GFP+ live cells. ILD and LFN Nef viruses were compared for statistical significance at days 4 and 7 post-infection. Bars show mean and lines join paired results from the same PBMC donor. Error bars show mean ± SEM. Groups were compared using paired *t*-test (ns, P>0.05; *, P<0.05; **, P<0.01; ***, P<0.001).

replication) by flow cytometry to identify Gag+ or GFP+ target cells (Figure 4.4A). Target cells were identified as live single cells positive for Target dye (gating strategy shown in Figure 3.5). Quantifying Gag-expressing target cells (Figure 4.4B), showed that ILD Nef virus (CD3 downmodulation) spread equally well as its LFN counterpart (retained CD3 expression), thus showing similar levels of cell-cell spread regardless of their ability to downmodulate CD3 expression (Figure 4.4B). Notably, ILD and LFN Nef viruses showed slightly decreased viral spread (Gag+ target cells) compared to NL4.3 Nef virus (≈19% vs ≈25% Gag+ target cells, 1.3-fold reduction; p=0.029). Treating co-cultures with the RT inhibitor Efavirenz resulted in an approximately 5-fold reduction of Gag+ target cells (Figure 4.4C), indicating that this assay predominantly measures productive infection. Measuring infection levels by LTR-driven expression of GFP reporter also showed similar levels of cell-cell spread by ILD and LFN Nef viruses (Figure 4.4D). When measuring GFP expression it was noted that SIVmac Nef viruses showed similar levels of viral spread compared to NL4.3 Nef virus (2.9% vs 2.5% GFP+ target cells; p=0.717) that was by contrast to measuring Gag expression. Treating co-cultures with Efavirenz almost completely abrogated detection of GFP+ target cells (Figure 4.4E), again showing that this assay is measuring productive infection. To extend the analysis of viral spread between ILD and LFN Nef viruses over time, a long-term spreading infection assay was performed. To do this, primary CD4+ T cells were infected with virus and infection levels adjusted to 2% GFP+ cells at 24h post-infection with autologous uninfected cells to equalise infection levels (Figure 4.4F). Viral spread was then measured by quantifying the percentage of Gag+ or GFP+ cells by flow cytometry over 7 days post-infection. ILD and LFN Nef viruses again showed similar levels of viral spread and replication kinetics as measured by expression of both Gag and GFP (Figure 4.4G-H). Taken together, these data show that the spread of ILD and LFN SIVmac Nef viruses that differ in their ability to downregulate CD3 are similar, and that there is no apparent correlation between CD3 expression on infected cells and cell-cell spread. These data are not in agreement with observations in Chapter 3 using SIVsmm Nef chimeric viruses, which showed CD3-dependent differences in cell-cell spread. Thus, further experiments in this Chapter were done to reconcile these differences.

Viral cell-cell spread takes place at virological synapses – VS (Jolly et al., 2004). Thus, to further examine the lack of a difference in cell-cell spread of ILD and LFN viruses, formation of VS in the donor-target cell co-cultures was measured. Primary CD4+ T cells infected with NL4.3, ILD and LFN Nef viruses were mixed with autologous uninfected pre-labelled target T cells, incubated on coverslips for 1h, stained and analysed by

immunofluorescent microscopy. As shown in Figure 4.5, examination of VS formation revealed no difference in the frequency or appearance of VS formed between ILD and LFN Nef viruses and target T cells (Figure 4.5D). This is consistent with no differences being observed in cell-cell spread.

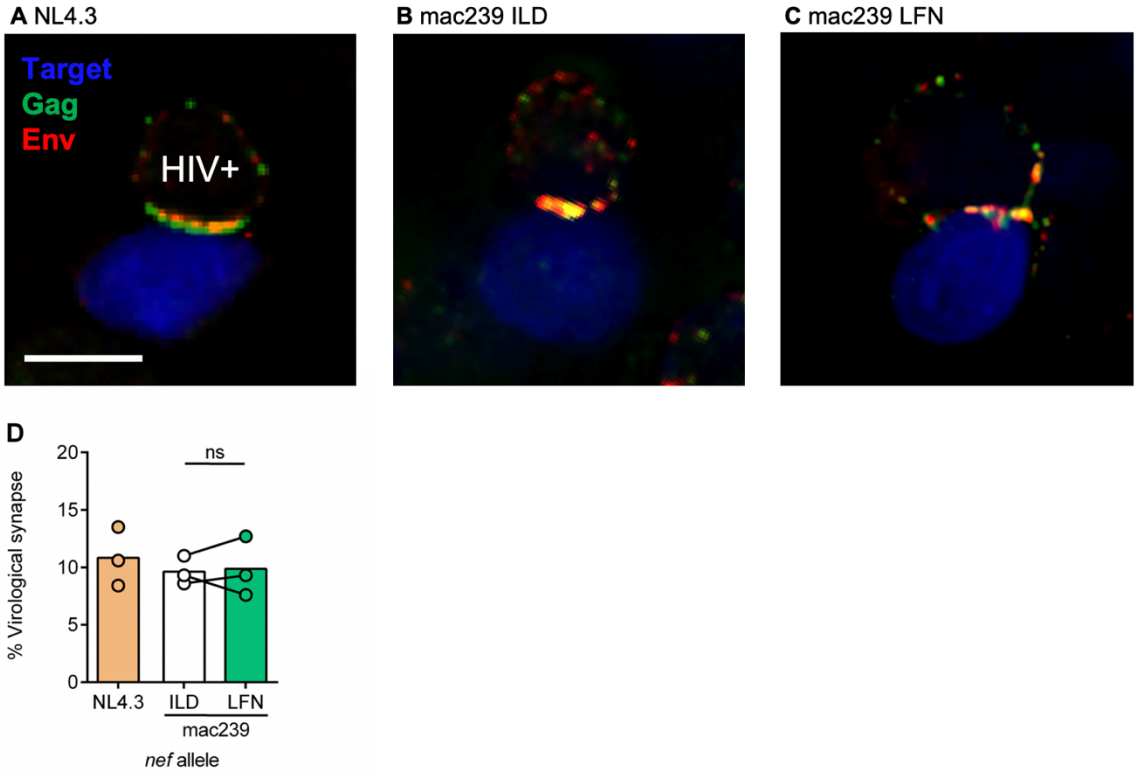

Figure 4.5: CD4+ T cells infected with Nef chimeric viruses form virological synapses at similar frequencies

CD4+ T cells were infected with Nef chimeric viruses for 48h. Autologous uninfected target cells were labelled with cell tracing dye and mixed with infected donor cells at 1:1 ratio. Cells were incubated on coverslips for 1h before fixation and antibody staining for immunofluorescence microscopy. Virological synapse (VS) was defined as infected donor cell-target cell conjugate with Gag and Env polarised towards the cell-cell contact. **(A-C)** Target cell dye is shown in blue, Gag is shown in green and Env is shown in red Scale bar is 5 μm. Shown are representative images (single xy slice) of VS for **(A)** NL4.3, **(B)**, ILD, and **(C)** LFN SIVmac Nef chimeric viruses. **(D)** Quantification of microscopy data. Shown is percentage of conjugates forming VS out of all donor-target cell conjugates. Minimum of 30 VS were counted for each PBMC donor. Bars show mean and lines join paired results from the same PBMC donor. Groups were compared using paired *t*-test (ns, $P>0.05$; *, $P<0.05$).

To investigate whether cell activation was masking CD3-dependent differences in viral spread, donor CD4+ T cells were treated with IL-7 to make them permissive to infection without causing robust T cell activation (as described in Chapter 3) and then co-cultured

with autologous uninfected, IL-7 treated, pre-labelled target cells (Figure 4.6A). Viral spread was quantified by flow cytometry 48h post-mix. Similar to what was seen using CD3/CD28 activated cells, both ILD and LFN Nef viruses showed similar levels of cell-cell spread when infection quantified either by percentage of Gag+ or GFP+ target cells (Figure 4.6B-C). Notably, ILD and LFN Nef viruses showed a more pronounced decrease in cell-cell spread compared to NL4.3 Nef virus (5% vs 10% Gag+ target cells, 2-fold reduction, p=0.017), whereas this effect was less apparent with CD3/CD28 activated CD4+ T cells (19% vs 25% Gag+ target cells, 1.3-fold reduction; Figure 4.4). Comparing IL-7 and CD3/CD28 activation experiments, cell-cell spread using IL-7 treated cells showed a lower percentage of either Gag+ (19% vs 5%, 3.6-fold reduction) or GFP+ (2.5% vs 0.5%, 5-fold reduction) target cells overall. Taken together, these data show that mode of T cell activation does not change the relative differences in viral spread of ILD and LFN Nef viruses with differential CD3 modulation; however, the mode of T cell activation does affect the absolute levels of viral spread, presumably by altering cellular permissivity as shown in Chapter 3.

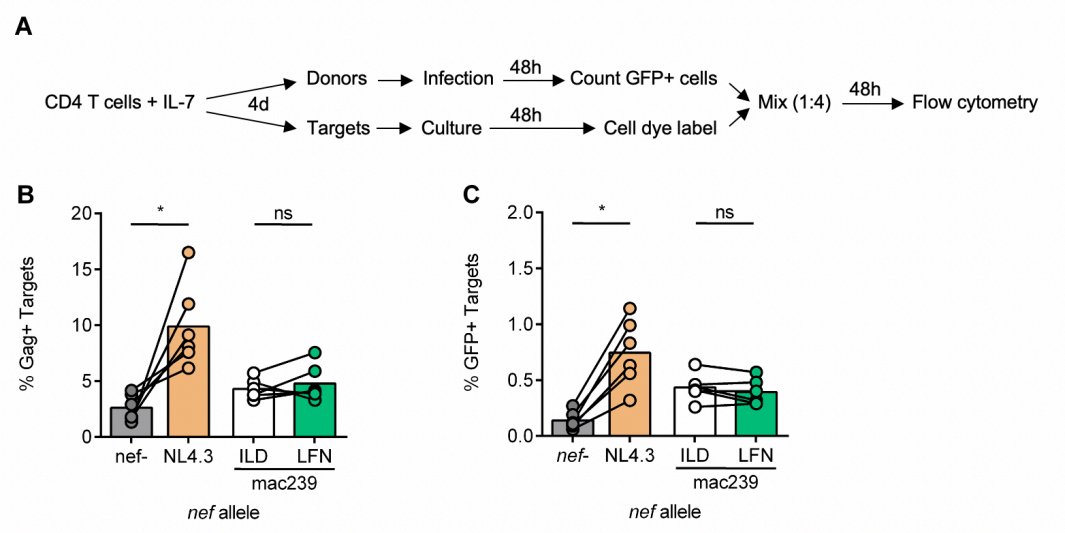

Figure 4.6: Cell-cell spread of SIVmac Nef chimeric viruses in IL-7 treated cells

(A) Schematic of the cell-cell spread assay. Primary CD4+ T cells were treated with IL-7 for 4 days. Donor cells were infected with Nef mutant viruses for 48h and analysed by flow cytometry to count GFP+ cells. Target cells were labelled with cell dye and mixed with infected donor cells in 1:4 ratio (GFP+ donor cell:target cell). Cells were analysed by flow cytometry at 48h post-mix. **(B)** Percentage of Gag+ target cells. **(C)** Percentage of GFP+ target cells. Bars show mean and lines join paired results from the same PBMC donor. Groups were compared using paired *t*-test (ns, P>0.05; *, P<0.05; **, P<0.01; ***, P<0.001).

4.2.3 Retained CD3 expression of SIVmac Nef viruses results in decreased Env expression and virion infectivity

To investigate why Nef-mediated modulation of CD3 expression does not affect viral spread of SIVmac viruses, virus release from infected cells and virion infectivity were analysed. CD4+ T cells were infected with SIVmac Nef chimeric viruses for 48h before virus containing culture supernatants and infected cells were collected and analysed. Virus release/budding from infected cells was quantified by measuring the amount RT activity present in the supernatants using an SG-PERT assay. RT activity measurements were normalised to the number of infected (GFP+) cells as quantified by flow cytometry. Figure 4.7A shows that cells infected with LFN virus (retained CD3 expression) showed significantly more virus release compared to cells infected with ILD virus (CD3 downmodulation). By contrast, quantification of virion infectivity measured by titrating the supernatants on HeLa-TZMbl reporter cell line revealed significantly greater virion infectivity of ILD Nef virus (CD3 downmodulation), compared to its LFN Nef counterpart (Figure 4.7B). As expected, NL4.3 Nef virus displayed significantly higher virion infectivity compared to *nef*-defective virus that can be attributed to the lack of SERINC antagonism (Rosa et al., 2015; Usami et al., 2015). For this analysis, the RLU values were normalised to supernatant RT activity to account for any differences in viral budding. When normalising RLU values to number of infected (GFP+) cells (to account for differences in infection levels) ILD and LFN Nef viruses showed similar supernatant infectivity (Figure 4.7C). This indicates that reduced virion infectivity of LFN Nef virus is compensated by increased virus release to yield similar levels of total supernatant infectivity compared to ILD Nef virus, which likely explains the similar levels of cell-cell spread observed for these viruses. Notably, observations here are in stark contrast to SIVsmm Nef data, which showed that retained CD3 expression resulted in increased virion infectivity and broadly similar levels of virus release.

Next, I sought to gain insight why virions produced in the presence of CD3 expression were less infectious. Having already excluded differences in SERINC5 antagonism (Figure 4.3), experiments were performed to measure Env expression, processing and incorporation into virions, similar to Chapter 3. CD4+ T cells infected with Nef chimeric viruses for 48h and then cell culture supernatants and cells were harvested for analysis. Immunoblot analysis of sucrose-gradient purified virions showed decreased incorporation of both Env subunits, gp120 and gp41 into nascent particles in LFN viruses (retained CD3 expression) compared to the ILD Nef counterpart (Figure 4.8A-C).

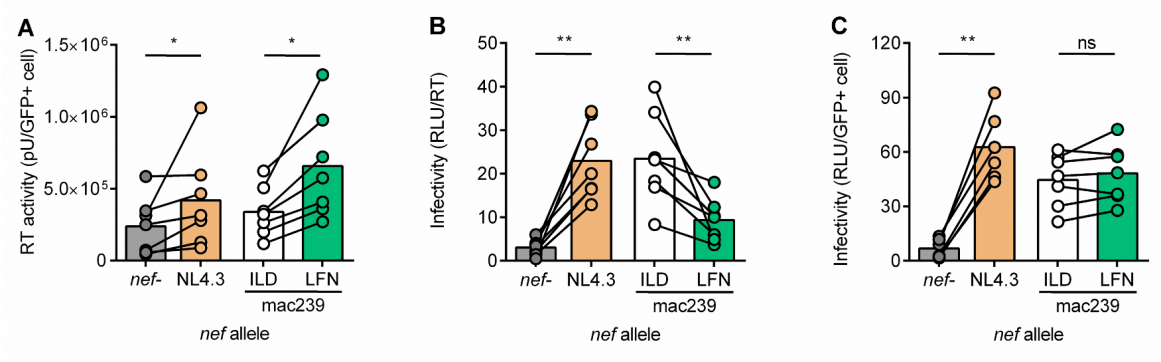

Figure 4.7: Virion infectivity and virus release of SIVmac Nef chimeric viruses

Primary CD4+ T cells were infected with Nef chimeric viruses and culture supernatants collected at 48h post-infection. Number of GFP+ cells in cell culture was analysed by flow cytometry. **(A)** Virus release was measured by supernatant RT activity and normalised to number of infected GFP+ cells. **(B)** Virion infectivity (RLUs) was measured using HeLa-TZMbl reporter cell assay and normalised to supernatant RT activity as measured in (A). **(C)** Supernatant infectivity (RLUs) was measured as in (B) and normalised to number of infected GFP+ cells (as measured in (A)). Bars show mean and lines join paired results from the same PBMC donor. Groups were compared using paired *t*-test (ns, P>0.05; *, P<0.05; **, P<0.01; ***, P<0.001).

Quantification of immunoblots by densitometry analysis of three independently prepared viral preparations from three independent PBMC donors showed a significant decrease in Env gp120 and gp41 incorporation into virions when normalised by the viral capsid protein Gag p24. This decrease in Env content is consistent with observation that this virus is less infectious (Figure 4.7). To understand the differences in Env virion incorporation, Env synthesis and processing were examined by immunoblot analysis of cell lysates (Figure 4.8D). Infected cells were analysed by flow cytometry to confirm similar levels of infection between Nef chimeric viruses (Figure 4.8E). Quantifying ratio of gp160/gp120 showed no difference in processing between ILD and LFN Nef viruses (Figure 4.8F). Env synthesis was quantified as ratio of total Env (gp160 + gp120) or gp41 normalised to cellular protein tubulin (Figure 4.8G-H). LFN Nef virus showed a decrease in Env synthesis compared to ILD Nef virus. By contrast, quantifying Gag expression, ILD and LFN Nef viruses showed similar ratios of Gag protein p55 normalised to tubulin (Figure 4.8I). Consistent with this observation, quantifying ratios of total Env (gp160 + gp120) or gp41 normalised to Gag protein p55 again showed decreased levels of Env for LFN Nef virus compared to its ILD counterpart (Figure 4.8J-K). Taken together, these results suggest that retained CD3 expression of LFN Nef virus results in decreased Env synthesis and Env incorporation into nascent virions, which is consistent with decreased virion infectivity of the SIVmac LFN virus. By contrast increased virus release of LFN Nef

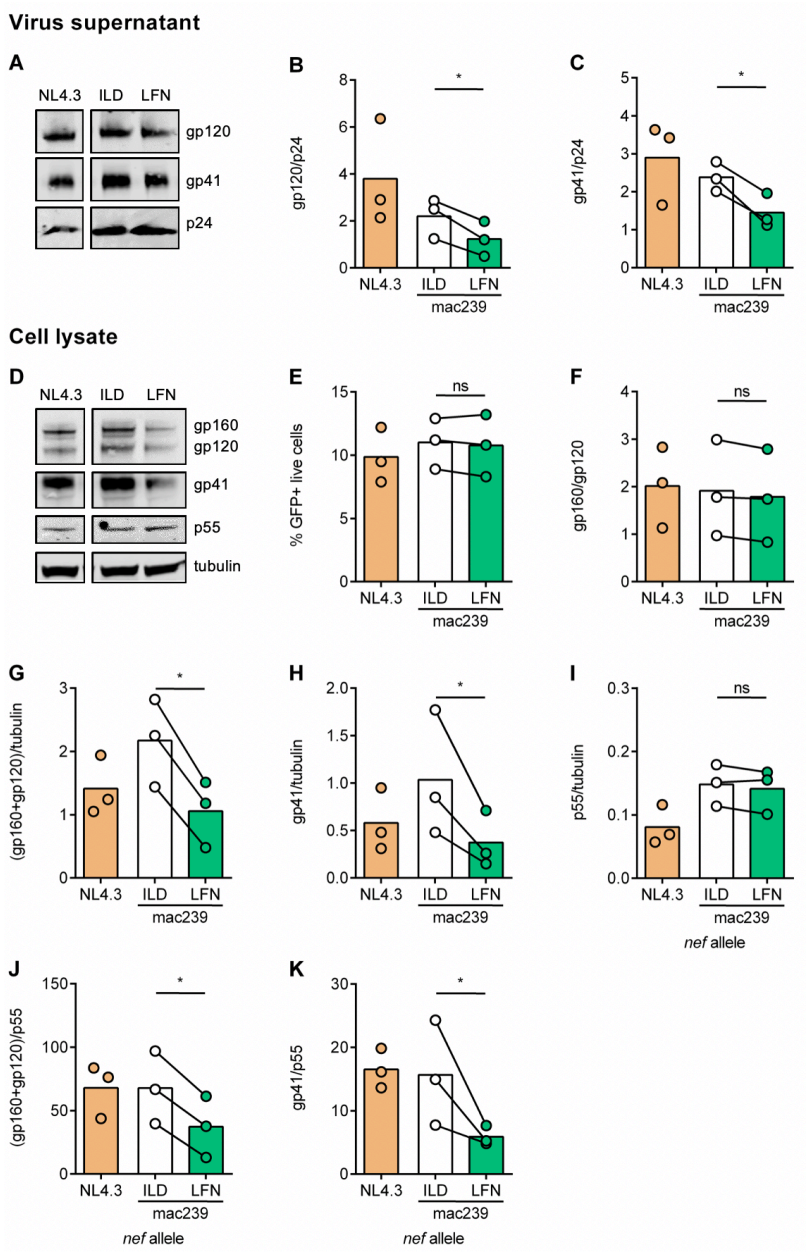

Figure 4.8: Env virion incorporation, synthesis and processing of SIVmac Nef chimeric viruses

Primary CD4+ T cells were infected with Nef chimeric viruses. Cells and culture supernatants were collected at 48h post-infection for immunoblot and flow cytometry analysis. **(A-C)** Immunoblotting of virus purified from cell culture supernatants. **(A)** Representative immunoblot shows detection of Env gp120, Env gp41 and Gag p24. **(B)** Quantification of gp120 incorporation normalised to p24. **(C)** Quantification of gp41 incorporation normalised to p24. **(D-K)** Immunoblot analysis of infected cell lysates. **(D)** Representative immunoblot shows detection of Env gp160, Env gp120, Env gp41, Gag p55 and tubulin. **(E)** Percentage of GFP+ live cells in the infected cell cultures as measured by flow cytometry prior to cell lysis. **(F)** Quantification of Env cleavage, shown as ratio of gp160/gp120. **(G)** Quantification of Env (gp160+gp120) expression normalised to tubulin. **(H)** Quantification of Env gp41 expression normalised to tubulin. **(I)** Quantification of Gag p55 expression normalised to tubulin. **(J)** Quantification of Env (gp160+120) normalised to p55. **(K)** Quantification of Env gp41 expression normalised to p55. Bars show mean and lines join paired results from the same PBMC donor. Groups were compared using paired *t*-test (ns, P>0.05; *, P<0.05; **, P<0.01; ***, P<0.001).

virus does not correlate with increased synthesis of Gag protein in the cell, which suggest other mechanisms are likely influencing viral budding.

Having observed differences in Env protein expression by immunoblotting, this phenotype was further examined using quantitative PCR and flow cytometry. First, the expression of Env and Gag mRNA was analysed by qRT-PCR. As above, CD4+ T cells were infected for 48h and analysed by flow cytometry to confirm similar infection levels between Nef chimeric viruses (Figure 4.9A). Percentage of infected (GFP+) cells was equalised to 8% in all infected cultures (using autologous uninfected cells) to facilitate the comparison between viruses and PBMC donors. Env and Gag mRNA expression was normalised to a housekeeping gene GAPDH mRNA levels. Decreased expression of Env mRNA was observed in cells infected with LFN Nef virus, which retain CD3 expression, compared to ILD Nef virus (Figure 4.9B). By contrast, ILD and LFN Nef viruses showed similar levels of Gag mRNA expression (Figure 4.9C). Consistent with this, decreased Env mRNA expression was observed when normalised to Gag mRNA (Figure 4.9D). These data are in agreement with the immunoblot analysis and show that retained CD3 expression results in decreased expression of Env mRNA and similar expression of Gag mRNA, suggesting that the decrease in Env protein is likely due to decreased transcription from the *env* gene.

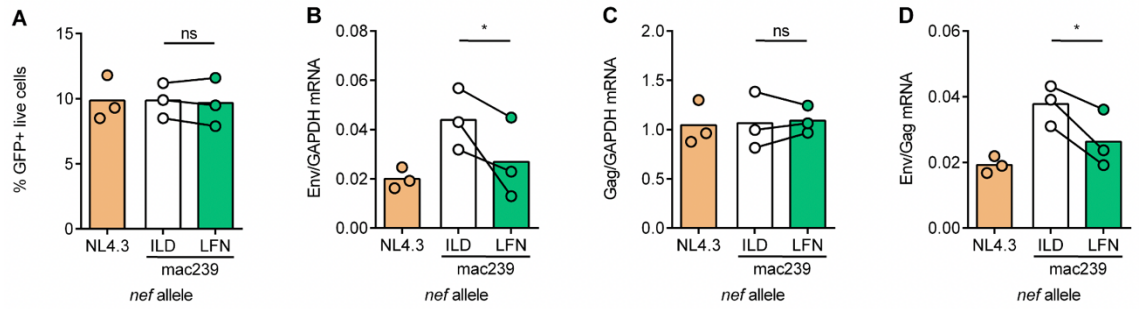

Figure 4.9: Env and Gag mRNA expression of SIVmac Nef chimeric viruses

Primary CD4+ T cells infected with Nef chimeric viruses were collected at 48h post-infection for flow cytometry analysis to equalise percentage of GFP+ live cells (8%) in all samples using autologous uninfected cells. Cells were analysed by qRT-PCR for Env, Gag, and GAPDH mRNA expression. **(A)** Percentage of GFP+ live cells before mixing with autologous uninfected cells. **(B)** Env mRNA relative expression normalized to GAPDH. **(C)** Gag mRNA relative expression normalized to GAPDH. **(D)** Env mRNA relative expression normalized to Gag. Bars show mean and lines join paired results from the same PBMC donor. Groups were compared using paired *t*-test (ns, P>0.05; *, P<0.05; **, P<0.01; ***, P<0.001).

Env is expressed on the plasma membrane of infected cells where it gets incorporated into viral particles as they bud from the cell surface. Decreased Env incorporation by LFN virus may therefore reflect a decrease in Env surface expression on infected cells. To test this, and further validate the immunoblot and qPCR data, Env protein expression was analysed by flow cytometry. CD4+ T cells were infected for 48h and analysed by flow cytometry to detect surface Env expression. As described in Chapter 3, surface staining was performed using two conformation-sensitive, broadly neutralising antibodies (bnAbs) that recognise functional Env trimers: PGT151 (cleaved trimer) and PG9 (trimer apex) (Burton et al., 2009; Falkowska et al., 2014). Decreased expression of surface Env (as recognised by both antibodies and quantified by the Env MFI) was observed on cells infected with LFN virus, which retains CD3 expression, when compared to ILD Nef virus (Figure 4.10). This is consistent with decreased levels of total intracellular Env (immunoblot) and decreased expression of Env mRNA for LFN Nef virus. This is also consistent with (and might explain) lower Env virion incorporation and decreased infectivity of LFN Nef virus.

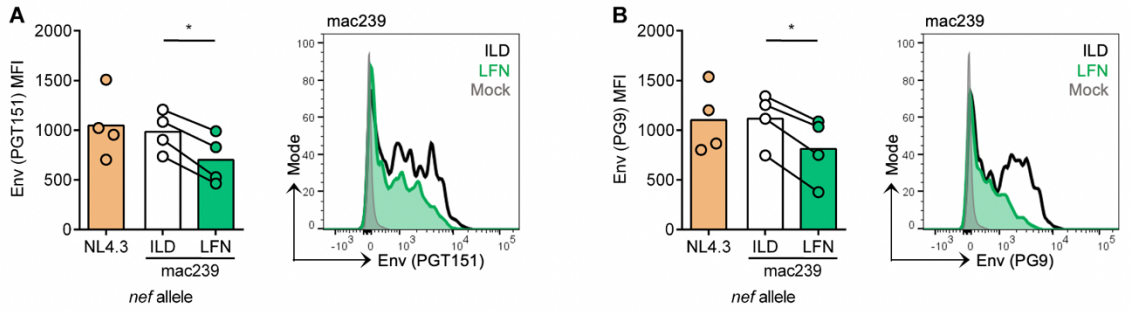

Figure 4.10: Surface Env expression of SIVmac Nef chimeric viruses

Primary CD4+ T cells infected with Nef chimeric viruses were collected at 48h post-infection for flow cytometry analysis of surface Env expression. Expression (MFI) of surface Env as detected by **(A)** PGT151 Ab, and **(B)** PG9 Ab. Right-hand side panels show representative flow cytometry plots. Mock is uninfected control. Bars show mean and lines join paired results from the same PBMC donor. Groups were compared using paired *t*-test (ns, P>0.05; *, P<0.05; **, P<0.01; ***, P<0.001).

To test whether increased Env trimer surface expression correlates with increased Env virion incorporation (as measured by immunoblot analysis), incorporation of functional Env trimers into virions was analysed by antibody neutralisation assay. Equal amounts of infectious virus produced from CD4+ T cells were titrated against increasing doses of antibodies to obtain neutralisation curves and to calculate IC_{50} values. LFN Nef virus, which retain CD3 expression, was easier to neutralise and showed lower IC_{50} values

compared to ILD Nef virus (Figure 4.11A-B) that is consistent with decreased Env trimer incorporation into virions. This result is in agreement with the immunoblot analysis where decreased Env virion incorporation into LFN Nef virions was observed (Figure 4.8). Furthermore, no differences in IC_{50} values were observed between ILD and LFN Nef viruses produced by 293T cells (Figure 4.11C). This was expected given that these viruses are equally infectious when produced from 293T cells (Figure 4.2) and that they express equal levels of surface Env on 293T cells (Figure 4.11D). Taken together, these results show that retained CD3 expression on infected CD4+ T cells results in production of virus that is easier to neutralise, indicative of less Env in viral particles, which correlates with decreased Env surface expression and Env virion incorporation.

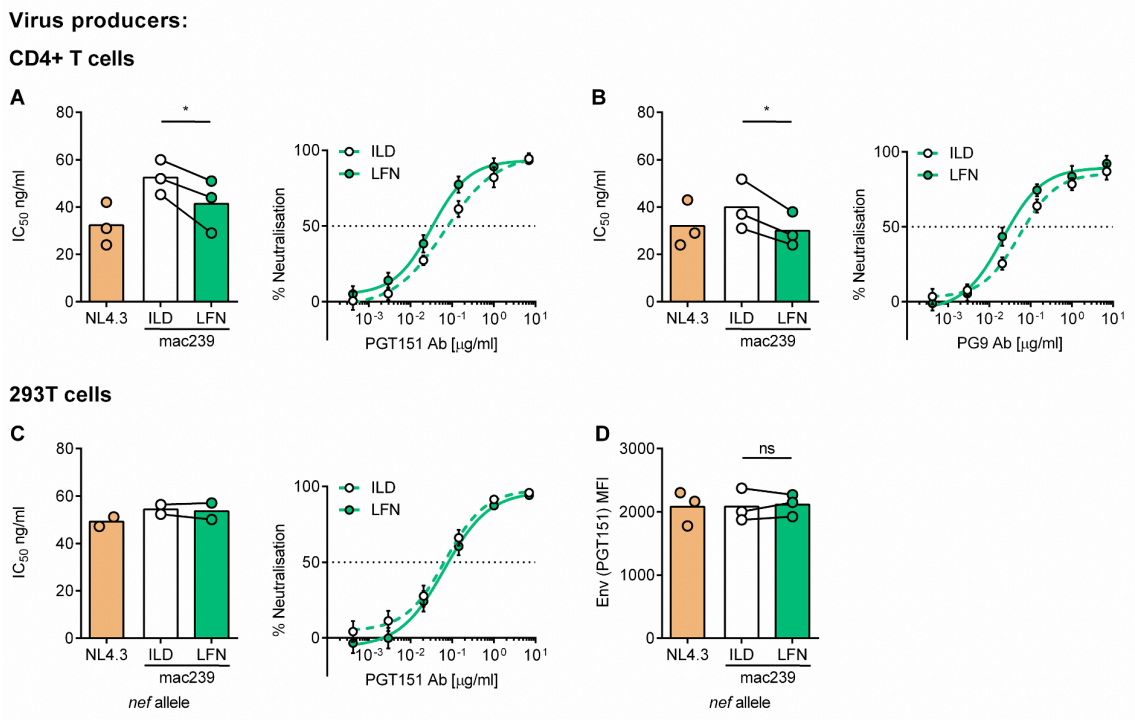

Figure 4.11: Neutralisation of SIVmac Nef chimeric viruses

Virus produced from primary CD4+ T cells and HEK293T cells was analysed by neutralisation assays. These were performed using HeLa-TZMbl reporter cell line with equal amounts of infectious supernatant and increasing amounts of bnAbs. IC_{50} values were calculated by non-linear regression analysis of the neutralisation curves. **(A-B)** Primary CD4+ T cells were infected with Nef chimeric viruses and cell culture supernatants were collected at 48h post-infection. Shown are IC_{50} values for **(A)** PGT151 Ab, and **(B)** PG9 Ab. **(C)** HEK293T cells were transfected with Nef chimeric proviruses and virus supernatants collected at 48h post-transfection. Shown are IC_{50} values for PGT151 Ab. Right-hand panels show representative examples of neutralisation curves. **(D)** HEK239T cells were analysed for surface expression (MFI) of Env (PGT151 Ab) at 48h post-transfection. Bars show mean and lines join paired results from the same PBMC donor. Error bars show mean ± SD. Groups were compared using paired *t*-test (ns, P>0.05; *, P<0.05).

4.2.4 Viral spread of SIVmac Nef chimeric viruses in Jurkat T cells

To test whether the effect of CD3 modulation on Env expression and viral infectivity was specific to primary CD4+ T cells, key experiments were repeated with Jurkat T cells. Jurkat cells were infected with Nef chimeric viruses and analysed by flow cytometry 48-post infection. It was confirmed that ILD Nef virus was able to downmodulate CD3 expression in these cells, while LFN Nef virus and the NL4.3 WT control retained CD3 expression (Figure 4.12A), as expected. Figure 4.12B-C shows there was no difference in cell-cell spread between ILD and LDN Nef viruses in Jurkat cells when measured by either Gag+ or GFP+ target cells. Next, virus release and viral infectivity were measured at 48h post-infection as described in Figure 4.7. Increased levels of virus release (Figure 4.12D) were detected from cells infected with LFN Nef virus (retained CD3 expression) compared to ILD Nef virus (CD3 downmodulation). By contrast, quantification of virion infectivity (RLU/RT) revealed significantly lower virion infectivity of LFN Nef virus compared to its LFN Nef counterpart (Figure 4.12E). Finally, analysing total supernatant infectivity (RLU/GFP+ cell), which accounts for differences in both virion infectivity and virus budding showed that ILD and LFN Nef viruses have similar supernatant infectivity (Figure 4.12F). This suggests that reduced virion infectivity of LFN Nef virus is compensated by increased virus release to yield similar levels of total supernatant infectivity compared to ILD Nef virus. This likely explains the similar levels of cell-cell spread observed for these viruses., LFN Nef virus also showed decreased levels of surface Env expression (detected by PGT151 and PG9 Abs) compared to ILD Nef virus (Figure 4.12G-H), which possibly explains decreased virion infectivity of this virus. Together these data show that Env expression, virion infectivity, virus release, and viral spread of SIVmac Nef chimeric viruses are similar between virus-infected Jurkat T cells and primary CD4+ T cells. This is again by contrast to SIVsmm Nef chimeric viruses (Chapter 3), where differences were observed between Jurkat T cells and primary CD4+ T cells in cell-cell spread, Env expression and virion infectivity.

4.2.5 T cell activation during cell-cell spread of SIVmac Nef chimeric viruses

Similar to Chapter 3, I next sought to investigate the effects of CD3 downmodulation on T cell activation during cell-cell spread. To do so, the same experimental setup was used as for the cell-cell spread assay described in Figure 4.4. The expression of activation markers in infected (GFP+) donor and target cell population after 0h and 24h of co-culture (allowing for cell-cell contact and VS formation) was measured. Figure 4.13A-D

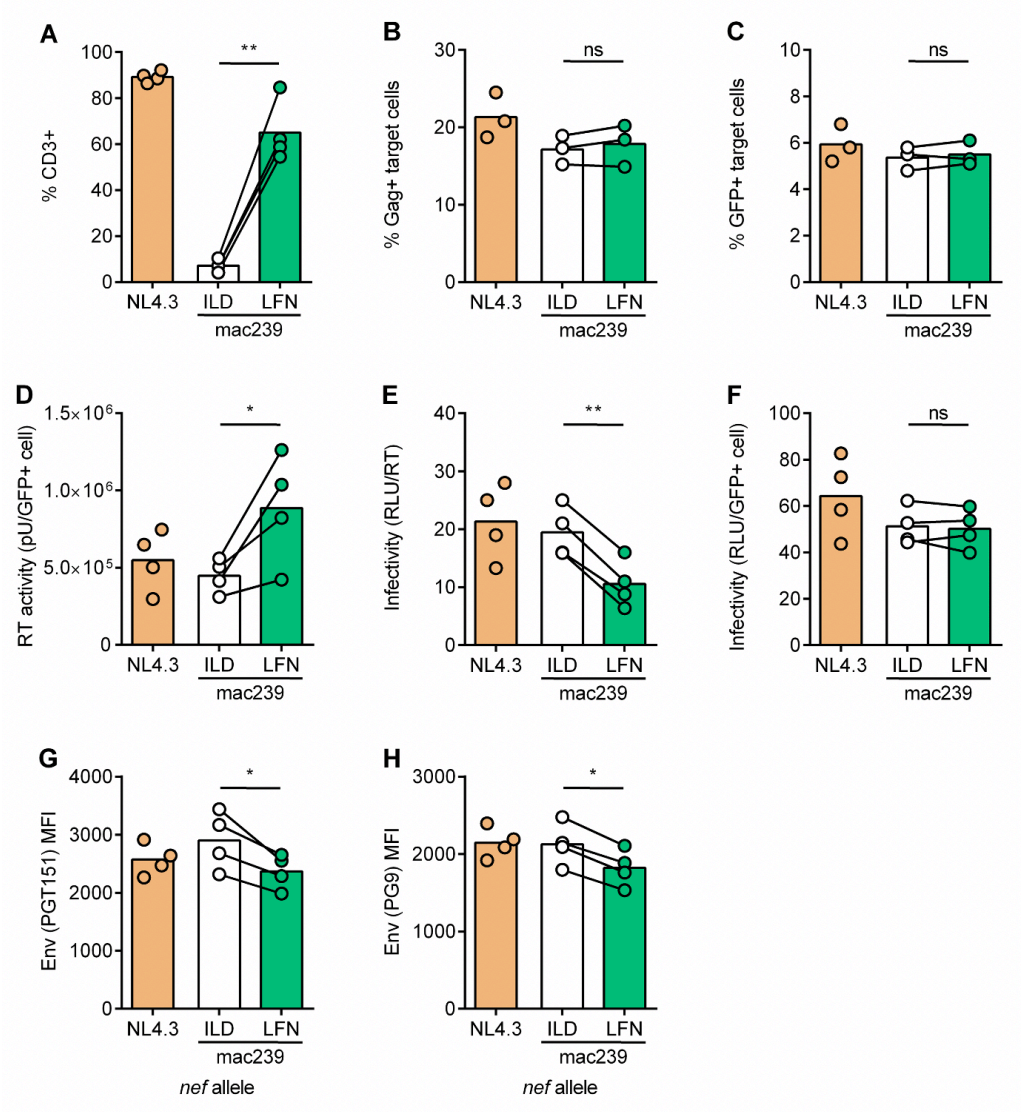

Figure 4.12: Viral spread, Env expression, virion infectivity and release of SIVmac Nef chimeric viruses in Jurkat T cells

Jurkat T cells were infected with Nef chimeric viruses were analysed by flow cytometry 48h post-infection. **(A)** Percentage of CD3+ cells in infected (GFP+) population. **(B-C)** Jurkat cells infected with indicated viruses were mixed with autologous pre-labelled target cells and analysed by flow cytometry at 24h post-mix as described in Figure 3.6. Shown is percentage of **(B)** Gag+ target cells, and **(C)** GFP+ target cells at 24h post-mix. **(D-F)** Virus supernatant was collected at 48h post-infection and analysed for virus release and virion infectivity as described in Figure 3.10. **(D)** Virus release was measured by supernatant RT activity and normalised to number of infected GFP+ cells. **(E)** Virion infectivity (RLUs) was measured using HeLa-TZMbl reporter cell assay and normalised to supernatant RT activity as measured in (D). **(F)** Supernatant infectivity (RLUs) was measured as in (E) and normalised to number of infected GFP+ cells (as measured in (D)). **(G-H)** Infected (GFP+) Jurkat cells were analysed at 48h post-infection for surface expression (MFI) of Env as detected by **(G)** PGT151 Ab, and **(G)** PG9 Ab. Bars show mean and lines join paired results from the same experiment. Groups were compared using paired *t*-test (ns, P>0.05; *, P<0.05; **, P<0.01; ***, P<0.001).

shows increased expression of CD69, phospho-S6, CD38, and PD-1 in NL4.3 Nef virus infected donor cells compared to uninfected (mock) cells, which was already apparent at 0h post-mix (48h post-infection). This may reflect activation of cell signalling at the VS or modulation of T cell activation by viral infection (Cavrois et al., 2017; Corneau et al., 2017; Len et al., 2017; Pardons et al., 2019; Rato et al., 2017). Notably, expression of CD69 and phospho-S6 in donor cells infected with LFN Nef virus, which retain CD3 expression, was greater than that observed for its ILD Nef counterpart, suggesting a contribution of CD3 expression to this phenotype. Comparing expression of CD69 and phospho-S6 at 0h and 24h post-mix (allowing for cell-cell spread and VS formation) shows increased expression of both markers over time in all infected cell cultures (Figure 4.13E-F); however, the increase was greater in LFN Nef infected cells, which retain CD3 expression and are thus better able to trigger TCR signalling. The small increase observed in ILD Nef infected cells is likely due to incomplete CD3 downmodulation by these viruses (Figure 4.2D). This increase in cell activation over time (as measured by CD69 expression and S6 phosphorylation) is consistent with the hypothesis that continuous donor-target cell contact is triggering T cell activation, which is increased by retained CD3 expression. By contrast, expression of CD38 and PD-1 remained similar between ILD and LFN Nef virus infected donor cells at 0h post-mix (Figure 4.13C-D) and at 24h post mix (Figure 4.13G-H). Next, target cells in the co-culture were also analysed, and a similar trend was seen in the newly infected target cell population, which showed increased expression of CD69, phospho-S6, CD38, and PD-1 compared to uninfected (mock) control (Figure 4.13I-L). As expected, target cells did not show any CD3-dependent differences in the expression of activation markers, as target cells in all infected cell cultures express CD3, and should thus respond similarly to cell-cell spread induced activation. Figure 4.14 shows similar analysis but using an expanded panel of surface markers (CD25, CD95, CD98 and Glut 1) as described in Chapter 3. These data show that increased expression of all markers was observed in all infected cell cultures in both donor and target cells compared to mock infected control (Figure 4.14). Notably, no significant differences in expression of these markers were observed between ILD and LFN Nef viruses in donor cells either at 0h or 24h post-mix or in target cells, which is similar to what was observed for expression of CD38 and PD-1 (Figure 4.13). This suggests that upregulation of these markers is independent of cell-cell spread and VS formation, and is likely caused by infection alone. This is consistent with previous observations showing that HIV-1 infected cells show increased activation phenotype (Cavrois et al., 2017; Corneau et al., 2017; Pardons et al., 2019). Another possibility

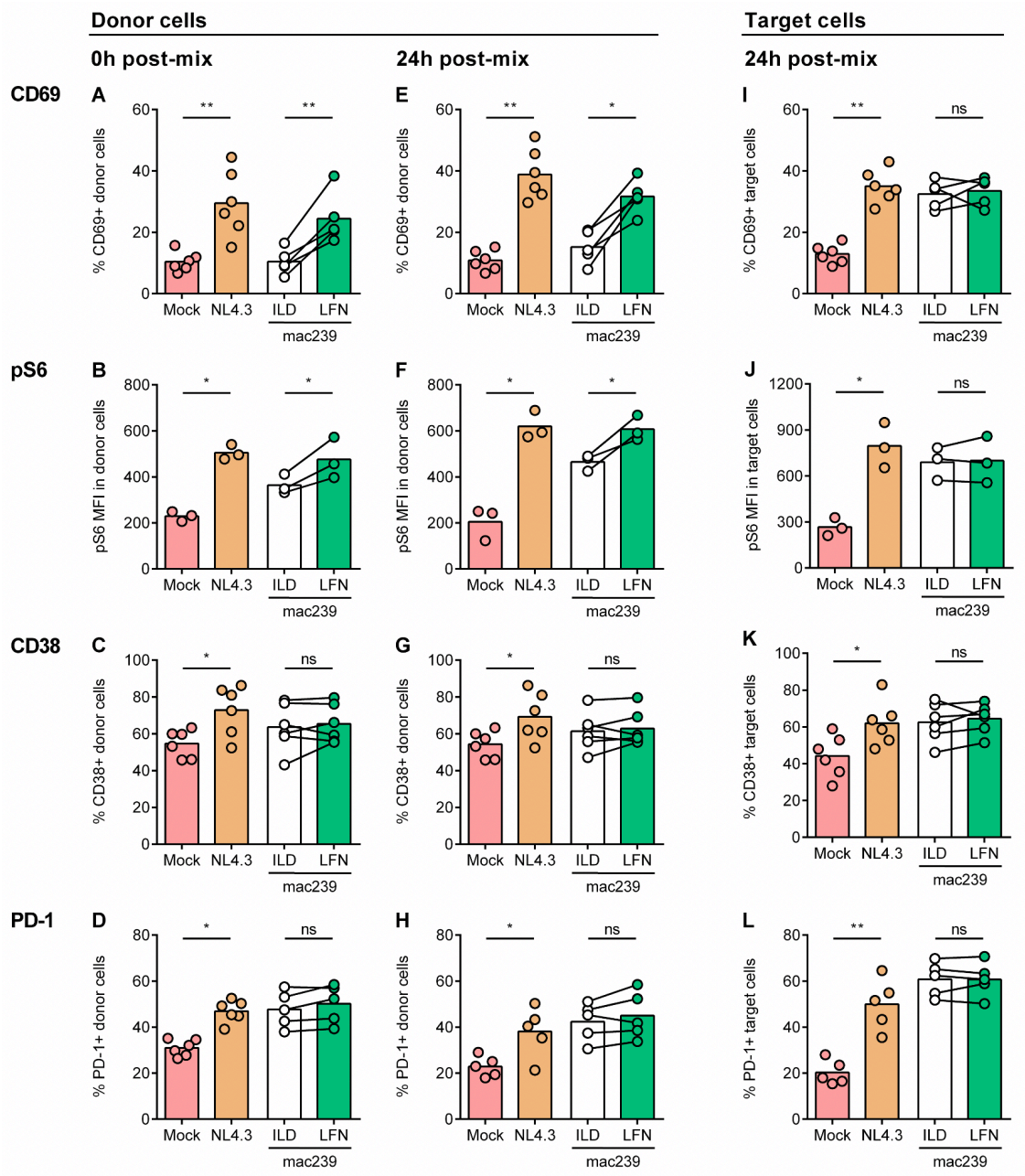

Figure 4.13: T cell activation (CD69, phospho-S6, CD38, PD-1) during cell-cell spread in donor and target cells infected with SIVmac Nef chimeric viruses

Primary CD4+ T cells infected with indicated viruses were mixed with autologous pre-labelled target cells and analysed by flow cytometry 24h post-mix as described in Figure 3.6. **(A-D)** Infected (GFP+) donor cell population was analysed for expression of activation markers at 0h post-mix. Shown is percentage of positive donor cells for **(A)** CD69, **(B)** MFI of phospho-S6 (pS6), **(C)** CD38, and **(D)** PD-1. **(E-H)** Infected (GFP+) donor cell population was analysed for expression of activation markers at 24h post-mix. Shown is percentage of positive donor cells for **(E)** CD69, **(F)** MFI of phospho-S6 (pS6), **(G)** CD38, and **(H)** PD-1. **(I-L)** Infected (GFP+) target cell population was analysed for expression of activation markers at 24h post-mix. Shown is percentage of positive target cells for **(I)** CD69, **(J)** MFI of phospho-S6 (pS6), **(K)** CD38, and **(L)** PD-1. Mock is uninfected control and total live population of donor or target cells was analysed. Bars show mean and lines join paired results from the same PBMC donor. Groups were compared using paired *t*-test (ns, P>0.05; *, P<0.05; **, P<0.01; ***, P<0.001).

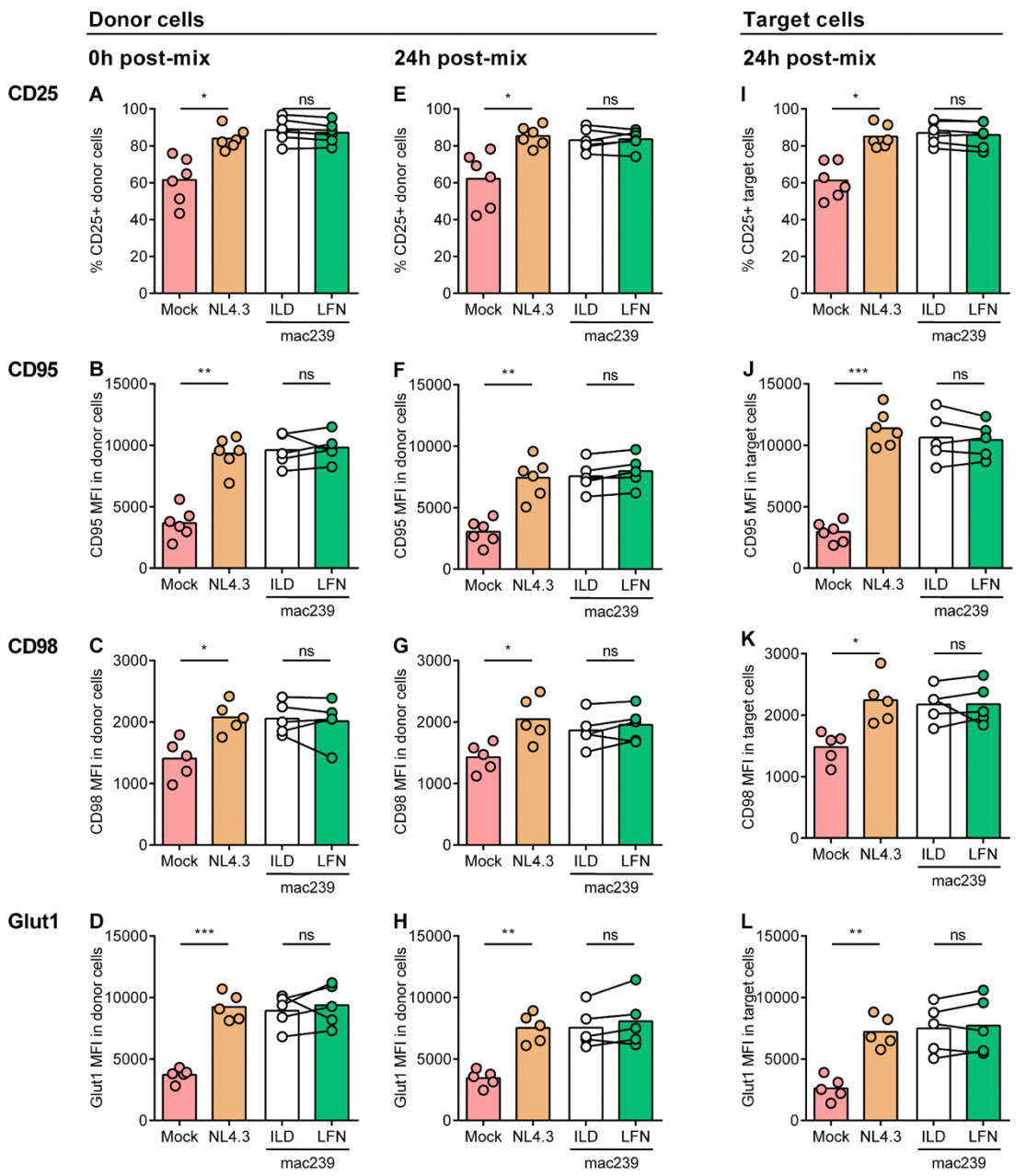

Figure 4.14: T cell activation (CD25, CD95, CD98, Glut1) during cell-cell spread in donor and target cells infected with SIVmac Nef chimeric viruses

Primary CD4+ T cells infected with indicated viruses were mixed with autologous pre-labelled target cells and analysed by flow cytometry 24h post-mix as described in Figure 4.4. **(A-D)** Infected (GFP+) donor cell population was analysed for expression of activation markers at 0h post-mix. Show is percentage of positive donor cells for **(A)** CD25, and MFI of **(B)** CD95, **(C)** CD98, and **(D)** Glut1. **(E-H)** Infected (GFP+) donor cell population was analysed for expression of activation markers at 24h post-mix. Show is percentage of positive donor cells for **(E)** CD25, and MFI of **(F)** CD95, **(G)** CD98, and **(H)** Glut1. **(I-L)** Infected (GFP+) target cell population was analysed for expression of activation markers at 24h post-mix. Show is percentage of positive target cells for **(I)** CD25, and MFI of **(J)** CD95, **(K)** CD98, and **(L)** Glut1. Mock is uninfected control and total live population of donor or target cells was analysed. Bars show mean and lines join paired results from the same PBMC donor. Groups were compared using paired *t*-test (ns, P>0.05; *, P<0.05; **, P<0.01; ***, P<0.001).

is that cells with high expression of CD38/PD-1/CD25/CD95/CD98/Glut1, i.e. highly-activated cells are preferentially infected or are better able to support productive infection (Rato et al., 2017).

HIV-1 viral gene expression is tightly linked to T cell activation (Gagne et al., 2019; Sauter et al., 2015; Shan et al., 2017; Stevenson et al., 1990; Weiss et al., 2014). Having observed some CD3-dependent differences in T cell activation during cell-cell spread, it was investigated whether increased expression of CD69 and phospho-S6 correlates with increased viral (or GFP-reporter) gene expression in cells that retain CD3 expression. As above, LTR-driven expression of Gag and GFP was measured in infected donor and target cells during cell-cell spread. ILD and LFN Nef virus infected donor cells showed similar levels of Gag expression (MFI) at 0h and 24h post-mix (Figure 4.15A-B). This is consistent with observation that these cells also showed similar levels of Gag protein and Gag mRNA by immunoblot and qPCR analysis (Figure 4.8Figure 4.9). By contrast, GFP MFI was higher in LFN Nef virus infected donor cells (retained CD3 expression) compared to ILD Nef virus at 0h and 24h post-mix (Figure 4.15D-E), suggesting a contribution of CD3 expression to this phenotype. This also correlates with increased expression of CD69 and phospho-S6 activation markers by these cells. Analysis of newly infected target cells showed no differences in expression of Gag or GFP between ILD and LFN Nef viruses, consistent with equal levels of viral spread and expression of activation markers by these cells.

4.2.6 Phosphorylation changes in ZAP70, ERK, AKT and S6 during virological synapse formation of SIVmac Nef viruses

To further explore CD3-dependent changes in T cell activation during cell-cell spread, activation of TCR signalling at the VS was examined. Previous work has shown that HIV-1 activates TCR signalling at the virological synapse to support viral spread (Len et al., 2017). Since SIVsmm and SIVmac Nef chimeric viruses showed different phenotypes in regard to viral spread, viral gene expression and T cell activation, it was investigated whether there is also difference in TCR signalling at the VS. As described in Chapter 3, a flow cytometry-based assay was developed to enable a high-throughput and quantitative analysis of TCR signalling at the virological synapse. Briefly, primary CD4+ T cells were infected (donor cells) and mixed with pre-labelled uninfected target cells and allowed to interact over a time course until formaldehyde fixation.

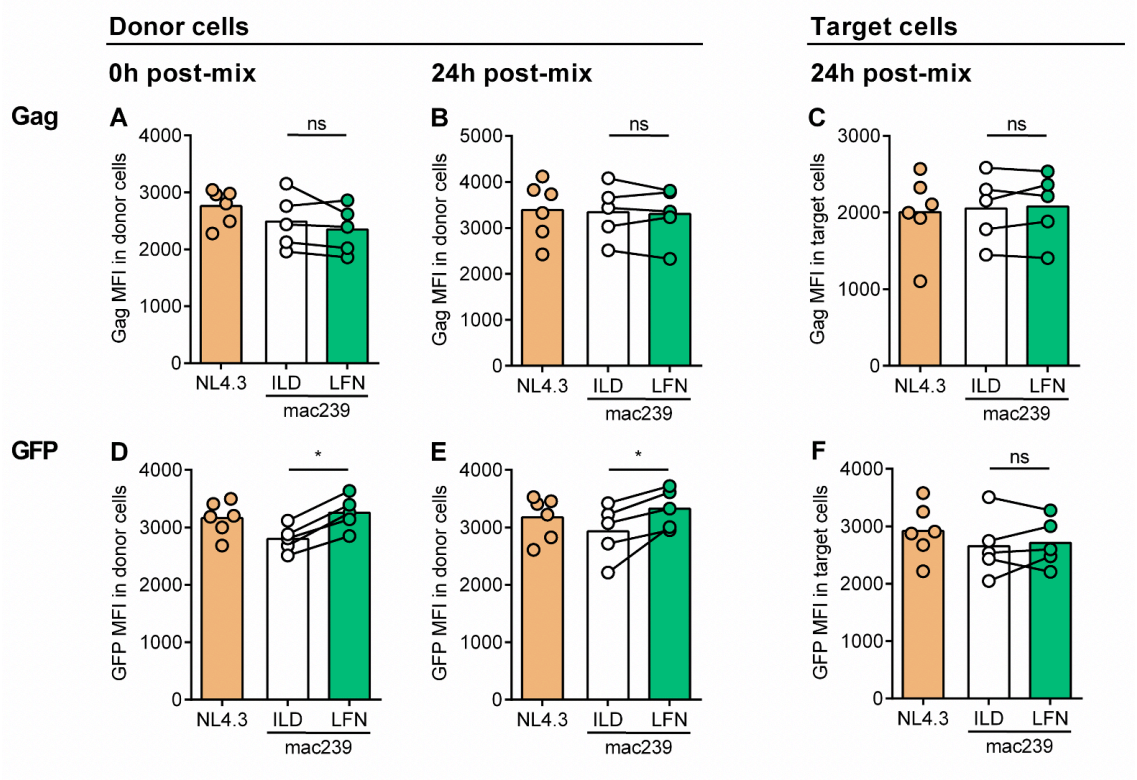

Figure 4.15: Expression of GFP and Gag during cell-cell spread in donor and target cells infected with SIVmac Nef chimeric viruses

Primary CD4+ T cells infected with indicated viruses were mixed with autologous pre-labelled target cells and analysed by flow cytometry 0h and 24h post-mix as described in Figure 3.6. **(A)** Gag MFI in Gag+ donor cells at 0h post-mix. **(B)** Gag MFI in Gag+ donor cells at 24h post-mix. **(C)** Gag MFI in Gag+ target cells at 24h post-mix. **(D)** GFP MFI in GFP+ donor cells at 0h post-mix. **(E)** GFP MFI in GFP+ donor cells at 24h post-mix. **(F)** GFP MFI in GFP+ target cells at 24h post-mix. Bars show mean and lines join paired results from the same PBMC donor. Groups were compared using paired *t*-test (ns, P>0.05; *, P<0.05; **, P<0.01; ***, P<0.001).

Infected donor-target conjugates were identified as live lymphocyte doublets that are positive for GFP (infected donor cell) and Target dye (target cell) expression (Figure 3.27). First, a time course experiment was performed using ILD and LFN Nef virus infected cells. Figure 4.16A-E shows that both ILD and LFN Nef virus infected donor-target cell conjugates displayed time-dependent changes in the phosphorylation of ZAP70, ERK, AKT, and S6 over 40mins, suggesting TCR signalling activation. However, when comparing the cells infected with either ILD and LFN Nef viruses the responses were identical, and a similar pattern and magnitude of phosphorylation for all five markers was observed. Graphing these data at the 20min time-point, alongside NL4.3 Nef virus and analysing multiple PBMC donors showed although time dependent changes in T cell signalling was observed (Fig. 4.16A-E), the phosphorylation of ZAP70, ERK, AKT and S6 in infected conjugates was similar between NL4.3, ILD and and LFN

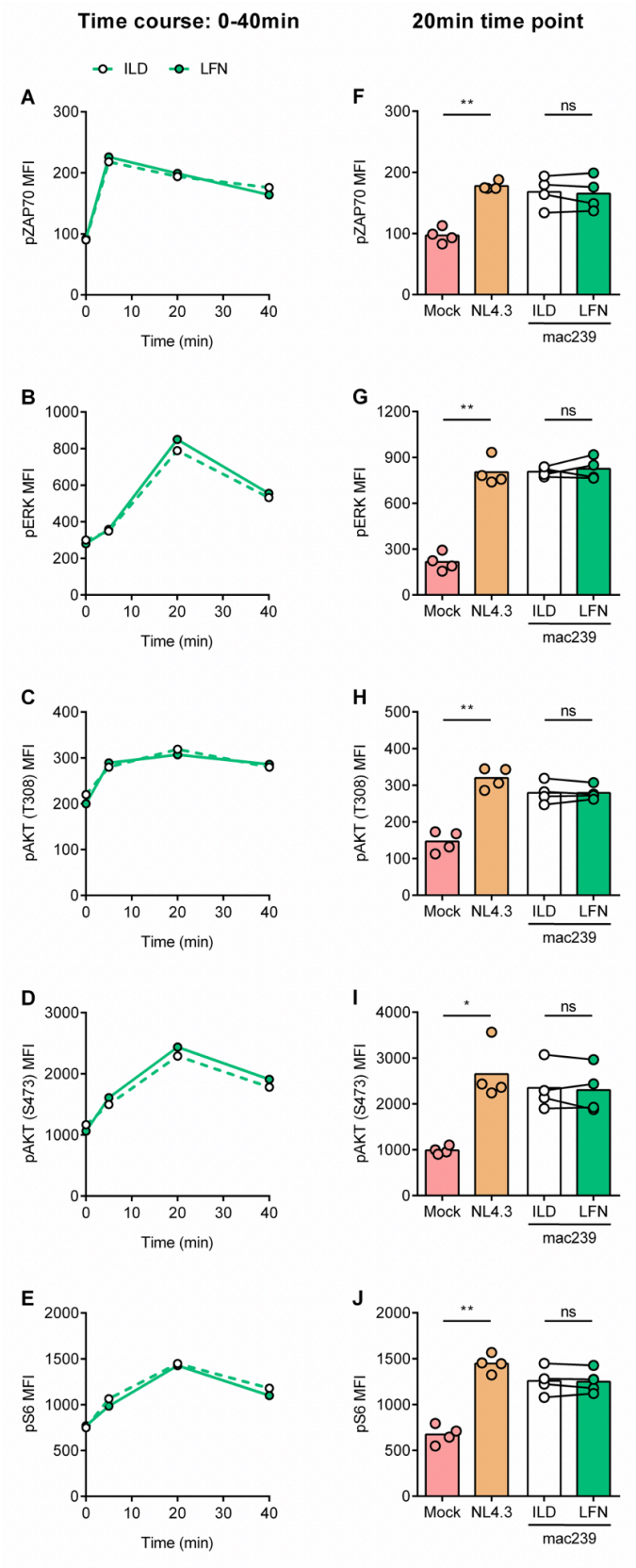

Figure 4.16: Phosphorylation of ZAP70, ERK, AKT and S6 in donor-target cell conjugates

Primary CD4+ T cells infected with Nef chimeric viruses were mixed with autologous pre-labelled target cells and analysed by flow cytometry to detect phosphorylation changes in pZAP70, pERK, pAKT, and pS6 as described in Figure 3.27. **(A-E)** Phosphorylation changes in infected donor cell-target cell conjugates at

0-40min post-mix. Shown is a representative example for SIVmac ILD and LFN Nef viruses (n=1). Shown are MFI values of **(A)** pZAP70 (Y319), **(B)** pERK (T202/Y204), **(C)** pAKT (T308), **(D)** pAKT (S473), and **(E)** pS6 (S235/S236). **(F-J)** Phosphorylation changes in infected donor cell-target cell conjugates at 20min post-mix. Shown are MFI values of **(F)** pZAP70 (Y319), **(G)** pERK (T202/Y204), **(H)** pAKT (T308), **(I)** pAKT (S473), and **(J)** pS6 (S235/S236). Mock is uninfected cells and total live doublet population was analysed. Bars show mean and lines join paired results from the same PBMC donor. Groups were compared using paired *t*-test (ns, P>0.05; *, P<0.05; **, P<0.01; ***, P<0.001).

Nef viruses (Figure 4.16F-J). This observation was surprising given the central role of CD3 expression in TCR signalling activation. It is also inconsistent with observed higher phosphorylation of S6 in LFN infected donor cells during cell-cell spread (Figure 4.13). Once again, the results also reveal differences between SIVmac Nef viruses (Chapter 4) and SIVsmm (Chapter 3).

Lck is a key upstream kinase in TCR signalling (reviewed in Dustin & Depoil, 2011). It has been reported that HIV and SIV Nef proteins can bind to Lck and cause its relocalisation from the plasma membrane to the TGN (Haller et al., 2007; Rudolph et al., 2009) through the interaction of PxxP motif in Nef with SH3 domain in Lck (Collette et al., 2000; Greenway et al., 1996; Haller et al., 2007). It has been proposed that this Lck relocalisation in turn results in increased T cell signalling (via activation of ERK); however precise mechanism remains unclear (Hung et al., 2007; Pan et al., 2012). Indeed, PxxP motif has been shown to be important for Nef-induced T cell hyperresponsiveness to stimulation (Fenard et al., 2005; Sauter et al., 2015; Schrager & Marsh, 1999) and to enhance viral spread (Carl et al., 2000; Fackler et al., 2006; Homann et al., 2009; Meuwissen et al., 2012). Although all SIVsmm and SIVmac *nef* alleles used in this thesis have an intact PxxP motif (Figure 4.1), other amino acid changes in these Nefs might affect Lck binding and thus modulation of T cell signalling that may explain differences in TCR signalling responses between viruses. To investigate the localisation of Lck, primary CD4+ T cells infected with Nef chimeric viruses were stained 48h post-infection for total intracellular Lck protein and analysed by immunofluorescence microscopy. As expected, uninfected (mock) and *nef*-defective control showed plasma membrane localisation of Lck, whilst NL4.3 Nef infected cells showed an intracellular accumulation of Lck and the appearance of larger Lck puncta (Haller et al., 2007; Rudolph et al., 2009), as well as Lck at the plasma membrane (Figure 4.17A-C). Similarly, both SIVmac ILD and LFN Nef viruses showed an intracellular accumulation of Lck, and no obvious difference in Lck staining or localisation were apparent between these mutant pairs (Figure 4.17D-E). For completeness, SIVsmm L4 Nef viruses were also examined and

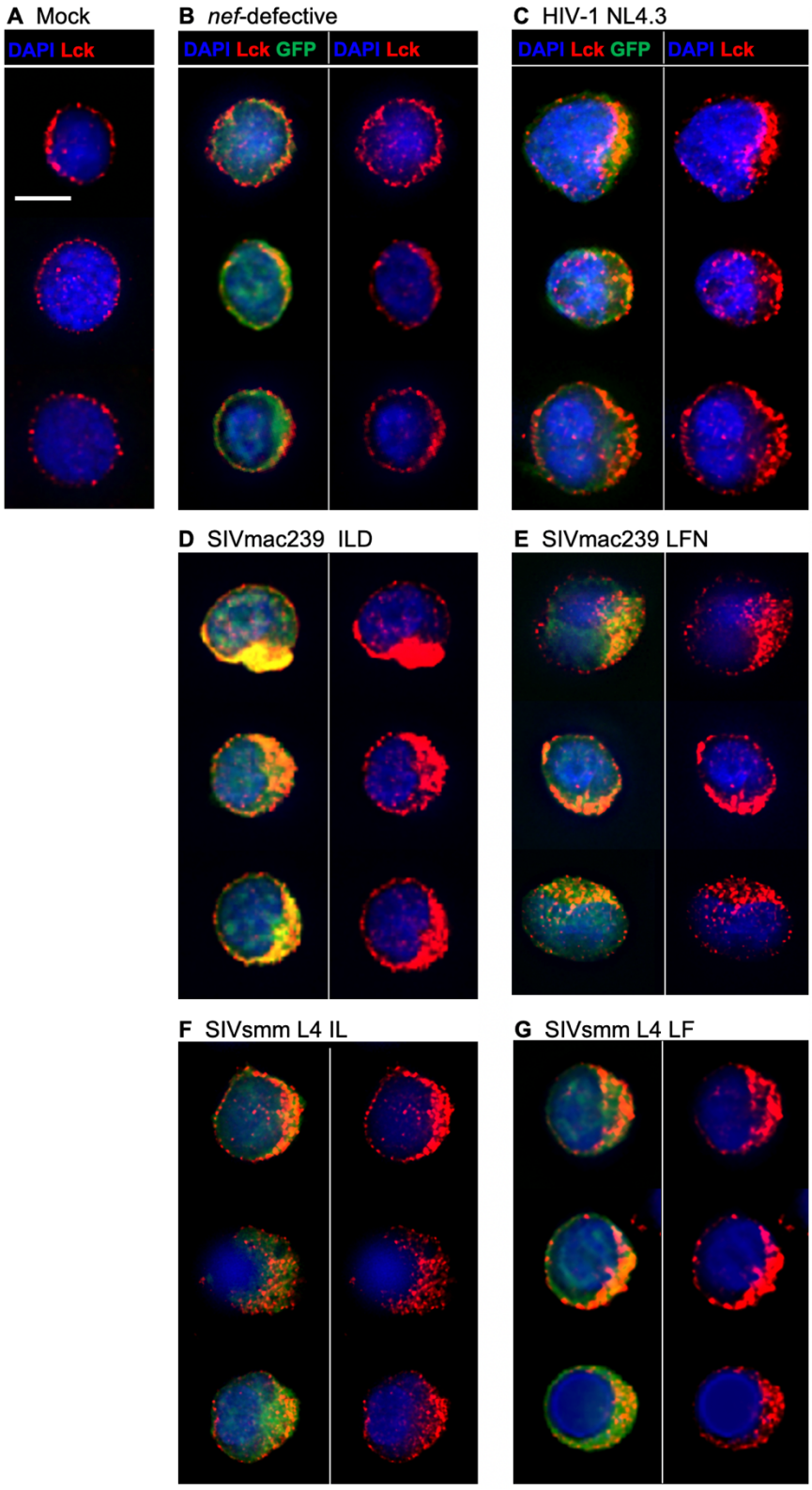

Figure 4.17: Lck relocalisation by Nef chimeric viruses

Primary CD4+ T cells were infected with indicated viruses for 48h and then incubated for 1h on coverslips before fixation and antibody staining for immunofluorescence microscopy. DAPI nuclear stain is shown in blue, Lck is shown in red and GFP is shown in green. Scale bar is 5 μm. Shown are representative images (single xy slice) of **(A)** uninfected (mock) cells, or cells infected with **(B)** *nef*-defective, **(C)** NL4.3, **(D)** SIVmac ILD, **(E)** SIVmac LFN, **(F)** SIVsmm L4 IL, and **(G)** SIVsmm L4 LF Nef chimeric viruses.

both IL and LF L4 Nef viruses induced intracellular Lck accumulation with no obvious differences between these mutant pairs (Figure 4.17F-G). These data show that all Nef-containing viruses examined induced a similar Lck localisation pattern and therefore further examination of Nef interaction with Lck was not pursued.

4.2.7 T cell death during cell-cell spread of SIVmac Nef chimeric viruses

Having observed in Chapter 3 that differences in CD3 downmodulation affected cell death during cell-cell spread of SIVsmm, cell death was next investigated in the context of SIVmac Nef virus infection. As described in Figure 4.4, flow cytometry was used to measure cell death (using a cell viability dye) in donor and target cells during cell-cell spread. LFN Nef virus infected donor cells (retained CD3 expression) showed similar levels of cell death compared to their ILD Nef infected counterparts at 0h and 24h post-mix (Figure 4.18A-B), which is consistent with similar levels of viral spread in these cultures. As expected, all infected cell cultures showed more cell death compared to mock infected control. Comparing donor cell death over time (0-24h post-mix), all infected cultures showed increase in the number of dead donor cells, most likely due to viral spread, which is consistent with previous observations showing cell-cell spread induced cell death (Galloway et al., 2015). A similar trend was seen in target cell population at 24h post-mix (Figure 4.18C). ILD and LFN Nef virus infected cultures showed similar levels of target cell death, again consistent with no differences in viral spread or cell activation. Overall, lower levels of cell death were seen for target cells compared to donor cells, with the latter having been infected for longer. Together these data show that T cell death is independent of CD3-modulation during cell-cell spread of SIVmac Nef viruses. This is again by contrast to the SIVsmm data which showed that retained CD3 expression resulted in increased cell death of donor and target cells, most likely due to increased cell-cell spread.

4.2.8 Validation of the phenotype of HIV-2 Nef chimeric viruses

The second part of this Chapter investigates viral spread of HIV-2 Nef chimeric viruses. D8 and A8 I Nef (CD3 downmodulation) and D8 and A8 T Nef (retained CD3 expression) chimeric viruses provided by our collaborator Frank Kirchhoff (Khalid et al., 2012) were first sequenced, which confirmed their sequence identity. To validate and characterise the HIV-2 Nef mutant viruses, 293T cells were transfected with viral plasmids and viruses

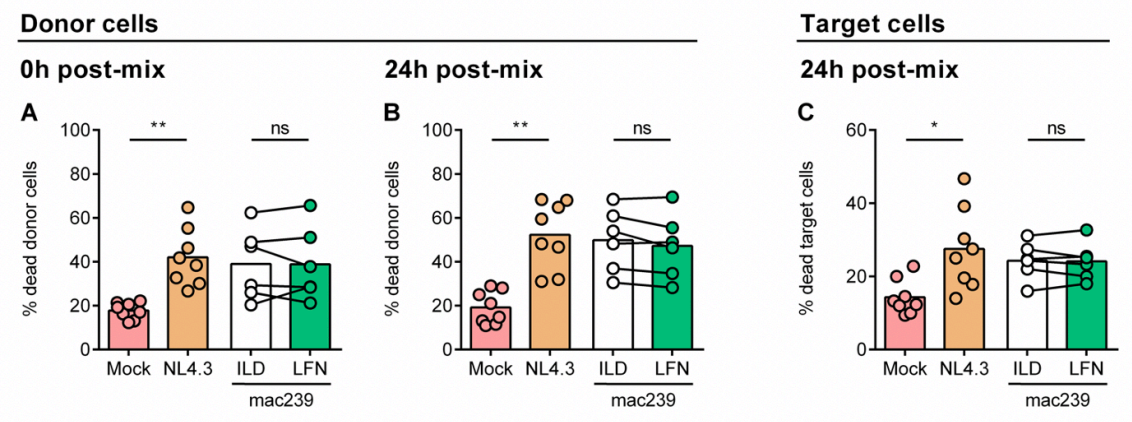

Figure 4.18: Cell death during cell-cell spread in donor and target cells infected with SIVmac Nef chimeric viruses

Primary CD4+ T cells infected with indicated viruses were mixed with autologous pre-labelled target cells and analysed by flow cytometry at 0h and 24h post-mix as described in Figure 3.6. **(A)** Percentage of dead donor cells at 0h post-mix. **(B)** Percentage of dead donor cells at 24h post-mix. **(B)** Percentage of dead target cells at 24h post-mix. Mock is uninfected control. Bars show mean and lines join paired results from the same PBMC donor. Groups were compared using paired *t*-test (ns, P>0.05; *, P<0.05; **, P<0.01; ***, P<0.001).

were titrated prior to infection of primary CD4+ T cells (as described in Figure 4.2). Figure 4.19A shows that all Nef chimeric proviruses produce infectious virus. Importantly, there was no difference in the relative infectivity of D8 and A8 mutant pair (I and T) Nef viruses. HIV-2 Nef viruses showed reduced infectivity compared to NL4.3 Nef virus (1.8-fold reduction; p=0.0057), which is consistent with previous observations that HIV-2 Nefs are less potent in enhancing virion infectivity due to weaker SERINC antagonism compared to HIV-1 Nef (Heigele et al., 2016; Khalid et al., 2012; Munch et al., 2005). Next, primary CD4+ T cells isolated from healthy PBMC donors were activated with anti-CD3/CD28 antibodies and infected with equal infectious doses of Nef chimeric viruses (*nef*-defective, NL4.3, D8 I and T, A8 I and T). After 48h primary CD4+ T cells were analysed by flow cytometry to quantify the percentage of infection and Nef activity. Analysis of infected primary CD+ T cells showed broadly similar percentages of Gag+ or GFP+ cells between cells infected with NL4.3 or HIV-2 Nef chimeric viruses (Figure 4.19B-C). As described in Chapter 3 (Figure 3.2), GFP+ cells better represent the population of productively infected cells, thus GFP expression was used in further experiments (unless otherwise stated) to identify infected cells.

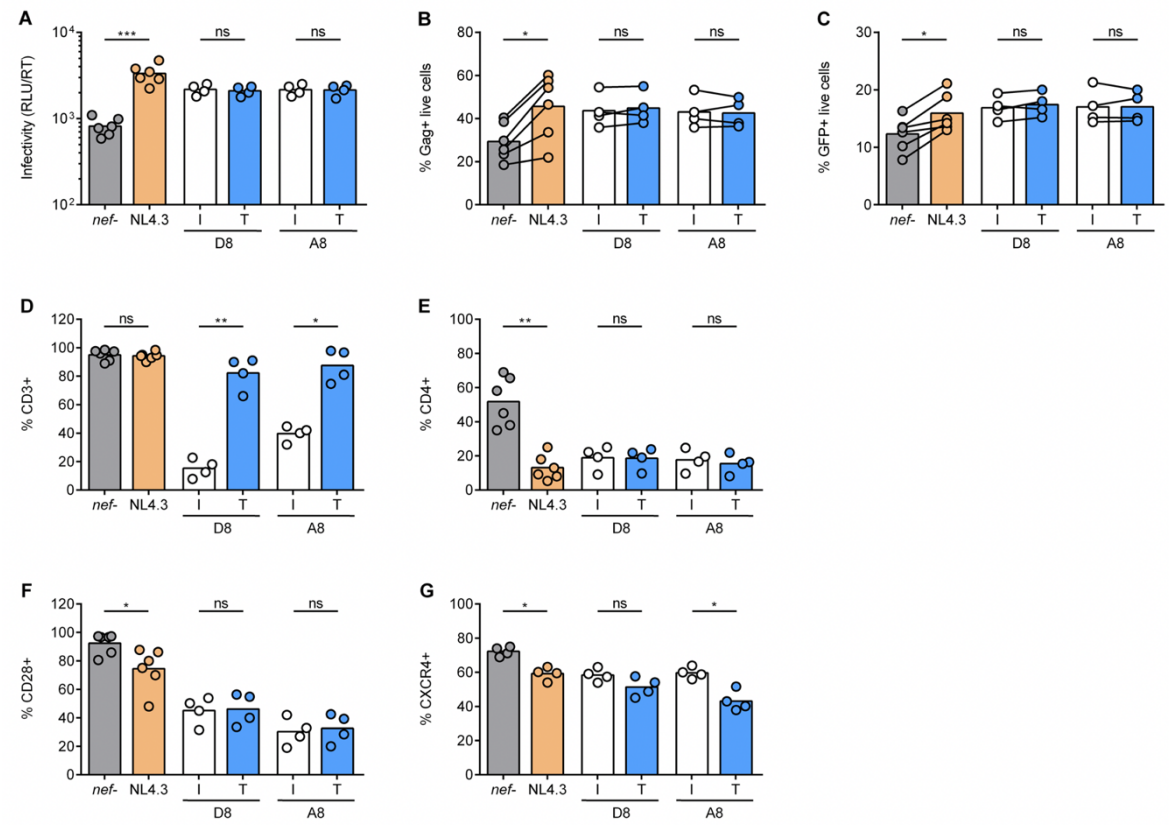

Figure 4.19: Validation of HIV-2 Nef chimeric viruses

(A) Nef chimeric viruses were produced by transfection of HEK293T cells. Viral infectivity (RLU) was measured by titration on HeLa-TZMbl reporter cell line and normalised to supernatant RT activity, a measure of viral content. **(B-G)** Primary CD4+ T cells were activated with anti-CD3/CD28 antibodies for 4-5 days, infected with Nef chimeric viruses for 48h and analysed by flow cytometry. **(B)** Percentage of Gag+ live cells. **(C)** Percentage of GFP+ live cells. Percentage of live, GFP+ cells positive for **(D)** CD3, **(E)** CD4, **(F)** CD28, and **(G)** CXCR4 surface markers. Bars show mean and lines join paired results from the same PBMC donor. Groups were compared using paired *t*-test (ns, P>0.05; *, P<0.05; **, P<0.01; ***, P<0.001).

To confirm the Nef phenotypes, primary CD4+ T cells infected with Nef chimeric viruses (or uninfected mock control) were analysed by flow cytometry to measure surface expression of CD3, CD4, CD28, and CXCR4. Figure 4.19D shows that, as expected, D8 and A8 I Nef expressing viruses were able to downmodulate surface expression of CD3; however, A8 I Nef was less able to downmodulate CD3 expression (≈40% CD3+ infected cells) compared to D8 I Nef (≈20% CD3+ infected cells), consistent with previous observations (Khalid et al., 2012; Yu et al., 2015). By contrast, D8 and A8 T Nefs were unable to downmodulate CD3 expression as evidenced by more than 90% of cells remaining CD3+, similar to the percentage of CD3+ cells in *nef*-defective and NL4.3 Nef virus infected cells, again as expected. CD4 surface staining (Figure 4.19E) showed that all *nef*-containing viruses (NL4.3, ILD and LFN) retained the ability to downmodulate

CD4 (≈20% CD4+ infected cells). Examination of CD28 showed that D8 and A8 mutant pair (I and T) Nef viruses downmodulated CD28 to similar extent (≈40% CD28+ infected cells), whereas NL4.3 Nef was less able to do so (≈70% CD28+ infected cells) (Figure 4.19F), in agreement with published data (Khalid et al., 2012; Munch et al., 2005; Yu et al., 2015). Similarly, NL4.3 Nef was also less able to downmodulate CXCR4 (≈60% CXCR4+ infected cells) (Figure 4.19G) compared to D8 and A8 Nef viruses, again as expected (Hrecka et al., 2005; Khalid et al., 2012). While it was observed that A8 T Nef virus appeared slightly better able to downmodulate CXCR4 compared to its I Nef counterpart, this difference was not significant for D8 mutant pair (I and T) Nef viruses. Together these results validate the expected phenotype of this panel of HIV-2 Nef chimeric viruses, and show that generation of I and T Nef mutants in D8 and A8 HIV-2 *nef* alleles by site-directed mutagenesis had specific effect on downmodulation of CD3, with a modest effect on CXCR4 downmodulation.

4.2.9 Viral spread of HIV-2 Nef chimeric viruses

To investigate the effect of CD3 downmodulation on cell-cell spread of HIV-2, primary CD4+ T cells infected with Nef chimeric viruses (donor cells) were co-cultured with autologous uninfected, pre-labelled target cells in 1:4 ratio as described in Figure 4.4. Viral spread was measured 24h post-mix (single round of replication) by flow cytometry to identify Gag+ or GFP+ target cells (Figure 4.20A). Analysing Gag expression in target cells showed that D8 and A8 I Nef viruses (CD3 downmodulation) showed similar levels of cell-cell spread compared to their T Nef counterparts, which retained CD3 expression (Figure 4.20B). Treating co-cultures with the RT inhibitor Efavirenz resulted in an approximately 5-fold reduction of Gag+ target cells (Figure 4.20C), confirming that this assay measures productive infection of target cells. Consistent with this, similar results were obtained when measuring infection levels by LTR-driven expression of GFP reporter, which also showed similar levels of cell-cell spread by D8 and A8 mutant pair (I and T) Nef viruses, regardless of their ability to downmodulate CD3 (Figure 4.4D). Treating co-cultures with Efavirenz almost completely abrogated detection of GFP+ target cells (Figure 4.20E). To examine the differences in viral spread between I and T mutant Nef viruses over time, a long-term spreading infection assay was performed as previously described in Figure 4.4. D8 and A8 mutant pair (I and T) Nef viruses again showed similar levels of viral spread and replication kinetics as measured by expression of both Gag and GFP up to day 7 post-infection (Figure 4.20G-H).

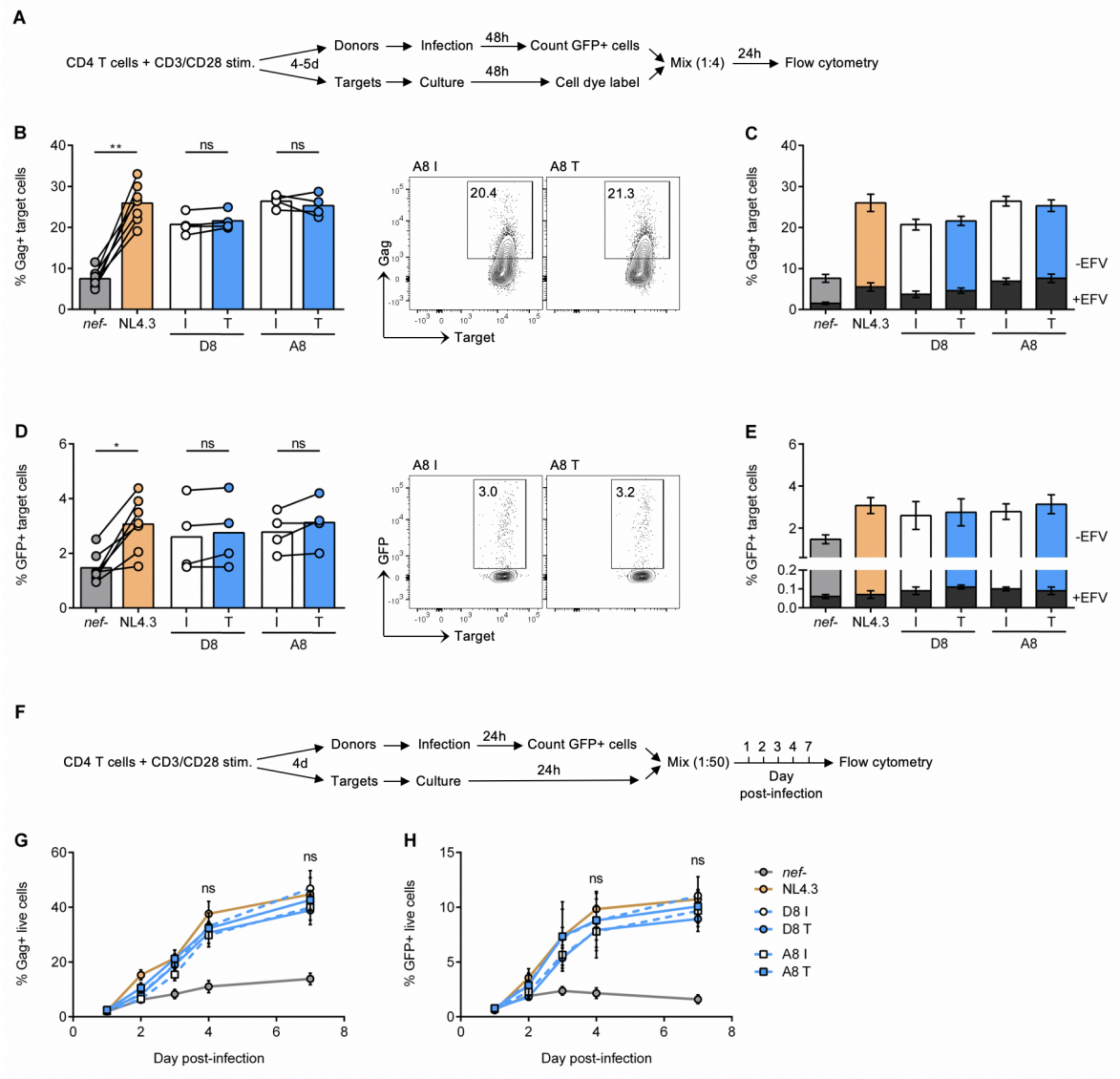

Figure 4.20: Cell-cell spread of HIV-2 Nef chimeric viruses

(A) Schematic of the 24h cell-cell spread assay (as described in Figure 3.6). CD4+ T cells infected with indicated viruses were mixed with autologous, pre-labelled target cells in 1:4 ratio (GFP+ donor cell:target cell). Cells were analysed by flow cytometry at 0h and 24h post-mix. **(B)** Percentage of Gag+ target cells. **(C)** Donor and target cells were co-cultured in the presence or absence of 5 μM Efavirenz (± EFV). Superimposed grey bars show percentage of Gag+ target cells in presence of Efavirenz. **(D)** Percentage of GFP+ target cells. **(E)** Percentage of GFP+ target cells in presence of 5 μM Efavirenz (superimposed grey bars). Shown are representative flow cytometry plots. **(F)** Schematic of the long-term cell-cell spread assay. CD4+ T cells were infected with Nef chimeric viruses for 24h and analysed by flow cytometry to count GFP+ cells. Infection levels in cell culture were adjusted to 2% GFP+ cells with autologous, unlabelled, uninfected cells. Spreading infection was quantified by flow cytometry until 7 days post-infection (n=3). **(G)** Percentage of Gag+ live cells. **(H)** Percentage of GFP+ live cells. ILD and LFN Nef viruses were compared for statistical significance at days 4 and 7 post-infection. Bars show mean and lines join paired results from the same PBMC donor. Error bars show mean ± SEM. Groups were compared using paired *t*-test (ns, P>0.05; *, P<0.05; **, P<0.01; ***, P<0.001).

Together these data show that there is no apparent correlation between CD3 expression on infected cells and viral spread of HIV-2 Nef viruses. This is consistent with previous observations of SIVmac Nef chimeric viruses (Figure 4.4); however, these data are again at odds with observations in Chapter 3 using SIVsmm Nef chimeric viruses, which showed CD3-dependent differences in cell-cell spread.

To investigate why Nef-mediated modulation of CD3 expression does not affect viral spread, virus release from infected cells and virion infectivity were analysed. CD4+ T cells were infected with Nef chimeric viruses for 48h before virus containing culture supernatants and infected cells were collected and analysed. As described in Figure 4.4, virus release/budding from infected cells was quantified by measuring the amount RT activity in the supernatants and normalised to the number of infected (GFP+) cells. Figure 4.21A shows similar levels of virus released from cells infected with D8 and A8 mutant pair Nef viruses. Similarly, quantification of virion infectivity measured by titrating the supernatants on HeLa-TZMbl reporter cell line revealed similar virion infectivity of D8 and A8 mutant pair Nef viruses (Figure 4.21B). D8 and A8 Nef mutant viruses showed lower virion infectivity when compared to NL4.3 Nef virus (2-fold reduction; $p=0.0084$), which is consistent with previous observations showing reduced virion infectivity of D8 and A8 Nef viruses when produced in 293T cells (Figure 4.19) and is most likely due to HIV-2 Nefs being weaker antagonists of SERINC compared to HIV-1 Nefs (Heigele et al., 2016). Consistent with similar levels of virus release and virion infectivity (RLU/RT), the D8 and A8 mutant pair Nef viruses showed similar levels of supernatant infectivity (RLU/GFP+ cell) (Figure 4.21C). The fact that these viruses have similar virion and supernatant infectivity likely explains why there was no difference observed in the cell-cell spread of D8 and A8 mutant pair viruses. Notably, despite these HIV-2 viruses having reduced virion infectivity, D8 I, D8 T, A8 I and A8 T viruses showed similar levels of cell-cell spread when compared to each other and to NL4.3 Nef virus (Figure 4.20). This suggests that highly efficient cell-cell spread might overcome reduced virion infectivity of HIV-2 Nef chimeric viruses.

To further explore cell-cell spread of HIV-2 Nef chimeric viruses, it was examined whether the lack of correlation between CD3 modulation and viral spread was specific to primary CD4+ T cells or whether this could also be observed using Jurkat cell line. To investigate this, Jurkat cells were infected with Nef chimeric viruses and analysed by flow cytometry 48h post-infection. It was confirmed that D8 and A8 I Nef virus were able

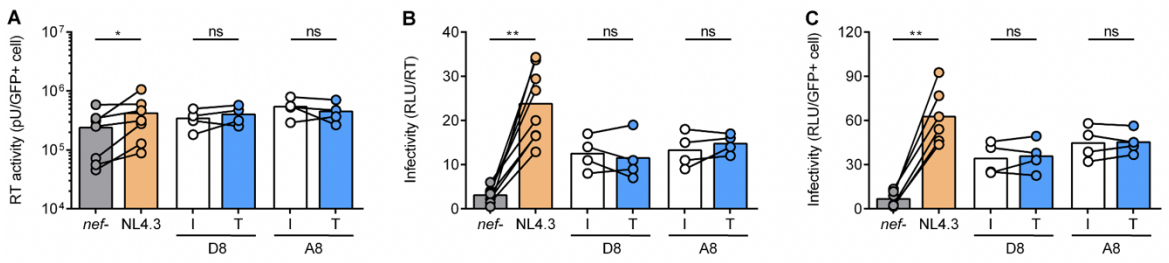

Figure 4.21: Virion infectivity and virus release of HIV-2 Nef chimeric viruses

Primary CD4+ T cells were infected with Nef chimeric viruses and culture supernatants collected at 48h post-infection. Number of GFP+ cells in cell culture was analysed by flow cytometry. **(A)** Virus release was measured by supernatant RT activity and normalised to number of infected GFP+ cells. **(B)** Virion infectivity (RLUs) was measured using HeLa-TZMbl reporter cell assay and normalised to supernatant RT activity as measured in (A). **(C)** Supernatant infectivity (RLUs) was measured as in (B) and normalised to number of infected GFP+ cells (as measured in (A)). Bars show mean and lines join paired results from the same PBMC donor. Groups were compared using paired *t*-test (ns, P>0.05; *, P<0.05; **, P<0.01; ***, P<0.001).

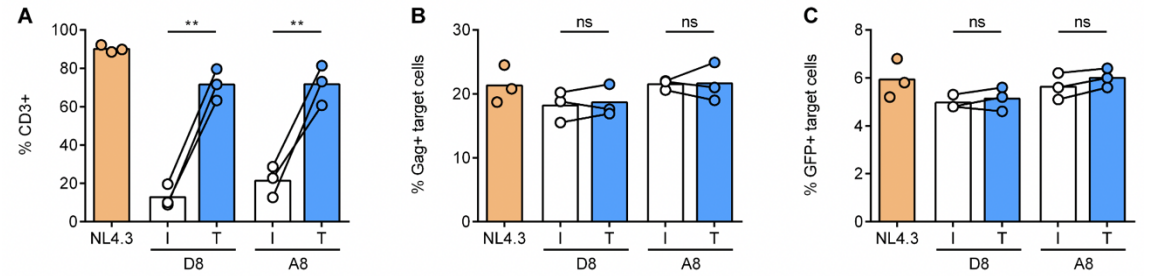

Figure 4.22: Viral spread of HIV-2 Nef chimeric viruses in Jurkat T cells

Jurkat T cells were infected with Nef chimeric viruses were analysed by flow cytometry 48h post-infection. **(A)** Percentage of CD3+ cells in infected (GFP+) population. **(B-C)** Jurkat cells infected with indicated viruses were mixed with autologous pre-labelled target cells and analysed by flow cytometry at 24h post-mix as described in Figure 3.6. Shown is percentage of **(B)** Gag+ target cells, and **(C)** GFP+ target cells at 24h post-mix. Bars show mean and lines join paired results from the same experiment. Groups were compared using paired *t*-test (ns, P>0.05; *, P<0.05; **, P<0.01; ***, P<0.001).

to downmodulate CD3 expression in these cells, while NL4.3 and D8 and A8 T Nef viruses retained CD3 expression (Figure 4.22A). Cell-cell spread was measured as described in Figure 4.4, which showed similar numbers of Gag+ or GFP+ target cells in all infected cultures (Figure 4.22B-C). This is consistent with observations in primary CD4+ T cells and further confirms that viral spread of HIV-2 Nef chimeric viruses does not correlate with CD3 expression on infected cells.

4.2.10 T cell activation during cell-cell spread of HIV-2 Nef chimeric viruses

Previous experiments in this Chapter and Chapter 3 showed CD3-dependent differences in T cell activation and viral gene expression in infected cells. Thus, it was further explored how retained CD3 expression affects T cell activation during cell-cell spread of HIV-2 Nef chimeric viruses. To do so, the same experimental setup was used as for the cell-cell spread assay described in Figure 4.4. The expression of activation markers in infected (GFP+) donor and target cell population after 0h and 24h of co-culture (allowing for cell-cell contact and VS formation) was measured. Figure 4.23A-C shows increased expression of CD69, CD38 and CD25, in NL4.3 and all HIV-2 Nef virus infected donor cells compared to uninfected (mock) cells, which was already apparent at 0h post-mix (48h post-infection), consistent with SIVmac data in Figure 4.13. Notably, expression of CD69 in donor cells infected with D8 and A8 T Nef viruses, which retain CD3 expression, was greater than that observed for their I Nef counterparts (CD3 downmodulation), suggesting a contribution of CD3 expression to this phenotype. Comparing expression of CD69 at 0h and 24h post-mix (allowing for cell-cell spread and VS formation) shows increased expression of this marker over time in all infected cell cultures (Figure 4.23A,D). However, the increase was greater in T Nef infected cells, which retain CD3 expression, and are thus better able to trigger TCR signalling. The small increase observed in I Nef infected cells is likely due to incomplete CD3 downmodulation by these viruses (Figure 4.19D). This increase in cell activation over time (as measured by CD69 expression) is consistent with the hypothesis that continuous donor-target cell contact is triggering T cell activation, which is increased by retained CD3 expression. By contrast, expression of CD38 and CD25 remained similar between I and T Nef virus infected donor cells at 0h post-mix (Figure 4.23B-C) and at 24h post-mix (Figure 4.23E-F). Similar results were seen using SIVmac Nef viruses and as described in Figure 4.13, this suggests that upregulation of these markers is independent of cell-cell spread and VS formation, and is likely caused by infection alone (Cavrois et al., 2017; Corneau et al., 2017; Pardons et al., 2019). Alternatively, highly-activated cells (high expression of CD38/CD25) are preferentially infected or are better able to support productive infection (Rato et al., 2017). Next, target cells in the co-culture were also analysed, and a similar trend was seen in the newly infected target cell population, which showed increased expression of CD69, CD38 and CD25 compared to uninfected (mock) control (Figure 4.23G-I). As expected, target cells did not show any CD3-dependent differences in the expression of activation markers, as target cells in all infected cell cultures express CD3, and should thus respond similarly to cell-cell spread induced activation.

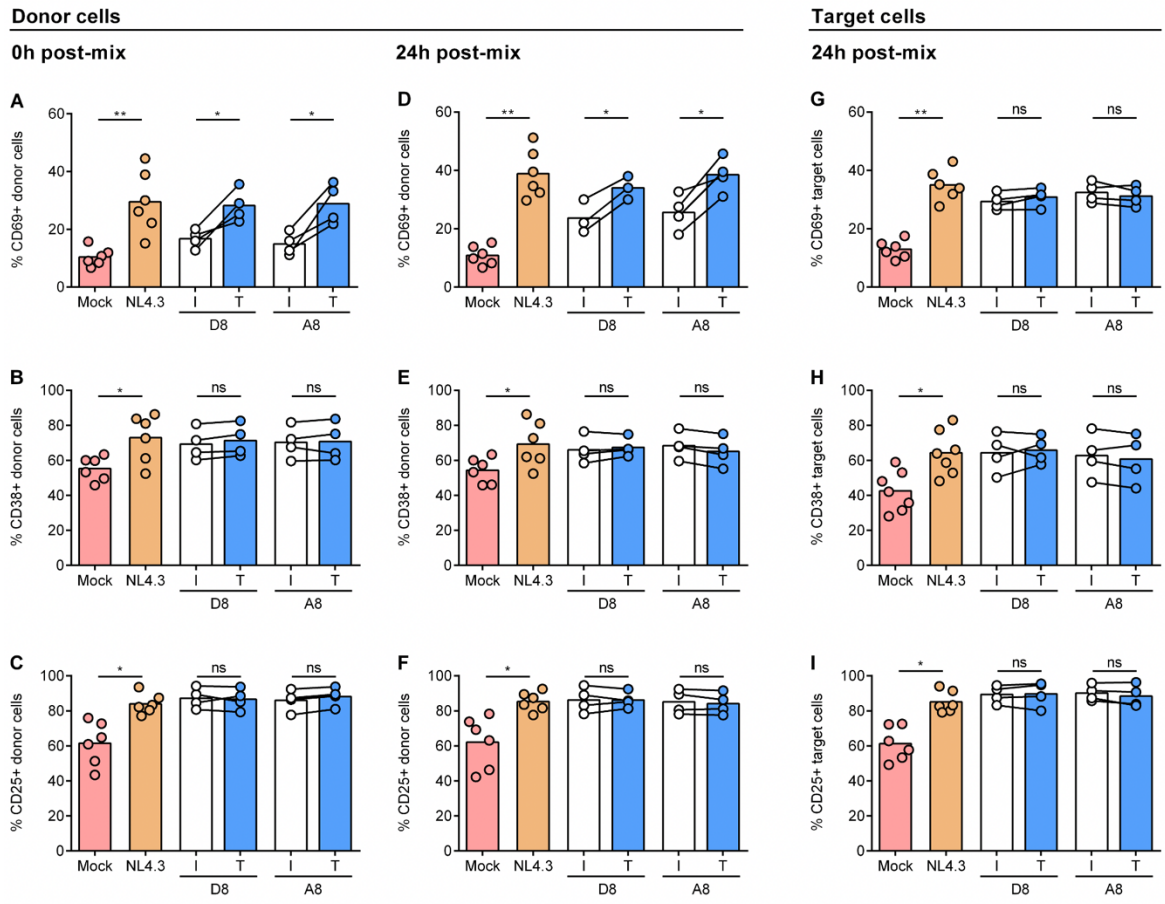

Figure 4.23: T cell activation (CD69, CD38, CD25) during cell-cell spread in donor and target cells infected with HIV-2 Nef chimeric viruses

Primary CD4+ T cells infected with indicated viruses were mixed with autologous pre-labelled target cells and analysed by flow cytometry 24h post-mix as described in Figure 3.6. **(A-C)** Infected (GFP+) donor cell population was analysed for expression of activation markers at 0h post-mix. Shown is percentage of positive donor cells for **(A)** CD69, **(B)** CD38, and **(C)** CD25. **(D-F)** Infected (GFP+) donor cell population was analysed for expression of activation markers at 24h post-mix. Shown is percentage of positive donor cells for **(D)** CD69, **(E)** CD38, and **(F)** CD25. **(G-I)** Infected (GFP+) target cell population was analysed for expression of activation markers at 24h post-mix. Shown is percentage of positive target cells for **(G)** CD69, **(H)** CD38, and **(I)** CD25. Mock is uninfected control and total live population of donor or target cells was analysed. Bars show mean and lines join paired results from the same PBMC donor. Groups were compared using paired *t*-test (ns, P>0.05; *, P<0.05; **, P<0.01; ***, P<0.001).

Having observed some CD3-dependent differences in T cell activation during cell-cell spread, it was next investigated whether increased expression of CD69 correlates with increased viral (or GFP-reporter) gene expression in cells that retain CD3 expression. As above, LTR-driven expression of Gag and GFP was measured in infected donor and target cells during cell-cell spread. D8 and A8 mutant pair Nef virus infected donor cells showed similar levels of Gag and GFP expression (MFI) at 0h and 24h post-mix (Figure 4.24). Interestingly, this does not correlate with increased expression of CD69 by these

cells, however it is consistent with no observed differences in virus release or virion infectivity by D8 and A8 mutant Nef viruses. Next, analysis of newly infected target cells (Figure 4.24C,F) showed no differences in expression of Gag or GFP between D8 and A8 mutant pair Nef viruses, consistent with equal levels of viral spread and expression of activation markers by these cells.

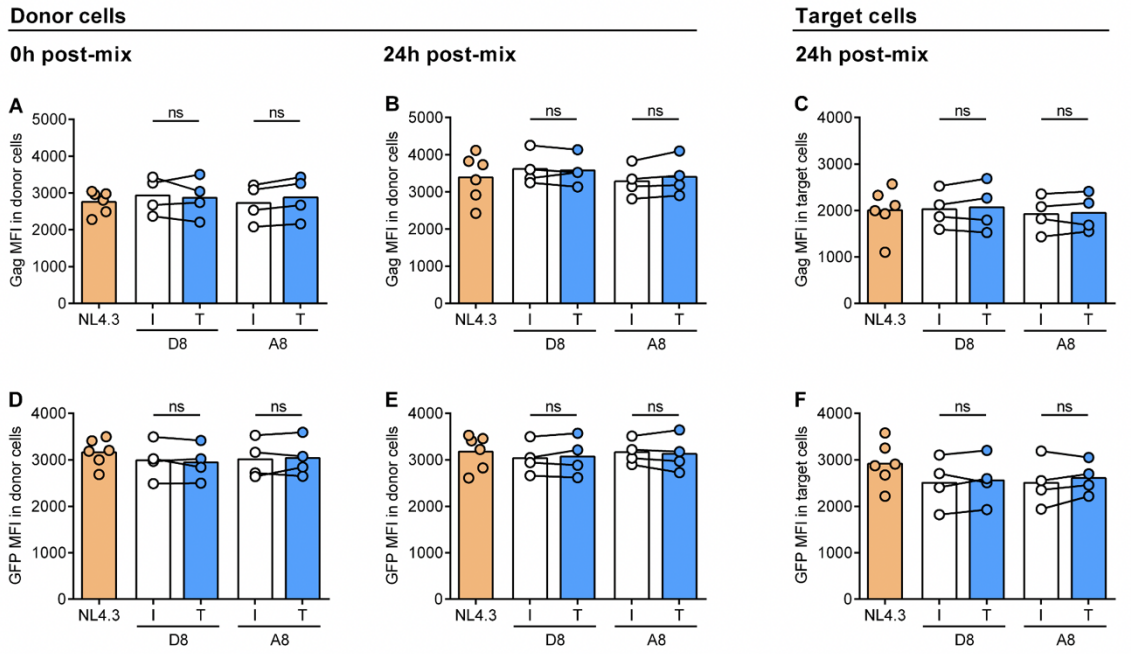

Figure 4.24: Expression of GFP and Gag during cell-cell spread in donor and target cells infected with HIV-2 Nef chimeric viruses

Primary CD4+ T cells infected with indicated viruses were mixed with autologous pre-labelled target cells and analysed by flow cytometry 0h and 24h post-mix as described in Figure 3.6. **(A)** Gag MFI in Gag+ donor cells at 0h post-mix. **(B)** Gag MFI in Gag+ donor cells at 24h post-mix. **(C)** Gag MFI in Gag+ target cells at 24h post-mix. **(D)** GFP MFI in GFP+ donor cells at 0h post-mix. **(E)** GFP MFI in GFP+ donor cells at 24h post-mix. **(F)** GFP MFI in GFP+ target cells at 24h post-mix. Bars show mean and lines join paired results from the same PBMC donor. Groups were compared using paired *t*-test (ns, P>0.05; *, P<0.05; **, P<0.01; ***, P<0.001).

4.2.11 T cell death during cell-cell spread of HIV-2 Nef chimeric viruses

Having observed no CD3-depedent differences in cell-cell spread and only a partial phenotype in T cell activation, it was investigated whether there is also no difference in cell death. As described in Figure 4.4, flow cytometry was used to measure cell death (using a cell viability dye) in donor and target cells during cell-cell spread. D8 and A8 T

Nef virus infected donor cells (retained CD3 expression) showed similar levels of cell death compared to their I Nef infected counterparts at 0h and 24h post-mix (Figure 4.25A-B), which is consistent with similar levels of viral spread in these cultures. As expected, all infected cell cultures showed more cell death compared to mock infected control. Comparing donor cell death over time (0-24h post-mix), all infected cultures showed increase in the number of dead donor cells, most likely due to viral spread. A similar trend was seen in target cell population at 24h post-mix (Figure 4.25C). D8 and A8 mutant pair Nef virus infected cultures showed similar levels of target cell death, again consistent with no differences in viral spread or cell activation. Together these data show that T cell death is independent of CD3-modulation during cell-cell spread of HIV-2 Nef viruses.

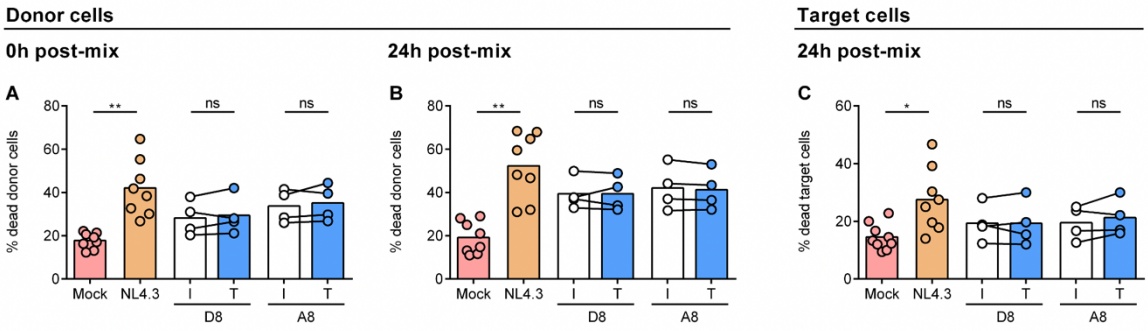

Figure 4.25: Cell death during cell-cell spread in donor and target cells infected with HIV-2 Nef chimeric viruses

Primary CD4+ T cells infected with indicated viruses were mixed with autologous pre-labelled target cells and analysed by flow cytometry at 0h and 24h post-mix as described in Figure 3.6. **(A)** Percentage of dead donor cells at 0h post-mix. **(B)** Percentage of dead donor cells at 24h post-mix. **(C)** Percentage of dead target cells at 24h post-mix. Mock is uninfected control. Bars show mean and lines join paired results from the same PBMC donor. Groups were compared using paired *t*-test (ns, P>0.05; *, P<0.05; **, P<0.01; ***, P<0.001).

4.3 Discussion

The results in this Chapter show the consequences of differential Nef-mediated CD3 downmodulation for HIV-1 viral spread, T cell activation and cell death using SIVmac and HIV-2 Nef chimeric viruses. It was hypothesised that retained CD3 expression on infected cells would result in triggering of TCR/CD3 signalling and T cell activation during the VS formation and cell-cell spread, thus supporting more efficient viral spread. Indeed, this hypothesis was supported by results in Chapter 3 using SIVsmm Nef chimeric viruses. By contrast, results in this Chapter show that cell-cell spread of SIVmac and

HIV-2 Nef chimeric viruses does not correlate with CD3 expression on infected cells. Notably, viruses that downmodulate CD3 (ILD and I Nefs) spread equally well as viruses with retained CD3 expression (LFN and T Nefs) and similar to NL4.3 Nef virus (retained CD3 expression), although SIVmac Nef viruses showed slightly reduced viral spread compared to NL4.3 Nef virus. This was not the case for SIVsmm viruses where CD3 downmodulation resulted in reduced viral spread. This suggests there are likely to be additional determinants (apart from CD3 downmodulation) in Nef that contribute to efficient cell-cell spread that may explain the differences between SIVsmm, SIVmac and HIV-2 Nef chimeric viruses and highlights additional species-specific differences between the *nef* alleles.

Retained CD3 expression of SIVmac LFN Nef virus resulted in increased virus release and decreased virion infectivity compared to ILF Nef virus (CD3 downmodulation). Importantly, reduced virion infectivity was not due to differences in Nef antagonism of SERINC5, as both SIVmac ILD and LFN Nef viruses showed similar ability to downmodulate SERINC5 expression, and were equally restricted by SERINC5 overexpression. Overall, total supernatant infectivity (accounting for differences in virus release and virion infectivity) was similar between the mutant pair viruses, which correlated with similar levels of viral spread. This suggests that somehow reduced virion infectivity of LFN virus was compensated with increased virus release, thus resulting in similar levels of viral spread. This is an intriguing observation and it is difficult to propose a mechanism that would explain how a triple point mutation in Nef that specifically affects CD3 downmodulation results in this phenotype, especially considering previous observations showing that retained CD3 expression of SIVsmm Nef viruses results in increased virion infectivity, but similar levels of virus release. This might suggest an additional yet unknown Nef-dependent link between viral budding and infectivity.

Retained CD3 expression and reduced virion infectivity of SIVmac LFN Nef virus correlated with decreased Env expression and decreased Env incorporation into virions. Env virion incorporation was measured directly by immunoblot analysis of purified virions and indirectly by Ab neutralisation assay, both of which showed decreased Env incorporation into LFN Nef virus. This was not due to differences in furin-mediated cleavage of Env gp160 as shown by immunoblot analysis of cell lysates. Decreased expression of Env was evident both on the transcriptional level (mRNA) and protein level. Importantly, flow cytometry analysis showed decreased levels of cell surface Env for LFN

Nef virus. Decreased expression of Env mRNA likely explains decreased Env synthesis in the cell, which in turn mediates reduced Env surface expression. Env is a limiting factor in viral infectivity due to low cell surface expression and low virion incorporation and mechanisms of Env virion incorporation are poorly understood (Checkley et al., 2011). However, disrupting Env endocytosis, which increases Env surface expression results in increased Env virion incorporation and virion infectivity (Day et al., 2004; Groppelli et al., 2014; Kirschman et al., 2018). This provides a plausible explanation how decreased surface Env expression results in decreased virion incorporation and virion infectivity of LFN Nef virus. However, it remains uncertain whether differences in Env expression are directly linked to CD3 downmodulation ability of ILD and LFN Nef viruses and not to some other effect of mutating these residues on Nef protein function. Experiments in Chapter 3 showed that RNAi-mediated CD3 depletion phenocopied Nef-mediated CD3 downmodulation effect on Env surface expression and virion infectivity of SIVsmm Nef chimeric viruses. Similar experiments are thus required to establish whether the same correlation exists for SIVmac Nef chimeric viruses.

By contrast to virion infectivity, retained CD3 expression of LFN Nef virus correlated with increased virus release as measured by RT activity in the culture supernatant. Interestingly, Gag expression was similar between ILD and LFN Nef viruses. This was apparent both on the transcriptional level (mRNA) and protein level as measured by immunoblot analysis of cell lysates and intracellular flow cytometry. This suggest that increased virus release is unlikely to be due to increased expression of Gag protein. Increased virus release could be mediated by increased Gag localisation to the plasma membrane (where the virions bud) or increased efficiency of viral budding mediated by ESCRT machinery (Halwani et al., 2003; Usami et al., 2009) and further experiments are required to test this possibility or how that might be regulated via Nef or CD3 modulation.

Examination of SIVmac Nef viruses in Jurkat cells showed that retained CD3 expression of LFN Nef virus correlated with increased virus release, but decreased virion infectivity and Env surface expression. This resulted in similar levels of supernatant infectivity and viral spread between ILD and LFN Nef viruses and shows the consistency of this phenotype between primary CD4+ T cells and Jurkat cells. This was not observed using SIVsmm Nef viruses, which showed no CD3-dependent differences in Env expression and virion infectivity in Jurkat cells. It was proposed this was perhaps due to the hyper-activated status of Jurkat cells (Gioia et al., 2018), which might be masking CD3-

modulation and cell activation-dependent effect on Env expression of SIVsmm viruses. By contrast, the consistency of SIVmac phenotype between primary CD4+ T cells and Jurkat cells might suggest that differences in virus release, Env expression and virion infectivity are not dependent on cell activation for SIVmac Nef viruses and it further highlights that SIVmac Nef is doing something different. Further experiments inducing T cell activation in infected cells (as done in Chapter 3) are required to explore the connection between T cell activation and SIVmac Nef function.

It is possible to suggest that SIVmac Nef is interacting with host cellular factors in a different manner compared to SIVsmm thus ILD/LFN mutations result in a different phenotype. To confirm the specificity of ILD/LFN mutations to CD3 downmodulation it was shown that ILD and LFN mutant pair viruses downmodulate CD4, CD28, SERINC5 (this thesis), and MHC-I (Joas et al., 2020; Yu et al., 2015) to a similar extent. A modest difference was observed in CXCR4 expression, which was downmodulated slightly better by LFN Nef (retained CD3 expression). However, the difference in downmodulation between ILD and LFN Nef viruses was small and experiments in this thesis are unlikely to be affected by differences in chemokine signalling and cell migration. Moreover, SIVsmm Nef viruses showed similar phenotype, further suggesting that differences in CXCR4 modulation are not responsible for observed differences between SIVsmm and SIVmac Nef viruses. However, it is possible that ILD and LFN Nefs (and compared to SIVsmm Nef) differ in their ability to interact with Src-family kinases: Lck, Fyn, Hck or Lyn (Collette et al., 2000; Saksela et al., 1995; Trible et al., 2006), PAK-2 (Rudolph et al., 2009; Stolp et al., 2010) or modulation of NF-κB signalling (Fortin et al., 2004; Sauter et al., 2015), which would change the host cell environment and could potentially explain the observed differences in virus release and virion infectivity. These activities of Nef were previously shown to be conserved between HIV-1, HIV-2, SIVsmm and SIVmac Nefs, however the effect size can vary significantly between different *nef* alleles (Collette et al., 2000; Rudolph et al., 2009; Sauter et al., 2015). Importantly, these Nef functions (except for Lck relocalisation, discussed below) have not been tested for the panel of *nef* alleles used in this thesis and further experiments are required to test this. Moreover, it cannot be excluded that Nef is interacting with a yet unidentified host cell factor, which could potentially account for differences in viral phenotypes observed here. Indeed, recent study showed that HIV-1 Nef promotes viral spread even in the absence of SERINC5/3 restriction or CD4 downmodulation (Wu et al., 2019), which hints that Nef has another yet unknown function. We cannot exclude the possibility that ILD and LFN Nef viruses have additional

different mutations in the viral NL4.3 backbone that were introduced during the cloning process by our collaborators in the Kirchhoff lab. Additional mutations in Env or Gag (or elsewhere in the genome) could potentially explain observed differences in Env expression and virus budding (independent of CD3-modulation) and full-length genome sequencing is required to exclude this possibility.

Retained CD3 expression on SIVmac LFN virus infected cells resulted in increased expression of CD69 and S6 phosphorylation during cell-cell spread, indicating increased T cell activation. This is consistent with SIVsmm Nef data and supports the hypothesis that VS formation triggers TCR signalling and cell activation during cell-cell spread in CD3-dependent manner. However, SIVsmm Nef viruses also showed CD3 dependent differences in expression of CD38 and PD-1, which was not observed in this Chapter. SIVmac showed high expression of CD38 and PD-1 regardless of CD3 downmodulation. This again shows that SIVmac Nef viruses are different compared to SIVsmm and may manipulate host cell factors in a different manner.

Consistent with increased cell activation as measured by expression of CD69 and phospho-S6, LFN Nef virus (retained CD3 expression) showed increased LTR-driven GFP expression, which might indicate increased viral gene expression. However, Gag mRNA and protein expression was similar between ILD and LFN Nef viruses and (as described earlier) LFN virus showed reduced expression of Env. Here we see a great disconnect between cell activation and viral gene (or GFP reporter) expression, which was not observed for SIVsmm Nef chimeric viruses and reasons for this remain hard to speculate.

Investigation of TCR signalling at the VS showed phosphorylation of ZAP70, ERK, AKT and S6 in infected donor-target cell conjugates, indication activation of TCR signalling. This is consistent with results in Chapter 3 using SIVsmm Nef viruses and previous observations showing triggering of TCR signalling at the VS (Len et al., 2017). Interestingly, ILD Nef virus, which downmodulates CD3, showed equally high levels of phosphorylation of ZAP70, ERK, AKT and S6 compared to LFN or NL4.3 Nef viruses (retained CD3 expression), which is surprising given the central role of CD3 in TCR signalling. This might suggest that CD3 expression is dispensable for TCR signalling activation at the VS of SIVmac Nef virus infected cells and reasons for this are unclear.

It is possible that SIVmac Nef is enhancing cell signalling in a different way (such as manipulation of Src-family kinases or modulation of NF-κB signalling as described above) so the effect of CD3 modulation is lost. This is inconsistent with SIVsmm data (Chapter 3), which showed that retained CD3 expression resulted in increased phosphorylation of ERK and S6 at the VS. Whether other cellular factors might contribute to the signalling activation remains to be investigated. Importantly, SIVmac ILD Nef virus does not completely downmodulate CD3 (≈20% CD3+ infected cells), thus it is possible that CD3-expressing infected cells preferentially form VS, which would skew the results. Further experiments using imaging flow cytometry (ImageStream) may help to dissect the role of CD3 expression and recruitment to the VS. Observing CD3-independent differences in TCR signalling is also inconsistent with increased cell activation as measured by CD69 and phospho-S6 expression in LFN Nef virus infected cells (retained CD3 expression) during cell-cell spread. Since signalling at the VS was independent of CD3 modulation it remains to be investigated how the retained CD3 expression results in increased cell activation later during cell-cell spread. Lck kinase is crucial for TCR signalling (Dustin & Depoil, 2011) and it has been shown that lentiviral Nef proteins bind to Lck and cause its relocalisation to the TGN, which was proposed to modulate T cell signalling and activation (Haller et al., 2007; Pan et al., 2012; Rudolph et al., 2009). Immunofluorescence analysis showed similar patterns of Lck relocalisation by SIVmac and SIVsmm Nef viruses irrespective of their CD3 downmodulation ability. This result suggested that observed differences in TCR signalling between the viruses are not due to differential Lck relocalisation. However, more quantitative analysis and using multiple PBMC donors is required to fully confirm there is no difference in Nef interaction with Lck. Moreover, Nef also interacts with other Src-family kinases (Hck, Lyn, Fyn) and PAK-2 to modulate cell signalling and activation (Collette et al., 2000; Olivieri et al., 2011; Saksela et al., 1995). It remains to be investigated whether SIVsmm and SIVmac Nefs used in this thesis have similar ability to interact with these kinases and how this might impact on TCR signalling.

A recent study (Joas et al., 2020) by our collaborator Frank Kirchhoff also showed no differences in viral spread of SIVmac ILD and LFN Nef chimeric viruses (same constructs as used in this thesis), which further confirms that SIVmac Nef mutant viruses spread equally well, regardless of their ability to downmodulate CD3. Joas et al. (2020) used a similar *in vitro* long-term spreading infection system using human primary CD4+ T cells as described in Figure 4.4F, which showed similar results, thus further validating observations in this Chapter. The second part of their study (Joas et al., 2020) described

in vivo infection of rhesus macaques infected with full-length SIVmac239 virus containing ILD or LFN mutations in *nef* gene. Viral replication was similar between ILD and LFN Nef viruses (irrespective of their CD3 downmodulation ability) in the acute phase of infection, which is consistent with *in vitro* observations using Nef chimeric viruses. However, retained CD3 expression by LFN Nef resulted in increased immune activation as measured by proinflammatory gene expression and cytokine secretion. Subsequently, some of the animals infected with LFN Nef virus (retained CD3 expression) showed reversions in the *nef* gene, mutating back to WT Nef able to downmodulate CD3. In the absence of *nef* reversions animals presented with attenuated course of infection and improved immune control of viral replication. These observations suggest that while SIVmac Nef CD3 downmodulation ability might be dispensable for viral replication directly, it is crucial for efficient immune evasion.

As observed for SIVmac Nef viruses, cell-cell spread of HIV-2 Nef chimeric viruses also does not correlate with CD3 expression on infected cells and viruses that downmodulate CD3 (D8 and A8 I Nef) spread equally well as viruses with retained CD3 expression (D8 and A8 T Nef, NL4.3 Nef). Consistent with this observation, HIV-2 Nef chimeric viruses showed similar levels of virus release and similar virion infectivity regardless of their ability to downmodulate CD3, which likely explains no differences in viral spread observed for these viruses. Notably, retained CD3 expression by SIVsmm, SIVmac and HIV-2 Nef viruses resulted in different effects on virion infectivity. For SIVsmm and SIVmac Nef viruses this was mapped to differences in Env expression and virion incorporation; however, this was not measured for HIV-2 Nef viruses. Given that all HIV-2 Nef viruses showed similar virion infectivity, it is likely that Env expression and virion incorporation will also be similar for these viruses. Retained CD3 expression on HIV-2 D8 and A8 T virus infected cells resulted in increased expression of CD69 during cell-cell spread, suggesting increased cell activation. This is consistent with SIVsmm and SIVmac data; however, the analysis of activation marker expression was not extensive and it cannot be excluded that other differences may arise. By contrast to SIVsmm and SIVmac data, HIV-2 Nef chimeric viruses did not show any CD3-dependent differences in Gag or GFP expression during cell-cell spread. This does not correlate with increased expression of CD69 in D8 and A8 T Nef virus infected cells (retained CD3 expression), suggesting that T cell activation might not impact on viral gene expression of HIV-2 Nef viruses; however, the analysis of HIV-2 Nef chimeric viruses was limited (since they showed no differences in viral spread or virion infectivity), thus further experiments are

required (as done in Chapter 3) to better define the relationship between CD3 downmodulation, cell activation and viral gene expression for HIV-2 Nef chimeric viruses.

Given the differences in viral spread, viral gene expression and T cell activation between *nef* alleles from the three lentiviral lineages tested here, a unifying mechanism that could explain all observations cannot be proposed. However, the data suggests that there are additional determinants in Nef (in addition to CD3 downmodulation) that impact on viral replication and T cell activation. Despite the main structural and functional motifs being conserved between the *nef* alleles, there are many changes in the amino acid sequence (Figure 4.1), which could affect Nef function. The C-terminal flexible loop, which contains the ExxxLL motif and is important for Nef interaction with cellular endocytic machinery (Munch et al., 2005), shows multiple differences between the *nef* alleles. However, given that all Nef chimeric viruses showed similar downmodulation ability of the major Nef targets, substitutions in this region unlikely explain the differences between the *nef* alleles observed here. Similarly, the unstructured N-terminal region (between the N-terminus and the PxxP motif) shows many differences (Figure 4.1); however this region is not well characterised and its role in Nef function remains poorly defined (Ananth et al., 2019; Fackler et al., 2006; Kirchhoff et al., 2004; Manrique et al., 2017; Munch et al., 2005). Future work making Nef chimers (e.g. swapping SIVsmm and SIVmac N-terminal regions of Nef) could help to establish whether differences between the *nef* alleles can be mapped to a particular region in Nef and thus help to identify the additional Nef determinants that impact on viral replication. It is important to note that naturally occurring SIVsmm causes a non-pathogenic infection in sooty mangebeys, whereas zoonotic transmissions to give SIVmac and HIV-2 result in pathogenic infections in rhesus macaques and humans (although HIV-2 is only moderately pathogenic in humans compared to HIV-1) (Gao et al., 1994; Frank Kirchhoff, 2009; Marlink et al., 1994; Murphey-Corb et al., 1986; Sodora et al., 2009). The adaptation of SIVsmm to a new host (macaques and humans) might have necessitated changes in Nef to better support viral replication in face of CD3 downmodulation. This is consistent with observations in this Chapter showing that SIVmac and HIV-2 viruses which downmodulate CD3 spread equally well as viruses that retain CD3 expression.

5 Conclusions and future work

5.1 Summary

The Nef protein of HIV-2 and most SIV lineages downmodulates the surface expression of CD3 - the signalling component of the TCR complex (Schindler et al., 2006). As described earlier, it was shown that CD3 downmodulation impairs signalling at the immunological synapse (Arhel et al., 2009) and may therefore interfere with antiviral responses and prevent aberrant immune activation during *in vivo* infection (Silvestri et al., 2003b; Sodora et al., 2009; Sumpter et al., 2007). However, this function of Nef was lost twice during the primate lentiviral evolution, most recently in the SIVcpz lineage that gave rise to the pandemic HIV-1 (Schindler et al., 2006). The reason why HIV-1 does not employ this potential immune evasion strategy remained poorly understood. It was previously shown that HIV-1 activates TCR/CD3 signalling during the VS formation and cell-cell spread, thus supporting more efficient viral spread (Len et al., 2017). Therefore, it was hypothesised that loss of Nef-mediated CD3 downmodulation in infected cells would result in triggering of TCR signalling and T cell activation during cell-cell spread, thus resulting in enhanced viral spread. Indeed, data in Chapter 3 showed that retained CD3 expression by SIVsmm Nef chimeric viruses is associated with increased viral replication and spread. Retained CD3 expression was associated with increased T cell activation and Env expression, resulting in increased viral infectivity, thus likely explaining enhanced viral spread. These observations provide a plausible explanation why the CD3 downmodulation ability of Nef was lost in HIV-1 lineage. In another words, retained CD3 expression on infected cells provides a replicative advantage for the virus. It is possible to speculate that SIVcpz and HIV-1 upon zoonotic transmissions to chimpanzees and humans required viral adaptations to enhance viral spread in the new host, possibly at the expense of additional means of immune evasion.

By contrast to SIVsmm Nef chimeric viruses, data in Chapter 4 shows that SIVmac and HIV-2 Nef chimeric viruses spread equally well, regardless of their ability to downmodulate CD3. This suggests that SIVmac and HIV-2 Nef proteins may have an additional ability to enhance viral spread, thus overriding the negative effect of CD3 downmodulation seen in SIVsmm Nef viruses. Further investigation is required to uncover the mechanism of CD3-independent enhancement of viral spread. Notably, SIVmac and HIV-2 transmitted from sooty mangabeys (SIVsmm) and are thus infections of non-natural hosts, macaques and humans. It is therefore plausible to speculate that additional changes in Nef may have occurred during adaptation of these viruses to a

new host that supported better viral replication, despite CD3 downmodulation. To explore this further and to better understand the impact of zoonotic transmissions on Nef function it would be interesting to observe the effect of CD3 downmodulation in the ancestral SIVcpz Nef or in Nefs from other SIV lineages. Given that both SIVcpz and HIV-1 do not downregulate CD3 and considering the evolutionary relationship, one may speculate that SIVcpz Nef engineered to downregulate may also show reduced cell-cell spread, but this is a hypothesis that will require further testing. Likewise, Nef proteins from other SIV lineages that are natural infections, like SIVsmm, may behave in a similar way and show reduced cell-cell spread compared to Nef mutant viruses that retain CD3 expression.

5.2 Relationship between Vpu and Nef function

Interestingly, the loss of Nef-mediated CD3 downmodulation in the lentiviral evolution appeared to coincide with acquisition of *vpu* gene. As described in detail in Chapter 1, one major function of Vpu is downmodulation of the host restriction factor tetherin, thus enhancing release of nascent virions from the cell surface (Neil et al., 2008; van Damme et al., 2008), but also preventing tetherin-mediated activation of NF-κB signalling (Galão et al., 2012). Another major function of Vpu is direct inhibition of NF-κB signalling by stabilising IκB and preventing NF-κB nuclear translocation and thus limiting interferon and ISG induction and innate immune responses (Akari et al., 2001; Langer et al., 2019; Sauter et al., 2015). Notably, lentiviruses that lack *vpu* gene have been shown to use Nef-mediated CD3 downmodulation as a strategy to prevent TCR signalling and consequently downstream NF-κB activation and thus limiting innate immune responses (Hotter et al., 2017; Schindler et al., 2006). This suggests that lentiviruses need a strategy to antagonise NF-κB activation and shows that viruses have evolved different mechanism and different accessory proteins to achieve this.

Vpu is only found in SIVcpz/HIV-1 lineage and in the lineage infecting closely related *Cercopithecus* monkeys: greater spot-nosed (SIVgsn), moustached (SIVmus) and mona (SIVmon) monkeys (Bibollet-Ruche et al., 2004). The origin of *vpu* gene is unclear, but phylogenetic analysis suggested that it was acquired by an early ancestor of SIVgsn/mus/mon lineage (Bailes et al., 2003). Since Nef proteins of closely related SIVdeb and SIVsyk (infecting DeBrazza and Sykes' monkeys) have the ability to downmodulate CD3, it was suggested that this ancestor of SIVgsn/mus/mon also had CD3 downmodulation ability, which was then lost upon acquisition of *vpu* gene (Frank

Kirchhoff, 2009). Phylogenetic analysis of *pol, env* and *nef* genes suggested that late ancestor of SIVgsn/mus/mon (containing Vpu and lacking CD3 downmodulation) recombined with the ancestor of SIVrcm (infecting red-capped mangebeys) to give an early ancestor of SIVcpz (Bailes et al., 2003). SIVcpz Nef is closely related to SIVrcm Nef, which is able to downmodulate CD3, therefore it was suggested that this early SIVcpz ancestor was able to downmodulate CD3 and that this ability was lost upon acquisition of *vpu* gene (after the recombination with SIVgsn/mus/mon) (Schindler et al., 2006). This was therefore the second loss of Nef-mediated CD3 downmodulation in lentiviral evolution.

Nef proteins from most SIV lineages are able to downmodulate tetherin in their respective hosts; however, SIVgsn/mon/mus Nefs are inactive in tetherin antagonism and instead use Vpu to downmodulate tetherin (Sauter et al., 2009; Zhang et al., 2009). Upon transmission to chimpanzees, SIVcpz Vpu was unable to antagonise chimpanzee tetherin, but instead SIVcpz evolved to use Nef to downmodulate tetherin (Sauter et al., 2009; Zhang et al., 2009). Upon subsequent transmission to humans, HIV-1 Nef protein was inactive against human tetherin, because of a short deletion in the cytoplasmic tail, which conferred resistance to Nef-mediated downmodulation (Zhang et al., 2009). HIV-1 M group thus evolved Vpu to antagonise tetherin (Neil et al., 2008; van Damme et al., 2008), and HIV-1 O group (despite having Vpu) evolved Nef to overcome human tetherin resistance (Kluge et al., 2014). By contrast HIV-2 (transmitted from SIVsmm) evolved Env to antagonise human tetherin (Heusinger et al., 2018; le Tortorec & Neil, 2009). This shows that tetherin antagonism is species-specific and while the mechanism of antagonism varies, this function is conserved in lentiviruses and thus suggest it is highly important for the virus.

Activation of NF-κB is necessary for efficient viral transcription as lentiviruses usually contain multiple NF-κB binding sites (Burnett et al., 2009; Williams et al., 2007). Thus, it was postulated that keeping both Vpu and Nef-mediated CD3 downmodulation (both preventing NF-κB activation) would result in poor viral replication. Therefore, it is possible to hypothesise that acquisition of Vpu necessitated or facilitated the loss of Nef-mediated CD3 downmodulation. Data in Chapter 3 are consistent with this hypothesis. Retained CD3 expression by SIVsmm Nef viruses resulted in increased T cell activation and viral gene expression, resulting in enhanced viral spread. These data therefore may help to explain why CD3 downmodulation was lost in HIV-1 lineage. For example, the

virus needs to balance cell activation for NF-κB-dependent proviral transcription with suppression of antiviral responses. As such, HIV-1 evolved to target NF-κB via Vpu instead of CD3 downmodulation, thus ensuring sufficient viral spread while supressing immune activation; however, further experiments are required to better understand the relationship between Vpu and Nef function. Since Vpu functions of tetherin and NF-κB antagonism are genetically separable (Sauter et al., 2015), it would be interesting to observe whether CD3 downmodulation results in improved viral spread in viruses that are specifically defective for Vpu-mediated NF-κB antagonism.

As mentioned above, activation of NF-κB is required for efficient viral replication; however, it can also result in expression of ISGs, resulting in innate immune response activation, thus inhibiting viral replication (Langer et al., 2019; Sauter et al., 2015). This suggests that lentiviruses need at least one strategy to antagonise NF-κB signalling to avoid innate immune responses, whether indirectly via Nef-mediated CD3 downmodulation or directly via Vpu. This is further exemplified by SIVolc and SIVcol (infecting olive colobus (olc) and guereza colobus (col) monkeys), which lack both Nef-mediated CD3 downmodulation and a *vpu* gene, but instead use Vpr to directly antagonise NF-κB signalling in a manner similar to Vpu (Hotter et al., 2017). However, new evidence is emerging that lentiviruses use additional mechanisms to antagonise NF-κB signalling. First, HIV-2 uses Vpx to target p65 subunit of NF-κB for degradation (Landsberg et al., 2018). This raises a question whether also other Vpx-containing viruses (i.e. SIVsmm, SIVmac, SIVrcm) use this mechanism to antagonise NF-κB and this remains to be investigated. Second, HIV-1 (which contains a *vpu* gene) also uses Vpr to inhibit NF-κB signalling, possibly by preventing its nuclear translocation (Khan et al., 2020). Taken together, this shows that the evolutionary relationships between lentiviral accessory protein function are highly complex and likely extend beyond the correlation between lack of Nef-mediated CD3 downmodulation and presence of a *vpu* gene. Lentiviruses need to finely balance the activation of NF-κB signalling to ensure optimal viral replication and as such have evolved several strategies to achieve this.

5.3 CD3, immune activation and viral pathogenicity

SIV infections in natural hosts are usually non-pathogenic and do not cause AIDS-like disease (Chahroudi et al., 2012; Kaur et al., 1998; Sumpter et al., 2007). While there are many possibilities for why the interplay between virus and host may have different

outcomes in different species, it has been proposed that this might be due to Nef-mediated CD3 downmodulation preventing aberrant immune activation in infected animals and thus mediating low pathogenicity of these viruses (Milush et al., 2007; Schmökel et al., 2013). However, sufficient evidence for low pathogenicity only exists for SIVsmm and SIVagm (infecting African green monkeys), which do not show CD4+ T cell depletion and do not develop disease despite high levels of viral replication (Silvestri et al., 2003b; Sodora et al., 2009). SIV infections in other monkey species have not been well studied, thus a clear link between CD3 downmodulation and lack of disease cannot be established. For example, it would be interesting to observe whether SIVgsn/mus/mon (which lack CD3 downmodulation ability) cause the disease in infected animals.

As described in Chapter 3, rare cases have been reported where loss of Nef-mediated CD3 downmodulation occurred in SIVsmm infected sooty mangabeys. This resulted in CD4+ T cell depletion and moderate immune activation; however, infected animals maintained relatively high viral loads and did not develop disease (Milush et al., 2007; Schindler et al., 2008; Schmökel et al., 2013). This might suggest that CD3 downmodulation in SIVsmm infection is not a crucial strategy to evade immune responses and further investigation is required to confirm this. Loss of Nef-mediated CD3 modulation also coincided with expanded Env co-receptor tropism, thus a direct link between retained CD3 expression and CD4+ T cell depletion could not be established (Schmökel et al., 2013). However, data in Chapter 3 showing that retained CD3 expression on infected cells resulted in increased T cell activation and cell death is consistent with these *in vivo* observations. Notably, loss of CD4+ T cells in sooty mangabeys did not result in AIDS-like disease, which was attributed to presence of functional double negative (CD4-CD8-) T helper cells (Milush et al., 2011; Sundaravaradan et al., 2013). Additionally, sooty mangabeys have been identified with low CCR5 co-receptor expression on memory T cells, defective TLR4 signalling and absence of ICAM-2 expression, which have been suggested to contribute to low pathogenicity of SIVsmm infection (Paiardini et al., 2011; Palesch et al., 2018). Like sooty mangabeys, African green monkeys also show certain level of adaptation to SIV infection. Low CD4 expression on memory T cells and presence of functional double-negative (CD4-CD8-) T helper cells have been suggested to have a protective role in SIVagm infection (Beaumier et al., 2009; Vinton et al., 2011). Infection with chimeric SIVagm that contained HIV-1 Nef (no CD3 downmodulation) and SIVgsn Vpu (to antagonise tetherin and NF-κB activation) showed increased levels of T cell activation

and inflammatory gene expression compared to WT virus that is able to downmodulate CD3 (Joas et al., 2018), consistent with protective role of CD3 downmodulation against aberrant immune activation. However, these viruses showed similar levels of viral replication and did not cause T cell depletion or disease, which suggest host factor adaptation that is protective against viral pathogenicity. Taken together, examination of SIVsmm and SIVagm infections indicates high level of host adaptation and perhaps suggests co-evolution between the virus and the host that prevents host pathology while maintaining sufficient viral replication. Furthermore, these observations argue that low pathogenicity of SIVsmm and SIVagm may not be simply due to Nef-mediated CD3 downmodulation, but instead may be related to specific host factors and unique features of the immune systems of sooty manganbeys and African green monkeys.

Unlike SIVsmm and SIVagm, SIVcpz and HIV-1 cause chronic immune activation, CD4+ T cell depletion and disease in chimpanzees and humans (Brenchley et al., 2006; Keele et al., 2009; Moir et al., 2011). As explained above, these viruses originated from zoonotic transmissions into non-natural hosts, and it has been suggested that the lack of virus-host adaptation may explain the high virulence and pathogenecity of these viruses. Interestingly, HIV-2 infection can cause disease in humans; however, it is generally considered less pathogenic compared to HIV-1, demonstrated by reduced viral loads, lower transmission rates and slower disease progression where the majority of infected individuals become long-term nonprogressors (Jaffar et al., 1997; Marlink et al., 1994; Nyamweya et al., 2013; Olesen et al., 2018; van der Loeff et al., 2010). HIV-2 Nef is able to downmodulate CD3 and this has been shown to have a protective role against CD4+ T cell depletion and aberrant immune activation (Khalid et al., 2012), but clearly it does not protect against disease progression in all infected individuals (Feldmann et al., 2009; Jaffar et al., 1997). Taken together, observations form *in vivo* infections of SIVsmm, SIVagm and HIV-2 suggest that CD3 downmodulation seems to be an important mechanism helping to reduce T cell activation and thus preventing aberrant immune activation. Data in this thesis showing that retained CD3 expression results in increased T cell activation is consistent with these observations. By contrast, CD3 downmodulation ability and its importance in reduced viral pathogenicity and efficient immune evasion is different in different viruses and host species. This illustrates highly complex interplay between the viral genes and between virus and host that remains incompletely understood. It is difficult to extrapolate *in vitro* data to *in vivo* observations; however, data in this thesis suggests that loss of Nef-mediated CD3 downmodulation in the HIV-1 lineage (and its SIVcpz ancestor) was beneficial for the virus to increase viral

replication, and thus selected for even at the expense of increased pathogenicity and less effective immune evasion.

5.4 Future directions

Data in Chapter 3 showed that increased Env expression and virion incorporation was the main factor mediating increased virion infectivity and viral spread. Moreover, retained CD3 expression resulted in faster kinetics of Env trafficking between the plasma membrane and the intracellular compartments. Previous work has shown that Env recycling through the TGN or endosomal recycling compartment (ERC) is important for Env virion incorporation (Groppelli et al., 2014; Kirschman et al., 2018). Questions that rise include the following: Does retained CD3 expression result in trafficking of Env through different intracellular compartments (TGN vs ERC)? Are there differences in trafficking to lysosomal compartment that would affect Env surface expression levels and consequently virion incorporation? Performing immunofluorescence microscopy co-localisation analysis would help to answer these questions. Another possibility is that retained CD3 expression (and signalling activation) results in more Env being recruited to the VS, which would also help to explain increased Env virion incorporation. Microscopy analysis of VS formation in Chapter 3 did not reveal any gross differences in Env levels at the VS; however, higher resolution and more quantitative imaging may help to address this question. Further analysis of CD3-dependent differences in Env localisation and trafficking would also help to increase our understanding of HIV-1 Env trafficking and virion incorporation in general. Moreover, whether Env directly interacts with CD3, which could impact on Env surface expression, could be explored further given that previous reports have suggested this interaction (Luo et al., 2016; Yakovian et al., 2018). Although my data showing increased Env internalisation in presence of CD3 expression argues against this hypothesis, more definitive experiments (such as co-immunoprecipitation or FRET) are required to determine whether there is direct Env-CD3 interaction.

Whether the effect of CD3 modulation on Env expression and virion incorporation is specific to the lab-adapted CXCR4-tropic NL4.3 strain remains to be tested. In light of this, can similar results be observed using a different Env or a different backbone altogether, particularly one of a primary CCR5-tropic viral isolate? Previous reports have also showed that HIV-1 transmitted founder viruses have higher Env incorporation and virion infectivity compared to chronic control viruses (Parrish et al., 2013). Thus, it would

also be interesting to observe whether there is different effect of CD3 modulation on transmitted founder compared to chronic control viruses. Furthermore, using chimeric viruses with CCR5 tropism would also help to answer the question whether observed differences in cell death were specific to CXCR4 tropism as was suggested in the original *in vivo* study that identified the SIVsmm *nef* alleles used in this thesis (Schmökel et al., 2013).

As described earlier in this Chapter, there might be a link between Nef and Vpu function in modulating NF-κB activation. Importantly, NF-κB activation was not measured in this thesis. Further experiments measuring phosphorylation or nuclear translocation of NF-κB would help to better understand the role of CD3 modulation on NF-κB activation during cell-cell spread. Another option is to create Nef chimeric viruses with Vpu mutants (R45K) specifically defective for NF-κB antagonism (Langer et al., 2019; Pickering et al., 2014) and measure viral spread and gene expression. Does CD3 downmodulation in R45K Vpu mutant result in enhanced viral spread? Does retained CD3 expression in R45K Vpu mutant result in innate immune response that inhibits viral spread? These experiments would thus help to better understand the relationship between Nef and Vpu function.

Data in Chapter 4 showed that SIVmac and HIV-2 Nef chimeric viruses spread equally well, regardless of their ability to downmodulate CD3. Is there another yet unknown function of Nef that contributes to enhanced viral spread? Indeed, a recent study suggested that Nef might have another previously unidentified function as it promotes viral spread even in the absence of SERINC restriction or CD4 downmodulation (Wu et al., 2019). Nef sequence analysis showed multiple differences between SIVsmm, SIVmac and HIV-2 Nefs, particularly in the poorly defined, unstructured N-terminal region. Making chimeric Nef constructs (e.g. swapping N-terminal domains) would help to map the differences between Nefs to a particular region in Nef. Further experiments could thus identify a particular sequence motif or a potential interaction with a host cell factor that would explain enhanced viral spread in face of CD3 downmodulation. Nef interaction with Src-family kinases, PAK2 and NF-κB stimulation have also been shown to affect T cell activation and viral spread (Collette et al., 2000; Fortin et al., 2004; Olivieri et al., 2011; Rudolph et al., 2009; Sauter et al., 2015). Therefore, further experiments are required to test these activities in the panel of Nef viruses used in this thesis. This

could also help to understand why there was no difference observed in TCR signalling between SIVmac Nef viruses.

SIVmac Nef chimeric viruses also showed an unusual phenotype in virus budding and Env expression compared to SIVsmm Nef viruses. Retained CD3 expression resulted in increased virus budding and further experiments are required to determine what factors mediate increased virus budding. Is there more Gag localised at the plasma membrane? Is it dependent on the activity of ESCRT machinery? Does CD3 downmodulation indirectly affect tetherin expression? Retained CD3 expression also resulted in decreased Env expression and virion infectivity. Is there a difference in Env internalisation and recycling? What is the effect of CD3 KD or stimulation of infected cells on Env expression? Performing these experiments (as described in Chapter 3) would thus help to better understand the relationship between CD3 expression, cell activation and Env expression in cell infected with SIVmac Nef chimeric viruses.

5.5 Final remarks

Lentiviruses have evolved in different hosts, and under different selective pressures, to support efficient replication and dissemination, while balancing this with the need to modulate the host environment towards immune evasion. To this end, lentiviruses have acquired and evolved different accessory genes to manipulate their host and increase viral fitness. Here I have explored the role of one such accessory protein: Nef and its ability to modulate surface expression of CD3, a key feature that differs amongst pandemic HIV-1 lineage and its ancestors. Collectively, the data in this thesis has highlighted the plasticity between different lentiviruses in Nef activity and reveals the evolution of multiple pathways available for these viruses to support efficient spread between T cells. While the interplay between virus and host is complex, this work highlights the value of comparative virology as an endeavour to gain new insight into the biology of HIV-1 and to inform our understanding into the evolution of an important human pathogen.

6 References

Achuthan, V., Perreira, J.M., Sowd, G.A., Puray-Chavez, M., McDougall, W.M., Paulucci-Holthauzen, A., Wu, X., Fadel, H.J., Poeschla, E.M., Multani, A.S., et al. (2018). Capsid-CPSF6 Interaction Licenses Nuclear HIV-1 Trafficking to Sites of Viral DNA Integration. Cell Host and Microbe *24*, 392-404.e8.

Agosto, L.M., Zhong, P., Munro, J., and Mothes, W. (2014). Highly Active Antiretroviral Therapies Are Effective against HIV-1 Cell-to-Cell Transmission. PLoS Pathogens *10*.

Agosto, L.M., Uchil, P.D., and Mothes, W. (2015). HIV cell-to-cell transmission: effects on pathogenesis and antiretroviral therapy. Trends in Microbiology *23*, 289–295.

Aiken, C., Konner, J., Landau, N.R., Lenburg, M.E., and Trono, D. (1994). Nef induces CD4 endocytosis: Requirement for a critical dileucine motif in the membrane-proximal CD4 cytoplasmic domain. Cell *76*, 853–864.

Akari, H., Fukumori, T., and Adachi, A. (2000). Cell-Dependent Requirement of Human Immunodeficiency Virus Type 1 gp41 Cytoplasmic Tail for Env Incorporation into Virions. Journal of Virology *74*, 4891–4893.

Akari, H., Bour, S., Kao, S., Adachi, A., and Strebel, K. (2001). The human immunodeficiency virus type 1 accessory protein Vpu induces apoptosis by suppressing the nuclear factor κB-dependent expression of antiapoptotic factors. Journal of Experimental Medicine *194*, 1299–1311.

Alfadhli, A., Barklis, R.L., and Barklis, E. (2009). HIV-1 matrix organizes as a hexamer of trimers on membranes containing phosphatidylinositol-(4,5)-bisphosphate. Virology *387*, 466–472.

Alfadhli, A., Staubus, A.O., Tedbury, P.R., Novikova, M., Freed, E.O., and Barklis, E. (2019). Analysis of HIV-1 Matrix-Envelope Cytoplasmic Tail Interactions. Journal of Virology *93*.

Alkhatib, G., Combadiere, C., Broder, C.C., Feng, Y., Kennedy, P.E., Murphy, P.M., and Berger, E.A. (1996). CC CKR5: A RANTES, MIP-1α, MIP-1β receptor as a fusion cofactor for macrophage-tropic HIV-1. Science *272*, 1955–1958.

Alvarez, R.A., Hamlin, R.E., Monroe, A., Moldt, B., Hotta, M.T., Rodriguez Caprio, G., Fierer, D.S., Simon, V., and Chen, B.K. (2014). HIV-1 Vpu Antagonism of Tetherin Inhibits Antibody-Dependent Cellular Cytotoxic Responses by Natural Killer Cells. Journal of Virology *88*, 6031–6046.

Anand, S.P., Grover, J.R., Tolbert, W.D., Prévost, J., Richard, J., Ding, S., Baril, S., Medjahed, H., Evans, D.T., Pazgier, M., et al. (2019). Antibody-Induced Internalization of HIV-1 Env Proteins Limits Surface Expression of the Closed Conformation of Env. Journal of Virology *93*.

Ananth, S., Morath, K., Trautz, B., Tibroni, N., Shytaj, I.L., Obermaier, B., Stolp, B., Lusic, M., and Fackler, O.T. (2019). Multifunctional Roles of the N-Terminal Region of HIV-1SF2Nef Are Mediated by Three Independent Protein Interaction Sites. Journal of Virology *94*.

Andreotti, A.H., Schwartzberg, P.L., Joseph, R.E., and Berg, L.J. (2010). T-cell signaling regulated by the Tec family kinase, Itk. Cold Spring Harbor Perspectives in Biology *2*.

Apetrei, C., Kaur, A., Lerche, N.W., Metzger, M., Pandrea, I., Hardcastle, J., Falkenstein, S., Bohm, R., Koehler, J., Traina-Dorge, V., et al. (2005). Molecular Epidemiology of Simian Immunodeficiency Virus SIVsm in U.S. Primate Centers Unravels the Origin of SIVmac and SIVstm. Journal of Virology *79*, 8991–9005.

Aramburu, J., Yaffe, M.B., López-Rodríguez, C., Cantley, L.C., Hogan, P.G., and Rao, A. (1999). Affinity-driven peptide selection of an NFAT inhibitor more selective than cyclosporin A. Science *285*, 2129–2133.

Arhel, N., Lehmann, M., Clauss, K., Nienhaus, G.U., Piguet, V., and Kirchhoff, F. (2009). The inability to disrupt the immunological synapse between infected human T cells and APCs distinguishes HIV-1 from most other primate lentiviruses. The Journal of Clinical Investigation *119*, 2965–2975.

Aries, S.P., Schaaf, B., Müller, C., Dennin, R.H., and Dalhoff, K. (1995). Fas (CD95) expression on CD4+ T cells from HIV-infected patients increases with disease progression. Journal of Molecular Medicine (Berlin, Germany) *73*, 591–593.

Arold, S.T., and Baur, A.S. (2001). Dynamic Nef and Nef dynamics: How structure could explain the complex activities of this small HIV protein. Trends in Biochemical Sciences *26*, 356–363.

Arold, S., O'Brien, R., Franken, P., Strub, M.P., Hoh, F., Dumas, C., and Ladbury, J.E. (1998). RT loop flexibility enhances the specificity of Src family SH3 domains for HIV-1 Nef. Biochemistry *37*, 14683–14691.

Arrighi, J.F., Pion, M., Garcia, E., Escola, J.M., van Kooyk, Y., Geijtenbeek, T.B., and Piguet, V. (2004). DC-SIGN-mediated infectious synapse formation enhances X4 HIV-1 transmission from dendritic cells to T cells. Journal of Experimental Medicine *200*, 1279–1288.

Autran, B., Carcelain, G., Li, T.S., Blanc, C., Mathez, D., Tubiana, R., Katlama, C., Debré, P., and Leibowitch, J. (1997). Positive effects of combined antiretroviral therapy on CD4+ T cell homeostasis and function in advanced HIV disease. Science *277*, 112–116.

Ayouba, A., Akoua-Koffi, C., Calvignac-Spencer, S., Esteban, A., Locatelli, S., Li, H., Li, Y., Hahn, B.H., Delaporte, E., Leendertz, F.H., et al. (2013). Evidence for continuing cross-species transmission of SIVsmm to humans. AIDS *27*, 2488–2491.

Bachand, F., Yao, X.J., Hrimech, M., Rougeau, N., and Cohen, É.A. (1999). Incorporation of Vpr into human immunodeficiency virus type 1 requires a direct interaction with the p6 domain of the p55 Gag precursor. Journal of Biological Chemistry *274*, 9083–9091.

Bailes, E., Gao, F., Bibollet-Ruche, F., Courgnaud, V., Peeters, M., Marx, P.A., Hahn, B.H., and Sharp, P.M. (2003). Hybrid Origin of SIV in Chimpanzees. Science *300*, 1713–1713.

Balagopalan, L., Kortum, R.L., Coussens, N.P., Barr, V.A., and Samelson, L.E. (2015). The linker for activation of T Cells (LAT) signaling hub: From signaling complexes to microclusters. Journal of Biological Chemistry *290*, 26422–26429.

Baldauf, H.-M., Pan, X., Erikson, E., Schmidt, S., Daddacha, W., Burggraf, M., Schenkova, K., Ambiel, I., Wabnitz, G., Gramberg, T., et al. (2012). SAMHD1 restricts HIV-1 infection in resting CD4+ T cells. Nature Medicine *18*, 1682–1688.

Baldauf, H.M., Stegmann, L., Schwarz, S.M., Ambiel, I., Trotard, M., Martin, M., Burggraf, M., Lenzi, G.M., Lejk, H., Pan, X., et al. (2017). Vpx overcomes a SAMHD1-independent block to HIV reverse transcription that is specific to resting CD4 T cells. Proceedings of the National Academy of Sciences of the United States of America *114*, 2729–2734.

Bandres, J.C., and Ratner, L. (1994). Human immunodeficiency virus type 1 Nef protein down-regulates transcription factors NF-kappa B and AP-1 in human T cells in vitro after T-cell receptor stimulation. Journal of Virology *68*, 3243–3249.

Bar, K.J., Li, H., Chamberland, A., Tremblay, C., Routy, J.P., Grayson, T., Sun, C., Wang, S., Learn, G.H., Morgan, C.J., et al. (2010). Wide Variation in the Multiplicity of HIV-1 Infection among Injection Drug Users. Journal of Virology *84*, 6241–6247.

Barda-Saad, M., Shirasu, N., Pauker, M.H., Hassan, N., Perl, O., Balbo, A., Yamaguchi, H., Houtman, J.C.D., Appella, E., Schuck, P., et al. (2010). Cooperative interactions at the SLP-76 complex are critical for actin polymerization. The EMBO Journal *29*, 2315–2328.

Barré-Sinoussi, F., Chermann, J.C., Rey, F., Nugeyre, M.T., Chamaret, S., Gruest, J., Dauguet, C., Axler-Blin, C., Vézinet-Brun, F., Rouzioux, C., et al. (1983). Isolation of a T-lymphotropic retrovirus from a patient at risk for acquired immune deficiency syndrome (AIDS). Science *220*, 868–871.

Baxter, A.E., Russell, R.A., Duncan, C.J.A., Moore, M.D., Willberg, C.B., Pablos, J.L., Finzi, A., Kaufmann, D.E., Ochsenbauer, C., Kappes, J.C., et al. (2014). Macrophage infection via selective capture of HIV-1-infected CD4+ T cells. Cell Host and Microbe *16*, 711–721.

Beaumier, C.M., Harris, L.D., Goldstein, S., Klatt, N.R., Whitted, S., McGinty, J., Apetrei, C., Pandrea, I., Hirsch, V.M., and Brenchley, J.M. (2009). CD4 downregulation by memory CD4+ T cells in vivo renders African green monkeys resistant to progressive SIVagm infection. Nature Medicine *15*, 879–885.

Bego, M.G., Mercier, J., and Cohen, E.A. (2012). Virus-Activated Interferon Regulatory Factor 7 Upregulates Expression of the Interferon-Regulated BST2 Gene Independently of Interferon Signaling. Journal of Virology *86*, 3513–3527.

Beitari, S., Ding, S., Pan, Q., Finzi, A., and Liang, C. (2017). Effect of HIV-1 Env on SERINC5 Antagonism. Journal of Virology *91*.

Bejarano, D.A., Peng, K., Laketa, V., Börner, K., Jost, K.L., Lucic, B., Glass, B., Lusic, M., Müller, B., and Kräusslich, H.G. (2019). HIV-1 nuclear import in macrophages is regulated by CPSF6-capsid interactions at the nuclear pore complex. ELife *8*.

Bell, S.M., and Bedford, T. (2017). Modern-day SIV viral diversity generated by extensive recombination and cross-species transmission. PLOS Pathogens *13*, e1006466.

Bennett, A.E., Narayan, K., Shi, D., Hartnell, L.M., Gousset, K., He, H., Lowekamp, B.C., Yoo, T.S., Bliss, D., Freed, E.O., et al. (2009). Ion-abrasion scanning electron microscopy reveals surface-connected tubular conduits in HIV-infected macrophages. PLoS Pathogens *5*.

Berg, R.K., Melchjorsen, J., Rintahaka, J., Diget, E., Søby, S., Horan, K.A., Gorelick, R.J., Matikainen, S., Larsen, C.S., Ostergaard, L., et al. (2012). Genomic HIV RNA induces innate immune responses through RIG-I-dependent sensing of secondary-structured RNA. PLoS ONE *7*.

Berger, G., Lawrence, M., Hué, S., and Neil, S.J.D. (2015). G 2 /M Cell Cycle Arrest Correlates with Primate Lentiviral Vpr Interaction with the SLX4 Complex . Journal of Virology *89*, 230–240.

Berkhout, B., Silverman, R.H., and Jeang, K.T. (1989). Tat trans-activates the human immunodeficiency virus through a nascent RNA target. Cell *59*, 273–282.

Berlioz-Torrent, C., Shacklett, B.L., Erdtmann, L., Delamarre, L., Bouchaert, I., Sonigo, P., Dokhelar, M.C., and Benarous, R. (1999). Interactions of the Cytoplasmic Domains of Human and Simian Retroviral Transmembrane Proteins with Components of the Clathrin Adaptor Complexes Modulate Intracellular and Cell Surface Expression of Envelope Glycoproteins. Journal of Virology *73*, 1350–1361.

Berman, P.W., Nunes, W.M., and Haffar, O.K. (1988). Expression of membrane-associated and secreted variants of gp160 of human immunodeficiency virus type 1 in vitro and in continuous cell lines. Journal of Virology *62*, 3135–3142.

Bernstein, H.B., Tucker, S.P., Hunter, E., Schutzbach, J.S., and Compans, R.W. (1994). Human immunodeficiency virus type 1 envelope glycoprotein is modified by O-linked oligosaccharides. Journal of Virology *68*, 463–468.

Berridge, M.J., and Irvine, R.F. (1984). Inositol trisphosphate, a novel second messenger in cellular signal transduction. Nature *312*, 315–321.

Bhattacharya, J., Repik, A., and Clapham, P.R. (2006). Gag Regulates Association of Human Immunodeficiency Virus Type 1 Envelope with Detergent-Resistant Membranes. Journal of Virology *80*, 5292–5300.

Bibollet-Ruche, F., Bailes, E., Gao, F., Pourrut, X., Barlow, K.L., Clewley, J.P., Mwenda, J.M., Langat, D.K., Chege, G.K., McClure, H.M., et al. (2004). New simian immunodeficiency virus infecting De Brazza's monkeys (Cercopithecus neglectus): evidence for a cercopithecus monkey virus clade. Journal of Virology *78*, 7748–7762.

Bichel, K., Price, A.J., Schaller, T., Towers, G.J., Freund, S.M.V., and James, L.C. (2013). HIV-1 capsid undergoes coupled binding and isomerization by the nuclear pore protein NUP358. Retrovirology *10*.

Bishop, K.N., Verma, M., Kim, E.Y., Wolinsky, S.M., and Malim, M.H. (2008). APOBEC3G inhibits elongation of HIV-1 reverse transcripts. PLoS Pathogens *4*.

Bivona, T.G., Pérez de Castro, I., Ahearn, I.M., Grana, T.M., Chiu, V.K., Lockyer, P.J., Cullen, P.J., Pellicer, A., Cox, A.D., and Philips, M.R. (2003). Phospholipase Cγ activates Ras on the Golgi apparatus by means of RasGRP1. Nature *424*, 694–698.

Bjorkman, P.J., Saper, M.A., Samraoui, B., Bennett, W.S., Strominger, J.L., and Wiley, D.C. (1987). Structure of the human class I histocompatibility antigen, HLA-A2. Nature *329*, 506–512.

Bleck, M., Itano, M.S., Johnson, D.S., Thomas, V.K., North, A.J., Bieniasz, P.D., and Simon, S.M. (2014). Temporal and spatial organization of ESCRT protein recruitment during HIV-1 budding. Proceedings of the National Academy of Sciences of the United States of America *111*, 12211–12216.

Boge, M., Wyss, S., Bonifacino, J.S., and Thali, M. (1998). A membrane-proximal tyrosine-based signal mediates internalization of the HIV-1 envelope glycoprotein via interaction with the AP-2 clathrin adaptor. Journal of Biological Chemistry *273*, 15773–15778.

Bolinger, C., and Boris-Lawrie, K. (2009). Mechanisms employed by retroviruses to exploit host factors for translational control of a complicated proteome. Retrovirology *6*.

Bour, S., Schubert, U., and Strebel, K. (1995). The human immunodeficiency virus type 1 Vpu protein specifically binds to the cytoplasmic domain of CD4: implications for the mechanism of degradation. Journal of Virology *69*, 1510–1520.

Braun, E., Hotter, D., Koepke, L., Zech, F., Groß, R., Sparrer, K.M.J., Müller, J.A., Pfaller, C.K., Heusinger, E., Wombacher, R., et al. (2019). Guanylate-Binding Proteins 2 and 5 Exert Broad Antiviral Activity by Inhibiting Furin-Mediated Processing of Viral Envelope Proteins. Cell Reports *27*, 2092-2104.e10.

Brenchley, J.M., Schacker, T.W., Ruff, L.E., Price, D.A., Taylor, J.H., Beilman, G.J., Nguyen, P.L., Khoruts, A., Larson, M., Haase, A.T., et al. (2004a). CD4+ T cell depletion during all stages of

HIV disease occurs predominantly in the gastrointestinal tract. Journal of Experimental Medicine *200*, 749–759.

Brenchley, J.M., Hill, B.J., Ambrozak, D.R., Price, D.A., Guenaga, F.J., Casazza, J.P., Kuruppu, J., Yazdani, J., Migueles, S.A., Connors, M., et al. (2004b). T-Cell Subsets That Harbor Human Immunodeficiency Virus (HIV) In Vivo: Implications for HIV Pathogenesis. Journal of Virology *78*, 1160–1168.

Brenchley, J.M., Price, D.A., and Douek, D.C. (2006a). HIV disease: fallout from a mucosal catastrophe? Nature Immunology *7*, 235–239.

Brenchley, J.M., Price, D.A., Schacker, T.W., Asher, T.E., Silvestri, G., Rao, S., Kazzaz, Z., Bornstein, E., Lambotte, O., Altmann, D., et al. (2006b). Microbial translocation is a cause of systemic immune activation in chronic HIV infection. Nature Medicine *12*, 1365–1371.

Brenchley, J.M., Silvestri, G., and Douek, D.C. (2010). Perspective Nonprogressive and Progressive Primate Immunodeficiency Lentivirus Infections. Immunity *32*, 737–742.

Briggs, J.A.G., Wilk, T., Welker, R., Kräusslich, H.G., and Fuller, S.D. (2003). Structural organization of authentic, mature HIV-1 virions and cores. EMBO Journal *22*, 1707–1715.

Brod, S.A., Purvee, M., Benjamin, D., and Hafler, D.A. (1990). T-T cell interactions are mediated by adhesion molecules. European Journal of Immunology *20*, 2259–2268.

Brown, P.O., Bowerman, B., Varmus, H.E., and Bishop, J.M. (1989). Retroviral integration: Structure of the initial covalent product and its precursor, and a role for the viral IN protein. Proceedings of the National Academy of Sciences of the United States of America *86*, 2525–2529.

Brumme, Z.L., Goodrich, J., Mayer, H.B., Brumme, C.J., Henrick, B.M., Wynhoven, B., Asselin, J.J., Cheung, P.K., Hogg, R.S., Montaner, J.S.G., et al. (2005). Molecular and Clinical Epidemiology of CXCR4-Using HIV-1 in a Large Population of Antiretroviral-Naive Individuals. The Journal of Infectious Diseases *192*, 466–474.

Bui, K.H., von Appen, A., Diguilio, A.L., Ori, A., Sparks, L., Mackmull, M.T., Bock, T., Hagen, W., Andrés-Pons, A., Glavy, J.S., et al. (2013). Integrated structural analysis of the human nuclear pore complex scaffold. Cell *155*, 1233–1243.

Burdick, R.C., Li, C., Munshi, M.H., Rawson, J.M.O., Nagashima, K., Hu, W.S., and Pathak, V.K. (2020). HIV-1 uncoats in the nucleus near sites of integration. Proceedings of the National Academy of Sciences of the United States of America *117*, 5486–5493.

Burnett, J.C., Miller-Jensen, K., Shah, P.S., Arkin, A.P., and Schaffer, D. v. (2009). Control of Stochastic Gene Expression by Host Factors at the HIV Promoter. PLoS Pathogens *5*, e1000260.

Burton, D.R., and Hangartner, L. (2016). Broadly Neutralizing Antibodies to HIV and Their Role in Vaccine Design. Annual Review of Immunology *34*, 635–659.

Burton, D.R., Walker, L.M., Phogat, S.K., Chan-Hui, P.Y., Wagner, D., Phung, P., Goss, J.L., Wrin, T., Simek, M.D., Fling, S., et al. (2009). Broad and potent neutralizing antibodies from an african donor reveal a new HIV-1 vaccine target. Science *326*, 285–289.

Busnadiego, I., Kane, M., Rihn, S.J., Preugschas, H.F., Hughes, J., Blanco-Melo, D., Strouvelle, V.P., Zang, T.M., Willett, B.J., Boutell, C., et al. (2014). Host and Viral Determinants of Mx2 Antiretroviral Activity. Journal of Virology *88*, 7738–7752.

Butte, M.J., Keir, M.E., Phamduy, T.B., Sharpe, A.H., and Freeman, G.J. (2007). Programmed Death-1 Ligand 1 Interacts Specifically with the B7-1 Costimulatory Molecule to Inhibit T Cell Responses. Immunity *27*, 111–122.

Buttler, C.A., Pezeshkian, N., Fernandez, M. v., Aaron, J., Norman, S., Freed, E.O., and van Engelenburg, S.B. (2018). Single molecule fate of HIV-1 envelope reveals late-stage viral lattice incorporation. Nature Communications *9*, 1861.

Byland, R., Vance, P.J., Hoxie, J.A., and Marsh, M. (2007). A conserved dileucine motif mediates clathrin and AP-2-dependent endocytosis of the HIV-1 envelope protein. Molecular Biology of the Cell *18*, 414–425.

Call, M.E., Pyrdol, J., Wiedmann, M., and Wucherpfennig, K.W. (2002). The organizing principle in the formation of the T cell receptor-CD3 complex. Cell *111*, 967–979.

Cameron, P.U., Freudenthal, P.S., Barker, J.M., Gezelter, S., Inaba, K., and Steinman, R.M. (1992). Dendritic cells exposed to human immunodeficiency virus type-1 transmit a vigorous cytopathic infection to CD4+ T cells. Science *257*, 383–387.

Carl, S., Iafrate, A.J., Lang, S.M., Stolte, N., Stahl-Hennig, C., Matz-Rensing, K., Fuchs, D., Skowronski, J., and Kirchhoff, F. (2000). Simian Immunodeficiency Virus Containing Mutations in N-Terminal Tyrosine Residues and in the PxxP Motif in Nef Replicates Efficiently in Rhesus Macaques. Journal of Virology *74*, 4155–4164.

Carr, J.M., Hocking, H., Li, P., and Burrell, C.J. (1999). Rapid and efficient cell-to-cell transmission of human immunodeficiency virus infection from monocyte-derived macrophages to peripheral blood lymphocytes. Virology *265*, 319–329.

Caruso, A., Licenziati, S., Corulli, M., Canaris, A.D., de Francesco, M.A., Fiorentini, S., Peroni, L., Fallacara, F., Dima, F., Balsari, A., et al. (1997). Flow cytometric analysis of activation markers on stimulated T cells and their correlation with cell proliferation. Cytometry *27*, 71–76.

Castro, K.G., Ward, J.W., Slutsker, L., Buehler, J.W., Jaffe, H.W., Berkelman, R.L., and Curran, J.W. (1993). 1993 revised classification system for hiv infection and expanded surveillance case definition for aids among adolescents and adults. Clinical Infectious Diseases *17*, 802–810.

Cavrois, M., Banerjee, T., Mukherjee, G., Raman, N., Hussien, R., Rodriguez, B.A., Vasquez, J., Spitzer, M.H., Lazarus, N.H., Jones, J.J., et al. (2017). Mass Cytometric Analysis of HIV Entry, Replication, and Remodeling in Tissue CD4+ T Cells. Cell Reports *20*, 984–998.

Chahroudi, A., Bosinger, S.E., Vanderford, T.H., Paiardini, M., and Silvestri, G. (2012). Natural SIV hosts: Showing AIDS the door. Science *335*, 1188–1193.

Chan, D.C., Fass, D., Berger, J.M., and Kim, P.S. (1997). Core structure of gp41 from the HIV envelope glycoprotein. Cell *89*, 263–273.

Chang, V.T., Fernandes, R.A., Ganzinger, K.A., Lee, S.F., Siebold, C., McColl, J., Jönsson, P., Palayret, M., Harlos, K., Coles, C.H., et al. (2016). Initiation of T cell signaling by CD45 segregation at “close contacts.” Nature Immunology *17*, 574–582.

Chapman, N.M., and Chi, H. (2015). mTOR links environmental signals to T cell fate decisions. Frontiers in Immunology *6*.

Charneau, P., Alizon, M., and Clavel, F. (1992). A second origin of DNA plus-strand synthesis is required for optimal human immunodeficiency virus replication. Journal of Virology *66*, 2814–2820.

Chastagner, P., Moreau, J.L., Jacques, Y., Tanaka, T., Miyasaka, M., Kondo, M., Sugamura, K., and Thèze, J. (1996). Lack of intermediate-affinity interleukin-2 receptor in mice leads to dependence on interleukin-2 receptor alpha, beta and gamma chain expression for T cell growth. European Journal of Immunology *26*, 201–206.

Checkley, M.A., Luttge, B.G., and Freed, E.O. (2011). HIV-1 Envelope Glycoprotein Biosynthesis, Trafficking, and Incorporation. Journal of Molecular Biology *410*, 582–608.

Checkley, M.A., Luttge, B.G., Mercredi, P.Y., Kyere, S.K., Donlan, J., Murakami, T., Summers, M.F., Cocklin, S., and Freed, E.O. (2013). Reevaluation of the Requirement for TIP47 in Human Immunodeficiency Virus Type 1 Envelope Glycoprotein Incorporation. Journal of Virology *87*, 3561–3570.

Chen, L., and Flies, D.B. (2013). Molecular mechanisms of T cell co-stimulation and co-inhibition. Nature Reviews Immunology *13*, 227–242.

Chen, J., Nikolaitchik, O., Singh, J., Wright, A., Bencsics, C.E., Coffin, J.M., Ni, N., Lockett, S., Pathak, V.K., and Hu, W.S. (2009). High efficiency of HIV-1 genomic RNA packaging and heterozygote formation revealed by single virion analysis. Proceedings of the National Academy of Sciences of the United States of America *106*, 13535–13540.

Chen, N.Y., Zhou, L., Gane, P.J., Opp, S., Ball, N.J., Nicastro, G., Zufferey, M., Buffone, C., Luban, J., Selwood, D., et al. (2016). HIV-1 capsid is involved in post-nuclear entry steps. Retrovirology *13*.

Chen, P., Hubner, W., Spinelli, M.A., and Chen, B.K. (2007). Predominant Mode of Human Immunodeficiency Virus Transfer between T Cells Is Mediated by Sustained Env-Dependent Neutralization-Resistant Virological Synapses. Journal of Virology *81*, 12582–12595.

Cherepanov, P., Maertens, G., Proost, P., Devreese, B., van Beeumen, J., Engelborghs, Y., de Clercq, E., and Debyser, Z. (2003). HIV-1 integrase forms stable tetramers and associates with LEDGF/p75 protein in human cells. Journal of Biological Chemistry *278*, 372–381.

Chikuma, S., Terawaki, S., Hayashi, T., Nabeshima, R., Yoshida, T., Shibayama, S., Okazaki, T., and Honjo, T. (2009). PD-1-Mediated Suppression of IL-2 Production Induces CD8 + T Cell Anergy In Vivo . The Journal of Immunology *182*, 6682–6689.

Chini, E.N., Chini, C.C.S., Kato, I., Takasawa, S., and Okamoto, H. (2002). CD38 is the major enzyme responsible for synthesis of nicotinic acid - Adenine dinucleotide phosphate in mammalian tissues. Biochemical Journal *362*, 125–130.

Chiu, Y.-L., and Greene, W.C. (2008). The APOBEC3 Cytidine Deaminases: An Innate Defensive Network Opposing Exogenous Retroviruses and Endogenous Retroelements. Annual Review of Immunology *26*, 317–353.

Chojnacki, J., Staudt, T., Glass, B., Bingen, P., Engelhardt, J., Anders, M., Schneider, J., Müller, B., Hell, S.W., and Kräusslich, H.G. (2012). Maturation-dependent HIV-1 surface protein redistribution revealed by fluorescence nanoscopy. Science *338*, 524–528.

Chojnacki, J., Waithe, D., Carravilla, P., Huarte, N., Galiani, S., Enderlein, J., and Eggeling, C. (2017). Envelope glycoprotein mobility on HIV-1 particles depends on the virus maturation state. Nature Communications *8*.

Chougui, G., Munir-Matloob, S., Matkovic, R., Martin, M.M., Morel, M., Lahouassa, H., Leduc, M., Ramirez, B.C., Etienne, L., and Margottin-Goguet, F. (2018). HIV-2/SIV viral protein X counteracts HUSH repressor complex. Nature Microbiology *3*, 891–897.

Chowers, M.Y., Spina, C.A., Kwoh, T.J., Fitch, N.J., Richman, D.D., and Guatelli, J.C. (1994). Optimal infectivity in vitro of human immunodeficiency virus type 1 requires an intact nef gene. Journal of Virology *68*, 2906–2914.

Chu, E.P.F., Elso, C.M., Pollock, A.H., Alsayb, M.A., Mackin, L., Thomas, H.E., Kay, T.W.H., Silveira, P.A., Mansell, A.S., Gaus, K., et al. (2017). Disruption of Serinc1, which facilitates serine-derived lipid synthesis, fails to alter macrophage function, lymphocyte proliferation or autoimmune disease susceptibility. Molecular Immunology *82*, 19–33.

Chung, S., and Strominger, J.L. (1995). Regulation of T-cell antigen receptor (TCR) α-chain expression by TCR β- chain transcripts. Proceedings of the National Academy of Sciences of the United States of America *92*, 3712–3716.

Chung, A., Rollman, E., Johansson, S., Kent, S., and Stratov, I. (2008). The Utility of ADCC Responses in HIV Infection. Current HIV Research *6*, 515–519.

Cihlar, T., and Fordyce, M. (2016). Current status and prospects of HIV treatment. Current Opinion in Virology *18*, 50–56.

st. Clair, M.H., Richards, C.A., Spector, T., Weinhold, K.J., Miller, W.H., Langlois, A.J., and Furman, P.A. (1987). 3'-Azido-3'-deoxythymidine triphosphate as an inhibitor and substrate of purified human immunodeficiency virus reverse transcriptase. Antimicrobial Agents and Chemotherapy *31*, 1972–1977.

Clavel, F., Guétard, D., Brun-Vézinet, F., Chamaret, S., Rey, M.A., Santos-Ferreira, M.O., Laurent, A.G., Dauguet, C., Katlama, C., Rouzioux, C., et al. (1986). Isolation of a new human retrovirus from West African patients with AIDS. Science *233*, 343–346.

Cocchi, F., DeVico, A.L., Garzino-Demo, A., Cara, A., Gallo, R.C., and Lusso, P. (1996). The V3 domain of the HIV–1 gp120 envelope glycoprotein is critical for chemokine–mediated blockade of infection. Nature Medicine *2*, 1244–1247.

Cocka, L.J., and Bates, P. (2012). Identification of Alternatively Translated Tetherin Isoforms with Differing Antiviral and Signaling Activities. PLoS Pathogens *8*.

Cohen, G.B., Gandhi, R.T., Davis, D.M., Mandelboim, O., Chen, B.K., Strominger, J.L., and Baltimore, D. (1999). The selective downregulation of class I major histocompatibility complex proteins by HIV-1 protects HIV-infected cells from NK cells. Immunity *10*, 661–671.

Cohen, M.S., Shaw, G.M., McMichael, A.J., and Haynes, B.F. (2011). Acute HIV-1 Infection. New England Journal of Medicine *364*, 1943–1954.

Coiras, M., Bermejo, M., Descours, B., Mateos, E., García-Pérez, J., López-Huertas, M.R., Lederman, M.M., Benkirane, M., and Alcamí, J. (2016). IL-7 Induces SAMHD1 Phosphorylation in CD4+ T Lymphocytes, Improving Early Steps of HIV-1 Life Cycle. Cell Reports *14*, 2100–2107.

Collette, Y., Arold, S., Picard, C., Janvier, K., Benichou, S., Benarous, R., Olive, D., and Dumas, C. (2000). HIV-2 and SIV Nef proteins target different Src family SH3 domains than does HIV-1 Nef because of a triple amino acid substitution. Journal of Biological Chemistry *275*, 4171–4176.

Collier, A.C., Coombs, R.W., Schoenfeld, D.A., Bassett, R.L., Timpone, J., Baruch, A., Jones, M., Facey, K., Whitacre, C., McAuliffe, V.J., et al. (1996). Treatment of human immunodeficiency virus infection with saquinavir, zidovudine, and zalcitabine. New England Journal of Medicine *334*, 1011–1017.

Compton, A.A., Malik, H.S., and Emerman, M. (2013). Host gene evolution traces the evolutionary history of ancient primate lentiviruses. Philosophical Transactions of the Royal Society B: Biological Sciences *368*.

Connor, R.I., Sheridan, K.E., Ceradini, D., Choe, S., and Landau, N.R. (1997). Change in coreceptor use correlates with disease progression in HIV-1- infected individuals. Journal of Experimental Medicine *185*, 621–628.

Corneau, A., Cosma, A., Even, S., Katlama, C., le Grand, R., Frachet, V., Blanc, C., and Autran, B. (2017). Comprehensive Mass Cytometry Analysis of Cell Cycle, Activation, and Coinhibitory Receptors Expression in CD4 T Cells from Healthy and HIV-Infected Individuals. Cytometry Part B - Clinical Cytometry *92*, 21–32.

Costello, P.S., Gallagher, M., and Cantrell, D.A. (2002). Sustained and dynamic inositol lipid metabolism inside and outside the immonological synapse. Nature Immunology *3*, 1082–1089.

Coudronniere, N., Villalba, M., Englund, N., and Altman, A. (2000). NF- B activation induced by T cell receptor/CD28 costimulation is mediated by protein kinase C- . Proceedings of the National Academy of Sciences *97*, 3394–3399.

Courtney, A.H., Lo, W.L., and Weiss, A. (2018). TCR Signaling: Mechanisms of Initiation and Propagation. Trends in Biochemical Sciences *43*, 108–123.

Craig, H.M., Pandori, M.W., and Guatelli, J.C. (1998). Interaction of HIV-1 Nef with the cellular dileucine-based sorting pathway is required for CD4 down-regulation and optimal viral infectivity. Proceedings of the National Academy of Sciences of the United States of America *95*, 11229–11234.

Cribier, A., Descours, B., Valadão, A.L.C., Laguette, N., and Benkirane, M. (2013). Phosphorylation of SAMHD1 by Cyclin A2/CDK1 Regulates Its Restriction Activity toward HIV-1. Cell Reports *3*, 1036–1043.

Crowley, L.C., Marfell, B.J., Scott, A.P., and Waterhouse, N.J. (2016). Quantitation of apoptosis and necrosis by annexin V binding, propidium iodide uptake, and flow cytometry. Cold Spring Harbor Protocols *2016*, 953–957.

Curtsinger, J.M., and Mescher, M.F. (2010). Inflammatory cytokines as a third signal for T cell activation. Current Opinion in Immunology *22*, 333–340.

Dai, W., Usami, Y., Wu, Y., and Göttlinger, H. (2018). A Long Cytoplasmic Loop Governs the Sensitivity of the Anti-viral Host Protein SERINC5 to HIV-1 Nef. Cell Reports *22*, 869–875.

van Damme, N., Goff, D., Katsura, C., Jorgenson, R.L., Mitchell, R., Johnson, M.C., Stephens, E.B., and Guatelli, J. (2008). The Interferon-Induced Protein BST-2 Restricts HIV-1 Release and Is Downregulated from the Cell Surface by the Viral Vpu Protein. Cell Host and Microbe *3*, 245–252.

Dang, Y., Wang, X., Esselman, W.J., and Zheng, Y.-H. (2006). Identification of APOBEC3DE as Another Antiretroviral Factor from the Human APOBEC Family. Journal of Virology *80*, 10522–10533.

Das, J., Ho, M., Zikherman, J., Govern, C., Yang, M., Weiss, A., Chakraborty, A.K., and Roose, J.P. (2009). Digital Signaling and Hysteresis Characterize Ras Activation in Lymphoid Cells. Cell *136*, 337–351.

Davis, S.J., and van der Merwe, P.A. (2006). The kinetic-segregation model: TCR triggering and beyond. Nature Immunology *7*, 803–809.

Day, J.R., Munk, C., and Guatelli, J.C. (2004). The Membrane-Proximal Tyrosine-Based Sorting Signal of Human Immunodeficiency Virus Type 1 gp41 Is Required for Optimal Viral Infectivity. Journal of Virology *78*, 1069–1079.

Deacon, N.J., Tsykin, A., Solomon, A., Smith, K., Ludford-Menting, M., Hooker, D.J., McPhee, D.A., Greenway, A.L., Ellett, A., Chatfield, C., et al. (1995). Genomic structure of an attenuated quasi species of HIV-1 from a blood transfusion donor and recipients. Science (New York, N.Y.) *270*, 988–991.

Demirov, D.G., and Freed, E.O. (2004). Retrovirus budding. Virus Research *106*, 87–102.

Deneka, M., Pelchen-Matthews, A., Byland, R., Ruiz-Mateos, E., and Marsh, M. (2007). In macrophages, HIV-1 assembles into an intracellular plasma membrane domain containing the tetraspanins CD81, CD9, and CD53. Journal of Cell Biology *177*, 329–341.

Deng, J., Mitsuki, Y.-Y., Shen, G., Ray, J.C., Cicala, C., Arthos, J., Dustin, M.L., Hioe, C.E., and Peters Veterans, J.J. (2016). HIV Envelope gp120 Alters T Cell Receptor Mobilization in the Immunological Synapse of Uninfected CD4 T Cells and Augments T Cell Activation.

Desai, T.M., Marin, M., Chin, C.R., Savidis, G., Brass, A.L., and Melikyan, G.B. (2014). IFITM3 Restricts Influenza A Virus Entry by Blocking the Formation of Fusion Pores following Virus-Endosome Hemifusion. PLoS Pathogens *10*.

Dicks, M.D.J., Betancor, G., Jimenez-Guardeño, J.M., Pessel-Vivares, L., Apolonia, L., Goujon, C., and Malim, M.H. (2018). Multiple components of the nuclear pore complex interact with the amino-terminus of MX2 to facilitate HIV-1 restriction. PLoS Pathogens *14*.

Dimitrov, D.S., Willey, R.L., Sato, H., Chang, L.J., Blumenthal, R., and Martin, M.A. (1993). Quantitation of human immunodeficiency virus type 1 infection kinetics. Journal of Virology *67*, 2182–2190.

Do, T., Murphy, G., Earl, L.A., del Prete, G.Q., Grandinetti, G., Li, G.-H., Estes, J.D., Rao, P., Trubey, C.M., Thomas, J., et al. (2014). Three-Dimensional Imaging of HIV-1 Virological Synapses Reveals Membrane Architectures Involved in Virus Transmission. Journal of Virology *88*, 10327–10339.

Doitsh, G., and Greene, W.C. (2016). Dissecting How CD4 T Cells Are Lost during HIV Infection. Cell Host and Microbe *19*, 280–291.

Doitsh, G., Galloway, N.L.K., Geng, X., Yang, Z., Monroe, K.M., Zepeda, O., Hunt, P.W., Hatano, H., Sowinski, S., Muñoz-Arias, I., et al. (2014). Cell death by pyroptosis drives CD4 T-cell depletion in HIV-1 infection. Nature *505*, 509–514.

Douek, D.C., Brenchley, J.M., Betts, M.R., Ambrozak, D.R., Hill, B.J., Okamoto, Y., Casazza, J.P., Kuruppu, J., Kunstman, K., Wolinsky, S., et al. (2002). HIV preferentially infects HIV-specific CD4+ T cells. Nature *417*, 95–98.

Dubay, J.W., Dubay, S.R., Shin, H.J., and Hunter, E. (1995). Analysis of the cleavage site of the human immunodeficiency virus type 1 glycoprotein: requirement of precursor cleavage for glycoprotein incorporation. Journal of Virology *69*, 4675–4682.

Dubé, M., Roy, B.B., Guiot-Guillain, P., Mercier, J., Binette, J., Leung, G., and Cohen, É.A. (2009). Suppression of Tetherin-Restricting Activity upon Human Immunodeficiency Virus Type 1 Particle Release Correlates with Localization of Vpu in the trans-Golgi Network. Journal of Virology *83*, 4574–4590.

Duncan, C.J.A., Russell, R.A., and Sattentau, Q.J. (2013). High multiplicity HIV-1 cell-to-cell transmission from macrophages to CD4+ T cells limits antiretroviral efficacy. AIDS *27*, 2201–2206.

Duncan, C.J.A., Williams, J.P., Schiffner, T., Gartner, K., Ochsenbauer, C., Kappes, J., Russell, R.A., Frater, J., and Sattentau, Q.J. (2014). High-Multiplicity HIV-1 Infection and Neutralizing

Antibody Evasion Mediated by the Macrophage-T Cell Virological Synapse. Journal of Virology *88*, 2025–2034.

Dunham, R., Pagliardini, P., Gordon, S., Sumpter, B., Engram, J., Moanna, A., Paiardini, M., Mandl, J.N., Lawson, B., Garg, S., et al. (2006). The AIDS resistance of naturally SIV-infected sooty mangabeys is independent of cellular immunity to the virus. Blood *108*, 209–217.

Dustin, M.L., and Depoil, D. (2011). New insights into the T cell synapse from single molecule techniques. Nature Reviews Immunology *11*, 672–684.

Dustin, M.L., Bromley, S.K., Kan, Z., Peterson, D.A., and Unanue, E.R. (1997). Antigen receptor engagement delivers a stop signal to migrating T lymphocytes. Proceedings of the National Academy of Sciences of the United States of America *94*, 3909–3913.

Duvall, M.G., Loré, K., Blaak, H., Ambrozak, D.A., Adams, W.C., Santos, K., Geldmacher, C., Mascola, J.R., McMichael, A.J., Jaye, A., et al. (2007). Dendritic Cells Are Less Susceptible to Human Immunodeficiency Virus Type 2 (HIV-2) Infection than to HIV-1 Infection. Journal of Virology *81*, 13486–13498.

Duvall, M.G., Precopio, M.L., Ambrozak, D.A., Jaye, A., McMichael, A.J., Whittle, H.C., Roederer, M., Rowland-Jones, S.L., and Koup, R.A. (2008). Polyfunctional T cell responses are a hallmark of HIV-2 infection. European Journal of Immunology *38*, 350–363.

Earl, P.L., Doms, R.W., and Moss, B. (1990). Oligomeric structure of the human immunodeficiency virus type 1 envelope glycoprotein. Proceedings of the National Academy of Sciences of the United States of America *87*, 648–652.

Egan, M.A., Carruth, L.M., Rowell, J.F., Yu, X., and Siliciano, R.F. (1996). Human immunodeficiency virus type 1 envelope protein endocytosis mediated by a highly conserved intrinsic internalization signal in the cytoplasmic domain of gp41 is suppressed in the presence of the Pr55gag precursor protein. Journal of Virology *70*, 6547–6556.

Emery, A., Zhou, S., Pollom, E., and Swanstrom, R. (2017). Characterizing HIV-1 Splicing by Using Next-Generation Sequencing. Journal of Virology *91*.

van Engelenburg, S.B., Shtengel, G., Sengupta, P., Waki, K., Jarnik, M., Ablan, S.D., Freed, E.O., Hess, H.F., and Lippincott-Schwartz, J. (2014). Distribution of ESCRT machinery at HIV assembly sites reveals virus scaffolding of ESCRT subunits. Science *343*, 653–656.

Espeseth, A.S., Felock, P., Wolfe, A., Witmer, M., Grobler, J., Anthony, N., Egbertson, M., Melamed, J.Y., Young, S., Hamill, T., et al. (2000). HIV-1 integrase inhibitors that compete with the target DNA substrate define a unique strand transfer conformation for integrase. Proceedings of the National Academy of Sciences of the United States of America *97*, 11244–11249.

Estes, J.D., Gordon, S.N., Zeng, M., Chahroudi, A.M., Dunham, R.M., Staprans, S.I., Reilly, C.S., Silvestri, G., and Haase, A.T. (2008). Early Resolution of Acute Immune Activation and Induction of PD-1 in SIV-Infected Sooty Mangabeys Distinguishes Nonpathogenic from Pathogenic Infection in Rhesus Macaques. The Journal of Immunology *180*, 6798–6807.

Etienne, L., Hahn, B.H., Sharp, P.M., Matsen, F.A., and Emerman, M. (2013). Gene loss and adaptation to hominids underlie the ancient origin of HIV-1. Cell Host and Microbe *14*, 85–92.

Eugenin, E.A., Gaskill, P.J., and Berman, J.W. (2009). Tunneling nanotubes (TNT) are induced by HIV-infection of macrophages: A potential mechanism for intercellular HIV trafficking. Cellular Immunology *254*, 142–148.

Evans, R., Lellouch, A.C., Svensson, L., McDowall, A., and Hogg, N. (2011). The integrin LFA-1 signals through ZAP-70 to regulate expression of high-affinity LFA-1 on T lymphocytes. Blood *117*, 3331–3342.

Fackler, O.T., Moris, A., Tibroni, N., Giese, S.I., Glass, B., Schwartz, O., and Kräusslich, H.G. (2006). Functional characterization of HIV-1 Nef mutants in the context of viral infection. Virology *351*, 322–339.

Falkowska, E., Le, K.M., Ramos, A., Doores, K.J., Lee, J.H., Blattner, C., Ramirez, A., Derking, R., vanGils, M.J., Liang, C.H., et al. (2014). Broadly neutralizing HIV antibodies define a glycan-dependent epitope on the prefusion conformation of gp41 on cleaved envelope trimers. Immunity *40*, 657–668.

Faria, N.R., Rambaut, A., Suchard, M.A., Baele, G., Bedford, T., Ward, M.J., Tatem, A.J., Sousa, J.D., Arinaminpathy, N., Pépin, J., et al. (2014). The early spread and epidemic ignition of HIV-1 in human populations. Science *346*, 56–61.

Feldmann, J., Leligdowicz, A., Jaye, A., Dong, T., Whittle, H., and Rowland-Jones, S.L. (2009). Downregulation of the T-Cell Receptor by Human Immunodeficiency Virus Type 2 Nef Does Not Protect against Disease Progression. Journal of Virology *83*, 12968–12972.

Felts, R.L., Narayan, K., Estes, J.D., Shi, D., Trubey, C.M., Fu, J., Hartnell, L.M., Ruthel, G.T., Schneider, D.K., Nagashima, K., et al. (2010). 3D visualization of HIV transfer at the virological synapse between dendritic cells and T cells. Proceedings of the National Academy of Sciences of the United States of America *107*, 13336–13341.

Fenard, D., Yonemoto, W., de Noronha, C., Cavrois, M., Williams, S.A., and Greene, W.C. (2005). Nef is physically recruited into the immunological synapse and potentiates T cell activation early after TCR engagement. Journal of Immunology (Baltimore, Md. : 1950) *175*, 6050–6057.

Feng, Y., Broder, C.C., Kennedy, P.E., and Berger, E.A. (1996). HIV-1 entry cofactor: Functional cDNA cloning of a seven-transmembrane, G protein-coupled receptor. Science *272*, 872–877.

Fiebig, E.W., Wright, D.J., Rawal, B.D., Garrett, P.E., Schumacher, R.T., Peddada, L., Heldebrant, C., Smith, R., Conrad, A., Kleinman, S.H., et al. (2003). Dynamics of HIV viremia and antibody seroconversion in plasma donors: Implications for diagnosis and staging of primary HIV infection. AIDS *17*, 1871–1879.

Finlay, D.K., Rosenzweig, E., Sinclair, L. v., Carmen, F.C., Hukelmann, J.L., Rolf, J., Panteleyev, A.A., Okkenhaug, K., and Cantrell, D.A. (2012). PDK1 regulation of mTOR and hypoxia-inducible factor 1 integrate metabolism and migration of CD8+ T cells. Journal of Experimental Medicine *209*, 2441–2453.

Fletcher, A.J., Christensen, D.E., Nelson, C., Tan, C.P., Schaller, T., Lehner, P.J., Sundquist, W.I., and Towers, G.J. (2015). TRIM 5α requires Ube2W to anchor Lys63-linked ubiquitin chains and restrict reverse transcription . The EMBO Journal *34*, 2078–2095.

Fletcher, C. v., Staskus, K., Wietgrefe, S.W., Rothenberger, M., Reilly, C., Chipman, J.G., Beilman, G.J., Khoruts, A., Thorkelson, A., Schmidt, T.E., et al. (2014). Persistent HIV-1 replication is associated with lower antiretroviral drug concentrations in lymphatic tissues. Proceedings of the National Academy of Sciences of the United States of America *111*, 2307–2312.

Ford, N., Irvine, C., Shubber, Z., Baggaley, R., Beanland, R., Vitoria, M., Doherty, M., Mills, E.J., and Calmy, A. (2014). Adherence to HIV postexposure prophylaxis: A systematic review and meta-analysis. AIDS *28*, 2721–2727.

Fortin, J.-F., Barat, C., Beauséjour, Y., Barbeau, B., and Tremblay, M.J. (2004). Hyper-responsiveness to Stimulation of Human Immunodeficiency Virus-infected CD4 $^{+}$ T Cells Requires Nef and Tat Virus Gene Products and Results from Higher NFAT, NF-κB, and AP-1 Induction. Journal of Biological Chemistry *279*, 39520–39531.

Foster, T.L., Wilson, H., Iyer, S.S., Coss, K., Doores, K., Smith, S., Kellam, P., Finzi, A., Borrow, P., Hahn, B.H., et al. (2016). Resistance of Transmitted Founder HIV-1 to IFITM-Mediated Restriction. Cell Host and Microbe *20*, 429–442.

Francis, A.C., and Melikyan, G.B. (2018). Single HIV-1 Imaging Reveals Progression of Infection through CA-Dependent Steps of Docking at the Nuclear Pore, Uncoating, and Nuclear Transport. Cell Host and Microbe *23*, 536-548.e6.

Frank, G.A., Narayan, K., Bess, J.W., del Prete, G.Q., Wu, X., Moran, A., Hartnell, L.M., Earl, L.A., Lifson, J.D., and Subramaniam, S. (2015). Maturation of the HIV-1 core by a non-diffusional phase transition. Nature Communications *6*.

Freed, E.O. (2015). HIV-1 assembly, release and maturation. Nature Reviews Microbiology *13*, 484–496.

Freed, E.O., and Martin, M.A. (1995). Virion incorporation of envelope glycoproteins with long but not short cytoplasmic tails is blocked by specific, single amino acid substitutions in the human immunodeficiency virus type 1 matrix. Journal of Virology *69*, 1984–1989.

Fribourgh, J.L., Nguyen, H.C., Matreyek, K.A., Alvarez, F.J.D., Summers, B.J., Dewdney, T.G., Aiken, C., Zhang, P., Engelman, A., and Xiong, Y. (2014). Structural insight into HIV-1 restriction by MxB. Cell Host and Microbe *16*, 627–638.

Friedman-Kien, AlvinE., Laubenstein, L., Marmor, M., Hymes, K.B., Green, J., Ragaz, A.F., Gottleib, J., Muggia, F., Demopoulos, R.I., and Weintraub, M. (1981). Kaposi's sarcoma and Pneumocystis pneumonia among homosexual men--New York City and California.

Fujii, K., Munshi, U.M., Ablan, S.D., Demirov, D.G., Soheilian, F., Nagashima, K., Stephen, A.G., Fisher, R.J., and Freed, E.O. (2009). Functional role of Alix in HIV-1 replication. Virology *391*, 284–292.

Fujita, H., Iwabu, Y., Tokunaga, K., and Tanaka, Y. (2013). Membrane-associated RING-CH (MARCH) 8 mediates the ubiquitination and lysosomal degradation of the transferrin receptor. Journal of Cell Science *126*, 2798–2809.

Fujiwara, T., and Mizuuchi, K. (1988). Retroviral DNA integration: Structure of an integration intermediate. Cell *54*, 497–504.

Furman, P.A., Fyfe, J.A., St Clair, M.H., Weinhold, K., Rideout, J.L., Freeman, G.A., Lehrman, S.N., Bolognesi, D.P., Broder, S., and Mitsuya, H. (1986). Phosphorylation of 3'-azido-3'-deoxythymidine and selective interaction of the 5'-triphosphate with human immunodeficiency virus reverse transcriptase. Proceedings of the National Academy of Sciences of the United States of America *83*, 8333–8337.

Gabuzda, D.H., Lawrence, K., Langhoff, E., Terwilliger, E., Dorfman, T., Haseltine, W.A., and Sodroski, J. (1992). Role of vif in replication of human immunodeficiency virus type 1 in CD4+ T lymphocytes. Journal of Virology *66*, 6489–6495.

Gagne, M., Michaels, D., Schiralli Lester, G.M., Gummuluru, S., Wong, W.W., and Henderson, A.J. (2019). Strength of T cell signaling regulates HIV-1 replication and establishment of latency. PLoS Pathogens *15*, e1007802.

Galão, R.P., le Tortorec, A., Pickering, S., Kueck, T., and Neil, S.J.D. (2012). Innate sensing of HIV-1 assembly by tetherin induces NFκB-dependent proinflammatory responses. Cell Host and Microbe *12*, 633–644.

Galão, R.P., Pickering, S., Curnock, R., and Neil, S.J.D. (2014). Retroviral retention activates a Syk-dependent HemITAM in Human tetherin. Cell Host and Microbe *16*, 291–303.

le Gall, S., Erdtmann, L., Benichou, S., Berlioz-Torrent, C., Liu, L., Benarous, R., Heard, J.M., and Schwartz, O. (1998). Nef interacts with the μ subunit of clathrin adaptor complexes and reveals a cryptic sorting signal in MHC I molecules. Immunity *8*, 483–495.

Galloway, N.L.K., Doitsh, G., Monroe, K.M., Yang, Z., Muñoz-Arias, I., Levy, D.N., and Greene, W.C. (2015). Cell-to-Cell Transmission of HIV-1 Is Required to Trigger Pyroptotic Death of Lymphoid-Tissue-Derived CD4 T Cells. Cell Reports *12*, 1555–1563.

Gao, F., Yue, L., Robertson, D.L., Hill, S.C., Hui, H., Biggar, R.J., Neequaye, A.E., Whelan, T.M., Ho, D.D., and Shaw, G.M. (1994). Genetic diversity of human immunodeficiency virus type 2: evidence for distinct sequence subtypes with differences in virus biology. Journal of Virology *68*, 7433–7447.

Gao, F., Balles, E., Robertson, D.L., Chen, Y., Rodenburg, C.M., Michael, S.F., Cummins, L.B., Arthur, L.O., Peeters, M., Shaw, G.M., et al. (1999). Origin of HIV-1 in the chimpanzee Pan troglodytes troglodytes. Nature *397*, 436–441.

Gao, G.F., Tormo, J., Gerth, U.C., Wyer, J.R., McMichael, A.J., Stuart, D.I., Bell, J.I., Jones, E.Y., and Jakobsen, B.K. (1997). Crystal structure of the complex between CD8αα human and HLA-A2. Nature *387*, 630–634.

Gao, Y., McKay, P.F., and Mann, J.F.S. (2018). Advances in HIV-1 vaccine development. Viruses *10*.

Garcia, J.V., and Miller, A.D. (1991). Serine phosphorylation-independent downregulation of cell-surface CD4 by nef. Nature *350*, 508–511.

Garrus, J.E., von Schwedler, U.K., Pornillos, O.W., Morham, S.G., Zavitz, K.H., Wang, H.E., Wettstein, D.A., Stray, K.M., Côté, M., Rich, R.L., et al. (2001). Tsg101 and the vacuolar protein sorting pathway are essential for HIV-1 budding. Cell *107*, 55–65.

Gaud, G., Lesourne, R., and Love, P.E. (2018). Regulatory mechanisms in T cell receptor signalling. Nature Reviews Immunology *18*, 485–497.

Geijtenbeek, T.B.H., Kwon, D.S., Torensma, R., van Vliet, S.J., van Duijnhoven, G.C.F., Middel, J., Cornelissen, I.L.M.H.A., Nottet, H.S.L.M., KewalRamani, V.N., Littman, D.R., et al. (2000). DC-SIGN, a dendritic cell-specific HIV-1-binding protein that enhances trans-infection of T cells. Cell *100*, 587–597.

Geis, F.K., and Goff, S.P. (2019). Unintegrated HIV-1 DNAs are loaded with core and linker histones and transcriptionally silenced. Proceedings of the National Academy of Sciences of the United States of America *116*, 23735–23742.

Gérard, A., Khan, O., Beemiller, P., Oswald, E., Hu, J., Matloubian, M., and Krummel, M.F. (2013). Secondary T cell-T cell synaptic interactions drive the differentiation of protective CD8+ T cells. Nature Immunology *14*, 356–363.

Geretti, A.M. (2006). HIV-1 subtypes: Epidemiology and significance for HIV management. Current Opinion in Infectious Diseases *19*, 1–7.

Geyer, M., Munte, C.E., Schorr, J., Kellner, R., and Kalbitzer, H.R. (1999). Structure of the anchor-domain of myristoylated and non-myristoylated HIV-1 Nef protein. Journal of Molecular Biology *289*, 123–138.

Gheysen, D., Jacobs, E., de Foresta, F., Thiriart, C., Francotte, M., Thines, D., and de Wilde, M. (1989). Assembly and release of HIV-1 precursor Pr55gag virus-like particles from recombinant baculovirus-infected insect cells. Cell *59*, 103–112.

Gioia, L., Siddique, A., Head, S.R., Salomon, D.R., and Su, A.I. (2018). A genome-wide survey of mutations in the Jurkat cell line. BMC Genomics *19*, 334.

Giorgi, J.V., Hultin, L.E., McKeating, J.A., Johnson, T.D., Owens, B., Jacobson, L.P., Shih, R., Lewis, J., Wiley, D.J., Phair, J.P., et al. (1999). Shorter Survival in Advanced Human Immunodeficiency Virus Type 1 Infection Is More Closely Associated with T Lymphocyte Activation than with Plasma Virus Burden or Virus Chemokine Coreceptor Usage. The Journal of Infectious Diseases *179*, 859–870.

Goila-Gaur, R., Khan, M.A., Miyagi, E., Kao, S., Opi, S., Takeuchi, H., and Strebel, K. (2008). HIV-1 Vif promotes the formation of high molecular mass APOBEC3G complexes. Virology *372*, 136–146.

Goldstein, S., Ourmanov, I., Brown, C.R., Plishka, R., Buckler-White, A., Byrum, R., and Hirsch, V.M. (2005). Plateau Levels of Viremia Correlate with the Degree of CD4+-T-Cell Loss in Simian Immunodeficiency Virus SIVagm-Infected Pigtailed Macaques: Variable Pathogenicity of Natural SIVagm Isolates. Journal of Virology *79*, 5153–5162.

Goldstone, D.C., Ennis-Adeniran, V., Hedden, J.J., Groom, H.C.T., Rice, G.I., Christodoulou, E., Walker, P.A., Kelly, G., Haire, L.F., Yap, M.W., et al. (2011). HIV-1 restriction factor SAMHD1 is a deoxynucleoside triphosphate triphosphohydrolase. Nature *480*, 379–382.

Gonen, R., Beach, D., Ainey, C., and Yablonski, D. (2005). T cell receptor-induced activation of phospholipase C-γ1 depends on a sequence-independent function of the P-I region of SLP-76. Journal of Biological Chemistry *280*, 8364–8370.

Goonetilleke, N., Liu, M.K.P., Salazar-Gonzalez, J.F., Ferrari, G., Giorgi, E., Ganusov, V. v., Keele, B.F., Learn, G.H., Turnbull, E.L., Salazar, M.G., et al. (2009). The first T cell response to transmitted/founder virus contributes to the control of acute viremia in HIV-1 infection. Journal of Experimental Medicine *206*, 1253–1272.

Gordon, S.N., Klatt, N.R., Bosinger, S.E., Brenchley, J.M., Milush, J.M., Engram, J.C., Dunham, R.M., Paiardini, M., Klucking, S., Danesh, A., et al. (2007). Severe Depletion of Mucosal CD4 + T Cells in AIDS-Free Simian Immunodeficiency Virus-Infected Sooty Mangabeys . The Journal of Immunology *179*, 3026–3034.

Gottlieb, G.S., Hawes, S.E., Agne, H.D., Stern, J.E., Critchlow, C.W., Kiviat, N.B., and Sow, P.S. (2006). Lower levels of HIV RNA in semen in HIV-2 compared with HIV-1 infection: Implications for differences in transmission. AIDS *20*, 895–900.

Gottlinger, H.G., Dorfman, T., Sodroski, J.G., and Haseltine, W.A. (1991). Effect of mutations affecting the p6 gag protein on human immunodeficiency virus particle release. Proceedings of the National Academy of Sciences of the United States of America *88*, 3195–3199.

Goujon, C., Moncorgé, O., Bauby, H., Doyle, T., Ward, C.C., Schaller, T., Hué, S., Barclay, W.S., Schulz, R., and Malim, M.H. (2013). Human MX2 is an interferon-induced post-entry inhibitor of HIV-1 infection. Nature *502*, 559–562.

Gousset, K., Ablan, S.D., Coren, L. v., Ono, A., Soheilian, F., Nagashima, K., Ott, D.E., and Freed, E.O. (2008). Real-time visualization of HIV-1 GAG trafficking in infected macrophages. PLoS Pathogens *4*.

Gratton, S., Cheynier, R., Dumaurier, M.J., Oksenhendler, E., and Wain-Hobson, S. (2000). Highly restricted spread of HIV-1 and multiply infected cells within splenic germinal centers. Proceedings of the National Academy of Sciences of the United States of America *97*, 14566–14571.

Greenwald, R.J., Freeman, G.J., and Sharpe, A.H. (2005). THE B7 FAMILY REVISITED. Annual Review of Immunology *23*, 515–548.

Greenway, A., Azad, A., Mills, J., and McPhee, D. (1996). Human immunodeficiency virus type 1 Nef binds directly to Lck and mitogen-activated protein kinase, inhibiting kinase activity. Journal of Virology *70*, 6701–6708.

Greenwood, E.J.D., Matheson, N.J., Wals, K., van den Boomen, D.J.H., Antrobus, R., Williamson, J.C., and Lehner, P.J. (2016). Temporal proteomic analysis of HIV infection reveals remodelling of the host phosphoproteome by lentiviral Vif variants. ELife *5*.

Greenwood, E.J.D., Williamson, J.C., Sienkiewicz, A., Naamati, A., Matheson, N.J., and Lehner, P.J. (2019). Promiscuous Targeting of Cellular Proteins by Vpr Drives Systems-Level Proteomic Remodeling in HIV-1 Infection. Cell Reports *27*, 1579-1596.e7.

Groot, F., Welsch, S., and Sattentau, Q.J. (2008). Efficient HIV-1 transmission from macrophages to T cells across transient virological synapses. Blood *111*, 4660–4663.

Groppelli, E., Len, A.C., Granger, L.A., and Jolly, C. (2014). Retromer Regulates HIV-1 Envelope Glycoprotein Trafficking and Incorporation into Virions. PLoS Pathogens *10*, e1004518.

Groppelli, E., Starling, S., and Jolly, C. (2015). Contact-Induced Mitochondrial Polarization Supports HIV-1 Virological Synapse Formation. Journal of Virology *89*, 14–24.

Gummuluru, S., Kinsey, C.M., and Emerman, M. (2000). An In Vitro Rapid-Turnover Assay for Human Immunodeficiency Virus Type 1 Replication Selects for Cell-to-Cell Spread of Virus. Journal of Virology *74*, 10882–10891.

Gupta, P., Balachandran, R., Ho, M., Enrico, A., and Rinaldo, C. (1989). Cell-to-cell transmission of human immunodeficiency virus type 1 in the presence of azidothymidine and neutralizing antibody. Journal of Virology *63*, 2361–2365.

Guzzo, C., Jung, M., Graveline, A., Banfield, B.W., and Gee, K. (2012). IL-27 increases BST-2 expression in human monocytes and T cells independently of type i IFN. Scientific Reports *2*, 1–8.

Hallenberger, S., Bosch, V., Angliker, H., Shaw, E., Klenk, H.D., and Garten, W. (1992). Inhibition of furin-mediated cleavage activation of HIV-1 glycoprotein gpl60. Nature *360*, 358–361.

Haller, C., Rauch, S., and Fackler, O.T. (2007). HIV-1 Nef employs two distinct mechanisms to modulate Lck subcellular localization and TCR induced actin remodeling. PLoS ONE *2*.

Halwani, R., Khorchid, A., Cen, S., and Kleiman, L. (2003). Rapid Localization of Gag/GagPol Complexes to Detergent-Resistant Membrane during the Assembly of Human Immunodeficiency Virus Type 1. Journal of Virology *77*, 3973–3984.

Hammonds, J., Wang, J.J., Yi, H., and Spearman, P. (2010). Immunoelectron microscopic evidence for tetherin/BST2 as the physical bridge between HIV-1 virions and the plasma membrane. PLoS Pathogens *6*.

Hanson, A., Sarr, A.D., Shea, A., Jones, N., Mboup, S., Kanki, P., and Cao, H. (2005). Distinct profile of T cell activation in HIV type 2 compared to HIV type 1 infection: Differential mechanism for immunoprotection. AIDS Research and Human Retroviruses *21*, 791–798.

Hanson, P.I., Shim, S., and Merrill, S.A. (2009). Cell biology of the ESCRT machinery. Current Opinion in Cell Biology *21*, 568–574.

Hare, S., Gupta, S.S., Valkov, E., Engelman, A., and Cherepanov, P. (2010). Retroviral intasome assembly and inhibition of DNA strand transfer. Nature *464*, 232–236.

Harris, R.S., Bishop, K.N., Sheehy, A.M., Craig, H.M., Petersen-Mahrt, S.K., Watt, I.N., Neuberger, M.S., and Malim, M.H. (2003). DNA deamination mediates innate immunity to retroviral infection. Cell *113*, 803–809.

Hatziioannou, T., Perez-Caballero, D., Cowan, S., and Bieniasz, P.D. (2005). Cyclophilin Interactions with Incoming Human Immunodeficiency Virus Type 1 Capsids with Opposing Effects on Infectivity in Human Cells. Journal of Virology *79*, 176–183.

Heigele, A., Kmiec, D., Regensburger, K., Langer, S., Peiffer, L., Stürzel, C.M., Sauter, D., Peeters, M., Pizzato, M., Learn, G.H., et al. (2016). The Potency of Nef-Mediated SERINC5 Antagonism Correlates with the Prevalence of Primate Lentiviruses in the Wild. Cell Host & Microbe *20*, 381–391.

Herbein, G., Varin, A., Larbi, A., Fortin, C., Mahlknecht, U., Fulop, T., and Aggarwal, B. (2008). Nef and TNFα are Coplayers that Favor HIV-1 Replication in Monocytic Cells and Primary Macrophages. Current HIV Research *6*, 117–129.

Herold, N., Anders-Össwein, M., Glass, B., Eckhardt, M., Müller, B., and Kräusslich, H.-G. (2014). HIV-1 entry in SupT1-R5, CEM-ss, and primary CD4+ T cells occurs at the plasma membrane and does not require endocytosis. Journal of Virology *88*, 13956–13970.

Heusinger, E., and Kirchhoff, F. (2017). Primate lentiviruses modulate NF-HIV, SIV, NF-κB, Nef, Vpu, Tat, LTRB activity by multiple mechanisms to fine-tune viral and cellular gene expression. Frontiers in Microbiology *8*.

Heusinger, E., Deppe, K., Sette, P., Krapp, C., Kmiec, D., Kluge, S.F., Marx, P.A., Apetrei, C., Kirchhoff, F., and Sauter, D. (2018). Preadaptation of Simian Immunodeficiency Virus SIVsmm Facilitated Env-Mediated Counteraction of Human Tetherin by Human Immunodeficiency Virus Type 2. Journal of Virology *92*.

Hirsch, V.M., Olmsted, R.A., Murphey-Corb, M., Purcell, R.H., and Johnson, P.R. (1989). An African primate lentivirus (SIVsmclosely related to HIV-2. Nature *339*, 389–392.

Hogg, N., Patzak, I., and Willenbrock, F. (2011). The insider's guide to leukocyte integrin signalling and function. Nature Reviews Immunology *11*, 416–426.

Hogue, I.B., Grover, J.R., Soheilian, F., Nagashima, K., and Ono, A. (2011). Gag induces the coalescence of clustered lipid rafts and tetraspanin-enriched microdomains at HIV-1 assembly sites on the plasma membrane. Journal of Virology *85*, 9749–9766.

Homann, S., Tibroni, N., Baumann, I., Sertel, S., Keppler, O.T., and Fackler, O.T. (2009). Determinants in HIV-1 Nef for enhancement of virus replication and depletion of CD4+ T lymphocytes in human lymphoid tissue ex vivo. Retrovirology *6*, 6.

Horejsi, V., Zhang, W., and Schraven, B. (2004). Transmembrane adaptor proteins: Organizers of immunoreceptor signalling. Nature Reviews Immunology *4*, 603–616.

Hotter, D., Krabbe, T., Reith, E., Gawanbacht, A., Rahm, N., Ayouba, A., van Driessche, B., van Lint, C., Peeters, M., Kirchhoff, F., et al. (2017). Primate lentiviruses use at least three alternative strategies to suppress NF-κB-mediated immune activation. PLoS Pathogens *13*, e1006598.

Howe, A.Y., Jung, J.U., and Desrosiers, R.C. (1998). Zeta chain of the T-cell receptor interacts with nef of simian immunodeficiency virus and human immunodeficiency virus type 2. Journal of Virology *72*, 9827–9834.

Hrecka, K., Swigut, T., Schindler, M., Kirchhoff, F., and Skowronski, J. (2005). Nef Proteins from Diverse Groups of Primate Lentiviruses Downmodulate CXCR4 To Inhibit Migration to the Chemokine Stromal Derived Factor 1. Journal of Virology *79*, 10650–10659.

Hrecka, K., Hao, C., Gierszewska, M., Swanson, S.K., Kesik-Brodacka, M., Srivastava, S., Florens, L., Washburn, M.P., and Skowronski, J. (2011). Vpx relieves inhibition of HIV-1 infection of macrophages mediated by the SAMHD1 protein. Nature *474*, 658–661.

Hu, W.S., and Hughes, S.H. (2012). HIV-1 reverse transcription. Cold Spring Harbor Perspectives in Medicine *2*.

Hua, J., and Cullen, B.R. (1997). Human immunodeficiency virus types 1 and 2 and simian immunodeficiency virus Nef use distinct but overlapping target sites for downregulation of cell surface CD4. Journal of Virology *71*, 6742.

Huang, J., Brameshuber, M., Zeng, X., Xie, J., Li, Q. jing, Chien, Y. hsiu, Valitutti, S., and Davis, M.M. (2013). A Single peptide-major histocompatibility complex ligand triggers digital cytokine secretion in CD4+ T Cells. Immunity *39*, 846–857.

Huang, M., Orenstein, J.M., Martin, M.A., and Freed, E.O. (1995). p6Gag is required for particle production from full-length human immunodeficiency virus type 1 molecular clones expressing protease. Journal of Virology *69*, 6810–6818.

Hubner, W., McNerney, G.P., Chen, P., Dale, B.M., Gordon, R.E., Chuang, F.Y.S., Li, X.-D., Asmuth, D.M., Huser, T., and Chen, B.K. (2009). Quantitative 3D Video Microscopy of HIV Transfer Across T Cell Virological Synapses. Science *323*, 1743–1747.

Hukelmann, J.L., Anderson, K.E., Sinclair, L. v., Grzes, K.M., Murillo, A.B., Hawkins, P.T., Stephens, L.R., Lamond, A.I., and Cantrell, D.A. (2016). The cytotoxic T cell proteome and its shaping by the kinase mTOR. Nature Immunology *17*, 104–112.

Hung, C.-H., Thomas, L., Ruby, C.E., Atkins, K.M., Morris, N.P., Knight, Z.A., Scholz, I., Barklis, E., Weinberg, A.D., Shokat, K.M., et al. (2007). HIV-1 Nef Assembles a Src Family Kinase-ZAP-70/Syk-PI3K Cascade to Downregulate Cell-Surface MHC-I. Cell Host & Microbe *1*, 121–133.

Hungnesi, O., Tjøtta, E., and Grinde, B. (1992). Mutations in the central polypurine tract of HIV-1 result in delayed replication. Virology *190*, 440–442.

Huthoff, H., Autore, F., Gallois-Montbrun, S., Fraternali, F., and Malim, M.H. (2009). RNA-dependent oligomerization of APOBEC3G Is required for restriction of HIV-1. PLoS Pathogens *5*.

Iafrate, A.J., Carl, S., Bronson, S., Stahl-Hennig, C., Swigut, T., Skowronski, J., and Kirchhoff, F. (2000). Disrupting Surfaces of Nef Required for Downregulation of CD4 and for Enhancement of Virion Infectivity Attenuates Simian Immunodeficiency Virus Replication In Vivo. Journal of Virology *74*, 9836–9844.

Iezzi, G., Karjalainen, K., and Lanzavecchia, A. (1998). The duration of antigenic stimulation determines the fate of naive and effector T cells. Immunity *8*, 89–95.

Igakura, T., Stinchcombe, J.C., Goon, P.K.C., Taylor, G.P., Weber, J.N., Griffiths, G.M., Tanaka, Y., Osame, M., and Bangham, C.R.M. (2003). Spread of HTLV-I between lymphocytes by virus-induced polarization of the cytoskeleton. Science *299*, 1713–1716.

Inder, K., Harding, A., Plowman, S.J., Philips, M.R., Parton, R.G., and Hancock, J.F. (2008). Activation of the MAPK module from different spatial locations generates distinct system outputs. Molecular Biology of the Cell *19*, 4776–4784.

Inuzuka, M., Hayakawa, M., and Ingi, T. (2005). Serinc, an activity-regulated protein family, incorporates serine into membrane lipid synthesis. Journal of Biological Chemistry *280*, 35776–35783.

Irving, B.A., and Weiss, A. (1991). The cytoplasmic domain of the T cell receptor ζ chain is sufficient to couple to receptor-associated signal transduction pathways. Cell *64*, 891–901.

Isel, C., Lanchy, J.M., le Grice, S.F., Ehresmann, C., Ehresmann, B., and Marquet, R. (1996). Specific initiation and switch to elongation of human immunodeficiency virus type 1 reverse transcription require the post-transcriptional modifications of primer tRNA3Lys. The EMBO Journal *15*, 917–924.

Izquierdo-Useros, N., Lorizate, M., Puertas, M.C., Rodriguez-Plata, M.T., Zangger, N., Erikson, E., Pino, M., Erkizia, I., Glass, B., Clotet, B., et al. (2012). Siglec-1 Is a Novel Dendritic Cell Receptor That Mediates HIV-1 Trans-Infection Through Recognition of Viral Membrane Gangliosides. PLoS Biology *10*.

Jacks, T., Power, M.D., Masiarz, F.R., Luciw, P.A., Barr, P.J., and Varmus, H.E. (1988). Characterization of ribosomal frameshifting in HIV-1 gag-pol expression. Nature *331*, 280–283.

Jacques, D.A., McEwan, W.A., Hilditch, L., Price, A.J., Towers, G.J., and James, L.C. (2016). HIV-1 uses dynamic capsid pores to import nucleotides and fuel encapsidated DNA synthesis. Nature *536*, 349–353.

Jaffar, S., Wilkins, A., Ngom, P.T., Sabally, S., Corrah, T., Bangali, J.E., Rolfe, M., and Whittle, H.C. (1997). Rate of decline of percentage CD4+ cells is faster in HIV-1 than in HIV-2 infection. Journal of Acquired Immune Deficiency Syndromes and Human Retrovirology *16*, 327–332.

James, J.R., and Vale, R.D. (2012). Biophysical mechanism of T-cell receptor triggering in a reconstituted system. Nature *487*, 64–69.

Janardhan, A., Swigut, T., Hill, B., Myers, M.P., and Skowronski, J. (2004). HIV-1 Nef Binds the DOCK2–ELMO1 Complex to Activate Rac and Inhibit Lymphocyte Chemotaxis. PLoS Biology *2*, e6.

Ji, X., Tang, C., Zhao, Q., Wang, W., Xiong, Y., and Goff, S.P. (2014). Structural basis of cellular dNTP regulation by SAMHD1. Proceedings of the National Academy of Sciences of the United States of America *111*, E4305–E4314.

Jia, B., Serra-Moreno, R., Neidermyer, W., Rahmberg, A., Mackey, J., Fofana, I. ben, Johnson, W.E., Westmoreland, S., and Evans, D.T. (2009). Species-Specific Activity of SIV Nef and HIV-1 Vpu in Overcoming Restriction by Tetherin/BST2. PLoS Pathogens *5*, e1000429.

Jia, R., Pan, Q., Ding, S., Rong, L., Liu, S.-L., Geng, Y., Qiao, W., and Liang, C. (2012a). The N-Terminal Region of IFITM3 Modulates Its Antiviral Activity by Regulating IFITM3 Cellular Localization. Journal of Virology *86*, 13697–13707.

Jia, X., Singh, R., Homann, S., Yang, H., Guatelli, J., and Xiong, Y. (2012b). Structural basis of evasion of cellular adaptive immunity by HIV-1 Nef. Nature Structural and Molecular Biology *19*, 701–706.

Jia, X., Weber, E., Tokarev, A., Lewinski, M., Rizk, M., Suarez, M., Guatelli, J., and Xiong, Y. (2014). Structural basis of HIV-1 Vpu-mediated BST2 antagonism via hijacking of the clathrin adaptor protein complex 1. ELife *2014*.

Jimenez-Guardeño, J.M., Apolonia, L., Betancor, G., and Malim, M.H. (2019). Immunoproteasome activation enables human TRIM5α restriction of HIV-1. Nature Microbiology *4*, 933–940.

Jin, J., Sherer, N.M., Heidecker, G., Derse, D., and Mothes, W. (2009). Assembly of the murine leukemia virus is directed towards sites of cell-cell contact. PLoS Biology *7*.

Jin, S.W., Alsahafi, N., Kuang, X.T., Swann, S.A., Toyoda, M., Göttlinger, H., Walker, B.D., Ueno, T., Finzi, A., Brumme, Z.L., et al. (2019). Natural HIV-1 Nef Polymorphisms Impair SERINC5 Downregulation Activity. Cell Reports *29*, 1449-1457.e5.

Joas, S., Parrish, E.H., Gnanadurai, C.W., Lump, E., Stürzel, C.M., Parrish, N.F., Learn, G.H., Sauermann, U., Neumann, B., Rensing, K.M., et al. (2018). Species-specific host factors rather than virus-intrinsic virulence determine primate lentiviral pathogenicity. Nature Communications *9*.

Joas, S., Sauermann, U., Roshani, B., Klippert, A., Daskalaki, M., Mätz-Rensing, K., Stolte-Leeb, N., Heigele, A., Tharp, G.K., Gupta, P.M., et al. (2020). Nef-Mediated CD3-TCR Downmodulation Dampens Acute Inflammation and Promotes SIV Immune Evasion. Cell Reports *30*, 2261-2274.e7.

Johnson, K.G., Bromley, S.K., Dustin, M.L., and Thomas, M.L. (2000). A supramolecular basis for CD45 tyrosine phosphatase regulation in sustained T cell activation. Proceedings of the National Academy of Sciences of the United States of America *97*, 10138–10143.

Jolly, C., and Sattentau, Q.J. (2004). Retroviral spread by induction of virological synapses. Traffic *5*, 643–650.

Jolly, C., and Sattentau, Q.J. (2005). Human Immunodeficiency Virus Type 1 Virological Synapse Formation in T Cells Requires Lipid Raft Integrity. Journal of Virology *79*, 12088–12094.

Jolly, C., and Sattentau, Q.J. (2007). Human Immunodeficiency Virus Type 1 Assembly, Budding, and Cell-Cell Spread in T Cells Take Place in Tetraspanin-Enriched Plasma Membrane Domains. Journal of Virology *81*, 7873–7884.

Jolly, C., Kashefi, K., Hollinshead, M., and Sattentau, Q.J. (2004). HIV-1 cell to cell transfer across an Env-induced, actin-dependent synapse. The Journal of Experimental Medicine *199*, 283–293.

Jolly, C., Mitar, I., and Sattentau, Q.J. (2007a). Adhesion molecule interactions facilitate human immunodeficiency virus type 1-induced virological synapse formation between T cells. Journal of Virology *81*, 13916–13921.

Jolly, C., Mitar, I., and Sattentau, Q.J. (2007b). Requirement for an intact T-cell actin and tubulin cytoskeleton for efficient assembly and spread of human immunodeficiency virus type 1. Journal of Virology *81*, 5547–5560.

Jolly, C., Booth, N.J., and Neil, S.J.D. (2010). Cell-cell spread of human immunodeficiency virus type 1 overcomes tetherin/BST-2-mediated restriction in T cells. Journal of Virology *84*, 12185–12199.

Jolly, C., Welsch, S., Michor, S., and Sattentau, Q.J. (2011). The Regulated Secretory Pathway in CD4+ T cells Contributes to Human Immunodeficiency Virus Type-1 Cell-to-Cell Spread at the Virological Synapse. PLoS Pathogens *7*, e1002226.

Jønsson, K.L., Laustsen, A., Krapp, C., Skipper, K.A., Thavachelvam, K., Hotter, D., Egedal, J.H., Kjolby, M., Mohammadi, P., Prabakaran, T., et al. (2017). IFI16 is required for DNA sensing in human macrophages by promoting production and function of cGAMP. Nature Communications *8*.

Josefsson, L., King, M.S., Makitalo, B., Brännström, J., Shao, W., Maldarelli, F., Kearney, M.F., Hu, W.S., Chen, J., Gaines, H., et al. (2011). Majority of CD4 + T cells from peripheral blood of HIV-1-infected individuals contain only one HIV DNA molecule. Proceedings of the National Academy of Sciences of the United States of America *108*, 11199–11204.

Josefsson, L., Palmer, S., Faria, N.R., Lemey, P., Casazza, J., Ambrozak, D., Kearney, M., Shao, W., Kottilil, S., Sneller, M., et al. (2013). Single Cell Analysis of Lymph Node Tissue from HIV-1 Infected Patients Reveals that the Majority of CD4+ T-cells Contain One HIV-1 DNA Molecule. PLoS Pathogens *9*.

Jouvenet, N., Bieniasz, P.D., and Simon, S.M. (2008). Imaging the biogenesis of individual HIV-1 virions in live cells. Nature *454*, 236–240.

Jouvenet, N., Neil, S.J.D., Zhadina, M., Zang, T., Kratovac, Z., Lee, Y., McNatt, M., Hatziioannou, T., and Bieniasz, P.D. (2009). Broad-Spectrum Inhibition of Retroviral and Filoviral Particle Release by Tetherin. Journal of Virology *83*, 1837–1844.

Jowett, J.B., Planelles, V., Poon, B., Shah, N.P., Chen, M.L., and Chen, I.S. (1995). The human immunodeficiency virus type 1 vpr gene arrests infected T cells in the G2 + M phase of the cell cycle. Journal of Virology *69*, 6304–6313.

Julien, J.P., Cupo, A., Sok, D., Stanfield, R.L., Lyumkis, D., Deller, M.C., Klasse, P.J., Burton, D.R., Sanders, R.W., Moore, J.P., et al. (2013). Crystal structure of a soluble cleaved HIV-1 envelope trimer. Science *342*, 1477–1483.

Jung, A., Maier, R., Vartanian, J.P., Bocharov, G., Jung, V., Fischer, U., Meese, E., Wain-Hobson, S., and Meyerhans, A. (2002). Multiply infected spleen cells in HIV patients. Nature *418*, 144.

Kambayashi, T., and Laufer, T.M. (2014). Atypical MHC class II-expressing antigen-presenting cells: Can anything replace a dendritic cell? Nature Reviews Immunology *14*, 719–730.

Kane, M., Yadav, S.S., Bitzegeio, J., Kutluay, S.B., Zang, T., Wilson, S.J., Schoggins, J.W., Rice, C.M., Yamashita, M., Hatziioannou, T., et al. (2013). MX2 is an interferon-induced inhibitor of HIV-1 infection. Nature *502*, 563–566.

Kane, M., Rebensburg, S. v., Takata, M.A., Zang, T.M., Yamashita, M., Kvaratskhelia, M., and Bieniasz, P.D. (2018). Nuclear pore heterogeneity influences HIV-1 infection and the antiviral activity of MX2. ELife *7*.

Kaplan, A.H., Zack, J.A., Knigge, M., Paul, D.A., Kempf, D.J., Norbeck, D.W., and Swanstrom, R. (1993). Partial inhibition of the human immunodeficiency virus type 1 protease results in aberrant virus assembly and the formation of noninfectious particles. Journal of Virology *67*, 4050–4055.

Karpinich, N.O., Tafani, M., Rothman, R.J., Russo, M.A., and Farber, J.L. (2002). The course of etoposide-induced apoptosis from damage to DNA and p53 activation to mitochondrial release of cytochrome c. Journal of Biological Chemistry *277*, 16547–16552.

Katz, D.H., Hamaoka, T., and Benacerraf, B. (1973). Cell interactions between histoincompatible T and B lymphocytes: II. Failure of physiologic cooperative interactions between T and B lymphocytes from allogeneic donor strains in humoral response to hapten-protein conjugates. Journal of Experimental Medicine *137*, 1405–1418.

Kaur, A., Grant, R.M., Means, R.E., McClure, H., Feinberg, M., and Johnson, R.P. (1998). Diverse host responses and outcomes following simian immunodeficiency virus SIVmac239 infection in sooty mangabeys and rhesus macaques. Journal of Virology *72*, 9597–9611.

Keckesova, Z., Ylinen, L.M.J., and Towers, G.J. (2006). Cyclophilin A renders human immunodeficiency virus type 1 sensitive to Old World monkey but not human TRIM5 alpha antiviral activity. Journal of Virology *80*, 4683–4690.

Keele, B.F., van Heuverswyn, F., Li, Y., Bailes, E., Takehisa, J., Santiago, M.L., Bibollet-Ruche, F., Chen, Y., Wain, L. v., Liegeois, F., et al. (2006). Chimpanzee reservoirs of pandemic and nonpandemic HIV-1. Science *313*, 523–526.

Keele, B.F., Giorgi, E.E., Salazar-Gonzalez, J.F., Decker, J.M., Pham, K.T., Salazar, M.G., Sun, C., Grayson, T., Wang, S., Li, H., et al. (2008). Identification and characterization of transmitted and early founder virus envelopes in primary HIV-1 infection. Proceedings of the National Academy of Sciences of the United States of America *105*, 7552–7557.

Keele, B.F., Jones, J.H., Terio, K.A., Estes, J.D., Rudicell, R.S., Wilson, M.L., Li, Y., Learn, G.H., Beasley, T.M., Schumacher-Stankey, J., et al. (2009). Increased mortality and AIDS-like immunopathology in wild chimpanzees infected with SIVcpz. Nature *460*, 515–519.

Kempf, D.J., Marsh, K.C., Denissen, J.F., McDonald, E., Vasavanonda, S., Flentge, C.A., Green, B.E., Fino, L., Park, C.H., Kong, X.P., et al. (1995). ABT-538 is a potent inhibitor of human immunodeficiency virus protease and has high oral bioavailability in humans. Proceedings of the National Academy of Sciences of the United States of America *92*, 2484–2488.

Kestler, H.W., Ringler, D.J., Mori, K., Panicali, D.L., Sehgal, P.K., Daniel, M.D., and Desrosiers, R.C. (1991). Importance of the nef gene for maintenance of high virus loads and for development of AIDS. Cell *65*, 651–662.

Khalid, M., Yu, H., Sauter, D., Usmani, S.M., Schmokel, J., Feldman, J., Gruters, R.A., van der Ende, M.E., Geyer, M., Rowland-Jones, S., et al. (2012). Efficient Nef-mediated downmodulation of TCR-CD3 and CD28 is associated with high CD4+ T cell counts in viremic HIV-2 infection. Journal of Virology *86*, 4906–4920.

Khan, H., Sumner, R.P., Rasaiyaah, J., Tan, C.P., Rodriguez-Plata, M.T., Tulleken, C. van, Fink, D., Zuliani-Alvarez, L., Thorne, L., Stirling, D., et al. (2020). HIV-1 Vpr antagonizes cGAS sensing by targeting karyopherin-mediated NF-κB/IRF3 nuclear transport. BioRxiv 2020.02.22.960757.

Kilzer, J.M., Stracker, T., Beitzel, B., Meek, K., Weitzman, M., and Bushman, F.D. (2003). Roles of host cell factors in circularization of retroviral DNA. Virology *314*, 460–467.

Kim, B.H., Shenoy, A.R., Kumar, P., Bradfield, C.J., and MacMicking, J.D. (2012). IFN-inducible GTPases in host cell defense. Cell Host and Microbe *12*, 432–444.

Kim, E.M., Lee, K.H., and Kim, J.W. (1999). The cytoplasmic domain of HIV-1 gp41 interacts with the carboxyl-terminal region of α-catenin. Molecules and Cells *9*, 281–285.

Kim, K., Dauphin, A., Komurlu, S., McCauley, S.M., Yurkovetskiy, L., Carbone, C., Diehl, W.E., Strambio-De-Castillia, C., Campbell, E.M., and Luban, J. (2019). Cyclophilin A protects HIV-1 from restriction by human TRIM5α. Nature Microbiology *4*, 2044–2051.

Kim, W.M., Sigalov, A.B., and Stern, L.J. (2010). Pseudo-merohedral twinning and noncrystallographic symmetry in orthorhombic crystals of SIVmac239 Nef core domain bound to different-length TCRζ fragments. Acta Crystallographica Section D: Biological Crystallography *66*, 163–175.

Kirchhoff, F. (2009). Is the high virulence of HIV-1 an unfortunate coincidence of primate lentiviral evolution? Nature Reviews Microbiology *7*, 467–476.

Kirchhoff, F., Desrosiers, R.C., Greenough, T.C., Sullivan, J.L., and Brettler, D.B. (1995). Absence of intact nef sequences in a long-term survivor with nonprogressive hiv-1 infection. New England Journal of Medicine *332*, 228–232.

Kirchhoff, F., Schindler, M., Bailer, N., Renkema, G.H., Saksela, K., Knoop, V., Muller-Trutwin, M.C., Santiago, M.L., Bibollet-Ruche, F., Dittmar, M.T., et al. (2004). Nef Proteins from Simian Immunodeficiency Virus-Infected Chimpanzees Interact with p21-Activated Kinase 2 and Modulate Cell Surface Expression of Various Human Receptors. Journal of Virology *78*, 6864–6874.

Kirschman, J., Qi, M., Ding, L., Hammonds, J., Dienger-Stambaugh, K., Wang, J.-J., Lapierre, L.A., Goldenring, J.R., and Spearman, P. (2018). HIV-1 Envelope Glycoprotein Trafficking through the Endosomal Recycling Compartment Is Required for Particle Incorporation. Journal of Virology *92*.

Klatt, N.R., Silvestri, G., and Hirsch, V. (2012). Nonpathogenic simian immunodeficiency virus infections. Cold Spring Harbor Perspectives in Medicine *2*.

Klaver, B., and Berkhout, B. (1994). Comparison of 5' and 3' long terminal repeat promoter function in human immunodeficiency virus. Journal of Virology *68*, 3830–3840.

Klimkait, T., Strebel, K., Hoggan, M.D., Martin, M.A., and Orenstein, J.M. (1990). The human immunodeficiency virus type 1-specific protein vpu is required for efficient virus maturation and release. Journal of Virology *64*, 621–629.

Kluge, S.F., Mack, K., Iyer, S.S., Pujol, F.M., Heigele, A., Learn, G.H., Usmani, S.M., Sauter, D., Joas, S., Hotter, D., et al. (2014). Nef proteins of epidemic HIV-1 group O strains antagonize human tetherin. Cell Host and Microbe *16*, 639–650.

Kmiec, D., Akbil, B., Ananth, S., Hotter, D., Sparrer, K.M.J., Stürzel, C.M., Trautz, B., Ayouba, A., Peeters, M., Yao, Z., et al. (2018). SIVcol Nef counteracts SERINC5 by promoting its proteasomal degradation but does not efficiently enhance HIV-1 replication in human CD4+ T cells and lymphoid tissue. PLoS Pathogens *14*.

Kohlstaedt, L.A., Wang, J., Friedman, J.M., Rice, P.A., and Steitz, T.A. (1992). Crystal structure at 3.5 Å resolution of HIV-1 reverse transcriptase complexed with an inhibitor. Science *256*, 1783–1790.

Koning, F.A., Newman, E.N.C., Kim, E.-Y., Kunstman, K.J., Wolinsky, S.M., and Malim, M.H. (2009). Defining APOBEC3 Expression Patterns in Human Tissues and Hematopoietic Cell Subsets. Journal of Virology *83*, 9474–9485.

Krapp, C., Hotter, D., Gawanbacht, A., McLaren, P.J., Kluge, S.F., Stürzel, C.M., Mack, K., Reith, E., Engelhart, S., Ciuffi, A., et al. (2016). Guanylate Binding Protein (GBP) 5 Is an Interferon-Inducible Inhibitor of HIV-1 Infectivity. Cell Host and Microbe *19*, 504–514.

Kratovac, Z., Virgen, C.A., Bibollet-Ruche, F., Hahn, B.H., Bieniasz, P.D., and Hatziioannou, T. (2008). Primate Lentivirus Capsid Sensitivity to TRIM5 Proteins. Journal of Virology *82*, 6772–6777.

Krautkrämer, E., Giese, S.I., Gasteier, J.E., Muranyi, W., and Fackler, O.T. (2004). Human immunodeficiency virus type 1 Nef activates p21-activated kinase via recruitment into lipid rafts. Journal of Virology *78*, 4085–4097.

Kruisbeek, A.M., Mond, J.J., Fowlkes, B.J., Carmen, J.A., Bridges, S., and Longo, D.L. (1985). Absence of the Lyt-2−, L3T4+ lineage of T cells in mice treated neonatally with anti-I-A correlates with absence of intrathymic I-A-bearing antigen-presenting cell function. Journal of Experimental Medicine *161*, 1029–1047.

Krummheuer, J., Johnson, A.T., Hauber, I., Kammler, S., Anderson, J.L., Hauber, J., Purcell, D.F.J., and Schaal, H. (2007). A minimal uORF within the HIV-1 vpu leader allows efficient translation initiation at the downstream env AUG. Virology *363*, 261–271.

Kucia, M., Jankowski, K., Reca, R., Wysoczynski, M., Bandura, L., Allendorf, D.J., Zhang, J., Ratajczak, J., and Ratajczak, M.Z. (2004). CXCR4-SDF-1 signalling, locomotion, chemotaxis and adhesion. Journal of Molecular Histology *35*, 233–245.

Kueck, T., and Neil, S.J.D. (2012). A cytoplasmic tail determinant in HIV-1 vpu mediates targeting of tetherin for endosomal degradation and counteracts interferon-induced restriction. PLoS Pathogens *8*.

Kueck, T., Foster, T.L., Weinelt, J., Sumner, J.C., Pickering, S., and Neil, S.J.D. (2015). Serine Phosphorylation of HIV-1 Vpu and Its Binding to Tetherin Regulates Interaction with Clathrin Adaptors. PLoS Pathogens *11*.

Kumar, B. v, Ma, W., Miron, M., Granot, T., Guyer, R.S., Carpenter, D.J., Senda, T., Sun, X., Ho, S.-H., Lerner, H., et al. (2017). Human Tissue-Resident Memory T Cells Are Defined by Core Transcriptional and Functional Signatures in Lymphoid and Mucosal Sites. Cell Reports *20*, 2921–2934.

Kupfer, A., and Singer, S.J. (1989). The specific interaction of helper T cells and antigen-presenting B cells. IV. Membrane and cytoskeletal reorganizations in the bound T cell as a function of antigen dose. Journal of Experimental Medicine *170*, 1697–1713.

Kupfer, A., Swain, S.L., and Singer, S.J. (1987). The specific direct interaction of helper t cells and antigen-presenting B cells: II . reorientation of the microtubule organizing center and reorganization of the membrane-associated cytoskeleton inside the bound helper T cells. Journal of Experimental Medicine *165*, 1565–1580.

Kupfer, H., Monks, C.K.F., and Kupfer, A. (1994). Small splenic B cells that bind to antigen-specific T helper (Th) cells and face the site of cytokine production in the Th cells selectively proliferate: Immunofluorescence microscopic studies of Th-B antigen-presenting cell interactions. Journal of Experimental Medicine *179*, 1507–1515.

Kupzig, S., Korolchuk, V., Rollason, R., Sugden, A., Wilde, A., and Banting, G. (2003). Bst-2/HM1.24 is a raft-associated apical membrane protein with an unusual topology. Traffic *4*, 694–709.

Kutluay, S.B., and Bieniasz, P.D. (2010). Analysis of the initiating events in HIV-1 particle assembly and genome packaging. PLoS Pathogens *6*, e1001200.

Kwon, Y. do, Finzi, A., Wu, X., Dogo-Isonagie, C., Lee, L.K., Moore, L.R., Schmidt, S.D., Stuckey, J., Yang, Y., Zhou, T., et al. (2012). Unliganded HIV-1 gp120 core structures assume the CD4-bound conformation with regulation by quaternary interactions and variable loops. Proceedings of the National Academy of Sciences of the United States of America *109*, 5663–5668.

Kwong, P.D., Wyatt, R., Robinson, J., Sweet, R.W., Sodroski, J., and Hendrickson, W.A. (1998). Structure of an HIV gp 120 envelope glycoprotein in complex with the CD4 receptor and a neutralizing human antibody. Nature *393*, 648–659.

Ladinsky, M.S., Kieffer, C., Olson, G., Deruaz, M., Vrbanac, V., Tager, A.M., Kwon, D.S., and Bjorkman, P.J. (2014). Electron Tomography of HIV-1 Infection in Gut-Associated Lymphoid Tissue. PLoS Pathogens *10*.

Laguette, N., Sobhian, B., Casartelli, N., Ringeard, M., Chable-Bessia, C., Ségéral, E., Yatim, A., Emiliani, S., Schwartz, O., and Benkirane, M. (2011). SAMHD1 is the dendritic- and myeloid-cell-specific HIV-1 restriction factor counteracted by Vpx. Nature *474*, 654–657.

Laguette, N., Brégnard, C., Hue, P., Basbous, J., Yatim, A., Larroque, M., Kirchhoff, F., Constantinou, A., Sobhian, B., and Benkirane, M. (2014). Premature activation of the slx4 complex by vpr promotes g2/m arrest and escape from innate immune sensing. Cell *156*, 134–145.

Lahaye, X., Satoh, T., Gentili, M., Cerboni, S., Conrad, C., Hurbain, I., ElMarjou, A., Lacabaratz, C., Lelièvre, J.D., and Manel, N. (2013). The Capsids of HIV-1 and HIV-2 Determine Immune Detection of the Viral cDNA by the Innate Sensor cGAS in Dendritic Cells. Immunity *39*, 1132–1142.

Lahouassa, H., Blondot, M.L., Chauveau, L., Chougui, G., Morel, M., Leduc, M., Guillonneau, F., Ramirez, B.C., Schwartz, O., and Margottin-Goguet, F. (2016). HIV-1 Vpr degrades the HLTF DNA translocase in T cells and macrophages. Proceedings of the National Academy of Sciences of the United States of America *113*, 5311–5316.

Lambert, A.A., Gilbert, C., Richard, M., Beaulieu, A.D., and Tremblay, M.J. (2008). The C-type lectin surface receptor DCIR acts as a new attachment factor for HIV-1 in dendritic cells and contributes to trans- and cis-infection pathways. Blood *112*, 1299–1307.

Landsberg, C.D., Megger, D.A., Hotter, D., Rückborn, M.U., Eilbrecht, M., Rashidi-Alavijeh, J., Howe, S., Heinrichs, S., Sauter, D., Sitek, B., et al. (2018). A Mass Spectrometry-Based Profiling of Interactomes of Viral DDB1- and Cullin Ubiquitin Ligase-Binding Proteins Reveals NF-κB Inhibitory Activity of the HIV-2-Encoded Vpx. Frontiers in Immunology *9*, 2978.

Lang, S.M., Iafrate, A.J., Stahl-Hennig, C., Kuhn, E.M., Nisslein, T., Kaup, F.J., Haupt, M., Hunsmann, G., Skowronski, J., and Kirchhoff, F. (1997). Association of simian immunodeficiency virus Nef with cellular serine/thereonine kinases is dispensable for the development of AIDS in rhesus macaques. Nature Medicine *3*, 860–865.

Langer, S., Hammer, C., Hopfensperger, K., Klein, L., Hotter, D., de Jesus, P.D., Herbert, K.M., Pache, L., Smith, N., van der Merwe, J.A., et al. (2019). HIV-1 Vpu is a potent transcriptional suppressor of NF-κB-elicited antiviral immune responses. ELife *8*.

Larder, B.A., Kemp, S.D., and Harrigan, P.R. (1995). Potential mechanism for sustained antiretroviral efficacy of AZT-3TC combination therapy. Science *269*, 696–699.

Lascano, J., Uchil, P.D., Mothes, W., and Luban, J. (2016). TRIM5 Retroviral Restriction Activity Correlates with the Ability To Induce Innate Immune Signaling. Journal of Virology *90*, 308–316.

Lee, C.H., Leung, B., Lemmon, M.A., Zheng, J., Cowburn, D., Kuriyan, J., and Saksela, K. (1995). A single amino acid in the SH3 domain of Hck determines its high affinity and specificity in binding to HIV-1 Nef protein. The EMBO Journal *14*, 5006–5015.

Lee, M.S., Glassman, C.R., Deshpande, N.R., Badgandi, H.B., Parrish, H.L., Uttamapinant, C., Stawski, P.S., Ting, A.Y., and Kuhns, M.S. (2015). A Mechanical Switch Couples T Cell Receptor Triggering to the Cytoplasmic Juxtamembrane Regions of CD3ζζ. Immunity *43*, 227–239.

Len, A.C.L., Starling, S., Shivkumar, M., and Jolly, C. (2017). HIV-1 Activates T Cell Signaling Independently of Antigen to Drive Viral Spread. Cell Reports *18*, 1062–1074.

Leonard, C.K., Spellman, M.W., Riddle, L., Harris, R.J., Thomas, J.N., and Gregory, T.J. (1990). Assignment of intrachain disulfide bonds and characterization of potential glycosylation sites of the type 1 recombinant human immunodeficiency virus envelope glycoprotein (gp120) expressed in Chinese hamster ovary cells. Journal of Biological Chemistry *265*, 10373–10382.

Leonard, J.A., Filzen, T., Carter, C.C., Schaefer, M., and Collins, K.L. (2011). HIV-1 Nef Disrupts Intracellular Trafficking of Major Histocompatibility Complex Class I, CD4, CD8, and CD28 by Distinct Pathways That Share Common Elements. Journal of Virology *85*, 6867–6881.

Letendre, S., Marquie-Beck, J., Capparelli, E., Best, B., Clifford, D., Collier, A.C., Gelman, B.B., McArthur, J.C., McCutchan, J.A., Morgello, S., et al. (2008). Validation of the CNS penetration-effectiveness rank for quantifying antiretroviral penetration into the central nervous system. Archives of Neurology *65*, 65–70.

Letko, M., Silvestri, G., Hahn, B.H., Bibollet-Ruche, F., Gokcumen, O., Simon, V., and Ooms, M. (2013). Vif Proteins from Diverse Primate Lentiviral Lineages Use the Same Binding Site in APOBEC3G. Journal of Virology *87*, 11861–11871.

Leung, K., Kim, J.O., Ganesh, L., Kabat, J., Schwartz, O., and Nabel, G.J. (2008). HIV-1 Assembly: Viral Glycoproteins Segregate Quantally to Lipid Rafts that Associate Individually with HIV-1 Capsids and Virions. Cell Host and Microbe *3*, 285–292.

Levy, J.A., Hoffman, A.D., Kramer, S.M., Landis, J.A., Shimabukuro, J.M., and Oshiro, L.S. (1984). Isolation of lymphocytopathic retroviruses from San Francisco patients with AIDS. Science *225*, 840–842.

Li, B., Stefano-Cole, K., Kuhrt, D.M., Gordon, S.N., Else, J.G., Mulenga, J., Allen, S., Sodora, D.L., Silvestri, G., and Derdeyn, C.A. (2010). Nonpathogenic Simian Immunodeficiency Virus Infection of Sooty Mangabeys Is Not Associated with High Levels of Autologous Neutralizing Antibodies. Journal of Virology *84*, 6248–6253.

Li, D., Molldrem, J.J., and Ma, Q. (2009). LFA-1 regulates CD8+ T cell activation via T cell receptor-mediated and LFA-1-mediated Erk1/2 signal pathways. Journal of Biological Chemistry *284*, 21001–21010.

Li, L., Olvera, J.M., Yoder, K.E., Mitchell, R.S., Butler, S.L., Lieber, M., Martin, S.L., and Bushman, F.D. (2001). Role of the non-homologous DNA end joining pathway in the early steps of retroviral infection. EMBO Journal *20*, 3272–3281.

Li, S., Hill, C.P., Sundquist, W.I., and Finch, J.T. (2000). Image reconstructions of helical assemblies of the HIV-1 CA protein. Nature *407*, 409–413.

Lightfoote, M.M., Coligan, J.E., Folks, T.M., Fauci, A.S., Martin, M.A., and Venkatesan, S. (1986). Structural characterization of reverse transcriptase and endonuclease polypeptides of the acquired immunodeficiency syndrome retrovirus. Journal of Virology *60*, 771.

Lim, E.S., Fregoso, O.I., McCoy, C.O., Matsen, F.A., Malik, H.S., and Emerman, M. (2012). The ability of primate lentiviruses to degrade the monocyte restriction factor SAMHD1 preceded the birth of the viral accessory protein Vpx. Cell Host and Microbe *11*, 194–204.

Linde, M.E., Colquhoun, D.R., Mohien, C.U., Kole, T., Aquino, V., Cotter, R., Edwards, N., Hildreth, J.E.K., and Graham, D.R. (2013). The conserved set of host proteins incorporated into HIV-1 virions suggests a common egress pathway in multiple cell types. Journal of Proteome Research *12*, 2045–2054.

Lioudyno, M.I., Kozak, J.A., Penna, A., Safrina, O., Zhang, S.L., Sen, D., Roos, J., Stauderman, K.A., and Cahalan, M.D. (2008). Orai1 and STIM1 move to the immunological synapse and are

up-regulated during T cell activation. Proceedings of the National Academy of Sciences of the United States of America *105*, 2011–2016.

Liu, B., Chen, W., Evavold, B.D., and Zhu, C. (2014). Accumulation of dynamic catch bonds between TCR and agonist peptide-MHC triggers T cell signaling. Cell *157*, 357–368.

Liu, C., Perilla, J.R., Ning, J., Lu, M., Hou, G., Ramalho, R., Himes, B.A., Zhao, G., Bedwell, G.J., Byeon, I.J., et al. (2016). Cyclophilin A stabilizes the HIV-1 capsid through a novel non-canonical binding site. Nature Communications *7*, 1–10.

Liu, N., Lee, C.H., Swigut, T., Grow, E., Gu, B., Bassik, M.C., and Wysocka, J. (2018). Selective silencing of euchromatic L1s revealed by genome-wide screens for L1 regulators. Nature *553*, 228–232.

Lockyer, P.J., Kupzig, S., and Cullen, P.J. (2001). CAPRI regulates ca2+-dependent inactivation of the Ras-MAPK pathway. Current Biology *11*, 981–986.

van der Loeff, M.F.S., Larke, N., Kaye, S., Berry, N., Ariyoshi, K., Alabi, A., van Tienen, C., Leligdowicz, A., Sarge-Njie, R., da Silva, Z., et al. (2010). Undetectable plasma viral load predicts normal survival in HIV-2-infected people in a West African village. Retrovirology *7*, 46.

Loisel-Meyer, S., Swainson, L., Craveiro, M., Oburoglu, L., Mongellaz, C., Costa, C., Martinez, M., Cosset, F.-L., Battini, J.-L., Herzenberg, L.A., et al. (2012). Glut1-mediated glucose transport regulates HIV infection. Proceedings of the National Academy of Sciences *109*, 2549–2554.

Lopez-Vergès, S., Camus, G., Blot, G., Beauvoir, R., Benarous, R., and Berlioz-Torrent, C. (2006). Tail-interacting protein TIP47 is a connector between Gag and Env and is required for Env incorporation into HIV-1 virions. Proceedings of the National Academy of Sciences of the United States of America *103*, 14947–14952.

Lu, J., Pan, Q., Rong, L., Liu, S.-L., and Liang, C. (2011a). The IFITM Proteins Inhibit HIV-1 Infection. Journal of Virology *85*, 2126–2137.

Lu, K., Heng, X., and Summers, M.F. (2011b). Structural determinants and mechanism of HIV-1 genome packaging. Journal of Molecular Biology *410*, 609–633.

Lu, X., Yu, H., Liu, S.H., Brodsky, F.M., and Peterlin, B.M. (1998). Interactions between HIV1 Nef and vacuolar ATPase facilitate the internalization of CD4. Immunity *8*, 647–656.

Luetkemeyer, A.F., Havlir, D. v, and Currier, J.S. (2010). Complications of HIV disease and antiretroviral treatment. Topics in HIV Medicine : A Publication of the International AIDS Society, USA *18*, 57–65.

Luo, Y., Jacobs, E.Y., Greco, T.M., Mohammed, K.D., Tong, T., Keegan, S., Binley, J.M., Cristea, I.M., Fenyö, D., Rout, M.P., et al. (2016). HIV-host interactome revealed directly from infected cells. Nature Microbiology *1*.

Lusic, M., and Siliciano, R.F. (2017). Nuclear landscape of HIV-1 infection and integration. Nature Reviews Microbiology *15*, 69–82.

Lyumkis, D., Julien, J.P., de Val, N., Cupo, A., Potter, C.S., Klasse, P.J., Burton, D.R., Sanders, R.W., Moore, J.P., Carragher, B., et al. (2013). Cryo-EM structure of a fully glycosylated soluble cleaved HIV-1 envelope trimer. Science *342*, 1484–1490.

Maddon, P.J., Dalgleish, A.G., McDougal, J.S., Clapham, P.R., Weiss, R.A., and Axel, R. (1986). The T4 gene encodes the AIDS virus receptor and is expressed in the immune system and the brain. Cell *47*, 333–348.

Magadán, J.G., Pérez-Victoria, F.J., Sougrat, R., Ye, Y., Strebel, K., and Bonifacino, J.S. (2010). Multilayered mechanism of CD4 downregulation by HIV-1 vpu involving distinct ER retention and ERAD targeting steps. PLoS Pathogens *6*, 1–18.

Malbec, M., Porrot, F., Rua, R., Horwitz, J., Klein, F., Halper-Stromberg, A., Scheid, J.F., Eden, C., Mouquet, H., Nussenzweig, M.C., et al. (2013). Broadly neutralizing antibodies that inhibit HIV-1 cell to cell transmission. Journal of Experimental Medicine *210*, 2813–2821.

Malim, M.H., Hauber, J., Le, S.Y., Maizel, J. v., and Cullen, B.R. (1989). The HIV-1 rev trans-activator acts through a structured target sequence to activate nuclear export of unspliced viral mRNA. Nature *338*, 254–257.

Manches, O., Frleta, D., and Bhardwaj, N. (2014). Dendritic cells in progression and pathology of HIV infection. Trends in Immunology *35*, 114–122.

Manganaro, L., Hong, P., Hernandez, M.M., Argyle, D., Mulder, L.C.F., Potla, U., Diaz-Griffero, F., Lee, B., Fernandez-Sesma, A., and Simon, V. (2018). IL-15 regulates susceptibility of CD4+ T cells to HIV infection. Proceedings of the National Academy of Sciences of the United States of America *115*, E9659–E9667.

Mangeat, B., Turelli, P., Caron, G., Friedli, M., Perrin, L., and Trono, D. (2003). Broad antiretroviral defence by human APOBEC3G through lethal editing of nascent reverse transcripts. Nature *424*, 99–103.

Mangino, G., Percario, Z.A., Fiorucci, G., Vaccari, G., Acconcia, F., Chiarabelli, C., Leone, S., Noto, A., Horenkamp, F.A., Manrique, S., et al. (2011). HIV-1 Nef induces proinflammatory state in macrophages through its acidic cluster domain: Involvement of TNF alpha receptor associated factor 2. PLoS ONE *6*.

Manning, B.D., and Toker, A. (2017). AKT/PKB Signaling: Navigating the Network. Cell *169*, 381–405.

Manrique, S., Sauter, D., Horenkamp, F.A., Lülf, S., Yu, H., Hotter, D., Anand, K., Kirchhoff, F., and Geyer, M. (2017). Endocytic sorting motif interactions involved in Nef-mediated downmodulation of CD4 and CD3. Nature Communications *8*, 442.

Margottin, F., Bour, S.P., Durand, H., Selig, L., Benichou, S., Richard, V., Thomas, D., Strebel, K., and Benarous, R. (1998). A novel human WD protein, h-βTrCP, that interacts with HIV-1 Vpu connects CD4 to the ER degradation pathway through an F-box motif. Molecular Cell *1*, 565–574.

Mariani, R., and Skowronski, J. (1993). CD4 down-regulation by nef alleles isolated from human immunodeficiency virus type 1-infected individuals. Proceedings of the National Academy of Sciences of the United States of America *90*, 5549–5553.

Marini, B., Kertesz-Farkas, A., Ali, H., Lucic, B., Lisek, K., Manganaro, L., Pongor, S., Luzzati, R., Recchia, A., Mavilio, F., et al. (2015). Nuclear architecture dictates HIV-1 integration site selection. Nature *521*, 227–231.

Marlink, R., Kanki, P., Thior, I., Travers, K., Eisen, G., Siby, T., Traore, I., Hsieh, C.C., Dia, M.C., Gueye, E.H., et al. (1994). Reduced rate of disease development after HIV-2 infection as compared to HIV-1. Science *265*, 1587–1590.

Martin, N., Welsch, S., Jolly, C., Briggs, J.A.G., Vaux, D., and Sattentau, Q.J. (2010). Virological synapse-mediated spread of human immunodeficiency virus type 1 between T cells is sensitive to entry inhibition. Journal of Virology *84*, 3516–3527.

Martin-Serrano, J., Zang, T., and Bieniasz, P.D. (2001). HIV-1 and Ebola virus encode small peptide motifs that recruit Tsg101 to sites of particle assembly to facilitate egress. Nature Medicine *7*, 1313–1319.

Matheson, N.J., Sumner, J., Wals, K., Rapiteanu, R., Weekes, M.P., Vigan, R., Weinelt, J., Schindler, M., Antrobus, R., Costa, A.S.H., et al. (2015). Cell Surface Proteomic Map of HIV Infection Reveals Antagonism of Amino Acid Metabolism by Vpu and Nef. Cell Host & Microbe *18*, 409–423.

Matloubian, M., Lo, C.G., Cinamon, G., Lesneski, M.J., Xu, Y., Brinkmann, V., Allende, M.L., Proia, R.L., and Cyster, J.G. (2004). Lymphocyte egress from thymus and peripheral lymphoid organs is dependent on S1P receptor 1. Nature *427*, 355–360.

Matreyek, K.A., Yücel, S.S., Li, X., and Engelman, A. (2013). Nucleoporin NUP153 Phenylalanine-Glycine Motifs Engage a Common Binding Pocket within the HIV-1 Capsid Protein to Mediate Lentiviral Infectivity. PLoS Pathogens *9*, e1003693.

Matusali, G., Potestà, M., Santoni, A., Cerboni, C., and Doria, M. (2012). The Human Immunodeficiency Virus Type 1 Nef and Vpu Proteins Downregulate the Natural Killer Cell-Activating Ligand PVR. Journal of Virology *86*, 4496–4504.

Maudet, C., Sourisce, A., Dragin, L., Lahouassa, H., Rain, J.C., Bouaziz, S., Ramirez, B.C., and Margottin-Goguet, F. (2013). HIV-1 Vpr Induces the Degradation of ZIP and sZIP, Adaptors of the NuRD Chromatin Remodeling Complex, by Hijacking DCAF1/VprBP. PLoS ONE *8*.

Mazurov, D., Ilinskaya, A., Heidecker, G., Lloyd, P., and Derse, D. (2010). Quantitative comparison of HTLV-1 and HIV-1 cell-to-cell infection with new replication dependent vectors. PLoS Pathogens *6*.

McCarthy, K.R., Kirmaier, A., Autissier, P., and Johnson, W.E. (2015). Evolutionary and Functional Analysis of Old World Primate TRIM5 Reveals the Ancient Emergence of Primate Lentiviruses and Convergent Evolution Targeting a Conserved Capsid Interface. PLoS Pathogens *11*.

McCoy, L.E., Quigley, A.F., Strokappe, N.M., Bulmer-Thomas, B., Seaman, M.S., Mortier, D., Rutten, L., Chander, N., Edwards, C.J., Ketteler, R., et al. (2012). Potent and broad neutralization of HIV-1 by a llama antibody elicited by immunization. Journal of Experimental Medicine *209*, 1091–1103.

McCoy, L.E., Groppelli, E., Blanchetot, C., de Haard, H., Verrips, T., Rutten, L., Weiss, R.A., and Jolly, C. (2014). Neutralisation of HIV-1 cell-cell spread by human and llama antibodies. Retrovirology *11*.

McDonald, D., Wu, L., Bohks, S.M., KewalRamani, V.N., Unutmaz, D., and Hope, T.J. (2003). Recruitment of HIV and its receptors to dendritic cell-T cell junctions. Science *300*, 1295–1297.

Mehandru, S., Poles, M.A., Tenner-Racz, K., Horowitz, A., Hurley, A., Hogan, C., Boden, D., Racz, P., and Markowitz, M. (2004). Primary HIV-1 infection is associated with preferential depletion of CD4+ T lymphocytes from effector sites in the gastrointestinal tract. Journal of Experimental Medicine *200*, 761–770.

Melikyan, G.B., Markosyan, R.M., Hemmati, H., Delmedico, M.K., Lambert, D.M., and Cohen, F.S. (2000). Evidence that the transition of HIV-1 gp41 into a six-helix bundle, not the bundle configuration, induces membrane fusion. Journal of Cell Biology *151*, 413–423.

Mercredi, P.Y., Bucca, N., Loeliger, B., Gaines, C.R., Mehta, M., Bhargava, P., Tedbury, P.R., Charlier, L., Floquet, N., Muriaux, D., et al. (2016). Structural and Molecular Determinants of Membrane Binding by the HIV-1 Matrix Protein. Journal of Molecular Biology *428*, 1637–1655.

Meuwissen, P.J., Stolp, B., Iannucci, V., Vermeire, J., Naessens, E., Saksela, K., Geyer, M., Vanham, G., Arien, K.K., Fackler, O.T., et al. (2012). Identification of a highly conserved valine-glycine-phenylalanine amino acid triplet required for HIV-1 Nef function. Retrovirology *9*, 34.

Milush, J.M., Reeves, J.D., Gordon, S.N., Zhou, D., Muthukumar, A., Kosub, D.A., Chacko, E., Giavedoni, L.D., Ibegbu, C.C., Cole, K.S., et al. (2007). Virally induced CD4+ T cell depletion is not sufficient to induce AIDS in a natural host. Journal of Immunology (Baltimore, Md. : 1950) *179*, 3047–3056.

Milush, J.M., Mir, K.D., Sundaravaradan, V., Gordon, S.N., Engram, J., Cano, C.A., Reeves, J.D., Anton, E., O'Neill, E., Butler, E., et al. (2011). Lack of clinical AIDS in SIV-infected sooty mangabeys with significant CD4+ T cell loss is associated with double-negative T cells. Journal of Clinical Investigation *121*, 1102–1110.

Mitchell, R.S., Katsura, C., Skasko, M.A., Fitzpatrick, K., Lau, D., Ruiz, A., Stephens, E.B., Margottin-Goguet, F., Benarous, R., and Guatelli, J.C. (2009). Vpu antagonizes BST-2-mediated restriction of HIV-1 release via β-TrCP and endo-lysosomal trafficking. PLoS Pathogens *5*.

Miyauchi, K., Kim, Y., Latinovic, O., Morozov, V., and Melikyan, G.B. (2009). HIV Enters Cells via Endocytosis and Dynamin-Dependent Fusion with Endosomes. Cell *137*, 433–444.

Mlcochova, P., Sutherland, K.A., Watters, S.A., Bertoli, C., Bruin, R.A., Rehwinkel, J., Neil, S.J., Lenzi, G.M., Kim, B., Khwaja, A., et al. (2017). A G1-like state allows HIV -1 to bypass SAMHD 1 restriction in macrophages . The EMBO Journal *36*, 604–616.

Moir, S., Chun, T.-W., and Fauci, A.S. (2011). Pathogenic Mechanisms of HIV Disease. Annual Review of Pathology: Mechanisms of Disease *6*, 223–248.

Molina, T.J., Kishihara, K., Siderovskid, D.P., van Ewijk, W., Narendran, A., Timms, E., Wakeham, A., Paige, C.J., Hartmann, K.U., Veillette, A., et al. (1992). Profound block in thymocyte development in mice lacking p56lck. Nature *357*, 161–164.

Moll, M., Andersson, S.K., Smed-Sörensen, A., and Sandberg, J.K. (2010). Inhibition of lipid antigen presentation in dendritic cells by HIV-1 Vpu interference with CD1d recycling from endosomal compartments. Blood *116*, 1876–1884.

Monks, C.R.F., Freiberg, B.A., Kupfer, H., Sciaky, N., and Kupfer, A. (1998). Three-dimensional segregation of supramolecular activation clusters in T cells. Nature *395*, 82–86.

Monroe, K.M., Yang, Z., Johnson, J.R., Geng, X., Doitsh, G., Krogan, N.J., and Greene, W.C. (2014). IFI16 DNA sensor is required for death of lymphoid CD4 T cells abortively infected with HIV. Science *343*, 428–432.

Montefiori, D.C. (2009). Measuring HIV neutralization in a luciferase reporter gene assay. Methods in Molecular Biology *485*, 395–405.

Montefiori, D.C., Robinson, W.E., and Mitchell, W.M. (1988). Role of protein N-glycosylation in pathogenesis of human immunodeficieny virus type 1. Proceedings of the National Academy of Sciences of the United States of America *85*, 9248–9252.

Moore, J.P., McKeating, J.A., Weiss, R.A., and Sattentau, Q.J. (1990). Dissociation of gp120 from HIV-1 virions induced by soluble CD4. Science *250*, 1139–1142.

Moore, J.P., Kitchen, S.G., Pugach, P., and Zack, J.A. (2004). The CCR5 and CXCR4 Coreceptors - Central to Understanding the Transmission and Pathogenesis of Human Immunodeficiency Virus Type 1 Infection. AIDS Research and Human Retroviruses *20*, 111–126.

Moore, M.D., Nikolaitchik, O.A., Chen, J., Hammarskjöld, M.L., Rekosh, D., and Hu, W.S. (2009). Probing the HIV-1 genomic RNA trafficking pathway and dimerization by genetic recombination and single virion analyses. PLoS Pathogens *5*, e1000627.

Moore, P.L., Crooks, E.T., Porter, L., Zhu, P., Cayanan, C.S., Grise, H., Corcoran, P., Zwick, M.B., Franti, M., Morris, L., et al. (2006). Nature of Nonfunctional Envelope Proteins on the Surface of Human Immunodeficiency Virus Type 1. Journal of Virology *80*, 2515–2528.

Mora, A., Komander, D., van Aalten, D.M.F., and Alessi, D.R. (2004). PDK1, the master regulator of AGC kinase signal transduction. Seminars in Cell and Developmental Biology *15*, 161–170.

Morris, K.L., Buffalo, C.Z., Stürzel, C.M., Heusinger, E., Kirchhoff, F., Ren, X., and Hurley, J.H. (2018). HIV-1 Nefs Are Cargo-Sensitive AP-1 Trimerization Switches in Tetherin Downregulation. Cell *174*, 659-671.e14.

Motamedi, M., Xu, L., and Elahi, S. (2016). Correlation of transferrin receptor (CD71) with Ki67 expression on stimulated human and mouse T cells: The kinetics of expression of T cell activation markers. Journal of Immunological Methods *437*, 43–52.

Mourez, T., Simon, F., and Plantiera, J.C. (2013). Non-M variants of human immunodeficiency virus type. Clinical Microbiology Reviews *26*, 448–461.

Mücksch, F., Laketa, V., Müller, B., Schultz, C., and Kräusslich, H.G. (2017). Synchronized HIV assembly by tunable PIP2 changes reveals PIP2 requirement for stable gag anchoring. ELife *6*.

Münch, J., Stolte, N., Fuchs, D., Stahl-Hennig, C., and Kirchhoff, F. (2001). Efficient Class I Major Histocompatibility Complex Down-Regulation by Simian Immunodeficiency Virus Nef Is Associated with a Strong Selective Advantage in Infected Rhesus Macaques. Journal of Virology *75*, 10532–10536.

Munch, J., Schindler, M., Wildum, S., Rucker, E., Bailer, N., Knoop, V., Novembre, F.J., and Kirchhoff, F. (2005). Primary Sooty Mangabey Simian Immunodeficiency Virus and Human Immunodeficiency Virus Type 2 nef Alleles Modulate Cell Surface Expression of Various Human Receptors and Enhance Viral Infectivity and Replication. Journal of Virology *79*, 10547–10560.

Münch, J., Rajan, D., Schindler, M., Specht, A., Rücker, E., Novembre, F.J., Nerrienet, E., Müller-Trutwin, M.C., Peeters, M., Hahn, B.H., et al. (2007). Nef-mediated enhancement of virion infectivity and stimulation of viral replication are fundamental properties of primate lentiviruses. Journal of Virology *81*, 13852–13864.

Munro, J.B., Gorman, J., Ma, X., Zhou, Z., Arthos, J., Burton, D.R., Koff, W.C., Courter, J.R., Smith, A.B., Kwong, P.D., et al. (2014). Conformational dynamics of single HIV-1 envelope trimers on the surface of native virions. Science *346*, 759–763.

Murakami, T., and Freed, E.O. (2000a). The long cytoplasmic tail of gp41 is required in a cell type-dependent manner for HIV-1 envelope glycoprotein incorporation into virions. Proceedings of the National Academy of Sciences of the United States of America *97*, 343–348.

Murakami, T., and Freed, E.O. (2000b). Genetic Evidence for an Interaction between Human Immunodeficiency Virus Type 1 Matrix and α-Helix 2 of the gp41 Cytoplasmic Tail. Journal of Virology *74*, 3548–3554.

Muranyi, W., Malkusch, S., Müller, B., Heilemann, M., and Kräusslich, H.G. (2013). Super-Resolution Microscopy Reveals Specific Recruitment of HIV-1 Envelope Proteins to Viral Assembly Sites Dependent on the Envelope C-Terminal Tail. PLoS Pathogens *9*.

Murooka, T.T., Deruaz, M., Marangoni, F., Vrbanac, V.D., Seung, E., von Andrian, U.H., Tager, A.M., Luster, A.D., and Mempel, T.R. (2012). HIV-infected T cells are migratory vehicles for viral dissemination. Nature *490*, 283–289.

Murphey-Corb, M., Martin, L.N., Rangan, S.R.S., Baskin, G.B., Gormus, B.J., Wolf, R.H., Andes, W.A., West, M., and Montelaro, R.C. (1986). Isolation of an HTLV-III-related retrovirus from macaques with simian AIDS and its possible origin in asymptomatic mangabeys. Nature *321*, 435–437.

Naamati, A., Williamson, J.C., Greenwood, E.J.D., Marelli, S., Lehner, P.J., and Matheson, N.J. (2019). Functional proteomic atlas of HIV infection in primary human CD4+ T cells. ELife *8*.

Nasioulas, G., Zolotukhin, A.S., Tabernero, C., Solomin, L., Cunningham, C.P., Pavlakis, G.N., and Felber, B.K. (1994). Elements distinct from human immunodeficiency virus type 1 splice sites are responsible for the Rev dependence of env mRNA. Journal of Virology *68*, 2986–2993.

Navé, B.T., Ouwens, D.M., Withers, D.J., Alessi, D.R., and Shepherd, P.R. (1999). Mammalian target of rapamycin is a direct target for protein kinase B: Identification of a convergence point for opposing effects of insulin and amino-acid deficiency on protein translation. Biochemical Journal *344*, 427–431.

Neil, S.J.D., Zang, T., and Bieniasz, P.D. (2008). Tetherin inhibits retrovirus release and is antagonized by HIV-1 Vpu. Nature *451*, 425–430.

Nguyen, D.H., and Hildreth, J.E.K. (2000). Evidence for Budding of Human Immunodeficiency Virus Type 1 Selectively from Glycolipid-Enriched Membrane Lipid Rafts. Journal of Virology *74*, 3264–3272.

Nicholas Llewellyn, G., Hogue, I.B., Grover, J.R., and Ono, A. (2010). Nucleocapsid Promotes Localization of HIV-1 gag to uropods that participate in virological synapses between T Cells. PLoS Pathogens *6*.

Niederman, T.M.J., Hastings, W.R., Luria, S., Bandres, J.C., and Ratner, L. (1993). HIV-1 Nef protein inhibits the recruitment of AP-1 DNA-binding activity in human T-cells. Virology *194*, 338–344.

Nii, T., Segawa, H., Taketani, Y., Tani, Y., Ohkido, M., Kishida, S., Ito, M., Endou, H., Kanai, Y., Takeda, E., et al. (2001). Molecular events involved in up-regulating human Na+-independent neutral amino acid transporter LAT1 during T-cell activation. Biochemical Journal *358*, 693–704.

Nika, K., Soldani, C., Salek, M., Paster, W., Gray, A., Etzensperger, R., Fugger, L., Polzella, P., Cerundolo, V., Dushek, O., et al. (2010). Constitutively active lck kinase in T cells drives antigen receptor signal transduction. Immunity *32*, 766–777.

Nikolaitchik, O.A., Dilley, K.A., Fu, W., Gorelick, R.J., Tai, S.H.S., Soheilian, F., Ptak, R.G., Nagashima, K., Pathak, V.K., and Hu, W.S. (2013). Dimeric RNA Recognition Regulates HIV-1 Genome Packaging. PLoS Pathogens *9*, e1003249.

Nikolic, D.S., Lehmann, M., Felts, R., Garcia, E., Blanchet, F.P., Subramaniam, S., and Piguet, V. (2011). HIV-1 activates Cdc42 and induces membrane extensions in immature dendritic cells to facilitate cell-to-cell virus propagation. Blood *118*, 4841–4852.

Noviello, C.M., Benichou, S., and Guatelli, J.C. (2008). Cooperative Binding of the Class I Major Histocompatibility Complex Cytoplasmic Domain and Human Immunodeficiency Virus Type 1 Nef to the Endosomal AP-1 Complex via Its μ Subunit. Journal of Virology *82*, 1249–1258.

Nunn, M.F., and Marsh, J.W. (1996). Human immunodeficiency virus type 1 Nef associates with a member of the p21-activated kinase family. Journal of Virology *70*, 6157.

Nuvor, S.V., van der Sande, M., Rowland-Jones, S., Whittle, H., and Jaye, A. (2006). Natural Killer Cell Function Is Well Preserved in Asymptomatic Human Immunodeficiency Virus Type 2 (HIV-2) Infection but Similar to That of HIV-1 Infection When CD4 T-Cell Counts Fall. Journal of Virology *80*, 2529–2538.

Nyamweya, S., Hegedus, A., Jaye, A., Rowland-Jones, S., Flanagan, K.L., and Macallan, D.C. (2013). Comparing HIV-1 and HIV-2 infection: Lessons for viral immunopathogenesis. Reviews in Medical Virology *23*, 221–240.

Odorizzi, P.M., and Wherry, E.J. (2012). Inhibitory Receptors on Lymphocytes: Insights from Infections. The Journal of Immunology *188*, 2957–2965.

van Oers, N.S.C., Killeen, N., and Welss, A. (1994). ZAP-70 is constitutively associated with tyrosine-phosphorylated TCR ζ in murine thymocytes and lymph node T cells. Immunity *1*, 675–685.

van Oers, N.S.C., Killeen, N., and Weiss, A. (1996). Lck regulates the tyrosine phosphorylation of the T cell receptor subunits and ZAP-70 in murine thymocytes. Journal of Experimental Medicine *183*, 1053–1062.

Okoye, A., Meier-Schellersheim, M., Brenchley, J.M., Hagen, S.I., Walker, J.M., Rohankhedkar, M., Lum, R., Edgar, J.B., Planer, S.L., Legasse, A., et al. (2007). Progressive CD4+ central-memory T cell decline results in CD4+ effector-memory insufficiency and overt disease in chronic SIV infection. Journal of Experimental Medicine *204*, 2171–2185.

Olesen, J.S., Jespersen, S., da Silva, Z.J., Rodrigues, A., Erikstrup, C., Aaby, P., Wejse, C., and Hønge, B.L. (2018). HIV-2 continues to decrease, whereas HIV-1 is stabilizing in Guinea-Bissau. AIDS *32*, 1193–1198.

Olivieri, K.C., Mukerji, J., and Gabuzda, D. (2011). Nef-mediated enhancement of cellular activation and human immunodeficiency virus type 1 replication in primary T cells is dependent on association with p21-activated kinase 2. Retrovirology *8*, 64.

Önfelt, B., Nedvetzki, S., Yanagi, K., and Davis, D.M. (2004). Cutting Edge: Membrane Nanotubes Connect Immune Cells. The Journal of Immunology *173*, 1511–1513.

Ono, A., Ablan, S.D., Lockett, S.J., Nagashima, K., and Freed, E.O. (2004). Phosphatidylinositol (4,5) bisphosphate regulates HIV-1 Gag targeting to the plasma membrane. Proceedings of the National Academy of Sciences of the United States of America *101*, 14889–14894.

Ozorowski, G., Pallesen, J., de Val, N., Lyumkis, D., Cottrell, C.A., Torres, J.L., Copps, J., Stanfield, R.L., Cupo, A., Pugach, P., et al. (2017). Open and closed structures reveal allostery and pliability in the HIV-1 envelope spike. Nature *547*, 360–361.

Paiardini, M., Cervasi, B., Reyes-Aviles, E., Micci, L., Ortiz, A.M., Chahroudi, A., Vinton, C., Gordon, S.N., Bosinger, S.E., Francella, N., et al. (2011). Low levels of SIV infection in sooty mangabey central memory CD4+ T cells are associated with limited CCR5 expression. Nature Medicine *17*, 830–836.

Palesch, D., Bosinger, S.E., Tharp, G.K., Vanderford, T.H., Paiardini, M., Chahroudi, A., Johnson, Z.P., Kirchhoff, F., Hahn, B.H., Norgren, R.B., et al. (2018). Sooty mangabey genome sequence provides insight into AIDS resistance in a natural SIV host. Nature *553*, 77–81.

Palmer, C.S., Duette, G.A., Wagner, M.C.E., Henstridge, D.C., Saleh, S., Pereira, C., Zhou, J., Simar, D., Lewin, S.R., Ostrowski, M., et al. (2017). Metabolically active CD4+ T cells expressing Glut1 and OX40 preferentially harbor HIV during in vitro infection. FEBS Letters *591*, 3319–3332.

Pan, X., Rudolph, J.M., Abraham, L., Habermann, A., Haller, C., Krijnse-Locker, J., and Fackler, O.T. (2012). HIV-1 Nef compensates for disorganization of the immunological synapse by inducing trans-Golgi network-associated Lck signaling. Blood *119*, 786–797.

Pancera, M., Zhou, T., Druz, A., Georgiev, I.S., Soto, C., Gorman, J., Huang, J., Acharya, P., Chuang, G.Y., Ofek, G., et al. (2014). Structure and immune recognition of trimeric pre-fusion HIV-1 Env. Nature *514*, 455–461.

Pandrea, I., Apetrei, C., Gordon, S., Barbercheck, J., Dufour, J., Bohm, R., Sumpter, B., Roques, P., Marx, P.A., Hirsch, V.M., et al. (2007a). Paucity of CD4+CCR5+ T cells is a typical feature of natural SIV hosts. Blood *109*, 1069–1076.

Pandrea, I. v., Gautam, R., Ribeiro, R.M., Brenchley, J.M., Butler, I.F., Pattison, M., Rasmussen, T., Marx, P.A., Silvestri, G., Lackner, A.A., et al. (2007b). Acute Loss of Intestinal CD4 + T Cells Is Not Predictive of Simian Immunodeficiency Virus Virulence . The Journal of Immunology *179*, 3035–3046.

Panganiban, A.T., and Fiore, D. (1988). Ordered interstrand and intrastrand DNA transfer during reverse transcription. Science *241*, 1064–1069.

Pardons, M., Baxter, A.E., Massanella, M., Pagliuzza, A., Fromentin, R., Dufour, C., Leyre, L., Routy, J.P., Kaufmann, D.E., and Chomont, N. (2019). Single-cell characterization and quantification of translation-competent viral reservoirs in treated and untreated HIV infection. PLoS Pathogens *15*.

Park, J.J., Omiya, R., Matsumura, Y., Sakoda, Y., Kuramasu, A., Augustine, M.M., Yao, S., Tsushima, F., Narazaki, H., Anand, S., et al. (2010). B7-H1/CD80 interaction is required for the induction and maintenance of peripheral T-cell tolerance. Blood *116*, 1291–1298.

Parrish, N.F., Gao, F., Li, H., Giorgi, E.E., Barbian, H.J., Parrish, E.H., Zajic, L., Iyer, S.S., Decker, J.M., Kumar, A., et al. (2013). Phenotypic properties of transmitted founder HIV-1. Proceedings of the National Academy of Sciences of the United States of America *110*, 6626–6633.

Passos, V., Zillinger, T., Casartelli, N., Wachs, A.S., Xu, S., Malassa, A., Steppich, K., Schilling, H., Franz, S., Todt, D., et al. (2019). Characterization of Endogenous SERINC5 Protein as Anti-HIV-1 Factor. Journal of Virology *93*.

Peeters, M., and Courgnaud, V. (2003). 2 Primate Lentiviruses in Africa Overview of Primate Lentiviruses and Their Evolution in Non-human Primates in Africa.

Pelosi, M., di Bartolo, V., Mounier, V., Mège, D., Pascussi, J.M., Dufour, E., Blondel, A., and Acuto, O. (1999). Tyrosine 319 in the interdomain B of ZAP-70 is a binding site for the Src homology 2 domain of Lck. Journal of Biological Chemistry *274*, 14229–14237.

Pende, M., Um, S.H., Mieulet, V., Sticker, M., Goss, V.L., Mestan, J., Mueller, M., Fumagalli, S., Kozma, S.C., and Thomas, G. (2004). S6K1-/-/S6K2-/- Mice Exhibit Perinatal Lethality and Rapamycin-Sensitive 5'-Terminal Oligopyrimidine mRNA Translation and Reveal a Mitogen-Activated Protein Kinase-Dependent S6 Kinase Pathway. Molecular and Cellular Biology *24*, 3112–3124.

Peng, K., Muranyi, W., Glass, B., Laketa, V., Yant, S.R., Tsai, L., Cihlar, T., Müller, B., and Kräusslich, H.G. (2014). Quantitative microscopy of functional HIV post-entry complexes reveals association of replication with the viral capsid. ELife *3*, e04114.

Perez-Caballero, D., Zang, T., Ebrahimi, A., McNatt, M.W., Gregory, D.A., Johnson, M.C., and Bieniasz, P.D. (2009). Tetherin Inhibits HIV-1 Release by Directly Tethering Virions to Cells. Cell *139*, 499–511.

Pertel, T., Hausmann, S., Morger, D., Züger, S., Guerra, J., Lascano, J., Reinhard, C., Santoni, F.A., Uchil, P.D., Chatel, L., et al. (2011). TRIM5 is an innate immune sensor for the retrovirus capsid lattice. Nature *472*, 361–365.

Perugi, F., Muriaux, D., Ramirez, B.C., Chabani, S., Decroly, E., Darlix, J.L., Blot, V., and Pique, C. (2009). Human discs large is a new negative regulator of human immunodeficiency virus-1 infectivity. Molecular Biology of the Cell *20*, 498–508.

Peterson, K., and Rowland-Jones, S. (2012). Novel agents for the treatment of HIV-2 infection. Antiviral Therapy *17*, 435–438.

Pettit, S.C., Moody, M.D., Wehbie, R.S., Kaplan, A.H., Nantermet, P. v, Klein, C.A., and Swanstrom, R. (1994). The p2 domain of human immunodeficiency virus type 1 Gag regulates sequential proteolytic processing and is required to produce fully infectious virions. Journal of Virology *68*, 8017–8027.

Pezeshkian, N., Groves, N.S., and van Engelenburg, S.B. (2019). Single-molecule imaging of HIV-1 envelope glycoprotein dynamics and Gag lattice association exposes determinants responsible for virus incorporation. Proceedings of the National Academy of Sciences of the United States of America *116*, 25269–25277.

Pickering, S., Hué, S., Kim, E.Y., Reddy, S., Wolinsky, S.M., and Neil, S.J.D. (2014). Preservation of Tetherin and CD4 Counter-Activities in Circulating Vpu Alleles despite Extensive Sequence Variation within HIV-1 Infected Individuals. PLoS Pathogens *10*.

Pielak, R.M., O'Donoghue, G.P., Lin, J.J., Alfieri, K.N., Fay, N.C., Low-Nam, S.T., and Groves, J.T. (2017). Early T cell receptor signals globally modulate ligand: receptor affinities during antigen discrimination. Proceedings of the National Academy of Sciences of the United States of America *114*, 12190–12195.

Piguet, V., Gu, F., Foti, M., Demaurex, N., Gruenberg, J., Carpentier, J.L., and Trono, D. (1999). Nef-induced CD4 degradation: A diacidic-based motif in Nef functions as a lysosomal targeting signal through the binding of β-COP in endosomes. Cell *97*, 63–73.

Piguet, V., Wan, L., Borel, C., Mangasarian, A., Demaurex, N., Thomas, G., and Trono, D. (2000). HIV-1 Nef protein binds to the cellular protein PACS-1 to downregulate class I major histocompatibility complexes. Nature Cell Biology *2*, 163–167.

Pitcher, C., Höning, S., Fingerhut, A., Bowers, K., and Marsh, M. (1999). Cluster of differentiation antigen 4 (CD4) endocytosis and adaptor complex binding require activation of the CD4 endocytosis signal by serine phosphorylation. Molecular Biology of the Cell *10*, 677–691.

Pitman, M.C., Y Lau, J.S., McMahon, J.H., and Lewin, S.R. (2018). Review Barriers and strategies to achieve a cure for HIV.

Pizzato, M., Erlwein, O., Bonsall, D., Kaye, S., Muir, D., and McClure, M.O. (2009). A one-step SYBR Green I-based product-enhanced reverse transcriptase assay for the quantitation of retroviruses in cell culture supernatants. Journal of Virological Methods *156*, 1–7.

Plantier, J.C., Leoz, M., Dickerson, J.E., de Oliveira, F., Cordonnier, F., Lemée, V., Damond, F., Robertson, D.L., and Simon, F. (2009). A new human immunodeficiency virus derived from gorillas. Nature Medicine *15*, 871–872.

Pollpeter, D., Parsons, M., Sobala, A.E., Coxhead, S., Lang, R.D., Bruns, A.M., Papaioannou, S., McDonnell, J.M., Apolonia, L., Chowdhury, J.A., et al. (2018). Deep sequencing of HIV-1 reverse transcripts reveals the multifaceted antiviral functions of APOBEC3G. Nature Microbiology *3*, 220–233.

Poo, W.J., Conrad, L., and Janeway, C.A. (1988). Receptor-directed focusing of lymphokine release by helper T cells. Nature *332*, 378–380.

Pope, M., Betjes, M.G.H., Romani, N., Hirmand, H., Cameron, P.U., Hoffman, L., Gezelter, S., Schuler, G., and Steinman, R.M. (1994). Conjugates of dendritic cells and memory T lymphocytes from skin facilitate productive infection with HIV-1. Cell *78*, 389–398.

Popper, S.J., Sarr, A.D., Guèye-Ndiaye, A., Mboup, S., Essex, M.E., and Kanki, P.J. (2000). Low Plasma Human Immunodeficiency Virus Type 2 Viral Load Is Independent of Proviral Load: Low Virus Production In Vivo. Journal of Virology *74*, 1554–1557.

del Portillo, A., Tripodi, J., Najfeld, V., Wodarz, D., Levy, D.N., and Chen, B.K. (2011). Multiploid Inheritance of HIV-1 during Cell-to-Cell Infection. Journal of Virology *85*, 7169–7176.

Prévost, J., Richard, J., Medjahed, H., Alexander, A., Jones, J., Kappes, J.C., Ochsenbauer, C., and Finzi, A. (2018). Incomplete Downregulation of CD4 Expression Affects HIV-1 Env Conformation and Antibody-Dependent Cellular Cytotoxicity Responses. Journal of Virology *92*, e00484-18.

Price, A.J., Fletcher, A.J., Schaller, T., Elliott, T., Lee, K.E., KewalRamani, V.N., Chin, J.W., Towers, G.J., and James, L.C. (2012). CPSF6 Defines a Conserved Capsid Interface that Modulates HIV-1 Replication. PLoS Pathogens *8*, e1002896.

Price, A.J., Jacques, D.A., McEwan, W.A., Fletcher, A.J., Essig, S., Chin, J.W., Halambage, U.D., Aiken, C., and James, L.C. (2014). Host Cofactors and Pharmacologic Ligands Share an Essential Interface in HIV-1 Capsid That Is Lost upon Disassembly. PLoS Pathogens *10*, e1004459.

Pye, V.E., Rosa, A., Bertelli, C., Struwe, W.B., Maslen, S.L., Corey, R., Liko, I., Hassall, M., Mattiuzzo, G., Ballandras-Colas, A., et al. (2020). A bipartite structural organization defines the SERINC family of HIV-1 restriction factors. Nature Structural and Molecular Biology *27*, 78–83.

Qi, M., Williams, J.A., Chu, H., Chen, X., Wang, J.J., Ding, L., Akhirome, E., Wen, X., Lapierre, L.A., Goldenring, J.R., et al. (2013). Rab11-FIP1C and Rab14 Direct Plasma Membrane Sorting and Particle Incorporation of the HIV-1 Envelope Glycoprotein Complex. PLoS Pathogens *9*.

Qi, M., Chu, H., Chen, X., Choi, J., Wen, X., Hammonds, J., Ding, L., Hunter, E., and Spearman, P. (2015). A tyrosine-based motif in the HIV-1 envelope glycoprotein tail mediates cell-type- and Rab11-FIP1C-dependent incorporation into virions. Proceedings of the National Academy of Sciences of the United States of America *112*, 7575–7580.

Quintana, A., Schwindling, C., Wenning, A.S., Becherer, U., Rettig, J., Schwarz, E.C., and Hoth, M. (2007). T cell activation requires mitochondrial translocation to the immunological synapse. Proceedings of the National Academy of Sciences of the United States of America *104*, 14418–14423.

Ramming, A., Thümmler, K., Schulze-Koops, H., and Skapenko, A. (2009). Homotypic T-cell/T-cell interaction induces T-cell activation, proliferation, and differentiation. Human Immunology *70*, 873–881.

Ramsay, G., and Cantrell, D. (2015). Environmental and metabolic sensors that control T cell biology. Frontiers in Immunology *6*.

Rankovic, S., Varadarajan, J., Ramalho, R., Aiken, C., and Rousso, I. (2017). Reverse Transcription Mechanically Initiates HIV-1 Capsid Disassembly. Journal of Virology *91*.

Rasaiyaah, J., Tan, C.P., Fletcher, A.J., Price, A.J., Blondeau, C., Hilditch, L., Jacques, D.A., Selwood, D.L., James, L.C., Noursadeghi, M., et al. (2013). HIV-1 evades innate immune recognition through specific cofactor recruitment. Nature *503*, 402–405.

Rato, S., Rausell, A., Muñoz, M., Telenti, A., and Ciuffi, A. (2017). Single-cell analysis identifies cellular markers of the HIV permissive cell. PLOS Pathogens *13*, e1006678.

Rey-Cuillé, M.A., Berthier, J.L., Bomsel-Demontoy, M.C., Chaduc, Y., Montagnier, L., Hovanessian, A.G., and Chakrabarti, L.A. (1998). Simian immunodeficiency virus replicates to high levels in sooty mangabeys without inducing disease. Journal of Virology *72*, 3872–3886.

Richardson, M.W., Carroll, R.G., Stremlau, M., Korokhov, N., Humeau, L.M., Silvestri, G., Sodroski, J., and Riley, J.L. (2008). Mode of Transmission Affects the Sensitivity of Human Immunodeficiency Virus Type 1 to Restriction by Rhesus TRIM5α. Journal of Virology *82*, 11117–11128.

Riddick, N.E., Hermann, E.A., Loftin, L.M., Elliott, S.T., Wey, W.C., Cervasi, B., Taaffe, J., Engram, J.C., Li, B., Else, J.G., et al. (2010). A Novel CCR5 Mutation Common in Sooty Mangabeys Reveals SIVsmm Infection of CCR5-Null Natural Hosts and Efficient Alternative Coreceptor Use In Vivo. PLoS Pathogens *6*, e1001064.

Rittner, K., Churcher, M.J., Gait, M.J., and Karn, J. (1995). The human immunodeficiency virus long terminal repeat includes a specialised initiator element which is required for tat-responsive transcription. Journal of Molecular Biology *248*, 562–580.

Robb, M.L., Rerks-Ngarm, S., Nitayaphan, S., Pitisuttithum, P., Kaewkungwal, J., Kunasol, P., Khamboonruang, C., Thongcharoen, P., Morgan, P., Benenson, M., et al. (2012). Risk behaviour and time as covariates for efficacy of the HIV vaccine regimen ALVAC-HIV (vCP1521) and AIDSVAX B/E: A post-hoc analysis of the Thai phase 3 efficacy trial RV 144. The Lancet Infectious Diseases *12*, 531–537.

Robb, R.J., Munck, A., and Smith, K.A. (1981). T cell growth factor receptors: Quantitation, specificity, and biological relevance. Journal of Experimental Medicine *154*, 1455–1474.

Robbez-Masson, L., Tie, C.H.C., Conde, L., Tunbak, H., Husovsky, C., Tchasovnikarova, I.A., Timms, R.T., Herrero, J., Lehner, P.J., and Rowe, H.M. (2018). The hush complex cooperates with trim28 to repress young retrotransposons and new genes. Genome Research *28*, 836–845.

Rodriguez, S.K., Sarr, A.D., MacNeil, A., Thakore-Meloni, S., Gueye-Ndiaye, A., Traoré, I., Dia, M.C., Mboup, S., and Kanki, P.J. (2007). Comparison of Heterologous Neutralizing Antibody Responses of Human Immunodeficiency Virus Type 1 (HIV-1)- and HIV-2-Infected Senegalese Patients: Distinct Patterns of Breadth and Magnitude Distinguish HIV-1 and HIV-2 Infections. Journal of Virology *81*, 5331–5338.

Roeth, J.F., Kasper, M.R., Filzen, T.M., and Collins, K.L. (2004). HIV-1 Nef disrupts MHC-I trafficking by recruiting AP-1 to the MHC-I cytoplasmic tail. Journal of Cell Biology *167*, 903–913.

Romani, B., Baygloo, N.S., Aghasadeghi, M.R., and Allahbakhshi, E. (2015). HIV-1 Vpr protein enhances proteasomal degradation of MCM10 DNA replication factor through the Cul4-DDB1[VprBP] E3 ubiquitin ligase to induce G2/M cell cycle arrest. Journal of Biological Chemistry *290*, 17380–17389.

Rosa, A., Chande, A., Ziglio, S., de Sanctis, V., Bertorelli, R., Goh, S.L., McCauley, S.M., Nowosielska, A., Antonarakis, S.E., Luban, J., et al. (2015). HIV-1 Nef promotes infection by excluding SERINC5 from virion incorporation. Nature *526*, 212–217.

Rosen, O., Sharon, M., Quadt-Akabayov, S.R., and Anglister, J. (2006). Molecular switch for alternative conformations of the HIV-1 V3 region: Implications for phenotype conversion.

Proceedings of the National Academy of Sciences of the United States of America *103*, 13950–13955.

Ross, T.M., Oran, A.E., and Cullen, B.R. (1999). Inhibition of HIV-1 progeny virion release by cell-surface CD4 is relieved by expression of the viral Nef protein. Current Biology *9*, 613–621.

Roux, P.P., Shahbazian, D., Vu, H., Holz, M.K., Cohen, M.S., Taunton, J., Sonenberg, N., and Blenis, J. (2007). RAS/ERK signaling promotes site-specific ribosomal protein S6 phosphorylation via RSK and stimulates cap-dependent translation. Journal of Biological Chemistry *282*, 14056–14064.

le Rouzic, E., Belaïdouni, N., Estrabaud, E., Morel, M., Rain, J.C., Transy, C., and Margottin-Goguet, F. (2007). HIV1 Vpr arrests the cell cycle by recruiting DCAF1/VprBP, a receptor of the Cul4-DDB1 ubiquitin ligase. Cell Cycle *6*, 182–188.

Roy, N.H., Lambele, M., Chan, J., Symeonides, M., and Thali, M. (2014). Ezrin Is a Component of the HIV-1 Virological Presynapse and Contributes to the Inhibition of Cell-Cell Fusion. Journal of Virology *88*, 7645–7658.

Rudd, C.E., Taylor, A., and Schneider, H. (2009). CD28 and CTLA-4 coreceptor expression and signal transduction. Immunological Reviews *229*, 12–26.

Rudnicka, D., Feldmann, J., Porrot, F., Wietgrefe, S., Guadagnini, S., Prévost, M.-C., Estaquier, J., Haase, A.T., Sol-Foulon, N., and Schwartz, O. (2009). Simultaneous Cell-to-Cell Transmission of Human Immunodeficiency Virus to Multiple Targets through Polysynapses. Journal of Virology *83*, 6234–6246.

Rudolph, J.M., Eickel, N., Haller, C., Schindler, M., and Fackler, O.T. (2009). Inhibition of T-Cell Receptor-Induced Actin Remodeling and Relocalization of Lck Are Evolutionarily Conserved Activities of Lentiviral Nef Proteins. Journal of Virology *83*, 11528–11539.

Russell, R.A., Martin, N., Mitar, I., Jones, E., and Sattentau, Q.J. (2013). Multiple proviral integration events after virological synapse-mediated HIV-1 spread. Virology *443*, 143–149.

Saad, J.S., Miller, J., Tai, J., Kim, A., Ghanam, R.H., and Summers, M.F. (2006). Structural basis for targeting HIV-1 Gag proteins to the plasma membrane for virus assembly. Proceedings of the National Academy of Sciences of the United States of America *103*, 11364–11369.

Sabatos, C.A., Doh, J., Chakravarti, S., Friedman, R.S., Pandurangi, P.G., Tooley, A.J., and Krummel, M.F. (2008). A Synaptic Basis for Paracrine Interleukin-2 Signaling during Homotypic T Cell Interaction. Immunity *29*, 238–248.

Sabin, C., Corti, D., Buzon, V., Seaman, M.S., Hulsik, D.L., Hinz, A., Vanzetta, F., Agatic, G., Silacci, C., Mainetti, L., et al. (2010). Crystal structure and size-dependent neutralization properties of HK20, a human monoclonal antibody binding to the highly conserved heptad repeat 1 of gp41. PLoS Pathogens *6*.

Saenz, D.T., Loewen, N., Peretz, M., Whitwam, T., Barraza, R., Howell, K.G., Holmes, J.M., Good, M., and Poeschla, E.M. (2004). Unintegrated Lentivirus DNA Persistence and Accessibility to Expression in Nondividing Cells: Analysis with Class I Integrase Mutants. Journal of Virology *78*, 2906–2920.

Sakai, Y., Doi, N., Miyazaki, Y., Adachi, A., and Nomaguchi, M. (2016). Phylogenetic insights into the functional relationship between primate lentiviral reverse transcriptase and accessory proteins Vpx/Vpr. Frontiers in Microbiology *7*.

Saksela, K., Cheng, G., and Baltimore, D. (1995). Proline-rich (PxxP) motifs in HIV-1 Nef bind to SH3 domains of a subset of Src kinases and are required for the enhanced growth of Nef+ viruses but not for down-regulation of CD4. The EMBO Journal *14*, 484–491.

Sakuma, T., Noda, T., Urata, S., Kawaoka, Y., and Yasuda, J. (2009). Inhibition of Lassa and Marburg Virus Production by Tetherin. Journal of Virology *83*, 2382–2385.

Salazar-Gonzalez, J.F., Salazar, M.G., Keele, B.F., Learn, G.H., Giorgi, E.E., Li, H., Decker, J.M., Wang, S., Baalwa, J., Kraus, M.H., et al. (2009). Genetic identity, biological phenotype, and evolutionary pathways of transmitted/founder viruses in acute and early HIV-1 infection. Journal of Experimental Medicine *206*, 1273–1289.

Sanders, R.W., and Moore, J.P. (2017). Native-like Env trimers as a platform for HIV-1 vaccine design. Immunological Reviews *275*, 161–182.

Sandgren, K.J., Smed-Sörensen, A., Forsell, M.N., Soldemo, M., Adams, W.C., Liang, F., Perbeck, L., Koup, R.A., Wyatt, R.T., Karlsson Hedestam, G.B., et al. (2013). Human Plasmacytoid Dendritic Cells Efficiently Capture HIV-1 Envelope Glycoproteins via CD4 for Antigen Presentation. The Journal of Immunology *191*, 60–69.

Saphire, A.C.S., Bobardt, M.D., Zhang, Z., David, G., and Gallay, P.A. (2001). Syndecans Serve as Attachment Receptors for Human Immunodeficiency Virus Type 1 on Macrophages. Journal of Virology *75*, 9187–9200.

Sato, H., Orensteint, J., Dimitrov, D., and Martin, M. (1992). Cell-to-cell spread of HIV-1 occurs within minutes and may not involve the participation of virus particles. Virology *186*, 712–724.

Sattentau, Q. (2008). Avoiding the void: cell-to-cell spread of human viruses. Nature Reviews Microbiology *6*, 815–826.

Sauter, D., and Kirchhoff, F. (2014). Properties of Human and Simian Immunodeficiency Viruses. In Natural Hosts of SIV: Implication in AIDS, (Elsevier Inc.), pp. 69–84.

Sauter, D., and Kirchhoff, F. (2019). Key Viral Adaptations Preceding the AIDS Pandemic. Cell Host and Microbe *25*, 27–38.

Sauter, D., Schindler, M., Specht, A., Landford, W.N., Münch, J., Kim, K.A., Votteler, J., Schubert, U., Bibollet-Ruche, F., Keele, B.F., et al. (2009). Tetherin-Driven Adaptation of Vpu and Nef Function and the Evolution of Pandemic and Nonpandemic HIV-1 Strains. Cell Host and Microbe *6*, 409–421.

Sauter, D., Hotter, D., Van Driessche, B., Stürzel, C.M., Kluge, S.F., Wildum, S., Yu, H., Baumann, B., Wirth, T., Plantier, J.-C., et al. (2015). Differential Regulation of NF-κB-Mediated Proviral and Antiviral Host Gene Expression by Primate Lentiviral Nef and Vpu Proteins. Cell Reports *10*, 586–599.

Schacker, T., Collier, A.C., Hughes, J., Shea, T., and Corey, L. (1996). Annals of Internal Medicine: Clinical and Epidemiologic Features of Primary HIV Infection. Annals of Internal Medicine *125*, 257–264.

Schacker, T., Little, S., Connick, E., Gebhard-Mitchell, K., Zhang, Z., Krieger, J., Pryor, J., Havlir, D., Wong, J.K., Richman, D., et al. (2000). Rapid Accumulation of Human Immunodeficiency Virus (HIV) in Lymphatic Tissue Reservoirs during Acute and Early HIV Infection: Implications for Timing of Antiretroviral Therapy. The Journal of Infectious Diseases *181*, 354–357.

Schacker, T., Little, S., Connick, E., Gebhard, K., Zhang, Z., Krieger, J., Pryor, J., Havlir, D., Wong, J.K., Schooley, R.T., et al. (2001). Productive Infection of T Cells in Lymphoid Tissues

during Primary and Early Human Immunodeficiency Virus Infection. The Journal of Infectious Diseases *183*, 555–562.

Schaefer, T.M., Bell, I., Fallert, B.A., and Reinhart, T.A. (2000). The T-Cell Receptor ζ Chain Contains Two Homologous Domains with Which Simian Immunodeficiency Virus Nef Interacts and Mediates Down-Modulation. Journal of Virology *74*, 3273–3283.

Schaller, T., Ocwieja, K.E., Rasaiyaah, J., Price, A.J., Brady, T.L., Roth, S.L., Hué, S., Fletcher, A.J., Lee, K.E., KewalRamani, V.N., et al. (2011). HIV-1 capsid-cyclophilin interactions determine nuclear import pathway, integration targeting and replication efficiency. PLoS Pathogens *7*.

Schindler, M., Münch, J., Kutsch, O., Li, H., Santiago, M.L., Bibollet-Ruche, F., Müller-Trutwin, M.C., Novembre, F.J., Peeters, M., Courgnaud, V., et al. (2006). Nef-Mediated Suppression of T Cell Activation Was Lost in a Lentiviral Lineage that Gave Rise to HIV-1. Cell *125*, 1055–1067.

Schindler, M., Schmökel, J., Specht, A., Li, H., Münch, J., Khalid, M., Sodora, D.L., Hahn, B.H., Silvestri, G., and Kirchhoff, F. (2008). Inefficient Nef-Mediated Downmodulation of CD3 and MHC-I Correlates with Loss of CD4+ T Cells in Natural SIV Infection. PLoS Pathogens *4*, e1000107.

Schmökel, J., Li, H., Shabir, A., Yu, H., Geyer, M., Silvestri, G., Sodora, D.L., Hahn, B.H., and Kirchhoff, F. (2013). Link between primate lentiviral coreceptor usage and Nef function. Cell Reports *5*, 997–1009.

Schneider, U., Schwenk, H. -U, and Bornkamm, G. (1977). Characterization of EBV-genome negative “null” and “T” cell lines derived from children with acute lymphoblastic leukemia and leukemic transformed non-Hodgkin lymphoma. International Journal of Cancer *19*, 621–626.

Schoenborn, J.R., Tan, Y.X., Zhang, C., Shokat, K.M., and Weiss, A. (2011). Feedback circuits monitor and adjust basal Lck-dependent events in T cell receptor signaling. Science Signaling *4*, ra59–ra59.

Schoggins, J.W., Wilson, S.J., Panis, M., Murphy, M.Y., Jones, C.T., Bieniasz, P., and Rice, C.M. (2011). A diverse range of gene products are effectors of the type i interferon antiviral response. Nature *472*, 481–485.

Schrager, J.A., and Marsh, J.W. (1999). HIV-1 Nef increases T cell activation in a stimulus-dependent manner. Proceedings of the National Academy of Sciences of the United States of America *96*, 8167–8172.

Schröfelbauer, B., Yu, Q., Zeitlin, S.G., and Landau, N.R. (2005). Human Immunodeficiency Virus Type 1 Vpr Induces the Degradation of the UNG and SMUG Uracil-DNA Glycosylases. Journal of Virology *79*, 10978–10987.

Schubert, U., Henklein, P., Boldyreff, B., Wingender, E., Strebel, K., and Porstmann, T. (1994). The human immunodeficiency virus type 1 encoded Vpu protein is phosphorylated by casein kinase-2 (CK-2) at positions ser52 and ser56 within a predicted α-helix-turn-α-helix-motif. Journal of Molecular Biology *236*, 16–25.

Schubert, U., Clouse, K.A., and Strebel, K. (1995). Augmentation of virus secretion by the human immunodeficiency virus type 1 Vpu protein is cell type independent and occurs in cultured human primary macrophages and lymphocytes. Journal of Virology *69*, 7699–7711.

Schubert, U., Antón, L.C., Bačík, I., Cox, J.H., Bour, S., Bennink, J.R., Orlowski, M., Strebel, K., and Yewdell, J.W. (1998). CD4 Glycoprotein Degradation Induced by Human Immunodeficiency Virus Type 1 Vpu Protein Requires the Function of Proteasomes and the Ubiquitin-Conjugating Pathway. Journal of Virology *72*, 2280–2288.

Schulte, B., Buffone, C., Opp, S., di Nunzio, F., de Souza Aranha Vieira, D.A., Brandariz-Nuñez, A., and Diaz-Griffero, F. (2015). Restriction of HIV-1 Requires the N-Terminal Region of MxB as a Capsid-Binding Motif but Not as a Nuclear Localization Signal. Journal of Virology *89*, 8599–8610.

Schulte, B., Selyutina, A., Opp, S., Herschhorn, A., Sodroski, J.G., Pizzato, M., and Diaz-Griffero, F. (2018). Localization to detergent-resistant membranes and HIV-1 core entry inhibition correlate with HIV-1 restriction by SERINC5. Virology *515*, 52–65.

Schwartz, O., Maréchal, V., le Gall, S., Lemonnier, F., and Heard, J.M. (1996). Endocytosis of major histocompatibility complex class I molecules is induced by the HIV-1 Nef protein. Nature Medicine *2*, 338–342.

Schwartz, S., Felber, B.K., Fenyö, E.M., and Pavlakis, G.N. (1990). Env and Vpu proteins of human immunodeficiency virus type 1 are produced from multiple bicistronic mRNAs. Journal of Virology *64*, 5448–5456.

Schwefel, D., Groom, H.C.T., Boucherit, V.C., Christodoulou, E., Walker, P.A., Stoye, J.P., Bishop, K.N., and Taylor, I.A. (2014). Structural basis of lentiviral subversion of a cellular protein degradation pathway. Nature *505*, 234–238.

Seddon, B., Legname, G., Tomlinson, P., and Zamoyska, R. (2000). Long-term survival but impaired homeostatic proliferation of naive T cells in the absence of p56(lck). Science *290*, 127–131.

Selig, L., Pages, J.-C., Tanchou, V., Prévéral, S., Berlioz-Torrent, C., Liu, L.X., Erdtmann, L., Darlix, J.-L., Benarous, R., and Benichou, S. (1999). Interaction with the p6 Domain of the Gag Precursor Mediates Incorporation into Virions of Vpr and Vpx Proteins from Primate Lentiviruses. Journal of Virology *73*, 592–600.

Serra-Moreno, R., Zimmermann, K., Stern, L.J., and Evans, D.T. (2013). Tetherin/BST-2 Antagonism by Nef Depends on a Direct Physical Interaction between Nef and Tetherin, and on Clathrin-mediated Endocytosis. PLoS Pathogens *9*.

Sewald, X., Gonzalez, D.G., Haberman, A.M., and Mothes, W. (2012). In vivo imaging of virological synapses. Nature Communications *3*.

Sewald, X., Ladinsky, M.S., Uchil, P.D., Beloor, J., Pi, R., Herrmann, C., Motamedi, N., Murooka, T.T., Brehm, M.A., Greiner, D.L., et al. (2015). Retroviruses use CD169-mediated trans-infection of permissive lymphocytes to establish infection. Science *350*, 563–567.

Shah, A.H., Sowrirajan, B., Davis, Z.B., Ward, J.P., Campbell, E.M., Planelles, V., and Barker, E. (2010). Degranulation of natural killer cells following interaction with HIV-1-infected cells is hindered by downmodulation of NTB-A by Vpu. Cell Host and Microbe *8*, 397–409.

Shaik, M.M., Peng, H., Lu, J., Rits-Volloch, S., Xu, C., Liao, M., and Chen, B. (2019). Structural basis of coreceptor recognition by HIV-1 envelope spike. Nature *565*, 318–323.

Shan, L., Deng, K., Gao, H., Xing, S., Capoferri, A.A., Durand, C.M., Rabi, S.A., Laird, G.M., Kim, M., Hosmane, N.N., et al. (2017). Transcriptional Reprogramming during Effector-to-Memory Transition Renders CD4+ T Cells Permissive for Latent HIV-1 Infection. Immunity *47*, 766-775.e3.

Sharova, N., Swingler, C., Sharkey, M., and Stevenson, M. (2005). Macrophages archive HIV-1 virions for dissemination in trans. EMBO Journal *24*, 2481–2489.

Sharp, P.M., and Hahn, B.H. (2011). Origins of HIV and the AIDS pandemic. Cold Spring Harbor Perspectives in Medicine *1*.

Shaw, G.M., and Hunter, E. (2012). HIV transmission. Cold Spring Harbor Perspectives in Medicine *2*.

Shaw, J.P., Utz, P.J., Durand, D.B., Toole, J.J., Emmel, E.A., and Crabtree, G.R. (2010). Identification of a putative regulator of early T cell activation genes. Journal of Immunology *185*, 4972–4975.

Sheehy, A.M., Gaddis, N.C., Choi, J.D., and Malim, M.H. (2002). Isolation of a human gene that inhibits HIV-1 infection and is suppressed by the viral Vif protein. Nature *418*, 646–650.

Sheehy, A.M., Gaddis, N.C., and Malim, M.H. (2003). The antiretroviral enzyme APOBEC3G is degraded by the proteasome in response to HIV-1 Vif. Nature Medicine *9*, 1404–1407.

Sherer, N.M., Lehmann, M.J., Jimenez-Soto, L.F., Horensavitz, C., Pypaert, M., and Mothes, W. (2007). Retroviruses can establish filopodial bridges for efficient cell-to-cell transmission. Nature Cell Biology *9*, 310–315.

Shi, J., Xiong, R., Zhou, T., Su, P., Zhang, X., Qiu, X., Li, H., Li, S., Yu, C., Wang, B., et al. (2018). HIV-1 Nef Antagonizes SERINC5 Restriction by Downregulation of SERINC5 via the Endosome/Lysosome System. Journal of Virology *92*.

Shi, Y., Brandin, E., Vincic, E., Jansson, M., Blaxhult, A., Glyllensten, K., Moberg, L., Broström, C., Fenyö, E.M., and Albert, J. (2005). Evolution of human immunodeficiency virus type 2 coreceptor usage, autologous neutralization, envelope sequence and glycosylation. Journal of General Virology *86*, 3385–3396.

Sigal, A., Kim, J.T., Balazs, A.B., Dekel, E., Mayo, A., Milo, R., and Baltimore, D. (2011). Cell-to-cell spread of HIV permits ongoing replication despite antiretroviral therapy. Nature *477*, 95–99.

Silvestri, G., Sodora, D.L., Koup, R.A., Paiardini, M., O'Neil, S.P., McClure, H.M., Staprans, S.I., and Feinberg, M.B. (2003a). Nonpathogenic SIV Infection of Sooty Mangabeys Is Characterized by Limited Bystander Immunopathology Despite Chronic High-Level Viremia. Immunity *18*, 441–452.

Silvestri, G., Sodora, D.L., Koup, R.A., Paiardini, M., O'Neil, S.P., McClure, H.M., Staprans, S.I., and Feinberg, M.B. (2003b). Nonpathogenic SIV infection of sooty mangabeys is characterized by limited bystander immunopathology despite chronic high-level viremia. Immunity *18*, 441–452.

Simon, F., Mauclère, P., Roques, P., Loussert-Ajaka, I., Müller-Trutwin, M.C., Saragosti, S., Georges-Courbot, M.C., Barré-Sinoussi, F., and Brun-VÉZINET, F. (1998). Identification of a new human immunodeficiency virus type 1 distinct from group M and group O. Nature Medicine *4*, 1032–1037.

Sims, T.N., Soos, T.J., Xenias, H.S., Dubin-Thaler, B., Hofman, J.M., Waite, J.C., Cameron, T.O., Thomas, V.K., Varma, R., Wiggins, C.H., et al. (2007). Opposing Effects of PKCθ and WASp on Symmetry Breaking and Relocation of the Immunological Synapse. Cell *129*, 773–785.

Sinclair, L. v., Rolf, J., Emslie, E., Shi, Y.B., Taylor, P.M., and Cantrell, D.A. (2013). Control of amino-acid transport by antigen receptors coordinates the metabolic reprogramming essential for T cell differentiation. Nature Immunology *14*, 500–508.

Smalls-Mantey, A., Connors, M., and Sattentau, Q.J. (2013). Comparative Efficiency of HIV-1-Infected T Cell Killing by NK Cells, Monocytes and Neutrophils. PLoS ONE *8*.

Smed-Sörensen, A., Loré, K., Vasudevan, J., Louder, M.K., Andersson, J., Mascola, J.R., Spetz, A.-L., and Koup, R.A. (2005). Differential Susceptibility to Human Immunodeficiency Virus Type 1 Infection of Myeloid and Plasmacytoid Dendritic Cells. Journal of Virology *79*, 8861–8869.

Sodora, D.L., Allan, J.S., Apetrei, C., Brenchley, J.M., Douek, D.C., Else, J.G., Estes, J.D., Hahn, B.H., Hirsch, V.M., Kaur, A., et al. (2009). Toward an AIDS vaccine: Lessons from natural simian immunodeficiency virus infections of African nonhuman primate hosts. Nature Medicine *15*, 861–865.

Soede, R.D.M., Wijnands, Y.M., van Kouteren-Cobzaru, I., and Roos, E. (1998). ZAP-70 tyrosine kinase is required for LFA-1-dependent T cell migration. Journal of Cell Biology *142*, 1371–1379.

Sokolskaja, E., Sayah, D.M., and Luban, J. (2004). Target Cell Cyclophilin A Modulates Human Immunodeficiency Virus Type 1 Infectivity. Journal of Virology *78*, 12800–12808.

Sol-Foulon, N., Sourisseau, M., Porrot, F., Thoulouze, M.I., Trouillet, C., Nobile, C., Blanchet, F., di Bartolo, V., Noraz, N., Taylor, N., et al. (2007). ZAP-70 kinase regulates HIV cell-to-cell spread and virological synapse formation. EMBO Journal *26*, 516–526.

Sood, C., Marin, M., Chande, A., Pizzato, M., and Melikyan, G.B. (2017). SERINC5 protein inhibits HIV-1 fusion pore formation by promoting functional inactivation of envelope glycoproteins. Journal of Biological Chemistry *292*, 6014–6026.

Soriano, V., Gomes, P., Heneine, W., Holguín, A., Doruana, M., Antunes, R., Mansinho, K., Switzer, W.M., Araujo, C., Shanmugam, V., et al. (2000). Human immunodeficiency virus type 2 (HIV-2) in Portugal: Clinical spectrum, circulating subtypes, virus isolation, and plasma viral load. Journal of Medical Virology *61*, 111–116.

Sourisseau, M., Sol-Foulon, N., Porrot, F., Blanchet, F., and Schwartz, O. (2007). Inefficient human immunodeficiency virus replication in mobile lymphocytes. Journal of Virology *81*, 1000–1012.

Sousa, A.E., Carneiro, J., Meier-Schellersheim, M., Grossman, Z., and Victorino, R.M.M. (2002). CD4 T Cell Depletion Is Linked Directly to Immune Activation in the Pathogenesis of HIV-1 and HIV-2 but Only Indirectly to the Viral Load. The Journal of Immunology *169*, 3400–3406.

Sowinski, S., Jolly, C., Berninghausen, O., Purbhoo, M.A., Chauveau, A., Köhler, K., Oddos, S., Eissmann, P., Brodsky, F.M., Hopkins, C., et al. (2008). Membrane nanotubes physically connect T cells over long distances presenting a novel route for HIV-1 transmission. Nature Cell Biology *10*, 211–219.

Srivastava, S., Swanson, S.K., Manel, N., Florens, L., Washburn, M.P., and Skowronski, J. (2008). Lentiviral Vpx accessory factor targets VprBP/DCAF1 substrate adaptor for cullin 4 E3 ubiquitin ligase to enable macrophage infection. PLoS Pathogens *4*.

Starling, S., and Jolly, C. (2016). LFA-1 Engagement Triggers T Cell Polarization at the HIV-1 Virological Synapse. Journal of Virology *90*, 9841–9854.

Stevenson, M., Stanwick, T.L., Dempsey, M.P., and Lamonica, C.A. (1990). HIV-1 replication is controlled at the level of T cell activation and proviral integration. The EMBO Journal *9*, 1551–1560.

van Stigt Thans, T., Akko, J.I., Niehrs, A., Garcia-Beltran, W.F., Richert, L., Stürzel, C.M., Ford, C.T., Li, H., Ochsenbauer, C., Kappes, J.C., et al. (2019). Primary HIV-1 Strains Use Nef To Downmodulate HLA-E Surface Expression. Journal of Virology *93*.

Stokoe, D., Stephens, L.R., Copeland, T., Gaffney, P.R.J., Reese, C.B., Painter, G.F., Holmes, A.B., McCormick, F., and Hawkins, P.T. (1997). Dual role of phosphatidylinositol-3,4,5-trisphosphate in the activation of protein kinase B. Science *277*, 567–570.

Stolp, B., Reichman-Fried, M., Abraham, L., Pan, X., Giese, S.I., Hannemann, S., Goulimari, P., Raz, E., Grosse, R., and Fackler, O.T. (2009). HIV-1 Nef Interferes with Host Cell Motility by Deregulation of Cofilin. Cell Host and Microbe *6*, 174–186.

Stolp, B., Abraham, L., Rudolph, J.M., and Fackler, O.T. (2010). Lentiviral Nef Proteins Utilize PAK2-Mediated Deregulation of Cofilin as a General Strategy To Interfere with Actin Remodeling. Journal of Virology *84*, 3935–3948.

Stopak, K., de Noronha, C., Yonemoto, W., and Greene, W.C. (2003). HIV-1 Vif blocks the antiviral activity of APOBEC3G by impairing both its translation and intracellular stability. Molecular Cell *12*, 591–601.

Stover, M.G., and Watson, R.R. (2015). Animal Lentiviruses: Models for Human Immunodeficiency Viruses and Nutrition. In Health of HIV Infected People: Food, Nutrition and Lifestyle without Antiretroviral Drugs, (Elsevier Inc.), pp. 349–365.

Straus, D.B., and Weiss, A. (1992). Genetic evidence for the involvement of the lck tyrosine kinase in signal transduction through the T cell antigen receptor. Cell *70*, 585–593.

Stremlau, M., Owens, C.M., Perron, M.J., Kiessling, M., Autissier, P., and Sodroski, J. (2004). The cytoplasmic body component TRIM5α restricts HIV-1 infection in Old World monkeys. Nature *427*, 848–853.

Stremlau, M., Perron, M., Lee, M., Li, Y., Song, B., Javanbakht, H., Diaz-Griffero, F., Anderson, D.J., Sundquist, W.I., and Sodroski, J. (2006). Specific recognition and accelerated uncoating of retroviral capsids by the TRIM5α restriction factor. Proceedings of the National Academy of Sciences of the United States of America *103*, 5514–5519.

Sugden, S., Bego, M., Pham, T., and Cohen, É. (2016). Remodeling of the Host Cell Plasma Membrane by HIV-1 Nef and Vpu: A Strategy to Ensure Viral Fitness and Persistence. Viruses *8*, 67.

Sumner, R.P., Thorne, L.G., Fink, D.L., Khan, H., Milne, R.S., and Towers, G.J. (2017). Are evolution and the intracellular innate immune system key determinants in HIV transmission? Frontiers in Immunology *8*.

Sumpter, B., Dunham, R., Gordon, S., Engram, J., Hennessy, M., Kinter, A., Paiardini, M., Cervasi, B., Klatt, N., McClure, H., et al. (2007). Correlates of preserved CD4(+) T cell homeostasis during natural, nonpathogenic simian immunodeficiency virus infection of sooty mangabeys: implications for AIDS pathogenesis. Journal of Immunology (Baltimore, Md. : 1950) *178*, 1680–1691.

Sundaravaradan, V., Saleem, R., Micci, L., Gasper, M.A., Ortiz, A.M., Else, J., Silvestri, G., Paiardini, M., Aitchison, J.D., and Sodora, D.L. (2013). Multifunctional double-negative T cells in sooty mangabeys mediate T-helper functions irrespective of SIV infection. PLoS Pathogens *9*, e1003441.

Swain, S.L., Howard, M., Kappler, J., Marrack, P., Watson, J., Booth, R., Wetzel, G.D., and Dutton, R.W. (1983). Evidence for two distinct classes of murine B cell growth factors with activities in different functional assays. Journal of Experimental Medicine *158*, 822–835.

Swigut, T., Iafrate, A.J., Muench, J., Kirchhoff, F., and Skowronski, J. (2000). Simian and Human Immunodeficiency Virus Nef Proteins Use Different Surfaces To Downregulate Class I Major Histocompatibility Complex Antigen Expression. Journal of Virology *74*, 5691–5701.

Swigut, T., Shohdy, N., and Skowronski, J. (2001). Mechanism for down-regulation of CD28 by Nef. The EMBO Journal *20*, 1593–1604.

Swigut, T., Greenberg, M., and Skowronski, J. (2003). Cooperative Interactions of Simian Immunodeficiency Virus Nef, AP-2, and CD3-ζ Mediate the Selective Induction of T-Cell Receptor-CD3 Endocytosis. Journal of Virology *77*, 8116–8126.

Swigut, T., Alexander, L., Morgan, J., Lifson, J., Mansfield, K.G., Lang, S., Johnson, R.P., Skowronski, J., and Desrosiers, R. (2004). Impact of Nef-Mediated Downregulation of Major Histocompatibility Complex Class I on Immune Response to Simian Immunodeficiency Virus. Journal of Virology *78*, 13335–13344.

Tada, T., Zhang, Y., Koyama, T., Tobiume, M., Tsunetsugu-Yokota, Y., Yamaoka, S., Fujita, H., and Tokunaga, K. (2015). March8 inhibits HIV-1 infection by reducing virion incorporation of envelope glycoproteins. Nature Medicine *21*, 1502–1507.

Takehisa, J., Kraus, M.H., Ayouba, A., Bailes, E., van Heuverswyn, F., Decker, J.M., Li, Y., Rudicell, R.S., Learn, G.H., Neel, C., et al. (2009). Origin and Biology of Simian Immunodeficiency Virus in Wild-Living Western Gorillas. Journal of Virology *83*, 1635–1648.

Takeuchi, J.S., Perche, B., Migraine, J., Mercier-Delarue, S., Ponscarme, D., Simon, F., Clavel, F., and Labrosse, B. (2013). High level of susceptibility to human TRIM5α conferred by HIV-2 capsid sequences. Retrovirology *10*.

Tchasovnikarova, I.A., Timms, R.T., Matheson, N.J., Wals, K., Antrobus, R., Göttgens, B., Dougan, G., Dawson, M.A., and Lehner, P.J. (2015). Epigenetic silencing by the HUSH complex mediates position-effect variegation in human cells. Science *348*, 1481–1485.

Tedbury, P.R., Ablan, S.D., and Freed, E.O. (2013). Global Rescue of Defects in HIV-1 Envelope Glycoprotein Incorporation: Implications for Matrix Structure. PLoS Pathogens *9*, e1003739.

Terahara, K., Yamamoto, T., Mitsuki, Y. ya, Shibusawa, K., Ishige, M., Mizukoshi, F., Kobayashi, K., and Tsunetsugu-Yokota, Y. (2012). Fluorescent reporter signals, EGFP, and DsRED, encoded in HIV-1 facilitate the detection of productively infected cells and cell-associated viral replication levels. Frontiers in Microbiology *2*.

Thiébaut, R., Matheron, S., Taieb, A., Brun-Vezinet, F., Chêne, G., and Autran, B. (2011). Long-term nonprogressors and elite controllers in the ANRS CO5 HIV-2 cohort. AIDS *25*, 865–867.

Thierry, S., Thierry, E., Subra, F., Deprez, E., Leh, H., Bury-Moné, S., and Delelis, O. (2016). Opposite transcriptional regulation of integrated vs unintegrated HIV genomes by the NF-κB pathway. Scientific Reports *6*, 25678.

Tilton, J.C., and Doms, R.W. (2010). Entry inhibitors in the treatment of HIV-1 infection. Antiviral Research *85*, 91–100.

Titanji, B.K., Aasa-Chapman, M., Pillay, D., and Jolly, C. (2013). Protease inhibitors effectively block cell-to-cell spread of HIV-1 between T cells. Retrovirology *10*, 161.

Titanji, B.K., Pillay, D., and Jolly, C. (2017). Combination antiretroviral therapy and cell–cell spread of wild-type and drug-resistant human immunodeficiency virus-1. Journal of General Virology *98*, 821–834.

Tokunaga, K., Kojima, A., Kurata, T., Ikuta, K., Akari, H., Koyama, A.H., Kawamura, M., Inubushi, R., Shimano, R., and Adachi, A. (1998). Enhancement of human immunodeficiency virus type 1 infectivity by Nef is producer cell-dependent. Journal of General Virology *79*, 2447–2453.

le Tortorec, A., and Neil, S.J.D. (2009). Antagonism to and intracellular sequestration of human tetherin by the human immunodeficiency virus type 2 envelope glycoprotein. Journal of Virology *83*, 11966–11978.

Trautz, B., Pierini, V., Wombacher, R., Stolp, B., Chase, A.J., Pizzato, M., and Fackler, O.T. (2016). The Antagonism of HIV-1 Nef to SERINC5 Particle Infectivity Restriction Involves the Counteraction of Virion-Associated Pools of the Restriction Factor. Journal of Virology *90*, 10915–10927.

Trautz, B., Wiedemann, H., Lüchtenborg, C., Pierini, V., Kranich, J., Glass, B., Kräusslich, H.G., Brocker, T., Pizzato, M., Ruggieri, A., et al. (2017). The host-cell restriction factor SERINC5 restricts HIV-1 infectivity without altering the lipid composition and organization of viral particles. Journal of Biological Chemistry *292*, 13702–13713.

Trickey, A., May, M.T., Vehreschild, J.J., Obel, N., Gill, M.J., Crane, H.M., Boesecke, C., Patterson, S., Grabar, S., Cazanave, C., et al. (2017). Survival of HIV-positive patients starting antiretroviral therapy between 1996 and 2013: a collaborative analysis of cohort studies. The Lancet HIV *4*, e349–e356.

Tristem, M., Marshall, C., Karpas, A., Petrik, J., and Hill, F. (1990). Origin of vpx in lentiviruses [14]. Nature *347*, 341–342.

Turville, S.G., Santos, J.J., Frank, I., Cameron, P.U., Wilkinson, J., Miranda-Saksena, M., Dable, J., Stõssel, H., Romani, N., Piatak, M., et al. (2004). Immunodeficiency virus uptake, turnover, and 2-phase transfer in human dendritic cells. Blood *103*, 2170–2179.

Tze, L.E., Horikawa, K., Domaschenz, H., Howard, D.R., Roots, C.M., Rigby, R.J., Way, D.A., Ohmura-Hoshino, M., Ishido, S., Andoniou, C.E., et al. (2011). CD83 increases MHC II and CD86 on dendritic cells by opposing IL-10 - Driven MARCH1-mediated ubiquitination and degradation. Journal of Experimental Medicine *208*, 149–165.

UNAIDS fact sheet. Global HIV and AIDS statistics — 2019 fact sheet | UNAIDS. Published 2019. Accessed May 28, 2020. https://www.unaids.org/en/resources/fact-sheet

Usami, Y., and Göttlinger, H. (2013). HIV-1 nef responsiveness is determined by env variable regions involved in trimer association and correlates with neutralization sensitivity. Cell Reports *5*, 802–812.

Usami, Y., Popov, S., Popova, E., Inoue, M., Weissenhorn, W., and Göttlinger, H.G. (2009). The ESCRT pathway and HIV-1 budding. Biochemical Society Transactions *37*, 181–184.

Usami, Y., Wu, Y., and Göttlinger, H.G. (2015). SERINC3 and SERINC5 restrict HIV-1 infectivity and are counteracted by Nef. Nature *526*, 218–223.

Valitutti, S., Miller, S., Cella, M., Padovan, E., and Lanzavecchia, A. (1995). Serial triggering of many T-cell receptors by a few peptide-MHC complexes. Nature *375*, 148–151.

Vanhaesebroeck, B., Leevers, S.J., Panayotou, G., Waterfield, M.D., and Waterfield, M.D. (1997). Phosphoinositide 3-kinases: A conserved family of signal transducers. Trends in Biochemical Sciences *22*, 267–272.

Varma, R., Campi, G., Yokosuka, T., Saito, T., and Dustin, M.L. (2006). T Cell Receptor-Proximal Signals Are Sustained in Peripheral Microclusters and Terminated in the Central Supramolecular Activation Cluster. Immunity *25*, 117–127.

Vasiliver-Shamis, G., Cho, M.W., Hioe, C.E., and Dustin, M.L. (2009). Human immunodeficiency virus type 1 envelope gp120-induced partial T-cell receptor signaling creates an F-actin-depleted zone in the virological synapse. Journal of Virology *83*, 11341–11355.

Veazey, R.S., Mansfield, K.G., Tham, I.C., Carville, A.C., Shvetz, D.E., Forand, A.E., and Lackner, A.A. (2000). Dynamics of CCR5 Expression by CD4+ T Cells in Lymphoid Tissues during Simian Immunodeficiency Virus Infection. Journal of Virology *74*, 11001–11007.

Veillette, A., Bookman, M.A., Horak, E.M., and Bolen, J.B. (1988). The CD4 and CD8 T cell surface antigens are associated with the internal membrane tyrosine-protein kinase p56lck. Cell *55*, 301–308.

Veillette, M., Desormeaux, A., Medjahed, H., Gharsallah, N.-E., Coutu, M., Baalwa, J., Guan, Y., Lewis, G., Ferrari, G., Hahn, B.H., et al. (2014). Interaction with Cellular CD4 Exposes HIV-1 Envelope Epitopes Targeted by Antibody-Dependent Cell-Mediated Cytotoxicity. Journal of Virology *88*, 2633–2644.

Venzke, S., Michel, N., Allespach, I., Fackler, O.T., and Keppler, O.T. (2006). Expression of Nef Downregulates CXCR4, the Major Coreceptor of Human Immunodeficiency Virus, from the Surfaces of Target Cells and Thereby Enhances Resistance to Superinfection. Journal of Virology *80*, 11141–11152.

Vigan, R., and Neil, S.J.D. (2010). Determinants of Tetherin Antagonism in the Transmembrane Domain of the Human Immunodeficiency Virus Type 1 Vpu Protein. Journal of Virology *84*, 12958–12970.

Vinton, C., Klatt, N.R., Harris, L.D., Briant, J.A., Sanders-Beer, B.E., Herbert, R., Woodward, R., Silvestri, G., Pandrea, I., Apetrei, C., et al. (2011). CD4-Like Immunological Function by CD4- T Cells in Multiple Natural Hosts of Simian Immunodeficiency Virus. Journal of Virology *85*, 8702–8708.

Visseaux, B., Damond, F., Matheron, S., Descamps, D., and Charpentier, C. (2016). Hiv-2 molecular epidemiology. Infection, Genetics and Evolution *46*, 233–240.

Wang, Y., and Prywes, R. (2000). Activation of the c-fos enhancer by the Erk MAP kinase pathway through two sequence elements: The c-fos AP-1 and p62(TCF) sites. Oncogene *19*, 1379–1385.

Wang, J.K., Kiyokawa, E., Verdin, E., and Trono, D. (2000). The Nef protein of HIV-1 associates with rafts and primes T cells for activation. Proceedings of the National Academy of Sciences of the United States of America *97*, 394–399.

Wang, Y., Pan, Q., Ding, S., Wang, Z., Yu, J., Finzi, A., Liu, S.-L., and Liang, C. (2017). The V3 Loop of HIV-1 Env Determines Viral Susceptibility to IFITM3 Impairment of Viral Infectivity. Journal of Virology *91*.

Ward, A.B., and Wilson, I.A. (2017). The HIV-1 envelope glycoprotein structure: nailing down a moving target. Immunological Reviews *275*, 21–32.

Ward, S.G., Westwick, J., Hall, N.D., and Sansom, D.M. (1993). Ligation of CD28 receptor by B7 induces formation of D-3 phosphoinositides in T lymphocytes independently of T cell receptor/CD3 activation. European Journal of Immunology *23*, 2572–2577.

Watson, A., Ranchalis, J., Travis, B., McClure, J., Sutton, W., Johnson, P.R., Hu, S.L., and Haigwood, N.L. (1997). Plasma viremia in macaques infected with simian immunodeficiency virus: plasma viral load early in infection predicts survival. Journal of Virology *71*, 284–290.

Watters, S.A., Mlcochova, P., and Gupta, R.K. (2013). Macrophages: The neglected barrier to eradication. Current Opinion in Infectious Diseases *26*, 561–566.

Wei, P., Garber, M.E., Fang, S.M., Fischer, W.H., and Jones, K.A. (1998). A novel CDK9-associated C-type cyclin interacts directly with HIV-1 Tat and mediates its high-affinity, loop-specific binding to TAR RNA. Cell *92*, 451–462.

Wei, X., Decker, J.M., Liu, H., Zhang, Z., Arani, R.B., Kilby, J.M., Saag, M.S., Wu, X., Shaw, G.M., and Kappes, J.C. (2002). Emergence of resistant human immunodeficiency virus type 1 in

patients receiving fusion inhibitor (T-20) monotherapy. Antimicrobial Agents and Chemotherapy *46*, 1896–1905.

Wei, X., Decker, J.M., Wang, S., Hui, H., Kappes, J.C., Wu, X., Salazar-Gonzalez, J.F., Salazar, M.G., Kilby, J.M., Saag, M.S., et al. (2003). Antibody neutralization and escape by HIV-1. Nature *422*, 307–312.

Weinelt, J., and Neil, S.J.D. (2014). Differential Sensitivities of Tetherin Isoforms to Counteraction by Primate Lentiviruses. Journal of Virology *88*, 5845–5858.

Weiss, L., Chevalier, M.F., Assoumou, L., Didier, C., Girard, P.-M., Piketty, C., Costagliola, D., and Rouzioux, C. (2014). T-cell activation positively correlates with cell-associated HIV-DNA level in viremic patients with primary or chronic HIV-1 infection. AIDS *28*, 1683–1687.

Weng, J., Krementsov, D.N., Khurana, S., Roy, N.H., and Thali, M. (2009). Formation of Syncytia Is Repressed by Tetraspanins in Human Immunodeficiency Virus Type 1-Producing Cells. Journal of Virology *83*, 7467–7474.

Wildum, S., Schindler, M., Munch, J., and Kirchhoff, F. (2006). Contribution of Vpu, Env, and Nef to CD4 Down-Modulation and Resistance of Human Immunodeficiency Virus Type 1-Infected T Cells to Superinfection. Journal of Virology *80*, 8047–8059.

van Wilgenburg, B., Moore, M.D., James, W.S., and Cowley, S.A. (2014). The productive entry pathway of HIV-1 in macrophages is dependent on endocytosis through lipid rafts containing CD4. PLoS ONE *9*.

Willey, R.L., Maldarelli, F., Martin, M.A., and Strebel, K. (1992). Human immunodeficiency virus type 1 Vpu protein induces rapid degradation of CD4. Journal of Virology *66*, 7193–7200.

Williams, S.A., Kwon, H., Chen, L.-F., and Greene, W.C. (2007). Sustained induction of NF-kappa B is required for efficient expression of latent human immunodeficiency virus type 1. Journal of Virology *81*, 6043–6056.

Wilton, J., Senn, H., Sharma, M., and Tan, D.H.S. (2015). Pre-exposure prophylaxis for sexually-acquired HIV risk management: A review. HIV/AIDS - Research and Palliative Care *7*, 125–136.

Witte, V., Laffert, B., Gintschel, P., Krautkrämer, E., Blume, K., Fackler, O.T., and Baur, A.S. (2008). Induction of HIV Transcription by Nef Involves Lck Activation and Protein Kinase Cθ Raft Recruitment Leading to Activation of ERK1/2 but Not NFκB. The Journal of Immunology *181*, 8425–8432.

de Witte, L., Bobardt, M., Chatterji, U., Degeest, G., David, G., Geijtenbeek, T.B.H., and Gallay, P. (2007). Syndecan-3 is a dendritic cell-specific attachment receptor for HIV-1. Proceedings of the National Academy of Sciences of the United States of America *104*, 19464–19469.

Wlodawer, A., and Erickson, J.W. (1993). Structure-Based Inhibitors of HIV-1 Protease. Annual Review of Biochemistry *62*, 543–585.

Worobey, M., Gemmel, M., Teuwen, D.E., Haselkorn, T., Kunstman, K., Bunce, M., Muyembe, J.J., Kabongo, J.M.M., Kalengayi, R.M., van Marck, E., et al. (2008). Direct evidence of extensive diversity of HIV-1 in Kinshasa by 1960. Nature *455*, 661–664.

Wu, W.L., Grotefend, C.R., Tsai, M.T., Wang, Y.L., Radic, V., Eoh, H., and Huang, I.C. (2017). Δ20 IFITM2 differentially restricts X4 and R5 HIV-1. Proceedings of the National Academy of Sciences of the United States of America *114*, 7112–7117.

Wu, Y., Olety, B., Weiss, E.R., Popova, E., Yamanaka, H., and Göttlinger, H. (2019). Potent enhancement of HIV-1 replication by nef in the absence of SERINC3 and SERINC5. MBio *10*.

Wyss, S., Berlioz-Torrent, C., Boge, M., Blot, G., Honing, S., Benarous, R., and Thali, M. (2001). The Highly Conserved C-Terminal Dileucine Motif in the Cytosolic Domain of the Human Immunodeficiency Virus Type 1 Envelope Glycoprotein Is Critical for Its Association with the AP-1 Clathrin Adapter. Journal of Virology *75*, 2982–2992.

Yakovian, O., Schwarzer, R., Sajman, J., Neve-Oz, Y., Razvag, Y., Herrmann, A., and Sherman, E. (2018). Gp41 dynamically interacts with the TCR in the immune synapse and promotes early T cell activation. Scientific Reports *8*.

Yamamoto, N., Okada, M., Koyanagi, Y., Kannagi, M., and Hinuma, Y. (1982). Transformation of human leukocytes by cocultivation with an adult T cell leukemia virus producer cell line. Science *217*, 737–739.

Ylinen, L.M.J., Keckesova, Z., Wilson, S.J., Ranasinghe, S., and Towers, G.J. (2005). Differential Restriction of Human Immunodeficiency Virus Type 2 and Simian Immunodeficiency Virus SIVmac by TRIM5α Alleles. Journal of Virology *79*, 11580–11587.

Yoh, S.M., Schneider, M., Seifried, J., Soonthornvacharin, S., Akleh, R.E., Olivieri, K.C., de Jesus, P.D., Ruan, C., de Castro, E., Ruiz, P.A., et al. (2015). PQBP1 is a proximal sensor of the cGAS-dependent innate response to HIV-1. Cell *161*, 1293–1305.

Yokosuka, T., Takamatsu, M., Kobayashi-Imanishi, W., Hashimoto-Tane, A., Azuma, M., and Saito, T. (2012). Programmed cell death 1 forms negative costimulatory microclusters that directly inhibit T cell receptor signaling by recruiting phosphatase SHP2. Journal of Experimental Medicine *209*, 1201–1217.

Yoon, K., and Kim, S. (1999). Lack of negative influence on the cellular transcription factors NF-κB and AP-1 by the Nef protein of human immunodeficiency virus type 1. Journal of General Virology *80*, 2951–2956.

Younas, M., Psomas, C., Reynes, J., and Corbeau, P. (2016). Immune activation in the course of HIV-1 infection: Causes, phenotypes and persistence under therapy. HIV Medicine *17*, 89–105.

Yu, G., and Felsted, R.L. (1992). Effect of myristoylation on p27nef subcellular distribution and suppression of HIV-LTR transcription. Virology *187*, 46–55.

Yu, H., Khalid, M., Heigele, A., Schmökel, J., M. Usmani, S., van der Merwe, J., Münch, J., Silvestri, G., and Kirchhoff, F. (2015). Lentiviral Nef Proteins Manipulate T Cells in a Subset-Specific Manner. Journal of Virology *89*, 1986–2001.

Yu, X., Yu, Y., Liu, B., Luo, K., Kong, W., Mao, P., and Yu, X.F. (2003). Induction of APOBEC3G Ubiquitination and Degradation by an HIV-1 Vif-Cul5-SCF Complex. Science *302*, 1056–1060.

Yuan, W., Li, X., Kasterka, M., Gorny, M.K., Zolla-Pazner, S., and Sodroski, J. (2009). Oligomer-specific conformations of the Human Immunodeficiency Virus (HIV-1) gp41 envelope glycoprotein ectodomain recognized by human monoclonal antibodies. AIDS Research and Human Retroviruses *25*, 319–328.

Yurkovetskiy, L., Guney, M.H., Kim, K., Goh, S.L., McCauley, S., Dauphin, A., Diehl, W.E., and Luban, J. (2018). Primate immunodeficiency virus proteins Vpx and Vpr counteract transcriptional repression of proviruses by the HUSH complex. Nature Microbiology *3*, 1354–1361.

Zhan, Y., Carrington, E.M., Zhang, Y., Heinzel, S., and Lew, A.M. (2017). Life and death of activated T cells: How are they different from naïve T Cells? Frontiers in Immunology *8*.

Zhang, F., Wilson, S.J., Landford, W.C., Virgen, B., Gregory, D., Johnson, M.C., Munch, J., Kirchhoff, F., Bieniasz, P.D., and Hatziioannou, T. (2009). Nef Proteins from Simian Immunodeficiency Viruses Are Tetherin Antagonists. Cell Host and Microbe *6*, 54–67.

Zhang, F., Landford, W.N., Ng, M., McNatt, M.W., Bieniasz, P.D., and Hatziioannou, T. (2011). SIV Nef proteins recruit the AP-2 complex to antagonize Tetherin and facilitate virion release. PLoS Pathogens *7*.

Zhang, N., Hartig, H., Dzhagalov, I., Draper, D., and He, Y.W. (2005). The role of apoptosis in the development and function of T lymphocytes. Cell Research *15*, 749–769.

Zhang, W., Du, J., Evans, S.L., Yu, Y., and Yu, X.F. (2012). T-cell differentiation factor CBF-β regulates HIV-1 Vif-mediated evasion of host restriction. Nature *481*, 376–379.

Zhang, Y., Tada, T., Ozono, S., Yao, W., Tanaka, M., Yamaoka, S., Kishigami, S., Fujita, H., and Tokunaga, K. (2019). Membrane-associated RING-CH (March) 1 and 2 are March family members that inhibit HIV-1 infection. Journal of Biological Chemistry *294*, 3397–3405.

Zhang, Z., Gu, Q., de Manuel Montero, M., Bravo, I.G., Marques-Bonet, T., Häussinger, D., and Münk, C. (2017). Stably expressed APOBEC3H forms a barrier for cross-species transmission of simian immunodeficiency virus of chimpanzee to humans. PLOS Pathogens *13*, e1006746.

Zhao, G., Perilla, J.R., Yufenyuy, E.L., Meng, X., Chen, B., Ning, J., Ahn, J., Gronenborn, A.M., Schulten, K., Aiken, C., et al. (2013). Mature HIV-1 capsid structure by cryo-electron microscopy and all-atom molecular dynamics. Nature *497*, 643–646.

Zheng, Y.-H., Irwin, D., Kurosu, T., Tokunaga, K., Sata, T., and Peterlin, B.M. (2004). Human APOBEC3F Is Another Host Factor That Blocks Human Immunodeficiency Virus Type 1 Replication. Journal of Virology *78*, 6073–6076.

Zhong, P., Agosto, L.M., Ilinskaya, A., Dorjbal, B., Truong, R., Derse, D., Uchil, P.D., Heidecker, G., and Mothes, W. (2013). Cell-to-Cell Transmission Can Overcome Multiple Donor and Target Cell Barriers Imposed on Cell-Free HIV. PLoS ONE *8*.

Zhou, X., DeLucia, M., and Ahn, J. (2016). SLX4-SLX1 protein-independent down-regulation of MUS81-EME1 protein by HIV-1 viral protein R (Vpr). Journal of Biological Chemistry *291*, 16936–16947.

Zhu, P., Chertova, E., Bess, J., Lifson, J.D., Arthur, L.O., Liu, J., Taylor, K.A., and Roux, K.H. (2003). Electron tomography analysis of envelope glycoprotein trimers on HIV and simian immunodeficiency virus virions. Proceedings of the National Academy of Sciences of the United States of America *100*, 15812–15817.

Zhu, Y., Wang, G.Z., Cingöz, O., and Goff, S.P. (2018). NP220 mediates silencing of unintegrated retroviral DNA. Nature *564*, 278–282.